# C-H Functionalisation Mediated by Aluminium and Iridium

Lyall, Catherine

*Award date:*
2014

*Awarding institution:*
University of Bath

# C-H Functionalisation Mediated by Aluminium and Iridium

Catherine Louise Lyall

A thesis submitted for the degree of Doctor of Philosophy

University of Bath

Department of Chemistry

May 2014

# Table of Contents

# Acknowledgements

First and foremost, to thank Simon, who coaxed me into this PhD initially and has unwaveringly supported me throughout. His guidance and teaching, as well as instruction to always have a fire extinguisher to hand, has been much appreciated.

To acknowledge the one-time right hand men of Simon, Mario and Matthew, without whom more reactions would have ended badly. To Mario in particular, who always put himself second over three years of working together.

Thank you to Dan for the introduction to the wonderful world of naphthalenediimides, as well as constant encouragement.

To those people who helped where my knowledge is limited. John, for NMRs, refills of liquid nitrogen and a friendly face. Mary, for X-ray crystallography, excess tissues and being a fabulous role-model. Ian and Makoto, for computational modelling and interesting discussions.

To those who provided equipment and showed me how to use it. Liam, in particular, for explaining how to use a variety of microwave reactors. The Whittlesey group for providing their glove-box and the Burrows group for allowing me to use their microwave.

To the ladies that started this adventure with me, Julia and Kat, without whom days would be duller, the lab would be quieter and my ability to hold it all together would be compromised.

To those students who worked so hard on the project. To Montse, who started the NDI chapter rolling, and never gave up. To Camilla, who suffered induction by fire to column chromatography.

To the other undergraduate students who have been subjected to my supervision; Michael, my guinea-pig; Nick W, who came back for more and Nick L, whose enthusiasm is unstoppable.

To the other students of the Lewis Group; Paul, Anthony G, Monika, Kate B (now T), George, Anthony T and Max who have brightened up my days.

To Kate L, who has been there for the seven years of ups and downs of university life. She has turned me into a person who is phased by very few things. To Sarah, a constant rock, always willing to minimise her own issues to listen to complaints about mine.

To housemates past; Anna, Jim, Kat, Liz and Michael, for putting up with me. Especially to Anna and Liz, for help with Barney.

To my Mum and Dad, for constant support despite my inability to express exactly what I'm doing.

This is dedicated to my fiancé Alex. For patience that knows no bounds.

# Abbreviations

| | |
|---|---|
| $^{11}B$ | Boron eleven |
| $^{19}F$ | Fluorine nineteen |
| $^{13}C$ | Carbon thirteen |
| $^{1}H$ | Proton |
| 9-BBN | 9-Borabicyclo[3.3.1]nonane |
| °C | Degrees centigrade |
| Ac | Acetyl |
| AcOH | Acetic acid |
| Ar | Aryl functional group |
| Å | Angstrom ($10^{-10}$ m) |
| BQ | 1,4-benzoquinone |
| $^{n}Bu$ | *normal*-Butyl |
| $^{t}Bu$ | *tertiary*-Butyl |
| cap | caprolactam |
| Cat. | Catalytic |
| Cbz | Carboxybenzyl |
| cod | 1,4-cyclooctadiene |
| coe | cyclooctene |
| COSY | Correlation spectroscopy |
| Cp | Cyclopentadienyl |
| Cp* | Pentamethylcyclopentadienyl |
| Cy | Cyclohexyl |
| d | doublet |
| DBN | 1,5-Diazabicyclo[4.3.0]non-5-ene |
| DCE | 1,2-Dichloroethane |

| | |
|---|---|
| DCM | Dichloromethane |
| DEG | Diethylene glycol |
| DMA | *N,N*-dimethylacetamide |
| DMF | *N,N*-dimethylformamide |
| DNP | Dinitrophenyl |
| DOSP | *N*-(*para*-dodecylphenylsulfonyl)proline |
| $\Delta$ | Heat |
| $E^+$ | Electrophile |
| EDA | ethyldiazoacetate |
| EDG | Electron donating group |
| ee | enantiomeric excess |
| eq. | Equivalents |
| Et | Ethyl |
| EtOH | Ethanol |
| EWG | Electron withdrawing group |
| FGI | Functional Group Interconversion |
| h | Hours |
| $H^+$ | Brønsted acid |
| H2BC | Heteronuclear 2 Bond Correlation |
| HMBC | Heteronuclear Multiple Bond Correlation |
| HSQC | Heteronuclear Single Quantum Correlation |
| $h\upsilon$ | Light |
| Hz | Hertz |
| IPr | *N,N*-bis(2,6-diisopropylphenyl)imidazol-2-ylidene |
| IR | Infra-red |
| ln | natural log |
| L | ligand |

| | |
|---|---|
| LP | Lone pair |
| M | Metal centre |
| M (unit) | Molar |
| *m* | *meta* |
| m | multiplet |
| m (unit) | metres |
| *m*CPBA | *meta*-chloroperbenzoic acid |
| Me | Methyl |
| Mes | Mesityl |
| MeOH | Methanol |
| MHz | Megahertz |
| min | Minutes |
| mmol | millimoles |
| mol | moles |
| MS | Mass spectrometry |
| µw | Microwave |
| NBS | *N*-Bromosuccinimide |
| NDA | Naphthalene-1,4,5,8-dianhydride |
| NDI | Naphthalene-1,4,5,8-diimide |
| NMR | Nuclear Magnetic Resonance |
| NOE | Nuclear Overhauser effect |
| NOESY | Nuclear Overhauser effect spectroscopy |
| Nuc | Nucleophile |
| *o* | *ortho* |
| Oct | Octyl |
| OEt | Ethoxy |
| OMe | Methoxy |

| | |
|---|---|
| *p* | *para* |
| PCM | Polarizable Continuum Model |
| PDI | Perylenediimide |
| PENDANT | Polarisation ENhancement During Attached Nucleus Testing |
| Ph | Phenyl |
| pin | pinacol |
| Piv | Pivaloyl (trimethyl acetyl) |
| ppm | Parts per million |
| q | quartet |
| R | Functional group |
| $R_f$ | Retention factor |
| RF | Radio frequency |
| rt | Room temperature |
| s | singlet |
| t | triplet |
| TBAF | tetrabutylammonium fluoride |
| TBS | *tertiary*-butyldimethylsilyl |
| TFDO | methyl(trifluoromethyl)dioxirane |
| THF | Tetrahydrofuran |
| THP | Tetrahydropyran |
| TMANO | Trimethylamine-*N*-oxide |
| Tol | Toluene |
| Ts | *p*-tolylsulfonyl |
| TsOH | *p*-tolylsulfonic acid |
| UV | Ultra-violet |
| W | Watts |
| X | Halogen |

# Declaration of material from a previously submitted thesis and of work done in conjunction with others

Computational modeling in Chapter two is performed by Dr Makoto Sato and Professor Ian Williams.

Computational modeling in Chapter three is performed by Dr G. Dan Pantoş. In the same chapter, identification of the enol ether product from the Baddeley reaction of bicyclohexyl was described in a project report by this author for the degree of MChem Chemistry for Drug Discovery.

This work is clearly outlined and credited in the text of the thesis where it is referred to.

Some experimental procedures referred to in Chapter four were first carried out by Monserrat Pérez-Salvia (Eramus student, Oct 2011-April 2012) and Camilla Shotton (Summer student, July-August 2012), under my supervision. These experimental procedures are detailed in Chapter five, where these students are credited.

# Abstract

This thesis investigates the use of aluminium trichloride and acetyl chloride to functionalise saturated hydrocarbons and probe the mechanism by which this functionalisation occurs. It also looks at the use of iridium catalysis to form carbon-boron bonds from carbon-hydrogen bonds in naphthalenediimides or NDIs.

Chapter one reviews work published in the field of carbon-hydrogen bond functionalisation; from the traditional reactions of hydrocarbons as simple as combustion to cutting-edge selective C-H activation in natural product synthesis.

Chapter two investigates experimentally the mechanism of the “Baddeley reaction”; the low-temperature interaction of decalin with aluminium trichloride and acetyl chloride, identifying key intermediates on the mechanistic pathway and the order of reaction in acylating reagent and substrate.

Chapter three applies the Baddeley methodology to other saturated hydrocarbons, selected for certain commonalities with decalin based on the mechanism established. The results of these reactions include unusual sketetal rearrangements and the synthesis of novel compounds.

Chapter four focuses on C-H borylation of NDIs at the naphthalene core; optimisation of the reaction uses microwave heating and both mono-borylated and di-borylated isomers can be synthesised. These boronic esters formed are suitable starting materials for further reactions; examples of possible Suzuki reactions are detailed.

Chapter five details experimental procedures associated with the work of the previous three chapters.

# A History of Functionalising Carbon-Hydrogen Bonds

## 1.1 Why Carbon-Hydrogen Bonds?

Carbon-hydrogen bonds in their various forms are the most common type of bond in organic chemistry. It makes sense therefore, that it is a desire of many chemists to be able to select one carbon-hydrogen bond from many in a molecule and transform it into a carbon-carbon bond, or indeed a bond to any atom other than hydrogen. For many reasons, this goal is still unobtainable, although over recent decades great advances have been made in the field of functionalising carbon-hydrogen bonds.[1, 2, 3]

Traditional organic chemistry has been mostly focused on functional group interconversion (FGI), where an already functionalised bond (for example, carbon-bromine) can be modified to form another functionalised bond (for example, carbon-oxygen). An outline of some typical functional group interconversions is shown in Scheme 1.

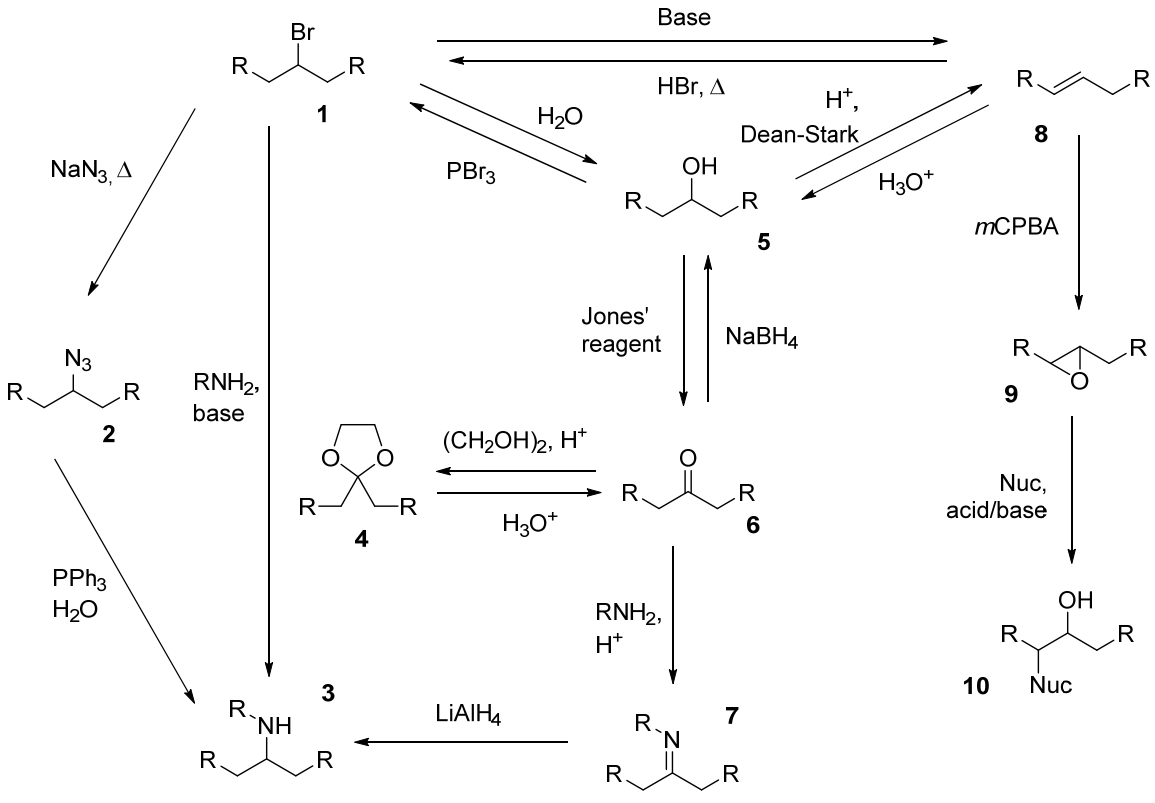


**Scheme 1: Some functional group interconversions.[4]**

Whilst advances in FGI have provided routes to complex molecules and natural products where none have existed before, it is apparent that the ability to directly convert carbon-hydrogen bonds to functionalised bonds could dramatically reduce the number of steps in a synthetic route, saving time, resources and expense.

## 1.2 Traditional Reactions of Hydrocarbons

Hydrocarbons (those molecules that are made up entirely of hydrogen and carbon) are typically sourced from crude oil; they are one of the main feedstocks for production of organic chemicals. They can be classified by their hybridisation; alkanes, composed of $sp^3$ hydbridised carbon atoms which are fully saturated; alkenes, containing at least two adjacent $sp^2$ hybridised carbon atoms with a double bond between them; aromatics, consisting of $sp^2$ carbons which follow Hückel's Rule for aromaticity – typically those aromatic hydrocarbons sourced from crude oil would contain a benzene ring; and alkynes, those molecules with at least one sp hydbridised carbon-carbon triple bond.

Some of the traditional reactions that these molecules undergo do involve the replacement of a carbon-hydrogen bond with a carbon-other atom bond, such as electrophilic aromatic substitution, but others take advantage of reducing the multiple bonds to single bonds leaving the carbon-hydrogen bonds untouched. With the least reactive group, the alkanes, the processes either involve free radicals or have limited use for organic synthesis.

Table 1 shows the homolytic bond dissociation energies of a variety of hydrocarbons; aliphatic, alkenic, alkynic and aromatic. This indicates the relative ease of cleaving tertiary aliphatic C-H bonds versus secondary aliphatic C-H bonds, which in turn have lower bond dissociation energies than primary aliphatic C-H bonds.

| Bond | Bond dissociation enthalpy (kJ $mol^{-1}$) | Bond | Bond dissociation enthalpy (kJ $mol^{-1}$) |
|---|---|---|---|
| 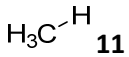 **11** | 439.7 | 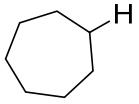 **17** | 387.0 |
| 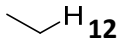 **12** | 410.9 | 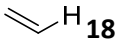 **18** | 460.2 |
| 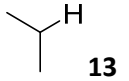 **13** | 397.9 | 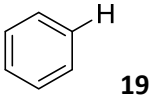 **19** | 464.0 |
| 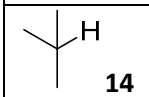 **14** | 389.9 | 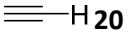 **20** | 552.3 |
| 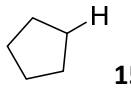 **15** | 395.4 | 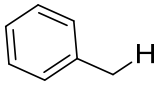 **21** | 368.2 |
| 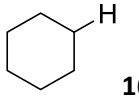 **16** | 399.6 | | |

**Table 1: Bond dissociation energies (kJ $mol^{-1}$) for a variety of carbon-hydrogen bonds.[5]**

## 1.2.1 Aromatic Hydrocarbons

### *1.2.1.1 Electrophilic Aromatic Substitution*

Aromatic hydrocarbons contain the most reactive carbon-hydrogen bonds. Typically, this is not due to these carbon-hydrogen bonds being weaker, as often the opposite is true.[3,5,6] However, the aromatic π system offers additional stabilisation to positively charged intermediates, which is not available in other hydrocarbons. The phenomenon of electrophilic aromatic substitution takes advantage of this π system stabilisation and many examples of this type of reaction are taught at undergraduate level.

Some representative examples are shown in Scheme 2; reaction of benzene with aluminium trichloride and acetyl chloride[7] (Friedel–Crafts Acylation) to give acylated benzene, **22**; reaction of benzene with halogens and the relevant iron trihalide to form halobenzene, **23**; sulfonation of benzene with oleum to form **24**; alkylation of benzene with ethene and an acid catalyst yielding **25**; finally, nitration of benzene with nitric acid and a sulfuric acid catalyst to give nitrobenzene **26**.[4]

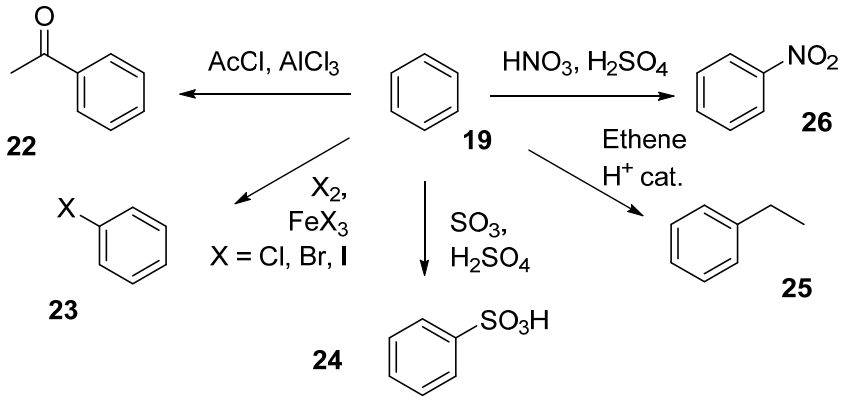


**Scheme 2: Examples of Electrophilic Aromatic Substitution ($S_EAr$).**

These reactions are subject to problems when the substrates are more complex than benzene. Firstly, the selectivity of the reactions can be controlled to some extent by directing functional groups around the ring, but these effects can be competing and give rise to multiple products. Functional groups which are electron-donating by resonance, such as $–NH_2$, direct the electrophilic aromatic substitution to occur at the *ortho* and *para* positions as well as speeding up the rate of the reaction. Scheme 3 shows the resonance structures of aniline, **27**, which illustrate the increased partial negative charges in the *ortho* and *para* positions.

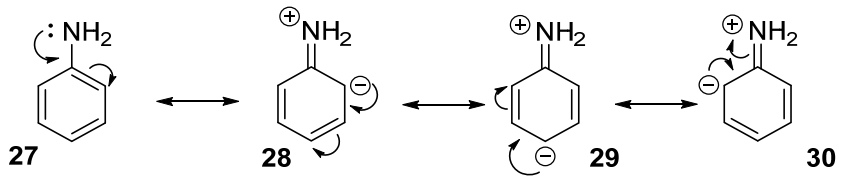


**Scheme 3: Resonance structures of aniline.**

Strongly electron-withdrawing groups, such as $–NO_2$, destabilise the *ortho* and *para* positions to electrophilic aromatic substitution by increasing the partial positive charge on these carbons, as shown in Scheme 4. As a result, the *meta* position is comparatively more reactive towards substitution but the reaction is slower.

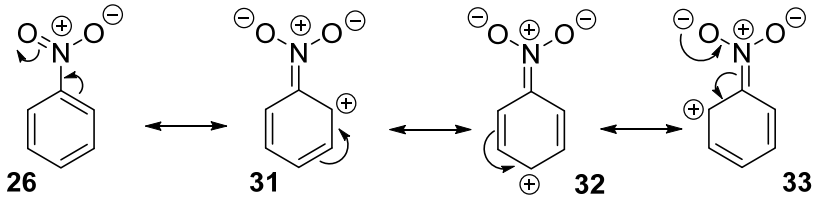


**Scheme 4: Resonance structures of nitrobenzene.**

Secondly, the reaction conditions are harsh. This can cause issues when subjecting aromatic molecules that contain other functional groups to the reactions, as some sensitive functional groups cannot stand up to these conditions.

### *1.2.1.2 Dearomatisation*

The Birch Reduction is a well-known reaction in organic chemistry, which is unusual in its ability to reduce aromatic rings to nonaromatic 1,4-cyclohexadienes.[8] The reaction conditions use sodium or lithium metal dissolved in liquid ammonia, generating the metal cations and solvated electrons. These solvated electrons are able to reduce the aromatic rings via the mechanism illustrated in Scheme 5.

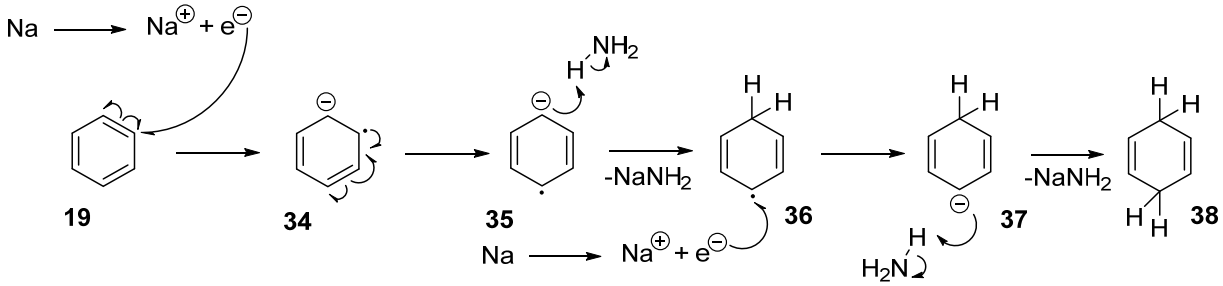


**Scheme 5: Mechanism of Birch Reduction of benzene.**

Aromatic hydrocarbons can be hydrogenated under high pressures of hydrogen and over heterogeneous metal catalysts, to give fully saturated rings, for example, benzene through to cyclohexane.

Whilst these reductions can be useful for accessing certain skeletal structures, the reaction conditions are again harsh, and applicability in more complex structures is limited. Any functional groups present which are susceptible to reduction would be reduced, so use of protecting groups would be required or said functional groups would need to be introduced in a later synthetic step.

Another possible method of removing aromaticity from aromatic rings is via microbial arene oxidation. An early example of this process was using *Pseudomonas putida*, oxidising benzene

to dihydrocatechol.[9] Ley and coworkers[10] used this process in the synthesis of racemic pinitol, as shown in Scheme 6.

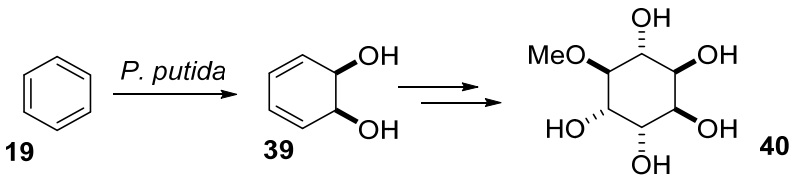


**Scheme 6: Synthesis of (±)-pinitol involving microbial oxidation of benzene with *P. putida* to dihydrocatechol.[9,10]**

### *1.2.1.3 Photochemistry*

It is possible to excite arenes with light, leading to photocycloadditions with alkenes. These can be [2+2], [3+2] or [4+2] cycloadditions; these reactions give products functionalised in the *ortho*, *meta* and *para* positions respectively.[11,12,13] [4+2] photocycloadditions, which can be considered to be photo-Diels–Alder reactions, are relatively uncommon in comparison to the [2+2] and [3+2] additions, and are disallowed by the Woodward-Hoffman rules.[4]

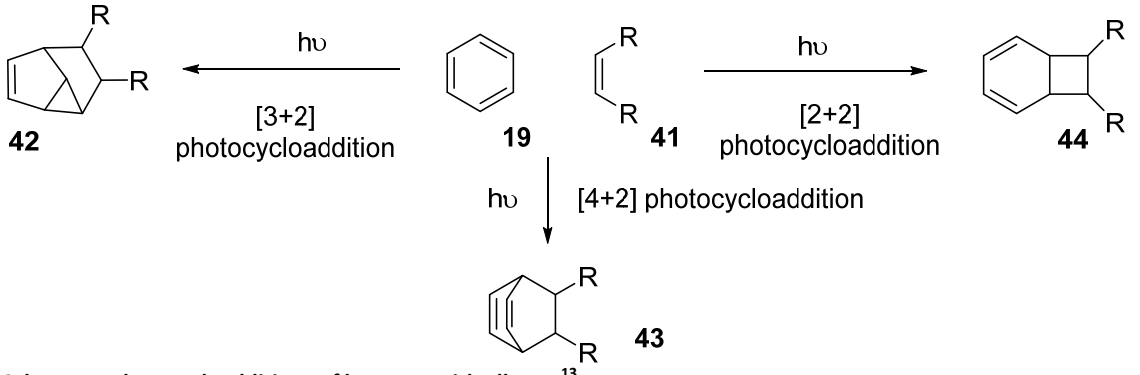


**Scheme 7: Photocycloadditions of benzene with alkenes[13]**

## 1.2.2 Alkenes and Alkynes

### *1.2.2.1 Addition of diatoms*

Both alkenes and alkynes undergo hydrogenation readily in the presence of hydrogen over metal catalysts, generally requiring significantly less hydrogen pressure than arenes. In the case of alkynes, selective conditions can be applied so that only one molecule of hydrogen is added across each triple bond, affording the alkene, rather than being fully saturated through to the alkane. The Lindlar catalyst (palladium on $CaCO_3$ or $BaSO_4$ with lead additives)[14] is used to hydrogenate alkynes through to *cis*-alkenes and Birch Reduction conditions (sodium in liquid ammonia) can be used to reduce alkynes to *trans*-alkenes, illustrated in Scheme 8.

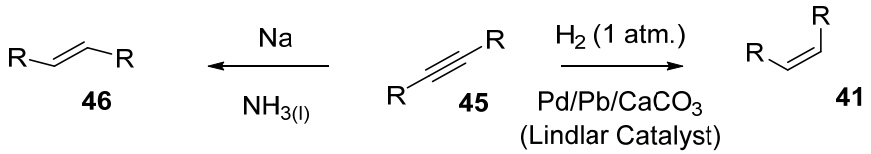


**Scheme 8: Selective reduction of alkynes to *cis*- and *trans*-alkenes.**

Alkenes react with halogens to give saturated 1,2-dihalides. Similarly, alkynes react with excess halogens to form the 1,1,2,2-tetrahalides. The discolouration of bromine water is used as a simple test for the presence of multiple bonds.

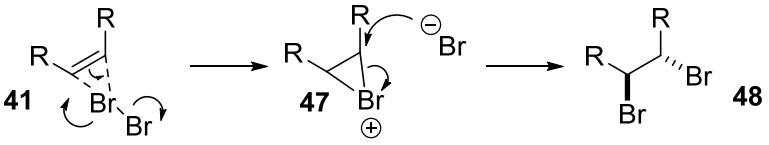


**Scheme 9: Mechanism for addition of bromine across an alkene.**

### *1.2.2.2 Markownikoff's Rule*

Addition of HX molecules across double or triple bonds follow Markowikoff's rule when the reaction proceeds via a carbocation intermediate. Markownikoff's rule[15] states that the hydrogen atom will be added to the carbon with most hydrogens already present, and the non-hydrogen moiety will be added to the carbon atom in a state of higher substitution.

### *1.2.2.3 Anti-Markownikoff Additions*

For additions which do not proceed via a carbocation intermediate, Markownikoff's rule is not followed. In these cases, it may be possible to use the anti-Markownikoff addition reaction followed by a substitution reaction to form an anti-Markownikoff product selectively, albeit via an additional synthetic step compared with the Markownikoff addition reaction. An example of anti-Markownikoff addition across a double bond is hydroboration, the mechanism for which is shown in Scheme 10. The borane approaches with the steric bulk of the borane ($-BR_2$) nearing the alkene carbon atom that is least hindered. This allows the small hydrogen atom to add to more substituted carbon, unlike in Markownikoff additions.

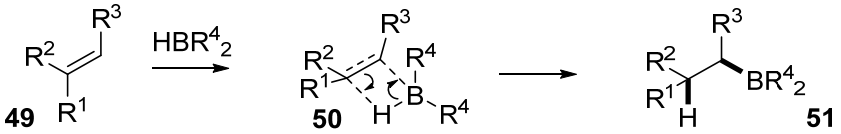


**Scheme 10: Hydroboration mechanism.**

## 1.2.3 Alkanes

Alkanes are the least reactive of the hydrocarbons, being fully $sp^3$ hybridised with no unsaturation to exploit. Alkanes can undergo combustion in the presence of oxygen to give carbon dioxide and water. In the event of combustion in the presence of insufficient oxygen, carbon monoxide can be formed. These reactions are not useful for chemical synthesis, although do find significant uses in the energy and automotive industries.

### *1.2.3.1 Cracking*

Cracking is a process that is applied to long chain alkanes that are generally less useful for combustion. Thermal cracking involves high temperatures and pressures; the chemical reactions involved are mainly based on free radical reactions. The products from cracking depend on the starting alkanes, but are a mixture of shorter chain alkanes and alkenes.

Catalytic cracking involves passing the same long chain alkanes over solid catalysts (for example, zeolite based) to again afford shorter chain alkanes and alkenes.[16]

### *1.2.3.2 Free Radical Halogenation*

The industrial method for synthesising the common laboratory solvents chloroform and dichloromethane involve the free radical halogenation of methane with chlorine. The initiation step involves irradiating chlorine with UV light causing homolytic cleavage of the chlorine-chlorine bond. This generates two chlorine radicals.

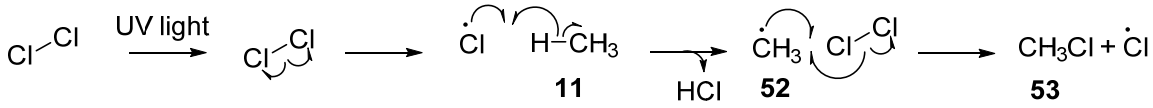


**Scheme 11: Free radical chlorination of methane yielding methyl chloride.**

As shown in Scheme 11, the chlorine radical then abstracts a hydrogen radical from methane, forming hydrogen chloride and a methyl radical. The methyl radical can either react with a chlorine molecule as shown, propagating the chain reaction by generating another chlorine radical or terminate the reaction by reacting with a previously formed chlorine radical. In the presence of excess chlorine, the methyl chloride can continue reacting via the same mechanism to form dichloromethane, chloroform and carbon tetrachloride. It is also possible to form ethane via the termination of two methyl radicals, which is not a desirable outcome from the process.

Performing this reaction on longer chain alkanes is possible, but as chlorine can be substituted at any position on the chain, a mixture of products is formed. This lack of selectivity, along with difficulties limiting the number of chlorines added to any one molecule mean the reaction is of little use with higher molecular weight alkanes.

## 1.3 C-H Activation

C-H activation is the broad and generally accepted term for reactions where a carbon-hydrogen bond has a metal centre inserted into it, “activating” the carbon-hydrogen bond. Whilst there are other means to replace a carbon-hydrogen bond under metal-free conditions, such as the previously discussed electrophilic aromatic substitution and free radical halogenations, C-H activation has been the main technique that has been developed over recent decades to yield selective and useful functionalisation of carbon-hydrogen bonds.

In his 1997 review,[3] Shilov divided C-H activation reactions into three classes; those that undergo “true” C-H activation by inserting a metal centre into a carbon-hydrogen bond, causing formation of a metal-carbon bond; those reactions where a carbon-hydrogen bond is cleaved, but a metal-carbon bond is not subsequently formed; and finally, those reactions where a metal promotes reactivity of another reagent which then goes on to break the carbon-hydrogen bond. Most C-H activation reactions studied today using transition metals fall into the first category, and it is this cateogory that is the generally accepted definition of C-H activation.

In the first instance, this discussion will focus on the activation of carbon-hydrogen bonds in aromatic or alkenic molecules. Although research into C-H activation of both aromatic and aliphatic hydrocarbons began at similar times in the late 1950's and early 1960's, initial reactions were stoichiometric; C-H activation of aromatic substrates progressed to using catalytic systems sooner.

### 1.3.1 Early Oxidative Addition Reactions

Scheme 12 shows an example of C-H activation of an aryl carbon-hydrogen bond from 1970.[17] In this case, the authors propose the tungsten molecule first reduces one of the double bonds present in the isoprene. This initial step results in a tungsten molecule which is coordinatively unsaturated and oxidative addition of the benzene carbon-hydrogen bond can occur. Oxidative addition of carbon-hydrogen bonds across a metal centre is still a common mechanism in C-H activation reactions being discovered today.

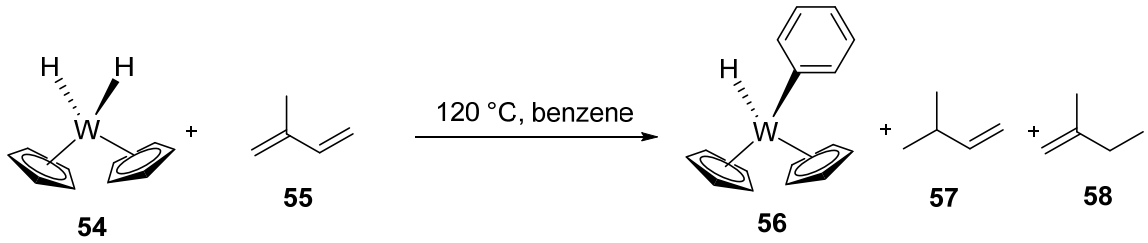


**Scheme 12: An early example of stoichiometric C-H activation of benzene with a tungsten metal centre.[17]**

Prior to this work, Chatt and coworkers[18] had investigated in 1959 the use of ruthenium complexes to mediate hydrogen-deuterium exchange in naphthalene compounds, where the ruthenium centre would insert into a carbon-hydrogen bond, as shown in Scheme 13. Further reaction of this complex with deuterium chloride would form the deuterated naphthalene and *cis*-[$RuCl_2(Me_2PCH_2CH_2PMe_2)_2$].

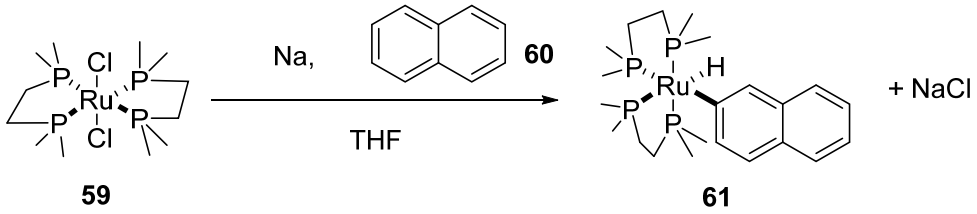


**Scheme 13: Reaction of a ruthenium complex with sodium naphthalenide to give C-H activation of naphthalene in the 2-position.[18]**

This work was expanded upon using platinum complexes, in the studies by Hodges and Garnett.[19] The authors showed (Scheme 14) the use of platinum salts to activate C-H bonds of benzene and polycyclic hydrocarbons such as naphthalene and pyrene. Facile loss of hydrogen chloride from these platinum complexes would allow for addition of deuterium chloride in a subsequent reaction, and the authors showed this exchange to be catalytic; multiple deuterations of one aromatic molecule could occur.

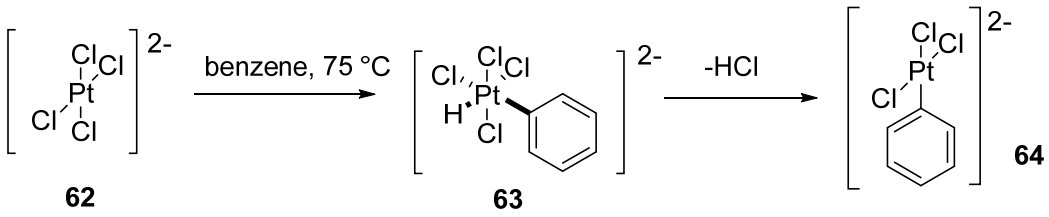


62 63 64

**Scheme 14: An example of the C-H activation technique used by Hodges and Garnett[19] showing the reaction of square planar platinum salts with benzene.**

In a reaction using $(C_5H_5)_2TaH_3$ Tebbe *et al.*[20] illustrated for the first time that gaseous hydrogen could be used to exchange C-D bonds in deuterated benzene. It was also possible to exchange C-H aryl bonds for C-D bonds with the use of gaseous deuterium and $(PhPEt_2)_2IrH_5$. The extent of the reaction was measured in quantities of $D_2$, HD and $H_2$ present in the sealed reactions; the organic products were not isolated.

The four examples shown of early work were pioneering, but these reactions only illustrated either the conversion of a carbon-hydrogen bond into a carbon-metal bond in a stoichiometric manner or the replacement of a carbon-hydrogen bond with a carbon-deuterium bond.

In order for C-H activation reactions to have synthetic utility in the wider organic chemistry community, it would need to be possible to replace carbon-hydrogen bonds with functionality frequently seen in organic molecules; carbon-carbon, carbon-oxygen and carbon-nitrogen bonds would be of particular interest.

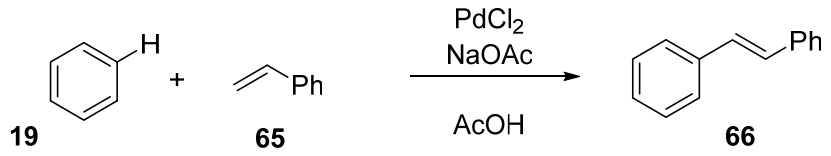


19 65 66

**Scheme 15: Moritani–Fujiwara reaction.[21,22]**

Scheme 15 shows one of the first C-H activation reaction to form carbon-carbon bonds, discovered by Moritani and Fujiwara.[21,22] The initial studies were stoichiometric, using a pre-formed styrene-$PdCl_2$ complex,[21] but the work was extended swiftly to include a variety of substituted benzenes as well as different palladium complexes; both palladium (II) chloride and palladium (II) acetate.

Which carbon-hydrogen bond was activated in the substituted benzenes substrates initially proved to follow a pattern based on which substituents were present, largely in common with the regioselectivity observed with electrophilic aromatic substitution, depicted in Table 2.

| Substituted benzene | *trans*-stilbene product | Yield |
|---|---|---|
| 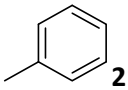 **21** | 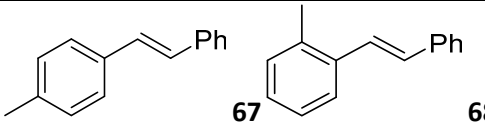 **67** **68** | 58% *para*<br>3% *ortho* |
| 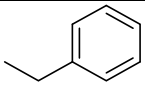 **25** | 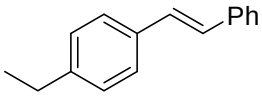 **69** | 52% *para* |

| | | |
|---|---|---|
| 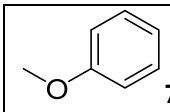 **70** | 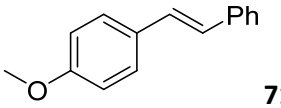 **71** | 61% *para* |
| 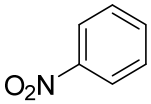 **26** | 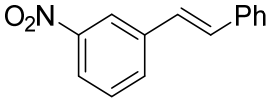 **72** | 60% *meta* |
| 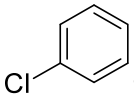 **73** | 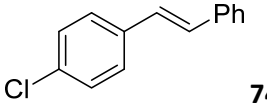 **74**<br> 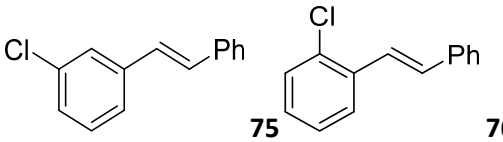 **75** **76** | 30% *para*<br>20% *meta*<br>12% *ortho* |

**Table 2: Outcomes of Moritani–Fujiwara reactions with substituted benzenes and styrene, using $Pd(OAc)_2$.[22]**

The outcomes of the reactions of toluene, ethylbenzene and anisole were in line with the *ortho* and *para* directing nature of these substituents. The reaction of nitrobenzene gave *meta*-nitro-*trans*-stilbene, consistent with the nitro group withdrawing electron-density from the *ortho* and *para* positions. The reaction of chlorobenzene proved to be anomalous though, giving a mixture of *ortho*, *meta* and *para* substituted *trans*-stilbenes. The authors suggested the unexpected *meta* product could be caused by coordination of the chlorine atom to the palladium complex. The lone pair of electrons usually able to transfer electron-density to the *ortho* and *para* positions would be otherwise engaged with forming a dative bond to the palladium, leaving the chlorobenzene to react as though it were an unsubstituted arene.

The Moritani–Fujiwara reaction has been studied intensively over the decades since it was first discovered; catalytic versions with high regioselectivity and mild conditions are now known, such as the example in Scheme 16.

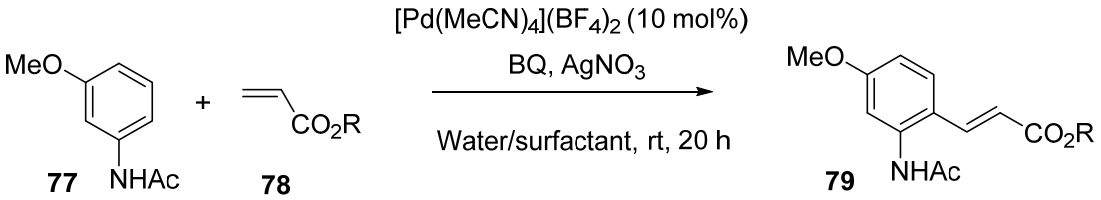


**Scheme 16: An example of a modern Moritani–Fujiwara reaction.[23]**

### 1.3.2 Agostic Bonding

Agostic bonds were the first indication that C-H activation of aliphatic carbon-hydrogen bonds may be possible.[1] "Agostic" is the term used to define two-electron, three-centre bonding between a metal, a carbon and a hydrogen atom.[24,25] This definition does not include three-centre-two-electron bonds that are commonly seen between "boron-hydrogen-boron" atoms, although the structures are similar.

Figure 1 shows an X-ray crystal structure as determined by Green, Prout and coworkers,[26] illustrating an agostic bond between a carbon-hydrogen bond from the methyl group of a ligand and a titanium metal centre in the complex $Ti(Me_2PCH_2CH_2PMe_2)EtCl_3$. The angle of the Ti(1)-C(1)-C(2) is shown to be 85.9(6)°, significantly smaller than the expected value of 109.5°

that would be present if there were no additional interactions. The distance between the Ti centre and the hydrogen atom labelled H(5) was only 2.29(2) Å, a shorter length than the bond between Ti(1) and C(1) at 2.408(3) Å.

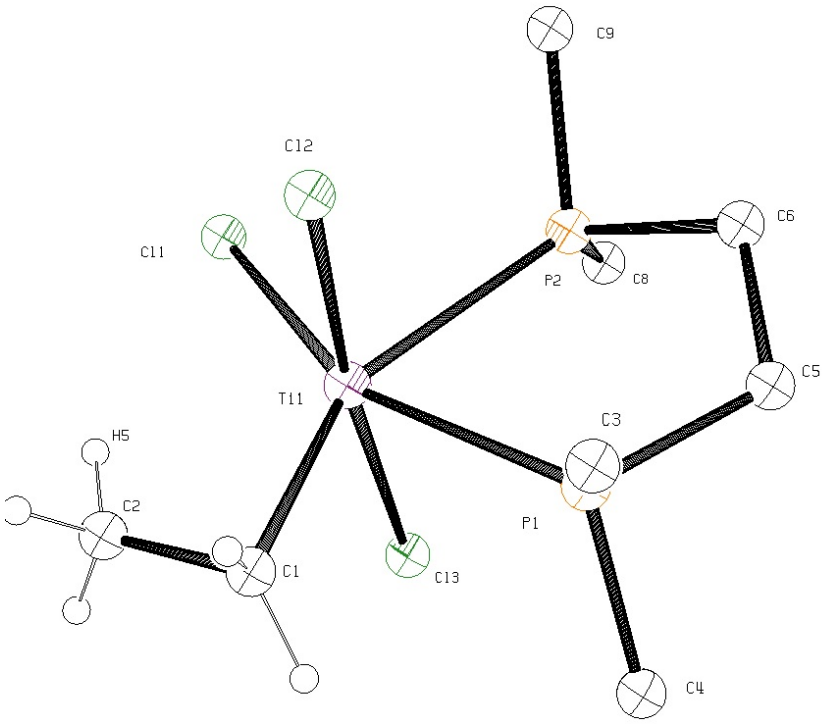


**Figure 1: Green, Prout and coworkers' X-ray crystal structure of $Ti(Me_2PCH_2CH_2PMe_2)EtCl_3$ with agostic bond interaction between C(2)-H(5) bond and the titanium metal centre.[26] Ellipsoids are shown at 30% probability.**

Certainly, with proof of this type of interaction now in hand, it seemed more achievable that other metal systems could be designed that could facilitate this type of interaction (as was done in this example; with a low valency, small ligands and a $d^0$ electron count at the titanium centre) thus in turn creating systems that could see insertion of the metal into the C-H bond.

### 1.3.3 σ-complexes of C-H Bonds to Metals

In a step further than agostic interactions between metals and ligands, one could envisage the possibility of external C-H bonds interacting in a similar manner without the C-H bond being part of a ligand that was already coordinated to the metal.

There is some evidence in early systems that σ-complexes are being formed prior to oxidative addition, where the metal interacts with the electrons in the carbon-hydrogen sigma-bond, but the bond is not yet cleaved. An example is shown in Scheme 17,[27,28] where identification of the species present was undertaken using IR spectroscopy – in particular a study of the peaks relating to the carbonyl ligands.

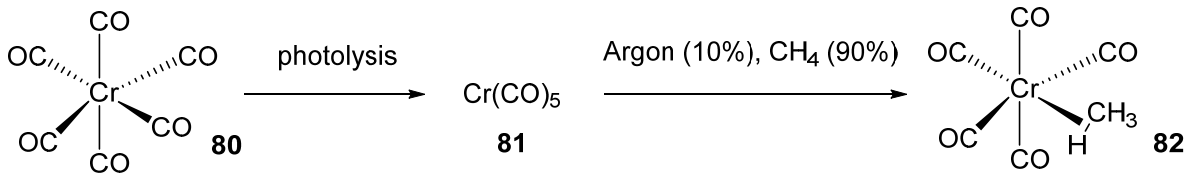


**Scheme 17: Interaction of chromium pentacarbonyl with methane.[27]**

Another example of evidence for a sigma-complex is that of the tungsten complex seen in Scheme 18.[29,30] This complex, although not involving a carbon-hydrogen bond and instead involving a hydrogen-hydrogen bond was stable enough to be analysed by NMR spectroscopy, showing conversion between the sigma-complex and the oxidative addition product of hydrogen to the tungsten centre.

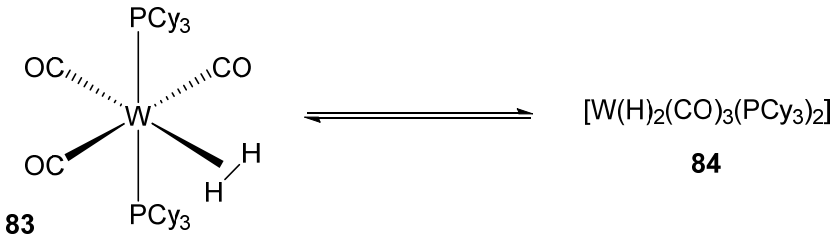


**Scheme 18: Kubas complex showing the interaction of hydrogen with a tungsten complex; equilibrating between a sigma-complex and oxidative cleavage of the dihydrogen bond.[30]**

### 1.3.4 Problems for C-H Activation of Aliphatic C-H Bonds

The major problems facing chemists seeking to activate aliphatic C-H bonds included selectivity and reactivity. These were (and indeed are) problems faced by those wishing to functionalise aromatic carbon-hydrogen bonds as well, but to a lesser degree, due to their higher reactivity.

In order to add functionality to a specific aliphatic carbon-hydrogen bond, one would need a catalytic metal centre which was sufficiently reactive to insert into the carbon-hydrogen bond in question but that would also undergo reductive elimination to release an activated molecule.

Further to this, additional functional groups within the starting molecule would need to be less inclined to react with the metal centre than the desired carbon-hydrogen bond. In terms of activating alkanes, this point is not particularly relevant; the activation of alkanes themselves is certainly desirable in terms of increasing the use of crude oil fractions, but of course not all molecules containing aliphatic carbon-hydrogen bonds are alkanes.

In order to use C-H activation reactions in the late stages of a complex synthesis of natural products, agrochemicals or pharmaceuticals, other functional groups present in the molecules would need to remain untouched. C-H activation at mild temperatures and conditions would also be desirable traits.

Finally, selectivity is a big issue for C-H activation chemistry. This can be overcome by working with molecules where only one site is available for activation, or where there is a preference for a weaker C-H bond (for example, as seen in Table 1, tertiary $sp^3$ carbon-hydrogen bonds

have a bond dissociation energy of around 389 kJ $mol^{-1}$, compared with primary $sp^3$ carbon-hydrogen bonds at around 410 kJ $mol^{-1}$). However, in cases where there are multiple possible sites for activation, with similar bond strengths, the interactions of nearby functional groups or more complex ligands can be employed to enhance selectivity, which will be discussed later.

### 1.3.5 Shilov and Catalytica Systems

A catalytic system that was somewhat overlooked at the time of its original publication was that by Shilov and colleagues, [31,32,33] the overall transformation of which was from methane to methanol, shown in Scheme 19 below. The main disadvantage to this system is the use of the platinum (IV) salt as a stoichiometric oxidant, which is prohibitively expensive.

The insertion of the platinum centre into the methane carbon-hydrogen bond is thought to occur via electrophilic addition.[1] These electrophilic addition C-H activation reactions typically use late transition metals in polar solvents forming HX and RX from RH. In this first example, one could consider attack on the methyl group by chloride or water, forming methyl chloride (this species could then undergo nucleophilic substitution with water to form methanol) or methanol directly.

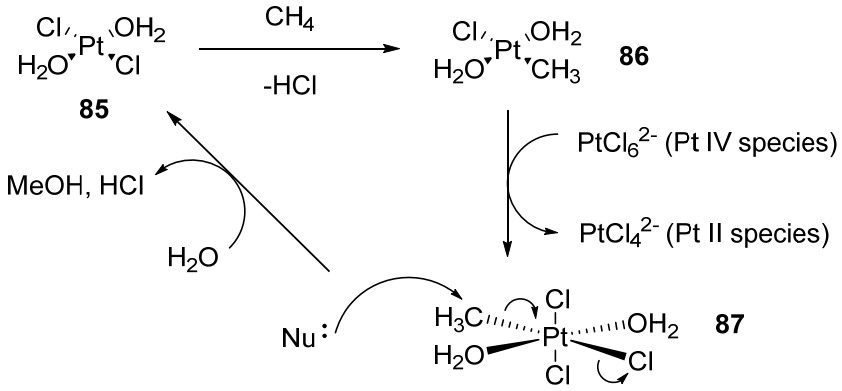


**Scheme 19: Shilov system for conversion of methane to methanol.[1]**

Much more recently, another system devised for oxidation of methane to methanol is the Catalytica system.[34] This process was reported in 1998 by Periana and coworkers and is outlined in Scheme 20 and Figure 2.

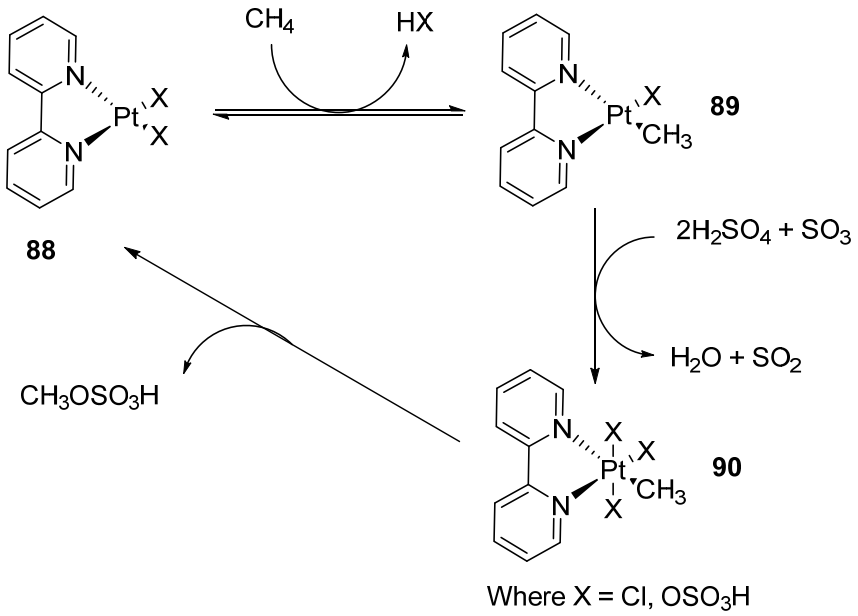


**Scheme 20: Catalytica system for transformation of methane into methane bisulfate.[34,1]**

Thallium, gold, palladium and platinum were all screened as potential catalysts by the authors, with thallium and gold requiring stoichiometric quantities whilst palladium and platinum were catalytic. This system does not directly oxidise methane to methanol, but instead to methyl bisulfate which can then be hydrolysed to methanol in water, shown in Figure 2.

**Step 2:** $MeOSO_3H + H_2O \longrightarrow MeOH + H_2SO_4$

**Step 3:** $SO_2 + 1/2\ O_2 \longrightarrow SO_3$

**Overall:** $CH_4 + 1/2\ O_2 \longrightarrow MeOH$

**Figure 2: Hydrolysis of methyl bisulfate to methanol and reoxidation of sulfur dioxide to sulfur trioxide.[1]**

In an extension to this work, Periana *et al.*[35] were able to form acetic acid from two methane molecules. This work was precedented by the rhodium catalysed method of Lin and coworkers[36] as well as the reactions identified by Shul'pin *et al.*[37] using vanadium catalysis. However, the fundamental difference is that in these earlier methods, only the methyl carbon of the acetic acid originated from methane, whereas the carbonyl carbon was derived from carbon monoxide[36,37] or a carbon dioxide molecule.[37] These three systems for conversion of methane to acetic acid are shown in Scheme 21.

Periana *et al*.[35] proposed several mechanisms for the reaction, and found their results were in line with the electrophilic C-H activation of methane to form a methyl-palladium species, and postulated that a "CO" moiety formed *in situ* would react to give acetic acid.

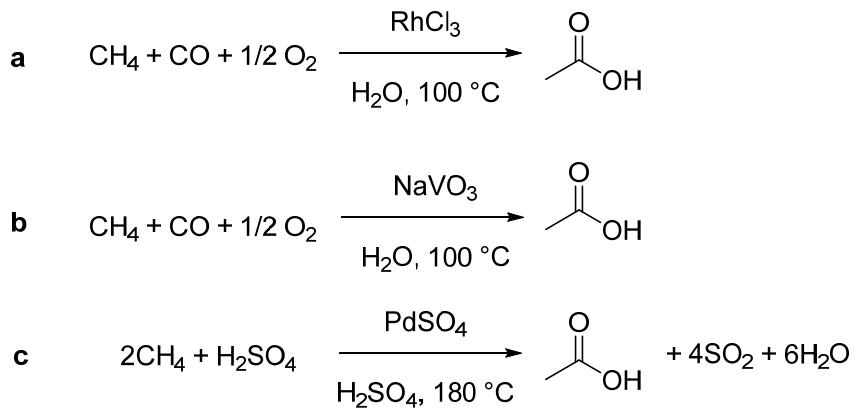


**Scheme 21: Examples of C-H activation reactions from methane to acetic acid; (a) Lin's rhodium catalysed method[36] (b) Shul'pin's vanadium catalysed method[37] (c) Periana's palladium catalysed method.[35]**

### 1.3.6 C-H Activation Using Metal-Carbenoids

Another mechanism for the cleavage of aryl carbon-hydrogen bonds is by means of carbenes. This type of C-H functionalisation could fall into either the category of cleavage of a C-H bond without formation of a carbon-metal bond, or the category of a metal activating a reactive species.

Typically, these carbenes are generated by extrusion of nitrogen from a diazo-compound in conjunction with a metal catalyst, forming a metal-carbenoid species. The metal used in the vast majority of this type of reaction is rhodium and the reactions are very well used for intramolecular C-H activation; in that the diazo-group and the C-H bond to be activated are on the same molecule.[38]

Early examples of these reactions in the late 1950s and 1960s were unexpected;[39,40] treatment of diazomethyl ketones with copper oxide or silver benzoate (reaction shown in Scheme 22) generated primary carbenes adjacent to the carbonyl, which subsequently inserted into a nearby carbon-hydrogen bond.

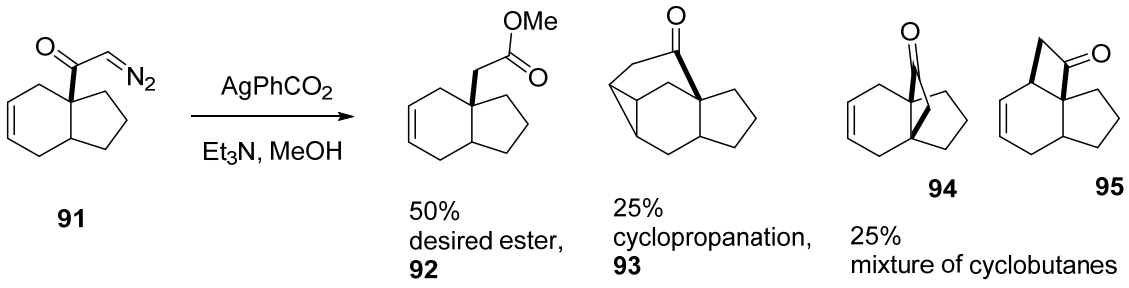


**Scheme 22: Products from an attempted Arndt–Eistert homologation, including some C-H insertion products.[40]**

The cyclopropane formation, via insertion of a carbene into a double bond, is another well-known reaction on decomposition of diazomethyl ketones.[41] The two cyclobutanone structures produced form via insertion of the carbene into the tertiary carbon-hydrogen bond or the allylic carbon-hydrogen bond respectively.

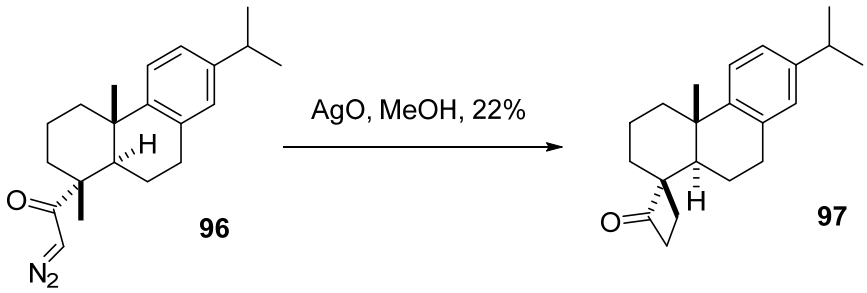


**Scheme 23: Unexpected cyclobutanone product of an attempted Wolff rearrangement, formed via C-H insertion.[42]**

Wenkert and coworkers[42] also discovered anomalous results when attempting Wolff rearrangements of diazomethyl ketones, this time in the presence of silver oxide (Scheme 23). They expanded on their original findings over a decade later,[43] illustrating the use of these carbon-hydrogen insertions in synthesis, using the dirhodium (II) tetraacetate complex as the catalyst. The carbene could have inserted into any of the three carbon-hydrogen bonds highlighted in Scheme 24, however the reaction is selective for the carbon-hydrogen bond shown in red. The authors postulate this selectivity is based on the allylic nature of this carbon-hydrogen bond.

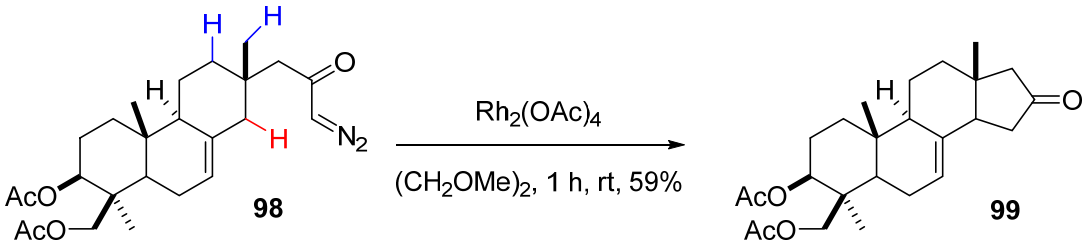


**Scheme 24: Use of a rhodium catalyst to induce C-H insertion forming the cyclopentanone ring of the steroid structure.[43]**

After another decade of research, work had shown diazoacetoacetate and related compounds (β-keto-α-diazophosphonates and β-keto-α-diazosulfones) could be used to form cyclopentanone scaffolds using rhodium (II) catalysts rather than the initially-described copper or silver catalysts;[44,45,46] significantly greater regioselectivity was then established by Doyle and colleagues[47] using diazoacetoacetates with catalytic dirhodium (II) caprolactam, in the syntheses of various five-membered lactones.

The less electron-donating nature of the caprolactam ligand (in comparison to the acetate ligand) was anticipated to favour insertion into the more electron-rich carbon-hydrogen bond site. This was found to be true in some cases (examples 1 and 3 in Table 3) where insertion into a tertiary or secondary C-H bond was preferred over a primary C-H bond. In example 2 however, preference was exhibited for a secondary C-H bond over a tertiary C-H bond and in example 4 some selectivity for a primary C-H bond was shown over a benzylic C-H bond,

indicating the electronic influence of the catalyst was not the only factor at play. The authors suggest that conformational strain in some compounds may be relevant to the question of which carbon-hydrogen bonds are preferred for insertion.

| | Starting diazoacetoacetate | Major product | Minor product |
|---|---|---|---|
| 1 | 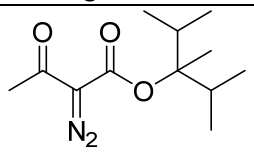 **100** | 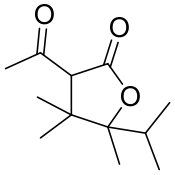 **101**, 99% | 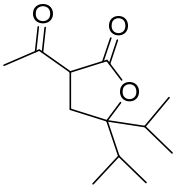 **102**, 1% |
| 2 | 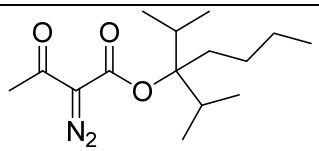 **103** | 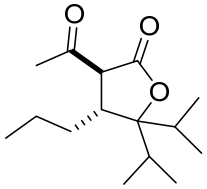 **104**, 96% | 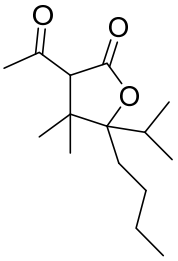 **105**, 4% |
| 3 | 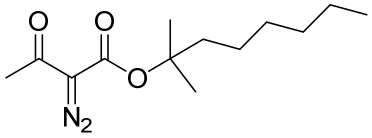 **106** | 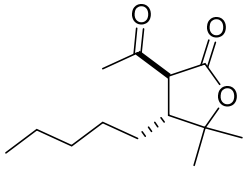 **107**, 92% | 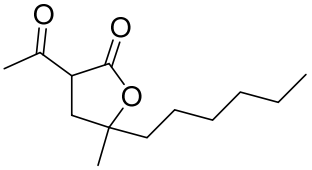 **108**, 8% |
| 4 | 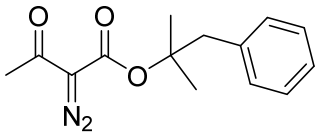 **109** | 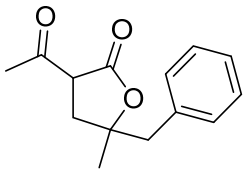 **110**, 70% | 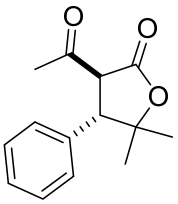 **111**, 30% |

**Table 3: Examples of competing C-H insertion reactions with $Rh_2(cap)_4$ (1 mol%) in $C_6H_6$ at 80 °C. Diastereomeric ratios were not calculated; major diastereomers were assigned where shown.[47]**

Use of alternative rhodium (II) catalysts was also shown to reverse the regioselectivity of the reaction in certain cases; for example, with dirhodium (II) perfluorobutyrate (a more electron withdrawing ligand than caprolactam and acetate) the first example in Table 3 gave a 39:61 ratio of **101**:**102**.

The generally accepted mechanism for nitrogen extrusion and carbene formation from the diazoacetoacetates and similar structures is as shown in Scheme 25.

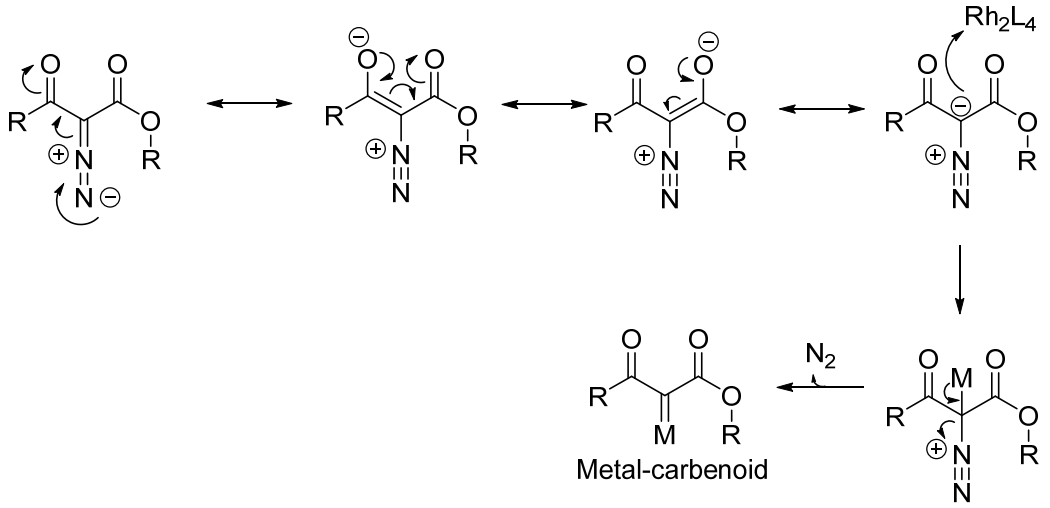


**Scheme 25: Mechanism for extrusion of nitrogen from a diazoacetoacetate to form a metal-carbenoid;[48] resonance structures of diazoacetoacetates are shown.**

Enantioselective examples of this type of carbene insertion into carbon-hydrogen bonds are known, including examples from complex natural product synthesis, one of which is illustrated in Scheme 26.[49]

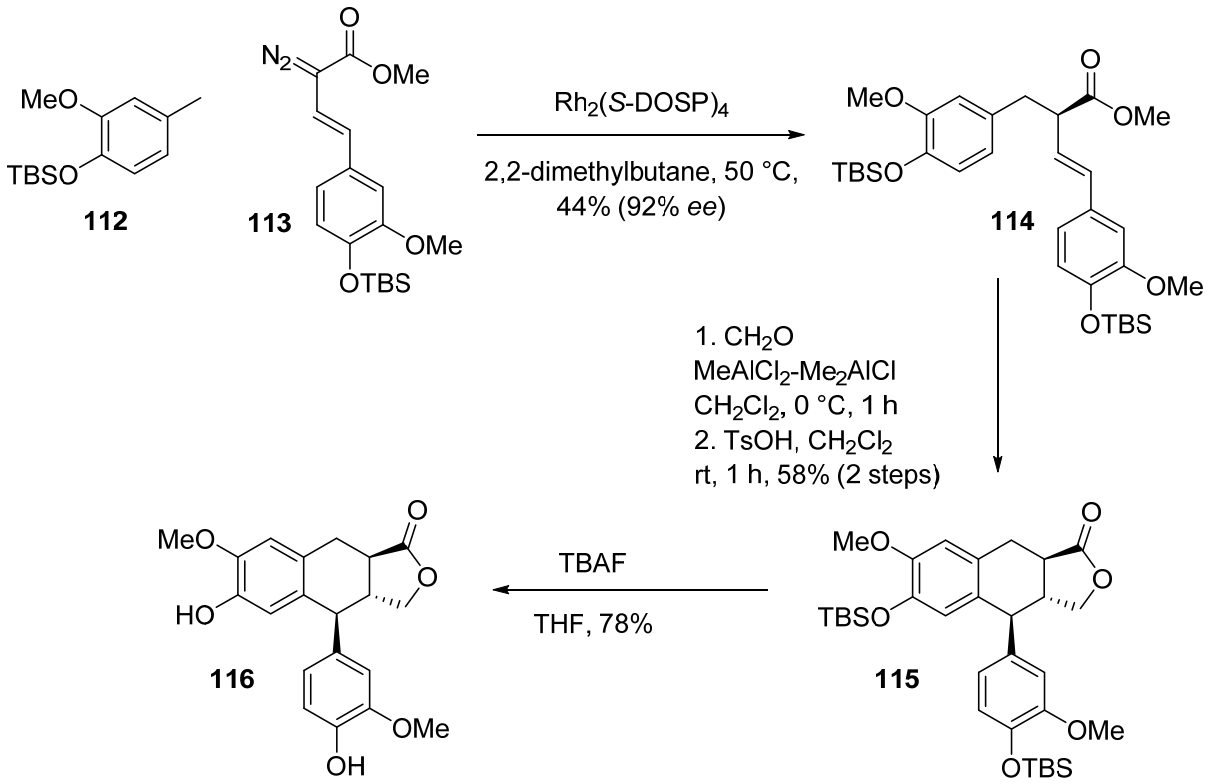


**Scheme 26: A concise synthesis of (−)-α-Conidendrin using C-H insertion as the key step with enantioselective control.[49]**

This is an example using a metal-carbenoid that has an electron donating group on one adjacent carbon and an electron withdrawing group on the other adjacent carbon, unlike those

previously discussed for use in intramolecular C-H insertion reactions; the diazoacetoacetates and related compounds have two adjacent electron withdrawing groups.

The enhanced stabilisation of the metal-carbenoid that these donor/acceptor groups provide decreases problems seen with reaction of metal-carbenoids with acceptor/acceptor groups, such as dimerisation of the carbenes. This increased stabilisation allows the somewhat slower intermolecular C-H insertion reactions to proceed, vastly expanding the scope of these carbene insertion reactions.

### 1.3.7 C-H Activation to Form C-B Bonds

Hartwig *et al.* studied C-H activation of primary C-H bonds using a rhodium catalyst, to give organoboron complexes in high yields with good selectivity.[50] Scheme 27 illustrates the functional group tolerance of the reaction; ethers, tertiary amines and fluorine atoms are all untouched. The reactions were performed without solvent, hence producing less waste.

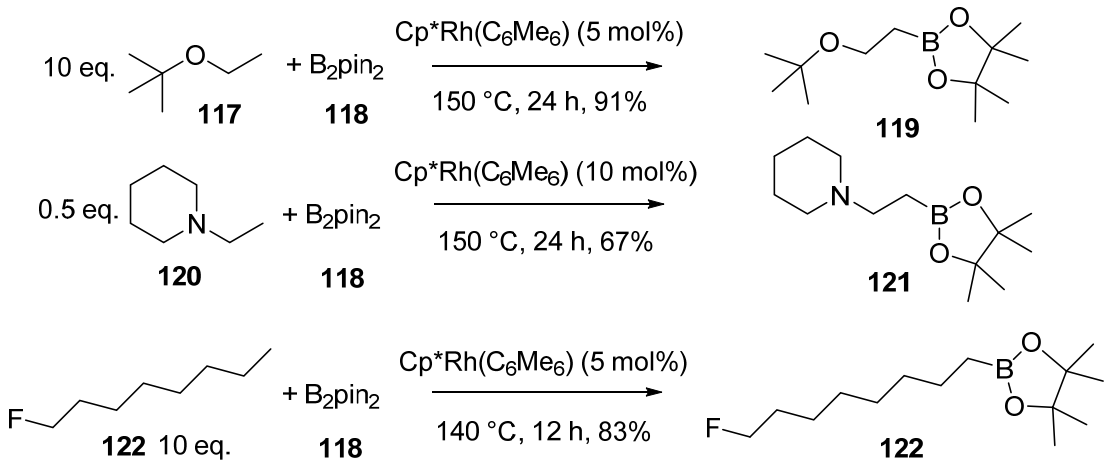


**Scheme 27: Examples of catalytic regioselective CH-activation to form organoboron compounds.[50]**

As organoboranes can act as reagents in Suzuki reactions, ultimately forming new carbon-carbon bonds, or be converted to the corresponding alcohol with sodium hydroxide and hydrogen peroxide, the products of these reactions are potentially useful for further organic synthesis. Hartwig and colleagues demonstrated this by taking the above products forwards using a palladium catalysed cross-coupling with 1-bromo-4-*tert*-butylbenzene in yields of up to 87%.

This work was followed up in 2010 by a study into the preference of rhodium cyclopentadienyl catalysts for primary C-H bonds over secondary C-H bonds.[51] Using isotope exchange studies (hydrogen/deuterium) the authors were able to conclude that the insertion of the rhodium catalyst into the C-H bond was reversible, and was observed to insert at both primary and secondary positions on the alkyl chain.

This was followed by irreversible C-B bond formation. Computational modelling indicated there was a lower energy of the transition state between the primary alkyl intermediate and the corresponding terminal organoborane product than the corresponding transition state between the secondary alkyl intermediate and its product.

With this information, the authors found that formation of the primary C-B bond would be kinetically favourable, whilst secondary alkyl intermediates would often revert to the original alkane before undergoing further CH-activation, hence the high selectivities observed. Other factors in support of this conclusion include the high energy barrier to the formation of the *cis* secondary alkyl boryl rhodium complex, a requirement for the formation of the C-B bond.

Another commonly used transition metal for the conversion of carbon-hydrogen bonds into carbon-boron bonds is iridium. The established mechanism for the borylation of C-H bonds via iridium catalysis is seen in Scheme 28.[52] Well established pre-catalysts used include the dimers $[Ir(cod)(Cl)]_2$ and $[Ir(cod)OMe]_2$ where iridium (I) is present.

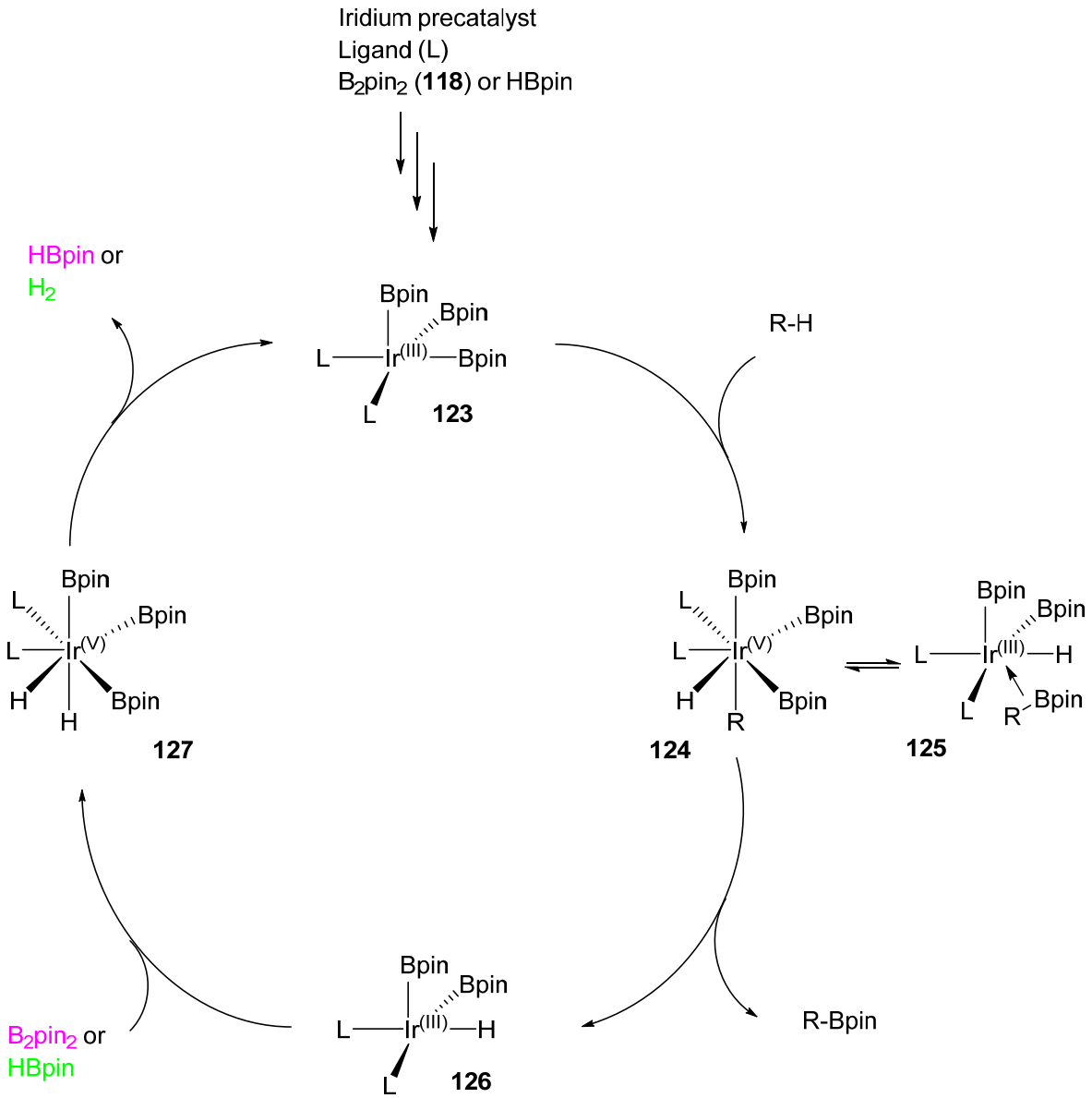


**Scheme 28: Mechanism for C-H borylation via iridium catalysis.[52]**

The catalyst is formed by cleavage of the boron-boron or boron-hydrogen bond in the boron containing species. Bis(pinacolato)diboron **118** is a commonly used reagent; use of boronic

esters rather than boronic acids reduces the formation of the problematic trimeric byproduct formed by condensation of boronic acids. The catalyst is an iridium(III) species which undergoes oxidative addition with an aryl or alkyl carbon-hydrogen bond to form an iridium(V) complex.

Reductive elimination of the desired alkyl or aryl boronic ester can then occur; reducing the iridium complex to iridum(III), but now containing a iridium-hydrogen bond. Addition of another equivalent of bis(pinacolato)diboron reoxidises the iridium to iridium(V). This species then undergoes another reductive elimination to reform the catalyst, and generate a molecule of pinacolborane (shown in pink).

In a later catalytic cycle, the pinacolborane generated can reoxidise the iridium (III) species to iridium (V); reductive elimination can then generate hydrogen (shown in green). It is possible to use pinacolborane as a boron source directly, although it is significantly less air stable. Whilst this mechanism has been studied extensively,[53,54,55] applications in this field are still expanding.

In 2014, Hartwig and colleagues continue to investigate and overcome the challenges of forming carbon-boron bonds from carbon-hydrogen bonds. In particular, the functionalisation of heteroaromatic rings can be difficult due to their inclination to act as ligands towards transition metal catalysts, rather than undergoing oxidative addition, and this has been Hartwig's most recent investigation to date.[56]

In their mechanistic investigation, the authors found, as they had expected, that en route from the pre-catalyst to the active catalyst, a ligand (in their example, cyclooctene or 1,4-cyclooctadiene) was reversibly replaced by the nitrogen-containing substrate. This heteroaromatic would then be displaced to form the active catalyst and undergo oxidative addition in the manner of non-heteroaromatic molecules. This slightly different mechanism is seen in Scheme 29.

With a simple heteroaromatic (3-picoline **131**) the reaction would then proceed as normal, but with molecules containing more steric hindrance (for example, benzoxazoles) around the nitrogen moiety the situation was shown to be more complex. The increased steric hindrance caused a lower affinity for binding to the iridium centre, meaning en route from the pre-catalyst the complex showed a preference for coordinating to the alkene rather than the heteroaromatic – this gave a small dependence of the rate on the concentration of heteroaromatic (the order of reaction was found to be approximately 0.4, compared to the zero-order dependence on 3-picoline).

A somewhat larger problem was the similar affinity for binding to the iridium centre between the starting heteroaromatic and the borylated heteroaromatic. In the 3-picoline example, the borylated heteroaromatic showed much lower affinity for the iridium. With the benzoxazole, it seemed likely product inhibition could occur if the catalyst turnover could be limited by coordination to the product.

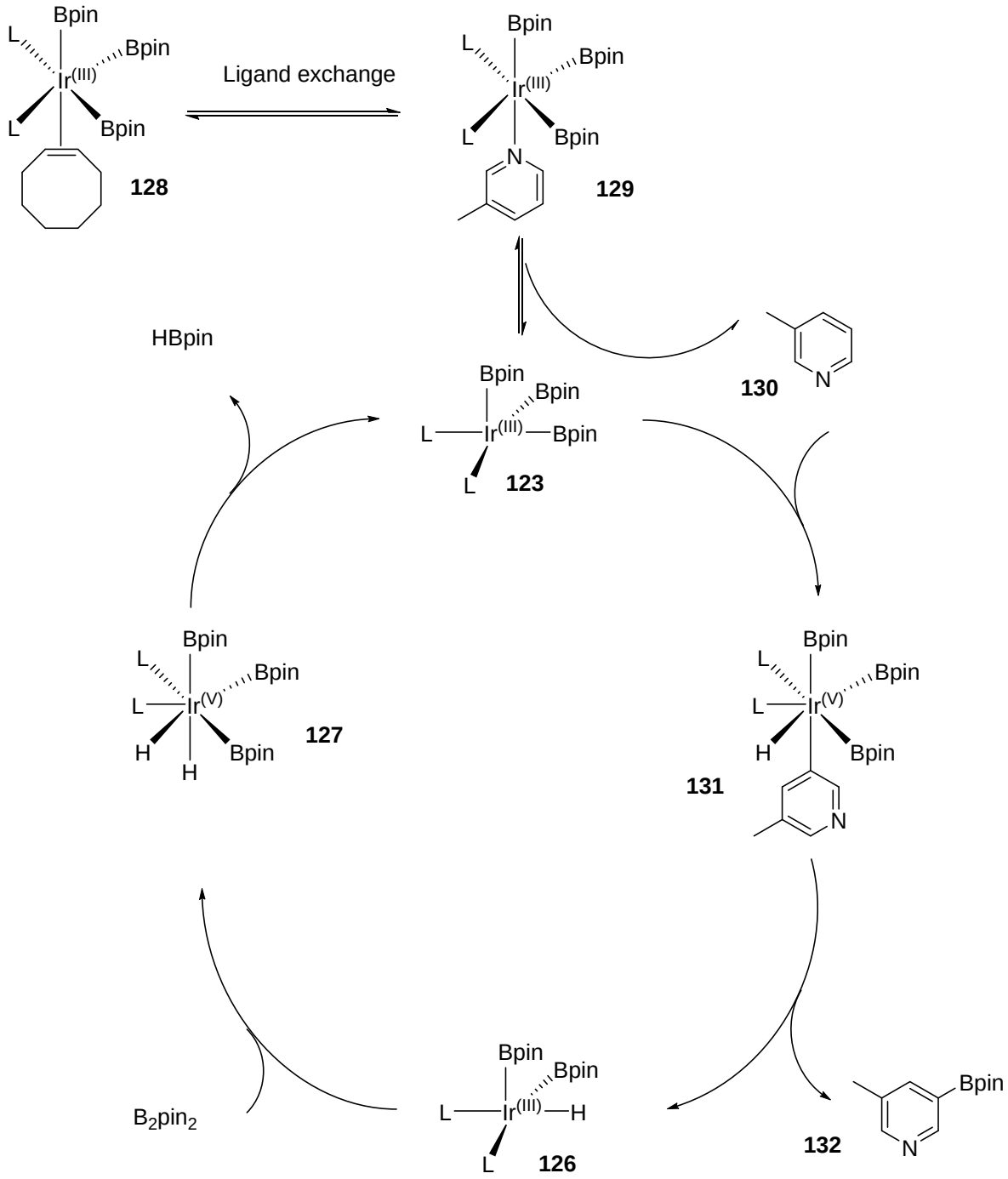


**Scheme 29: C-H borylation mechanism for heteroaromatics.[56]**

Three key rules for the C-H borylation of heteroaromatic compounds have been established; these are shown pictorially in Figure 3. Rule one shows that sites α- or *ortho*- to basic nitrogen or NH functionality will not be borylated. Rule two indicates the preferential borylation of carbon-hydrogen bonds that are *ortho* to oxygen or sulfur. Rule three outlined the preference for unhindered carbon-hydrogen bonds over those more hindered; a fact previously established for borylation of non-heteroaromatic compounds which still holds true.

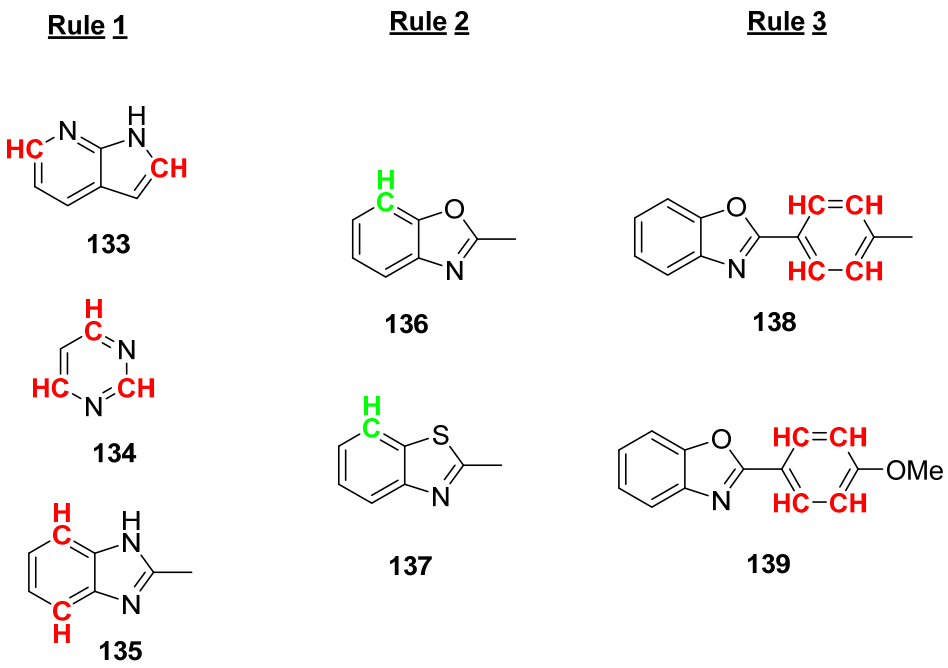


**Figure 3: Rules for regioselectivity of C-H borylation of heteroaromatic compounds, where green C-H bonds represent sites where borylation is favoured and red C-H bonds represent sites where no borylation occurs.[56]**

As previously mentioned, it has also been shown to be possible to use rhodium based catalysts for this type of C-H activation, although in these examples the catalytic cycle is proposed to involve rhodium (I) and rhodium (III) complexes.[57,58,59]

### 1.3.8 C-H Activation Towards Dehydrogenation of Alkanes

Lui *et al.*[60] identified the first catalytic C-H activation of linear alkanes to form terminal alkenes. The transfer dehydrogenation mechanism proposed in Scheme 30 proceeds via oxidative addition of a C-H bond to the iridium "pincer" catalyst followed by β-hydride elimination.

As terminal alkenes are monosubstituted, they are less thermodynamically favoured than internal disubstituted alkenes, however the terminal C-H bond shows a higher affinity for oxidative addition. Unfortunately, the iridium catalyst is also able to catalyse isomerisation of terminal alkenes, so internal alkenes are obtained as a byproduct over time.

The best result the group obtained used 0.5 M 1-decene as the hydrogen acceptor and *tert*-butyl groups as R-groups on the catalyst, where after 15 min >95% terminal alkene was formed, dropping to 68% after 120 min. It is suggested that further modification of the catalyst/acceptor combination may be able to prevent isomerisation and therefore allow formation of a higher proportion of monosubstituted alkene.

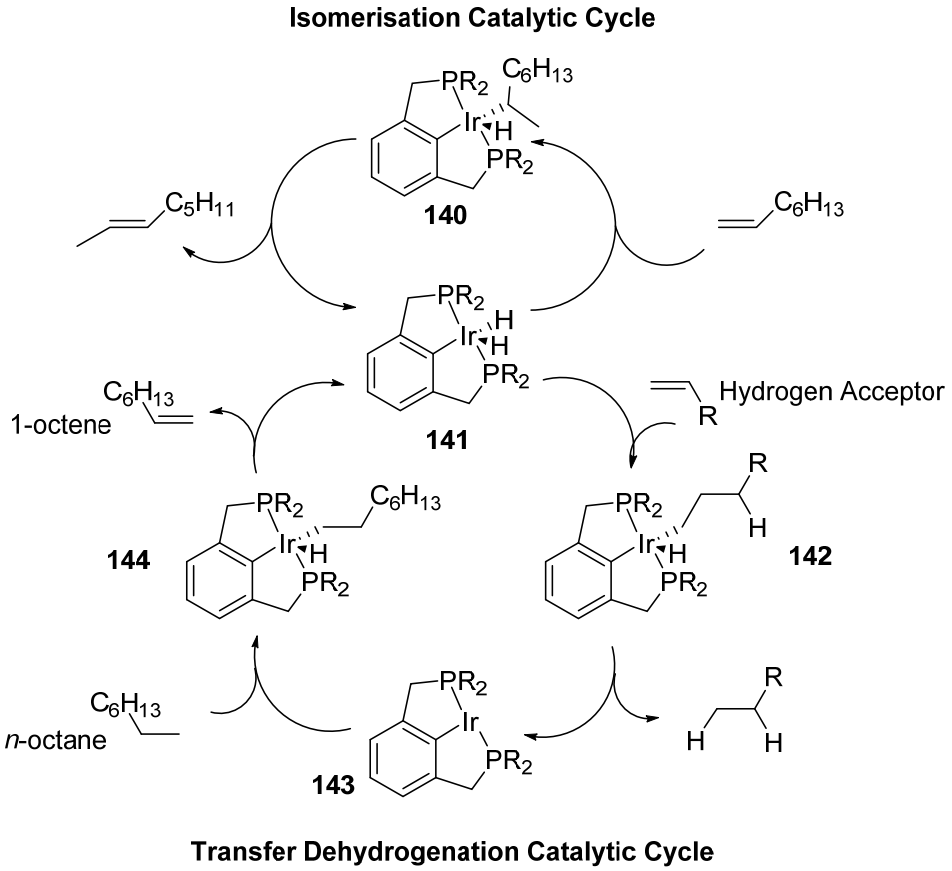


**Scheme 30: Catalytic cycle for dehydrogenation of linear alkanes.[60]**

### 1.3.9 Introducing Nitrogen Functionality via C-H Activation

As well as uses of C-H activation for forming carbon-carbon bonds, carbon-boron bonds and dehydrogenating $sp^3$ C-H bonds, it has also been possible to introduce nitrogen functionality. An example of intramolecular amination of alkyl C-H bonds to form cyclic carbamates[61] is shown in Scheme 31.

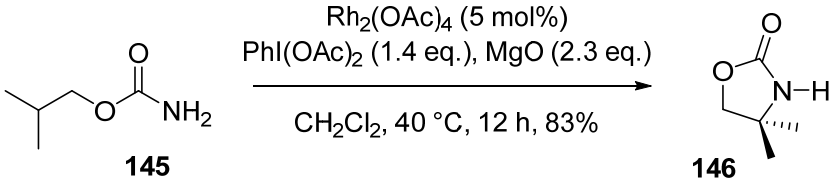


**Scheme 31: An example of CH-amination to afford cyclic carbamates.[61]**

Intermolecular alkyl CH-amination is more challenging, although examples were first established in the 1980s with Breslow *et al.*[62] using a manganese catalyst and a pre-synthesised nitrene source (PhI=NTs) to form *N*-cyclohexyl-*p*-toluenesulphonamide from cyclohexane. Che and co-workers[63] expanded on this work in 2000 using a catalyst that did not require the pre-synthesis of the nitrene precursor, examples of which are shown in Scheme 32. Interestingly, the cyclohexene double bond did not undergo aziridination under these reaction conditions.

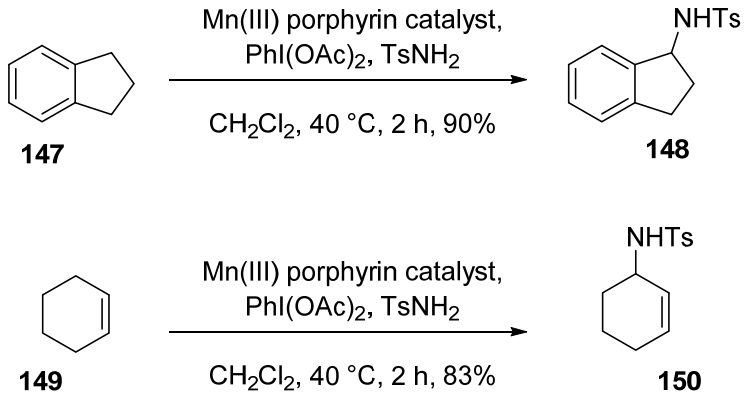


**Scheme 32: Examples of C-H amination.[63]**

### 1.3.10 Selective C-H Activation of Aliphatic Bonds

Recent work by White *et al.*[64] in 2007 shows how far the field has come in terms of selectively oxidising alkyl C-H bonds. The authors developed an iron catalyst that would selectively oxidise tertiary C-H bonds to tertiary alcohols. In the absence of 3° bonds, secondary C-H bonds were oxidised to ketones, an example of which is shown in Scheme 33b. Using optically pure substrates resulted in enantiomerically pure alcohols, seen in Scheme 33c.

Where more than one tertiary site was available for activation, the proximity to electron withdrawing groups was a factor in determining which site would be oxidised preferentially. Generally, the sites furthest from EWGs were oxidised in at least 5:1 selectivity, for example, oxidation of a tertiary site with an -OAc group at the β-carbon. Oxidation with 99:1 selectivity was observed where an acid or methyl ester group was used on the α-carbon.

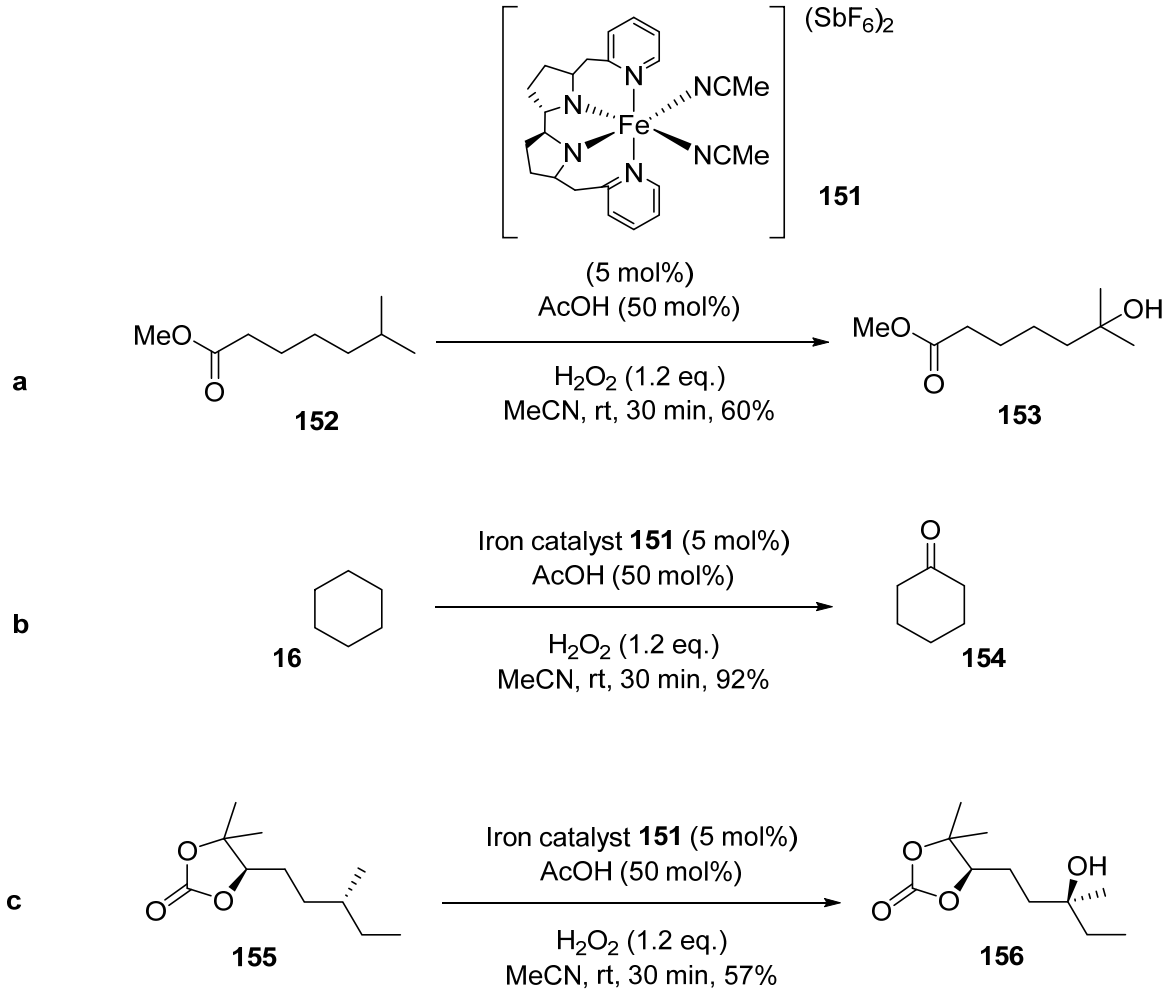


**Scheme 33: Examples of selective aliphatic C-H oxidation.[64]**

However, carboxylic acid groups on the γ-carbon to a tertiary or secondary site directed oxidation to these sites, which were then able to lactonise, as illustrated in Scheme 34, also demonstrating the use of this C-H activation on more complex molecules.

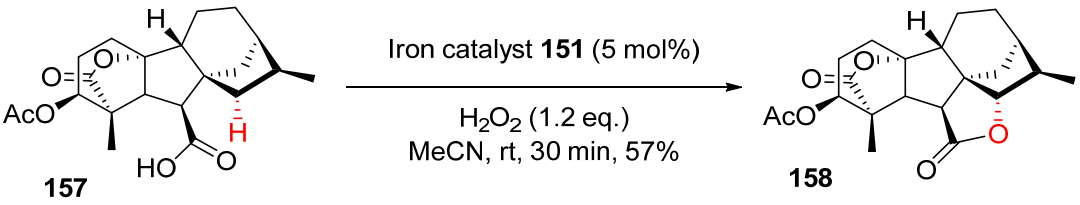


**Scheme 34: Example of C-H activation followed by lactonisation.**[64]

The final consideration that was taken into account was that of steric bulk, due to the bulkiness of the catalyst. It was determined that increased steric bulk at the tertiary site favoured formation of a ketone at a less hindered secondary site instead.

In 2009, Baran *et al.*[65] published a review considering the aspect of strain relief in reactions where alkanes undergo oxidation, determining that the selectivities of these reactions could be explained in terms of which isomer has most strain relief in the transition state during oxidation. In the example below (Scheme 35) *cis*-decalin was found to react with 91:9 selectivity at the tertiary C-H bond over secondary C-H bonds. However, the ratio for the comparative *trans*-decalin reaction was 62.5:37.5.[66]

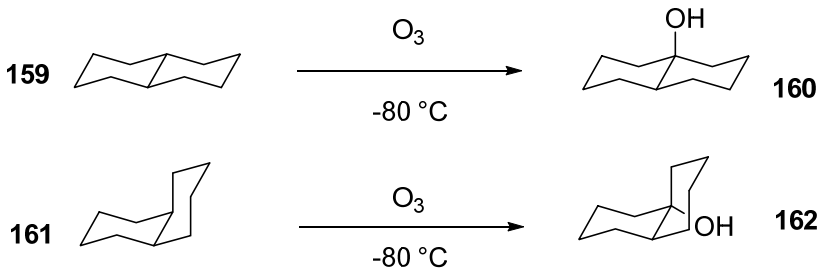


**Scheme 35: Reaction of *cis*- and *trans*- decalin with ozone.**[66]

A further review was published by Baran[67] in 2011, discussing the factors operating in selective C-H oxidation. Specifically, he outlines the preference for oxidation of primary methyl groups over secondary methylene sites by transition metal reagents, the functionalisation of sites distal from an EWG as opposed to those proximal and the steric hindrance at each site, similarly outlined by White.[64]

However, in addition to this, he examines the effects of conjugation and hyperconjugation. Although oxidising reagents that do not contain metals tend to have a preference for tertiary sites, the hyperconjugation effects of a cyclopropane ring allows oxidation at a secondary site α- to the cyclopropane rather than the tertiary site of the cyclopropane itself, an example of which is shown below in Scheme 36.[68]

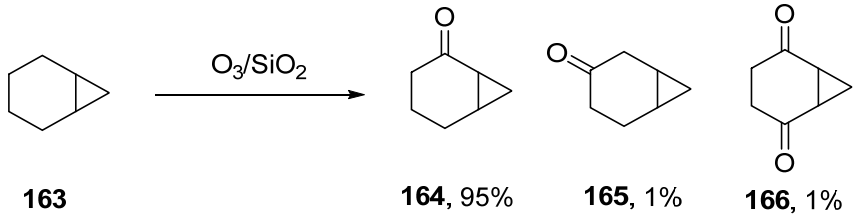


**Scheme 36: An example of the effect of hyperconjugation on C-H oxidation selectivity.**[68]

Heteroatoms have also been used to direct the oxidation of $sp^3$ C-H bonds, for example, THF and THP can be activated by several reagent systems to give functionalisation at the α-carbon only,[69,70] as illustrated in Scheme 37, showing both oxidation and C-C bond formation.

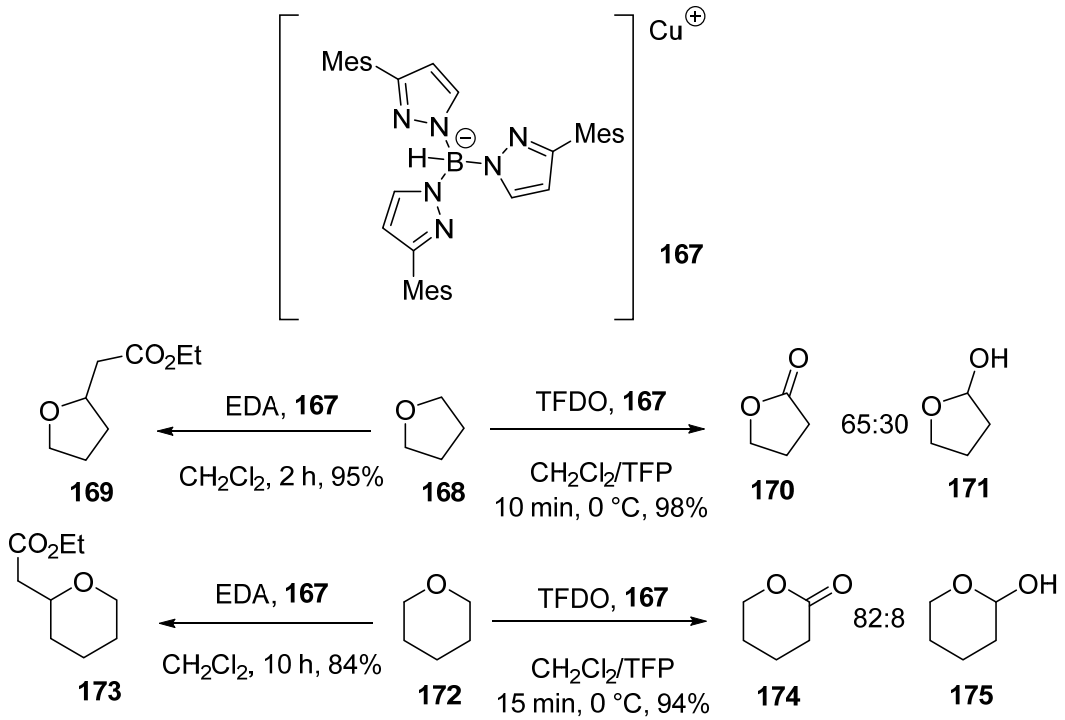


**Scheme 37: Examples of C-H activation at α-carbon to heteroatom with copper catalyst shown above.[69,70]**

### 1.3.11 Use of Base Metals to effect C-H functionalisation

Due to the depletion of already scarce transition metals, such as iridium, rhodium, palladium and platinum,[71] it would be ideal to use more common metals to mediate carbon-hydrogen bond activation. White's use of iron catalysts[64] showed excellent promise that this would be possible, and since then many groups have investigated these possibilities.

The most abundant metals include aluminium, iron and titanium[71] but of these it is clear that transition metals which are easy to handle with the ability to incorporate chiral ligands have an advantage.

Very recently in 2013, it has been shown by Mazzacano and Mankad[72] that iron can be used in conjunction with copper or zinc to catalyse borylation of aromatic carbon-hydrogen bonds. Regioselectivity in this reaction proved to be troublesome, as has been seen previous in C-H borylation reactions with iridium and rhodium catalysts. The results of this work are seen in Scheme 38 and Table 4.

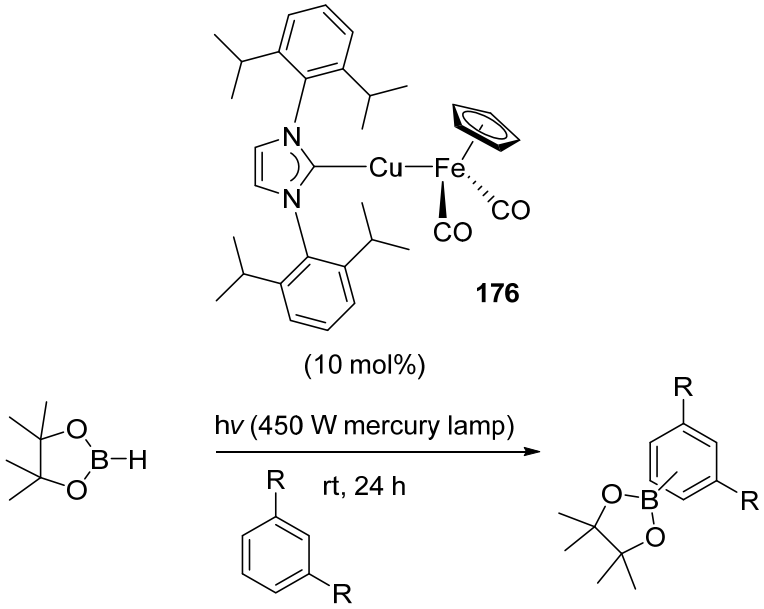


**Scheme 38: Reaction scheme for C-H borylation using an iron/copper catalyst.[72]**

| Starting arene | Major Product | Minor Product(s) | Yield |
|---|---|---|---|
|  **19** | 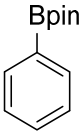 **177** | | 71% |
| 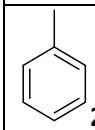 **21** | 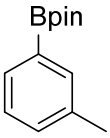 **178** | 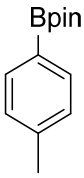 **179** | 83%<br>62:38 *meta*:*para* |
| 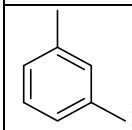 **180** | 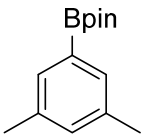 **181** | | 46% |
| 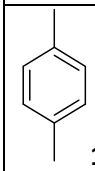 **182** | 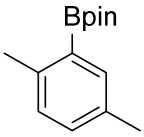 **183** | | 6% |
| 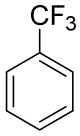 **184** | 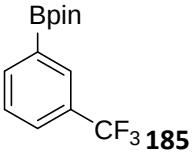 **185** | 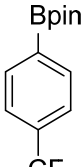 **186** | 25%<br>66:33 *meta*:*para* |
| 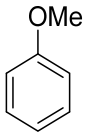 **70** | 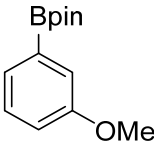 **187** | 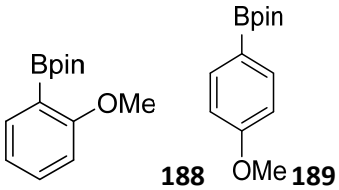 **188** **189** | 41%<br>71:21:2<br>*meta*:*para*:*ortho* |

**Table 4: Results of C-H borylation of simple arenes with a copper and iron catalyst under a 450 W mercury lamp[72]**

It was only in the example with anisole that a small quantity of *ortho*-substituted product was detected, it is likely this is formed due to coordination of the oxygen to the catalyst. All the other examples reported appear to be controlled by steric hindrance primarily.

A 2014 review by Li[73] looked at recent advances in the use of iron as a catalyst for carbon-hydrogen bond activation. Examples of aliphatic carbon-hydrogen bonds included those shown in Scheme 39[74] where the authors employed iron nonacarbonyl as a catalyst with yields ranging from 52-98% over a one hour reaction time.

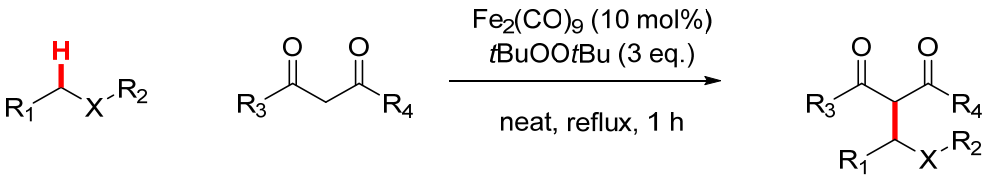


**Scheme 39: A general scheme for the use of iron nonacarbonyl to catalyse C-H activation of C-H adjacent to a heteroatom. X=S, O, N. [74]**

It is also possible to activate benzylic carbon-hydrogen bonds, something that has been challenging to achieve via C-H borylation methodology, where preference is seen for the aryl carbon-hydrogen bonds instead. Using ferrous chloride as the catalyst in conjunction with *N*-bromosuccinamide, Zhao and coworkers[75] were able to functionalise the benzylic C-H bond of ethyl benzene and diphenylmethane to form secondary amides and secondary sulfonamides; examples are shown in Table 5.

| Starting material | Primary amide | Product | Yield |
|---|---|---|---|
| 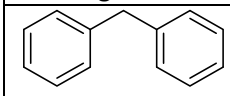 **190** | 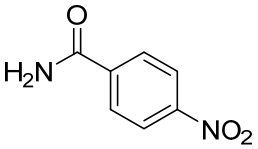 **191** | 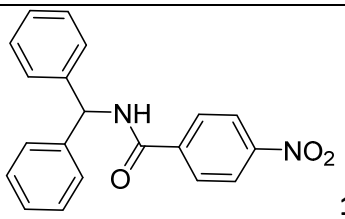 **192** | 81% |
| 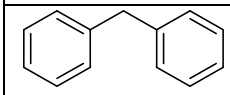 **190** | 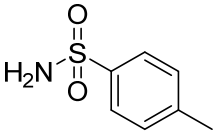 **193** | 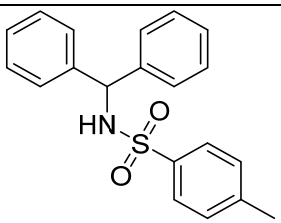 **194** | 75% |
| 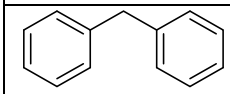 **190** | 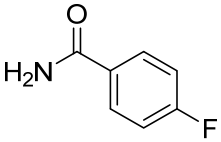 **195** | 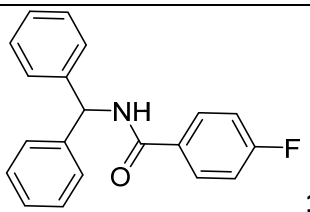 **196** | 77% |
| 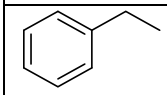 **25** | 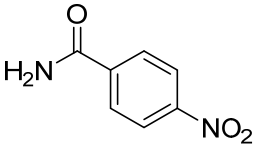 **191** | 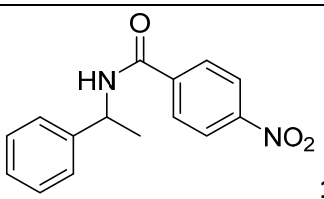 **197** | 60% |
| 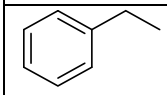 **25** | 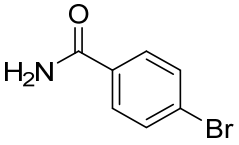 **198** | 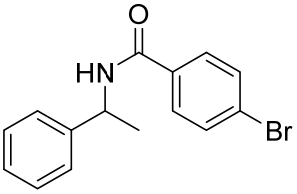 **199** | 68% |
| 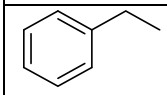 **25** | 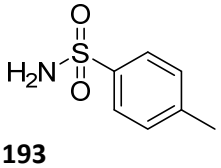 **193** | 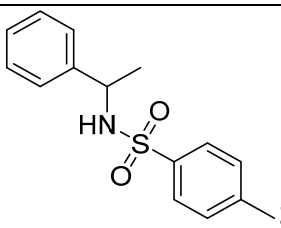 **200** | 64% |

**Table 5: Reaction of benzylic C-H bonds with primary amides and sulfonamides with $FeCl_2$ (10 mol%) and NBS (1.1 eq.) in EtOAc for 6-8 h at 50 °C.[75]**

Regarding the mechanism of this reaction, the authors propose there is no direct insertion of iron into the carbon-hydrogen bond being activated, as seen in Scheme 40.

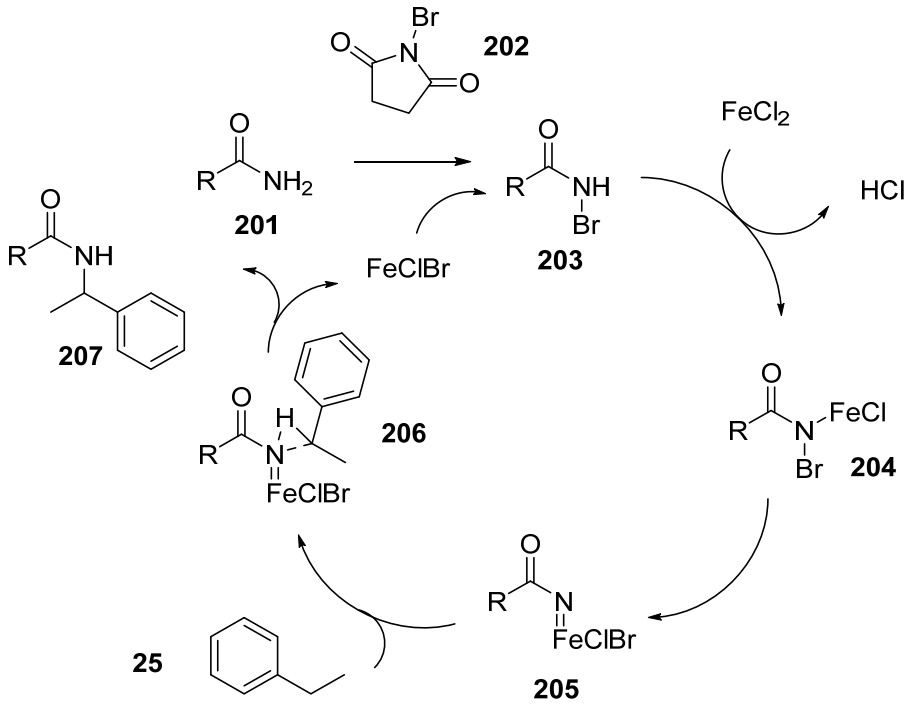


**Scheme 40: Mechanism proposed for C-H activation of benzylic positions by ferrous chloride and NBS.[75]**

Whilst the advances in the field of functionalizing carbon-hydrogen bonds have been vast, there is still scope for many additional advances to be made. The recent trend away from using scarce and expensive metals is massively beneficial for those who may want to utilise these methodologies in the decades to come, but there is much more work to be done to match the versatility of the rare transition metals often used.

Furthermore, there is scope to develop current methodologies for use with previously unexplored substrates which contain carbon-hydrogen bonds that are particularly inaccessible. The following three chapters detail the results of my investigations into functionalising carbon-hydrogen bonds using both aluminium and iridium mediated methodology.

# Mechanistic Investigations into the Acylation of Decalin with Aluminium Trichloride

## 2.1 Introduction

### 2.1.1 Acylation of Unsaturated Hydrocarbons

Acylation and alkylation of aromatic hydrocarbons was initially reported by Friedel and Crafts in the late 19th century, using acid chlorides or alkyl chlorides and aluminium trichloride, an early example of which is shown in Scheme 41.7

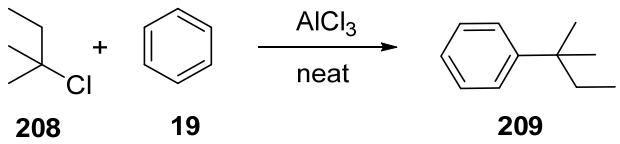


**Scheme 41: Reaction of benzene with amyl chloride in the presence of aluminium trichloride, first described in 1877.[7]**

The mechanism has been determined; nucleophilic attack on the "$R^+$" species by the aromatic system is followed by deprotonation. The reaction is made possible by the delocalised system of π electrons stabilising the intermediate carbocation (Scheme 42).

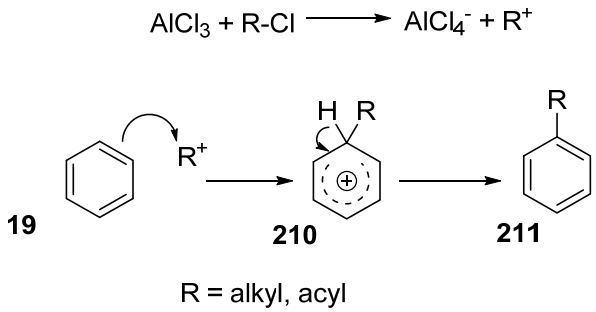


**Scheme 42: Mechanism of the Friedel-Crafts reaction.[4,7]**

As previously discussed, the substituents around the aromatic ring in an electrophilic aromatic substitution reaction can impact on the outcome of the reaction; electron-donating groups direct the electrophile to the *ortho* and *para* positions and electron-withdrawing groups disfavor reaction at the *ortho* and *para* positions, giving rise to an increase in substitution at the *meta* position.

This reaction is ubiquitous in organic chemistry - many examples of extensions to the methodology can be found; using metal catalysts such as ferric chloride,[77] zinc oxide,[78] zirconium tetrachloride,[79] indium tribromide[80] and titanium tetrachloride.[81] Non-metal Lewis

acid catalysts have also been developed, including boron trifluoride.[82,83,84,85] The reaction can be performed in a microwave and under solvent-free conditions.[86,87,88]

Applications employing many different types of aromatic rings can also be found; there are many examples of electron-rich[89,90] arenes undergoing Friedel–Crafts acylations and alkylations as well as fewer examples of electron-poor[91,92] aromatic molecules. Variants of the Friedel–Crafts acylations and alkylations have been used extensively towards synthesis of complex molecules.

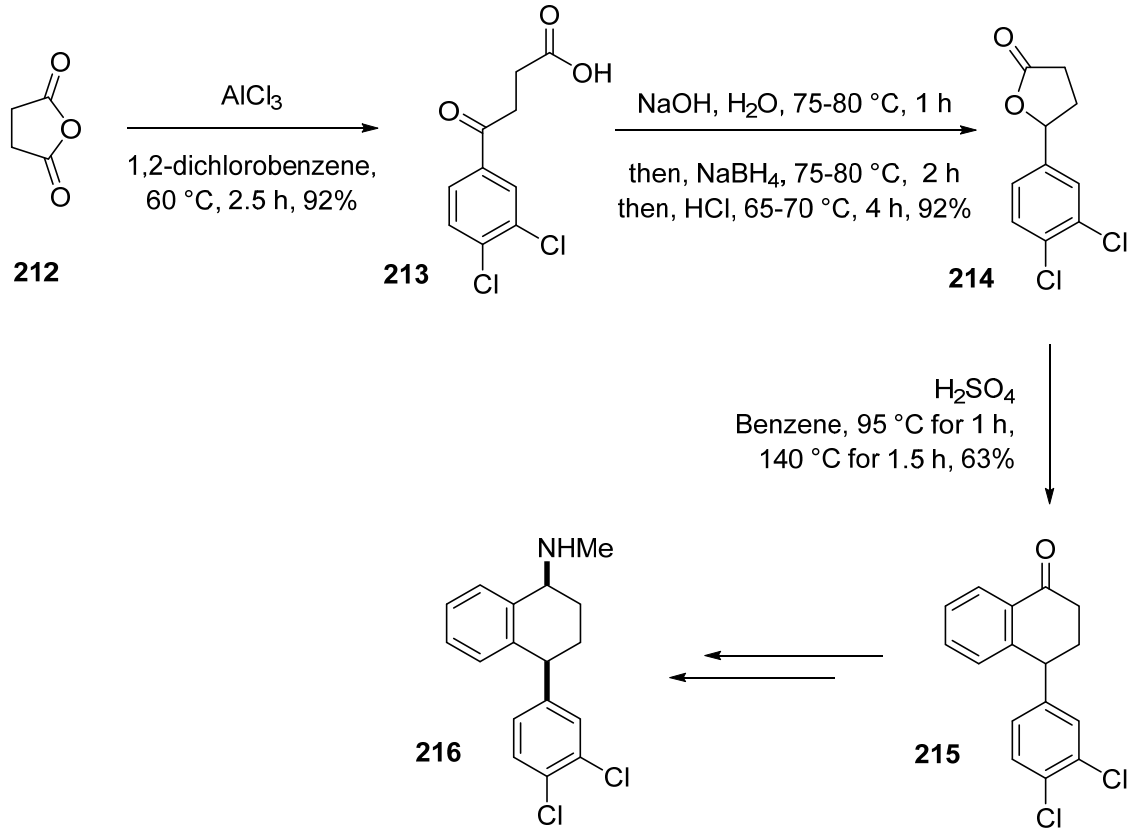


**Scheme 43: Use of Friedel–Crafts acylation in the formal synthesis of (±)-sertraline, 216.[93]**

Scheme 43 shows the use of Friedel–Crafts acylation in the formal synthesis of (±)-sertraline, **216**, an anti-depressant. In this 1990 synthesis,[93] Friedel–Crafts acylation using succinic anhydride as an acyl halide analogue is followed by reduction and cyclisation to form the lactone, **214**. An additional Friedel–Crafts acylation/alkylation step using a Brønsted acid promoter rather than a Lewis acid as seen in step one yields the desired tetralone product, **215**.

More recently in 2011, use of a tandem Prins / Friedel–Crafts acylation has been utilised in a formal synthesis of (–)-Haouamine A, as outlined in Scheme 44.[94] Reducing the number of steps in the synthesis of this alkaloid was of interest due to its potent anticancer activity. In a cyclisation mediated by aluminium triflate in nitromethane, a 65% yield of the tricyclic product, **218**, was obtained as a mixture of diastereomers. Swern oxidation followed by simultaneous hydrodebromination and removal of the Cbz protecting group via hydrogenation led to an intermediate (**220**) in Fürstner's total synthesis of (–)-Haouamine A, **221**.[95]

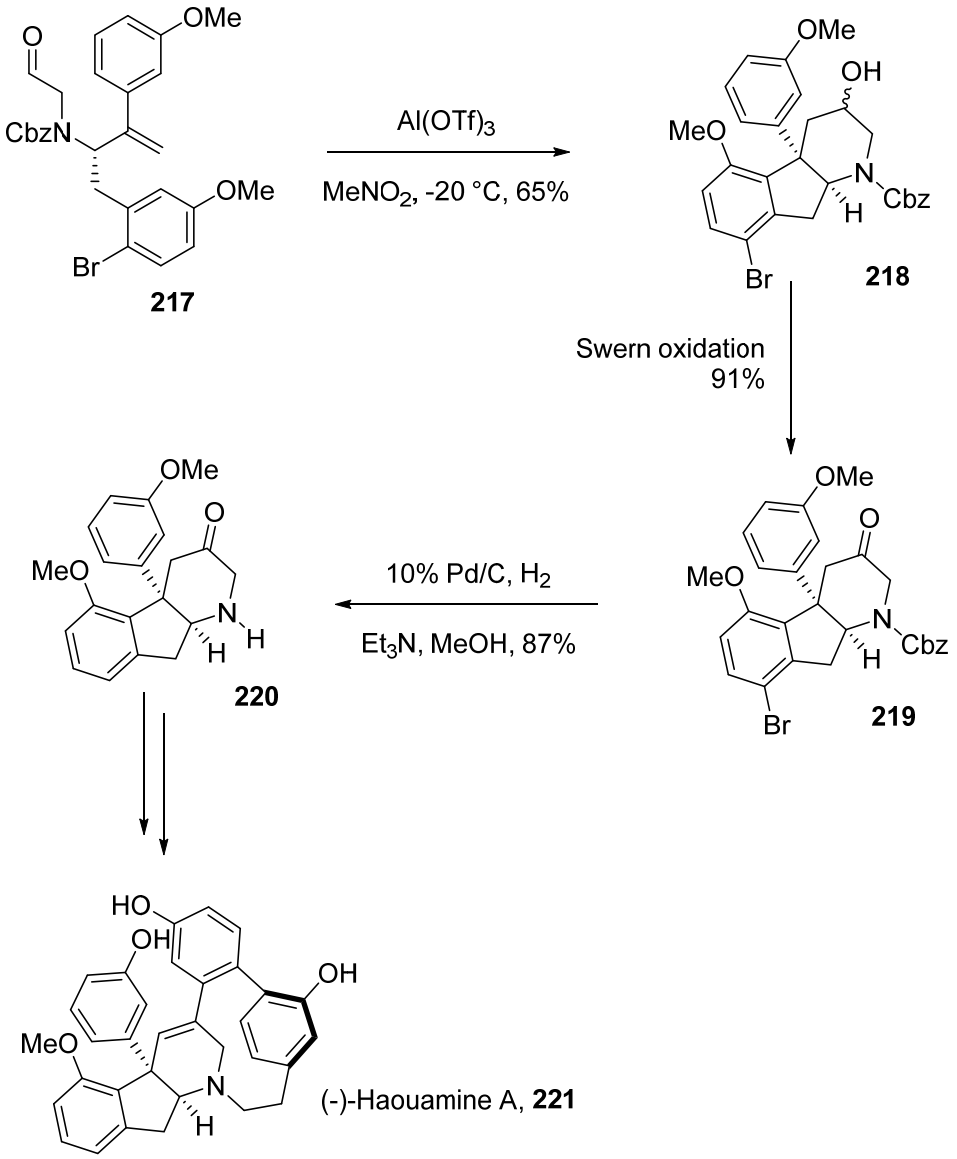


**Scheme 44: Formal synthesis of (–)-Haouamine A, using tandem Prins / Friedel–Crafts acylation in step one**[94]

Another example of use of Friedel–Crafts acylation in synthesis was established in the total synthesis of diptoindonesin G, **225**, although somewhat serendipitously on this occasion. During efforts to demethylate the aromatic methoxy groups, Kim and Kim[96] discovered that as well as demethylation, they could achieve Friedel–Crafts acylation at the 2-position of the dimethoxybenzene ring.

Using the mild conditions seen in Scheme 45, demethylation was only achieved at one methoxy moiety, forming **223**. The authors were happy to proceed with this compound due to the later demethylation step required after introduction of another methoxy group in the palladium catalysed cross-coupling C-H activation reaction that followed.

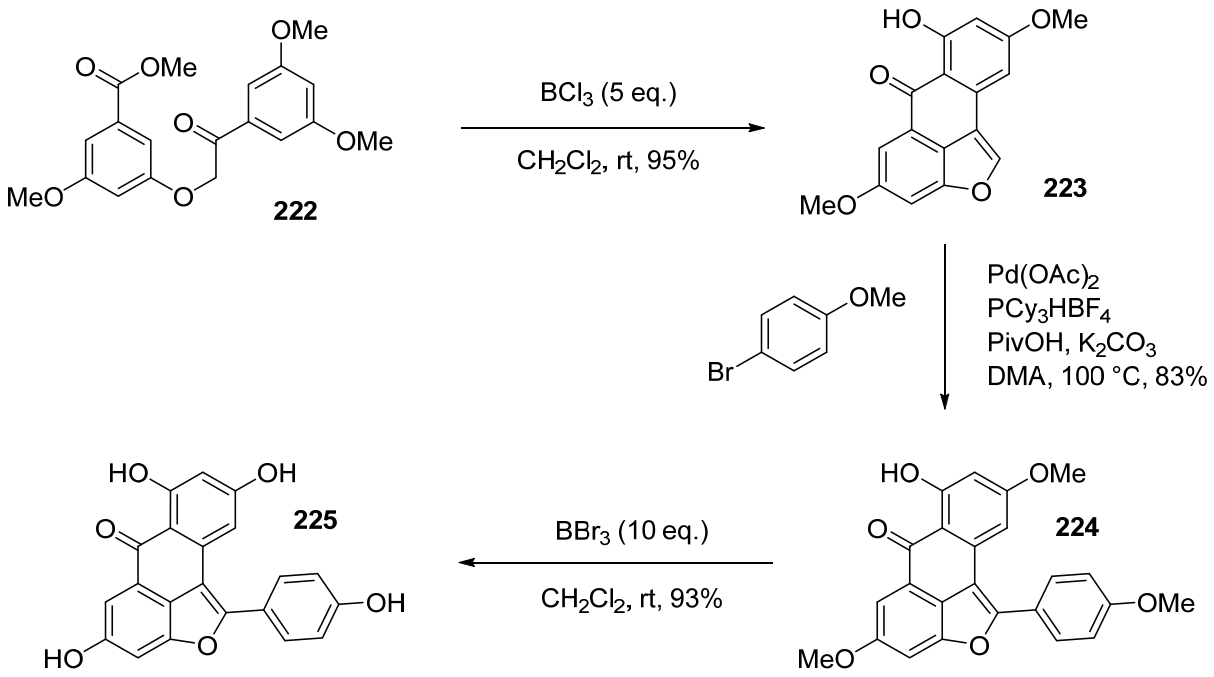


**Scheme 45: Synthesis of diptoindonesin G (225) using $BCl_3$ as a Lewis acid for Friedel–Crafts acylation and concomitant demethylation[96]**

Functionalisation of alkenes by Friedel–Crafts acylating and alkylating reagents is well precedented in the literature.[97-109] An example of some of the previous work undertaken is shown in Scheme 46, with the results outlined in Table 6.

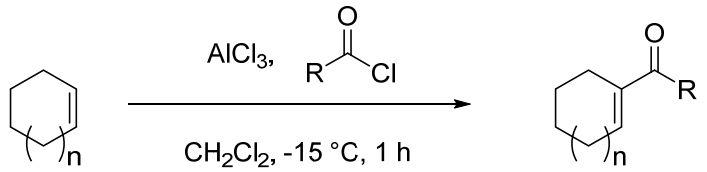


**Scheme 46: An example of Friedel-Crafts acylation of alkenes, using cycloheptene and cyclooctene[99]**

| Starting material | Acyl chloride | Yield (%) |
|---|---|---|
| n = 2 | R =Me | 70 |
| n = 2 | R = Et | 58 |
| n = 2 | R = Pr | 45 |
| n = 2 | R = Ph | 50 |
| n = 2 | R = $CH_2CH_2COOMe$ | 26 |
| n = 2 | R = $CH_2CH_2Cl$ | 60 |
| n = 2 | R = $CH_2CH_2CH_2Cl$ | 54 |
| n = 3 | R = Me | 48 |
| n = 3 | R = Ph | 33 |

**Table 6: Results of the reaction outlined in Scheme 46[99]**

It seems likely that these reactions of alkenes with aluminium trichloride and acyl chlorides proceed in a similar manner to their aromatic counterparts. Although alkenes do not have a π-system to stabilise the intermediate carbocation, the alkene can nevertheless act as a nucleophile towards the "$R^+$" species. Following this attack, loss of a proton from the acylated carbon reforms the alkene and neutralises the positive charge, as seen in Scheme 48.

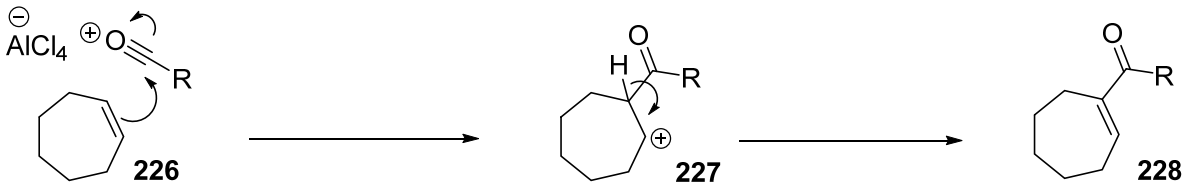


**Scheme 47: Mechanism for the acylation of cycloheptene by aluminium trichloride and an acyl chloride[99]**

Conversely, it would appear that the Friedel–Crafts acylation of alkanes seems less plausible due to the lack of nucleophilic functional groups on the substrate.

### 2.1.2 Acylation of Saturated Hydrocarbons

Despite these Friedel–Crafts acylations of alkanes seeming less likely to occur than those of aromatics and alkenes, there are in fact several examples in the literature of their existence.[110-123]

Tabushi *et al.*[111] were able to isolate 1-acetyl-2-methyl-cyclopentene, **233**, from cyclohexane. They propose a mechanism shown in Scheme 48 initiated by hydride abstraction from one of the carbons, followed by skeletal rearrangement of the cyclohexane secondary carbocation, **229**, forming the methylcyclopentane tertiary carbocation, **230**. This goes on to form 1-methylcyclopentene, **231**, as an intermediate. The alkene then attacks a second equivalent of acyl cation, forming a tertiary carbocation, **232**, and finally losing a proton to form the observed product.

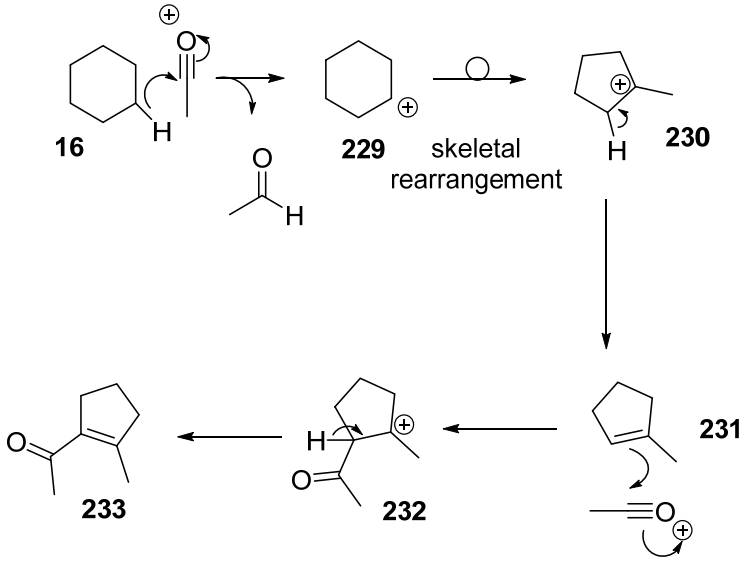


**Scheme 48: Proposed mechanism for the acylation of cyclohexane to yield 1-acetyl-2-methylcyclopentene[111]**

In a publication later the same year,[112] the authors showed methylcyclopentane to undergo acylation and yield 1-acetyl-2-methyl-cyclopentene as well. This supported the proposed skeletal rearrangement shown above, as abstraction of a hydride from methylcyclopentane would occur primarily at the tertiary position to give the same tertiary carbocation intermediate.

This reaction was later used by Harding and coworkers[119] in the two-step synthesis of 2-methyl-cyclopentene-1-carboxylic acid from cyclohexane with an overall 29% yield.

It was later reported in 1981 that a second product of the acylation of cyclohexane had been identified.[115] This product is 1,3-diacetyl-2-methylcyclopentene, **235**, shown in Scheme 49. Furthermore, the authors established that the both the mono- and di-acylated products from the acylation of cyclohexane were also produced from the acylation of methylcyclopentane, **234**, as well as 1-methylcyclopentene, **231**. The acylation of 1-methylcyclopentene proceeded under less forcing reaction temperatures of -75 °C to -30 °C. This gives further evidence for the above mechanism, as the methylcyclopentene intermediate proposed is seen to yield the same products. As anticipated, this implies the rate limiting step is the initial hydride abstraction.

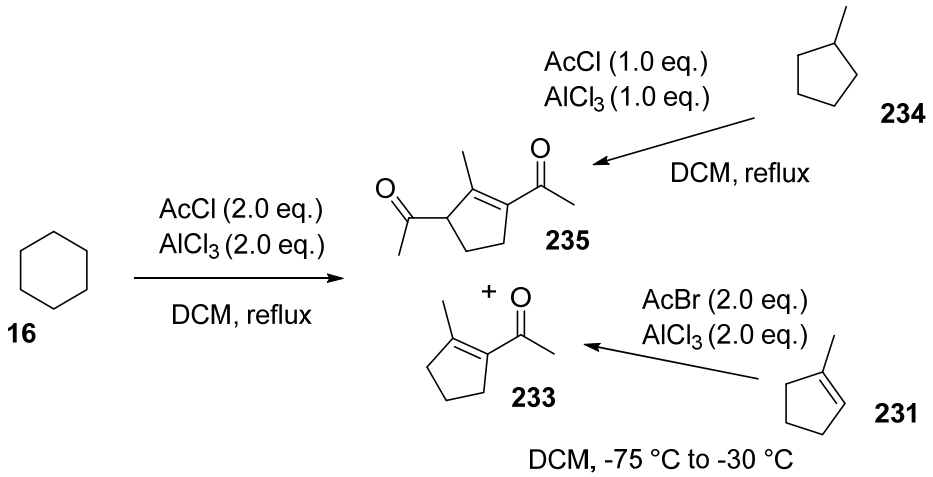


**Scheme 49: Reactions of various hydrocarbons to yield 1-acetyl-2-methylcyclopentene, 233, and 1,3-diacetyl-2-methylcyclopentane, 235.**[111,112,116]

With all of the starting hydrocarbons, it was found that the monoacylated product, **233**, was the major product, with the yields of product decreasing with the increased complexity of the reaction mechanism, i.e., methylcyclopentene where no hydride abstraction or skeletal rearrangement was required gave 60% yield and methylcyclopentane gave 50% yield with no skeletal rearrangement needed; cyclohexane gave 40%. They were also able to identify that some of the acetyl chloride, where used, was reduced to ethyl acetate.

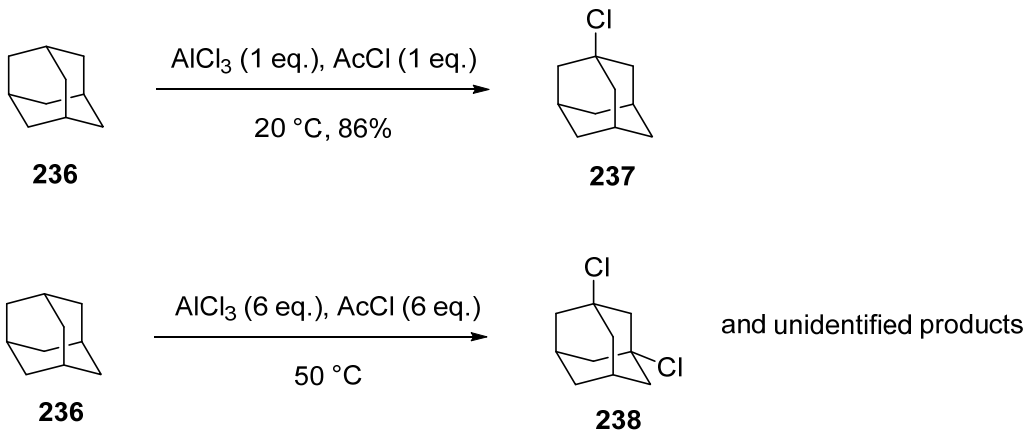


**Scheme 50: Reactions of adamantane with Friedel–Crafts acylating reagents.**[124]

With alkanes that are not inclined to form alkenes, such as adamantane, **236**, shown in Scheme 50, it is found that chlorination occurs instead of acylation.[124,125] Due to the ring strain that would be invoked by the loss of a proton from the tertiary carbocation, the tertiary carbocation is attacked by a chloride anion to form 1-chloroadamantane, **237**, or 1,3-dichloroadamantane, **238**, under more forcing conditions. The authors identified a byproduct from the reaction as the aldehyde formed from the acid chloride. Tabushi *et al*.[124] were able to effect this transition using acetyl chloride, butyryl and isobutyryl chloride as well as cyclohexanecarbonyl chloride.

### 2.1.3 Acylation of Decalin

The acylation of decalin was first reported by Baddeley and Wrench in the 1950s and further articles regarding this interaction were published shortly afterwards.[126-135] It was observed that multiple acylation products were formed at room temperature, using an excess of aluminium trichloride to acetyl chloride.

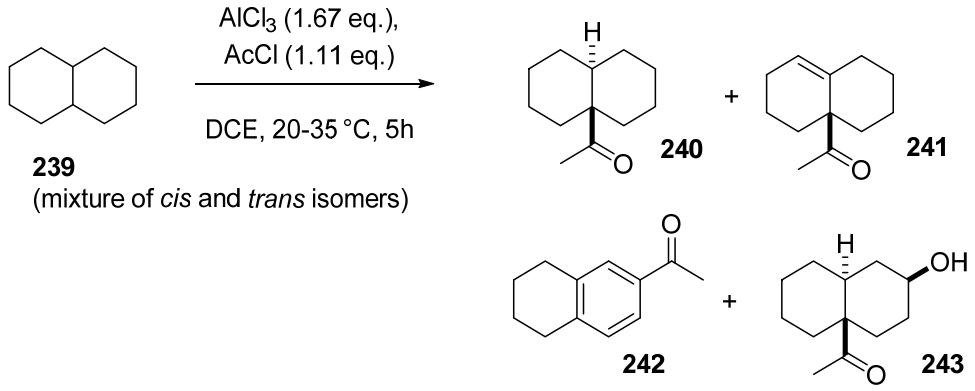


**Scheme 51: Baddeley and Wrench's initial investigation into the acylation of decalin with Friedel-Crafts acylating reagents.[126]**

The reason for the complexity of products was identified to be a use of excess aluminium chloride in relation to acetyl chloride; the number of equivalents of which was reduced accordingly (2.4 equivalents of AcCl and 1.5 equivalents of $AlCl_3$) and in conjunction with a decrease in the reaction temperature it was found to be possible to isolate cleanly a major product of the optimised reaction, an enol ether (**244**) which had not been observed under the previous reaction conditions.[127]

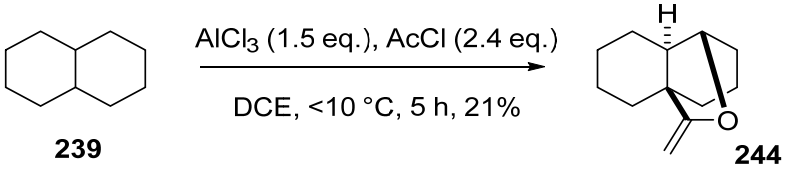


**Scheme 52: Baddeley's optimised reaction conditions yield the enol ether product, 244.[127]**

Decalin is functionalised at both a tertiary and a specific secondary site in this reaction and this reaction appears to have an unusual reaction mechanism in comparison with other acylation of alkanes, yielding an enol ether instead of α,β-unsaturated ketones.

The reaction has an advantage over C-H activation using transition metal catalysts as the Lewis acid used to mediate this reaction is $AlCl_3$, which is inexpensive in comparison with most transition metals.

It was of interest to investigate the mechanism of this unusual reaction to give insight into whether this reaction could be applied to other substrates, broadening the scope of compounds that one could use for future synthesis. The results contained in this chapter are the results of a detailed experimental, kinetic and computational analysis of the reaction.

## 2.2 Mechanisms

### 2.2.1 Baddeley's Postulated Mechanism

It was proposed by Baddeley that the formation of the enol ether would proceed as illustrated in Scheme 53 below. Initial abstraction of the hydride from the tertiary position of the decalin gives rise to the most stable carbocation, **245**. Loss of a proton from the remaining tertiary position yields the tetrasubstituted alkene ($\Delta^{9,10}$ octalin, **246**). This alkene can then attack a second equivalent of the acylium cation, acylating the decalin at tertiary position and forming a quaternary centre (**247**). The resulting positive charge is attacked by the oxygen lone pair, which would give a four-membered ring containing a carbon-oxygen double bond in which the oxygen is cationic, **248**. Isomerisation to a five-membered ring, presumably via a hydride shift and migration of the carbon-oxygen single bond yields the precursor to the enol ether, **249**; loss of a proton from the methyl group to form an *exo*-methylene then gives the neutral enol ether.

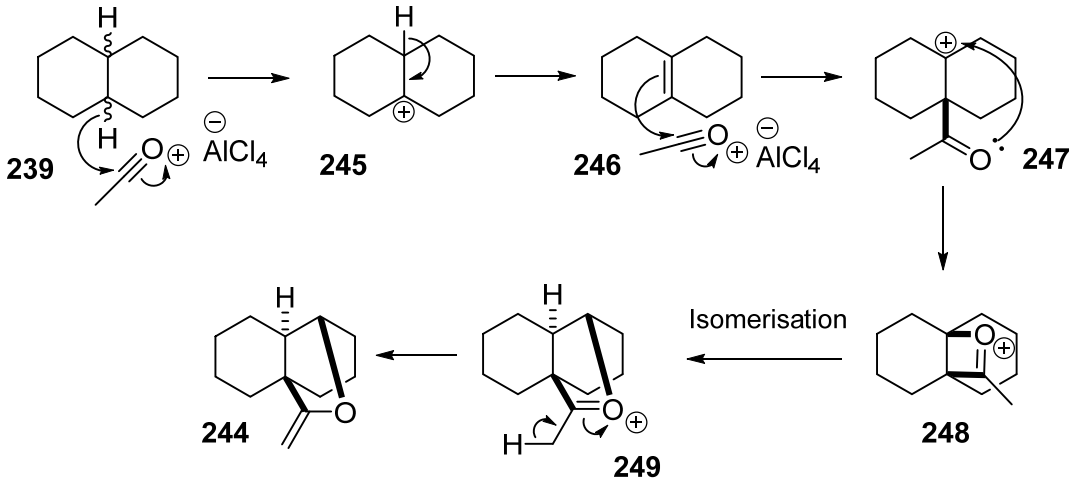


**Scheme 53: Formation of the enol ether, 244, from decalin, as proposed by Baddeley.[130]**

Whilst it was thought that the initial steps of the mechanism were plausible, no evidence was presented to support the identity of the proposed hydride-abstracting species or the presence of the alkene intermediate, **246**. Further to this, the ring strain present in the intermediate containing the four-membered ring, **248**, would be significantly increased over a simple cyclobutane due to the presence of the double bond and the rigidity of the decalin backbone.

### 2.2.2 Santelli's Postulated Mechanism

Later, in 1991, Santelli *et al.*,[122] proposed a different mechanism for the formation of the enol ether, shown in Scheme 54. Hydride abstraction and subsequent loss of a proton to form $\Delta^{9,10}$ octalin proceeded as per Baddeley's mechanism. Attack of the acetyl chloride moiety, rather than the acylium cation was next, with the chloride hypothesized to not be lost at this point. Instead the anionic oxygen would be stabilised by donation of electrons to the Lewis acidic aluminium trichloride. The oxygen aluminium bond would then attack the carbon *adjacent* to the positive charge and a [1,2]-hydride shift would occur. Finally, the neutral molecule formed would undergo loss of hydrochloric acid to generate the enol ether.

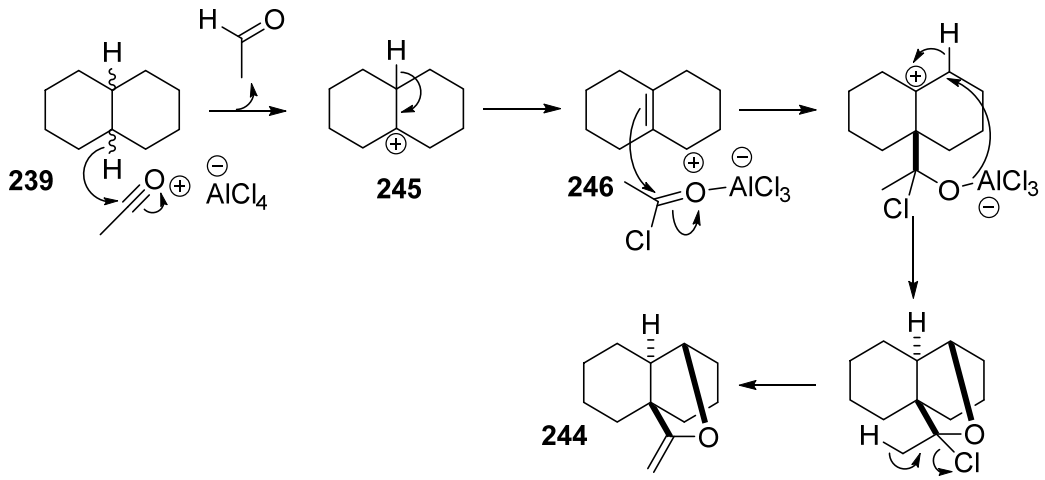


**Scheme 54: Formation of the enol ether, 244, from decalin, as proposed by Santelli.[122]**

The [1,2]-hydride shift illustrated in this mechanism seems more feasible as it removes the need to invoke the four-membered ring intermediate seen in Baddeley's mechanism. However, attack on the acetyl chloride by the alkene is more curious; with 2.4 equivalents of acetyl chloride in the reaction mixture and only 1.5 equivalents of aluminium trichloride, some acetyl chloride would potentially be expected to be present in its original neutral form. However, the more reactive acylium cation would still be present in at least 0.5 equivalents. This assumes 1.0 equivalent of acetyl chloride is converted to acetaldehyde and that the hydride abstraction is not the rate limiting step, otherwise more acylium cation would still be available. In addition, all 1.5 equivalents of aluminium trichloride would be expected to exist as the anionic aluminium tetrachloride, dramatically reducing its ability to act as a Lewis acid.

### 2.2.3 Our Postulated Mechanism

The mechanism outlined in Scheme 55 is our proposed mechanism for the formation of the enol ether. Hydride abstraction and deprotonation leading to the presence of the alkene, **246**, is as per the mechanisms of both Baddeley and Santelli. We propose the alkene then attacks an acylium ion, forming the cationic intermediate seen in Baddeley's postulated mechanism, **247**. Further to this, it is postulated that a [1,2]-hydride shift, as seen in Santelli's mechanism, occurs either in a concerted fashion with attack of the oxygen lone pair at the carbon adjacent to the tertiary carbocation or in a two step process. Finally, loss of a proton yields the enol ether, **244**.

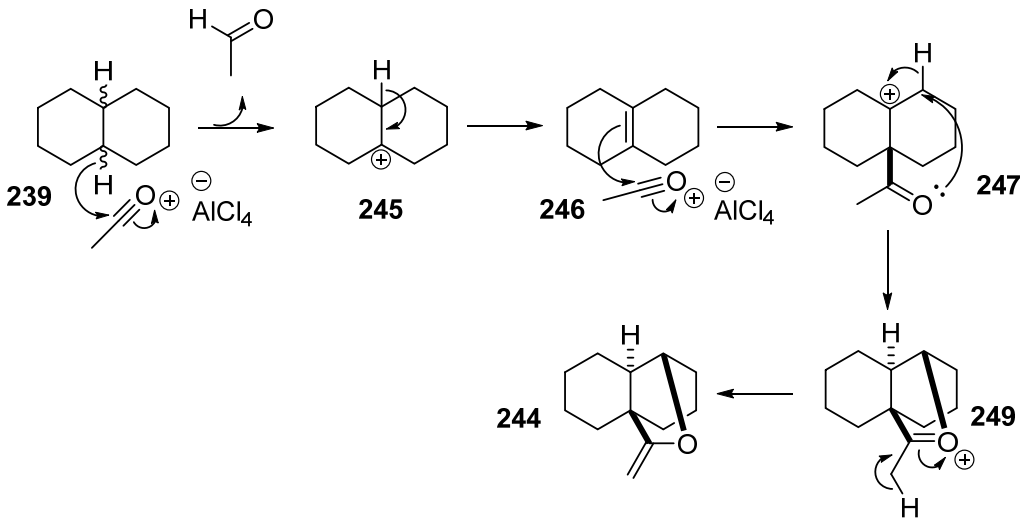


**Scheme 55: Our proposed mechanism for the formation of the enol ether, 244.**

There is a precedent for carbocation rearrangements involving hydride and alkyl shifts, such as those commonly observed in the biosynthesis of terpenes. There have been many examples of these shifts studied by computational modelling.[136] Scheme 56 illustrates rearrangements occurring in the biosynthesis of 5-epi-aristolochene and premnaspirodiene from farnesyl diphosphate, **250**.[137]

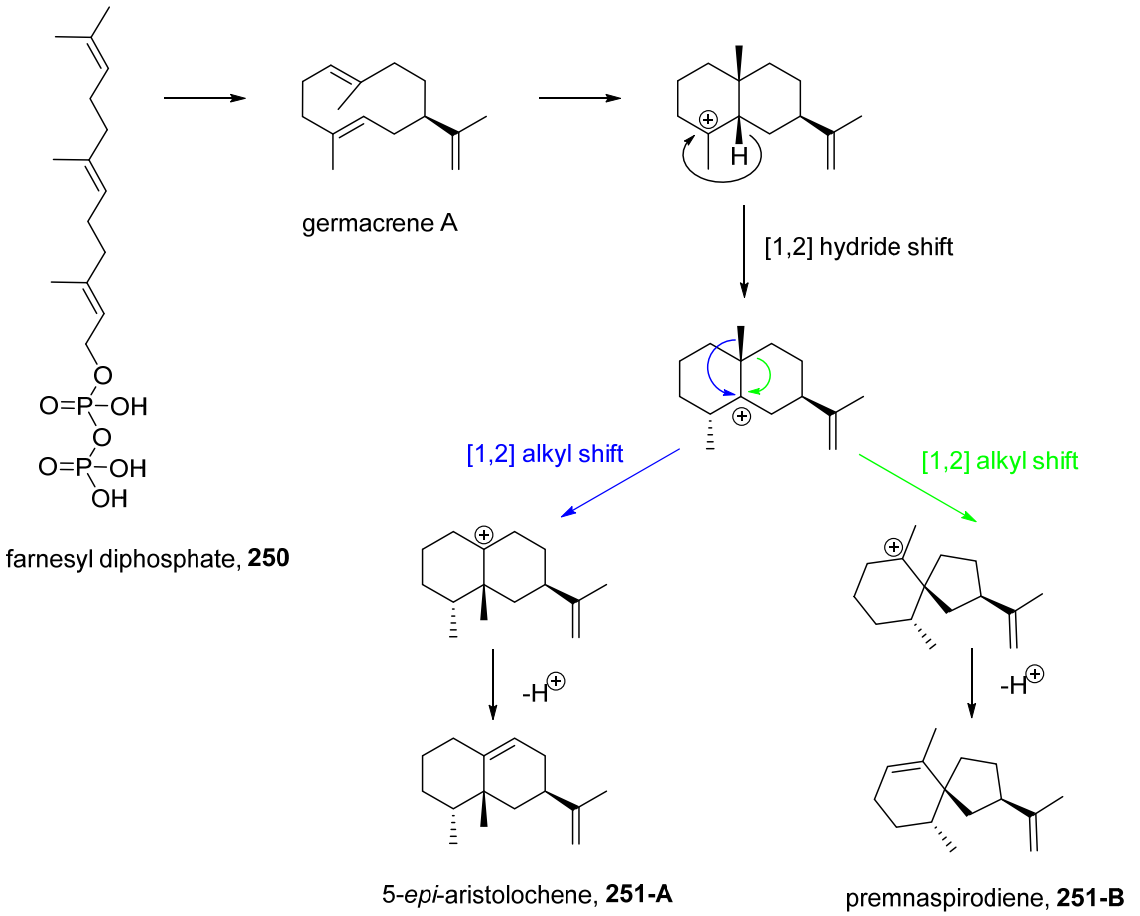


**Scheme 56: Biosynthetic pathway towards 251-A and 251-B, showing carbocation rearrangements. Computational modelling was performed using B3LYP/6-31G(d).[136,137]**

### 2.2.4 Additional Products from the Baddeley Reaction

In our hands, it was possible to identify the presence of another product derived from the enol ether, a chloroketone, **252**, shown in Scheme 57 whose existence had been reported previously by Baddeley, but only on reaction of the purified enol ether with hydrochloric acid.[129] Due to the infancy of the technique at the time of Baddeley's work, no NMR data were reported for any compounds synthesised.

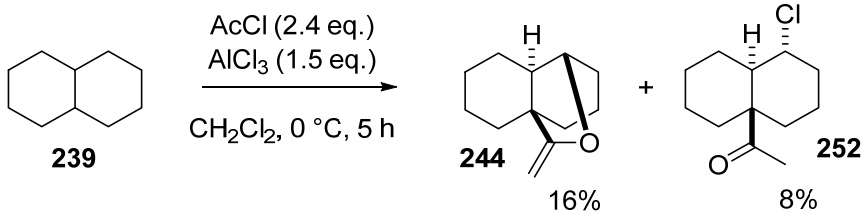


**Scheme 57: Reaction of decalin with aluminium trichloride and acetyl chloride under Baddeley's optimised reaction conditions giving enol ether, 244, and chloroketone, 252.**

The structure of the chloroketone, **252**, was elucidated via analysis of the NMR spectra obtained. The proton NMR spectrum (Figure 4) showed a singlet peak at 1.98 ppm, consistent with a methyl group adjacent to a ketone. This indicated the decalin skeleton had been monoacylated. Based on the mechanism for the formation of the enol ether, acylation is most likely to occur at the ring junction.

The peak at 4.51 ppm was of particular interest due to the downfield chemical shift. This indicated the proton in question was geminal to a heteroatom. Under the reaction conditions, possible heteroatoms included oxygen or chlorine. No indication of an alcohol proton is observed in the proton NMR spectrum, so it seems likely the heteroatom concerned is chlorine, although this alone is not conclusive.

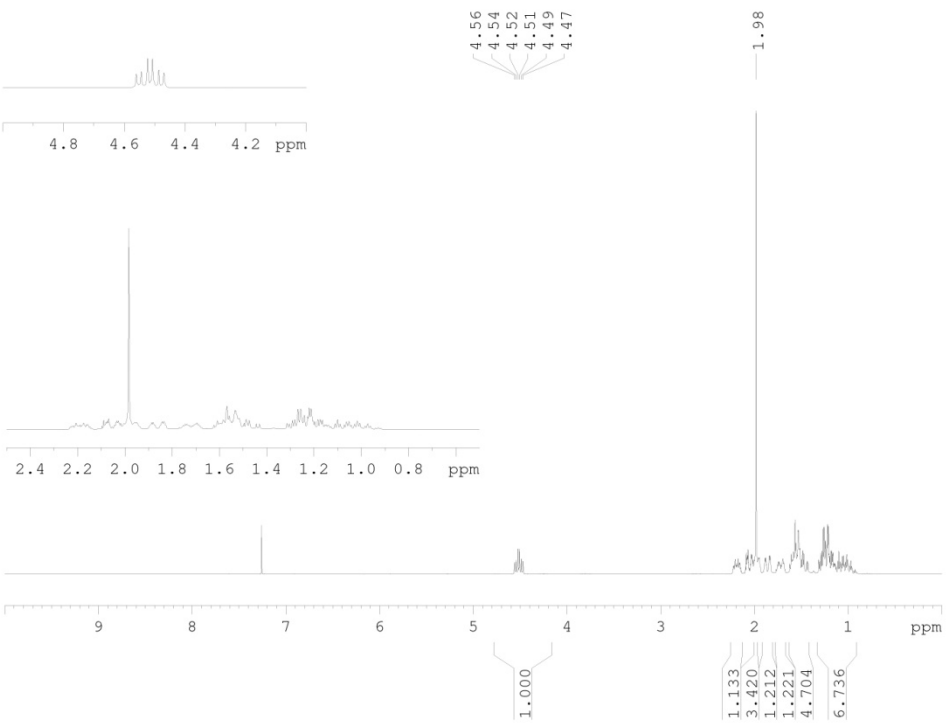


**Figure 4: Proton NMR spectrum of chloroketone.**

The splitting pattern observed is an apparent triplet of doublets, with $^{3}J$ coupling constants of 11.0 Hz and 5.0 Hz respectively. The proton is therefore coupling to three adjacent protons; the only possible location of the bicyclic ring skeleton that the proton could be positioned in order to couple to three protons is adjacent to the tertiary ring junction as seen in Figure 5.

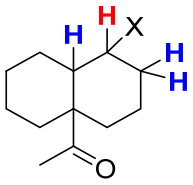


**Figure 5: Location of proton (red) corresponding to peak at 4.51 ppm, coupling to the three protons shown in blue.**

Figure 6 shows the possible relative stereochemistries and conformations of the compound with the heteroatom located α- to the tertiary ring junction carbon. Structures **252-A** and **252-B** have a *trans*-decalin backbone and **252-C** and **252-D** are *cis*-decalins. Due to the conformationally locked bicyclic ring structures, the coupling of the protons outlined in red to the protons shown in green and blue can be predicted using the Karplus equation.[138,139] This equation looks at the relationship between dihedral angles and $^{3}J$ coupling constants, where dihedral angles of 0° and 180° command the largest coupling constants and dihedral angles of 90° are associated with the smallest coupling constants, near to zero. The exact coupling

constants depend on the precise nature of the molecule, but an indication of the angles involved can be inferred.

In the possible structures, compounds **252-B** and **252-C** have dihedral angles between the red proton and adjacent protons of approximately 60 ° in all cases, and would present as a doublet of doublet of doublets. As the $^{3}J$ coupling constants would be very close in magnitude, the splitting pattern may look like a quartet.

In the case of compound **252-D**, the red proton would couple to the blue proton with a large $^{3}J$ value and the two green protons with a smaller similar $^{3}J$ value; the splitting pattern from this conformation would likely present as an apparent doublet of triplets.

In the case of compound **252-A**, the red proton would couple to the two blue protons with a large $^{3}J$ value and the green proton with a smaller $^{3}J$ value; the splitting pattern from this conformation would likely present as a triplet of doublets; this matches the observed pattern seen in the proton NMR spectrum.

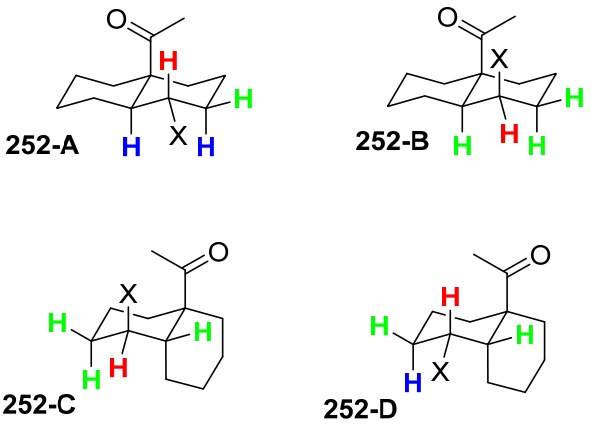


**Figure 6: Possible relative stereochemistries and conformations of the chloroketone, 252, with the proton of interest shown in red, protons with dihedral angles of ≈ 60 ° to the red proton shown in green, protons with dihedral angles of ≈ 180 ° shown in blue**

Upon examination of the carbon-13 NMR spectrum, shown in Figure 7, the peak at δ = 212.4 ppm confirms the presence of a ketone. The peaks at δ = 56.3 and 53.5 ppm correspond to the quaternary carbon and the tertiary carbon at the ring junction respectively and δ = 62.1 ppm corresponds to the carbon attached to the heteroatom. The remaining eight peaks in the aliphatic region correspond to the seven secondary carbons and the methyl group.

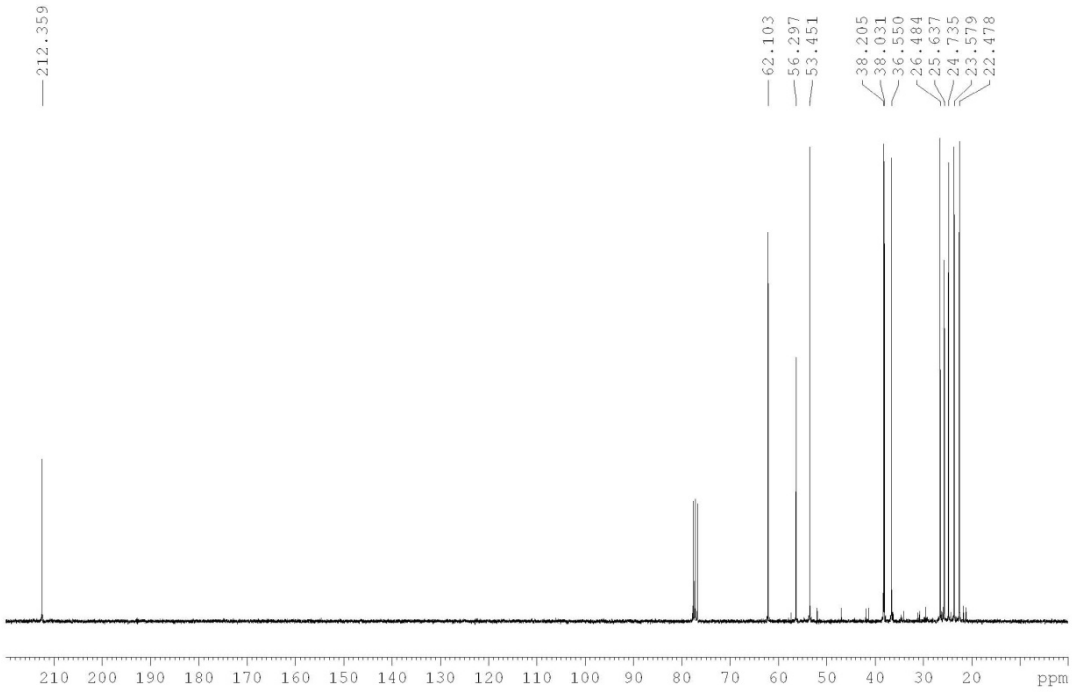


**Figure 7: Carbon-13 NMR spectrum of chloroketone 252.**

The enol ether was subjected to treatment with hydrochloric acid to induce ring opening to the chloroketone; the NMR data from the chloroketone, **252**, obtained from this reaction was compared with the sample isolated from the Baddeley reaction, confirming its identity.

## 2.3 Nature of the Acylating Species

In Scheme 53 to Scheme 55, the acylating/hydride abstracting species has been depicted as an acylium cation and aluminium tetrachloride anion in a 1:1 ratio. It was thought to be unlikely that the acylium cation would exist as a discrete species without some interaction with the aluminium tetrachloride anion. However, it was not clear whether a 1:1 ratio of anion to cation would exist alongside an additional 0.9 equivalents of acetyl chloride or if a more complex aggregate species would form.

The reaction was run in an NMR tube and proton NMR experiments taken at intervals overnight showed that the chemical shift of methyl group from the acylating species shifted significantly over the course of the reaction at 0 °C (Figure 8). This indicated that the species present at the beginning of the reaction was gradually changing as increasing amounts of “acylium cation” were used for hydride abstraction and acylation. No methyl peak was observed for acetyl chloride.

Other peaks seen in this region of the spectra include the methyl peak of cationic intermediate, **249**, at 3.07 ppm.

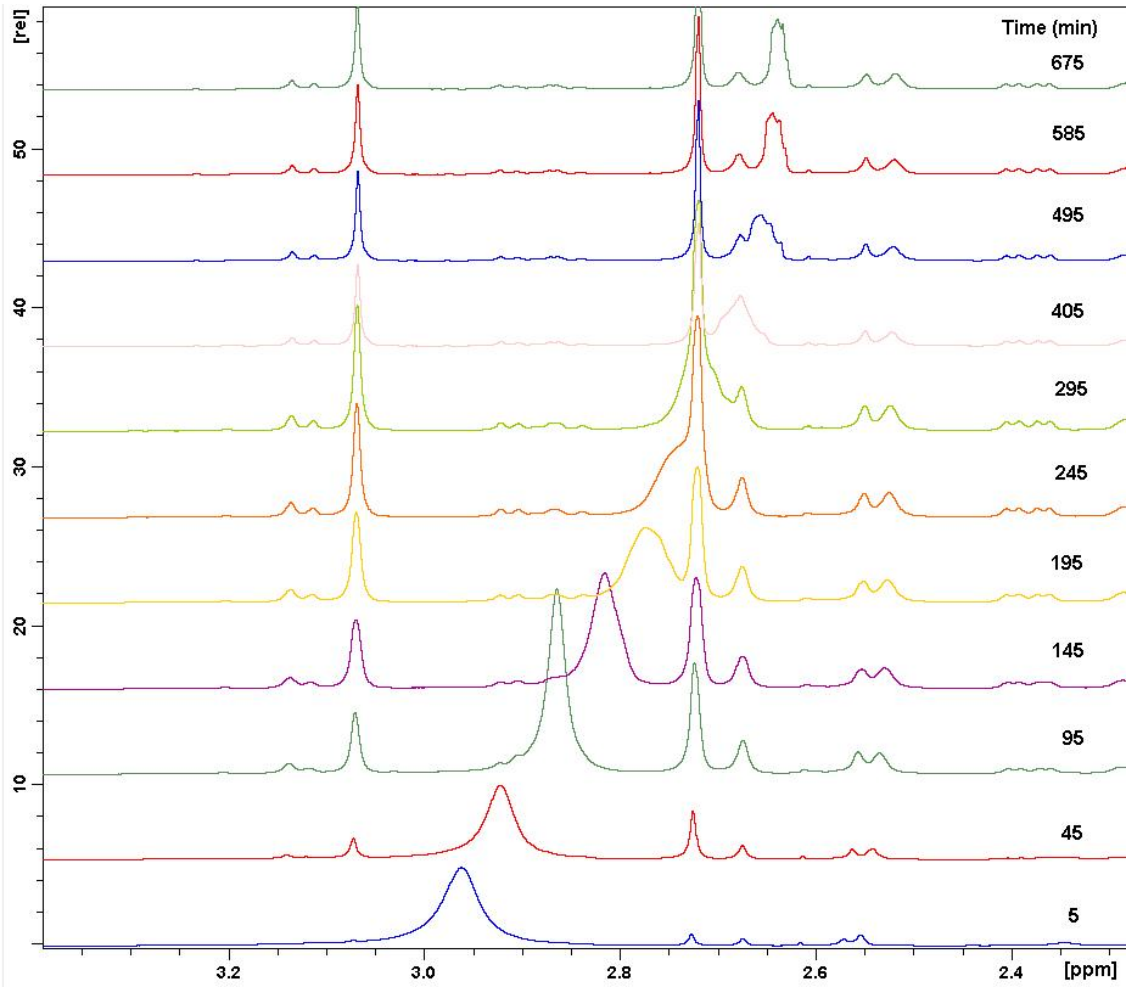


**Figure 8: Proton NMR spectrum of the Baddeley reaction of *cis*-decalin at 0 °C over time, showing the methyl group of the acylating species shifting from 2.96 ppm to 2.66 ppm.**

## 2.4 Hydride Abstraction

### 2.4.1 Acetaldehyde

The presence of acetaldehyde in the reaction mixture would serve as a good indication that both a hydride was being abstracted from decalin and that the hydride sink was the acylium ion. However, analysis of the crude reaction mixture after work-up by proton and carbon NMR showed no acetaldehyde peaks. It was considered that due to the low boiling point (20 °C) any acetaldehyde present would have been removed in the work up, so the absence of peaks in the NMRs was inconclusive. The paraldehyde trimer and metaldehyde tetramer were also not observed.

The reaction was performed using decanoyl chloride instead of acetyl chloride, with the hope that any decanal formed would be less volatile and would therefore be visible by NMR. Aldehyde peaks were indeed visible in the distillate of this reaction. This gave an indication that the hydride abstracted from the decalin was subsequently transferring to the acylium ion and resulting in formation of an aldehyde byproduct.

### 2.4.2 Aluminium Trichloride as a Hydride Abstractor

The presence of the aldehyde did not however confirm that the acylium ion is acting as the hydride abstractor, merely as the hydride sink. Another possible hydride abstractor present in the reaction mixture is aluminium trichloride, which has been reported previously in the literature to isomerise *cis*-decalin into *trans*-decalin.[140,141] This reaction presumably occurs via a hydride abstraction from the tertiary position of *cis*-decalin, and the subsequent carbocation then abstracts the hydride back from the $[HAlCl_3]^-$ anion, forming the more stable *trans*-decalin.

Repeating this reaction with a commercially available mixture of *cis*- and *trans*-decalin and 1.5 equivalents of aluminium trichloride (as per Baddeley's optimised reaction conditions) yielded only *trans*-decalin, as shown in Scheme 58. This illustrated the ability of the aluminium trichloride to act as a hydride transfer agent.

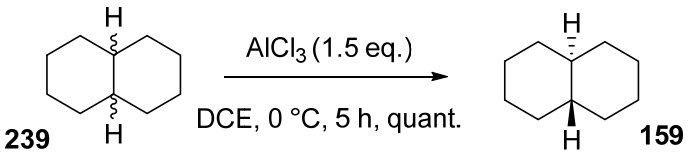


**Scheme 58: Isomerisation of decalin with $AlCl_3$ without acetyl chloride.**

However, it should be noted that the reaction conditions employed in the Baddeley reaction (1.5 equivalents of aluminium trichloride and 2.4 equivalents of acetyl chloride) enable a substantial proportion (if not the entirety) of the aluminium species to be present as the aluminium tetrachloride anion complexed to the acylium ion. This species would lack the ability to abstract a hydride as it already has a full octet and is negatively charged.

In conclusion, aluminium trichloride would be able to transfer a hydride from the decalin to the acylium ion, but is unlikely to be present in significant amounts under the reaction conditions employed.

### 2.4.3 Presence of 1-Chloroethyl Acetate Byproduct

A significant peak in the $^1H$ NMR spectrum of the crude reaction mixture was observed at $\delta$ = 6.51 ppm (quartet, $CDCl_3$), but the corresponding compound was not observed in any of the distillate fractions. This suggested the compound was particularly volatile and unlikely to be based on the decalin skeletal structure. Distillation without the use of vacuum allowed for isolation of the compound, which was subsequently identified as 1-chloroethyl acetate.

It is clear that the formation of 1-chloroethyl acetate requires two equivalents of acetyl chloride, but one equivalent *must be in the aldehyde oxidation state* in order for this reaction to occur. Control reactions carried out simply by mixing acetyl chloride and aluminium trichloride led only to the formation of the acylium ion.

However, reaction between acetyl chloride and acetaldehyde in the presence of aluminium trichloride yielded 1-chloroethyl acetate. This reaction had been observed previously in the literature using aluminium trichloride[142] or zinc dichloride[143] as the Lewis acid. From this we

could be sure that acetaldehyde was being produced as a byproduct of the Baddeley reaction and reacting further to form 1-chloroethyl acetate.

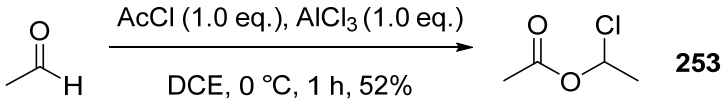


**Scheme 59: Reaction of acetaldehyde with acetyl chloride mediated with aluminium trichloride.**

### 2.4.4 *trans*-Crotonyl Chloride

Further proof was sought to establish whether the acylium ion was directly abstracting a hydride or if the hydride was abstracted by the aluminium trichloride and subsequently transferred onto the acylium ion.

Using *trans*-crotonyl chloride in the place of acetyl chloride was explored, as the cation formed from *trans*-crotonyl chloride would have more resonance stabilisation and hence less of a partial positive charge at the carbonyl carbon. In turn, this would reduce the ability of the cationic species to act as a hydride abstractor (Scheme 60).

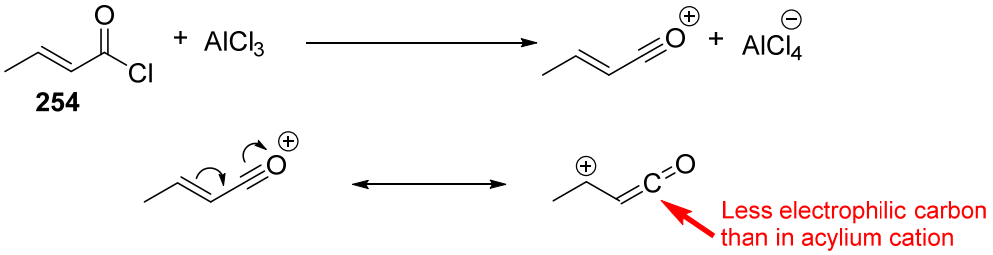


**Scheme 60: Proposed interaction of *trans*-crotonyl chloride with aluminium trichloride and the resonance stabilisation forms of the resulting cation.**

However, the advantage of using this system is that the aluminium trichloride would be converted to the tetrachloroaluminate species in the same manner as using the acetyl chloride / aluminium trichloride system. As a result, if the aluminium trichloride was acting as the hydride abstractor, hydride abstraction should still occur.

If the crotonyl cation were too stable to act as a hydride abstractor, it is plausible it may be resistant to nucleophilic attack by the alkene intermediate. If this were the case, hydride abstraction by the aluminium trichloride would result in isomerisation from *cis*-decalin to *trans*-decalin rather than formation of an analogous enol ether.

Under Baddeley's reaction conditions using crotonyl chloride instead of acetyl chloride, no reaction was observed; *cis*-decalin was also not converted to *trans*-decalin (Scheme 61).

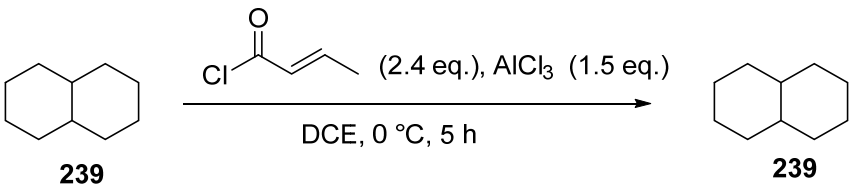


**Scheme 61: Attempted Baddeley reaction using *trans*-crotonyl chloride instead of acetyl chloride.**

To confirm that reaction of crotonyl chloride with aluminium trichloride had indeed taken place, acetyl chloride was added to the reaction mixture (Scheme 62). It was not expected that any further reaction would then occur, as if crotonyl chloride and aluminium trichloride had not formed the ionic complex then the presence of aluminium trichloride would have isomerised *cis*-decalin into *trans*-decalin. Indeed, as anticipated, no reaction was then observed upon the addition of acetyl chloride, indicating the aluminium trichloride was not available to convert the acetyl chloride into the acylium ion.

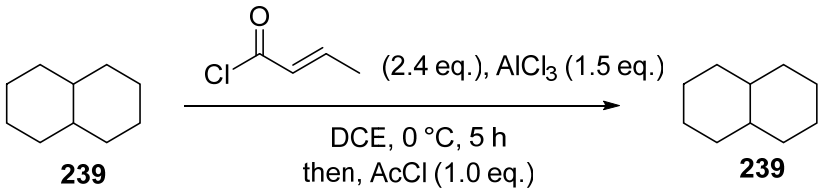


**Scheme 62: Attempted Baddeley reaction using *trans*-crotonyl chloride followed by acetyl chloride.**

Finally, a 1:1 mixture of acetyl chloride and aluminium trichloride was added to the reaction mixture containing decalin and the crotonyl chloride / aluminium trichloride mixture. From this, formation of the enol ether, **244**, was observed, as well as 1-chloroethyl crotonate, as shown in Scheme 63.

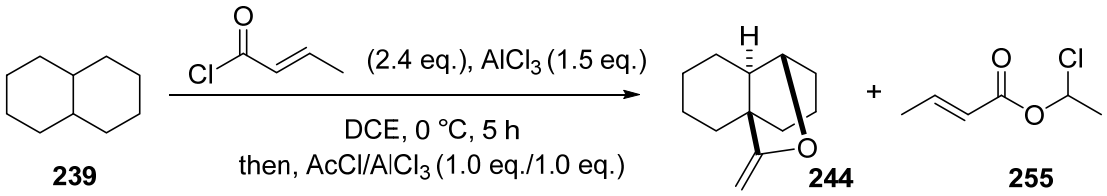


**Scheme 63: Sucessful control Baddeley reaction using *trans*-crotonyl chloride followed by acetyl chloride and aluminium trichloride (pre-mixed).**

A control reaction between acetaldehyde and crotonyl chloride in the presence of aluminium trichloride formed 1-chloroethyl crotonate, seen in Scheme 64.

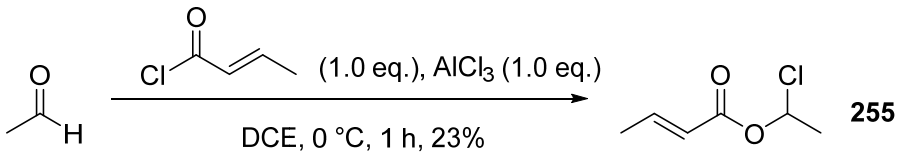


**Scheme 64: Reaction of acetaldehyde with *trans*-crotonyl chloride, mediated by aluminium trichloride.**

## 2.5 $\Delta^{9,10}$ Octalin Intermediate

### 2.5.1 Synthesis

$\Delta^{9,10}$ octalin, **246**, was independently synthesised via two different routes, as outlined in Scheme 65. Route A involved the Birch-like reduction of naphthalene to a mixture of tetralin, **257**, $\Delta^{1,9}$ octalin, **256**, and the desired $\Delta^{9,10}$ octalin, **246**. Tetralin was easily separated by column chromatography, but the monoalkenes were inseparable. Route B used 2-decahydronaphthol, **259**, as a starting material, which was dehydrated using orthophosphoric acid and phosphoric anhydride. Further subjection of the crude material to treatment with phosphoric anhydride caused isomerisation of the $\Delta^{1,2}$ octalin (**260**) to $\Delta^{1,9}$ octalin and $\Delta^{9,10}$ octalin. As in route A, direct separation of these two compounds was not possible, so the mixture was subjected to a selective hydroboration / oxidation reaction which resulted in $\Delta^{1,9}$octalin being converted to 1-decahydronaphthol, **258**, whereas $\Delta^{9,10}$ octalin was left untouched. These compounds could then be separated by distillation or column chromatography.

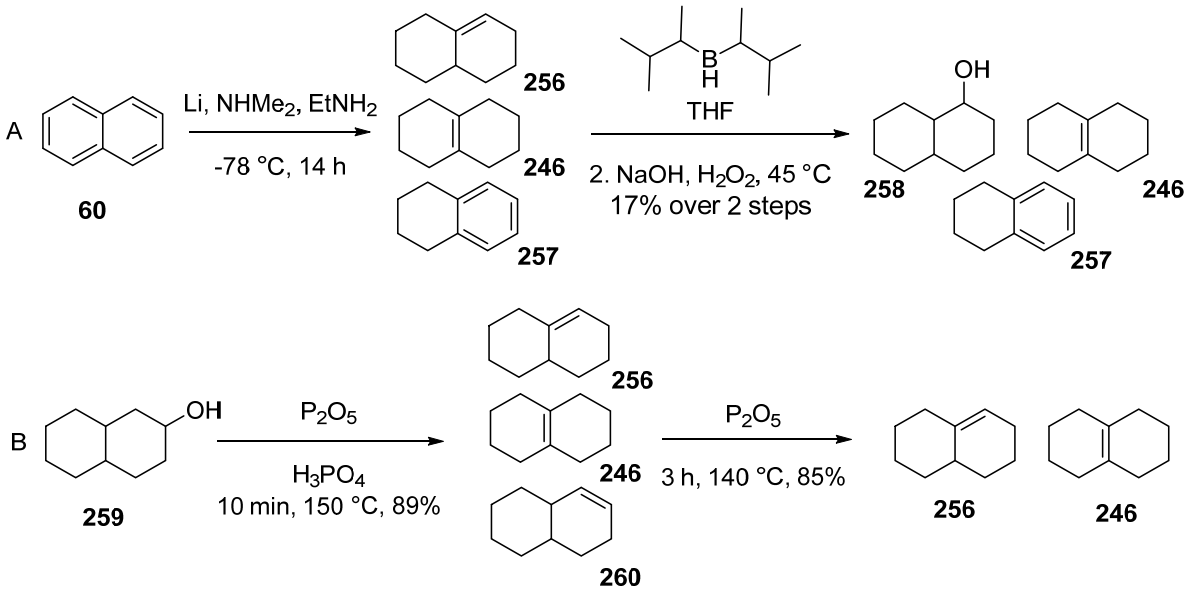


**Scheme 65: Synthesis of $\Delta^{9,10}$ Octalin[144]**

### 2.5.2 Reactivity of $\Delta^{9,10}$ Octalin

$\Delta^{9,10}$ octalin was treated with aluminium trichloride and acetyl chloride under slightly modified reaction conditions in order to discern whether the tetrasubstituted alkene, **246**, is a likely intermediate in the reaction mechanism.

Less acetyl chloride (1.0 eq.) and aluminium trichloride (1.0 eq.) were used to represent more accurately the amount of acylating reagent that would be present in the Baddeley reaction mixture after hydride abstraction and formation of 1-chlorethyl acetate. However, given the slow hydride abstraction step that precedes the formation of $\Delta^{9,10}$ octalin, the quantity of unreacted acylating species available to react with $\Delta^{9,10}$ octalin will be variable. Nonetheless, as seen in Scheme 66, the alkene reacts to give both enol ether and chloroketone.

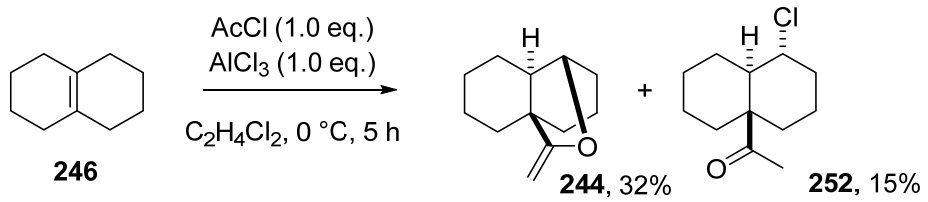


**Scheme 66: Reaction of $\Delta^{9,10}$ octalin with aluminium trichloride and acetyl chloride.**

It should be noted however, that the yields of these compounds are not as high as was anticipated. With one equivalent of acylating reagent present and only one equivalent of acylating reagent needed to proceed to completion with no hydride abstraction step, it was expected that the yield would be substantially higher than the reaction with decalin. A further curiosity was that both *cis*- and *trans*-decalin were recovered from the reaction in addition to the enol ether and chloroketone.

An explanation for this can be found in a computational modeling study performed by Ian Williams and Makoto Sato, the results of which can be viewed in Figure 9. It was discovered that the energy barrier to proceed from $\Delta^{9,10}$ octalin, **246**, to the tricyclic cationic intermediate, **249**, (before work-up) and the energy needed to recede from $\Delta^{9,10}$ octalin to back to decalin were similar. With respect to the octalin intermediate, the lowest Gibbs energy barrier for the forward reaction is 56 kJ $mol^{-1}$ and the reverse reaction to *cis*-decalin is 55 kJ $mol^{-1}$.

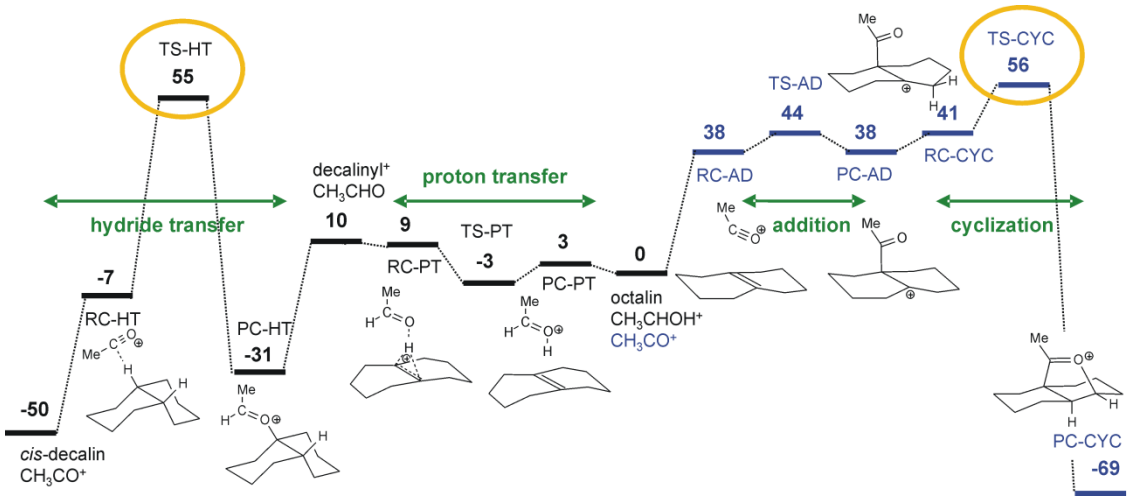


**Figure 9: MP2/cc-pVTZ//MP2/6-31+G* Gibbs energy profiles in PCM $CH_2Cl_2$. Computational modelling by Ian Williams and Makoto Sato showing the reaction profile of the Baddeley reaction starting from *cis*-decalin, relative to the $\Delta^{9,10}$ octalin intermediate.**

## 2.6 Kinetic Studies

It was possible (as previously mentioned) to monitor the Baddeley reaction in an NMR tube, using dichloromethane-$d_2$ as the solvent. Unfortunately, due to the overlapping peaks in the aliphatic region of the proton NMR spectra, it was not possible to monitor the consumption of decalin accurately. In lieu of this, it was possible to monitor the growth of distinctive peaks corresponding to one proton from 1-chloroethyl acetate, **253**, and one proton from the cationic intermediate, **249**. The cationic intermediate, **249**, can be considered a surrogate of the final enol ether product, which does not form until work-up of the reaction mixture.

Figure 10 shows the proton NMR spectrum of the Baddeley reaction, with the region from 5.8 – 6.8 ppm magnified. The doublet appearing at 6.08 ppm corresponds to the proton shown in red on the cationic intermediate, **249**. The quartet at 6.62 pm corresponds to the proton shown in blue from 1-chloroethyl acetate, **253**.

Due to the high reactivity of the reagents and the mass of overlapping peaks from 1.0 – 3.0 ppm, it was important to select an internal NMR standard that wouldn't react with the acylating reagents or be difficult to integrate due to the presence of nearby peaks.

Initially, the commonly-used tetramethylsilane was trialled for use as the internal standard. However, on mixing tetramethylsilane with a pre-mixed solution of acetyl chloride and aluminium trichloride in dichloromethane-$d_2$, it became apparent that a reaction was slowly occurring to form trimethylsilyl chloride. However, the reaction between tetramethylsilane and the acylating reagents did not appear to proceed further to form the di- or tri-chlorinated silanes. A similar reaction is known in the literature.[145]

With this information in hand, use of trimethylsilyl chloride as an internal standard was attempted. This compound proved to be unreactive under the reaction conditions and was henceforth employed as the standard.

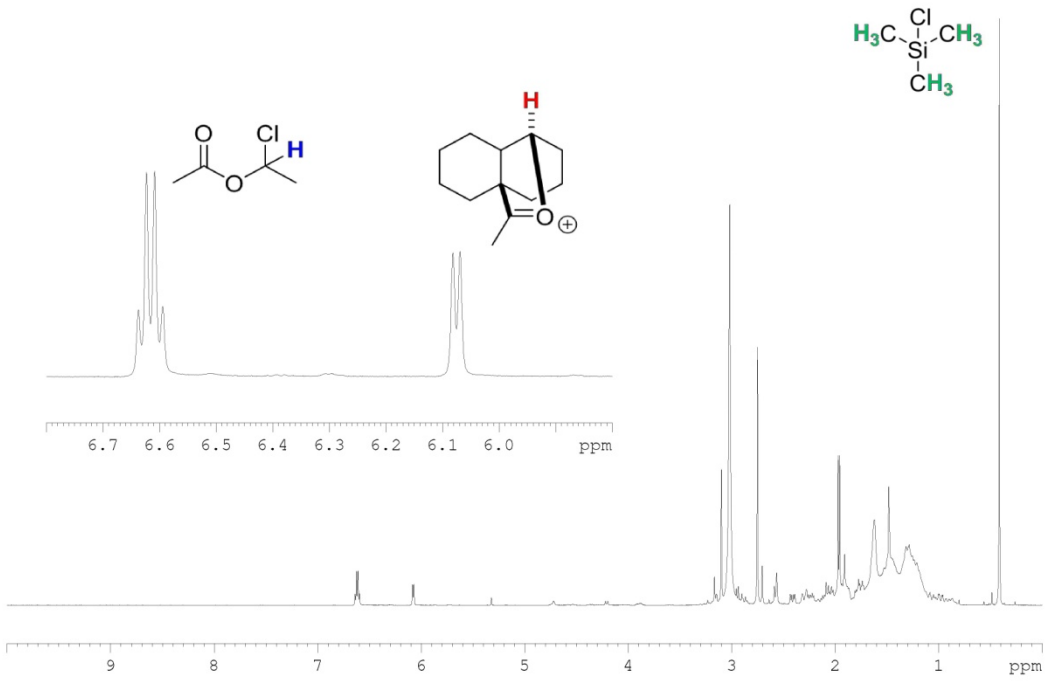


**Figure 10: Proton NMR spectra of Baddeley reaction (*cis*-Decalin) recorded on a Bruker Avance 400 MHz spectrometer at 273 K. Compounds with coloured protons are shown next to their corresponding diagnostic peaks.**

### 2.6.1 Reactivity of cis-Decalin and *trans*-Decalin

It had previously been observed by Santelli *et al.*[122] that *cis*-decalin, **161**, was the reactive isomer in the Baddeley reaction, on the basis that *trans*-decalin, **159**, was recovered unreacted from the reaction mixture when performed on a mixture of both isomers. On performing the reaction on *cis*- and *trans*-decalin independently, it was clear that *trans*-decalin was still reacting, albeit much more slowly. Over a typical five hour reaction time, *cis*-decalin was converted to products in 37% yield and *trans*-decalin just 4.5% yield, the breakdown of which can be seen in Table 7.

| Isomer | Conversion to enol ether, **244** | Conversion to chloroketone, **252** | Total conversion to products |
|---|---|---|---|
| *cis*-decalin, **161** | 27% | 10% | 37% |
| *trans*-decalin, **159** | 0.9% | 3.6% | 4.5% |

**Table 7: Comparison of a five hour Baddeley reaction at 273 K on both *cis*- and *trans*-decalin.**

A typical Baddeley reaction was performed in an NMR tube as previously discussed using both *cis*- and *trans*-decalin as substrates, to track the reaction conversion over time. The results of these experiments are shown in Graph 1 below.

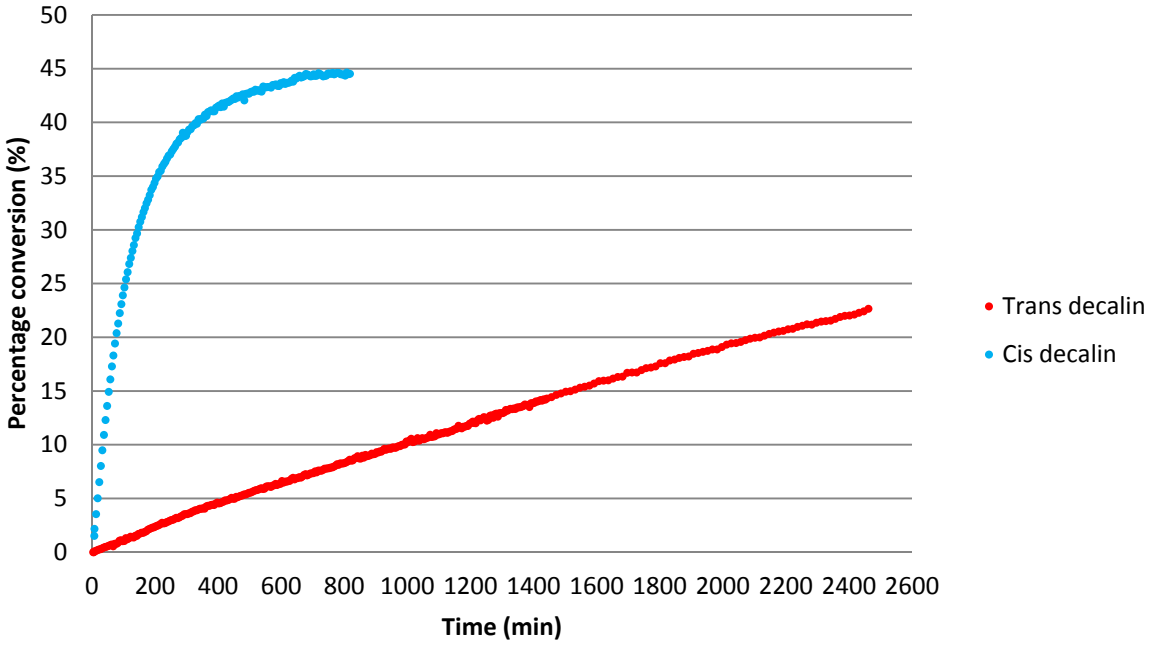


**Graph 1: Plot showing percentage conversion to cationic intermediate, 249, (%) against time (min) for both *cis*- and *trans*-decalin under Baddeley reaction conditions.**

As the reaction of *trans*-decalin proceeds significantly more slowly, only reaching 20% conversion after 35 hours compared with an hour and 15 minutes in the case of *cis*-decalin, the hydride abstraction from the tertiary position must be limiting the rate of reaction.

Once the tertiary hydride has been abstracted, the cation that is subsequently formed will be the same compound derived from either isomer. The mechanism from the tertiary carbocation onwards will be the same, regardless of which isomer was present initially.

Figure 11 (from the computational study performed by Ian Williams and Makoto Sato) shows the difference in energy required to abstract a tertiary hydride from *cis*-decalin ($\Delta G$ = 62 kJ $mol^{-1}$) and *trans*-decalin ($\Delta G$ = 82 kJ $mol^{-1}$). The energies are shown relative to $\Delta^{9,10}$ octalin, **246**, and protonated acetaldehyde.

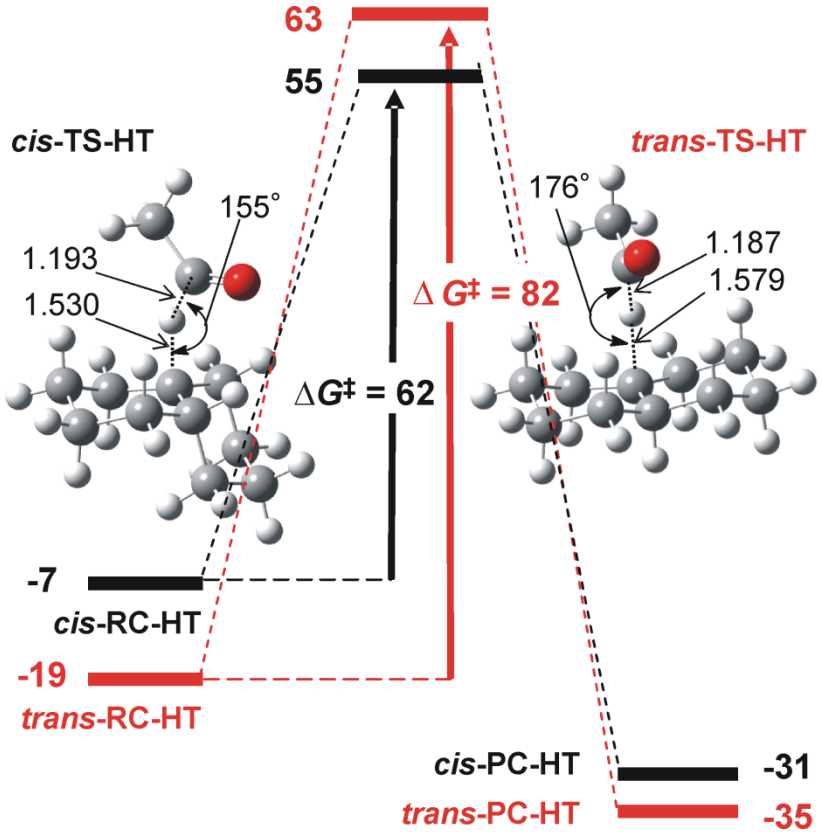


**Figure 11: MP2/cc-pVTZ//MP2/6-31+G* Gibbs energy profiles in PCM $CH_2Cl_2$ for hydride abstraction from *cis*- and *trans*-decalin. Bond lengths are in Å and angles in degrees. Energies are relative to separated $CH_3CHOH^+$ and octalin.**

### 2.6.2 Order of reaction in *cis*-Decalin

In order to investigate the reaction mechanism further, it was desirable to experimentally determine the order of reaction in *cis*-decalin and in the acylating reagent. Equation 1 was used as a starting point to substitute reagents into to give Equation 2, where *k* represents the overall rate constant at a given temperature.

$$Rate = k[A]^a[B]^b[C]^c$$

**(Equation 1)**

$$Rate = k[cis - decalin]^a[AcCl]^b[AlCl_3]^c$$

**(Equation 2)**

As acetyl chloride and aluminium trichloride were pre-mixed prior to the addition of decalin to form the acylating species, it was possible to consider them as a single entity as illustrated in Equation 3.

$$Rate = k[cis - decalin]^a[Acylating\ species]^b$$

**(Equation 3)**

One can use the method of initial rates to determine the order of the reaction in each reagent. This involves keeping the initial concentration of one reagent constant over several experiments where the initial concentration of the second reagent is varied. The initial rate can

then be calculated either by plotting a graph of decreasing concentration of starting material versus time, or increasing concentration of product versus time, and taking the gradient.

This modification of Equation 1 for initial rates can be represented by Equation 4 where $k_a$ is equal to the overall rate constant *k* multiplied by [B], which is now constant. This equation can be rearranged to the style of "y = mx + c" (Equation 5), such that plotting a graph of ln *initial rate* versus ln [A] will give a straight line with the gradient equal to the order of reaction in A (a).

$$Initial\ rate = \ k_a\ [A]^a$$

**(Equation 4)**

$$\ln initial\ rate = \ \ln k_a + \ a \ln[A]$$

**(Equation 5)**

Substituting *cis*-decalin into Equation 5 as the reagent of interest whilst keeping the concentration of the acylating species constant gives Equation 6.

$$\ln initial\ rate = \ \ln k_a + \ a \ln[cis - decalin]$$

**(Equation 6)**

A series of experiments were performed at concentrations outlined in Table 8. The concentration of the acylating species is based on the concentration of acetyl chloride, as the proton NMR shows only one methyl group environment. This indicates all of the acetyl chloride has been transformed into a partially positively charged species, rather than 62.5% being converted to an acylium ion and 37.5% remaining as acetyl chloride. One would expect to see this ratio of products if a 1:1 ionic complex were formed between the acylium cation and tetrachloroaluminate anion, as there is 62.5% aluminium trichloride added to the reaction mixture relative to 100% acetyl chloride.

| Experiment | *cis*-decalin (eq.) | [*cis*-decalin] (M) | AcCl:$AlCl_3$ (eq.) | [Acylating species] (M) |
|---|---|---|---|---|
| 1 | 0.40 | 0.5167 | 2.40:1.50 | 3.0999 |
| 2 | 0.60 | 0.7750 | 2.40:1.50 | 3.0999 |
| 3 | 0.80 | 1.0333 | 2.40:1.50 | 3.0999 |
| 4 | 1.00 | 1.2915 | 2.40:1.50 | 3.0999 |
| 5 | 1.40 | 1.8078 | 2.40:1.50 | 3.0999 |
| 6 | 1.60 | 2.0665 | 2.40:1.50 | 3.0999 |

**Table 8: Baddeley NMR experiments performed varying the concentration of *cis*-decalin, where equivalents of *cis*-decalin given are relative to the 1.00 equivalents of *cis*-decalin that would be present in the typical Baddeley reaction.**

Graph 2 shows the increasing concentration of the tricyclic cationic intermediate over 300 minutes with various concentrations of *cis*-decalin. As the rate-limiting step of the reaction was deduced to be the hydride abstraction (based on the difference in reactivity between *cis*- and *trans*-decalin), the rate limiting step in the formation of 1-chloroethyl acetate was also believed to be the hydride abstraction. As such, given it was also possible to follow the

formation of 1-chloroethyl acetate, **253** (Graph 3), these results could be used to calculate the order of this side-reaction in *cis*-decalin also.

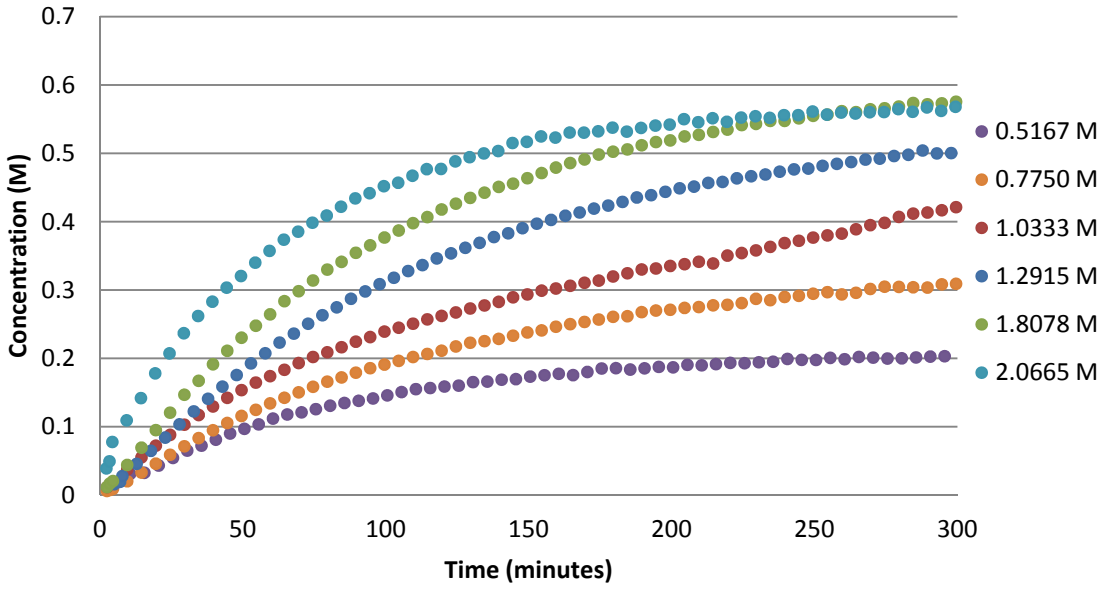


**Graph 2: Concentration of the cationic intermediate, 249, (M) versus time (minutes) with various concentration of *cis*-decalin over 300 minutes.**

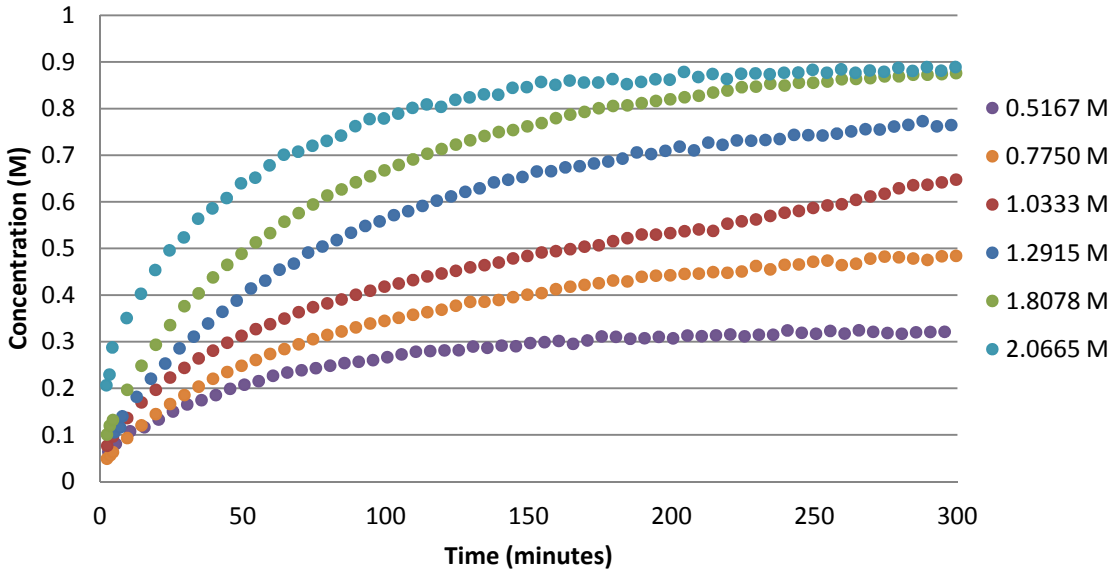


**Graph 3: Concentration of 1-chloroethyl acetate, 253, (M) versus time (minutes) with various concentration of *cis*-decalin over 300 minutes.**

Viewing the data points with less than 15% conversion to cationic intermediate, trendlines can be drawn that represent the initial rate of the reaction. 15% was selected in order to represent low conversion, but still use a reasonable number of data points. This data are shown with lines of best fit in Graph 4.

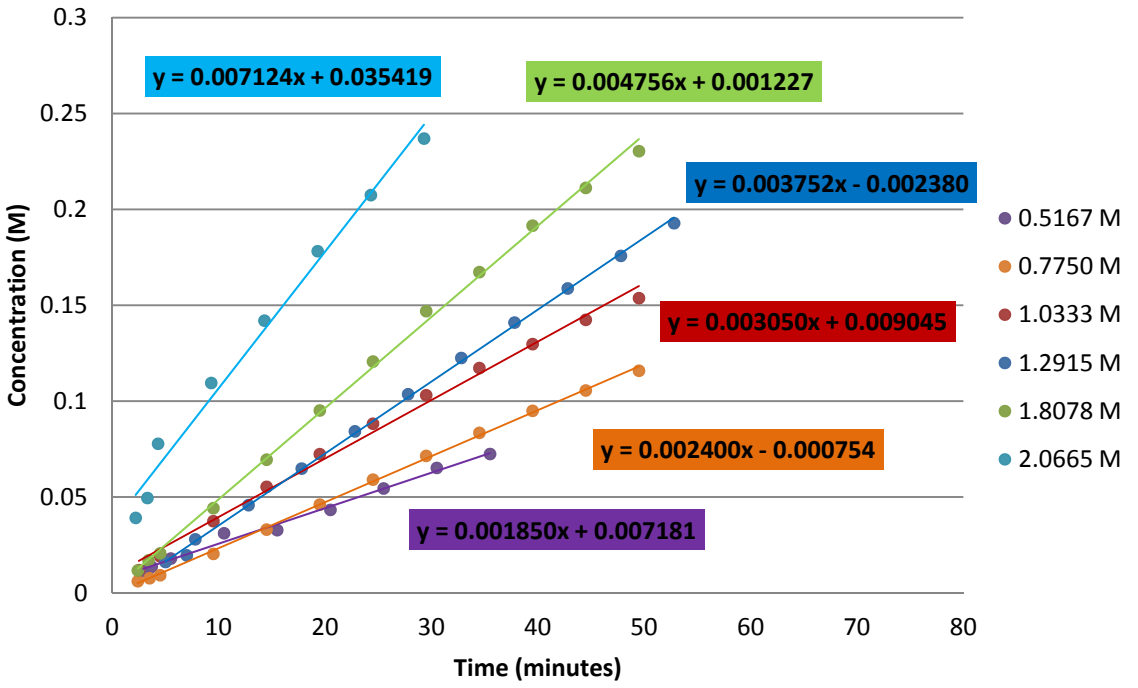


**Graph 4: Concentration of cationic intermediate, 249, (M) versus time (minutes) with various concentrations of *cis*-decalin illustrating initial rates as gradients of each trendline.**

The natural log of each of the initial rates of reaction was taken and plotted against the natural log of each initial concentration of *cis*-decalin; the results of this are shown in Graph 5. The gradient of this trendline represents the order of the reaction with respect to *cis*-decalin; it is first order within experimental error.

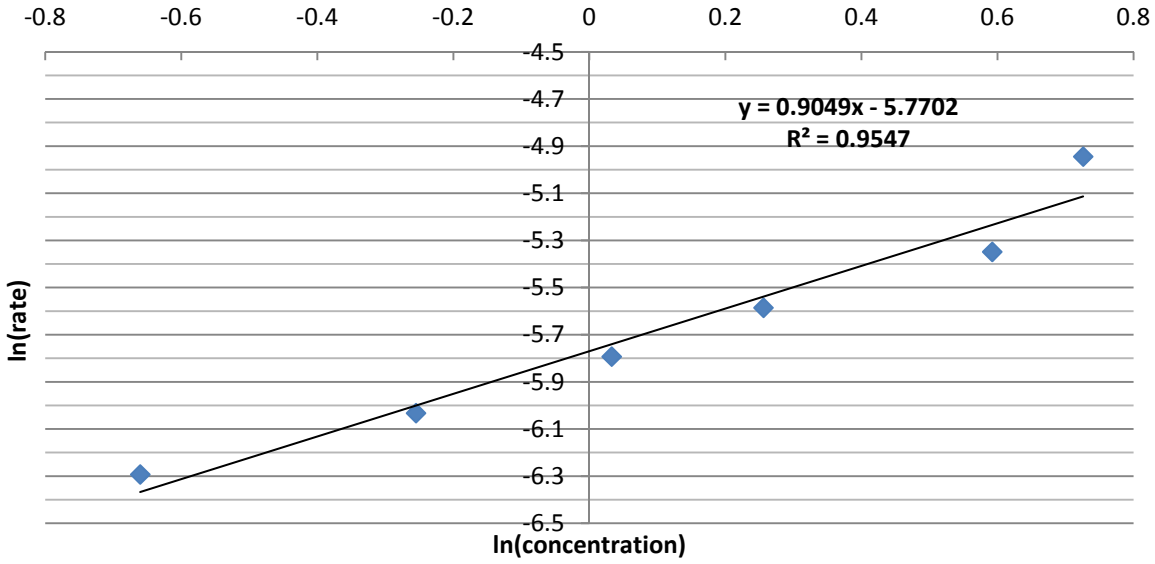


**Graph 5: Plot of ln(initial rate) versus ln(initial concentration) with various initial concentrations of *cis*-decalin based on the formation of the tricyclic cationic intermediate, 249.**

The conversion to 1-chloroethyl acetate was examined in a similar manner, although the reaction proceeded faster and in order to use a reasonable number of data points, conversion

under 20% was selected to represent initial rate. The initial rates are seen as gradients on the trendlines in Graph 6.

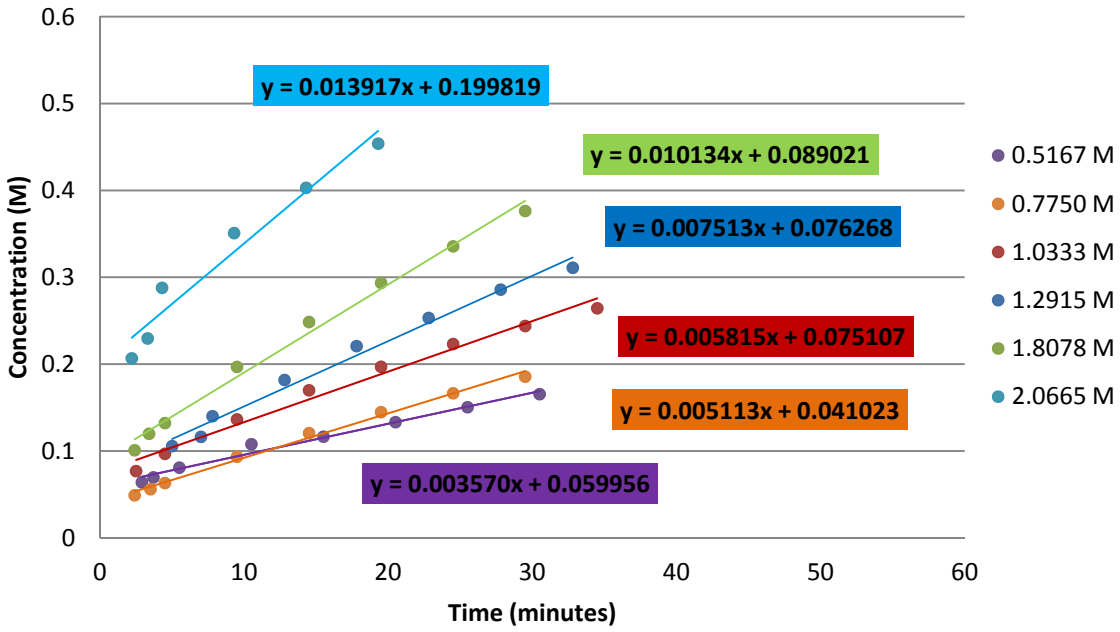


**Graph 6: Concentration of 1-chloroethyl acetate, 253, (M) versus time (minutes) with various concentrations of *cis*-decalin illustrating initial rates as gradients of each trendline.**

The natural log of each initial rate was calculated and plotted against the natural log of the initial concentration of *cis*-decalin, in the same manner as for the cationic intermediate. Graph 7 shows the gradient of the trendline to also be one within experimental error, indicating that the formation of 1-chloroethyl acetate is also first order in *cis*-decalin.

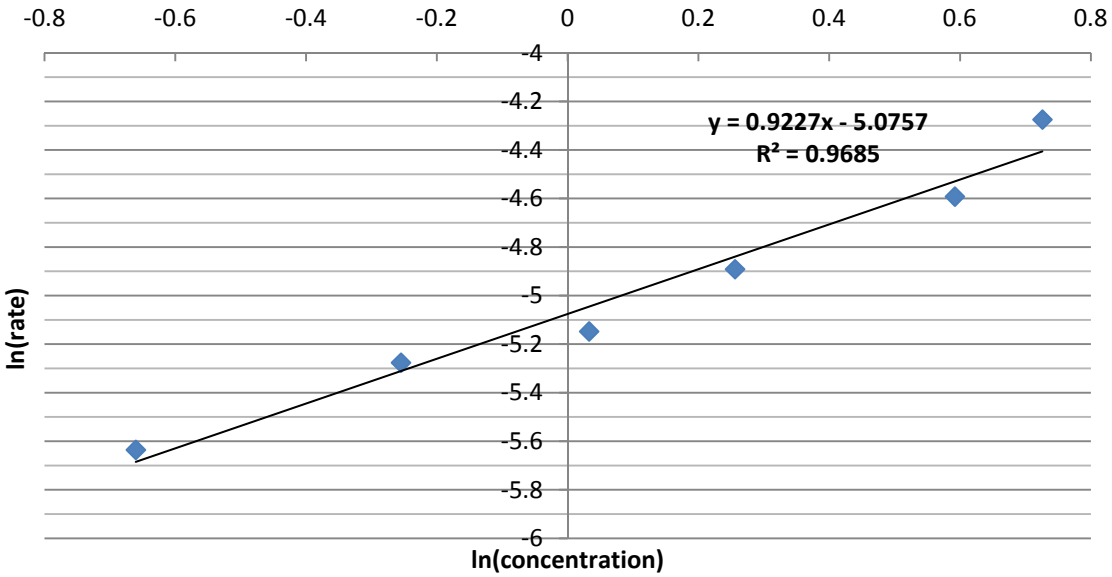


**Graph 7: Plot of ln(initial rate) versus ln(initial concentration) with various initial concentrations of *cis*-decalin based on the formation of the 1-chloroethyl acetate, 253.**

### 2.6.3 Order of reaction in acylating reagent

With the order of reaction in *cis*-decalin in hand, interest turned towards the order of reaction in the acylating reagent. Substituting the acylating species into Equation 5 to give Equation 7, a series of similar reactions were planned to those used for calculating the order of the reaction in *cis*-decalin.

$$\ln initial\ rate = \ln k_b + b \ln[Acylating\ species]$$

**(Equation 7)**

Table 9 outlines the experiments undertaken. As in previous experiments, the ratio of aluminium trichloride to acetyl chloride was kept at a constant 2.4:1.5, so that the acylating species formed in the first instance is consistent across all reactions.

| Experiment | *cis*-decalin (eq.) | [*cis*-decalin] (M) | AcCl:$AlCl_3$ (eq.) | [Acylating species] (M) |
|---|---|---|---|---|
| 1 | 1.00 | 1.2915 | 0.80:0.50 | 1.0332 |
| 2 | 1.00 | 1.2915 | 1.20:0.75 | 1.5498 |
| 3 | 1.00 | 1.2915 | 1.60:1.00 | 2.0665 |
| 4 | 1.00 | 1.2915 | 2.00:1.25 | 2.6559 |
| 5 | 1.00 | 1.2915 | 2.40:1.50 | 3.0999 |

**Table 9: Baddeley NMR experiments performed with various concentrations of acetyl chloride and aluminium trichloride.**

In the experiments varying *cis*-decalin, both higher and lower concentrations than the typical reaction (1.2915 M) were investigated. Attempts to increase the concentration of acylating reagent above the concentration used in the typical reaction (3.0999 M) proved implausible due to precipitation out of solution at 273 K. Unfortunately, this meant only concentrations below 3.0999 M could be studied.

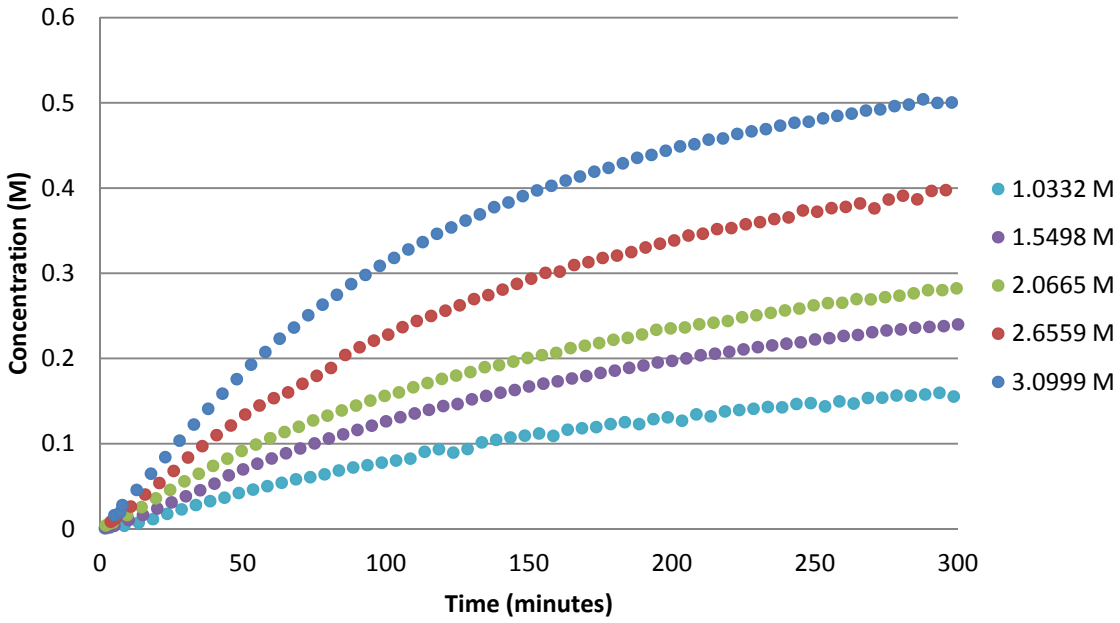


**Graph 8: Concentration of the cationic intermediate, 249 (M) versus time (minutes) with various concentration of acylating reagent over 300 minutes**

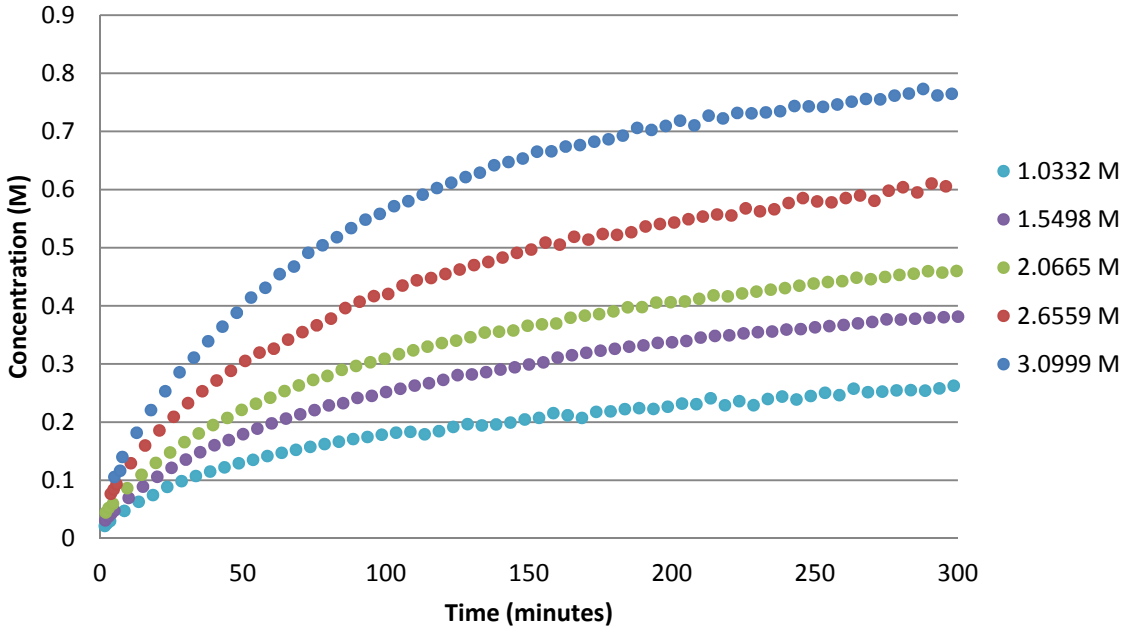


**Graph 9: Concentration of 1-chloroethyl acetate, 253 (M) versus time (minutes) with various concentration of acylating reagent over 300 minutes**

Graph 8 and Graph 9 show the growth in concentration of cationic intermediate and 1-chlorethyl acetate, respectively, over the first 300 minutes of the reaction.

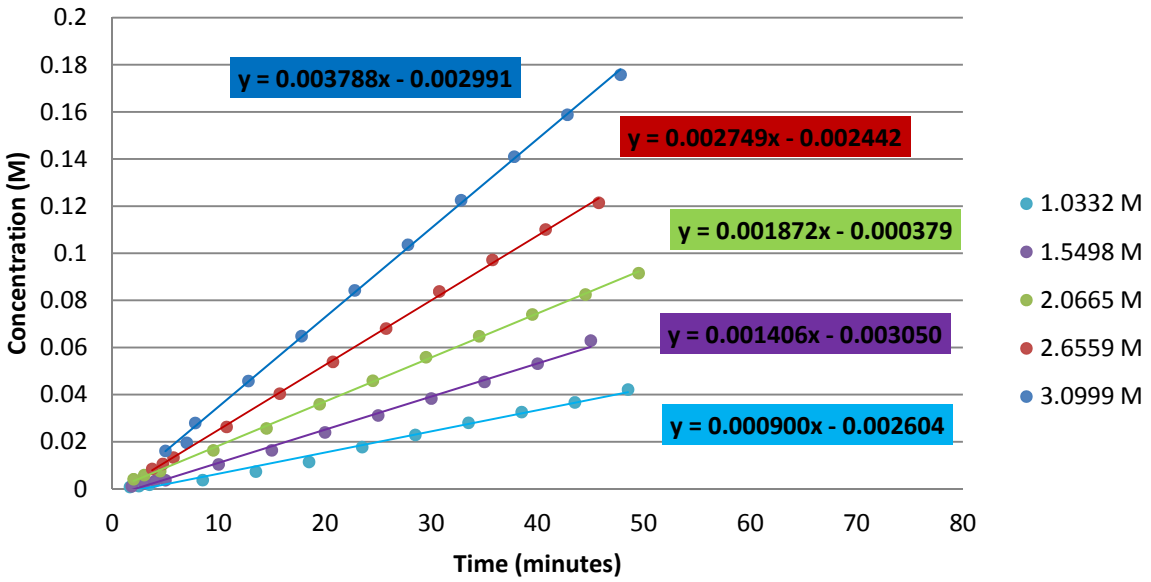


**Graph 10: Concentration of cationic intermediate (M) versus time (minutes) with various concentrations of acylating reagent illustrating initial rates as gradients of each trendline, 249.**

Initial rates are represented by the gradients of the trendlines in Graph 10. In this instance, as the starting concentration of *cis*-decalin was the same in each experiment, percentage conversion could not be used to establish how many data points to take. Instead data points over the first 50 minutes were used, allowing for a reasonable number of data points and a reasonable approximation to initial rates.

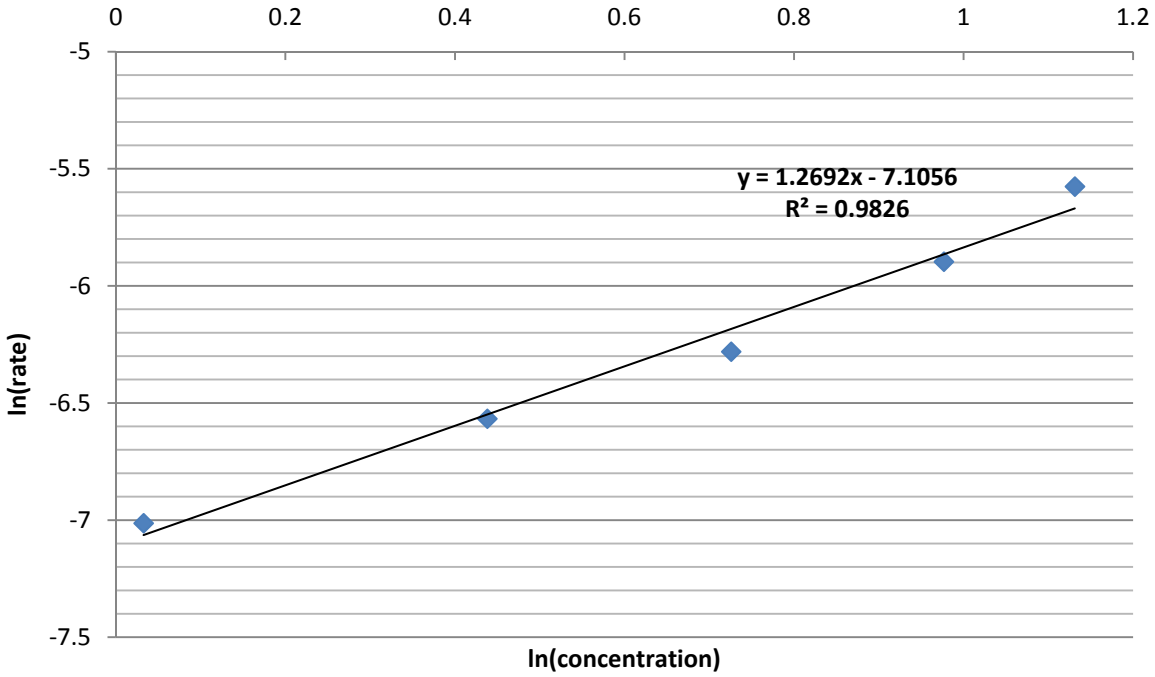


**Graph 11: Plot of ln(initial rate) versus ln(initial concentration) with various initial concentrations of acylating reagent based on the formation of the tricyclic cationic intermediate, 249.**

The initial rates calculated in Graph 10 were used to plot Graph 11, which shows the natural log of each of these initial rates against the natural log of the initial concentration of acylating species. The gradient of this trendline is 1.27 ± 0.10 which indicates that the order of the formation of cationic intermediate in acylating species is greater than one. The experimental error indicates that the order of reaction in acylating species is not likely to be the integer preceding or following (one or two) and is in fact a fractional order of reaction.

From this, it can be inferred that in the reaction with *cis*-decalin, the hydride abstraction from *cis*-decalin is not the only rate limiting step. If this were the case, the order of reaction in both *cis*-decalin and acylating species should be one, as only one molecule of each is involved in the step. Finding an order of more than one in the acylating reagent indicates another step in the mechanism that involves a second equivalent of acylating species is at least partially rate limiting.

Due to the large difference in energy required to remove a hydride from *cis*-decalin compared with *trans*-decalin (Figure 11), it is unlikely that this second partially rate limiting step would affect the rate in reactions involving *trans*-decalin.

The order of reaction in acylating species in the reaction forming 1-chloroethyl acetate was also investigated. Graph 12 shows the initial rates as gradients of the trendlines for the first 30 minutes of the reaction.

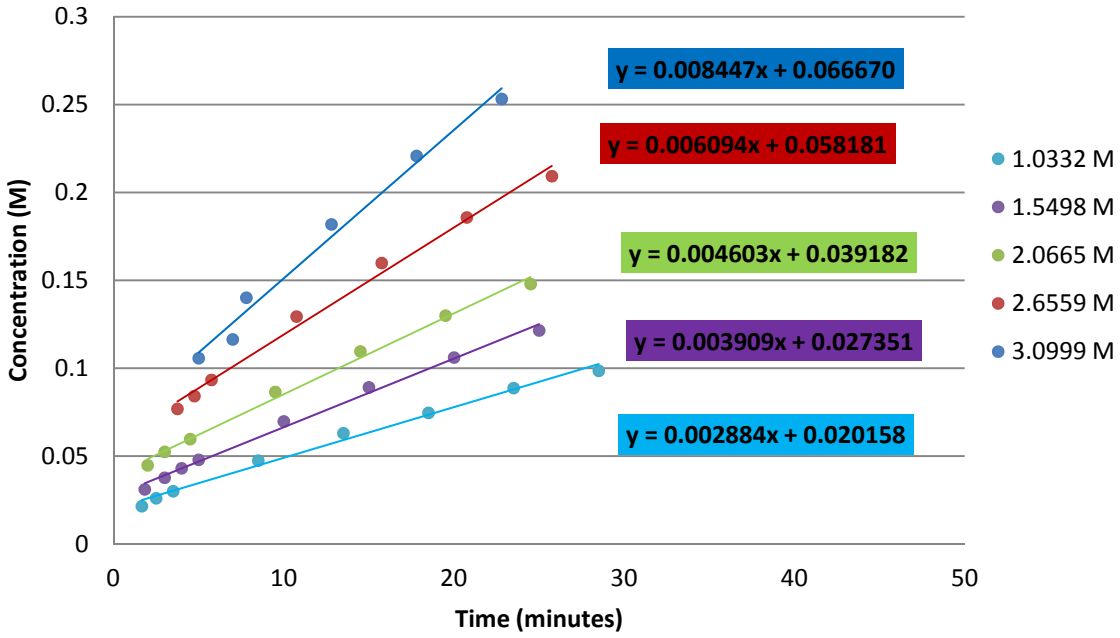


**Graph 12: Concentration of 1-chloroethyl acetate, 253 (M) versus time (minutes) with various concentrations of acylating reagent illustrating initial rates as gradients of each trendline.**

The data from Graph 12 was inserted into Equation 7 in order to plot Graph 13. From this graph, the gradient of the trendline was 0.92 ± 0.12, showing the order of this reaction in acylating reagent is one within experimental error.

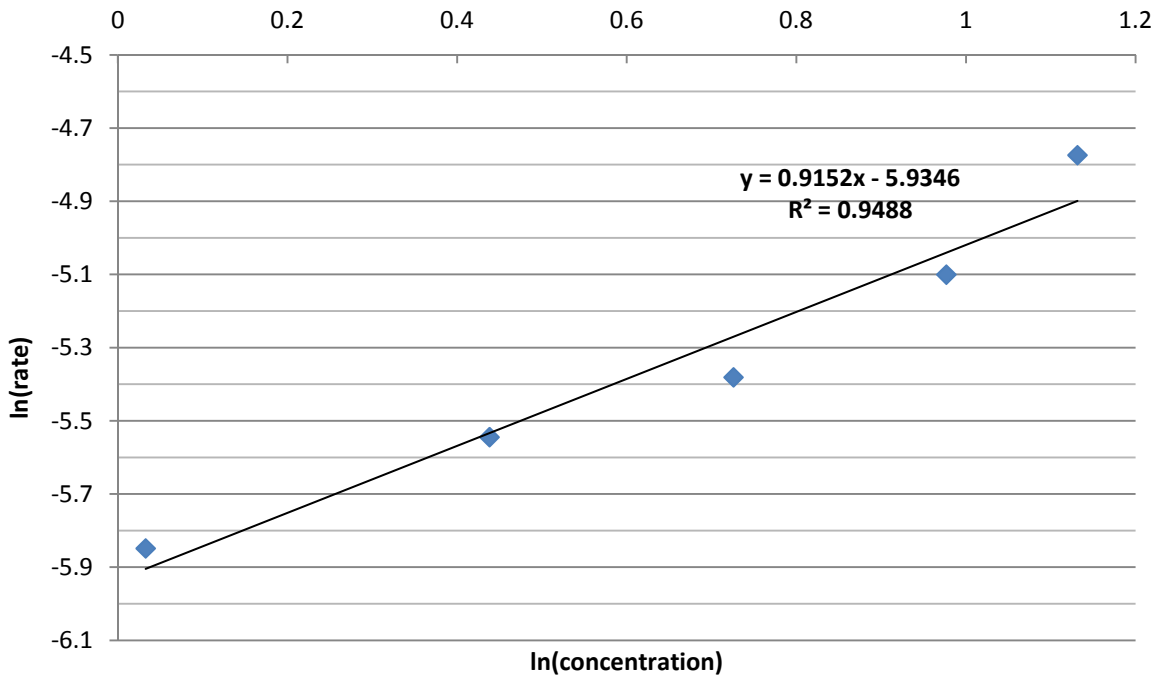


**Graph 13: Plot of ln(initial rate) versus ln(initial concentration) with varying initial concentrations of acylating reagent based on the formation of 1-chloroethyl acetate, 253.**

This gives us further confirmation that the fractional order of reaction in acylating reagent found for the formation of cationic intermediate, approximately 1.3, is not solely related to the hydride abstraction step.

As the reaction of acetaldehyde and acetyl chloride in the presence of aluminium trichloride is very fast – an immediate colour change is observed on addition of acetaldehyde to the pre-formed acylating reagent – it is reasonable to conclude that the abstraction of a hydride from decalin is the only limiting step in the formation of 1-chloroethyl acetate under the Baddeley conditions.

Therefore, if the reaction to form 1-chloroethyl acetate is first order in *cis*-decalin and first order in acylating reagent, the hydride abstraction step involves one molecule of *cis*-decalin and one molecule of acylating reagent, as one would expect from the proposed mechanism.

The other partially rate limiting step is one which involves another equivalent of acylating species, specifically, nucleophilic attack by the double bond of $\Delta^{9,10}$ octalin. As seen previously in Figure 9, computational modelling by Ian Williams and Makoto Sato shows that although the difference in Gibbs energy required for hydride abstraction from *cis*-decalin is most significant (62 kJ $mol^{-1}$), the lowest energy route for cyclisation (56 kJ $mol^{-1}$) is higher than the Gibbs energy needed to recede back to *cis*-decalin, which would indicate it is possible for both of these steps of the mechanism to impact on the rate of reaction.

It should also be noted that the computational modelling indicates a concerted mechanism is more likely than a stepwise mechanism, with regards to the [1,2]-hydride shift and cyclisation steps. This likely mechanism and the Gibbs energies calculated for this step are shown in Figure 12.

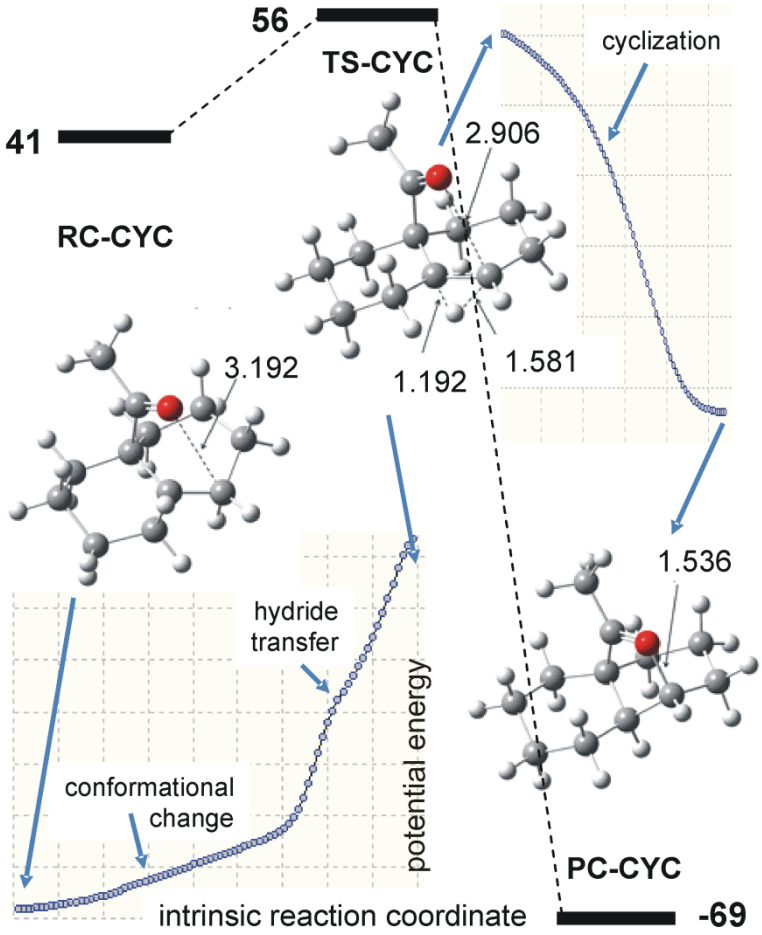


**Figure 12: Computational modelling (MP2/cc-pVTZ//MP2/6-31+G* Gibbs energy profiles in PCM $CH_2Cl_2$) by Ian Williams and Makoto Sato indicating the concerted mechanism of the [1,2]-hydride shift and cyclisation steps.**

It should also be considered that decalin recovered from the Baddley reaction after 5 hours was converted fully to *trans*-decalin, where the initial substrate was either *cis*-decalin or a commercially available mixture of the two decalins. This can be explained by considering the Gibbs energy barrier for the reverse reaction from $\Delta^{9,10}$ octalin to *trans*-decalin is only 62 $kJmol^{-1}$, not very dissimilar to the energy barriers from $\Delta^{9,10}$ octalin to *cis*-decalin or the tricyclic cationic intermediate. However, once converted to the more stable *trans*-decalin, the energy barrier needing to be conquered is substantially more, approximately 82 $kJmol^{-1}$.

## 2.7 Conclusions

It has been shown from these investigations that the mechanism we proposed for the Baddeley reaction of decalin is in line with the results obtained. The steps outlined in red in Scheme 67 have been studied experimentally;

- The presence of 1-chlorethyl acetate, **253**, showing abstraction of the hydride to form acetaldehyde
- Performing the reaction on the tetrasubstituted alkene intermediate, **246**, to yield the same products
- Observing the cationic tricyclic intermediate, **249**, in the proton and carbon-13 NMR spectra of the reaction mixture before work-up

The steps outlined in green show work studied using kinetics;

- The rate of reaction of *cis*-decalin, **161**, is much faster than *trans*-decalin, **159**.
- The rate limiting step is hydride abstraction in *trans*-decalin and hydride abstraction and a later step involving a second equivalent of acylium cation in *cis*-decalin

Computational work shown in blue;

- The cyclisation and [1,2]-hydride shift occurring in a concerted manner is likely
- The partial rate-limiting step in the reaction of *cis*-decalin could be due to formation of the tricyclic intermediate, **249**, from the alkene, **246**.

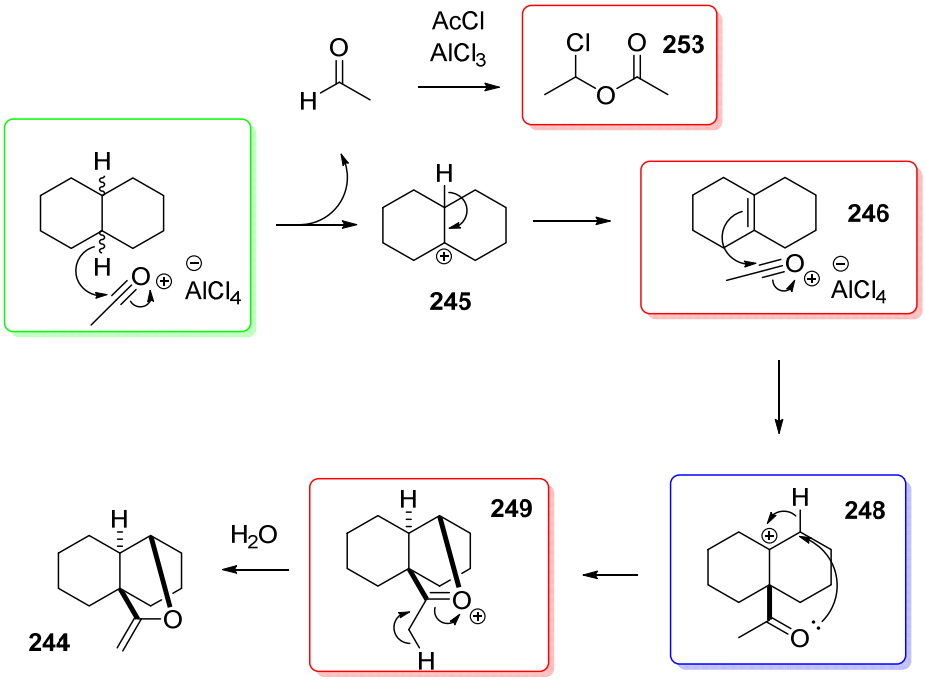


**Scheme 67: Mechanism for the Baddeley reaction with steps highlighted in red (experimental evidence), green (kinetic evidence) and blue (computational evidence).**

# Extending the Substrate Scope: Acylation of Saturated Hydrocarbons with Aluminium Trichloride

For the published work, please see Appendix 3. Lyall, C. L.; Uosis Martin, M.; Lowe, J. P.; Mahon, M. F.; Pantoş, G. D.; Lewis, S. E. *Org. Biomol. Chem.* **2013**, 11, 1157-1165.

## 3.1 Introduction

### 3.1.1 Use of the Baddeley Methodology in Synthesis

Baddeley showed multiple examples of reactions from the enol ether, **244**, synthesised from decalin, yielding a range of products that have potential uses in synthesis of more complex molecules (Scheme 68).

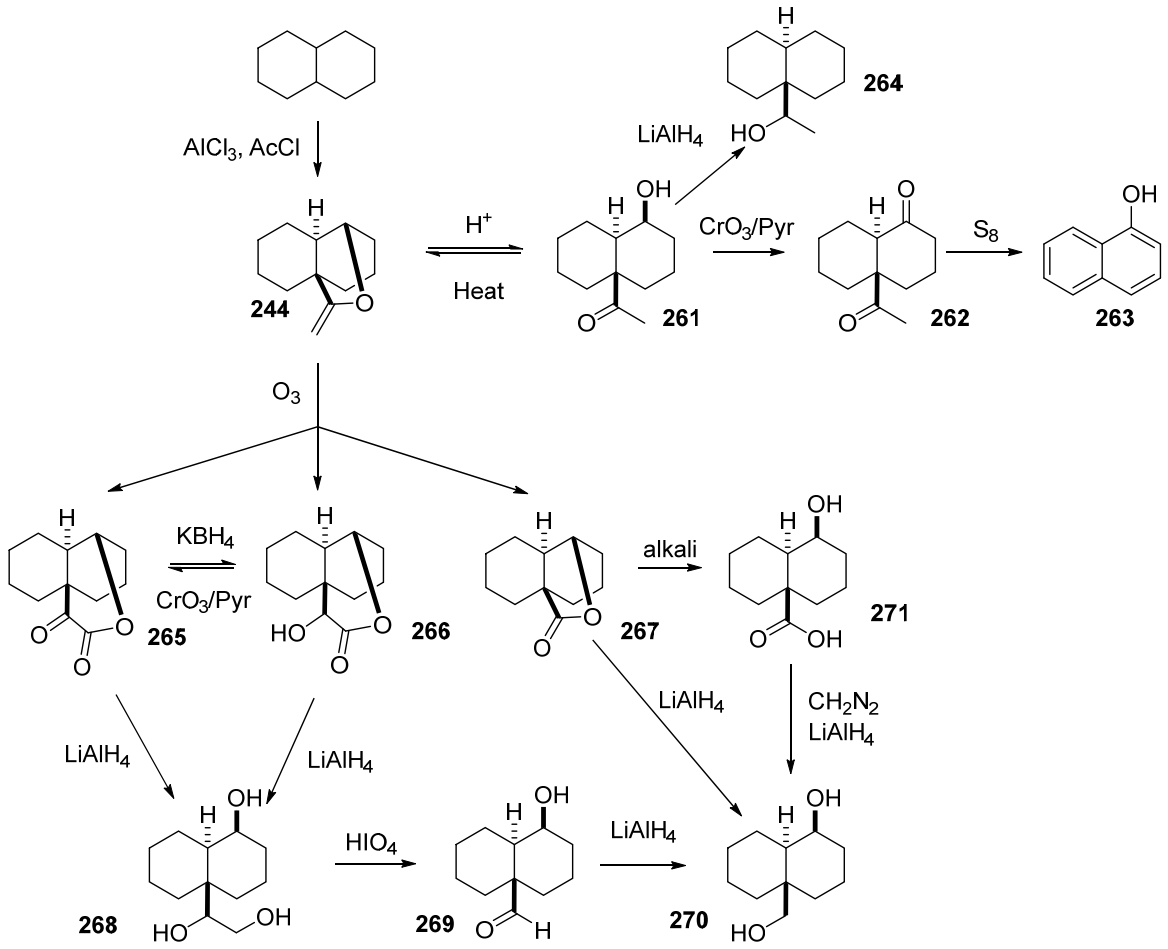


**Scheme 68: Reactions of the enol ether, 244, as shown by Baddeley**

In 2011, within the Lewis group,[146] the enol ether was used in synthesis in a model system looking at the synthesis of Complanadine A, **272**, seen in Figure 13.

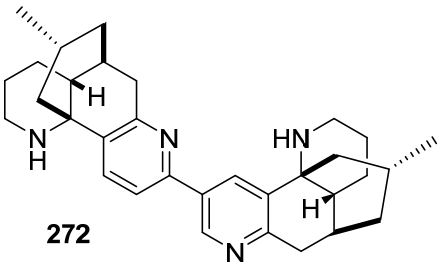


272

**Figure 13: Structure of Complanadine A, 272.**

The beginnings of this model system are shown in Scheme 69. Initial ring opening of the cyclic enol ether using sulfuric acid to give the hydroxyketone, **261**, is followed by formation of the hydrazone, **273**. This is the first step in the Shapiro reaction, which is followed by treatment with butyl lithium to form the alkenyl lithium and then protonation to give the alkene, **274**.

At this point the alcohol moiety undergoes treatment with oxalyl chloride and dimethylsulfoxide to form the ketone, **275**, (Swern oxidation), before the ketone formed is converted to the alkene via a Wittig reaction. This gave the authors the desired unsaturated hydrocarbon, **276**.

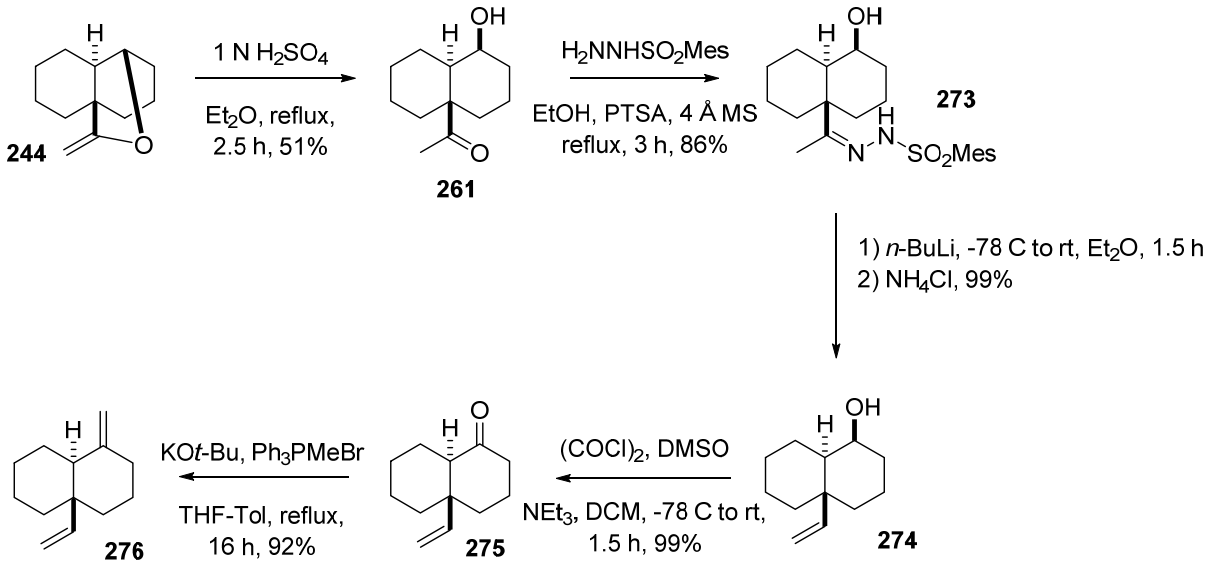


**Scheme 69: Use of the enol ether in synthesis; approaches towards to synthesis of Complanadine A, 272.**[146]

Further to this work, in 2013, the unsaturated hydrocarbon, **276**, formed from the enol ether in five steps in Scheme 69 was used to extend the model system further. As shown in Scheme 70,[147] a selective hydroboration / oxidation through to the mono-alcohol, **277**, in 85% yield over two steps. Another Swern oxidation gave the aldehyde, **278**, in 87% yield.

Reaction of the aldehyde, **278**, with an oxazole nucleophile gave a 1:1 mixture of diastereomers in 53% yield, which could then be subjected to microwave heating in the presence of excess DBN to form several products from a Kondrat'eva oxazole-olefin cycloaddition, giving the authors proof of concept for future synthesis of Complanadine A.

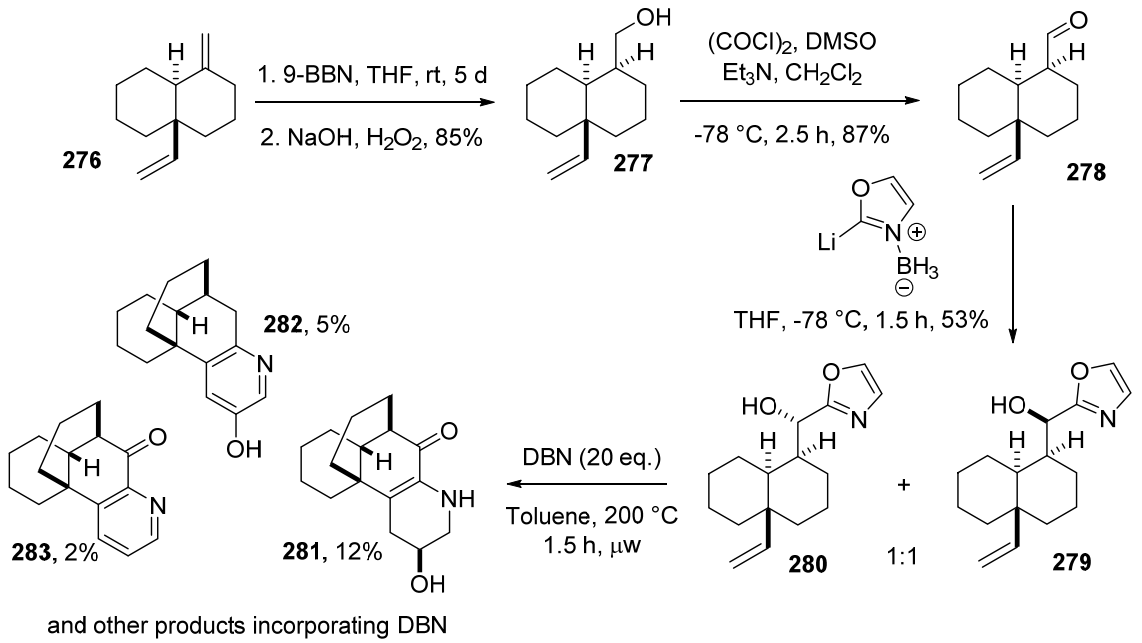


**Scheme 70: Use of the enol ether in synthesis; approaches towards to synthesis of Complanadine A, 272.**[147]

### 3.1.2 Previous Extensions of Baddeley's Methodology

Baddeley's original work has been expanded on, in the acylation of other bicyclic fused-ring saturated hydrocarbons, in particular hydrindane.[115,123] Rasburn (who had previously worked with Baddeley) and coworkers showed a variety of acylated products could be formed from hydrindane, as seen in Scheme 71.

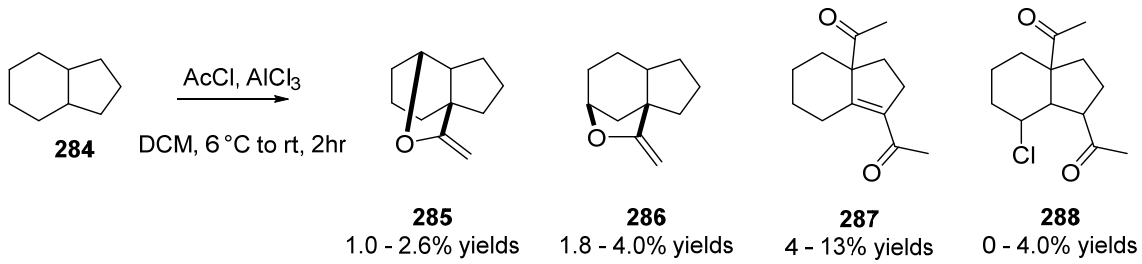


**Scheme 71: Reaction of hydrindane, 284, with Friedel-Crafts acylating reagents; relative stereochemistries were not established.**[123]

It is important to note however, that the ratio of acylating species to decalin used in Baddeley's optimised conditions was not maintained in the hydrindane reaction; neither was the ratio of acetyl chloride to aluminium trichloride.

Hydrindane used was a commercial mixture of *cis*- and *trans*-hydrindane, and unreacted hydrindane was recovered enriched in the *trans* isomer.

| | Decalin reaction | Hydrindane reaction |
|---|---|---|
| **AcCl equivalents** | 2.4 | 3.5 |
| **$AlCl_3$ equivalents** | 1.5 | 2.5 |
| **Reaction time** | 5 h | 80 – 130 min |
| **Reaction temperature** | 0 – 10 °C | 6 – 18 °C |

**Table 10: Differences in reaction conditions between Baddeley's decalin reaction and reaction of hydrindane**

Having established in the previous chapter how sensitive the reaction yields are to ratios of acylating reagent, in addition to the fact that Baddeley's work at room temperature that showed a much wider product variation, it should not come as a surprise that this work yielded multiple products.

Table 10 shows the key differences in reaction conditions between Baddeley's work and Rasburn's hydrindane reaction. In particular, it should be noted that the use of 3.5 equivalents of acetyl chloride could well be accountable for the diacylated products observed.

Scheme 72 shows some mechanistic rationale for the formation of the four products described in Rasburn's work; mechanisms are outlined in the article, however, not all steps depicted here are described in the original work.

The formation of both enol ethers seen indicate that it may be similarly likely in this instance to form a tetrasubstituted alkene intermediate (**293**, red arrows) and a trisubstituted alkene intermediate (**290**, blue arrows).

The possible mechanism shown for the formation of the enol ether, **286**, shown in blue involves formation of a secondary cation, **291,** in preference to a tertiary cation, which appears counter-intuitive; alternatively, the enol ether, **286**, outlined in blue could be formed via a tetrasubstituted intermediate, **293**, and a [1,4]-hydride shift rather than the [1,2]-hydride shift that forms the red enol ether, **285**. Without further mechanistic investigation in the form of isotopic labelling or computational modelling, it is not completely clear which may be occurring.

Overall, no other fused-ring or linked-ring saturated hydrocarbons had been investigated with the use of Friedel–Crafts reagents. This chapter identifies some key structures to which the Baddeley reaction could be applied, and the results of these reactions.

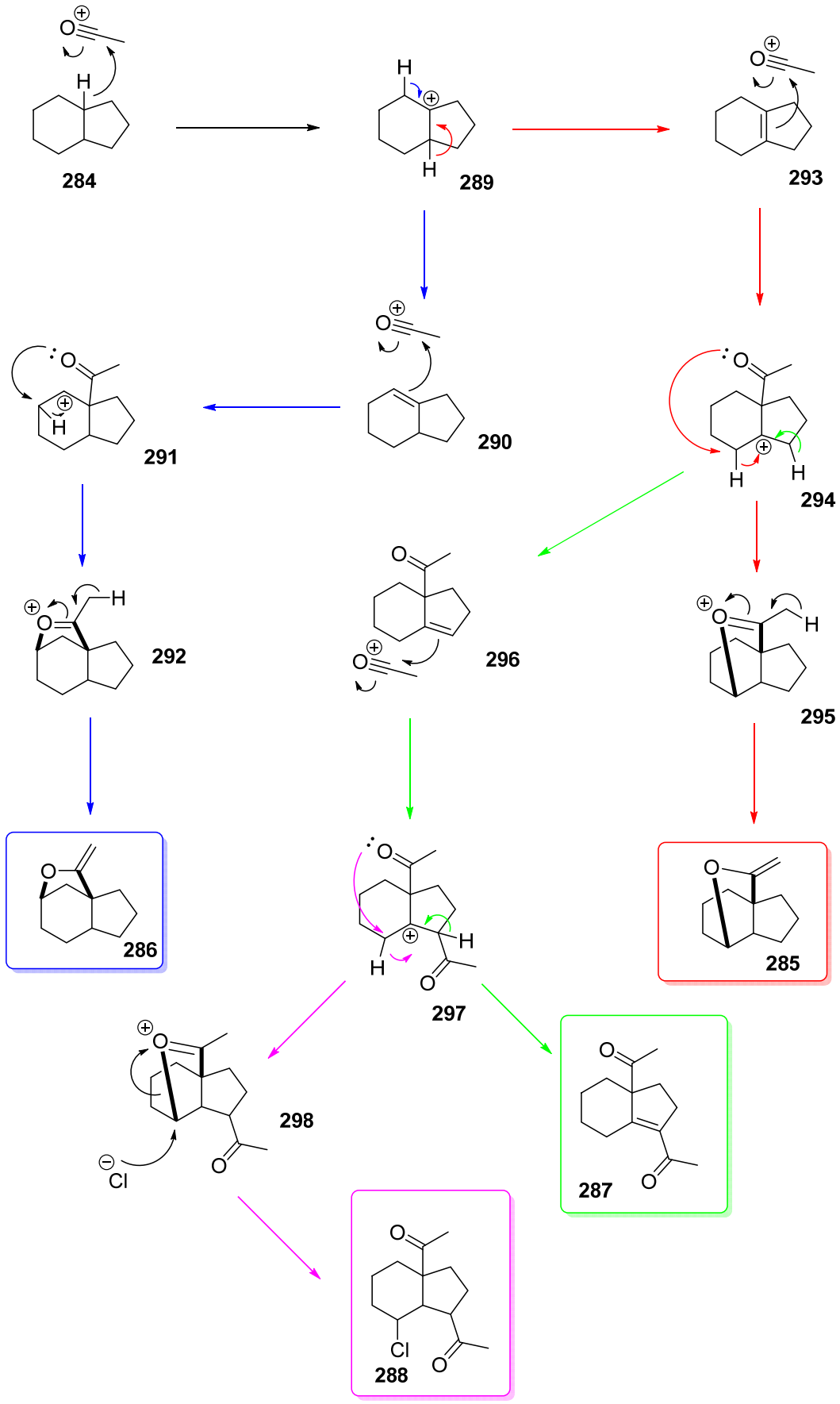


**Scheme 72: Possible mechanistic rationale for formation of enol ethers and diacylated compounds from hydrindane.**

## 3.2 Bicyclohexyl

### 3.2.1 Reaction with Acetyl Chloride and Aluminium Trichloride

Bicyclohexyl was sourced from Tokyo Chemical Industry (TCI); it is a relatively inexpensive hydrocarbon due to its formation from the reduction of readily available biphenyl. Bicyclohexyl was selected as a saturated hydrocarbon for study, due to its two adjacent tertiary carbons, with all other carbon centres being secondary.

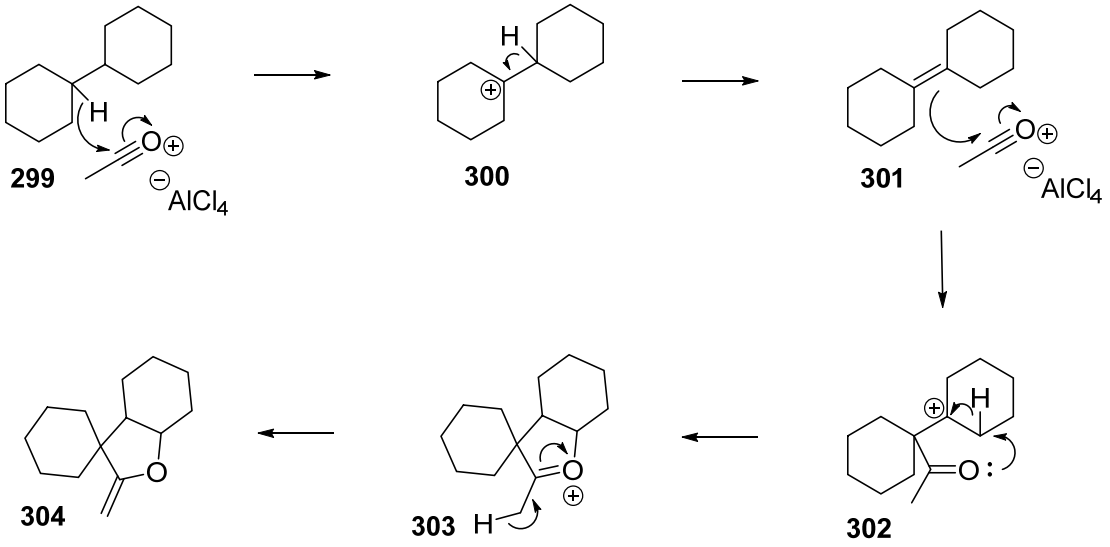


**Scheme 73: Postulated mechanism for Baddeley reaction of bicyclohexyl, 299.**

It was envisaged that a reaction would occur whereby initial hydride abstraction from one of the equivalent tertiary centres would occur, followed by deprotonation at the other tertiary position, leading to a tetrasubstituted alkene. Following this, one could predict that this alkene could attack a molecule of acylating reagent, leading to an intermediate where the cationic charge was at the remaining tertiary position. Subsequently, this acylated carbocation could undergo an intramolecular cyclisation, analogous to that seen with decalin. Attack of the oxygen lone pair onto the secondary carbon adjacent to the cationic charge could occur in conjunction with a [1,2]-hydride shift from the secondary carbon in question onto the positively charged tertiary position. This would give a tricyclic cationic intermediate analogous with that seen in the Baddeley reaction of decalin, which could be deprotonated to give the enol ether product via aqueous work-up (Scheme 73).

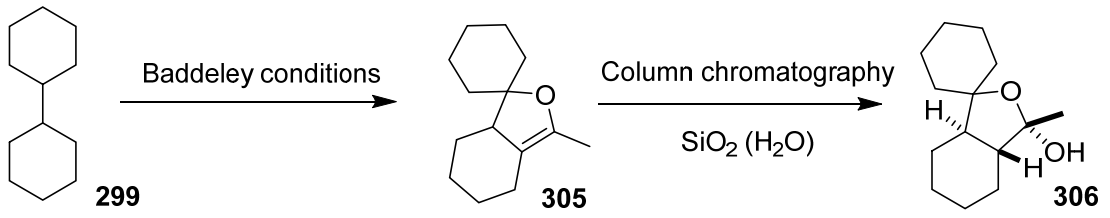


**Scheme 74: Actual enol ether product, 305, formed under Baddeley conditions with bicyclohexyl and hydrate, 306, formed via purification techniques.**

Baddeley's optimised conditions were used for the reaction and the preliminary results were disclosed in the author's previous Masters' thesis. Results of this work showed that a different product was formed to that postulated, seen in Scheme 74.

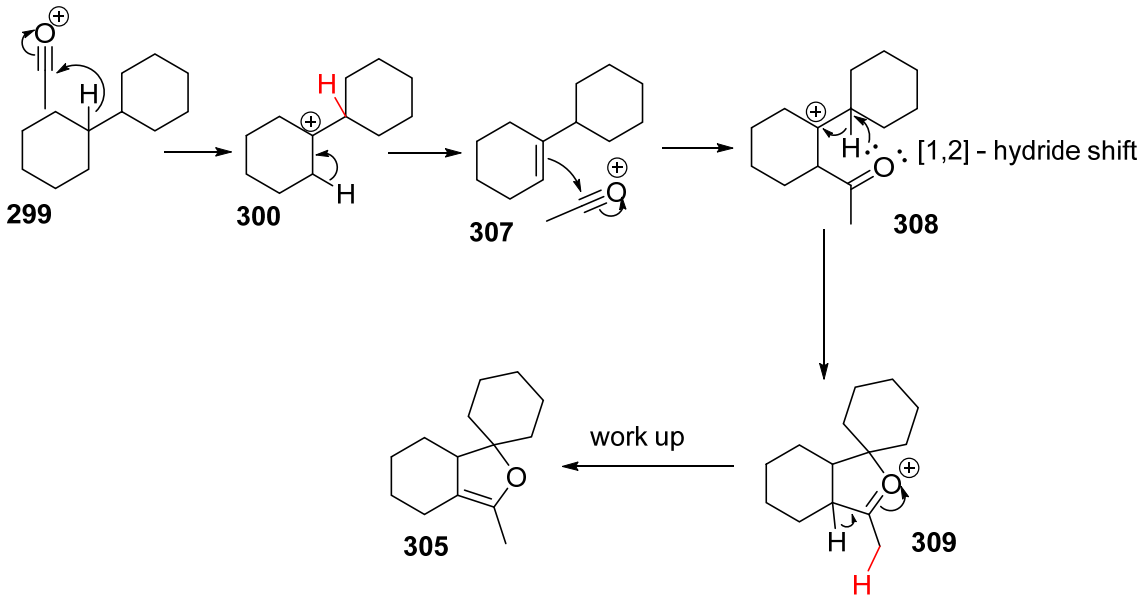


**Scheme 75: Mechanism proposed for the Baddeley reaction of bicyclohexyl through to the isolated product, 305.**

The mechanism for formation of this product is seen in Scheme 75, where the protons highlighted in red were those that would have been lost if the mechanism were analogous to the mechanism for the Baddeley reaction of decalin. This work was expanded in the current study, as detailed in the following sections.

### 3.2.2 Differences in the Mechanism for Bicylohexyl vs. Decalin

The two key differences between the expected mechanism (analogous to the decalin mechanism) and the actual mechanism noted in the Masters' work, were:

- Formation of a tri-subsituted alkene intermediate, **307**, rather than a tetra-substituted alkene intermediate, **301**, in the second step of the mechanism; and
- Loss of a proton from the adjacent tertiary site to form the final enol ether during work-up, rather than loss from the adjacent primary site.

The second of the differences is easier to explain than the first. The increased stability of a tetrasubstituted alkene over a distubstituted alkene as the final product would be expected for products formed under thermodynamic control, but it seems likely this product is formed under kinetic conditions – that the final deprotonation occurs on work-up and is irreversible. In this case, it is likely that the transition state is product-like; the energy barrier for a product-like transition state would be lower in comparison to a product-like transition state towards the disubstituted enol ether product. This transition state would be stabilised by additional hyperconjugation and inductive interactions that would be lacking in the analogous transition state towards formation of the disubstituted enol ether.

It should also be noted that in the case of decalin, a less stable disubstituted alkene is formed as the final product, but there is no alternative route through to any isomeric enol ether.

Scheme 76 shows that in the tricyclic cationic intermediate in the decalin reaction, the only deprotonation site available is the methyl group, which yields the 1,1-disubstituted alkene. Furthermore, it illustrates the two possible deprotonation sites of the bicyclohexyl-derived tricyclic cationic intermediate; the route shown in red deprotonates at the methyl group, which does not occur; and the route shown in green where the deprotonation of the adjacent tertiary carbon occurs, which is the route that is followed. The increased stability of the final product is a likely factor in this mechanistic step.

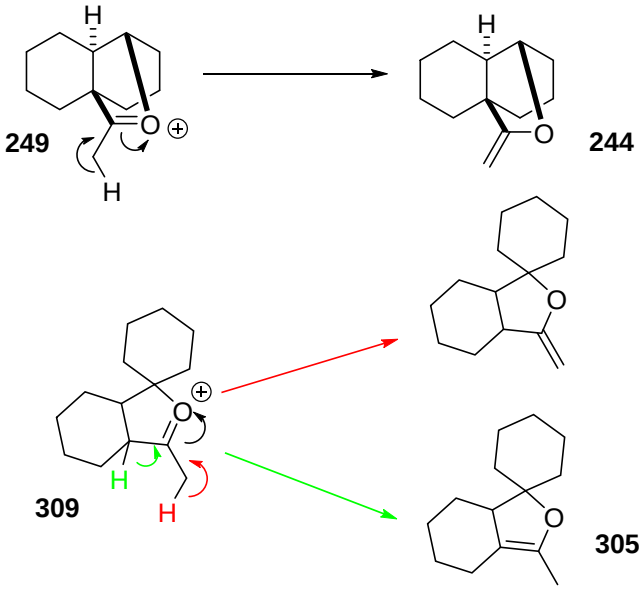


**Scheme 76: Possible deprotonation sites on work-up shown for both decalin and bicyclohexyl based tricyclic cationic intermediates, 249 and 309.**

The first difference between the two mechanisms is the loss of a proton from a tertiary carbocation to yield an alkene. In the decalin mechanism, a tetrasubstituted alkene is formed and in the bicyclohexyl example, a trisubstituted alkene is formed. Unlike the previous mechanistic divergence, where the pathway of reaction for decalin took was restricted by only having one protonated adjacent site, in this case both the bicyclohexyl carbocation and the decalin carbocation could form a tri- or a tetrasubstituted alkene.

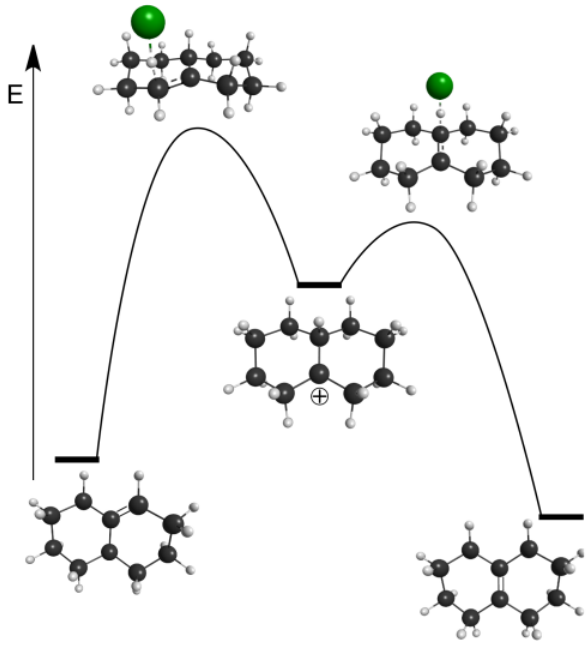


**Figure 14: Energy profile for the formation of tri (left, 256) and tetra (right, 246) substituted alkenes from the tertiary carbocation of decalin – DFT modelling at the M06/6-31G(d) basis set by G. Dan Pantoş**

Computational modelling was carried out by a collaborator, G. Dan Pantoş, on each of these systems, to establish the relative energy levels of the possible alkenes and their respective transition states. Figure 14 shows the schematic energy profile for the decalin mechanism and Figure 15 shows the energy profile for the bicyclohexyl mechanism.

Considering first the mechanism starting from decalin; the transition state for formation of the tetrasubstituted alkene ($\Delta^{9,10}$-octalin, **246**) from the starting tertiary carbocation was calculated to be significantly lower in energy (31.6 kJ $mol^{-1}$) than the analogous transition state through to the trisubstituted alkene ($\Delta^{1,9}$-octalin, **256**).

The relative energies are the opposite way around for the mechanism with bicyclohexyl as the starting alkane; formation of the trisubstituted alkene, **307**, is favoured over the tetrasubstituted alkene, **301**. The transition state through to the former alkene from the tertiary carbocation was found to be 10.8 kJ $mol^{-1}$ lower in energy than the corresponding transition state for formation of the tetrasubstituted alkene.

Also of note, in the bicyclohexyl example, the trisubstituted alkene, **307**, is the thermodynamic product, the tetrasubstituted alkene, **301**, being 2.4 kJ $mol^{-1}$ higher in energy. In the decalin mechanism, the tetrasubstituted alkene ($\Delta^{9,10}$-octalin, **246**) was determined to be lower in energy than the trisubstituted alkene ($\Delta^{1,9}$-octalin, **256**) by 6.7 kJ $mol^{-1}$.

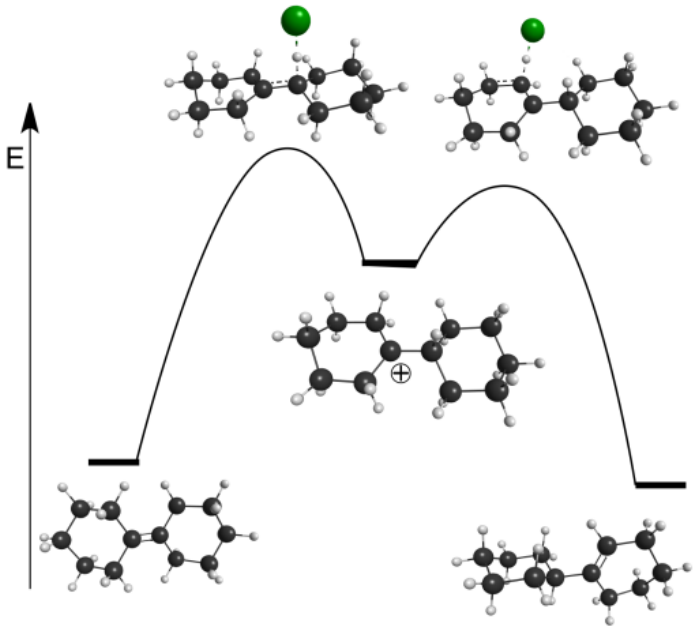


**Figure 15: Energy profile for the formation of tri (right, 307) and tetra (left, 301) substituted alkenes from the tertiary carbocation of bicyclohexyl – DFT modelling at the M06/6-31G(d) basis set by G. Dan Pantoş**

Despite the general increased stability of tetrasubstituted alkenes over trisubstituted alkenes, it seems reasonable in the case of bicyclohexyl the trisubstituted alkene might be slightly lower in energy. The tetrasubstituted alkene mean neither of the cyclohexane rings are fully $sp^3$ hybridised so cannot sit in the preferred chair conformation (minimising steric interactions) whereas the trisubstituted alkene only affects the conformation of the cyclohexene ring it is resident in.

Further to this, observing the optimised structures seen in Figure 15 for the two alkenes, steric interactions are inevitable between protons adjacent to the alkene in the tetrasubstituted case. In the trisubstituted structure, the second cyclohexane ring is able to align itself, via rotation around the ring-linking single bond, to minimise these steric clashes.

### 3.2.3 Alkene Intermediate

The trisubstituted alkene, **307**, was synthesised as shown in Scheme 77. Cyclohexylmagnesium bromide was synthesised from cyclohexylbromide and reacted *in situ* with cyclohexanone to form tertiary alcohol, **310**. Dehydration of **310** with $P_2O_5$ gave the desired alkene, **307**.

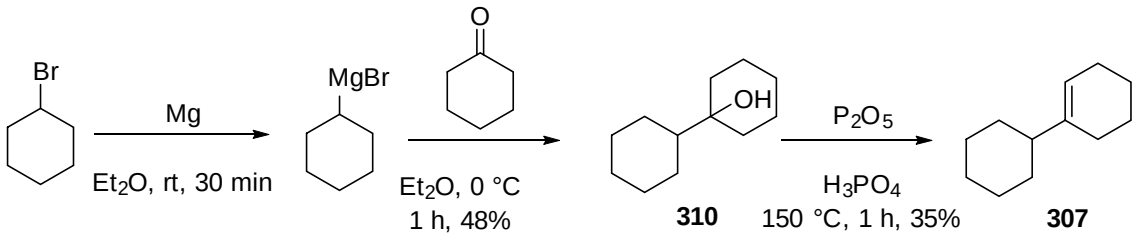


**Scheme 77: Synthesis of 307 from cyclohexylbromide.**

The alkene, **307**, was subjected to the amended Baddeley conditions as per the reaction of $\Delta^{9,10}$ octalin, **246**. This resulted in a 55% mixture of enol ether, **305**, and unsaturated ketone, **311** – the structural elucidation of **311** is outlined in the following section. This gave a strong indication that the alkene, **307**, was an intermediate in the reaction mechanism.

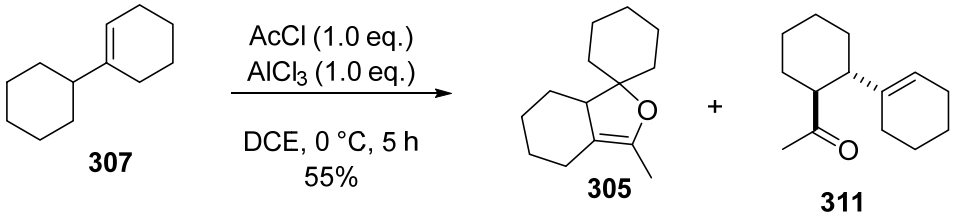


**Scheme 78: Amended Baddeley reaction of trisubstituted alkene intermediate, 307.**

### 3.2.4 Further Product Identification

Attempts to further purify the enol ether, **305**, formed via distillation caused a rearrangement of the product under higher temperatures. This rearrangement product would give additional confirmation of the structure of the enol ether from which it formed. Mass spectrometry indicates that the compound is isomeric with the originally formed enol ether.

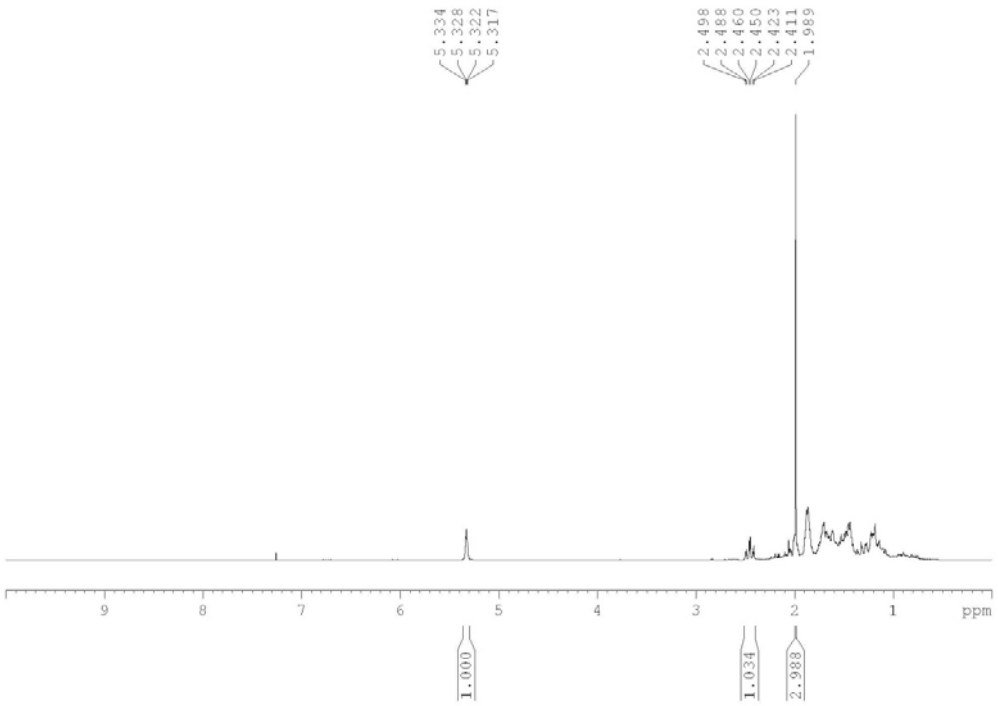


**Figure 16: Proton NMR of rearrangement product formed from enol ether, 305, on distillation at 104-108 °C**

Although most of the peaks seen in the proton NMR of the rearrangement product (Figure 16) are overlapping and represent aliphatic protons, there are some significant peaks at 2.0 ppm and above that are more helpful for structural elucidation.

The peak at 5.33 ppm represents one proton and falls in the alkenic region of the spectra. This is likely to indicate a trisubstituted alkene is present in the molecule. The singlet at 2.00 ppm integrates for three protons and is unlikely to correspond to anything other than a methyl group. Most interestingly however, the peak at 2.46 ppm is a triplet of doublets that integrates for one proton. This distinct splitting pattern may help determine the relative stereochemistry of the compound.

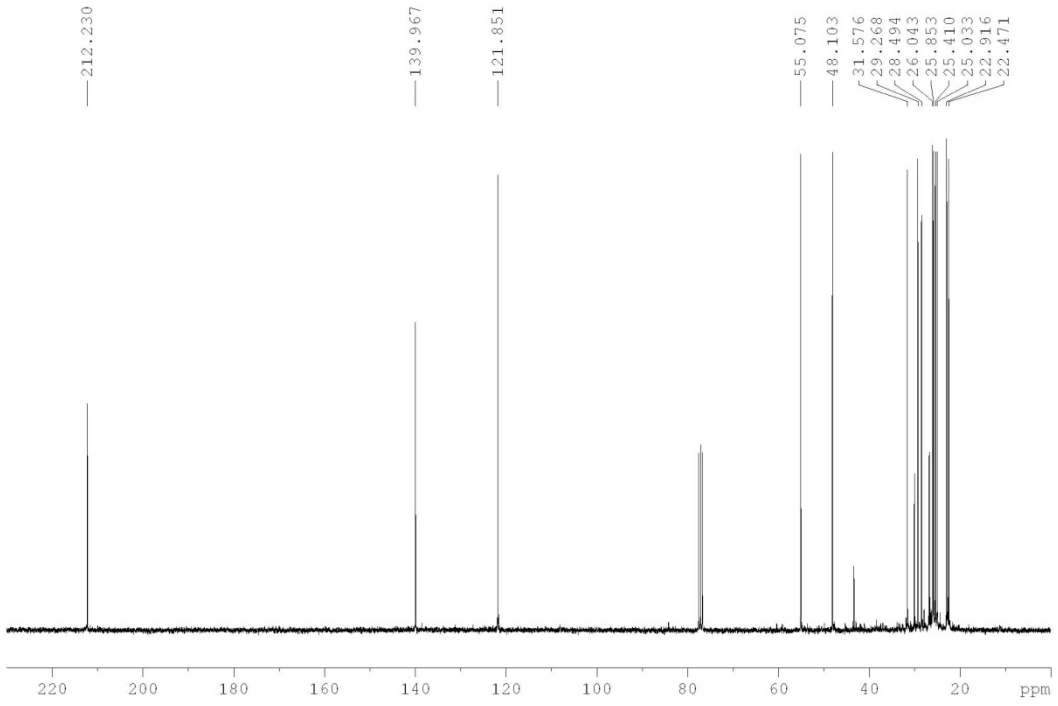


**Figure 17: Carbon-13 NMR spectrum of rearrangement product formed from enol ether, 305, on distillation at 104-108 °C.**

Figure 17 shows the carbon-13 NMR spectra of the rearrangement product. Whilst most of the peaks again fall into the aliphatic region and are not distinctive, there are some exceptions; the peak at δ = 212.2 ppm is indicative of a carbonyl carbon, either an aldehyde or a ketone. In this case no aldehyde proton is seen in the proton NMR, so a ketone is present.

The two peaks at δ = 140.0 and 121.9 ppm fall in the alkenic/aromatic region of the spectra, but the presence of only two of these peaks along with the lack of aromatic protons in the proton NMR adds to the evidence for the presence of an alkene.

With this evidence, alongside the lability of the ether moiety, it seems likely that the ether has ring opened to form the methyl ketone in addition to undergoing elimination to form an alkene functional group within the structure.

Scheme 79 shows a likely product that is consistent with the NMR data presented. The NMR data can be used further to discern the relative stereochemistries of the cyclohexene and methyl ketone moieties in relation to the cyclohexane ring to which they are both connected.

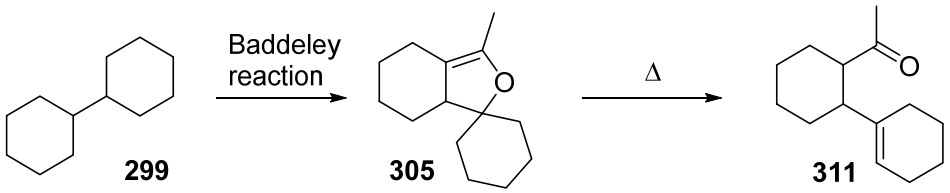


**Scheme 79: Scheme showing the reaction of bicylohexyl to γ,δ-unsaturated ketone, 311, via enol ether, 305.**

Figure 18 shows the possible relative stereochemistries of the γ,δ-unsaturated ketone, **311**. The proton illustrated in red is the proton observed in the proton NMR at 2.46 ppm. The blue protons are at a dihedral angle to the red proton of approximately 60° and the green protons are at a dihedral angle of approximately 180°. The apparent triplet of doublets splitting pattern observed indicates that of the three adjacent protons (illustrated in each structure by green and blue protons) two will have the same dihedral angle to the red proton, causing the triplet splitting; the other will have a different dihedral angle, causing the doublet splitting. The triplet splitting in question will actually be a doublet of doublets, but the close similarity of the dihedral angles (and therefore the coupling constants) cause the coupling to be seen as an effective triplet.

This immediately rules out the structures where all the adjacent protons have dihedral angles of approximately 60°: both the structure with *cis*-stereochemistry with the cyclohexene sitting equatorial (**311-B**) and the structure with *trans*-stereochemistry where both the cyclohexene and the methyl ketone occupy the axial positions (**311-C**). In these cases, an apparent quartet would be observed – it should be a doublet of doublet of doublets but due to all the dihedral angles (and hence coupling constants) being so similar the difference in the coupling constants would be unlikely to be distinguishable.

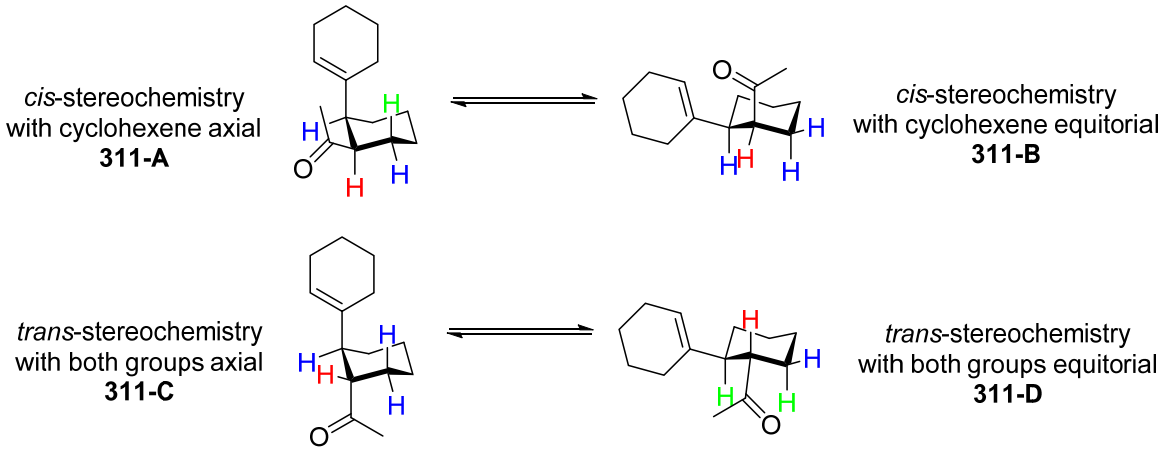


**Figure 18: Possible relative stereochemistries of the γ,δ-unsaturated ketone, 311, formed from the rearrangement of the enol ether formed from bicyclohexyl.**

The two possible structures that remain can be distinguished between using the Karplus equation.[138,139] This equation shows the relationship between $^{3}J$ coupling constants in proton NMR spectroscopy and dihedral angles. Although exact $^{3}J$ coupling constants depend on the

nature of the substrate, the overall pattern is the same. Those adjacent protons which have dihedral angles of 90° between them have the smallest $^{3}J$ coupling constants, whereas those with dihedral angles of 0° or 180° between them have the largest coupling constants.

In this example, the larger coupling constant is in the triplet (11 Hz) and the smaller coupling constant is in the doublet (3 Hz). This indicates that two adjacent protons are at an angle close to 180° (or 0°) and one adjacent proton is at an angle more likely to fall closer to 90° than 180° or 0°. From this, it can be seen that the structure with *cis*-stereochemistry with the cyclohexene group axial (**311-A**) would give the opposite splitting pattern (a doublet of triplets, where the larger $^{3}J$ coupling constant would be that of the doublet).

This leaves the structure with *trans*-stereochemistry and both methyl ketone and cyclohexene groups in the equatorial positions (**311-D**). This is very plausible, as the other structure with *trans*-stereochemistry would likely ring-flip to put both large substituents into the equatorial positions. Having larger groups in the axial plane causes more steric hindrance than the alternative conformer with only hydrogens in the axial positions.

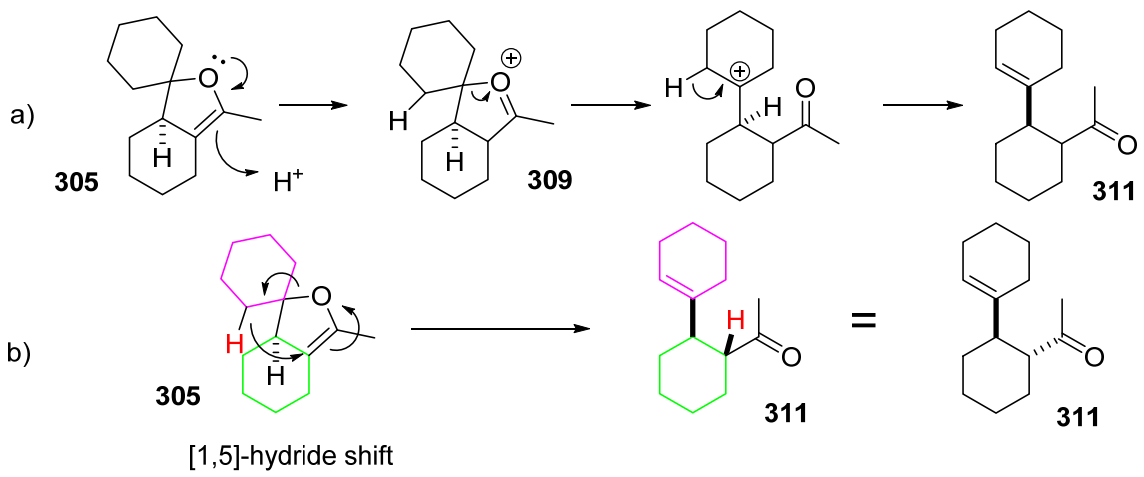


**Scheme 80: Possible mechanisms for the formation of the γ,δ-unsaturated ketone; a) a two-step process involving protonation of the enol ether, followed by elimination; b) a one-step process involving a 1,5-hydride shift.**

Scheme 80 shows two possible mechanisms for the formation of the γ,δ-unsaturated ketone from the enol ether formed in the first instance.

In the presence of acid, mechanism A seems like a much more viable route. However, whilst under distillation conditions, minimal acid is present. This does not completely eliminate the possibility of this mechanism however, as only a tiny amount of acid would be required due to its catalytic nature.

The second mechanism postulated is that of a [1,5]-hydride shift. Isotopic labelling or computational modelling would be required to determine which of the mechanisms (if either) were occurring.

With this ketone-containing product in hand, it was of interest to attempt to form a 2,4-dinitrophenyl hydrazone for further confirmation of the structure. Scheme 81 shows the formation of the relevant hydrazone.

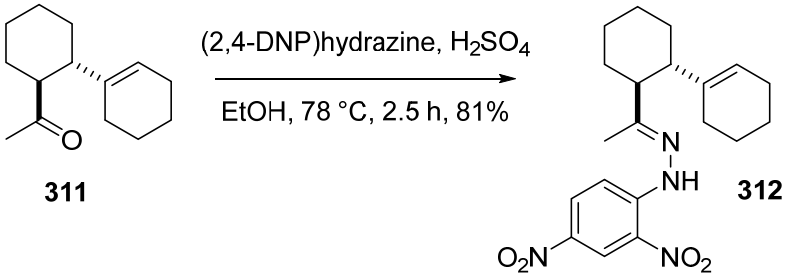


**Scheme 81: Acid catalysed hydrazone formation from γ,δ-unsaturated ketone and 2,4-dinitrophenyl hydrazine.**

The hydrazone product of this reaction was crystalline and it was possible to obtain an x-ray crystal structure of this compound, which is shown in Figure 19.

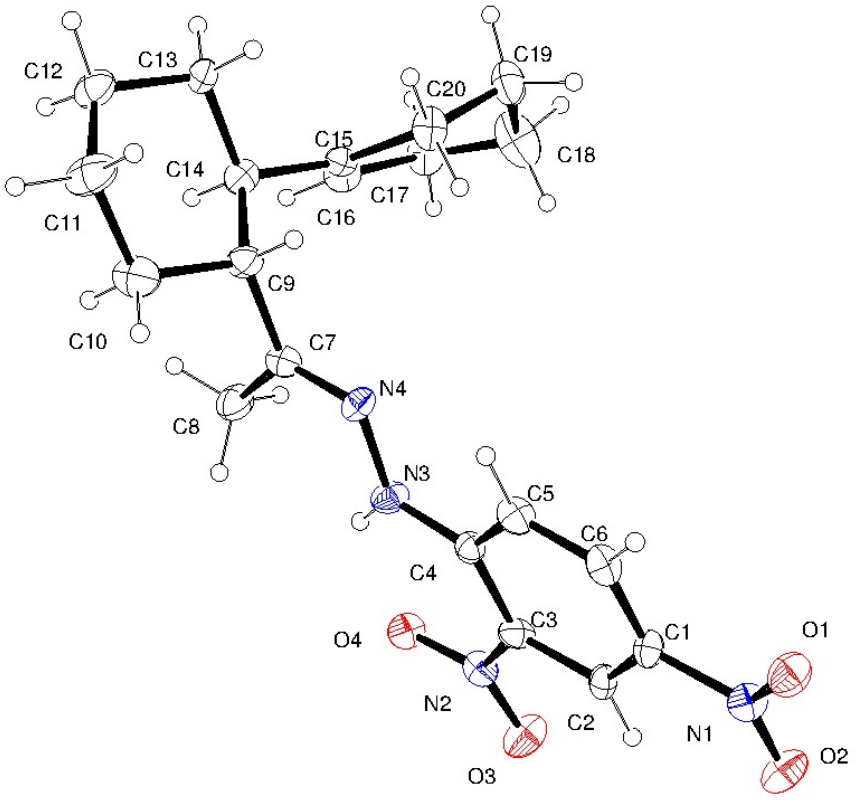


**Figure 19: X-ray crystal structure of the 2,4-DNP hydrazone derivative of the γ,δ-unsaturated ketone, 312. Carbons are represented in black, nitrogens in blue, oxygens in red and hydrogens in white. Ellipsoids are shown at 30% probability. Only one atom of the two in the unit cell is shown for clarity.**

It can be seen from this structure that the relative stereochemistry deduced from the NMR data is also present in the solid state; the cyclohexene and the hydrazone groups are seen *trans* to each other as well as both sitting in the equatorial plane.

## 3.3 Bicyclopentyl

### 3.3.1 Synthesis

The initially planned synthesis of bicyclopentyl involved the retrosynthesis shown in Scheme 82. This would firstly involve the Aldol condensation of cyclopentanone, the product of which was already in hand from previous work. Subsequent reduction of the ketone moiety via a Huang–Minlon[150] modification of the Wolff–Kishner[148,149] reduction would then be followed by reduction of the double bond through to the desired alkane.

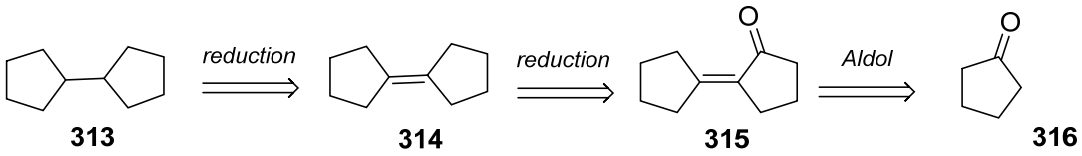


**Scheme 82: Retrosynthetic analysis of bicyclopentyl.**

Subjecting the α,β-unsaturated ketone to the Wolff–Kishner reduction was successful with regards to removal of the ketone group, but unexpectedly yielded a trisubstituted alkene product rather than the anticipated tetrasubstituted alkene; the reaction shown in Scheme 83.

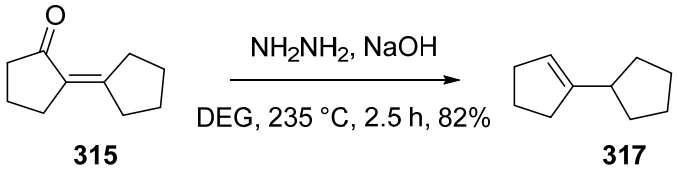


**Scheme 83: Wolff–Kishner Reduction (Huang–Minlon modification) on route to bicyclopentyl.**

This is precedented for α,β-unsaturated ketones undergoing Wolff–Kishner reduction; possible mechanisms for formation of both alkenes are shown in Scheme 84. The difference in the mechanisms comes after the formation of the secondary carbanion, which needs to be protonated in order to form the final product.

The secondary carbanion can be protonated directly (by a water molecule, for example), as shown via the red arrows in Scheme 84. Alternatively, as the negative charge is conjugated with the adjacent alkene, protonation at the other end of this allyl anion is also possible.

In this instance, it could be imagined that the transition state en route to the trisubstituted alkene would again be lower in energy than the transition state towards the tetrasubstituted isomer, **314**, despite the general trend for increased stability with increased substituation of alkenes. This transition state en route to the trisubstituted isomer, **317**, could be imagined to allow for less steric clashing of the protons adjacent to the alkene and for one cyclopentane ring to sit in its preferred envelope conformation; this is similar to the elimination preferences observed with the bicyclohexyl carbocation.

Fortunately, given that the next step involved reduction of the alkene regardless of its location, it was possible to proceed using this compound instead.

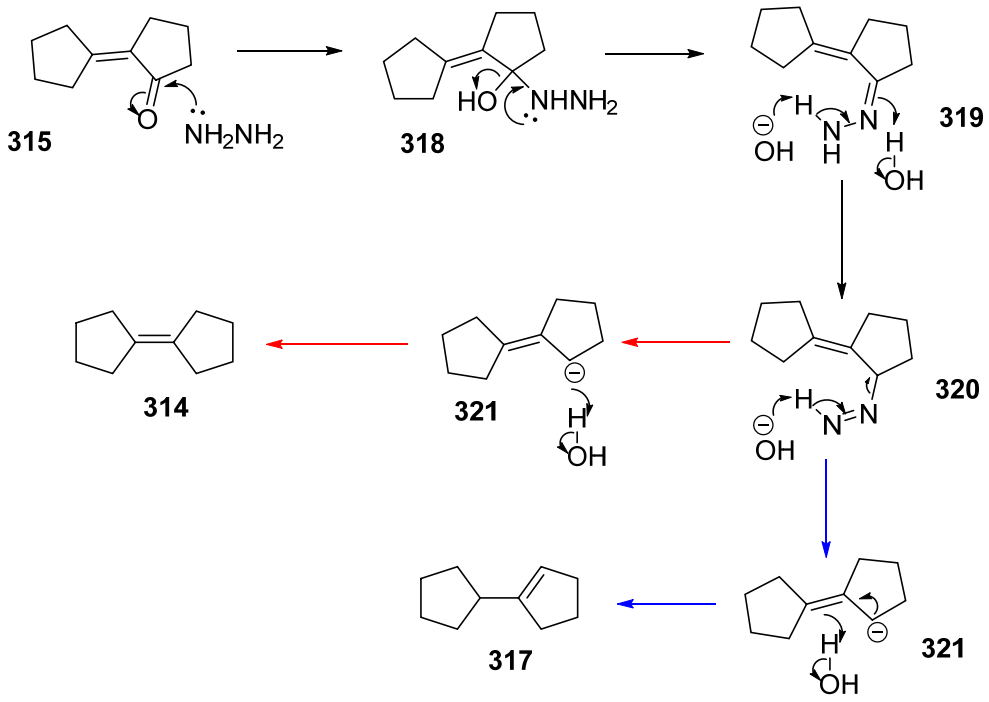


**Scheme 84: Mechanisms for the Wolff–Kishner Reduction of the α,β-unsaturated ketone, with red arrow representing the expected outcome and blue arrows representing the route to the product formed.**

Reduction of the alkene using a positive pressure of hydrogen over palladium on carbon was attempted, but the reduction did not proceed as smoothly as expected; Scheme 85. It was established that the incomplete reaction was due to the palladium used having become inactive.

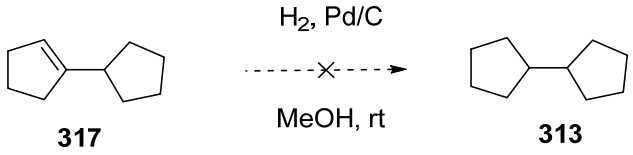


**Scheme 85: Attempted hydrogenation of 1-cyclopentylcyclopentene.**

In the meantime, bicyclopentyl, **313**, was also synthesised directly from the cross coupling of cyclopentyl bromide and cyclopentyl magnesium bromide, facilitated by $Fe(acac)_3$, as seen in Scheme 86.[151]

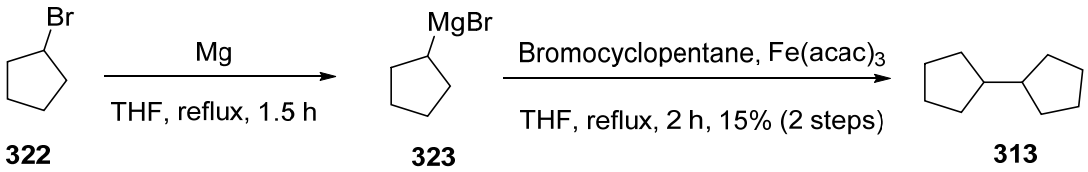


**Scheme 86: Synthesis of bicyclopentyl from bromocyclopentane.**

As could be expected from using Grignard reagents with available β-hydrides, the reaction did not proceed cleanly. The additional major product obtained was cyclopentene, formed via a β-hydride elimination. Another product was also observed, cyclopentane, most likely formed on

protonation of the Grignard reagent. Both of these side-products were fortunately easily separated from the desired bicyclopentyl via distillation.

Crucially, it was possible to perform this reaction on a multigram scale and obtain enough bicyclopentyl to proceed to the Baddeley reaction, despite the poor yields.

### 3.3.2 Expected Reaction with Acetyl Chloride and Aluminium Trichloride

It was anticipated that the reaction of bicyclopentyl, **313**, would proceed in a similar manner to the behavior of bicyclohexyl, **299**, under the Baddeley reaction conditions, an outline of which is seen in Scheme 87. An initial hydride abstraction from one of the two identical tertiary positions would occur, to form a tertiary carbocation. Following this, elimination of a proton would form an alkene; based on previous evidence of the stability of the two possible alkene isomers (seen in the Wolff–Kishner reduction), it seemed likely the trisubstituted alkene, **317**, would form, via loss of the proton coloured in blue. This would be analogous to the step in the bicyclohexyl mechanism.

This alkene could then attack a second equivalent of acylating reagent, forming a tertiary carbocation, **325**. This intermediate could then cyclise, via a [1,2]-hydride shift and attack of the oxygen lone-pair, to form **326**. This oxycationic intermediate would be present until work-up, at which time the loss of a proton could occur from either the methyl group (proton shown in red in the final step) or the adjacent tertiary site, shown in blue. The relative stability of the alkenes in the two possible isomers (1,1-disubstituted alkene, **328**, versus a tetrasubstituted alkene, **327**) indicates the formation of the tetrasubstituted alkene may be plausible, but increased ring strain in this isomer could offset the advantages of the tetrasubstituted alkene, leading to **328**.

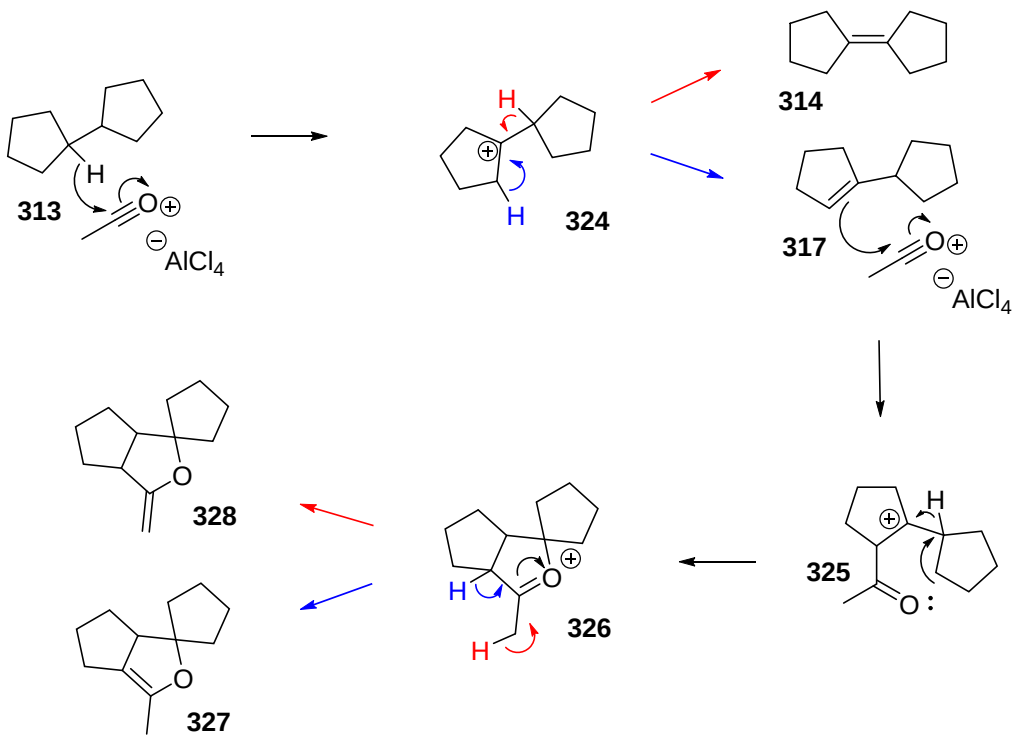


**Scheme 87: Possible mechanistic pathways envisaged for the Baddeley reaction of bicyclopentyl.**

### 3.3.3 Reaction with Acetyl Chloride and Aluminium Trichloride

The reaction of bicyclopentyl under the Baddeley reaction conditions was not as straightforward as we had imagined it might be. Having performed the reaction, the unpurified product was subjected to distillation to recover any unreacted starting material as well as isolate any enol ether formed.

Surprisingly, alongside the unreacted bicyclopentyl, both *cis*- and *trans*-decalin were recovered. As both bicyclopentyl and decalin have the molecular formula $C_{10}H_{18}$, they are isomeric, but the isomerisation from bicyclopentyl into decalin with the level of ease observed was certainly unexpected.

Turning to the isolated enol ether product, the proton NMR spectrum showed three distinct peaks each representing one proton away from the aliphatic region. Although all three of these shifts were downfield of the alkenic region, two of these were alkenic, showing typical chemical shifts for 1,1-disubstituted alkenes. The third was an individual proton adjacent to a heteroatom, as shown in Figure 20.

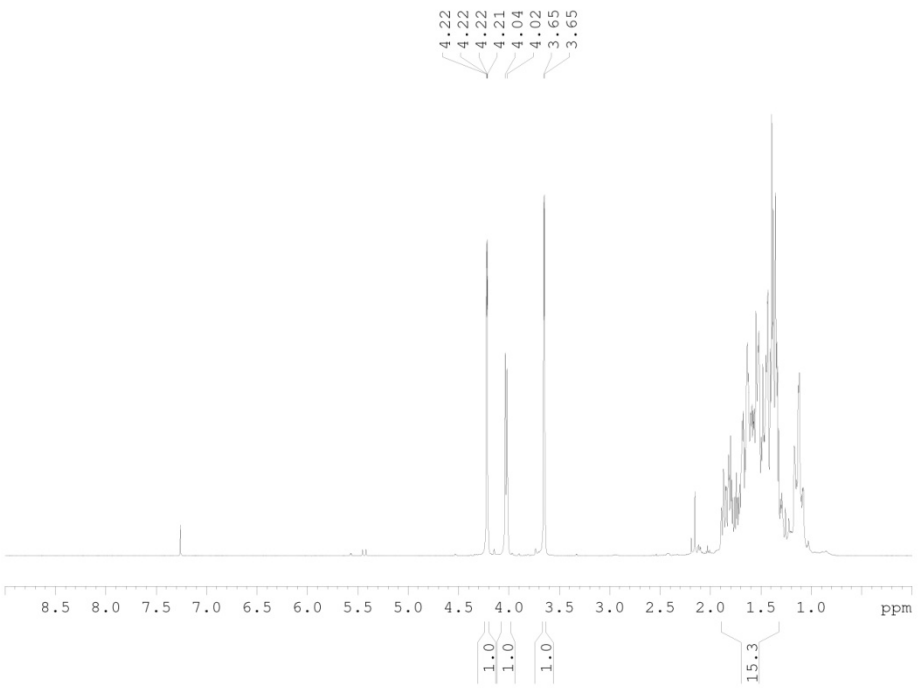


**Figure 20: Proton NMR spectrum of the enol ether obtained from the Baddeley reaction of bicyclopentyl.**

Whilst this proton NMR spectrum could have been consistent with a enol ether formed from bicyclopentyl; via a tetrasubstituted alkene intermediate followed in the final step of the reaction mechanism by loss of a methyl proton, this didn't seem to agree with the likelihood of the increased stability of a tri-substituted alkene intermediate. The chemical shifts and

coupling constants of the peaks were also identical to those of the enol ether formed on reaction of the acylating reagent with decalin.

In addition to this, the carbon-13 NMR spectrum gave identical chemical shifts to the enol ether formed in the original Baddeley reaction of decalin. Given that decalin had been recovered from the reaction mixture, it seemed that the respective enol ether had been synthesised as well.

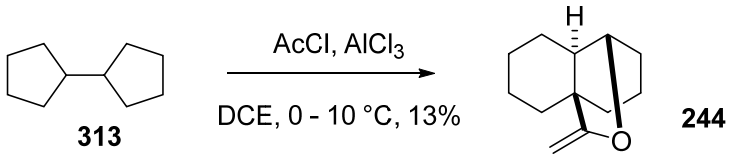


**Scheme 88: Baddeley reaction of bicyclopentyl, 313.**

Clearly, the mechanism from decalin through to the enol ether product would be the same as that previously discussed, however the isomerisation of bicyclopentyl to decalin was not as obvious.

The isomerisation had some precedent, wherein bicyclopentyl was isomerised to decalin (a mixture of *cis*- and *trans*-) mediated by aluminium trichloride.[152] Over six hours at 0 °C the authors found that the bicyclopentyl was primarily converted to *cis*-decalin, although at higher temperatures and longer reaction times (15 h at 100 °C) mostly *trans*-decalin was observed. This may be due to the isomerisation of *cis*-decalin to *trans*-decalin in the presence of aluminium trichloride as discussed beforehand.

Aluminium trichloride has the ability to act as a hydride abstractor, which is a trait in common with the acylating species formed from aluminium trichloride and acetyl chloride in the Baddeley reaction. It seems plausible therefore, that a mechanism for the isomerisation of bicyclopentyl to decalin would begin with abstraction of a hydride, most likely from the tertiary position. This is shown in Scheme 89 below.

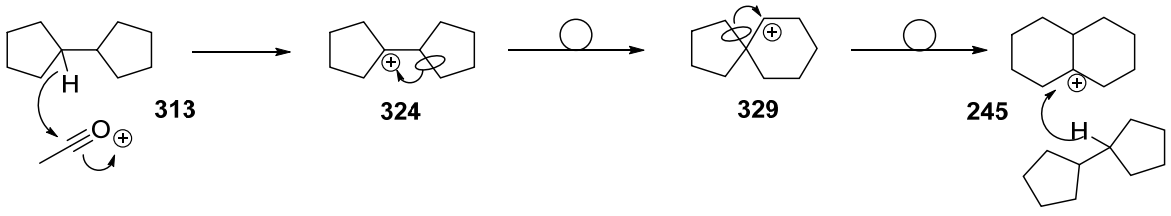


**Scheme 89: Possible mechanism for isomerisation of bicyclopentyl to decalin.**

Following on from the hydride abstraction, intramolecular migration of an adjacent carbon-carbon single bond could occur, changing the skeletal backbone of the alkane to a spirocyclic system with a five-membered and a six-membered ring, **329**. The six-membered ring would have a secondary carbocation adjacent to the quaternary centre; this secondary carbocation would have previously been the uncharged tertiary carbon.

This could be followed by a second migration of a carbon-carbon sigma bond, which in turn causes the positive charge to end up at the newly formed tertiary position; the carbon that would have been the quaternary centre in the previous step. This would certainly be a favourable step due to the removal of a secondary carbocation in favour of a more stable tertiary carbocation.

The tertiary carbocation, **245**, formed would have the same skeletal structure as decalin and is identical to the carbocation formed from decalin when abstracting a hydride. It could be envisaged that this carbocation could proceed to undergo the rest of the Baddeley reaction through to the enol ether.

Alternatively, it has previously been seen in the Baddeley reaction of decalin, the energy barrier between the $\Delta^{9,10}$ octalin intermediate, **246**, proceeding to the enol ether, **244**, is very similar to the energy barrier of the $\Delta^{9,10}$ octalin intermediate, **246**, regressing to decalin, either *cis* (**161**) or *trans* (**159**). The results of this reaction provide further evidence for this reversibility, as in order to form either isomer of decalin from bicyclopentyl, the mechanism must proceed via the carbocation, **245**.

In the mechanism shown in Scheme 89, the final step shows the decalin carbocation abstracting a hydride from another molecule of bicyclopentyl. This seems the most plausible source of hydrides to form decalin; however a hydride could also be abstracted from a solvent molecule or retrieved from acetaldehyde, which would reform the acylating species.

## 3.4 Bicyclo[5.3.0]decane

### 3.4.1 Synthesis

Initial retrosynthetic analysis (Scheme 90) of bicyclo[5.3.0]decane, **330**, envisioned the oxidation of $\Delta^{9,10}$ octalin, **246**, to cyclodecane-1,6-dione, **332**, which could undergo an Aldol reaction to install the [5.3.0] skeletal structure followed by reduction to the desired product.

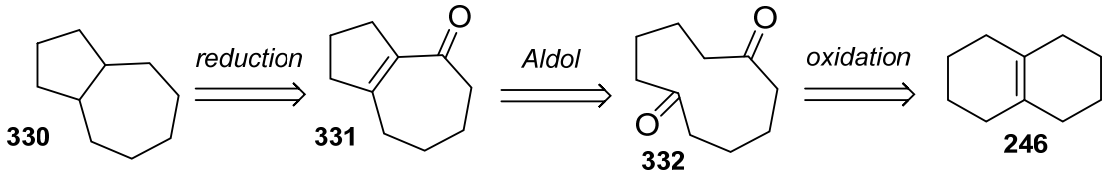


**Scheme 90: Retrosynthetic analysis of bicyclo[5.3.0]decane.**

Oxidation of $\Delta^{9,10}$ octalin was attempted using ruthenium tetroxide and sodium periodate which was successful using a mixture of carbon tetrachloride, acetonitrile and water as the solvent (Scheme 91).

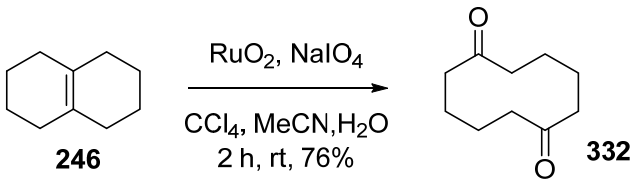


**Scheme 91: Oxidation of $\Delta^{9,10}$ octalin using ruthenium dioxide and sodium periodate in carbon tetrachloride, acetonitrile and water on a 200mg scale.**

However, due to the toxic nature of carbon tetrachloride, chloroform was used as a substitute solvent in subsequent reactions. This gave comparable yields on a small scale. It was desirable however, to scale up the reaction to multigram quantities. Upon scale up, using chloroform in the solvent mixture gave significantly lower yields, so an alternative route was investigated.

Ozonolysis of the $\Delta^{9,10}$ octalin was attempted; initial reactions gave substantial amounts of an undesired by-product, which was identified as the diperoxide.

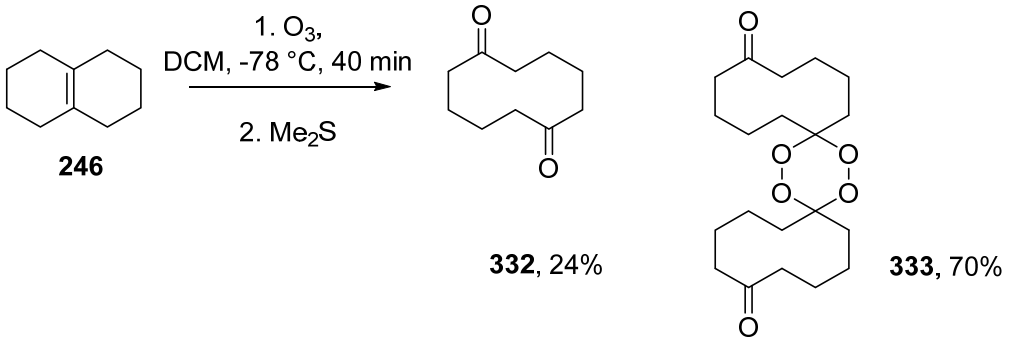


**Scheme 92: Initial ozonolysis of $\Delta^{9,10}$ octalin.**

It transpired that this compound had been observed previously as a by-product of the ozonolysis of $\Delta^{9,10}$ octalin. The authors were able to optimise the reaction conditions to limit the production of the diperoxide; the conditions therein were replicated and further improved for this work.

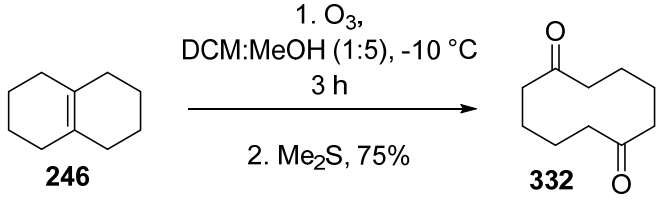


**Scheme 93: Ozonolysis of $\Delta^{9,10}$ octalin.**

The resulting cyclodecane-1,6-dione then underwent sodium carbonate mediated aldol condensation to form the α,β-unsaturated ketone in 88% yield, as shown in Scheme 94. This provided access to the desired 5,7 fused hydrocarbon skeleton.

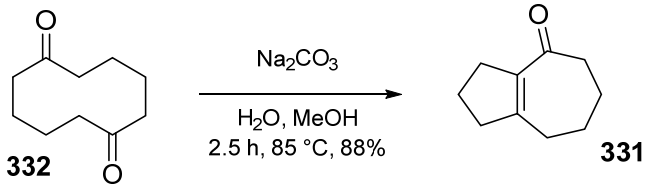


**Scheme 94: Base-mediated aldol condensation of cyclodecane-1,6-dione, 332.**

The reduction of the ketone via Wolff–Kishner reduction (Huang–Minlon modification) was performed, but only gave 36% yield. It was considered this could be related to the required reaction temperature of 235 °C and the boiling point of the enone (126-128 °C); other reductions were considered. As there is minimal other functionality elsewhere in the molecule, there were more options available than reducing a ketone with acid or base sensitive functional groups in the compound.

The ketone moiety was removed from α,β-unsaturated ketone by zinc metal reduction with hydrochloric acid (Clemmensen reduction[153]), and a mixture of tetrasubstituted and trisubstituted monoalkenes were formed in 63% yield. A small quantity of fully saturated alkane was also identified.

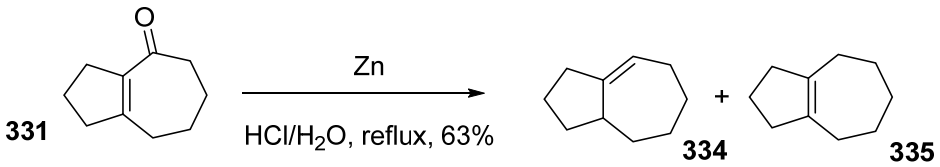


**Scheme 95: Reduction of the α,β-unsaturated ketone to form a mixture of alkenes, 334 and 335.**

As synthesis of the desired saturated hydrocarbon product would involve reduction of either of these alkenes, the unsaturated products were not separated; instead, they were taken forward together and subjected to hydrogenation over palladium on carbon. This gave the desired bicyclo[5.3.0]decane in 96% yield.

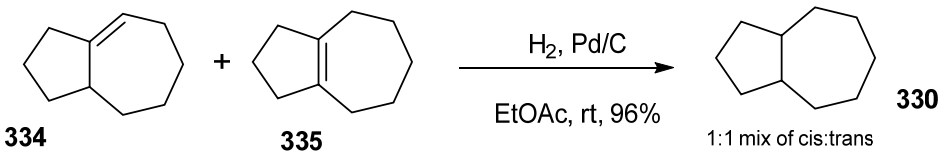


**Scheme 96: Hydrogenation of alkenes through to bicyclo[5.3.0]decane, 330.**

The ratio of *cis* to *trans* bicyclo[5.3.0]decane could not be established via proton NMR, due to the overlapping peaks. It was possible however to run a carbon-13 NMR with a long relaxation delay, in order to maintain reliable integration.

For example, the peaks in a carbon-13 NMR spectrum relating to quaternary carbon centres are often seen to be smaller than those peaks relating to methylene or methyl carbons. Atoms relax by dipole-dipole interaction with adjacent atoms (or nearby atoms). Hydrogen atoms are particularly amenable to accepting this interaction, so generally, the less substituted a carbon atom is, the faster it will relax.

Each scan that occurs emits a pulse of radio frequency (RF) through the sample; the length of time the pulse is emitted for is calibrated to cause the overall aligned magnetic field of the atoms to flip by a ceratin angle, say 30 °, towards the XY-plane. The magnetisation present in the XY plane is detected. This is seen as the free induction decay (FID) and Fourier transformed into the NMR spectra that we recognise. The signal we see is directly proportional to the magnetisation that was initially on the Z-axis.

However, if some atoms in the molecule do not have time to relax back to the z-axis between scans (for example, quaternary carbons) then less magnetisation will be along the Z-axis at the start of the next RF pulse. This pulse, in turn, will excite the now reduced Z magnetisation towards the XY-plane, and subsquently less magnetisation will be observed along the XY-plane. Less observed magnetisation results in a smaller signal in the final NMR spectrum.

Standard carbon-13 NMR experiments are run with a relaxation delay (D1) that may be shorter than the relaxation time required by some carbon atoms for full relaxation (typically described as five times T1, where T1 is the spin-lattice relaxation time constant). It is the short D1 that means the integration of a standard carbon-13 NMR experiment is not accurate. This shorter relaxation delay does however mean that carbon-13 NMR experiments can be acquired in a reasonable length of time, given the 1.1% natural abundance of $^{13}C$. Setting D1 to be at least five times T1 allows for carbon-13 NMR spectra that can be confidently integrated.

A further complication in integrating carbon-13 spectra arises from the proton decoupling that is invariably turned on throughout these experiments. The decoupling pulses, which constantly excite the proton spins, can result in spin polarisation being transferred between the decoupled protons and nearby carbon-13 atoms (through space, rather than through bonds) and is referred to as the Nuclear Overhauser Effect (nOe). This effect normally leads to an increase in relaxation rate for carbon-13 nuclei with protons nearby (i.e.attached) to them compared to quaternary atoms, and hence reduces the reliability of integration. It is not negated by increasing the relaxation delay, but can be negated using an inverse-gated pulse

sequence, where the decoupler is only turned on for the minimum time possible (during the acquisition) and turned off for the majority of the time between successive scans

Figure 21 shows the carbon-13 NMR spectrum obtained using an inverse-gated pulse sequence and a relaxation delay of one minute, where the integrations of the peaks are almost exactly one to one. Four peaks (δ = 24.0, 26.5, 26.6 and 31.7 ppm) represent one carbon each; the two carbons in *cis*- bicyclo[5.3.0]decane that are along the plane of symmetry and the comparable two carbons in *trans*- bicyclo[5.3.0]decane. The remaining eight peaks represent two carbons each; four environments in each isomer. The peaks at δ = 43.4 and 46.4 ppm are the tertiary centres.

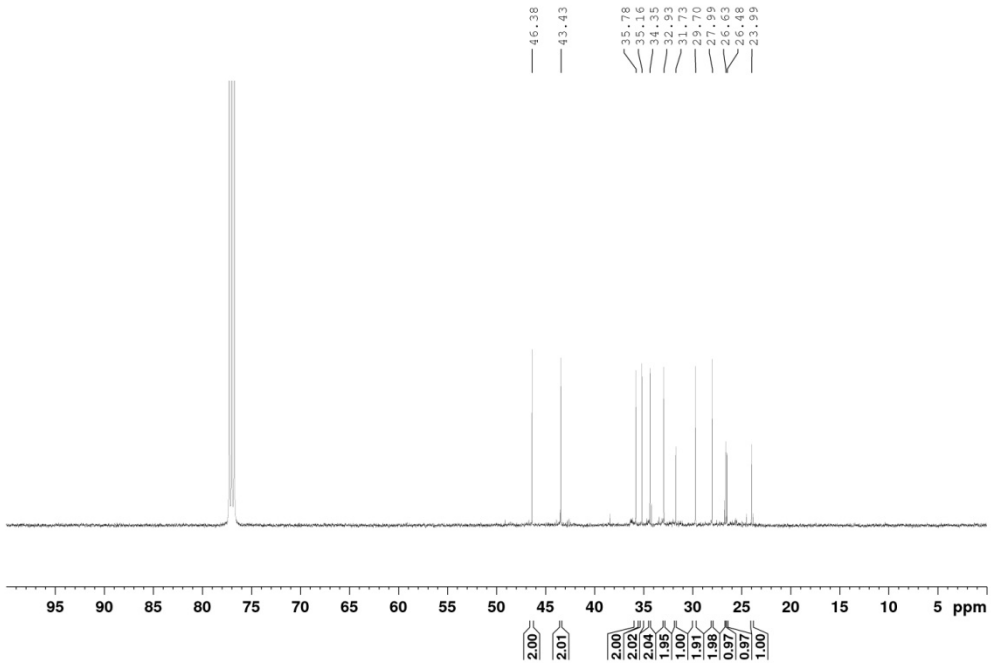


**Figure 21: Inverse-gated decoupled carbon-13 NMR spectrum of *cis* and *trans* bicyclo[5.3.0]decane with a D1 of 60 seconds, run in $CDCl_3$ at 500 MHz (298 K, 1024 scans)**

### 3.4.2 Reaction with Acetyl Chloride and Aluminium Trichloride

It was considered that on reaction with acetyl chloride and aluminium trichloride, bicyclo[5.3.0]decane could form two possible enol ethers with the 5,7-skeletal structure, **339** and **342**. The mechanisms for formation of these products would proceed in the same manner as the mechanism starting with decalin.

The two possible mechanisms for formation of these anticipated structures are shown in Scheme 97. After formation of the tetrasubstituted alkene intermediate, a hydride shift could occur from a methylene on the seven-membered ring (shown in blue, **340**) or from a methylene on the five-membered ring (illustrated in green,**337**).

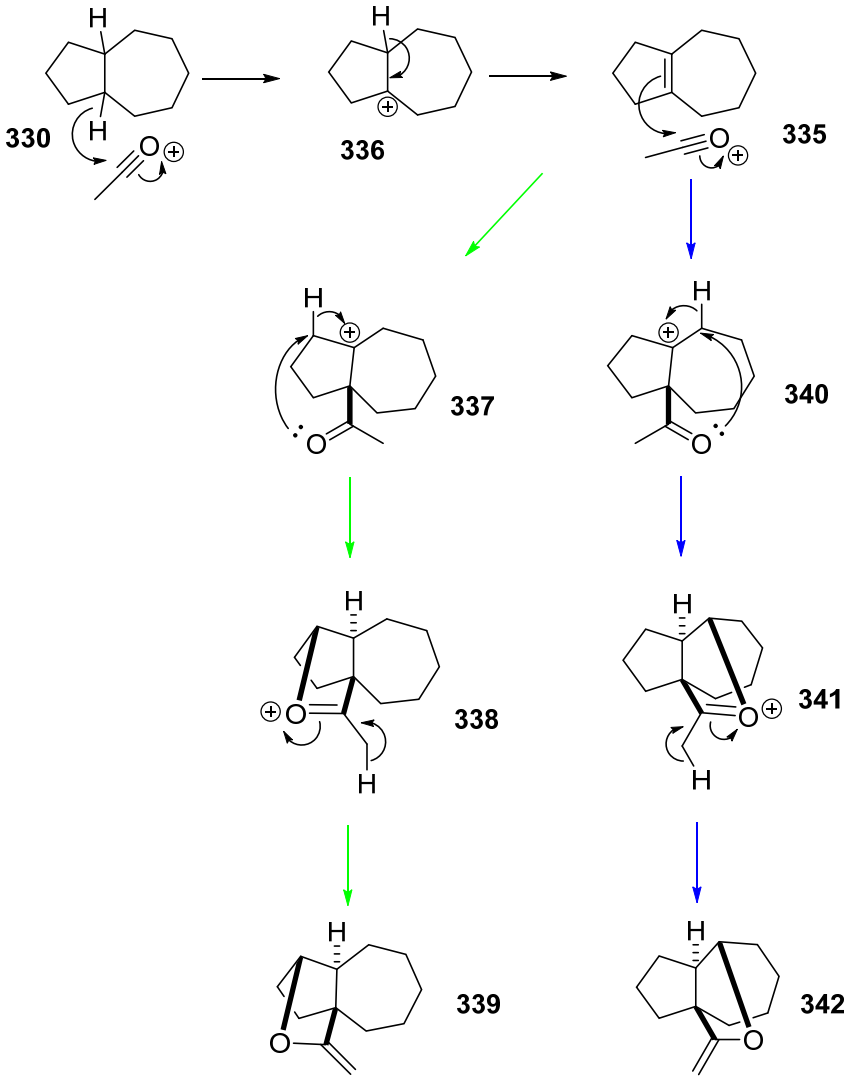


**Scheme 97: Possible mechanisms for formation of envisaged enol ethers from bicyclo[5.3.0]decane.**

However, on performing the reaction and subjecting the unpurified products to distillation under reduced pressure, it was found that the products synthesised in the reaction of bicyclo[5.3.0]decane with acetyl chloride and aluminium trichloride were in fact the enol ether previously synthesised from decalin and bicyclopentyl, as well as the chloroketone previously seen in the Baddeley reaction of decalin.

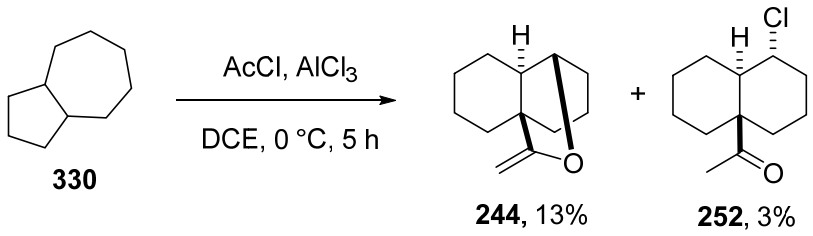


**Scheme 98: Products formed in the reaction of bicyclo[5.3.0]decane with acetyl chloride and aluminium trichloride.**

This had not been expected, but with hindsight it was plausible that this bicyclic saturated hydrocarbon containing 10 carbon centres would rearrange to decalin given the tendency of bicyclopentyl (also a 10 carbon bicyclic hydrocarbon) to isomerise to decalin.

The mechanism for this process was not as apparent as the mechanism for the isomerisation of bicyclopentyl. Clearly, it would be initiated by the abstraction of a hydride from a tertiary carbon to give the carbocation and end with the decalin-based tertiary carbocation which could then revert to decalin itself or proceed to form the enol ether.

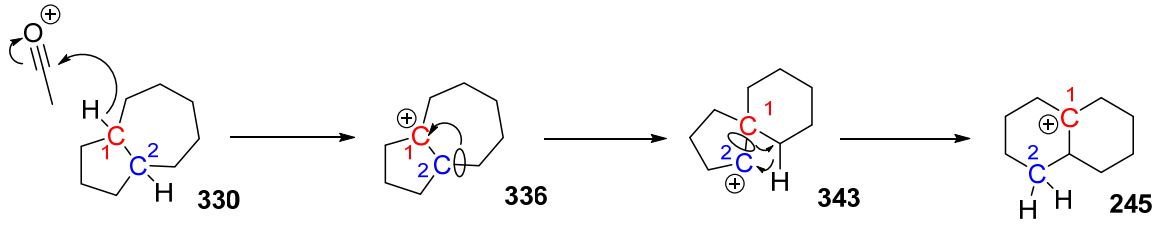


**Scheme 99: Possible mechanism for formation of the decalin skeletal structure from bicyclo[5.3.0]decane.**

Two plausible mechanisms are outlined in Scheme 99 and Scheme 100. Both begin with the well established abstraction of a hydride from the tertiary position to give **336**; in both schemes this tertiary position is shown as carbon one, in red. The other tertiary position is shown as carbon two, in blue, and these carbons are coloured throughout the mechanisms to illustrate where they end up in the final structure.

The mechanism shown in Scheme 99 is stepwise, and proceeds via a spirocyclic intermediate which contains a secondary carbocation, **343**, (formed by Wagner-Meerwein rearrangement). This intermediate would then undergo a [1,2]-carbon shift and a [1,2]-hydride shift, either simultaneously or step-wise, to give the decalin backbone with the cation residing in the tertiary position, **245**. In each step, as well as forming more stable six-membered rings, electrons move to neutralise the positive charge.

The mechanism in Scheme 100 may be more plausible, as in just one step a migration of a carbon-carbon bond and a [1,2]-hydride shift occur, leaving the tertiary carbocation, **245**. No relatively unstable spirocyclic intermediate is needed, nor a secondary carbocation. If this mechanism were correct however, no movement of electrons towards the positive charge would occur. This mechanism could be a candidate for further computational modelling.

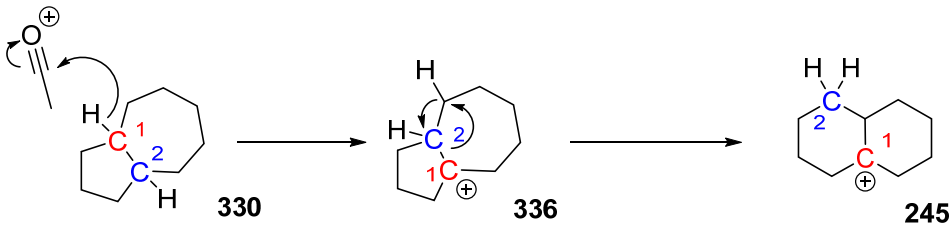


**Scheme 100: Possible concerted mechanism for of the decalin skeletal structure from bicyclo[5.3.0]decane.**

## 3.5 Bicyclo[5.4.0]undecane

### 3.5.1 Synthesis

Simple retrosynthetic analysis envisaged bicyclo[5.4.0]undecane would be formed from the reduction of commercially available 1-benzosuberone, as seen in Scheme 101.

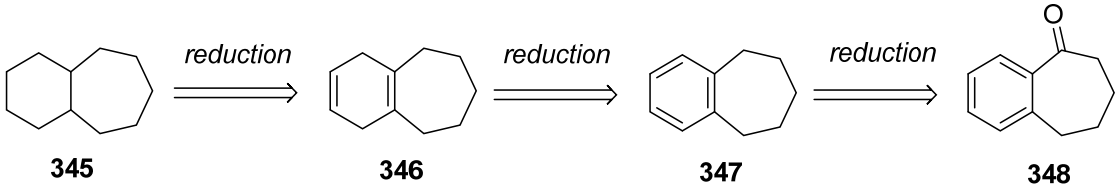


**Scheme 101: Retrosynthetic analysis of bicyclo[5.4.0]undecane, 345, from 1-benzosuberone, 348.**

Wolff–Kishner reduction (Huang–Minlon modification) of 1-benzosuberone, **348**, afforded the aromatic hydrocarbon, **347**, in 81% yield. This aromatic hydrocarbon was then subjected to Birch reduction which gave a 98% yield of a mixture of dienes. Separation of these compounds was not attempted as further reduction would take both through to the same desired compound.

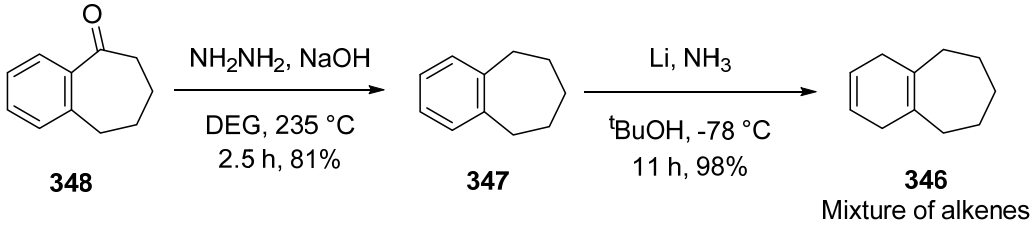


**Scheme 102: Reduction of 1-benzosuberone to a mixture of dienes via Wolff–Kishner and Birch reductions**

The next step of the synthetic route involved hydrogenation over palladium on carbon, which proved to be more challenging than expected. Rather than reducing the dienes to monoalkenes via the addition of one hydrogen molecule, followed by reduction of the monoalkene to the saturated hydrocarbon via addition of another hydrogen molecule across the remaining double bond, the dienes themselves acted as hydrogen transfer agents as well as the hydrogen.

This resulted in some of the starting material being rearomatised to the aromatic hydrocarbon previously subjected to Birch reduction. The remaining starting material was reduced to the monoalkene by addition of two hydrogen atoms; either from another diene or from a hydrogen molecule.

The monoalkenes were not separable by column chromatography, although it was possible to separate the aromatic hydrocarbon, which could subsequently be recycled. The monoalkenes would both give the desired saturated molecule on further hydrogenation so lack of separation was not an issue.

Resubjecting the monoalkene mixture to hydrogenation over palladium on carbon gave the desired alkane in 68% yield.

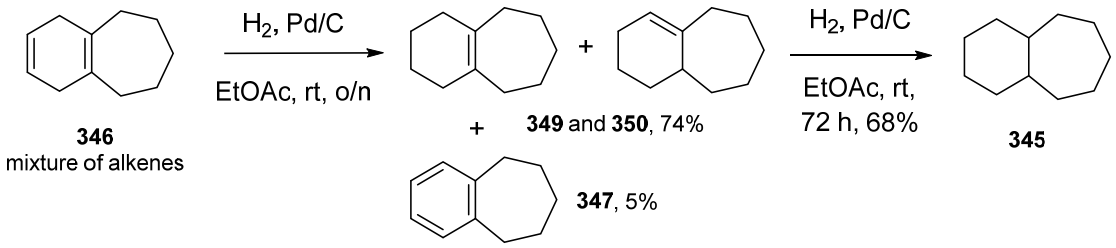


**Scheme 103: Synthesis of bicyclo[5.4.0]undecane.**

The hydrocarbon, **345**, was a mixture of *cis*- and *trans*-isomers. The ratio was established by $^{13}C$ NMR using an inverse gated pulse sequence and a long D1, as in the bicyclo[5.3.0]decane mixture, **330**, and is shown in Figure 22. This illustrates approximately a 1:3.4 ratio between isomers. It is likely, based on analogy between *cis*- and *trans*-decalin, that the minor isomer is *cis*-bicyclo[5.4.0]undecane, due to peak broadening in some secondary carbon peaks and the ring junction carbon at δ = 36.6 ppm (*cis*-decalin shows peak broadening in $CH_2$ peaks and the ring junction carbons present at δ = 36.4 ppm). *trans*-decalin shows no peak broadening at room temperature and the ring junction carbons present at δ = 43.8 ppm.

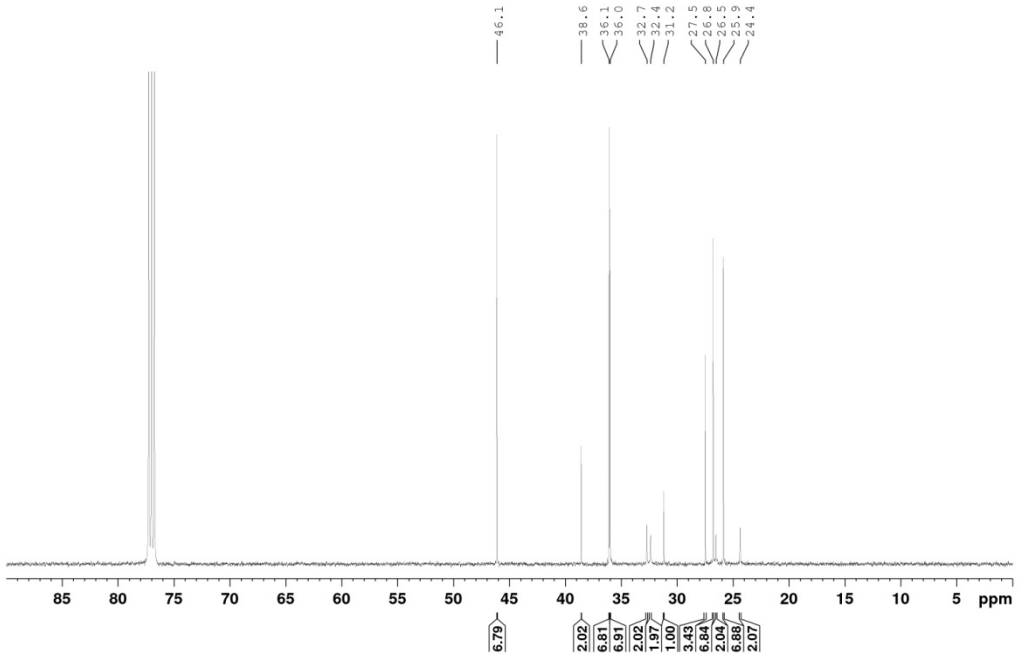


**Figure 22: Inverse-gated decoupled carbon-13 NMR spectrum of *cis* and *trans* bicyclo[5.4.0]undecane with a D1 of 60 seconds, run in $CDCl_3$ at 500 MHz (298 K, 512 scans)**

### 3.5.2 Reaction with Acetyl Chloride and Aluminium Trichloride

After distillation and column chromatography, the major product from the reaction was isolated. Although small amounts of characteristic enol ether peaks were seen in the crude proton NMR spectra, these enol ethers could not be isolated due to their limited quantity and instability towards column chromatography. The proton NMR spectrum of the major compound obtained is seen in Figure 23.

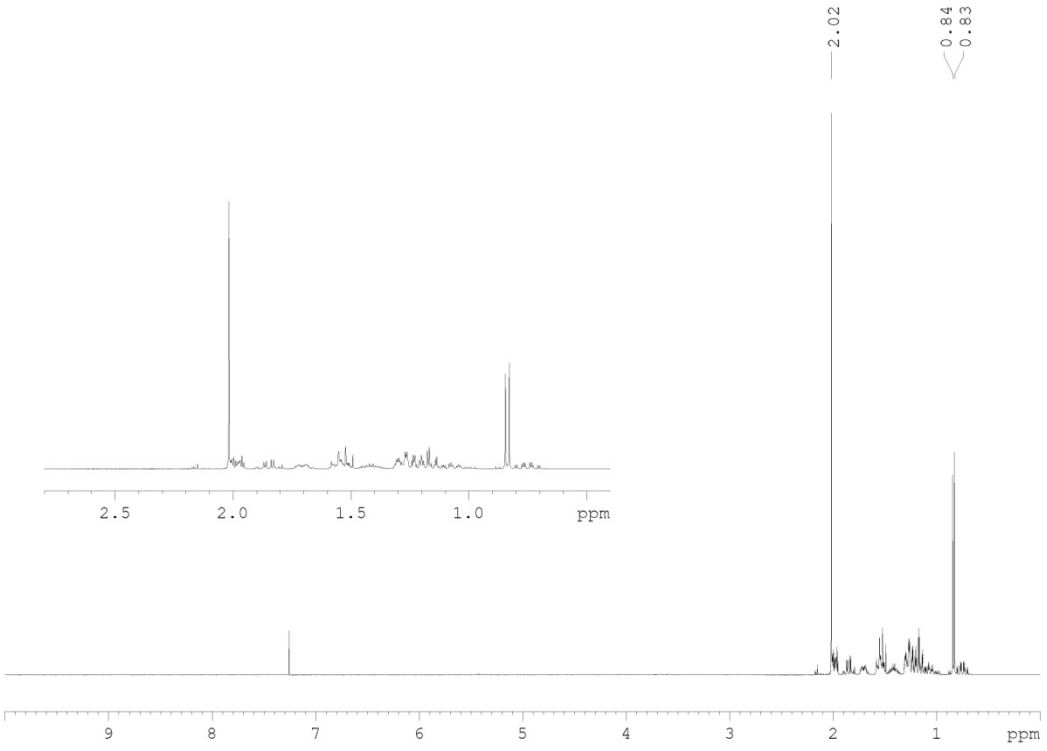


**Figure 23: Proton NMR spectrum of product from Baddeley reaction of bicyclo[5.4.0]undecane with insert showing 0.4-2.8 ppm at greater magnification**

The major product from the reaction was not easily identified. The first key observation from the proton NMR spectra was the presence of two methyl groups, one split into a doublet at 0.84 ppm, the other a singlet at 2.02 ppm. The methyl group presenting as a singlet is more downfield and corresponds with the chemical shift likely to be that of a methyl ketone.

The methyl group appearing as a doublet indicates it is located adjacent to a methine. This is indicative of skeletal rearrangement occurring, as no methyl groups were present in the initial hydrocarbon. Previous studies have shown that cycloheptane can be isomerised to methylcyclohexane in the presence of aluminium trichloride. It would not be unreasonable to imagine that the cycloheptane ring in this bicyclic system could rearrange to a more stable six-membered ring with a methyl group attached.

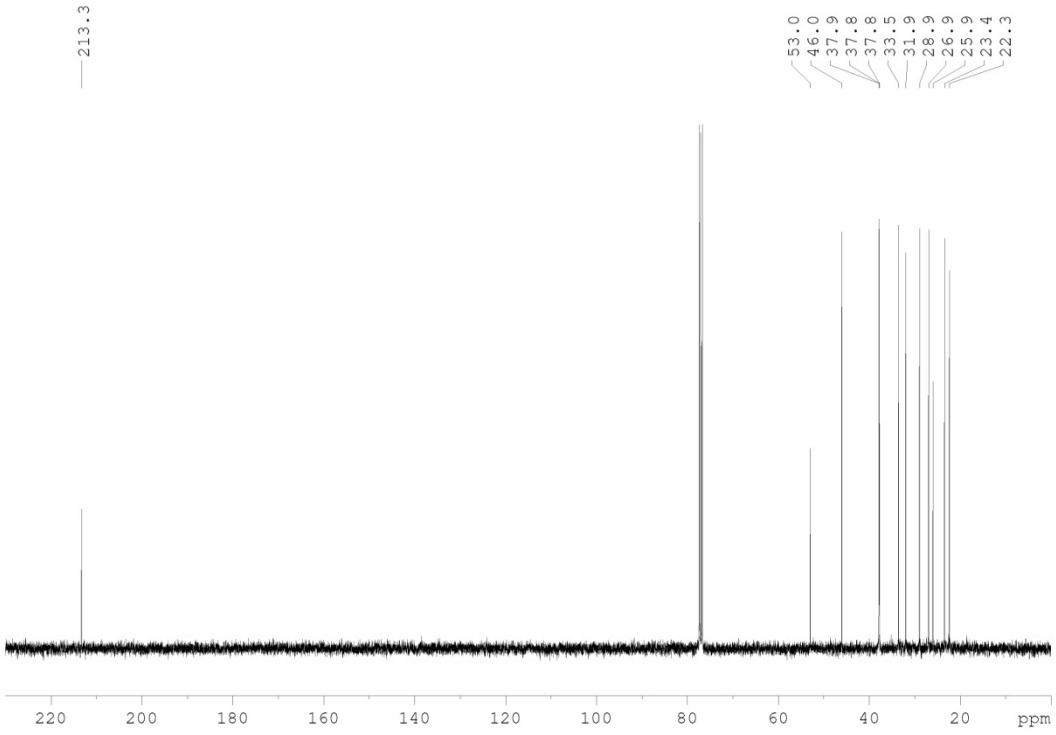


**Figure 24: Carbon-13 NMR spectrum of product from Baddeley reaction of bicyclo[5.4.0]undecane**

Figure 24 shows the $^{13}C$ NMR spectrum, which confirms the presence of a ketone moiety. Beyond this however, the only information able to be gleaned from the carbon-13 NMR spectrum is that the remaining carbons are aliphatic. The IR spectrum was also obtained, shown in Figure 25. This further confirmed the presence of a ketone and aliphatic carbon-hydrogen bonds, but little else.

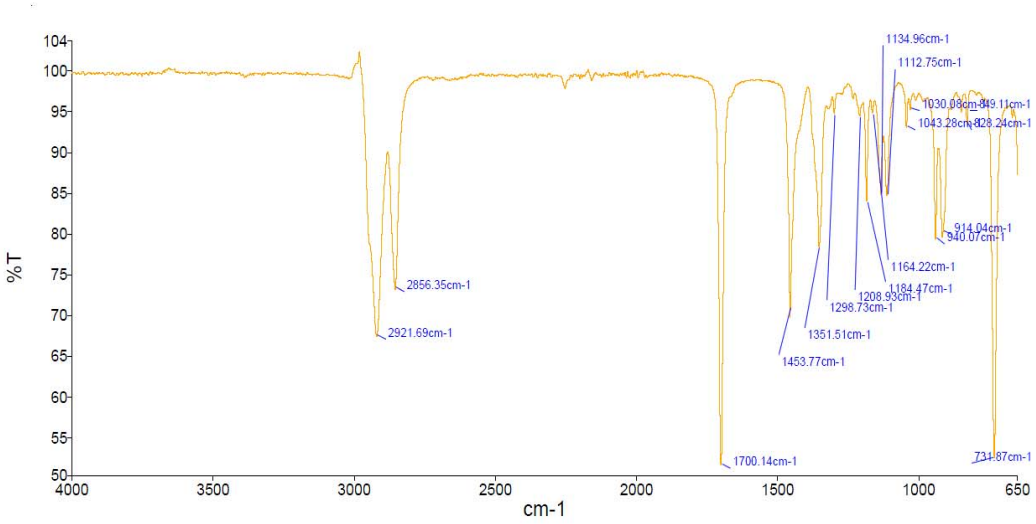


**Figure 25: IR spectrum of product from Baddeley reaction of bicyclo[5.4.0]undecane**

With this information, or lack thereof, in hand, more NMR data were obtained. It was determined from the PENDANT NMR spectrum (Figure 26) that the methyl ketone was attached to the ring junction of the bicyclic system. The spectrum indicates that four carbons in the molecule are tertiary or primary (δ = 46.0, 33.5, 25.9 and 22.3 ppm); two methyl groups, the methine carbon adjacent to one of the methyl groups and presumably one of the ring junction carbons. The other ring junction carbon is quaternary (δ = 52.9 ppm).

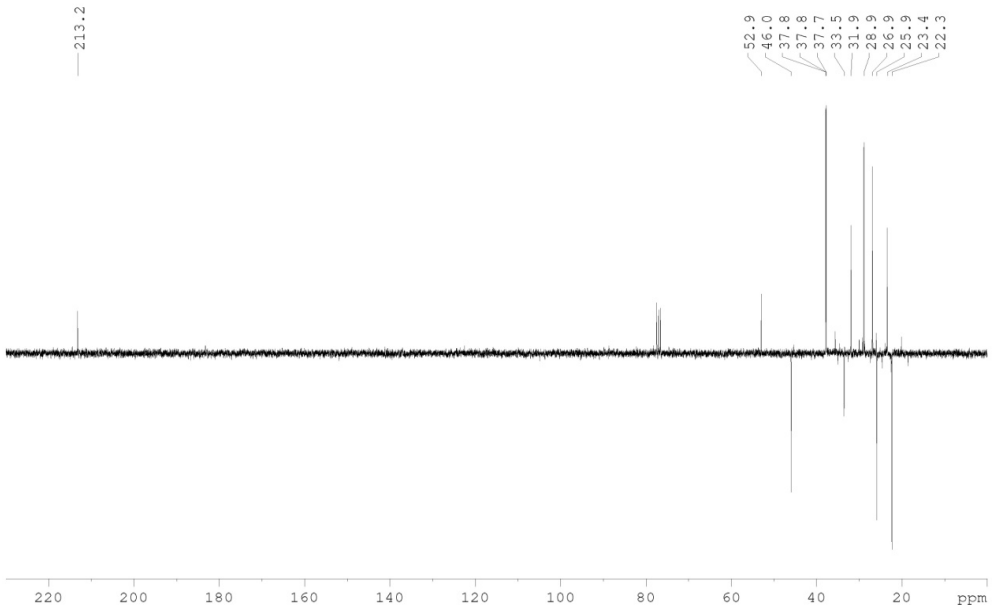


**Figure 26: PENDANT NMR spectrum of product from Baddeley reaction of bicyclo[5.4.0]undecane**

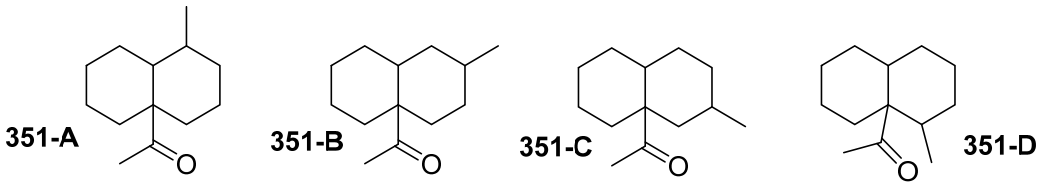


**Figure 27: Possible structures of the methyl ketone formed from the Baddeley reaction of bicyclo[5.4.0]undecane, not considering relative stereochemistry**

Figure 27 shows the four possible structures of the methyl ketone product. In order to establish which of these structures had been formed, and ideally the relative stereochemistry of the compound, 2D NMR data were obtained.

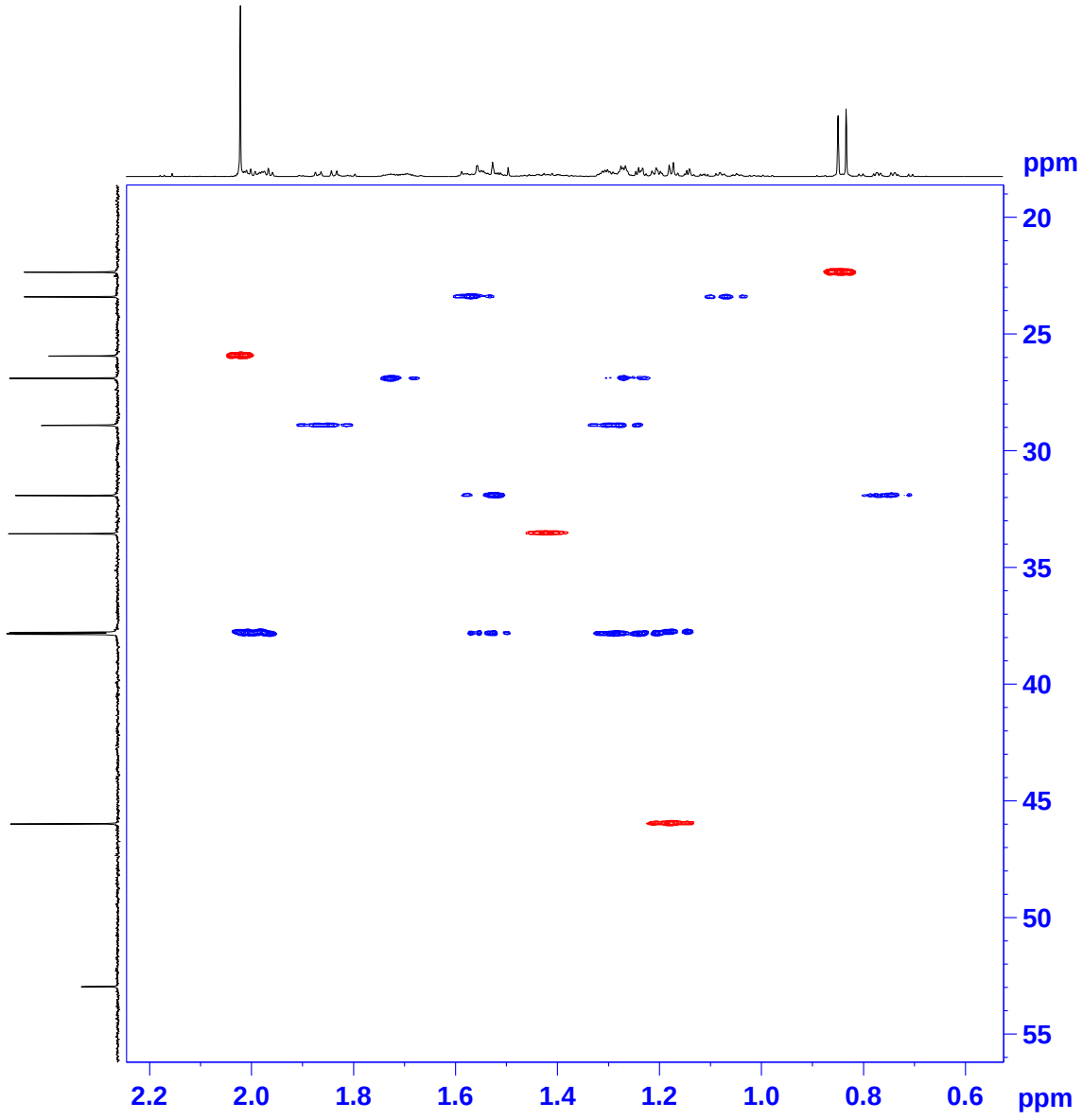


**Figure 28: Multiplicity edited HSQC NMR spectrum of methyl ketone, 351, formed from the Baddeley reaction of bicyclo[5.4.0]undecane**

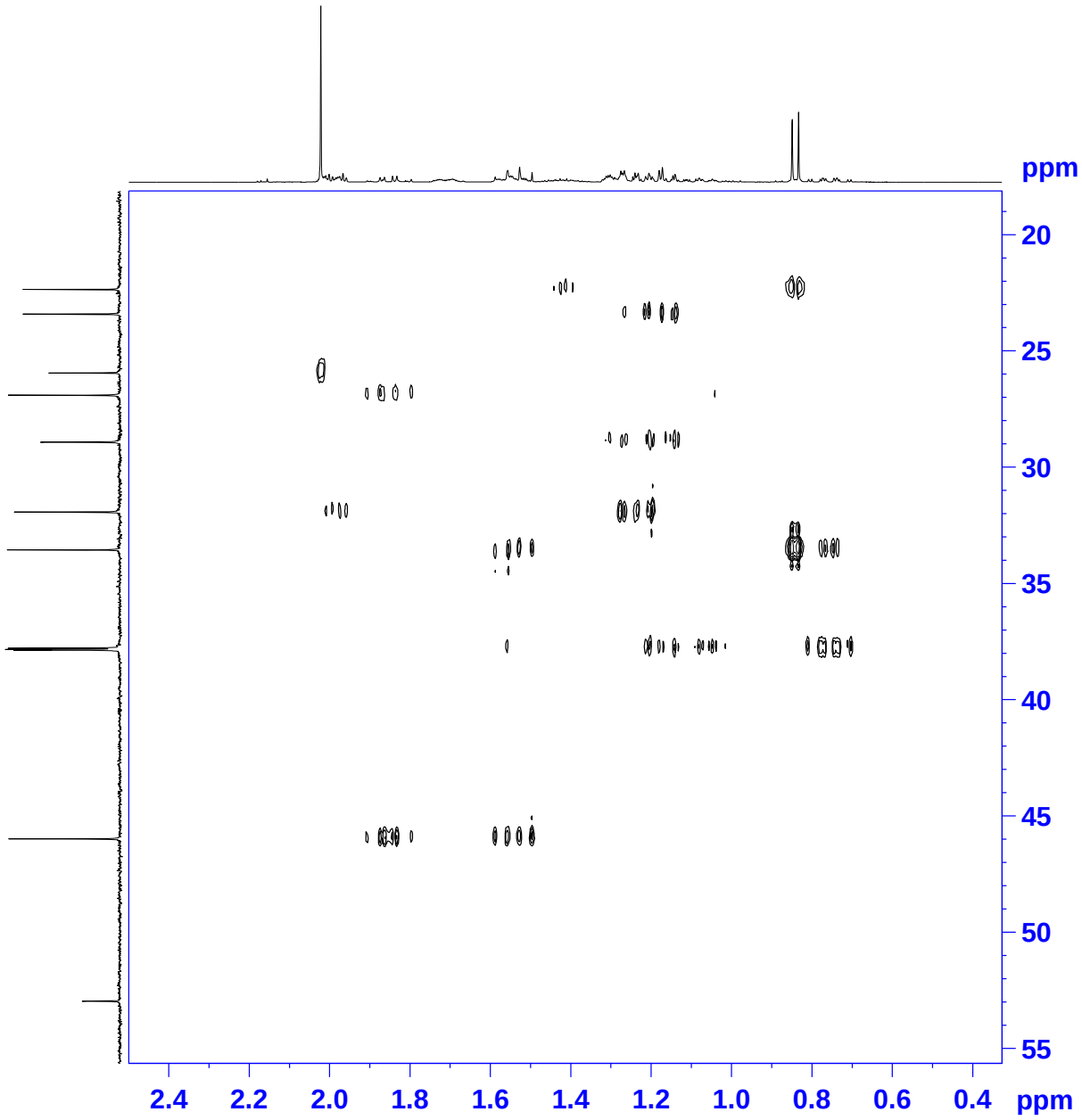


**Figure 29: H2BC NMR spectrum of methyl ketone, 351, formed from the Baddeley reaction of bicyclo[5.4.0]undecane**

Figure 28 and Figure 29 shows the HSQC and H2BC NMR spectra, respectively. H2BC specifically shows cross-peaks between protons and carbons that are separated by two bonds, where the carbons are not quaternary.[154,155] From this data as well as COSY (Figure 31) and NOESY spectra (Figure 32), it was possible to assign all the carbons in the molecule, as detailed in Table 11. This confirmed that the methyl group was positioned at the β-carbon to the tertiary ring junction carbon.

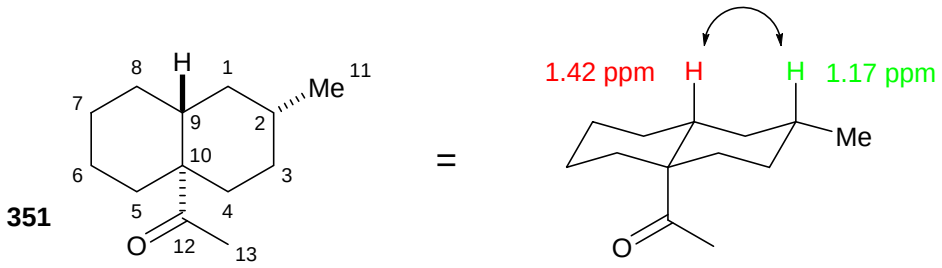


**Figure 30: Structure of methyl ketone compound, 351, showing NOESY correlations and atom numbering**

| Carbon number | Carbon-13 NMR peaks (ppm) | Proton NMR peaks (ppm) | Assignment detail |
|---|---|---|---|
| 1 | 37.9 | 1.54 (1H, m) 1.30 (1H, m) | COSY correlation to methine protons at 1.42 and 1.17, H2BC correlations from carbons at 46.1 and 33.5 to proton at 1.54 ppm |
| 2 | 33.5 | 1.42 (1H, m) | Methine adjacent to methyl |
| 3 | 31.9 | 1.54 (1H, m), 0.76 (1H, m) | COSY correlation to methine proton at 1.42 |
| 4 | 37.9 | 2.00 (1H, m), 1.22 (1H, m) | |
| 5 | 37.8 | 1.99 (1H, m), 1.18 (1H, m) | |
| 6 | 23.5 | 1.56 (1H, m), 1.08 (1H, m) | |
| 7 | 26.9 | 1.71 (1H, m), 1.27 (1H, m) | |
| 8 | 29.0 | 1.86 (1H, m), 1.28 (1H, m) | H2BC correlation between proton at 1.86 and carbon at 46.1 (tertiary ring junction) |
| 9 | 46.1 | 1.17 (1H, m) | Tertiary ring junction methine |
| 10 | 53.1 | None | Quaternary ring junction carbon |
| 11 | 22.4 | 0.84, 3H, d, *J* = 6.5 Hz | Methyl adjacent to methine |
| 12 | 213.2 | None | Carbonyl group |
| 13 | 26.0 | 2.02, 3H, s | Methyl group |

**Table 11: Assignment of NMR data for methyl ketone product, 351.**

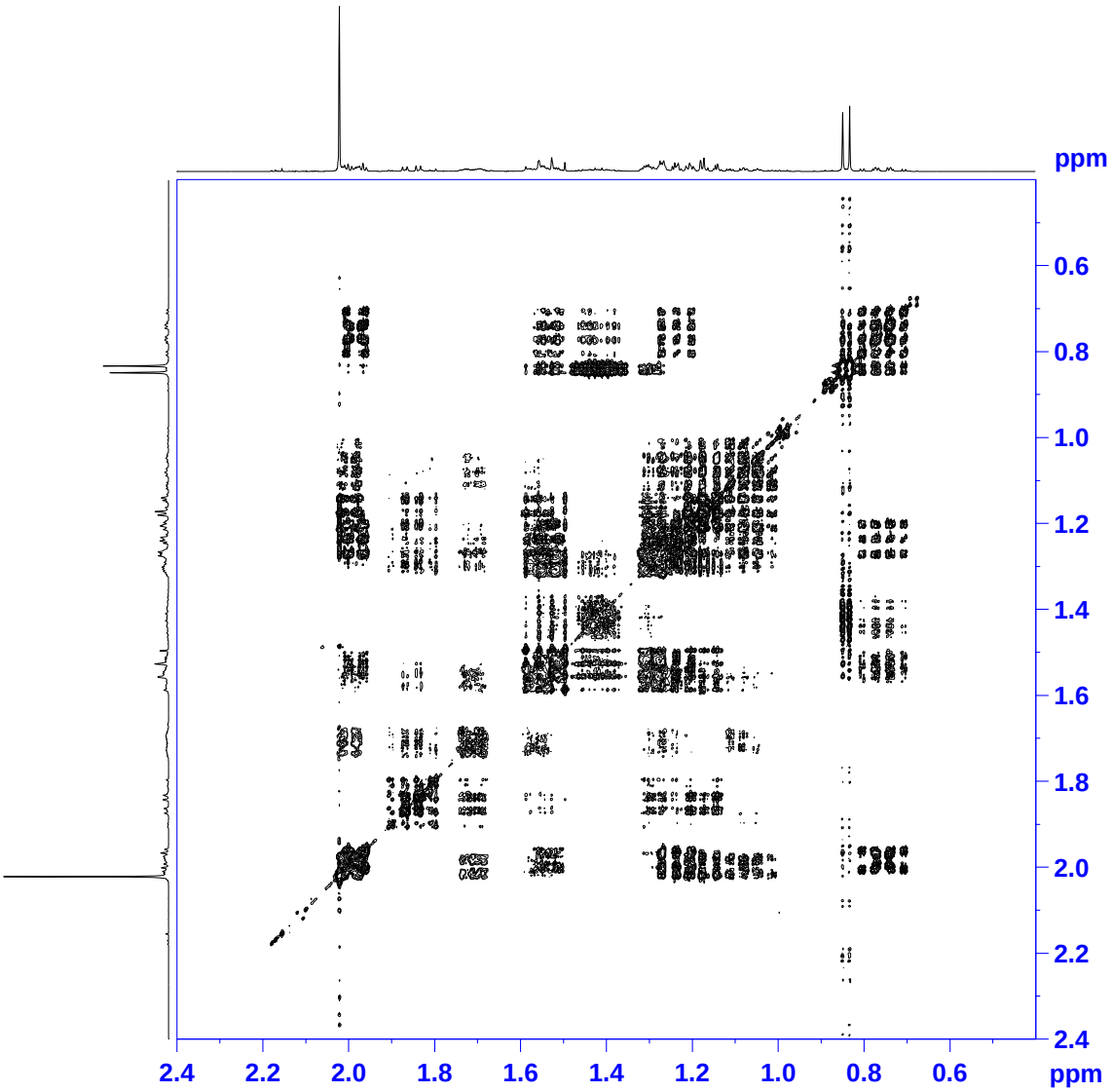


**Figure 31: COSY NMR spectrum of methyl ketone product, 351 (400 MHz, $CDCl_3$).**

The NOESY spectrum shown in Figure 32 has cross-peaks highlighted showing through-space interactions between the proton at 1.42 ppm (methine proton adjacent to methyl group) and 1.17 ppm (ring junction methine proton). It was anticipated that the bicyclic system would be *trans*-configured and adopt the chair-chair conformer, by analogy with previous examples and due to its increased stability over the *cis*-configuration. A lack of cross-peaks between the methine proton at 1.42 ppm and the methyl protons at 2.02 ppm indicates this is likely to be the case. This information indicates the relative stereochemistry of the methyl ketone product is as illustrated in Figure 30.

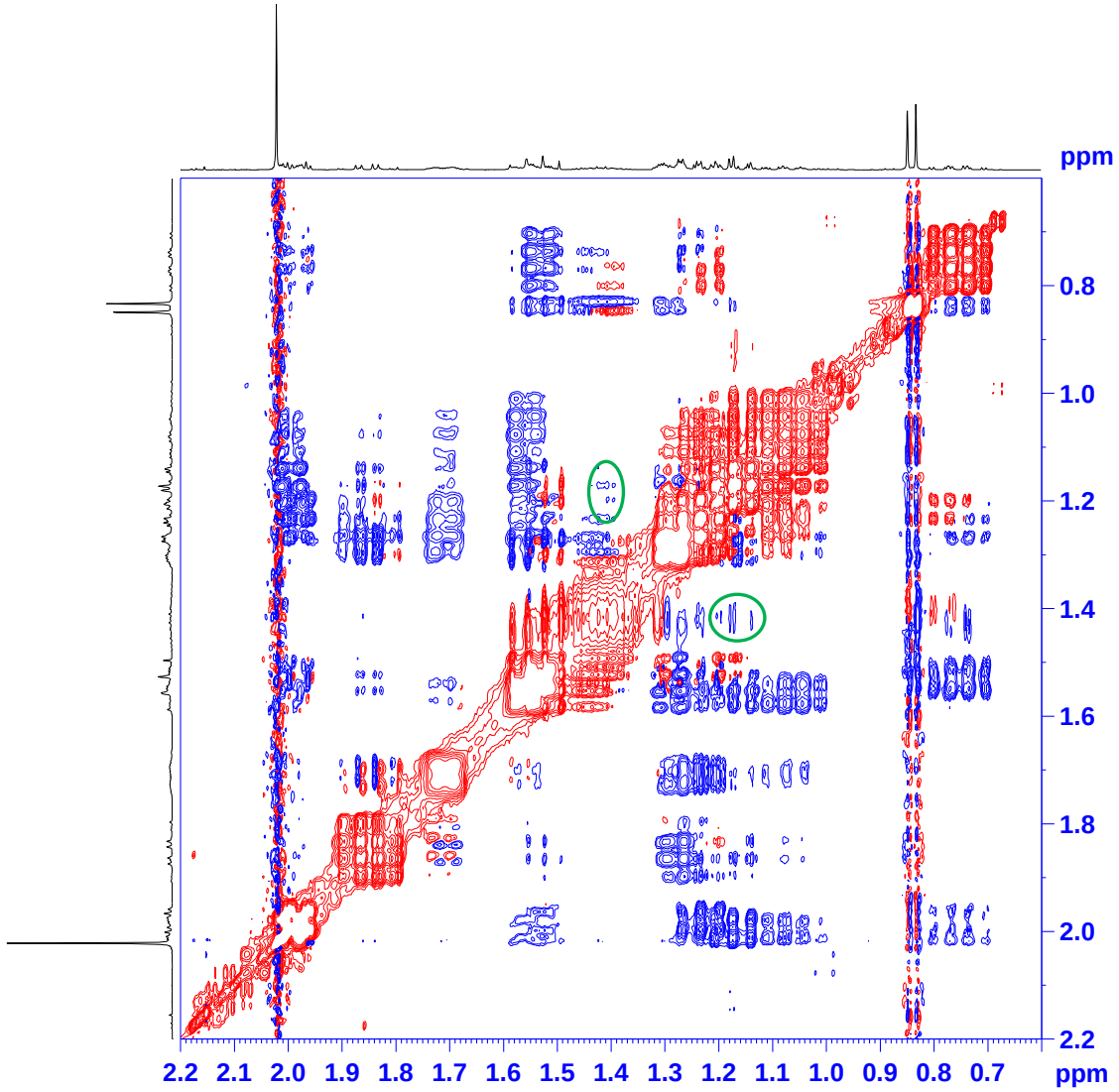


**Figure 32: NOESY NMR spectrum of methyl ketone product, 351 (400 MHz, $CDCl_3$).**

Scheme 104 shows a possible mechanistic explanation for the formation of methyl ketone **351.** It should be reiterated that whilst this was the major product of the reaction and the only compound isolated, it was not the only product formed, so other mechanistic pathways are likely to be occurring.

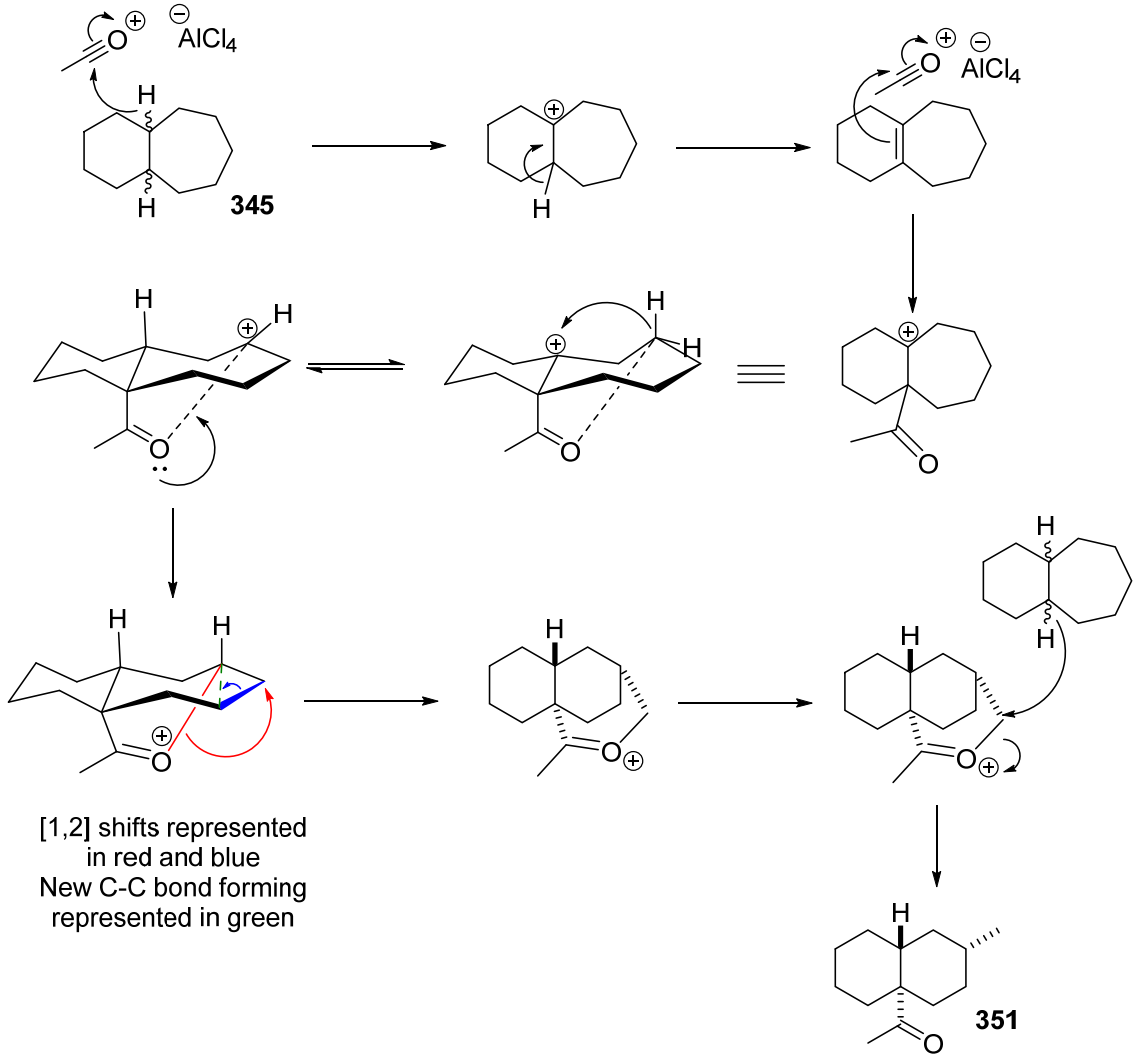


**Scheme 104: Possible mechanistic rationale for formation of 351 from bicyclo[4.5.0]undecane, 345.**

The [1,3]-hydride shift that occurs in preference to a [1,2]-hydride shift in this postulated mechanism also has precendence in the biosynthetic pathway of various terpenes.[136] An example of such a carbocation rearrangement is illustrated in Scheme 105, in the biosynthesis of α-amorphene.[156]

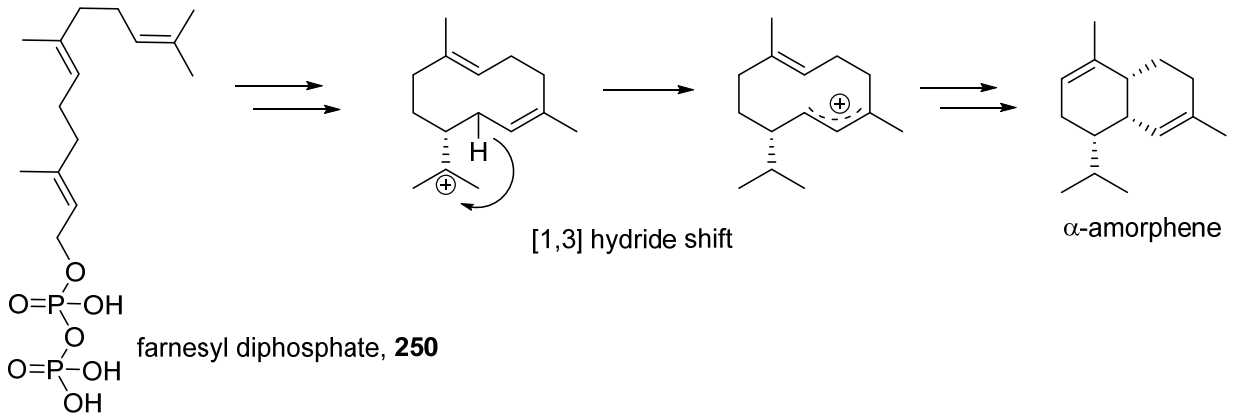


**Scheme 105: An example of a [1,3] hydride shift in one possible pathway towards α-amorphene modelled computationally (mPW1PW91/6-31+G(d,p)//B3LYP/6-31+G(d,p)).[156]**

## 3.6 Isopropylcyclohexane

### 3.6.1 Consideration of Plausible Mechanisms

Isopropylcyclohexane was sourced from TCI as a relatively inexpensive hydrocarbon, presumably due to its formation by reduction of the readily available cumene. It was considered that there was a wider range of products which could be formed from this reaction, due to the presence of two inequivalent tertiary centres.

It would be interesting to observe whether a hydride was more likely to be abstracted from the less hindered tertiary centre in the isopropyl group; although it would have slightly less inductive stabilisation for the carbocation subsequently formed, the cyclohexane would be able to adopt the preferred chair conformation. The other option would be abstraction of a hydride from the tertiary centre in the cyclohexane ring; somewhat more sterically hindered but with more inductive stabilisation for a tertiary carbocation in this position.

Scheme 106 shows the most likely products and their mechanisms of formation, although the list is not exhaustive. Only mechanisms starting with hydride abstraction from a tertiary centre were considered; this seemed a reasonable assumption given the lack of precedent for abstraction from a less substituted position.

Furthermore, on acylation of the double bond with the second equivalent of acylating species, mechanisms which resulted in an intermediate with a tertiary carbocation were deemed most plausible. Those which followed a mechanism containing a secondary or an even less likely primary carbocation are not shown.

Of the remaining mechanisms considered, six of the eight possible products were formed from a tri- or tetrasubstituted alkene intermediate, where there is precedent for both, either in the bicyclohexyl or decalin examples respectively. The remaining two compounds would have to be formed via a disubstituted alkene intermediate. There is no precedent for disubstituted alkene intermediates in the previous examples, but equally there have been no alternate pathways in the mechanisms of the other examples where it would be possible to form a disubstituted alkene, so although this seemed less likely to occur, it was not possible to discount this on the basis of a lack of a precedent.

In the case of isopropylcyclohexane, given the significantly increased number of plausible pathways, it seemed likely a mixture of products from various mechanistic routes could be formed; if this were the case, separating these would likely prove challenging.

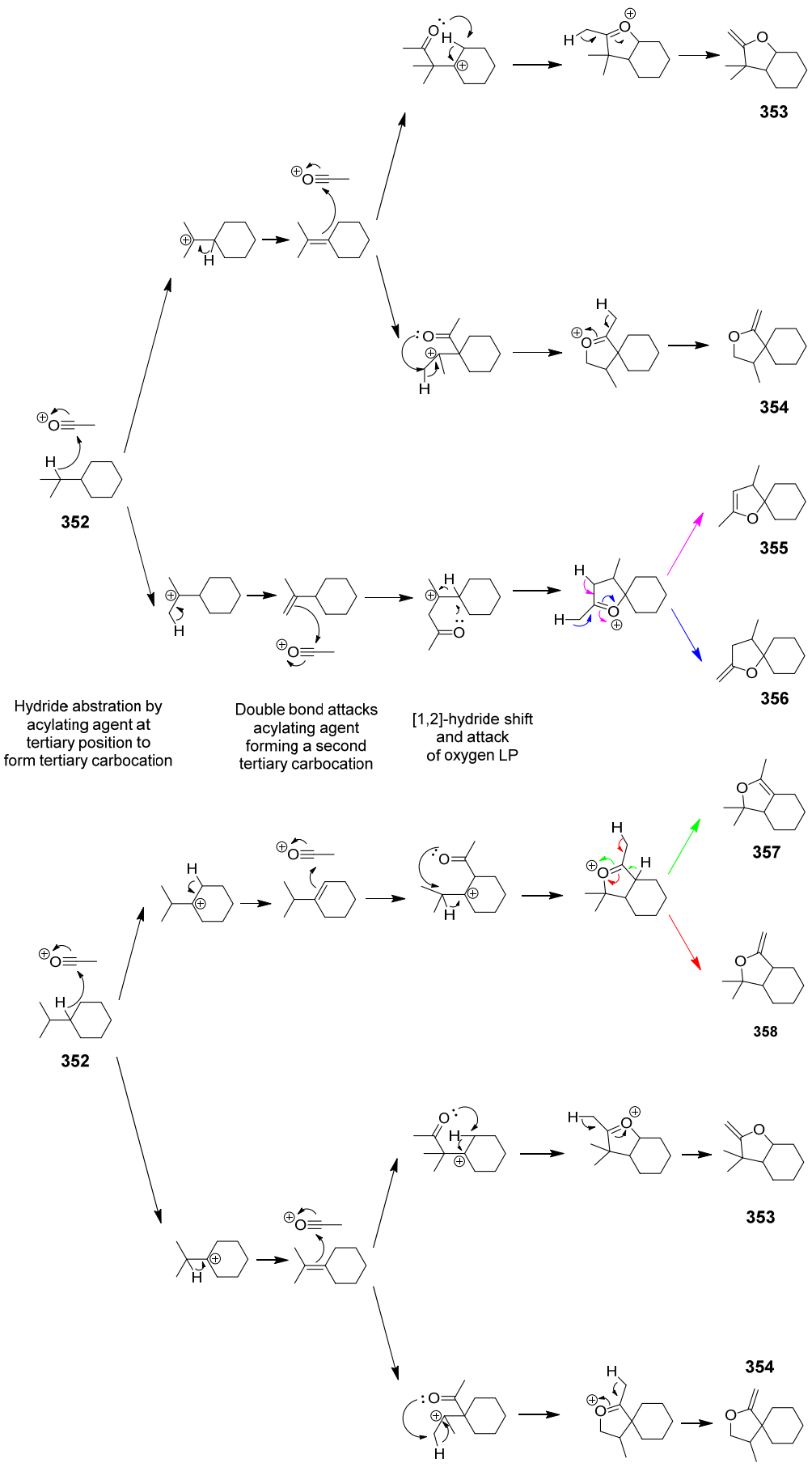


**Scheme 106: A consideration of possible enol ether products from the interaction of isopropylcyclohexane and AcCl:$AlCl_3$**

### 3.6.2 Reaction with Acetyl Chloride and Aluminium Trichloride

On reaction with aluminium trichloride and acetyl chloride, fortunately one major product predominated. It transpired that separation of this compound from the starting isopropylcyclohexane was difficult due to degradation of this enol ether compound on heating. It was however possible to characterise this product as a compound formed from one of the predicted mechanisms, as a mixture with the starting isopropylcyclohexane.

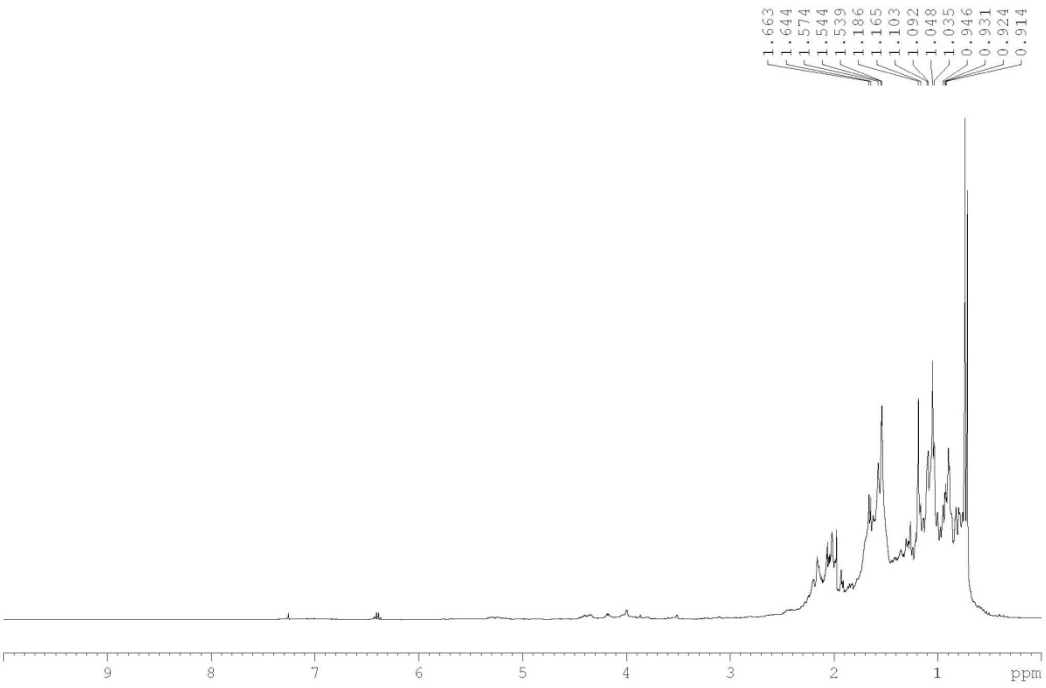


**Figure 33: Proton NMR spectrum of unpurified reaction mixture of isopropylcyclohexane and enol ether product; small quantities of 1-chloroethyl acetate can also be seen.**

No alkenic peaks were seen in the unpurified proton NMR spectrum (Figure 33), which gave a clear indication that either there were no alkenes present in the structure or that the alkenes that were present were tetrasubstituted. The carbon-13 NMR spectrum, seen in Figure 34, showed alkene peaks with chemical shifts which corresponded to the chemical shifts associated with previous enol ether alkenes. The peaks picked in the carbon-13 NMR spectrum do not include those associated with the starting isopropylcyclohexane, for clarity.

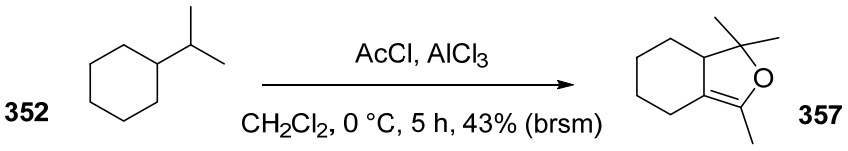


**Scheme 107: Reaction of isopropylcyclohexane with aluminium trichloride and acetyl chloride**

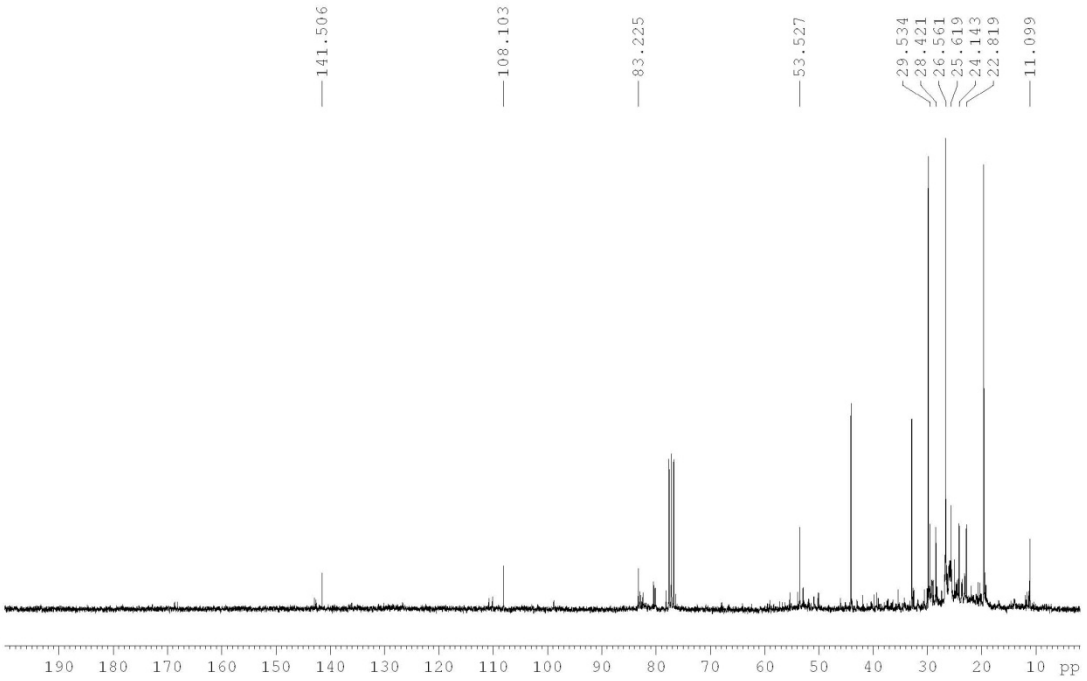


**Figure 34: Carbon-13 NMR spectrum of unpurified reaction mixture of isopropylcyclohexane and enol ether product, 357.**

From this it was possible to conclude that the only feasible mechanism (Scheme 108) was the analogous mechanism to the mechanism observed in the bicyclohexyl reaction. This is not particularly surprising given the similarity of the initial structures.

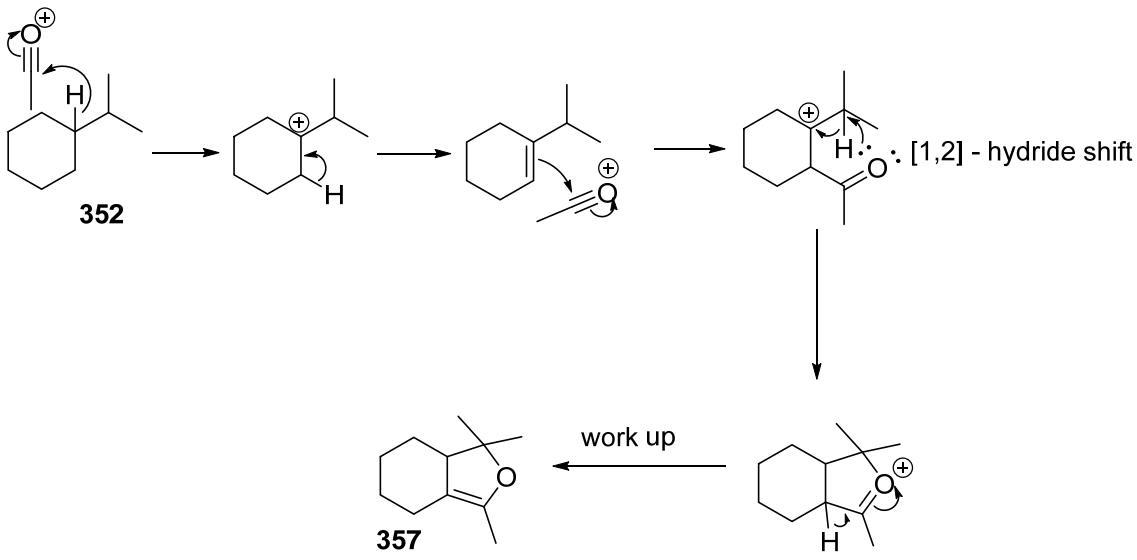


**Scheme 108: Mechanism of formation of enol ether 357 from isopropylcyclohexane.**

## 3.7 Conclusions

Work in this chapter has shown extension of the Baddeley methodology to other fused-ring saturated hydrocarbons, linked-ring saturated hydrocarbons and a monocyclic saturated hydrocarbon with an adjacent tertiary site. These reactions have yielded some novel products and some products previously identified, as well as unexpected mechanistic curiosities highlighting parallels between very similar hydrocarbons.

In the cases of bicyclopentyl and bicyclo[5.3.0]decane, it is unlikely these reactions would be of much synthetic value. Both of these compounds yield the same enol ether as decalin, but in lower yields and are not as inexpensively obtained as starting materials.

It may be that the reactions of bicyclohexyl, bicyclo[5.4.0]undecane and isopropylcyclohexane are of more synthetic use, although ease of ring opening of enol ether products may limit this. Certainly it is clear from this investigation that the enol ether derived from decalin is significantly more stable than it would appear at first glance, as well as more stable than analogous compounds.

# Core Functionalisation of Naphthalenediimides via Iridium Catalysed C-H Activation

## 4.1 Introduction

Naphthalenediimides are compounds with the basic structure shown in Figure 35. They have multiple uses in chemistry[157]; supramolecular chemistry and host-guest interactions,[158,159] dyes,[160] self-assembly of nanotubes[161] and sensors.[162]

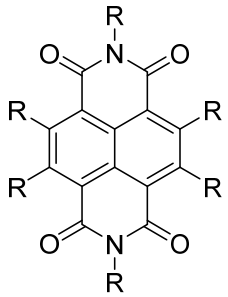


**Figure 35: Structure of naphthalenediimides (NDIs)**

Functionalisation of the core naphthalene rings has proved difficult due to the electron-poor nature of the naphthalene system. Typical methods for obtaining a core-functionalised NDI involve constructing the NDI with the functionalised bonds already in place. Scheme 109 shows a synthesis of 2,6-dichlorinated naphthalenediimides starting from pyrene.[163]

Initial chlorination of pyrene in all *ortho* substituted positions is followed by basic dechlorination to yield two hexachlorinated isomers, which were not separable. Oxidation of one isomer with fuming nitric acid leaving the other isomer untouched allowed for separation of the two compounds.

The single isomer of the hexachlorinated pyrene could then be oxidised to the dichlorinated naphthalene dianhydride. Condensation of this species with two equivalents of primary amine gave the core-dichlorinated naphthalenediimide. Overall, pyrene is converted to a naphthalenediimide in less than 4% yield over the five steps.

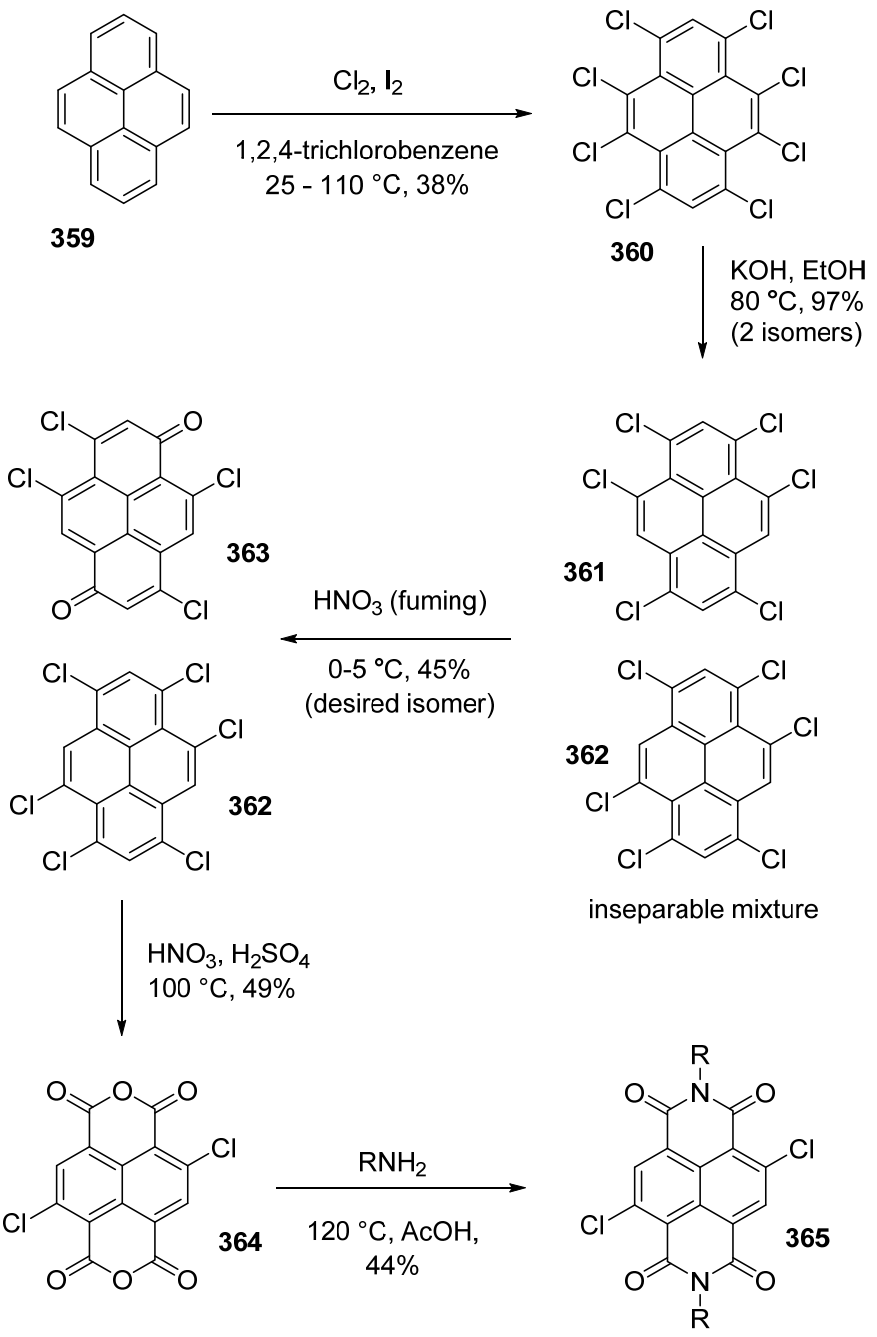


**Scheme 109: Synthesis of dichlorinated naphthalenediimides (R = 2,6-*i*PrC$_6$H$_3$-).**[163, 164]

Further reactions of the 2,6-dichlorinated naphthalenediimide can give access to other functional groups on the core naphthalene rings.[164] Using butylamine and varying the reaction conditions, nucleophilic substitution of either one or both chlorines could occur, to give the secondary amines. Similar selectivity was possible using sodium ethoxide as the nucleophile, to introduce either one or two ether groups.

The authors also found it was possible to take the mono-ether naphthalenediimide and subject it to butylamine at low temperature to substitute the previously untouched chlorine, outlined in Scheme 110.

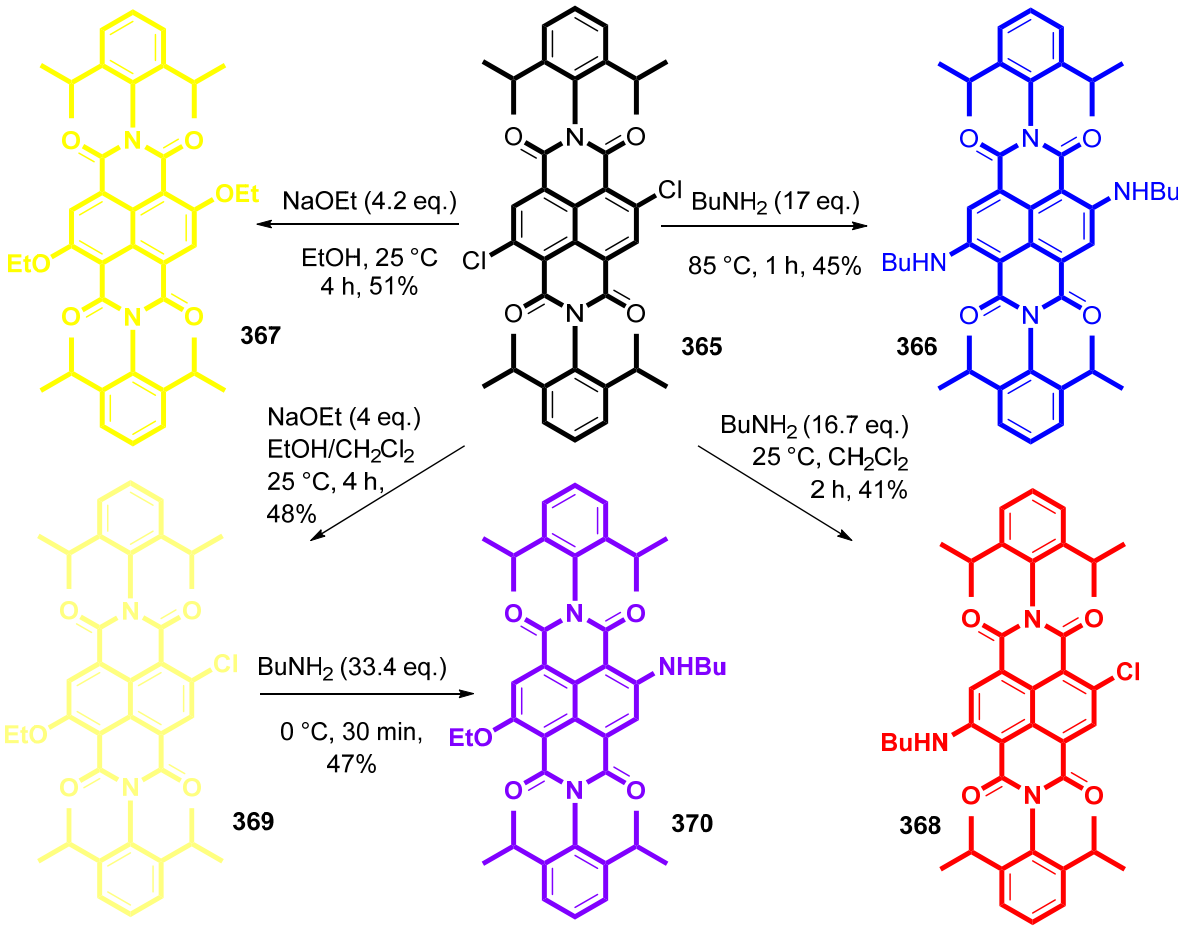


**Scheme 110: Synthesis of various core-functionalised NDIs.**[164]

These similar compounds exhibit a wide variety of optical properties; the starting dichloro NDI is yellowish-white with an absorbance maximum of 402 nm. The optical properties of the amine and ether derivatives are shown in Table 12. The range of optical properties and photoluminesence possible by core-functionalisation of the naphthalenediimides fuels the interest of the community in these molecules for use as fluorescent sensors and electroactive moieties in macromolecules.

| Compound | Colour (solid) | Absorbance max. (nm) |
|---|---|---|
| **366** diamine | Blue | 620 |
| **367** diether | Yellow | 469 |
| **368** mono amine | Red | 535 |
| **369** mono ether | Pale yellow | 440 |
| **370** amine ether | Violet | 552 |

**Table 12: Optical properties of NDIs shown in Scheme 110.**[164]

A more recent synthesis of core-functionalised NDIs is shown in Scheme 111.[165] Using dibromoisocyanuric acid as a brominating reagent in sulphuric acid at 130 °C, a 15 hour reaction time gives quantitative yield of one isomer of dibrominated naphthalenediimide. Unfortunately, due to poor solubility of the 2,6-dibromo naphthalene dianhydride, the following step to install the imide functionality only gave a 28% yield.

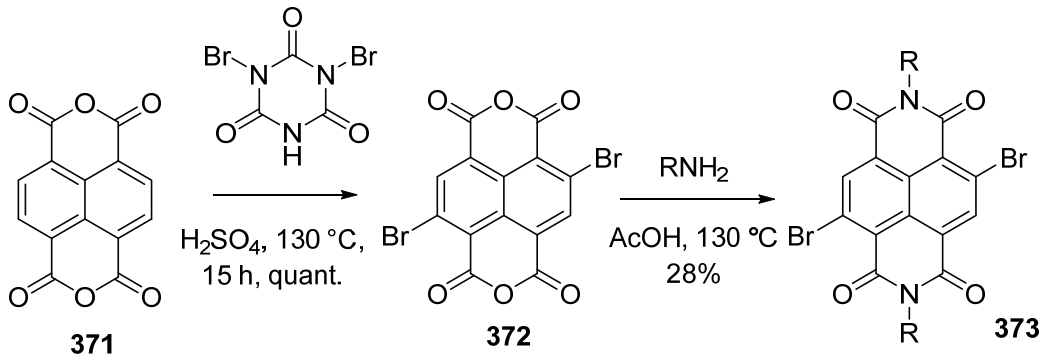


**Scheme 111: Synthesis of dibrominated naphthalenediimides (R- = $CH_3(CH_2)_7$-).**[165]

Having bromine substituents on the naphthalene core rather than chlorines gives scope for conversion into a wider range of functional groups. Use of aryl bromides in Suzuki or Stille couplings for example gives access to carbon-carbon bonds. These possibilities have been exploited in recent literature.[165,166]

Although it was possible to use the aryl chlorides in Suzuki couplings, the lengthy and low-yielding syntheses of the aryl chlorides was undesirable and the aryl bromides gave better yields in all examples.[166]

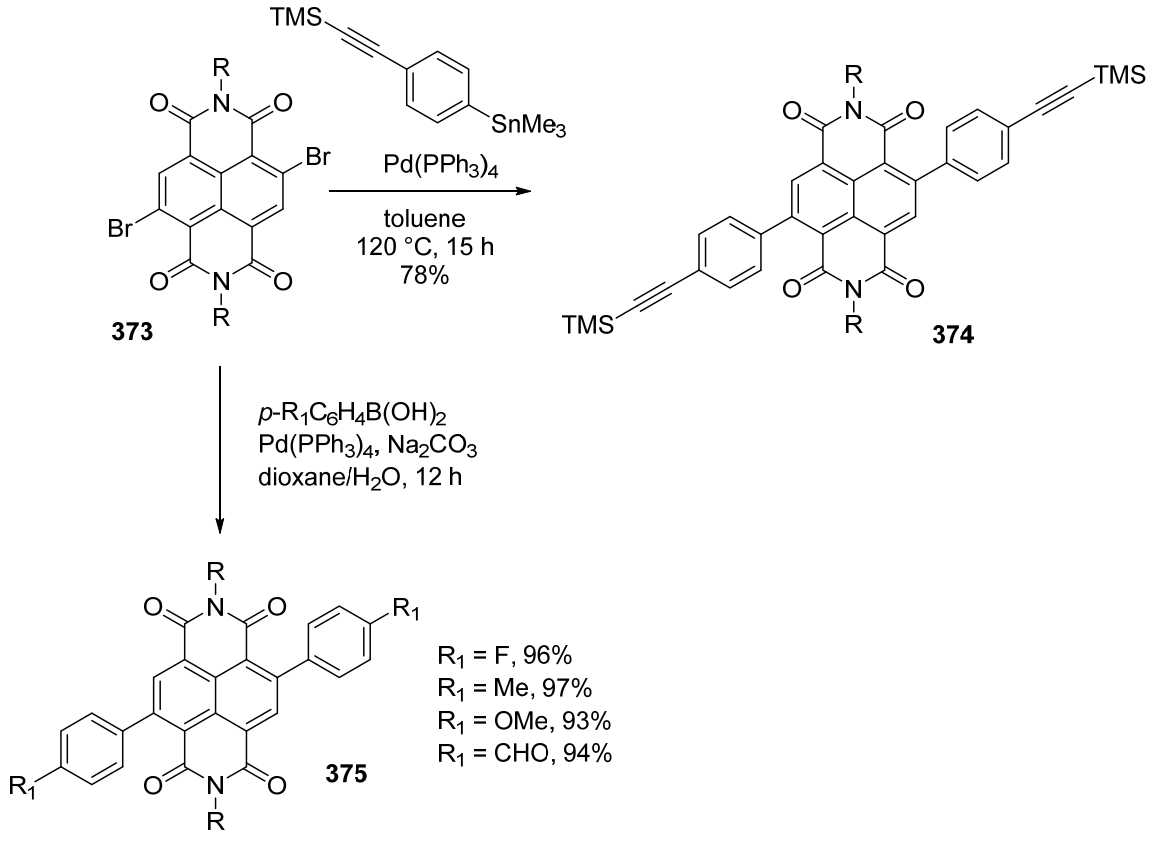


**Scheme 112: Use of 2,6-dibromo NDIs in Suzuki and Stille couplings (R- = $CH_3(CH_2)_7$-).**[165,166]

A mixture of mono-substituted and 2,6-di-brominated naphthalenediimides could be obtained by reacting naphthalene dianhydride with bromine and iodine in oleum, which were not separated, and subsequently condensing the brominated NDAs obtained with the relevant

amine, which were separated. The authors substituted the bromine(s) for nitrile groups using copper cyanide.[167]

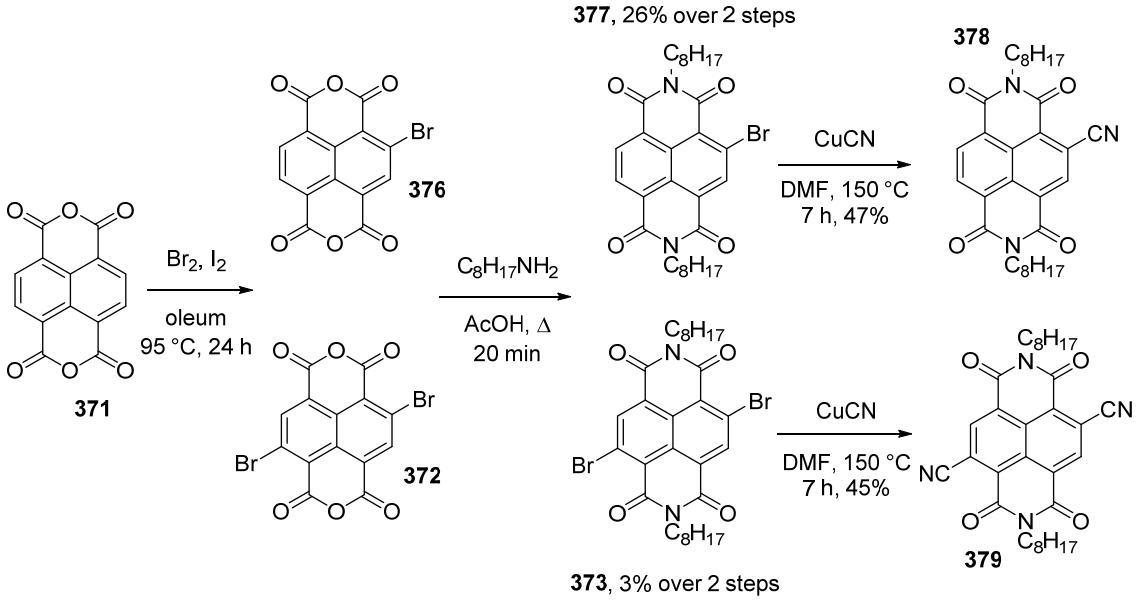


**Scheme 113: Functionalisation of NDA with bromine**[167]

This bromination technique was applied by Qian and coworkers to form core-perfluoroalkylated NDIs, over several steps.[168]

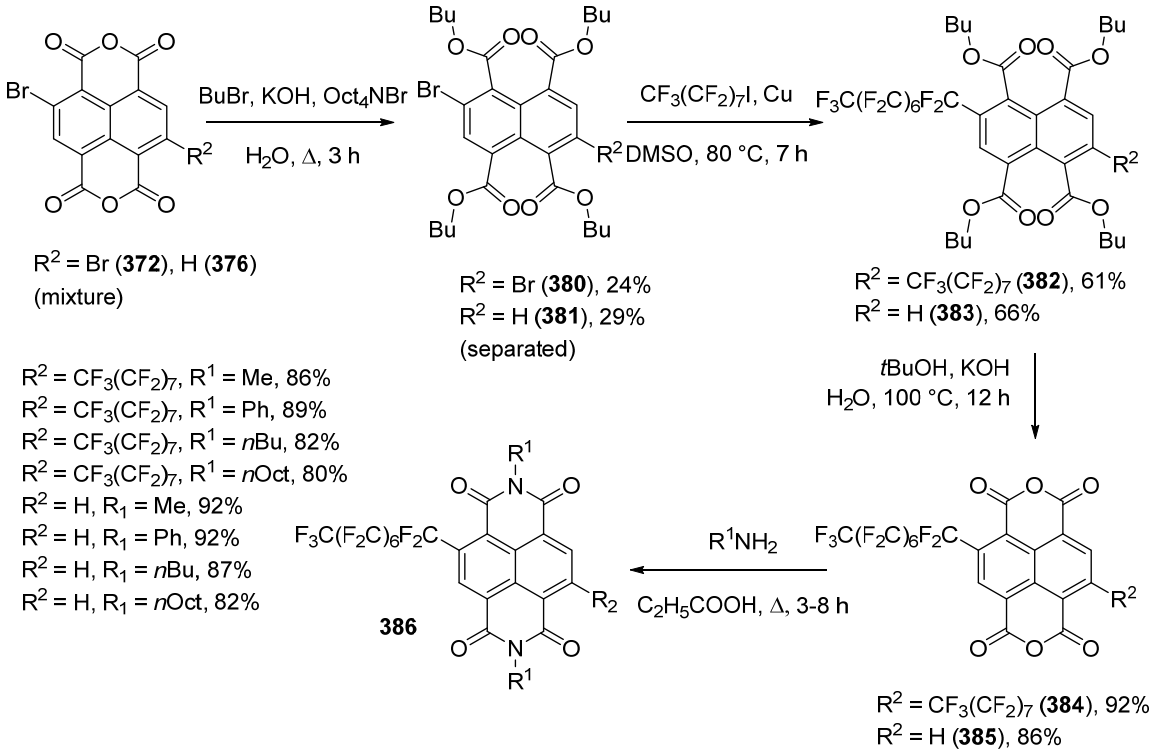


**Scheme 114: Synthesis of core-perfluoroalkylated NDIs.**[168]

It is worth noting that whilst mono-functionalised and di-functionalised NDIs have been synthesised, the only significant example of efficient synthesis of functionalisation in the 2,7-positions rather than the 2,6-positions is shown in Scheme 115.[169] This work provided a mixture of isomers via ruthenium catalysed C-H activation and was based on the previously reported C-H activation of the analogous perylenediimides.

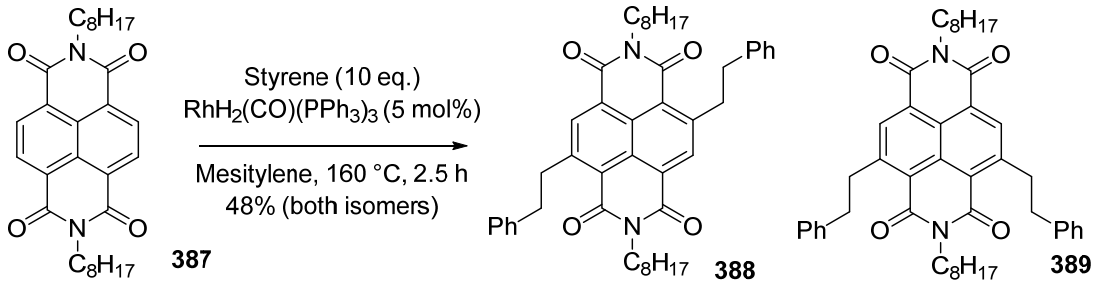


**Scheme 115: Ruthenium catalysed C-H activation of the NDI core carbon-hydrogen bonds.[169]**

Perylenediimides have a similar structure to the naphthalenediimides, but possess a perylene core rather than a naphthalene core. It has been possible to functionalise the core carbon-hydrogen bonds of the perylenediimides directly using C-H activation. [170,171]

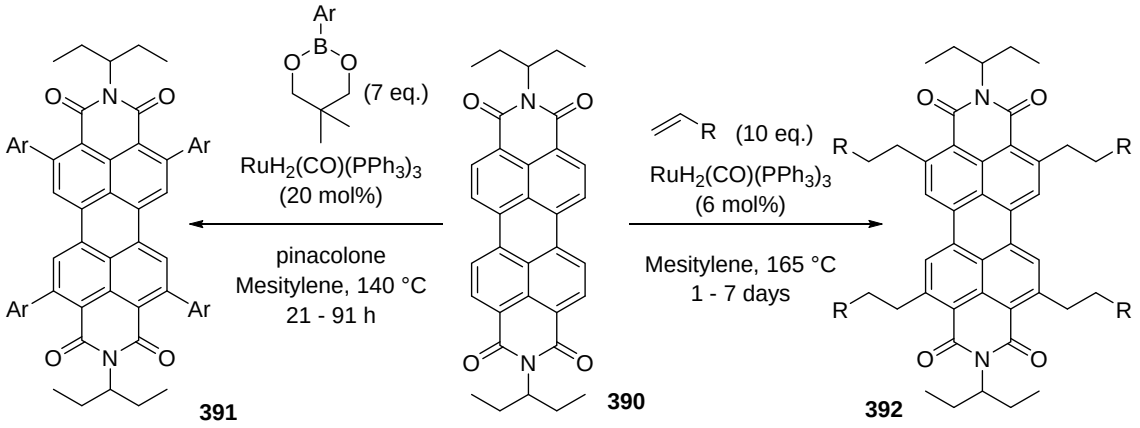


Ar = Ph,83%
Ar = *p*-$MeOC_6H_4$, 83%
Ar = *p*-$CF_3C_6H_4$, 75%
Ar = *p*-$MeC_6H_4$, 69%
Ar = *p*-$BrC_6H_4$, 12%

R = $SiMe_3$, 94%
R = $C_4H_9$, 50%
R = Cy, 69%
R = $Si(OMe)_3$, 95%

**Scheme 116: C-H activation of PDIs using ruthenium catalysis.[170,171]**

It had been observed in the literature more recently that it was possible to functionalise the carbon-hydrogen bonds of the perylene core of the perylenediimides (PDIs) via iridium catalysed C-H borylation as outlined in Scheme 117.[172] A similar synthesis using ruthenium catalysis was published shortly afterwards.[173]

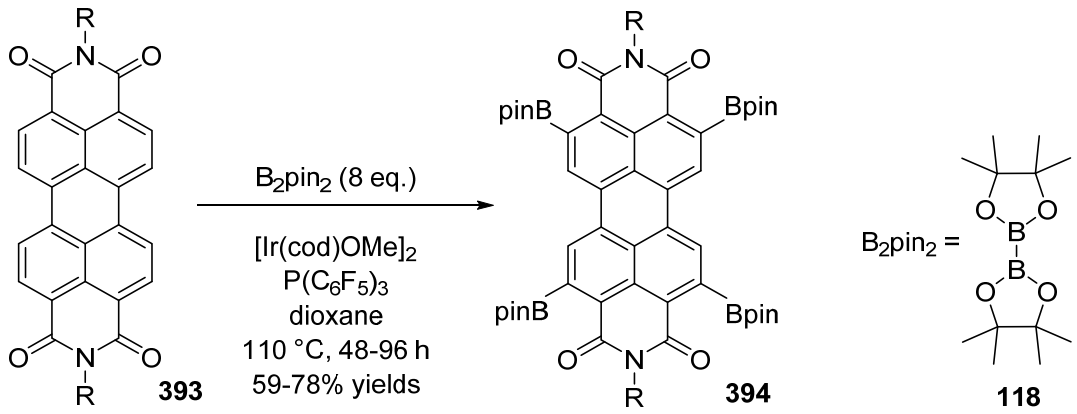


**Scheme 117: C-H activation of perylenediimides via iridium catalysed borylation.[172]**

This chapter details efforts to functionalise the carbon-hydrogen bonds of the naphthalene core via iridium catalysed C-H borylation.

## 4.2 Synthesis of Core-Unfunctionalised Naphthalenediimides

The synthesis of naphthalenediimides has been known for many decades. The general method for forming symmetrical NDIs involves condensing naphthalene-1,4,5,8-tetracarboxylic dianhydride (NDA) with two equivalents of primary amine. These reactions are carried out at high temperatures, as seen in Scheme 118.


**Scheme 118: Synthesis of symmetrical NDIs from condensation of NDA with primary amines under thermal heating conditions.**

More recently, the reaction has been studied under microwave conditions, shortening the reaction time to just five minutes in some cases.[174,175] This has significantly increased the ease with which these compounds can be accessed.

Using both of these techniques, several symmetrical naphthalenediimides were synthesised from NDA and the relevant amines.

| Amine | NDI product | Yield |
|---|---|---|
| 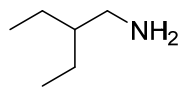 **396** | 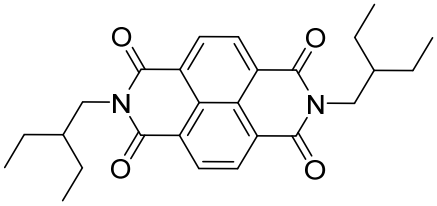 **397** | 91% |
| 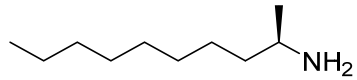 **398** | 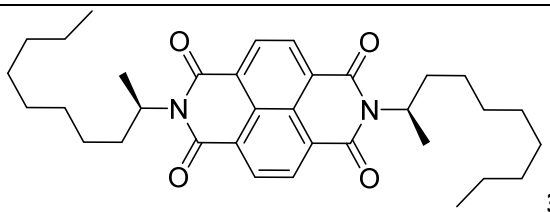 **399** | 93% |
| 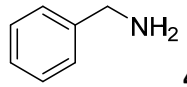 **400** | 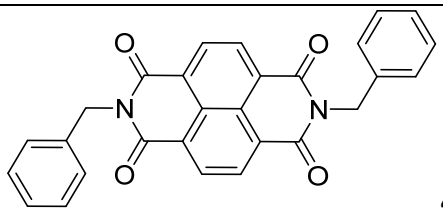 **401** | 96% |

**Table 13: NDIs synthesised for attempts at core C-H functionalisation.**

Non-symmetrical NDIs can also be synthesised, but require a stepwise procedure. Basic hydrolysis with potassium hydroxide of the NDA is performed to form naphthalene-1,4,5,8-tetracarboxylic acid; this compound can then be converted to the monoanhydride via pH adjustment to pH 6.2-6.4 and reaction with one equivalent of a primary amine, yielding the naphthalene dicarboxylic acid. The dicarboxylic acid can then be converted to the NDI by means of heating at a higher temperature with one equivalent of a different primary amine.

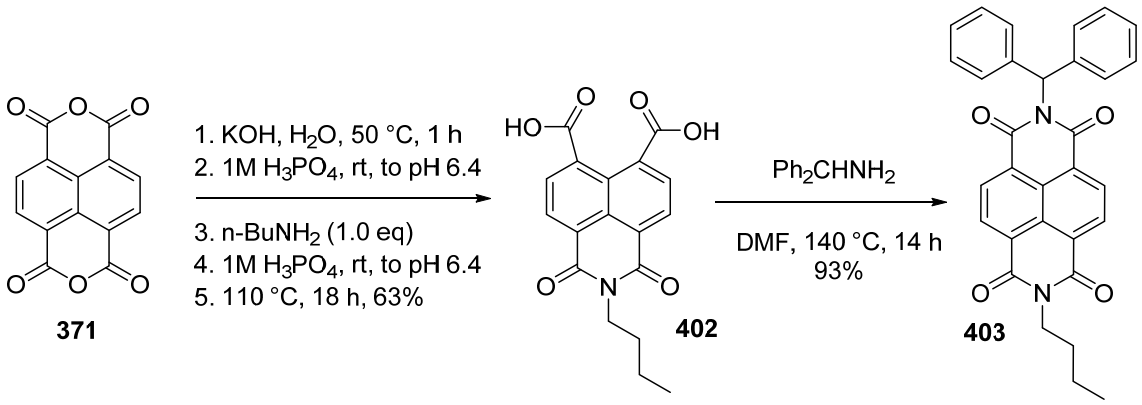


**Scheme 119: Synthesis of asymmetrical NDI with butyl group and benzhydryl group, 403.**

Initial attempts at condensation of benzhydrylamine with the naphthalene dianhydride in the first step were unsuccessful, leading to a mixture of compounds. Further reaction of this mixture of compounds with butylamine gave no significant amount of the desired naphthalenediimide, so the order of addition was converted to that shown in Scheme 119.

## 4.3 Functionalisation of the Naphthalene C-H Bonds

### 4.3.1 Optimisation of Reaction Conditions

It was thought that similar C-H activation methodology should be applicable to the naphthalenediimides as well as the perylenediimides, although it was not expected that a tetra-substituted naphthalene core would be formed due to the steric hindrance of the boronic ester. Once one core carbon-hydrogen bond was borylated, it seemed likely that the adjacent C-H bond would be too inaccessible and the regioselectivity in C-H borylation with iridium catalysis is often controlled by steric factors.

In the first instance, it was desirable to apply the methodology from the perylenediimides to naphthalenediimides, but there were some drawbacks to this methodology that would be useful to address.

The reaction time for C-H functionalisation of the perylene core of the PDIs was between 48 and 96 hours; it would be significantly better if this reaction could be performed within the working hours of one day, ideally within a few hours.

The PDI functionalisation reaction uses eight equivalents of bis(pinacolato)diboron where theoretically four should be the maximum required. In fact, based on the mechanism proposed for this type of reaction, if pinacolborane is able to act as a borylating reagent under these reaction conditions then one equivalent of bis(pinacolato)diboron should be able to borylate two C-H bonds; two equivalents of bis(pinacolato)diboron would be sufficient for this reaction.

Finally, use of dioxane as a solvent is not desirable, as it is a potential carcinogen and like other ethers, may form peroxides on extended contact with air. In optimising this reaction, it would be ideal to establish use of a safer solvent.

The methodology was initially applied to the NDI shown in Scheme 120. This reaction yielded a mixture of unfunctionalised NDI, **397**, mono-borylated NDI, **404**, and a 1:1 ratio of two isomers of di-borylated NDI, **405** and **406**.

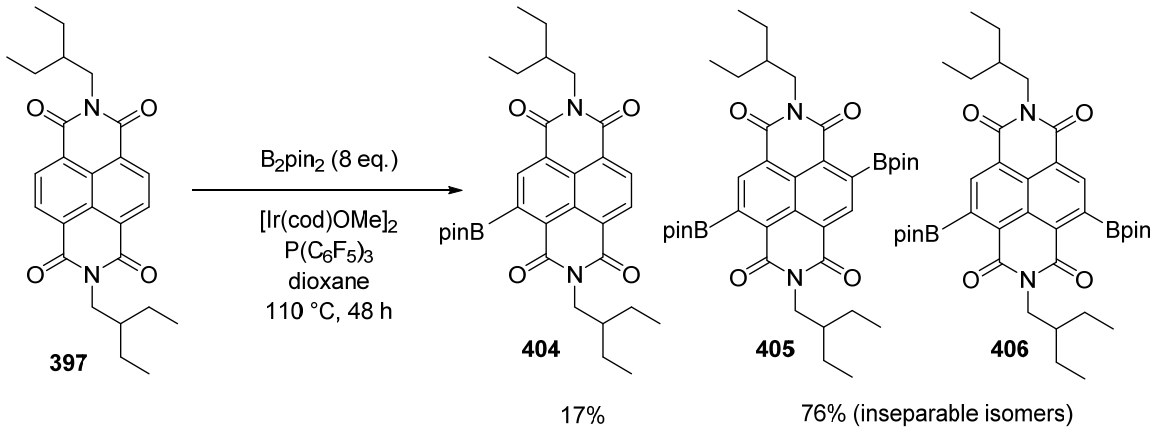


**Scheme 120: Application of PDI C-H borylation to a symmetrical NDI, 397.**

Reducing the reaction time to 24 hours gave a substantially reduced conversion to the diborylated material – 64% diborylated isomers and 28% of the monoborylated isomer. Use of

four equivalents of $B_2pin_2$ with 48 hours of conventional heating in dioxane had reduced the conversion to 25% diborylated isomers and 50% of the monoborylated isomer.

Use of a different solvent was considered, although the nature of the reaction meant the chosen solvent would have to fit within several criteria.

- No aryl carbon-hydrogen bonds. Due to the C-H activation occurring in the reaction, it was considered the solvent could be borylated in preference to the substrate. Common aromatic solvents such as toluene, benzene and pyridine were ruled out.
- No ligating ability. If the solvent were to ligate to iridium in preference to the ligands or reagents, this could affect the catalytic cycle or turnover. *N,N*-dimethylformamide and similar solvents could therefore be discounted.
- High boiling points were desirable. Although the use of microwave heating in a sealed tube allows solvents to be heated above their boiling points under pressure, it would be less hazardous to use a solvent with a medium to high boiling point initially. Diethyl ether, tetrahydrofuran, pentane and hexane would not meet this criterion.
- Ideally, the solvent would be easy to use under microwave conditions. It should either have a dipole moment or an easily induced dipole moment, in order to be efficiently heated.
- The naphthalenediimides (and of course other reagents) should be soluble in the solvent. NDIs tend to be more soluble in aromatic solvents, so these should be considered, the restrictions of the first criterion notwithstanding.
- Non-carcinogenic. The solvent used to replace dioxane should be less hazardous than dioxane.
- Conversion of substrate into product would need to be at least as high as with dioxane as the solvent.

With these restrictions in mind, it was considered that an aromatic solvent with no aryl carbon-hydrogen bonds would be ideal, but options were limited. Fully substituted benzene rings tend to have higher melting points than room temperature, for example, hexamethylbenzene has a melting point of 166 °C.[176] However, it seemed that hexafluorobenzene may be a suitable option.

Attempting the reaction using hexafluorobenzene as the solvent resulted in a similar conversion to dioxane (18% monoborylated and 76% diborylated products), so subsequent reactions were performed in this solvent.

In order to reduce the reaction time, it seemed that use of microwave heating could be beneficial. Strangely, using the same reaction conditions, but under microwave heating in dioxane at 110 °C for 14 hours, no reaction was observed.

Increasing the reaction temperature to 140 °C in hexafluorobenzene however did allow the reaction to proceed, in just two hours, with 84% conversion to diborylated material and 7% conversion to monoborylated material – better conversions to those observed after 48 hours with conventional heating.

Use of half the equivalents of bis(pinacolato)diboron was attempted as well; the prior functionalisation of perylenediimides had used eight equivalents of $B_2pin_2$ to functionalise four carbon-hydrogen bonds of the perylenediimide core. By analogy, it stood to reason that four

equivalents of $B_2pin_2$ should be able to functionalise two carbon-hydrogen bonds of the naphthalenediimide core. Reducing the amount of $B_2pin_2$ to four equivalents gave a 12% conversion to monoborylated product and 85% conversion to diborylated material.

A variety of ligands were used, the results of which are shown in Table 14. It was found that the phosphine ligands were significantly more effective than nitrogen based ligands. Triphenylphosphine gave a lower conversion to diborylated NDI than the perfluorinated ligand $P(C_6F_5)_3$; use of $P(C_6F_5)_3$ as the ligand was continued in subsequent optimisation.

| Ligand | Conversion to monoborylated NDI | Conversion to diborylated NDI | Total conversion |
|---|---|---|---|
| 2,2-bipy 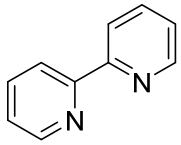 | 0% | 0% | 0% |
| 4,4,-ditertbutyl-2,2-bipy 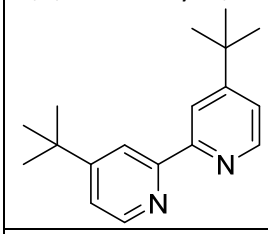 | 6% | 0% | 6% |
| $PPh_3$ 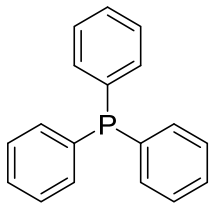 | 44% | 35% (1:1 ratio) | 79% |
| $P(C_6F_5)_3$ 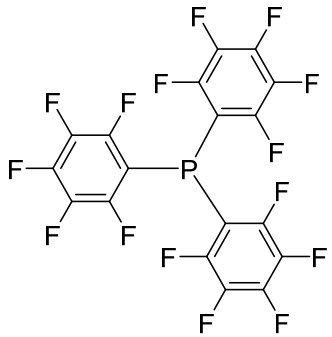 | 12% | 85% (1:1 ratio) | 97% |

**Table 14: Screening of ligands, using 4.0 eq. of $B_2pin_2$ and starting NDI 397 in $C_6F_6$. Conversions are calculated from 1H NMR integrations.**

At this point, the reaction was carried out using fewer equivalents of bis(pinacolato)diboron. Although high proportions of borylated material could be obtained using only two equivalents of $B_2pin_2$ (90%) the majority was monoborylated product; the results are outlined in Table 15. It was decided that in order to obtain maximum quantity of the diborylated NDI, the equivalents of $B_2pin_2$ used should remain at four equivalents.

| Equivalents of $B_2pin_2$ | Conversion to monoborylated NDI, **404** | Conversion to diborylated NDI (1:1, **405**:**406**) | Total conversion |
|---|---|---|---|
| 4.0 | 12% | 85% | 97% |
| 3.0 | 22% | 75% | 97% |
| 2.0 | 48% | 42% | 90% |
| 1.0 | 36% | 9% | 45% |

**Table 15: Screening of equivalents of $B_2pin_2$, using $P(C_6F_5)_3$ and starting NDI 397 in $C_6F_6$. Conversions are calculated from $^1$H NMR integrations.**

### 4.3.2 Separation of Products

Using silica gel column chromatography with dichloromethane and ethyl acetate eluent graduated from 0% to 10% ethyl acetate, it was possible to separate the starting naphthalenediimide, the mono-borylated naphthalenediimide and the di-borylated naphthalenediimides. Various solvent systems were used for silica gel column chromatography and in all cases residual $B_2pin_2$ "streaking" down the column was problematic, leaving a mixture of $B_2pin_2$ and product. On performing column chromatography more than once, it was possible to reduce the residual $B_2pin_2$ to a minimal amount.

Recrystallisation was attempted from acetonitrile and was partially successful, especially in cases where a significant proportion of unfunctionalised NDI remained; the unfunctionalised NDI would crystallise out of solution. Once conversion of the reaction was at over 90% this technique was less useful.

Unfortunately, separation of the two diborylated isomers (**405** and **406**) also proved challenging, as they co- eluted in all solvent systems used.

### 4.3.3 Use of Various N-substituted Naphthalenediimides

The optimised reaction was applied to several naphthalenediimides as seen in Table 16. As expected, using a different *N*-alkyl chain resulted in similar conversions.

Using an *N*-aryl group however, gave a lower conversion to the diborylated NDI. It is postulated that the phenyl rings and the naphthalene core may be able to attempt to "stack" and enhance π-π interactions, which may result in the naphthalene core being less available for borylation as the phenyl groups inhibit access.

It was pleasing to discover that no borylation of the phenyl rings occurred; borylation was limited only to the core naphthalene carbon-hydrogen bonds, despite these being more sterically hindered.

| Starting NDI | Conversion to monoborylated NDI | Conversion to diborylated NDI | Total conversion |
|---|---|---|---|
| 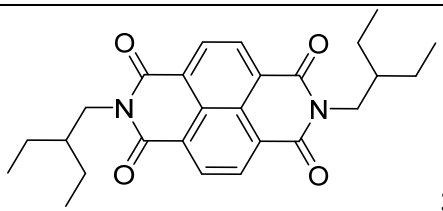 **397** | 12% (**404**) | 85% (1:1, **405**:**406**) | 97% |
| 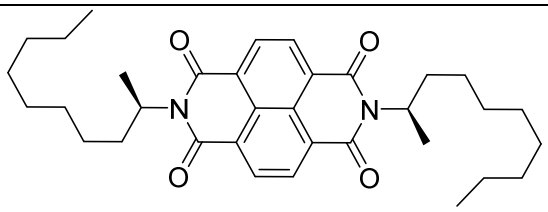 **399** | 16% (**407**) | 81% (1:1, **408**:**409**) | 97% |
| 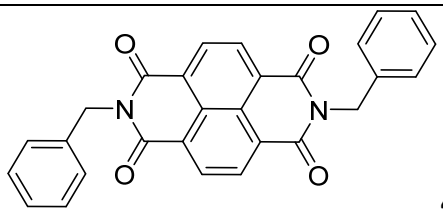 **401** | 42% (**410**) | 48% (1:1, **411**:**412**) | 90% |

**Table 16: Conversions of different NDI starting materials to borylated NDIs. Conversions are calculated from $^{1}$H NMR integrations.**

The reaction was then applied to NDI **403**, where the two R-groups attached the nitrogens were inequivalent. It was hoped that the bulky benzhydryl functionality could retard borylation at the two proximal carbon-hydrogen bonds and only form a single 2,7-substituted isomer, as seen in Scheme 121. The hydrogens shown in green represent those that would not be sterically hindered by the benzhydryl group and would therefore be accessible for CH-borylation. Those positions shown in red would be more hindered and less likely to be borylated.

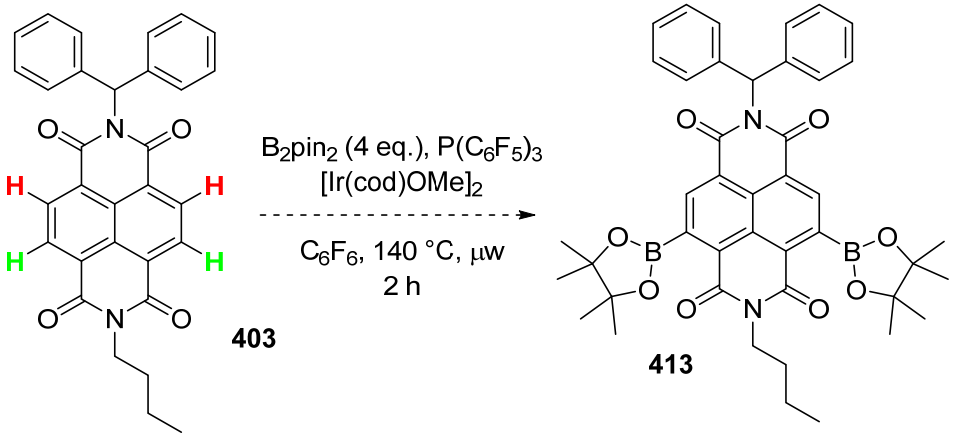


**Scheme 121: Reaction showing possible major isomer, 413, if steric hindrance of benzhydryl group is a factor, where hydrogens shown in red will be hindered and those shown in green will be more easily accessed.**

Alternatively, Scheme 122 shows the potential outcome if the benzhydryl group does not influence the regioselectivity of borylation in any way. In this case, there is an equal likelihood

that the first borylation will be of a carbon-hydrogen bond proximal to the butyl group or a carbon-hydrogen bond proximal to the benzhydryl group.

The second borylation would then occur at one of the non-adjacent positions, as access to the adjacent carbon-hydrogen bond is now inhibited by the steric bulk of the pinacolato group; this lack of reactivity has been seen in all previous examples of activation of the NDI core.

This would result in a statistical 1:2:1 mixture of isomers **413**:**416**:**417**.

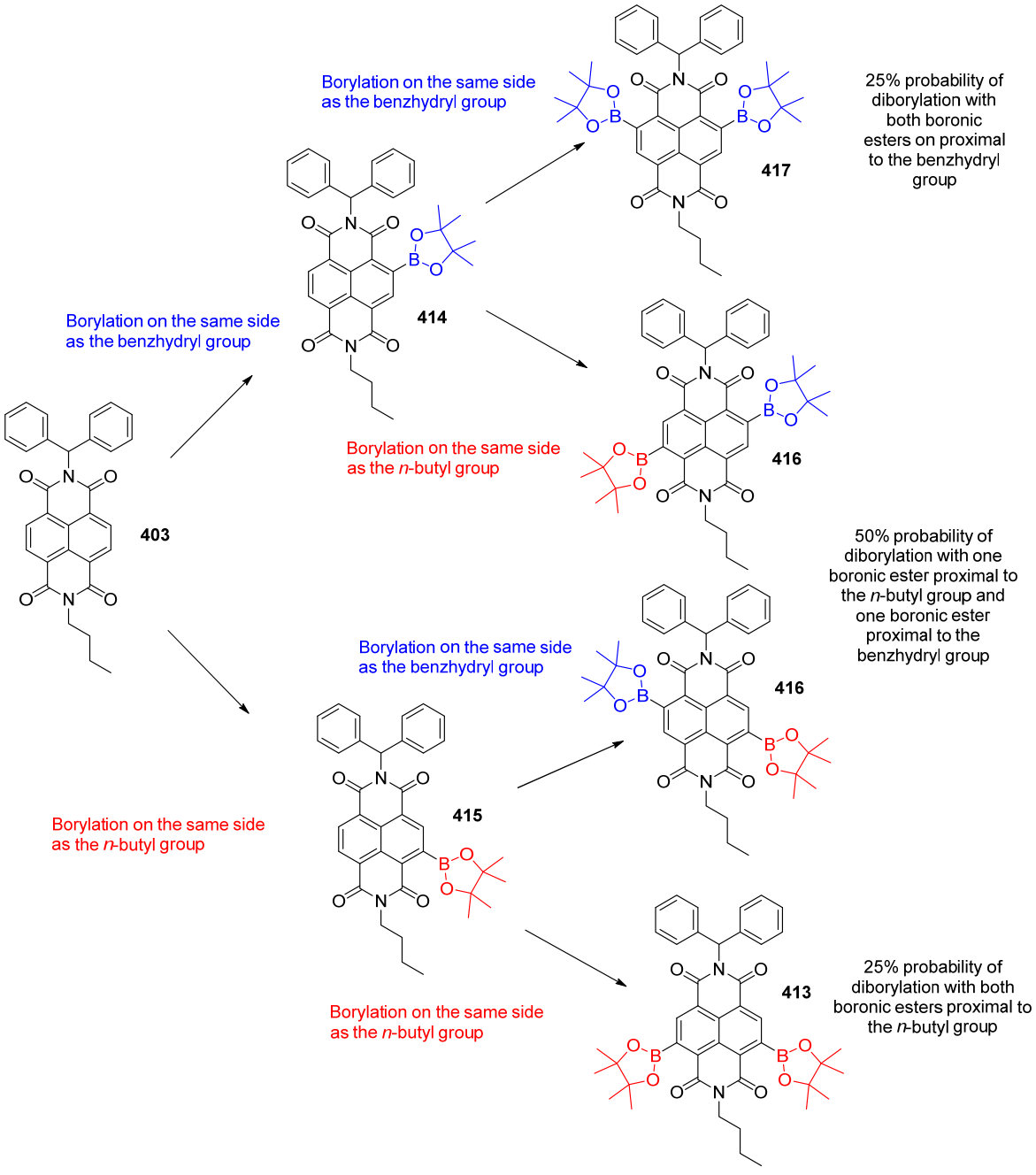


**Scheme 122: Statistical likelihood of product formation, assuming that no steric hinderance is caused by the presence of the benzhydryl group**

It transpires that the formation of products follows the statistical probabilities illustrated in Scheme 122, and no steric or electronic effect is discernable from use of the bulky benzhydryl group.

However, these di borylated isomers of the non-symmetrical NDI were somewhat separable via silica gel column chromatography and could be characterised, although small quantities of the other isomers remained (≈ 15%); this was a major advantage over use of symmetrical NDIs.

As the isomers were not crystalline and were synthesised in small quantities only, it seemed it may be possible to determine the location of the Bpin groups via HMBC NMR analysis, rather than attempts at recrystallisation and subsequent X-ray crystallography.

Three-bond HMBC correlations might be seen between the carbonyl carbons and the NDI core protons. The carbonyl carbons would also correlate to either the distinctive -C*H*$_2$N- group or the Ph$_2$C*H*N- group, allowing determination of which imide group contained the butyl group and which contained the benzhydryl group.

With compound **416**, it was anticipated that there would be four carbonyl environments due to the substitution of Bpin groups onto the core naphthalene and the lack of symmetry in the structure. The HMBC interactions that were observed are outlined in Figure 36 and Figure 37.

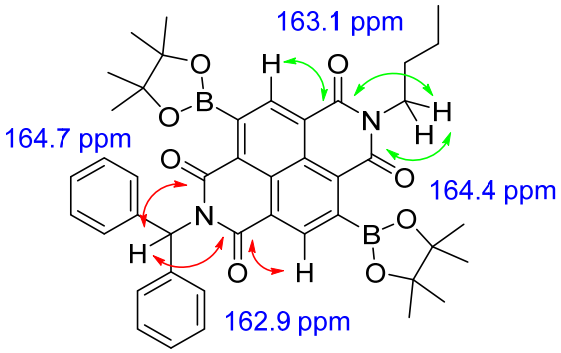


**Figure 36: Compound 416 showing HMBC interactions in red between protons and carbonyls in the *N*-benzhydryl imide and in green between protons and the *N*-butyl imide.**

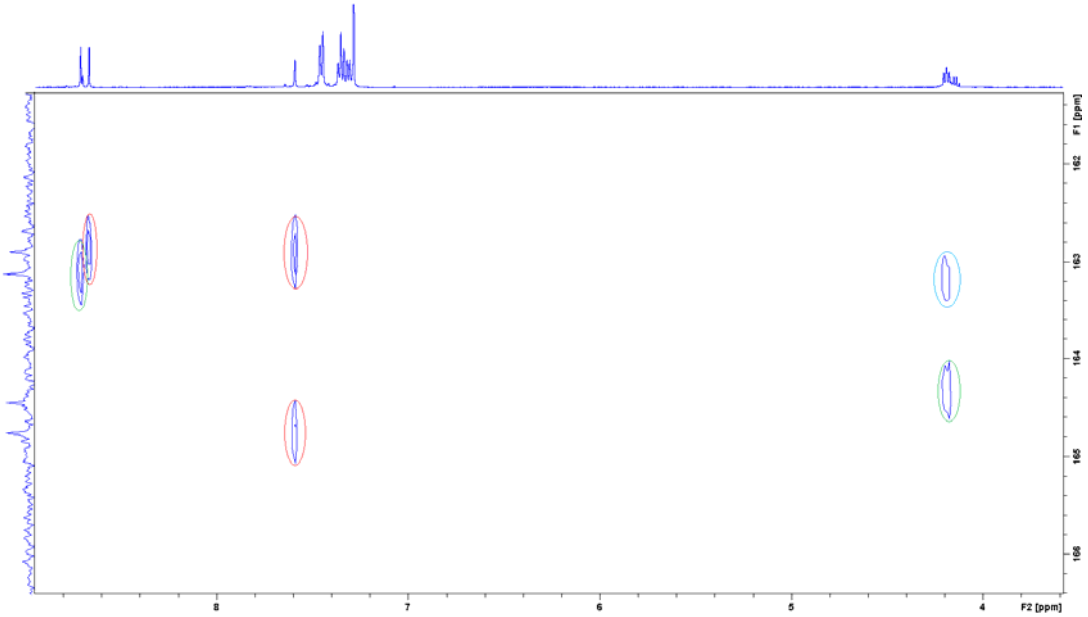


**Figure 37: HMBC NMR data for compound 416 showing the carbonyl region from 161-166 ppm in the carbon-13 axis (y) and 3.8-9.0 ppm in the proton axis (x). Correlations marked in green show interactions between protons and carbonyls on the *N*-butyl imide and those in red show interactions between protons at carbonyls on the *N*-benzhydryl imide.**

In the cases of compounds **413** and **417**, it was expected that there would be two carbonyl environments; where both carbonyls in the *N*-butyl imide group would be in the same environment and both carbonyls in the *N*-benzhydryl imide group would be in the same environment, due to the plane of symmetry in the molecules.

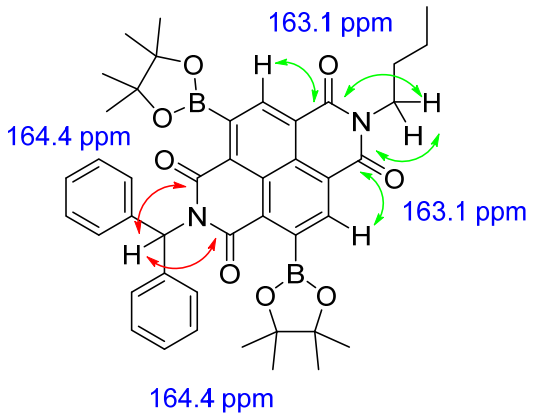


**Figure 38: Compound 417 showing HMBC interactions in red between protons and carbonyls in the *N*-benzhydryl imide and in green between protons and the *N*-butyl imide.**

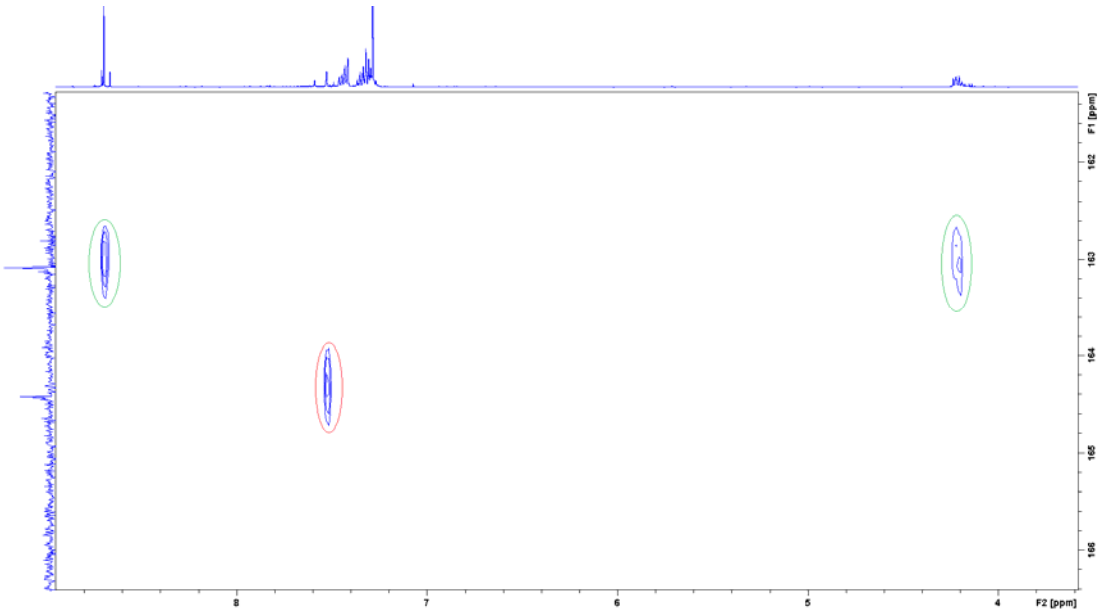


**Figure 39: HMBC NMR data for compound 417 showing the carbonyl region from 161-166 ppm in the carbon-13 axis (y) and 3.8-9.0 ppm in the proton axis (x). Correlations marked in green show interactions between protons and carbonyls on the *N*-butyl imide and those in red show interactions between protons at carbonyls on the *N*-benzhydryl imide.**

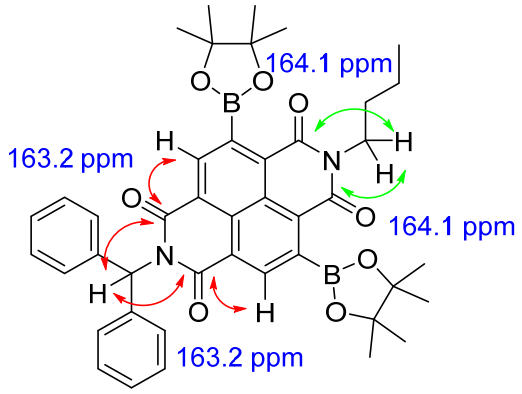


**Figure 40: Compound 413 showing HMBC interactions in red between protons and carbonyls in the *N*-benzhydryl imide and in green between protons and the *N*-butyl imide.**

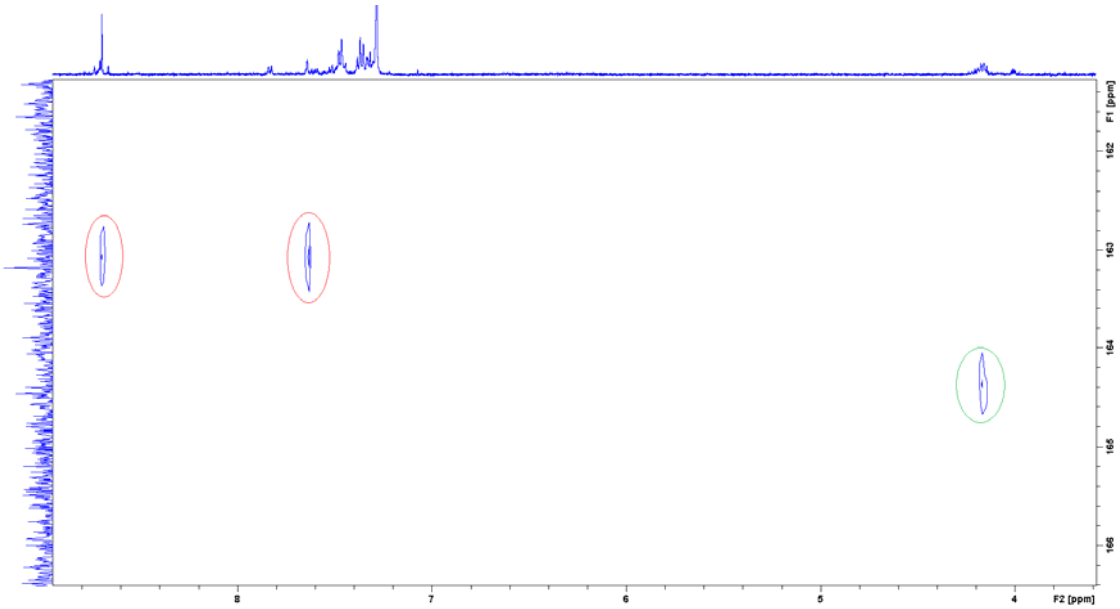


**Figure 41: HMBC NMR data for compound 413 showing the carbonyl region from 161-166 ppm in the carbon-13 axis (y) and 3.8-9.0 ppm in the proton axis (x). Correlations marked in green show interactions between protons and carbonyls on the *N*-butyl imide and those in red show interactions between protons at carbonyls on the *N*-benzhydryl imide.**

In the carbon-13 NMR spectrum of **413**, the peak at δ = 164.1 ppm unfortunately cannot be picked out due to the weak signal-to-noise ratio, but its presence is inferred from the cross-peak observed in the more sensitive HMBC experiment.

It was not possible to isolate any mono-borylated compounds from the C-H activation of **403**, but due to the overlapping peaks in the unpurified $^{1}$H NMR spectrum it would not be possible to say conclusively that none were formed in small quantities.

It was possible to unambiguously assign the separated diborylated isomers **413**, **416** and **417** using analysis of the HMBC spectra. Carbon-13 signals from carbon atoms adjacent to boron atoms were seen as broad peaks or not at all, due to the fast relaxation time which occurs when next to quadrupolar nuclei.

## 4.4 Attempts at C-H Activation of 1,4,5,8-tetracarboxylicnaphthalene dianhydride (NDA)

It was considered that it would be useful to activate directly the carbon-hydrogen bonds on the core naphthalene of NDA, **371**. This would give scope for producing a large quantity of mono or di borylated NDA which could then be transformed into diverse NDIs, including NDIs that may not be able to be borylated directly.

The major problem with any reactions of NDA is its insolubility. The compound is soluble in acetic acid and *N*,*N*-dimethylformamide at high temperatures, but these solvents are unlikely to be suitable for the C-H activation reaction.

Nonetheless, multiple reactions were attempted using hexafluorobenzene, dioxane and DMF as the solvents at up to 200 °C (under microwave heating with DMF). No conversion was observed with any of these reaction conditions.

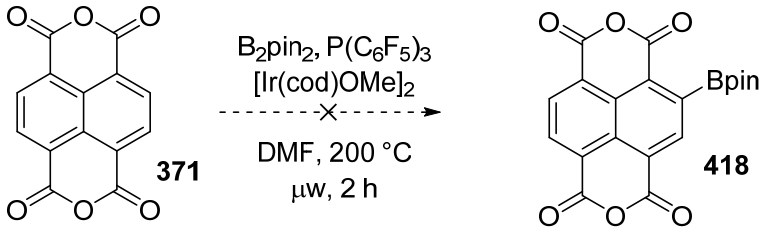


**Scheme 123: Attempted C-H borylation of NDA**

## 4.5 Further Reactions of the Borylated Naphthalenediimides

It was decided that to demonstrate the synthetic utility of the core-borylated naphthalenediimides, the molecules should be subjected to further derivatisations to convert the Bpin groups into other functionality.

Key reactions to attempt included Suzuki couplings and oxidations. The reactions would be attempted using mono-functionalised NDIs for simplicity, and also using the di-substituted NDIs that were able to be separated from other isomers, **413**, **416** and **417**.

Due to the comparatively high conversion of the *N*,*N*'-dibenzyl NDI, **401**, to the mono-borylated compound, **410** would be used as a starting NDI for Suzuki couplings, the general reaction scheme is shown in Scheme 124.[173]

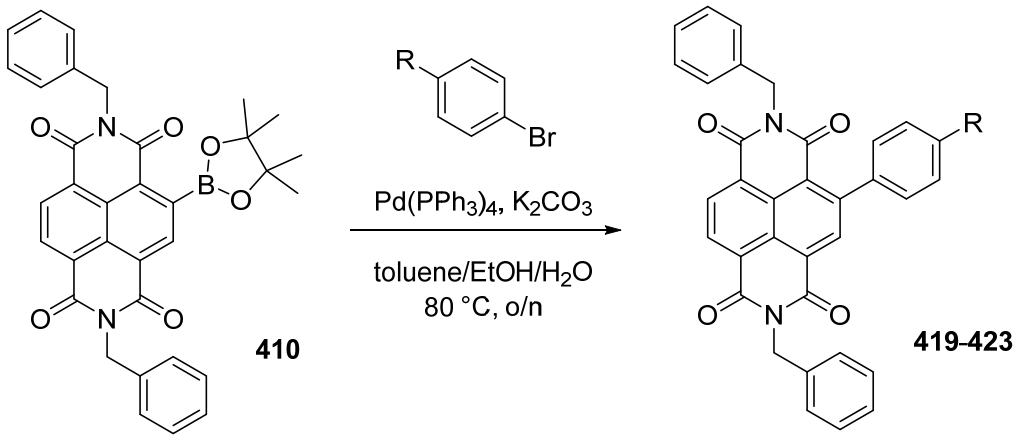


**Scheme 124: General scheme for Suzuki couplings.**[173]

Different *para*-substituted bromobenzenes were used as the Suzuki coupling partners; the results of these reactions are shown in Table 17. The reactions proceeded in moderate to good yield, with both electron withdrawing and electron donating substituents.

| ArBr coupling partner | Yield |
|---|---|
| 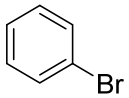 | 81% (**419**) |
| 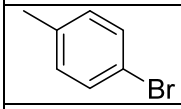 | 56% (**420**) |
| 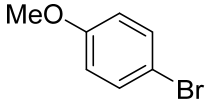 | 68% (**421**) |
| 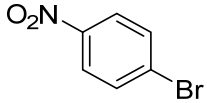 | 73% (**422**) |
| 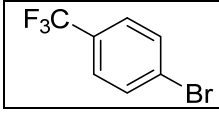 | 69% (**423**) |

**Table 17: Use of *para*-substituted bromobenzenes as coupling partners in the Suzuki reaction**

Suzuki reactions were also performed on the diborylated isomers of the non-symmetrical NDI, as illustrated in Scheme 125.

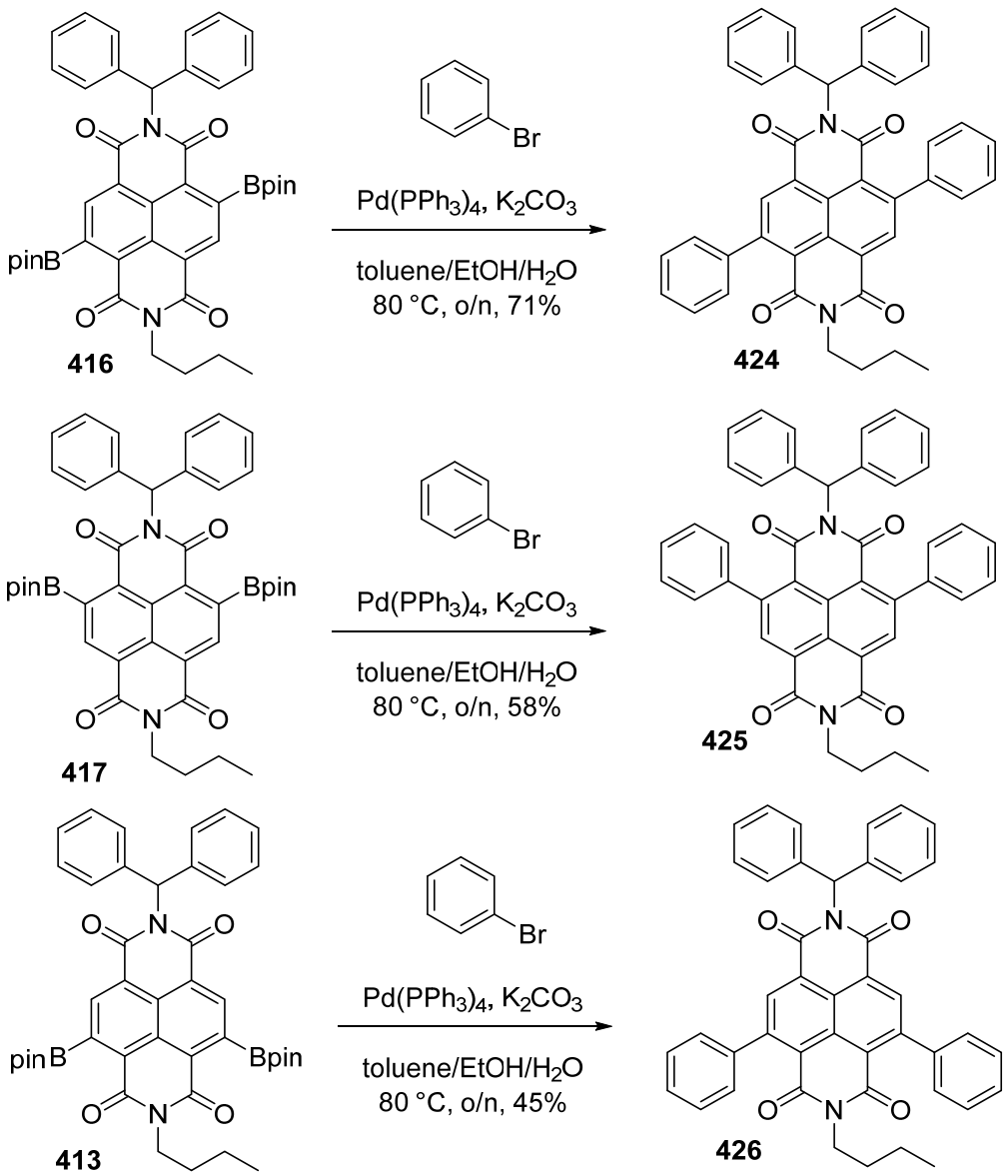


**Scheme 125: Suzuki reactions of diborylated NDI isomers**

In order to confirm the identity of the Suzuki products, HMBC NMR spectra were acquired and analysed for these compounds.

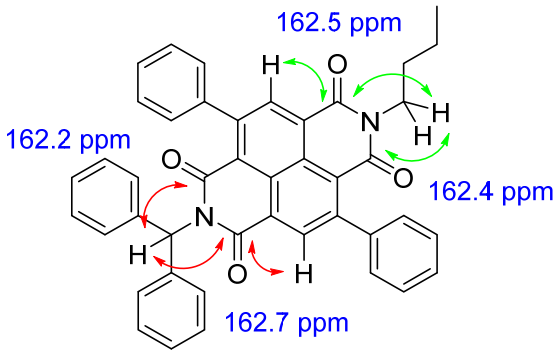


**Figure 42: Compound 424 showing HMBC interactions in red between protons and carbonyls in the *N*-benzhydryl imide and in green between protons and the *N*-butyl imide.**

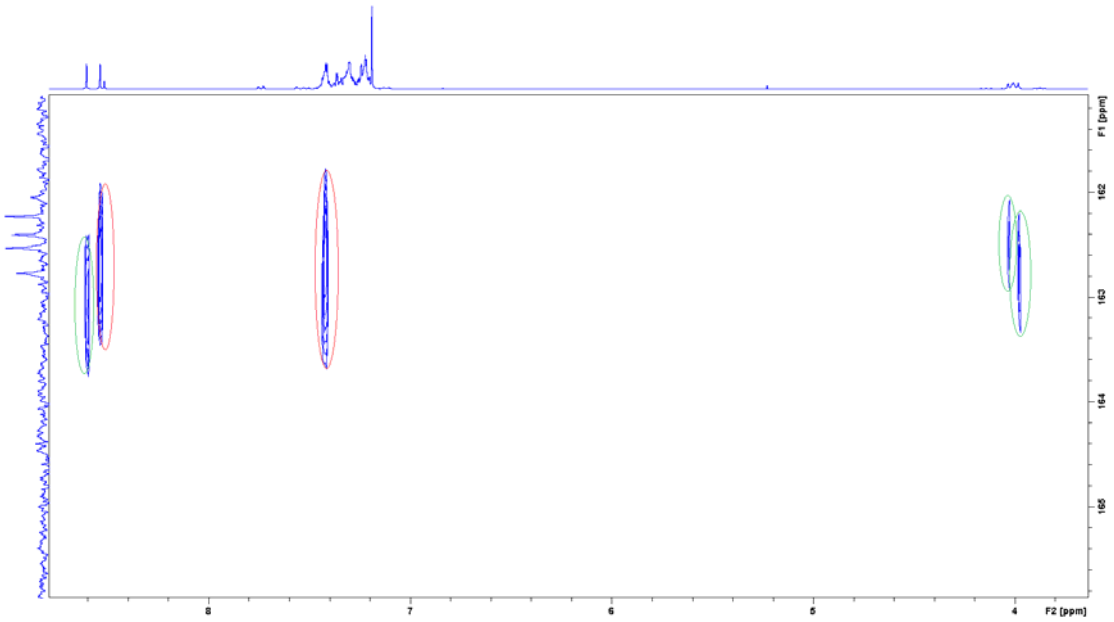


**Figure 43: HMBC NMR data for compound 424 showing the carbonyl region from 161-166 ppm in the carbon-13 axis (y) and 3.8-9.0 ppm in the proton axis (x). Correlations marked in green show interactions between protons and carbonyls on the *N*-butyl imide and those in red show interactions between protons at carbonyls on the *N*-benzhydryl imide.**

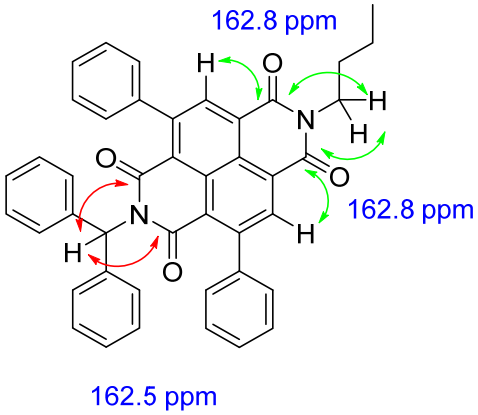


**Figure 44: Compound 425 showing HMBC interactions in red between protons and carbonyls in the *N*-benzhydryl imide and in green between protons and the *N*-butyl imide.**

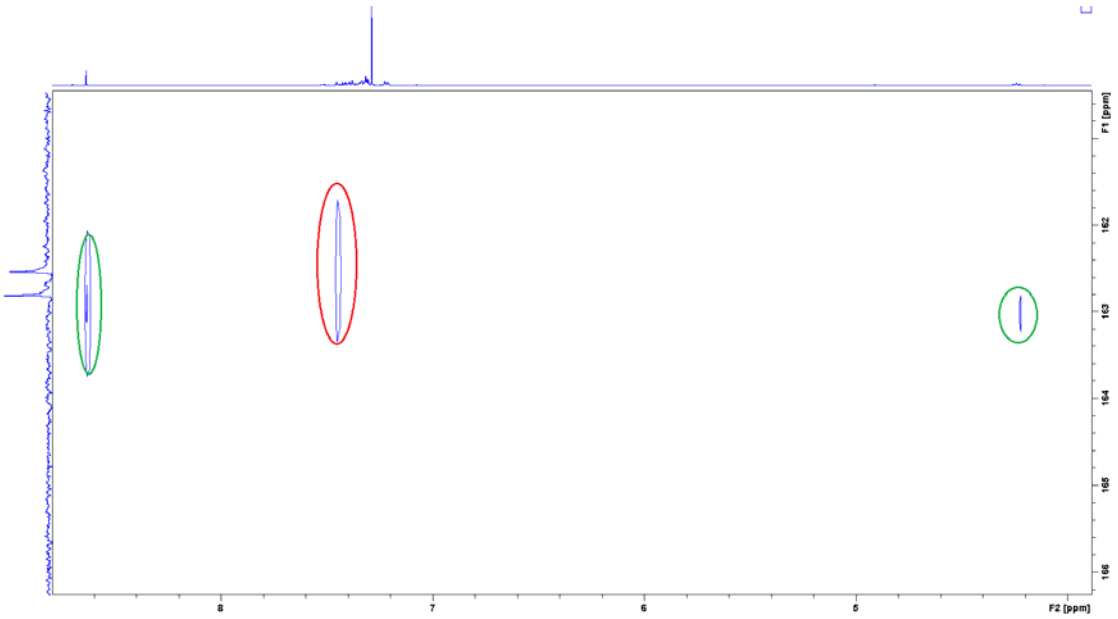


**Figure 45: HMBC NMR data for compound 425 showing the carbonyl region from 161-166 ppm in the carbon-13 axis (y) and 3.8-9.0 ppm in the proton axis (x). Correlations marked in green show interactions between protons and carbonyls on the *N*-butyl imide and those in red show interactions between protons at carbonyls on the *N*-benzhydryl imide.**

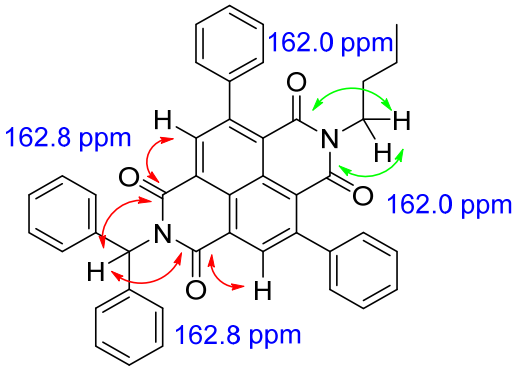


**Figure 46: Compound 426 showing HMBC interactions in red between protons and carbonyls in the *N*-benzhydryl imide and in green between protons and the *N*-butyl imide.**

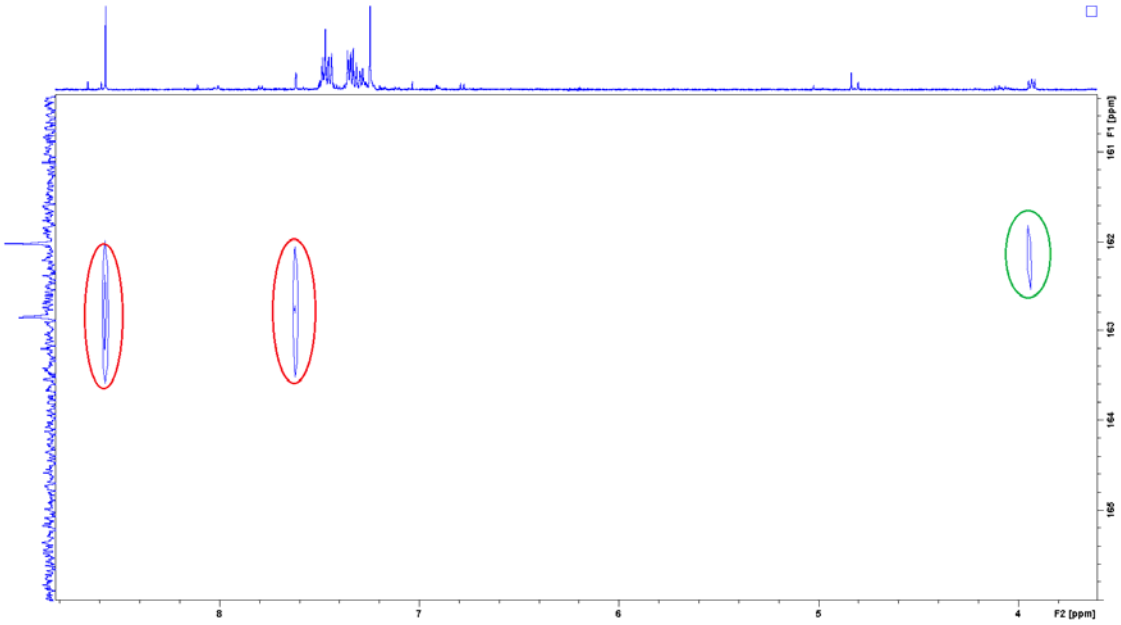


**Figure 47: HMBC NMR data for compound 426 showing the carbonyl region from 161-166 ppm in the carbon-13 axis (y) and 3.8-9.0 ppm in the proton axis (x). Correlations marked in green show interactions between protons and carbonyls on the *N*-butyl imide and those in red show interactions between protons at carbonyls on the *N*-benzhydryl imide.**

Oxidation of the boronic esters to alcohol moieties was less successful. Initial attempts used a common method of aqueous hydrogen peroxide and sodium hydroxide solution in tetrahydrofuran. This reaction resulted in crude material containing what appeared to be the desired product.

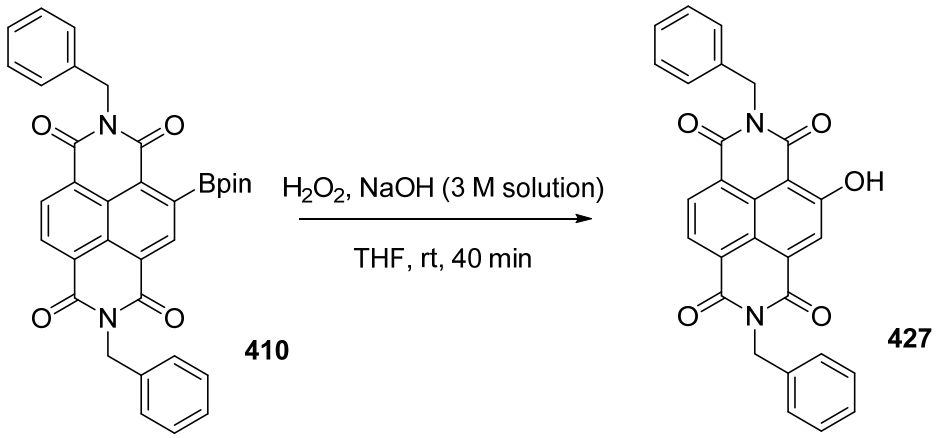


**Scheme 126: Attempted oxidation of boronic esters using hydrogen peroxide and sodium hydroxide**

Proton NMR showed the presence of a sharp peak very downfield at 12.81 ppm, which is consistent with the alcohol proton hydrogen bonding to the carbonyl oxygen in a favoured six-membered ring. This spectrum is shown in Figure 48.

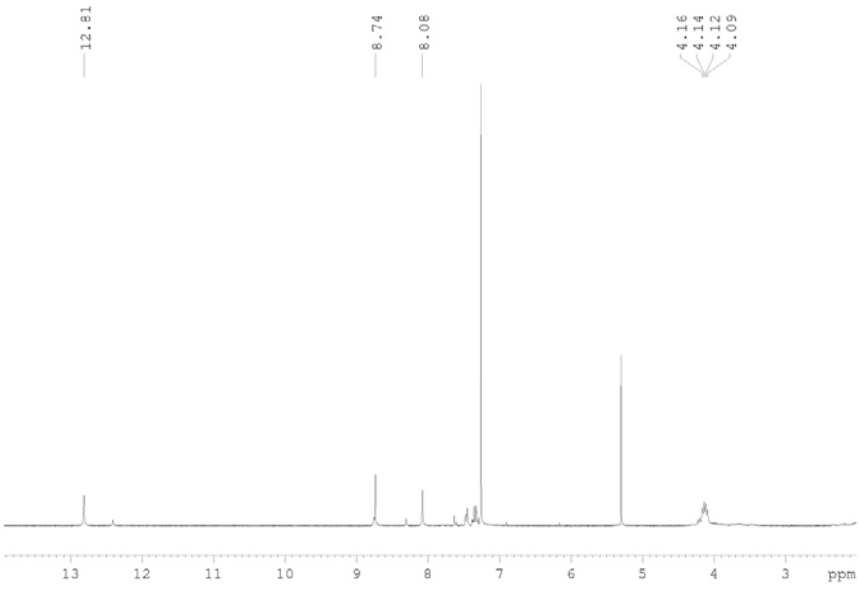


**Figure 48: Proton NMR at 300 MHz in $CDCl_3$ showing oxidation attempt before purification, with the key alcohol peak at 12.81 ppm**

Unfortunately, attempts at purifying this compound failed and the reaction was repeated using $NH_2OH.HCl$ and sodium hydroxide in ethanol, the technique that had been applied to the borylated perylenediimides to achieve the analogous oxidation.[172] This oxidation attempt effected no reaction and starting material was recovered.

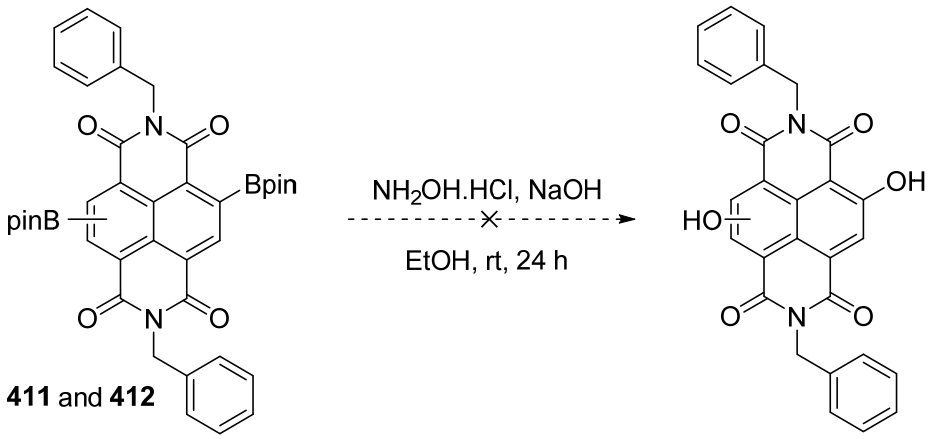


**Scheme 127: Attempted oxidation of boronic esters using $NH_2OH.HCl$ and NaOH**

Finally, the oxidation was attempted using trimethylamine-*N*-oxide (TMANO) in tetrahydrofuran. Interestingly, rather than forming the alcohol, the unfunctionalised NDI was formed in 100% yield, as shown in Scheme 128.

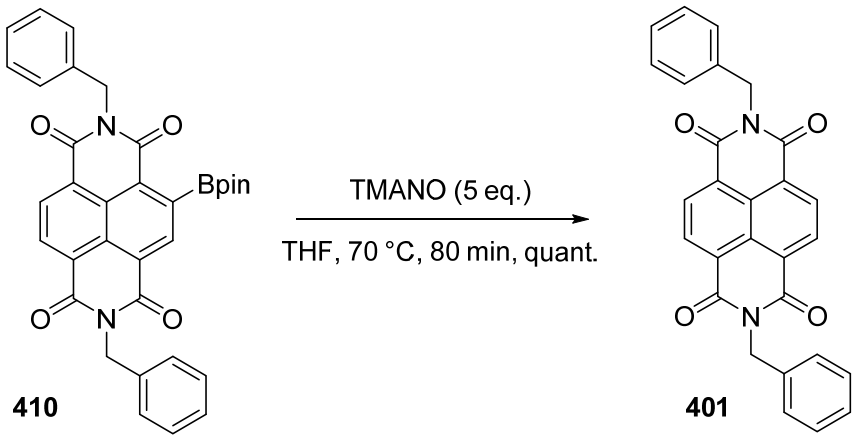


**Scheme 128: Unexpected protodeborylation of mono-borylated NDI 410 with TMANO.**

Attempts at direct fluorination of the boronic esters using methodology from Hartwig[177] and Ritter[178] were also unsuccessful.

## 4.6 Conclusions

It has been shown that the carbon-hydrogen bonds of the naphthalenediimides can be directly borylated via an iridium catalysed C-H activation method. Further to this, it has been observed that microwave heating can drastically increase the rate of this reaction, reducing the reaction time from 48 hours to just two hours.

Unfortunately, despite the reaction theoretically only requiring one equivalent of $B_2pin_2$ reagent, conversion to diborylated NDIs drops off dramatically when lowering the number of equivalents below four. It has however, been possible to use a solvent, hexafluorobenzene, that is not potentially carcinogenic unlike that used in previous reports, i.e., dioxane.

In this study it has not been possible to directly borylate the naphthalene core of NDA, most likely due to the lack of solubility of this compound.

The boronic esters formed can undergo Suzuki coupling reactions in moderate to good yields and oxidation of the boronic esters is also possible, although purification of the alcohol formed has not be successful to date.

Further to these reactions, it would be useful to use core-borylated NDIs in other applications. Naphthalenediimides are able to fluoresce. Use of fluorescent molecules as tags in sensing is well-precedented, and boronic acids can be used to detect sugars and related compounds.[179] Conversion of the boronic esters formed in this chapter could be converted to boronic acids and used for detection purposes. Further variation could be introduced by using a wider range of R-groups on the imide nitrogens.

NDIs have previously been explored in sensing, with a low molecular weight gelator containing a naphthalenediimide moiety. This gelator uses π-π stacking interactions to differentiate between the seven isomers of dihydroxynaphthalene.[162]

The boronic esters could be converted to other functional groups, such as ethers[180] via Chan-Lam coupling and primary amines[181] via nitration and reduction. Within a variety of areas of research utilising NDIs, for example, bio-imaging,[182] ligands for transition metals[183] and bulk-

heterojunction solar-cells,[184] it has proven useful to control and amend the electronic properties of the materials, so scope to modify the core naphthalene bonds in this manner should prove exceedingly valuable.

# Experimental Procedures

## 5.1 General Experimental Procedures

Reactions which required the use of anhydrous, inert atmosphere techniques were carried out under an atmosphere of nitrogen or argon. Reactions requiring glove-box techniques used an argon-filled mBraun labmaster (2005). Solvents were dried and degassed by passing through anhydrous alumina columns using an Innovative Technology Inc. PS-400-7 solvent purification system.

Petrol refers to petroleum ether, bp 40-60 °C. TLCs were performed using aluminium-backed plates precoated with Alugram® SIL G/UV and visualized by UV light (254 nm) and $KMnO_4$ followed by gentle warming. Flash column chromatography was carried out using Davisil LC 60Å silica gel (35-70 micron) purchased from Fisher Scientific.

IR spectra were recorded on a Perkin-Elmer 1600 FT IR spectrometer with absorbances quoted as ν in $cm^{-1}$. Mass spectra were recorded with a micrOTOF electrospray time-of-flight (ESI-TOF) mass spectrometer (Bruker Daltonik). Reactions performed in a microwave reactor used a Biotage initiator 2.0.

NMR spectra were run in $CDCl_3$ (unless otherwise specified) on Bruker Avance 250, 300, 400 or 500 MHz instruments at 298 K. Kinetic NMR experiments were run in $CD_2Cl_2$ on a Bruker Avance 400 MHz instrument at 273 K. $^1H$ and $^{13}C$ NMR spectra were calibrated to internal solvent signals ($CDCl_3$ using $^1H$ 7.26 and $^{13}C$ 77.0 ppm; DMSO-$d_6$ using $^1H$ 2.50 and $^{13}C$ 39.5 ppm; $CD_2Cl_2$ using $^1H$ 5.32 ppm); $^{19}F$ NMR spectra were calibrated to external $CFCl_3$ (0.00 ppm); $^{11}B$ NMR spectra were calibrated to external $BF_3.Et_2O$ (0.00 ppm).

Aluminium trichloride (98%, #206911), acetyl chloride (98%, #11,418-9) and 1,2-dichloroethane (99.8%, anhydrous, #284505) were purchased from Sigma-Aldrich. Dichoromethane-$d_2$ (>99.9%, #D-023) was purchased from Fluorochem Ltd. Hexafluorobenzene, which was purchased from Fluorochem Ltd. (Item #001356) and used as supplied.

## 5.2 Experimental Procedures Relating to Chapter 2

### 5.2.1 General procedure for Baddeley Reaction of Decalin

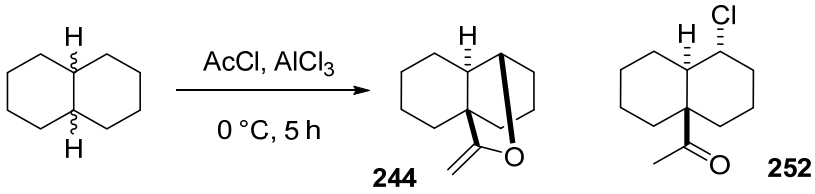


To a stirring suspension of $AlCl_3$ (1.5 eq.) in $CH_2ClCH_2Cl$ or $CH_2Cl_2$ was added gradually AcCl (2.4 eq.), yielding a pale yellow solution. The reaction mixture was cooled in an ice bath to 0 °C. Decalin (1.0 eq.) was added dropwise and stirred for 5 h at 0 °C. Colour change from yellow to orange observed. The reaction mixture was poured over a stirring ice-water slurry; colour changed through cherry-red to yellow and acidic gas evolved. Organic product extracted with $CH_2Cl_2$, combined and washed with brine, dried over $MgSO_4$ and concentrated under reduced pressure. Crude product purified by fractional distillation to give enol ether, **244** (90-95 °C, 3.0-3.1 Torr) and residue subjected to silica gel column chromatography to afford chloroketone, **252** ($R_f$ = 0.64 (90:10 petrol/EtOAc).

**Enol ether 244**: $\delta_H$ (250 MHz, $CDCl_3$) 4.22 (1H, dt, *J* = 1.5, 0.5 Hz, =C*H*$_2$), 4.03 (1H, d, *J* = 4.5Hz, -C*H*-O), 3.65 (1H, d, *J* = 1.5 Hz, =$CH_2$), 1.88-1.07 (15H, m); $\delta_C$ (75 MHz, $CDCl_3$) 166.0, 80.4, 76.9, 50.0, 46.2, 39.5, 31.3, 30.2, 26.5, 24.9, 22.1, 18.9; $\nu_{max}$ 2927, 2860, 1679, 1455, 1369, 1198, 1106 $cm^{-1}$; TOF-MS (ESI+) *m/z* calcd for $(C_{12}H_{18}O+H)^+$ 179.1435; found 179.1425.

**Chloroketone 252**: $\delta_H$ (300MHz, $CDCl_3$) 4.52 (1H, td, *J* = 11.5, 5.0 Hz, -CH-Cl), 1.98 (3H, s, -$CH_3$), 2.2-0.9 (15H, m); $\delta_C$ (75MHz, $CDCl_3$) 212.4, 62.1, 56.3, 53.5, 38.2, 38.0, 36.6, 26.5, 25.6, 24.7, 23.6, 22.5; $\nu_{max}$ 2934, 2858, 1699, 1458, 1363, 1126, 907, 728 $cm^{-1}$. TOF-MS (ESI+) *m/z* calcd for $(C_{12}H_{19}ClO+Na)^+$ 237.1017; found 237.0882.

#### *5.2.1.1 Baddeley Reaction with 1,2-dichloroethane*

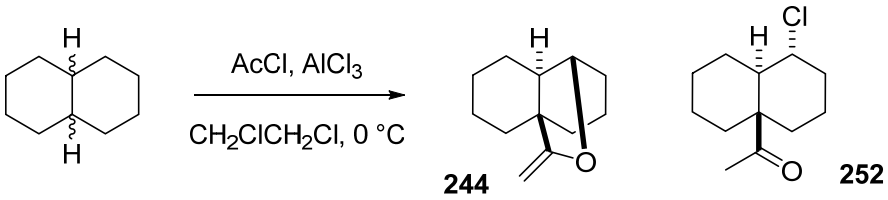


The general procedure for the Baddeley reaction was followed, using aluminium trichloride (116 g, 0.87 mol), acetyl chloride (109 g, 1.39 mol) and decalin (80 g, 0.58 mol) in 1,2-dichloroethane (230 mL). Enol ether, **244**, was obtained in 16% yield (16.8 g) and chloroketone, **252**, in 8% yield (10.0 g).

### *5.2.1.2 Baddeley Reaction with dichloromethane*

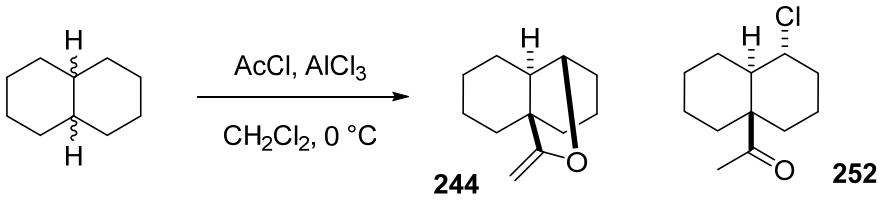


The general procedure for the Baddeley reaction was followed, using aluminium trichloride (36.2 g, 0.27 mol), acetyl chloride (34.1 g, 0.43 mol) and decalin (25.0 g, 0.18 mol) in dichloromethane (75 mL). Enol ether, **244**, was obtained in 15% yield (4.9 g) and chloroketone, **252**, in 6% yield (2.2 g).

### *5.2.1.3 Baddeley Reaction with cis-decalin*

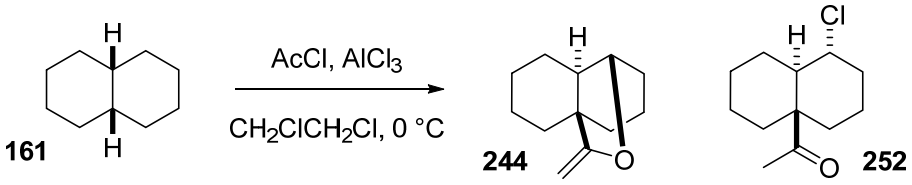


The general procedure for the Baddeley reaction was followed, using aluminium trichloride (65.0 g, 0.49 mol), acetyl chloride (61.3 g, 0.78 mol) and *cis*-decalin (38.6 g, 0.29 mol) in 1,2-dichloroethane (150 mL). Enol ether, **244**, was obtained in 27% yield (15.8 g) and chloroketone, **252**, in 10% yield (5.9 g).

### *5.2.1.4 Baddeley Reaction with trans-decalin*

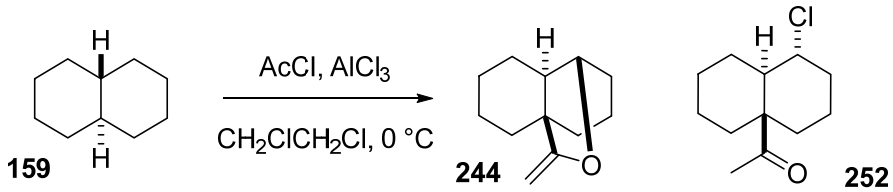


The general procedure for the Baddeley reaction was followed, using aluminium trichloride (58.0 g, 0.43 mol), acetyl chloride (54.0 g, 0.69 mol) and *trans*-decalin (38.6 g, 0.29 mol) in 1,2-dichloroethane (150 mL). Enol ether, **244**, was obtained in 0.9% yield (0.45 g) and chloroketone, **252**, in 3.6% yield (2.2 g).

### *5.2.1.5 Baddeley Reaction with Iron Trichloride*

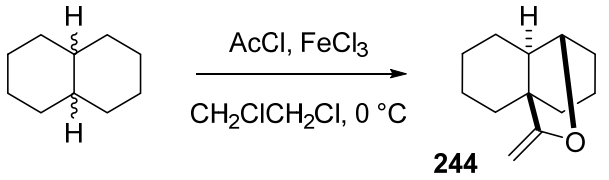


**244**

The general procedure for the Baddeley reaction was followed, using iron trichloride (50.0 g, 0.31 mol), acetyl chloride (38.7 g, 0.49 mol) and decalin (28.4 g, 0.21 mol) in 1,2-dichloroethane (150 mL). Enol ether, **244**, was obtained in 8.5% yield (3.2 g).

### *5.2.1.6 Baddeley Reaction with Zinc Chloride*

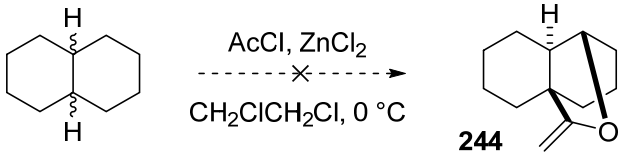


**244**

The general procedure for the Baddeley reaction was followed, using zinc dichloride (1.48 g, 10.8 mmol), acetyl chloride (1.36 g, 17.4 mmol) and decalin (1.0 g, 7.2 mmol) in 1,2-dichloroethane (5 mL). No reaction was observed and decalin was recovered unchanged.

### *5.2.1.7 Baddeley Reaction with Boron Trifluoride*

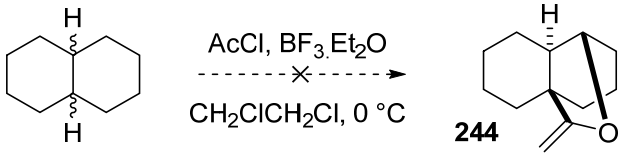


**244**

The general procedure for the Baddeley reaction was followed, using boron trifluoride etherate (1.54 g, 10.8 mmol), acetyl chloride (1.36 g, 17.4 mmol) and decalin (1.0 g, 7.2 mmol) in 1,2-dichloroethane (5 mL). No reaction was observed and decalin was recovered unchanged.

#### *5.2.1.8 Formation of Chloroketone 252 from enol ether 244*

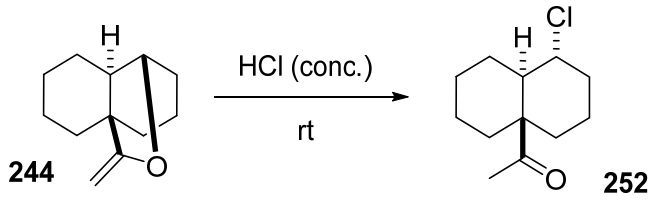


244 252

Enol ether **244** (1.0 eq., 1.03 g, 6.0 mmol) was added gradually to HCl (37%, 10 mL) and stirred at rt for 2 h. Colour change from colourless to yellow observed. The reaction mixture was diluted with $Et_2O$ and separated with $Et_2O$ washings. Organic layers combined and washed with brine, dried over $MgSO_4$ and concentrated under reduced pressure. Chloroketone **252** obtained in 99% yield (1.23g).

### 5.2.2 Control Reactions for Determination of Hydride Abstractor

#### *5.2.2.1 Baddeley Reaction without Acetyl Chloride*

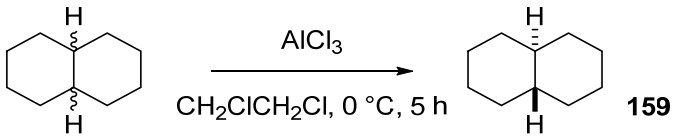


**159**

A stirring suspension of $AlCl_3$ (1.5 eq., 0.054 mol, 7.23 g) in $CH_2ClCH_2Cl$ (20 mL) was cooled to 0 °C over 20 min. Decalin (1.0 eq., 0.036 mol, 5.0 g) was added dropwise and the resulting solution was stirred at 0 °C for 5 h. Reaction mixture was poured over a stirring ice-water slurry, separated with $CH_2Cl_2$ washings, dried over $MgSO_4$ and concentrated under reduced pressure. Crude material flushed through silica pad with hexane to give *trans*-decalin **159** (4.48 g, 90%).

$\delta_H$ (300 MHz, $CDCl_3$) 1.70 (4H, m), 1.58 (4H, m), 1.23 (4H, m), 0.94 (6H, m); $\delta_C$ (75 MHz, $CDCl_3$) 43.8 (2C, CH), 34.5 (4C, $CH_2$), 27.0 (4C, $CH_2$).

#### *5.2.2.2 Reaction of Acetaldehyde with Aluminium Trichloride and Acetyl Chloride*

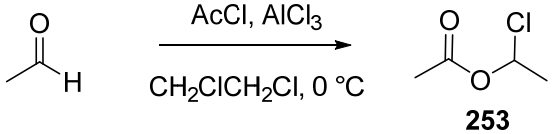


**253**

AcCl (1.0 eq., 6.90 g, 0.089 mol) was gradually added to a suspension of $AlCl_3$ (0.6 eq., 7.10 g, 0.053 mol) in $CH_2ClCH_2Cl$ (20 mL) and stirred for 20 min. The resulting yellow solution was cooled to 0 °C and acetaldehyde (1.0 eq., 3.90 g, 0.089 mol) was added dropwise over 10 min and an immediate colour change to orange was observed. The reaction mixture was stirred at

0 °C for a further 1 h with no further colour change. The resulting orange solution was gradually added to a vigorously stirred slurry of ice-water. Mixture was transferred to separating funnel and organic product was extracted with $CH_2ClCH_2Cl$ (2 × 50 mL). Organic extracts were combined and washed with ice-water (2 × 50 mL), dried over $MgSO_4$, and concentrated under reduced pressure. Product, **253**, is a colourless liquid (5.81 g, 52%)

**1-chloroethyl acetate 253**: $\delta_H$ (250 MHz, $CDCl_3$) 6.37 (1H, q, *J* = 6.0 Hz, –C*H*Cl), 1.96 (3H, s, -$CH_3$), 1.63 (3H, d, *J* = 6.0 Hz, -$CH_3$); $\delta_C$ (75 MHz, $CDCl_3$) 168.0 (-C=O, $4^o$), 80.3 (-C(O)(Cl), $3^o$), 24.7 ($CH_3$, $1^o$), 20.3 ($CH_3$, $1^o$); $^1$H and $^{13}$C NMR values correspond to literature values.[142]

### *5.2.2.3 Reaction of Acetaldehyde with Aluminium Trichloride and Crotonyl Chloride*

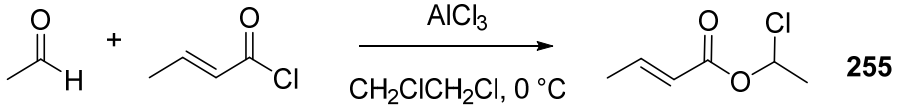


**255**

*trans*-Crotonyl chloride (1.0 eq., 9.30 g, 0.089 mol) was gradually added to a suspension of $AlCl_3$ (0.6 eq., 7.10 g, 0.053 mol) in $CH_2ClCH_2Cl$ (20 mL) and stirred for 20 min. The resulting yellow solution was cooled to 0 °C and acetaldehyde (1.0 eq., 3.90 g, 0.089 mol) was added dropwise over 10 min and an immediate colour change to orange was observed. The reaction mixture was stirred at 0 °C for a further 1 h with no further colour change. The resulting orange solution was gradually added to a vigorously stirred slurry of ice-water. Mixture was transferred to separating funnel and organic product was extracted with $CH_2Cl_2$ (2 × 50 mL), dried over $MgSO_4$, and concentrated under reduced pressure. Product **255** (3.05 g, 23%) was isolated as an oily liquid via silica gel column chromatography with eluent petrol:EtOAc (90:10, $R_f$ = 0.66).

**1-chloroethyl crotonate 255**: $\delta_H$ (250 MHz, $CDCl_3$) 7.06 (1H, dq, *J* = 15.5 Hz, 7.0 Hz, =C*H*Me), 6.57 (1H, q, *J* = 6.0 Hz, -C*H*Cl), 5.82 (1H, dq, *J* = 15.5 Hz, 2.0 Hz, =C*H*C(O)-), 1.88 (3H, dd, *J* = 7.0 Hz, 2.0 Hz, =CH*Me*), 1.77 (3H, d, *J* = 6.0 Hz, -CH(Cl)*Me*); $\delta_C$ (75 MHz, $CDCl_3$) 163.6 (*C*=O), 147.4 (Me*C*H=CHC(O)), 121.4 (MeCH=*C*HC(O)), 80.7 (-*C*(Cl)(O)), 25.1 (=CH*Me*), 18.1 (-CH(Cl)*Me*); $\nu_{max}$ 2981, 1736, 1653, 1443, 1294, 1241, 1158, 1082, 1023, 966; TOF-MS (ESI+) *m/z* calcd for $(C_6H_9ClO_2+H)^+$ 149.0364; found 149.0295.

### *5.2.2.4 Baddeley Reaction with Crotonyl Chloride*

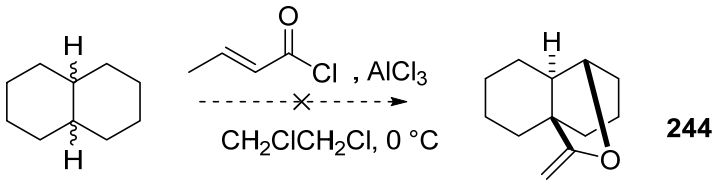


**244**

The general procedure for the Baddeley reaction was followed, using aluminium trichloride (7.2 g, 0.054 mol), *trans*-crotonyl chloride (9.1 g, 0.087 mol) and decalin (5.0 g, 0.036 mol) in 1,2-dichloroethane (20 mL). No reaction was observed and decalin was recovered unchanged.

### *5.2.2.5 Baddeley Reaction with Crotonyl Chloride then Acetyl Chloride*

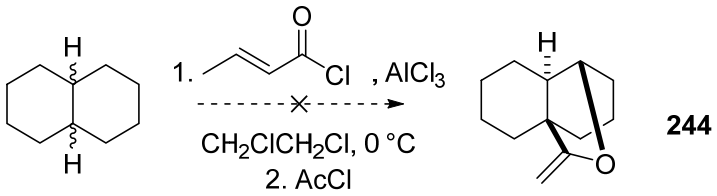


**244**

The general procedure for the Baddeley reaction was followed, using aluminium trichloride (7.2 g, 0.054 mol), *trans*-crotonyl chloride (9.1 g, 0.087 mol) and decalin (5.0 g, 0.036 mol) in 1,2-dichloroethane (20 mL). Acetyl chloride (1.0 eq., 2.8 g, 0.036 mol) was added after the addition of decalin. No reaction was observed and decalin was recovered unchanged.

### *5.2.2.6 Baddeley Reaction with Crotonyl Chloride, then Acetyl Chloride/Aluminium Trichloride*

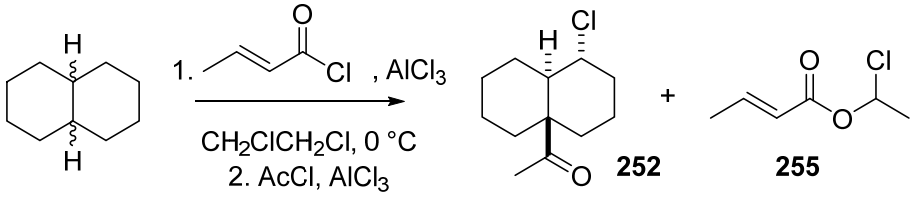


**252** **255**

The general procedure for the Baddeley reaction was followed, using aluminium trichloride (7.2 g, 0.054 mol), *trans*-crotonyl chloride (9.1 g, 0.087 mol) and decalin (5.0 g, 0.036 mol) in 1,2-dichloroethane (20 mL). A premixed solution of acetyl chloride (1.0 eq., 2.8 g, 0.036 mol) and aluminium trichloride (1.0 eq., 4.8 g, 0.036 mol) in 1,2-dichloroethane (10 mL) was added after the addition of decalin. Chloroketone **252** was obtained in 2.3% yield (177 mg) and 1-chloroethyl crotonate **255** was obtained in 3.4% yield (180 mg).

### 5.2.3 $\Delta^{9,10}$-Octalin

#### *5.2.3.1 Synthesis of $\Delta^{9,10}$-Octalin via Birch-like Reduction*

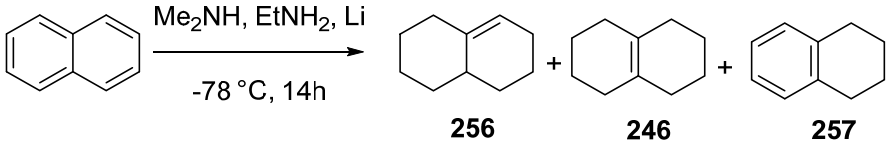


This reaction was performed in accordance with a literature procedure.[144]

Napthalene (1.0 eq., 25.6 g, 0.20 mol) was added to 50:50 $Me_2NH$:$EtNH_2$ (500 mL) in a stirring 3-necked 1 L round bottomed flask at 0 °C, attached to a coldfinger (dry ice and acetone). Lithium wire (8.3 eq., 11.6 g, 1.66 mol) was cut into 0.5 cm pieces and added piecewise to the reaction mixture. Lithium was not completely dissolved for 8 h. Reaction left to stir for 14 h after first addition of Li with ice bath removed. $MgSO_4$ drying tube added to dry-ice condenser and reaction mixture left to warm up overnight. Remaining solvent evaporated off with gentle warming under reduced pressure. The reaction mixture was quenched carefully with 500 mL water. The reaction mixture was filtered and washed with diethyl ether, separated and aqueous layer washed with 2 × 100 mL portions of diethyl ether. Organic layers combined, dried over $MgSO_4$ and concentrated under reduced pressure.

Crude material distilled to give a colourless oil containing $\Delta^{1,9}$ octalin, **256**, $\Delta^{9,10}$ octalin, **246**, and tetralin, **257**, at 50-54 °C (19.35g). Mixture taken forward to next step.

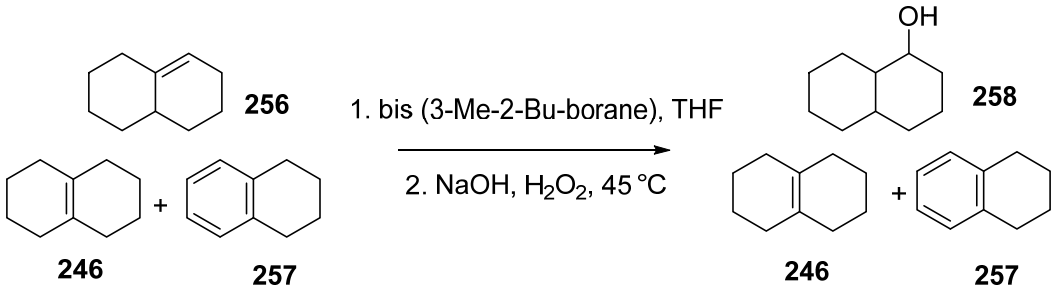


This reaction was performed in accordance with a literature procedure.[144]

To a suspension of $NaBH_4$ (2.3 eq., 2.35 g, 0.06 mol) in dry THF (78 mL) under Ar was first added 2-methyl-2-butene (6.1 eq., 11.55 g, 0.17 mol) and then, dropwise over 45 mins, boron trifluoride diethyl etherate (3.1 eq., 11.75 g, 0.08 mol) in THF (22 mL) was added. Effervescence was observed. To the bis(3-methylbutan-3-yl)borane produced was added the mixture of $\Delta^{1,9}$ octalin, **256**, $\Delta^{9,10}$ octalin, **246**, and tetralin, **257**, (containing $\Delta^{1,9}$ octalin, **256**, approx. 1.0 eq., 3.8 g, 0.03 mol) dropwise over 10 mins, and left to stir at rt for 3.5 h. Water (50 mL) was added over 20 min; an exothermic reaction with effervescence. NaOH (3.0 M, 35 mL) was added over 10 min, then $H_2O_2$ (30%, 35 mL) over 45 mins. The reaction mixture was heated to 45 $^{o}$C and stirred for 5 h, then left to cool overnight. The reaction mixture was diluted with diethyl ether and separated. Organic layers washed with brine, dried over $MgSO_4$, tested for peroxides using starch iodide paper and concentrated under reduced pressure.

Crude material distilled to give a colourless oil containing $\Delta^{9,10}$ octalin and tetralin at 65-70 °C. Column performed in 100% hexane to recover $\Delta^{9,10}$ octalin (4.74 g, 17.2% yield over 2 steps).

**$\Delta^{9,10}$ octalin 246**: $\delta_H$ (250 MHz, $CDCl_3$) 1.85 (8H, m, C$H_2$C$H_2$C=), 1.59 (8H, m, C$H_2$C=); $\delta_C$ (62.5 MHz, $CDCl_3$) 128.1, 30.6, 23.4.

Fraction B contained tetralin (5.21 g, 19.7% over 2 steps).

**Tetralin 257**: $\delta_H$ (300 MHz, $CDCl_3$) 7.29 (4H, m, Ar), 3.00 (4H, m, C$H_2$C=), 2.03 (4H, m, C$H_2$C$H_2$C=); $\delta_C$ (75 MHz, $CDCl_3$) 137.1, 129.2, 125.5, 29.5, 23.4.

Both sets of NMR data correspond to data published in the literature.[144,185,186]

### *5.2.3.2 Synthesis of Δ$^{9,10}$-Octalin via dehydration of 2-decahydronaphthol*

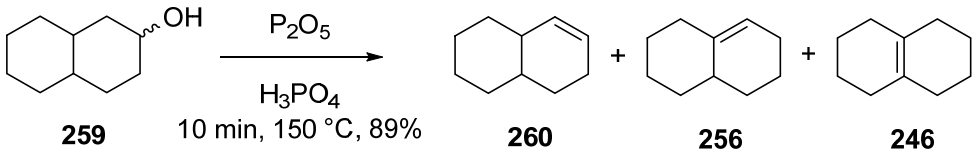


This reaction was performed in accordance with a literature procedure.[187, 188]

To a stirring solution of $P_2O_5$ (1.08 eq., 10.0 g, 0.070 mol) in $H_3PO_4$ (60 mL) was added slowly 2-decahydronaphthol (1.00 eq., 10.0 g, 0.065 mol). The resulting solution was heated to 150 °C for 10 minutes under Ar. A gentle vacuum was applied, and the resulting octalins were distilled off with steam via the gradual addition of water to the reaction vessel. The contents of the receiver flask were transferred to a separating funnel and the organic layer extracted with $Et_2O$ washings, combined, dried over $MgSO_4$ and concentrated under reduced pressure. The colourless oily liquid was identified as a mixture of $\Delta^{1,2}$, $\Delta^{1,9}$ and $\Delta^{9,10}$ octalins (7.92 g, 89% yield). Mixture taken forward to next step.

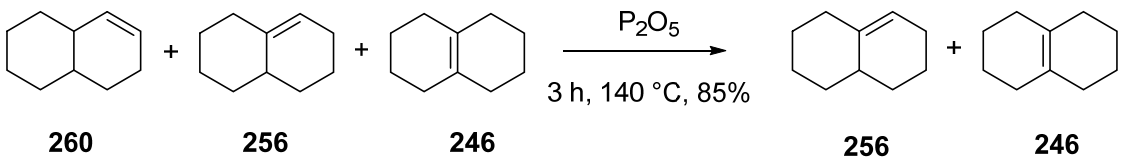


This reaction was performed in accordance with a literature procedure.[187, 188]

To the stirring mixture of $\Delta^{1,2}$, $\Delta^{1,9}$ and $\Delta^{9,10}$ octalins (1.00 eq., 37.4 g, 0.275 mol) was added $P_2O_5$ (0.32 eq., 12.5 g, 0.088 mol), and the resulting solution heated to 140 °C for 3 h under Ar. After cooling to rt, ice was added to the reaction mixture before transfer to separating funnel. Organic layer extracted with $Et_2O$ washings, dried over $MgSO_4$ and concentrated under reduced pressure. The oily liquid was identified as a mixture of $\Delta^{1,9}$ and $\Delta^{9,10}$ octalins (**256** and **246**) (31.68 g, 85% yield). Mixture taken forward to next step.

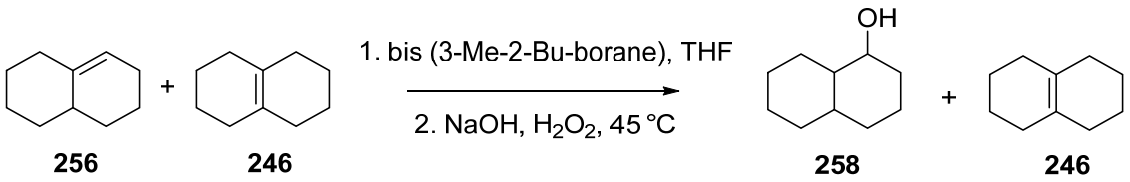


This reaction was performed in accordance with a literature procedure. [144]

To a suspension of $NaBH_4$ (2.3 eq., 3.37 g, 0.09 mol) in dry THF (100 mL) under Ar was first added 2-methyl-2-butene (6.1 eq., 16.6 g, 0.24 mol) and then, dropwise over 45 mins, boron trifluoride diethyl etherate (3.1 eq., 17.04 g, 0.12 mol) in THF (25 mL) was added. Effervescence was observed. To the bis(3-methylbutan-3-yl)borane produced is added the mixture of $\Delta^{1,9}$ octalin and $\Delta^{9,10}$ octalin (containing $\Delta^{1,9}$ octalin approx. 1.0 eq., 5.3 g, 0.04 mol) dropwise over 10 mins, and left to stir at rt for 3.5 h. Water (65 mL) added over 20 min; an exothermic reaction with effervescence. NaOH (3.0 M, 55 mL) added over 10 min, then $H_2O_2$ (30%, 55 mL) over 45 mins. The reaction mixture was heated to 45 $^oC$ and stirred for 5 h, then left to cool overnight. The reaction mixture was diluted with diethyl ether and separated. Organic layers washed with brine, dried over $MgSO_4$, tested for peroxides using starch iodide paper and concentrated under reduced pressure. Crude material distilled to give a colourless oil identified as $\Delta^{9,10}$ octalin at 60-67 °C, 80% (20.1 g). $^1H$ and $^{13}C$ NMR data corresponded with NMR data previously obtained.

### *5.2.3.3 Baddeley Reaction of $\Delta^{9,10}$-Octalin*

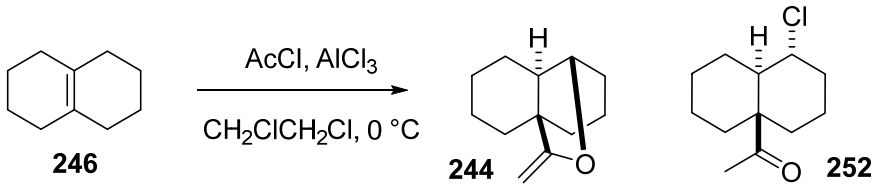


The general procedure for the Baddeley reaction was followed, using aluminium trichloride (1.0 eq., 9.8 g, 0.073 mol), acetyl chloride (1.0 eq., 5.8 g, 0.073 mol) and $\Delta^{9,10}$-octalin (1.0 eq., 10.0 g, 0.073 mol) in 1,2-dichloroethane (40 mL). Enol ether **244** was obtained in 32% yield (4.2 g) and chloroketone **252** was obtained in 15% yield (2.3 g).

### 5.2.4 General Procedure for NMR Scale Baddeley Reaction

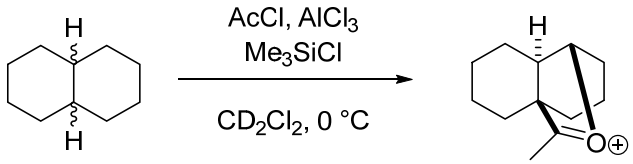


The NMR instrument (400 MHz, Bruker Avance II) was pre-cooled to 273 K. To a suspension of aluminium trichloride in 0.3 mL of $CD_2Cl_2$ was added acetyl chloride. The resulting clear solution was cooled to 273 K in an ice bath. Trimethylsilylchloride, dissolved in the remaining $CD_2Cl_2$, was added to the cooled solution as a standard and transferred to an NMR tube, with a total volume of 0.863 mL. The temperature of the NMR tube was maintained at 273 K. The NMR tube was inserted into the NMR instrument prior to addition of decalin to lock and shim the sample, then ejected. Decalin was injected into the NMR tube immediately prior to the second insertion into the instrument. After obtaining several initial spectra, spectra were recorded every 5 minutes for at least 300 minutes.

#### *5.2.4.1 Rate Comparison of cis and trans-Decalin*

| Experiment | Aluminium Trichloride | Acetyl Chloride | Decalin | Deuterated dichloromethane |
|---|---|---|---|---|
| *cis*-Decalin | 223 mg, 1.67 mmol | 210 mg, 2.68 mmol | 1.54 mg, 1.11 mmol | 0.500 mL |
| *trans*-Decalin | 223 mg, 1.67 mmol | 210 mg, 2.68 mmol | 154 mg, 1.11 mmol | 0.500 mL |

#### *5.2.4.2 Varying Concentrations of cis-Decalin*

| Experiment Number | Aluminium Trichloride | Acetyl Chloride | *cis*-Decalin | Deuterated dichloromethane | [*cis*-Decalin] |
|---|---|---|---|---|---|
| 1 | 223 mg, 1.67 mmol | 210 mg, 2.68 mmol | 62 mg, 0.45 mmol | 0.603 mL | 0.5167 M |
| 2 | 223 mg, 1.67 mmol | 210 mg, 2.68 mmol | 92 mg, 0.67 mmol | 0.570 mL | 0.7750 M |
| 3 | 223 mg, 1.67 mmol | 210 mg, 2.68 mmol | 123 mg, 0.89 mmol | 0.535 mL | 1.0333 M |
| 4 | 223 mg, 1.67 mmol | 210 mg, 2.68 mmol | 154 mg, 1.11 mmol | 0.500 mL | 1.2915 M |
| 5 | 223 mg, 1.67 mmol | 210 mg, 2.68 mmol | 216 mg, 1.56 mmol | 0.431 mL | 1.8078 M |
| 6 | 223 mg, 1.67 mmol | 210 mg, 2.68 mmol | 247 mg, 1.78 mmol | 0.400 mL | 2.0665 M |

#### *5.2.4.3 Varying Concentrations of Acetyl Chloride and Aluminium Trichloride*

| Experiment Number | Aluminium Trichloride | Acetyl Chloride | *cis*-Decalin | Deuterated dichloromethane | [acetyl chloride] |
|---|---|---|---|---|---|
| 1 | 74 mg, 0.56 mmol | 70 mg, 0.89 mmol | 154 mg, 1.11 mmol | 0.627 mL | 1.0332 M |
| 2 | 111 mg, 0.84 mmol | 105 mg, 1.34 mmol | 154 mg, 1.11 mmol | 0.596 mL | 1.5498 M |
| 3 | 149 mg, 1.11 mmol | 140 mg, 1.78 mmol | 154 mg, 1.11 mmol | 0.564 mL | 2.0665 M |
| 4 | 188 mg, 1.39 mmol | 175 mg, 2.23 mmol | 154 mg, 1.11 mmol | 0.532 mL | 2.6559 M |
| 5 | 223 mg, 1.67 mmol | 210 mg, 2.68 mmol | 154 mg, 1.11 mmol | 0.500 mL | 3.0999 M |

## 5.3 Experimental Procedures Relating to Chapter 3

### 5.3.1 Bicyclohexyl

#### *5.3.1.1 Baddeley reaction of Bicyclohexyl*

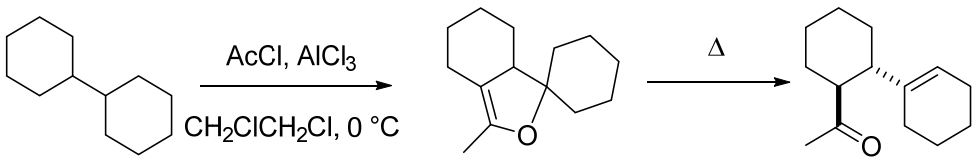


**299** **305** **311**

The general procedure for the Baddeley reaction was followed, using aluminium trichloride (240 g, 1.80 mol), acetyl chloride (226 g, 2.88 mol) and bicyclohexyl (200 g, 1.20 mol) in 1,2-dichloroethane (500 mL).

101 g bicyclohexyl (50%) was recovered by fractional distillation (1.4-1.5 Torr, 65-67 °C). Enol ether **305** and bicyclohexyl mixture was obtained in 33% yield brsm (40 g, 1.5-1.6 Torr, 73-76 °C).

Using higher distillation temperatures the enol ether **305** rearranged to give **311** (9.38g, 7.6% brsm) (1.5 Torr, 104-108 °C).

**Enol ether 305**: $\delta_H$ (250 MHz) 2.33-0.80 (19H, m [including 1.67 (3H, s, -$CH_3$)]) ppm; $\delta_C$ (75MHz) 141.7 (=*C*($CH_3$)-O, 4°), 108.4 (C=*C*-C, 4°), 84.4 (-C-O, 4°), 53.6, 38.3, 31.8, 27.8, 26.8, 26.7, 25.5, 24.2, 22.6, 22.5, 11.0 (-$CH_3$) ppm; $\nu_{max}$ (film) 2924, 2852, 1447, 1353, 1265, 1221, 1180, 1143, 1088, 1034, 953, 928, 890, 839, 815, 737 $cm^{-1}$; HRMS (ESI+) *m/z* calcd for $(C_{14}H_{22}O+H)^+$ 207.1743; found 207.1710.

**Unsaturated ketone 311**: $\delta_H$ (300 MHz) 5.34-5.31 (1H, m, =C*H*R), 2.46 (1H, app td, *J* 11.0 Hz, 2.5 Hz, C(O)-CH<), 2.18-0.72 (20H, m [including 1.99 (3H, s, -$CH_3$)]) ppm; $\delta_C$ (75 MHz) 212.4 (C=O), 139.9, 121.8, 55.1, 48.1, 31.5, 29.2, 28.5, 26.0, 25.8, 25.4, 25.0, 22.9, 22.4 ppm; $\nu_{max}$ 2923, 2854, 1705, 1447, 1355, 1244, 1220, 1161, 920, 882 $cm^{-1}$; HRMS (ESI+) *m/z* calcd for $(C_{14}H_{22}O+H)^+$ 207.1743; found 207.1765.

### *5.3.1.2 Hydrazone formation of 312*

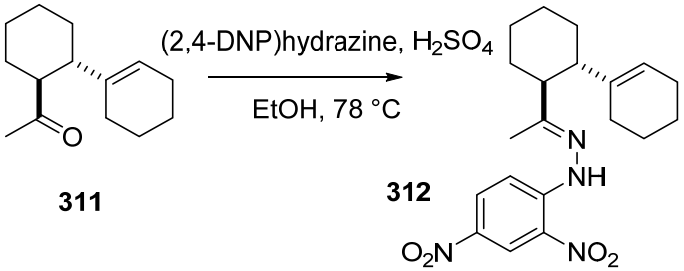


311 312

Ketone **311** (1.0 eq., 1.70 g, 8.24 mmol) was dissolved in ethanol (20 mL), stirring in a round-bottomed flask. (2,4-dinitrophenyl)hydrazine (1.5 eq., 2.50 g, 12.4 mmol) was added, resulting in a red/orange mixture. $H_2SO_4$ (0.5 eq., 0.40 g, 4.12 mmol) was added dropwise, then solution heated to reflux for 2.5 h. Further 2,4-dinitrophenyl)hydrazine (0.5 eq., 0.80 g, 4.12 mmol) added and reflux continued until reaction complete; orange precipitate observed in red solution. Precipitate separated from solution by vacuum filtration, and air-dried overnight. Pure product isolated by dissolving product / 2,4-DNP mixture in 95:5 petrol:EtOAc and removing 2,4-DNP (red crystals) by vacuum distillation. Solvent removed under reduced pressure to give crude product (yellow crystalline substance, 2.56 g, 81%), which was re-crystallised from hot ethanol to form crystals for x-ray analysis.

**Hydrazone 312**: $\delta_H$ (250 MHz, $CDCl_3$) 10.96 (1H, s, -NH), 9.12 (1H, d, *J* 2.5 Hz, aryl CH), 8.29 (1H, dd, *J* 9.5 Hz, 2.5 Hz, aryl CH), 7.93 (1H, d, *J* 9.5 Hz, aryl CH), 5.36 (1H, s, =C*H*R), 2.54 (1H, app td, *J* 11.0, 2.8Hz), 1.23 - 2.20 (20H, m [including 1.93 (3H, s, -$CH_3$)]) ppm; $\delta_C$ (75 MHz, $CDCl_3$) 161.6, 145.2, 140.2, 137.5, 129.9, 128.9, 123.6, 122.3, 116.3, 50.2, 49.7, 31.6, 30.5, 26.2, 25.6, 25.5, 24.6, 22.9, 22.6, 13.1; $\nu_{max}$ 3636, 2981, 2156, 2027, 1619, 1518, 133, 1139, 1074, 955$cm^{-1}$; TOF-MS (ESI+) *m/z* calcd for $(C_{20}H_{26}N_4O_4+Na)^+$ 409.1852; found 409.1868.

### *5.3.1.3 Formation of alcohol, 310*

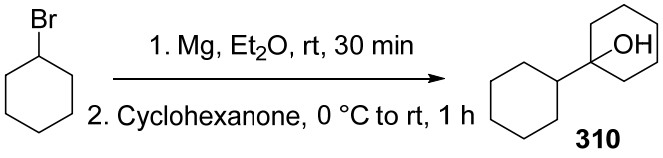


310

This reaction was performed in accordance with a literature procedure.[189]

Cyclohexylbromide (1.2 eq., 17.9 g, 0.110 mol) was added dropwise over 30 min to a stirring suspension of magnesium turnings (1.4 eq., 3.2 g, 0.132 mol) in diethyl ether (33 mL) and the reaction mixture turned silver. The reaction mixture was then cooled to 0 °C and cyclohexanone (1.0 eq., 9.0 g, 0.092 mol) dissolved in diethyl ether (7 mL) was added dropwise over 20 min. The reaction mixture was warmed to rt with stirring over 40 min. The reaction mixture was quenched with water (40 mL) and HCl (1 M, 40 mL then 6 M, 5mL). Organics extracted with diethyl ether, washed with sodium thiosulfate solution and water, then dried over $MgSO_4$ and concentrated under reduced pressure. Alcohol **310** was obtained by distillation (1.7 Torr, 88-92 °C) in 48% yield (8.03 g).

Alcohol **310**: $\delta_H$ (300 MHz, $CDCl_3$) 0.80-2.50 (m, 22 H); $\delta_C$ (75 MHz, $CDCl_3$) 73.0, 48.2, 34.3, 26.8, 26.6, 26.5, 26.0, 21.9. $^1H$ and $^{13}C$ NMR data correspond to literature data. [190]

### *5.3.1.4 Formation of cyclohexyl-1-cyclohexene, 307*

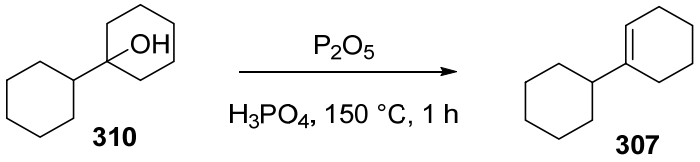


Alcohol **310** (1.0 eq., 8.0 g, 0.044 mol) was added to $P_2O_5$ (1.1 eq., 8.0 g, 0.050 mol) dissolved in $H_3PO_4$ (80 g) and heated to 150 °C for 1 h. Water and alkene **307** were then distilled off under reduced pressure. Organic layers extracted with hexane, neutralised with NaOH solution (1 M), washed with brine and dried over $MgSO_4$. Organic product was flushed through a silica pad using hexane eluent and identified as alkene **307.**

**Alkene 307**: $\delta_H$ (300 MHz, $CDCl_3$) 5.38-5.34 (1H, m, C=CH), 2.20-0.85 (19H, m); $\delta_C$ (75 MHz, $CDCl_3$) 143.1, 118.6, 45.8, 31.9, 30.1, 26.9, 26.8, 26.7, 26.5, 25.3, 23.2, 22.8. NMR data corresponds to literature values.[191]

### *5.3.1.5 Baddeley reaction of cyclohexyl-1-cyclohexene, 307*

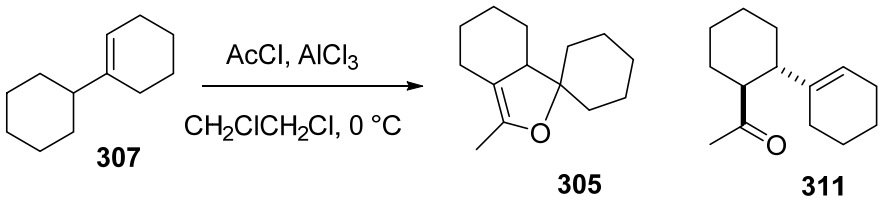


The general procedure for the Baddeley reaction was followed, using aluminium trichloride (1.0 eq., 2.03 g, 0.0152 mol), acetyl chloride (1.0 eq., 1.19 g, 0.0152 mol) and alkene **307** (2.50 g, 0.0152 mol) in 1,2-dichloroethane (10 mL). A mixture of enol ether **305** and unsaturated ketone **311** were obtained in 55% yield (1.72 g).

## 5.3.2 Bicyclopentyl

### *5.3.2.1 Aldol condensation of cyclopentanone*

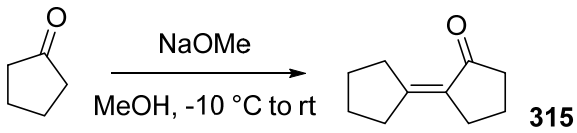


**315**

This reaction was adapted from a literature procedure.[192]

Cyclopentanone (1.0 eq., 79.0 g, 0.94 mol) was cooled to -10 °C in a 2-necked round bottom flask. NaOMe (0.5 eq., 25.0 g, 0.47 mol) was dissolved in methanol (100 mL) and added dropwise to the cyclopentanone. Whilst stirring, the resulting solution was warmed to rt over 16 h. The mixture was diluted with water, organic product was extracted with EtOAc; extracts were combined and dried over $MgSO_4$, and concentrated under reduced pressure. Fractional distillation gave [1,1-(bicyclopentylidene)]-2-one **315**, a pale-yellow oily liquid in 30% yield (21.3 g) at 1.5 Torr and 72-78 °C.

**Unsaturated Ketone 315**: $\delta_H$ (300 MHz, $CDCl_3$) 2.59 (2H, m, $-CH_2$), 2.36 (2H, m, $-CH_2$), 2.10 (4H, t, *J* 8.0 Hz, $-CH_2$), 1.73 (2H, quintet, *J* 7.5 Hz, $-CH_2$), 1.52 (4H, m, $-CH_2$); $\delta_C$ (75 MHz, $CDCl_3$) 206.5 (C=O), 157.8 (*C*=C-C=O), 127.4 (C=*C*-C=O), 39.3, 33.8, 32.0, 29.0, 26.5, 24.8, 19.6. $^1$H and $^{13}$C NMR data correspond to literature values.[193]

### *5.3.2.2 Formation of cyclopentyl-1-cyclopentene*

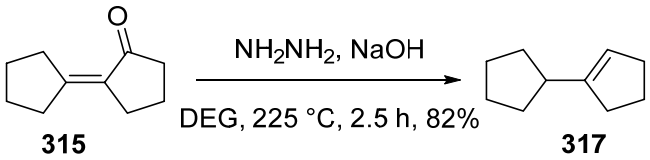


**315** **317**

[1,1-(bicyclopentylidene)]-2-one **315** (1.0 eq., 21.3 g, 0.14 mol), NaOH (4.0 eq., 22.7 g, 0.57 mol) and $NH_2NH_2.H_2O$ (3.3 eq., 29.3 g, 0.47 mol) were combined in diethylene glycol (200 mL) and refluxed at 100 °C for 1 h. Reflux apparatus was replaced with distillation apparatus; temperature of reaction flask was raised to 235 °C for 1.5 h and then allowed to cool to rt. The mixture formed was diluted with water, transferred to separating funnel and organic product was extracted with hexane (2 × 100 mL). Hexane extracts were combined and washed with brine, dried over $MgSO_4$, and concentrated under reduced pressure. A pale yellow oily liquid identified as cyclopentyl-1-cyclopentene **317** (15.8 g, 82%).

**Alkene 317**: $\delta_H$ (250 MHz, $CDCl_3$) 4.47 (1H, td, *J* 8.0, 2.5Hz =C*H*R), 1.96-0.63 (15H, m); $\delta_H$ (400 MHz, $CCl_4$) 4.85 (1H, m), 2.33 (1H, m), 1.6-2.2 (9H, m), 1.54 (3H, m), 1.36 (1H, m), 1.17 (1H, m); $\delta_C$ (75 MHz, $CDCl_3$) 99.7, 92.9, 43.9, 38.0, 31.5, 29.1, 28.3, 24.4, 24.0, 23.7. $^1$H NMR datum in $CCl_4$ corresponds to literature values.[194]

### *5.3.2.3 Iron-catalysed cross-coupling of cyclopentyl magnesium bromide and bromocyclopentane*

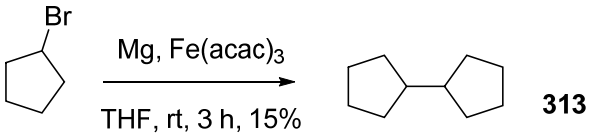


This reaction was adapted from a literature procedure.[151]

A suspension of Mg (1.2 eq., 10.9 g, 0.45 mol) in THF (300 mL) under Ar was stirring in an oven dried 1 L, 2-necked flask with water condenser. Cyclopentylbromide (1.0 eq., 55.9 g, 0.38 mol) was added slowly until reaction turned silver and effervesced, then added dropwise over 50 min and cooled to rt. The cyclopentylmagnesiumbromide in THF was then transferred dropwise by syringe to a red/orange solution of $Fe(acac)_3$ (1.0 mol%, 1.34 g, 38 mmol) and cyclopentylbromide (0.67 eq., 65.0 g, 0.25 mol) in THF (200 mL) under Ar which then turned black. The RM cooled to rt and was quenched with 1M HCl. Organic product extracted with $Et_2O$ (3 × 100 mL), combined and washed with $Na_2S_2O_3$ solution, dried over $MgSO_4$ and concentrated under reduced pressure. Bicyclopentyl **313** was identified as an oily liquid in 15% yield (5.2 g).

**313**: $\delta_H$ (250 MHz, $CDCl_3$) 1.74-1.69 (4H, m), 1.59-1.54 (10H, m), 1.16-1.11 (4H, m); $\delta_C$ (75 MHz, $CDCl_3$) 46.5, 32.0, 25.5. $^1H$ and $^{13}C$ NMR data correspond to literature values.[195]

### *5.3.2.4 Baddeley Reaction of bicyclopentyl*

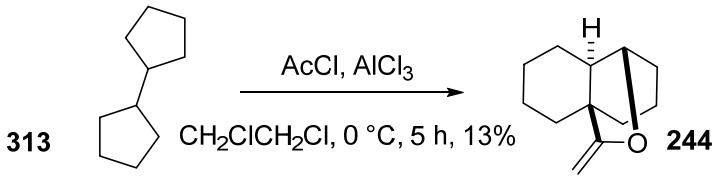


The general procedure for the Baddeley reaction was followed, using aluminium trichloride (5.8 g, 0.043 mol), acetyl chloride (5.5 g, 0.069 mol) and bicyclopentyl (4.0 g, 0.029 mol) in 1,2-dichloroethane (25 mL).

Crude product purified by distillation, bicyclopentyl and decalin mixture (1.24 g, 31%) at 3.0 Torr and 36 – 40 °C; enol ether (0.69 g, 13%) at 2.1 Torr, 60 – 70 °C.

**Enol ether 244**: $\delta_H$ (250 MHz, $CDCl_3$) 4.22 (1H, dt, *J* = 1.5, 0.5 Hz, =C*H*$_2$), 4.03 (1H, d, *J* = 4.5Hz, -C*H*-O), 3.65 (1H, d, *J* = 1.5 Hz, =$CH_2$), 1.88-1.07 (15H, m); $\delta_C$ (75 MHz, $CDCl_3$) 166.0, 80.4, 76.9, 50.0, 46.2, 39.5, 31.3, 30.2, 26.5, 24.9, 22.1, 18.9. $^1H$ and $^{13}C$ NMR data correspond to previously obtained data.

### 5.3.3 Bicyclo[5.3.0]decane

#### *5.3.3.1 Formation of cyclodecane-1,6-dione using ruthenium dioxide*

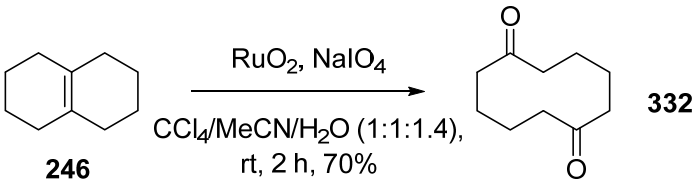


This reaction was performed in accordance with a literature procedure.[196]

$\Delta^{9,10}$ octalin **246** (1.0 eq., 4.08 g, 0.030 mol) was dissolved in a 1:1:1.4 $CCl_4$:MeCN:$H_2O$ (150 mL:150 mL: 215 mL) stirring solvent mixture under $N_2$, to which $RuO_2.H_2O$ and $NaIO_4$ were added. TLC after 45 min indicated all starting material was consumed. The reaction mixture was diluted with $H_2O$, transferred to separating funnel, extracted with $CH_2Cl_2$ (3 × 100 mL), dried over $MgSO_4$ and concentrated under reduced pressure. Crude material flushed through silica pad (90:10 hexane:EtOAc, $R_f$ = 0.38) to afford cyclodecane-1,6-dione **332** as a white crystalline solid in 70% yield (3.50 g).

**332**: $\delta_H$ (400 MHz, $CDCl_3$) 2.36-2.33 (8H, m, -C*H*$_2$C=O), 1.85-1.83 (8H, m, -C*H*$_2$); $\delta_C$ (75 MHz, $CDCl_3$) 214.3 (-*C*=O, 4$^o$), 42.3 (-*C*-C=O, 2$^o$), 23.6 (-*C*$H_2$-$CH_2$, 2$^o$). $^1$H and $^{13}$C NMR values correspond to literature values.[196,]

#### *5.3.3.2 Formation of cyclodecane-1,6-dione by ozonolysis*

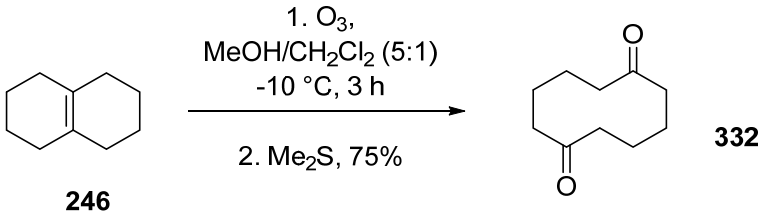


This reaction was adapted from a literature procedure.[197]

$\Delta^{9,10}$-Octalin **246** (1.0 eq., 9.00 g, 0.066 mol) dissolved in MeOH/$CH_2Cl_2$ (85 mL:15 mL) was cooled to -10 °C with stirring. Ozone was bubbled through reaction mixture into a potassium iodide trap. TLC showed all starting material consumed after 3 h. $Me_2S$ (1.5 eq., 6.15 g, 0.099 mol) was added to the reaction mixture and allowed to warm to rt. Solvent was removed under reduced pressure, crude material dissolved in $CH_2Cl_2$ and washed with $NaHCO_3$ solution. Organic layer dried over $MgSO_4$ and concentrated. The compound, **332**, was subjected to silica gel column chromatography (eluent petrol/EtOAc 95:5) and obtained in 75% yield (8.32 g). $^1$H NMR data corresponded with those previously obtained.

### *5.3.3.3 Intramolecular Aldol condensation of cyclodecane-1,6-dione, 332*

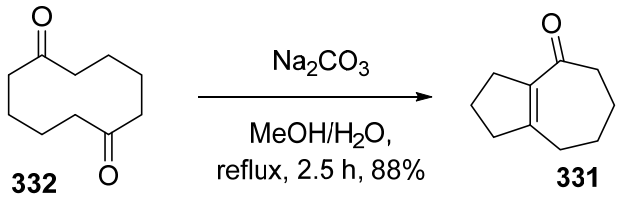


This reaction was performed in accordance with a literature procedure.[197]

Cyclodecane-1,6-dione **332** (1.0 eq., 3.50 g, 0.021 mol) dissolved in MeOH (11 mL) and 10% $Na_2CO_3$ solution (2.45 eq., 54 mL) and stirred at reflux for 2.5 h. After cooling to rt, organic layer extracted with $CH_2Cl_2$ (4 × 25 mL), dried over $MgSO_4$ and concentrated under reduced pressure. Crude material flushed through silica pad (100% pentane) to afford 2,3,5,6,7,8-hexahydroazulen-4(1H)-one **331** as a colourless oil (2.74 g, 88%).

**Unsaturated ketone 331**: $\delta_H$ (250 MHz, $CDCl_3$) 2.57 (6H, m), 2.42 (2H, bs), 1.77 (6H, m); $\delta_C$ (62.5 MHz, $CDCl_3$) 201.5 (-C=O, 4°), 159.1 (*C*=C-C=O, 4°), 138.6 (C=*C*-C=O, 4°), 44.0, 41.7, 34.0, 31.7, 26.0, 22.5, 21.3; $^1$H and $^{13}$C NMR values correspond to literature values.[197]

### *5.3.3.4 Wolff-Kishner Reduction of 2,3,5,6,7,8-hexahydroazulen-4(1H)-one, 331*

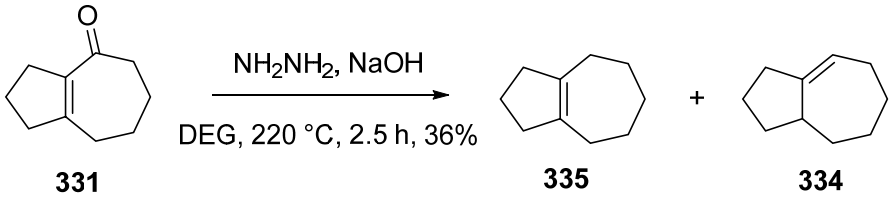


2,3,5,6,7,8-hexahydroazulen-4(1H)-one **331** (1.0 eq., 2.73 g, 0.018 mol) was dissolved in diethylene glycol (30 mL) under Ar with condenser, to which was added NaOH (4.0 eq., 2.91 g, 0.073 mol) and 80% $NH_2NH_2.H_2O$ (3.3 eq., 3.75 g, 0.060 mol). The stirring reaction mixture was heated to 100 °C for 1 h, then condenser removed and distillation glassware used to distill off $H_2O$ as the reaction mixture heated to 220 °C for a further 1.5 h. The reaction mixture was cooled to rt, reaction and receiver flask transferred to separating funnel, diluted with water and extracted with hexane (3 × 50 mL). Organic layers combined and washed with brine, dried over $MgSO_4$ and concentrated under reduced pressure. Crude product purified by flushing through silica pad with pentane (0.902 g, 36%). $^1$H NMR shows the presence of isomerised (trisubstituted) product **334** and $^{13}$C NMR shows a mixture of both isomers **334** and **335**.

### *5.3.3.5 Clemmensen Reduction of 2,3,5,6,7,8-hexahydroazulen-4(1H)-one, 331*

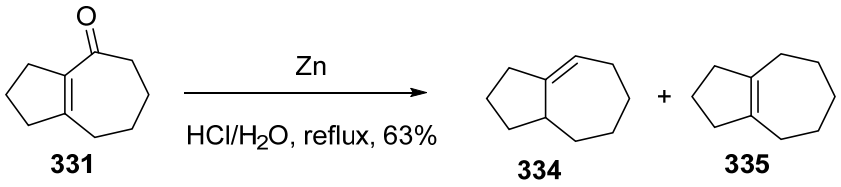


**331** **334** **335**

To a mixture of 2,3,5,6,7,8-hexahydroazulen-4(1H)-one **331** (1.0 eq., 4.50 g, 0.030 mol) and zinc powder (23.0 eq., 45 g, 0.690 mol) was gradually added an HCl solution (9 M, 187mL). Reaction mixture heated to reflux at 100 °C for 3 h. After cooling to rt, reaction mixture was carefully diluted by addition to 300 mL of water and transferred to a separating funnel. Organic layer extracted with pentane (3 × 100 mL), dried over $MgSO_4$ and concentrated under reduced pressure. The mixture of alkenes, **334** and **335** (2.58g, 63%, colourless oil) were taken forward to hydrogenation without further purification.

### *5.3.3.6 Hydrogenation of alkenes 334 and 335*

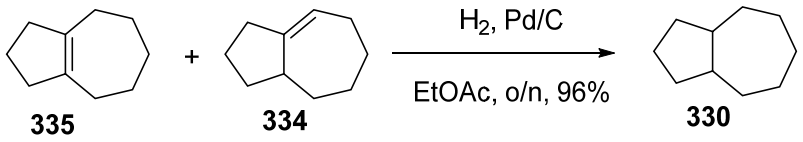


**335** **334** **330**

A mixture of alkenes, **335** and **334**, (1.0 eq., 2.80 g, 0.021 mol) were dissolved in EtOAc (80 mL) to which Pd/C (230 mg) was added. The reaction was allowed to stir at room temperature overnight under 1 atmosphere of $H_2$. Gas was then removed under vacuum, Pd/C removed by flushing reaction mixture through a celite pad and EtOAc removed under reduced pressure. A mixture of *cis* and *trans* bicyclo[5.3.0]decane **330** was identified as a colourless oil (2.74 g, 96%).

**Bicyclo[5.3.0]decane 330**: $\delta_H$ (300 MHz, $CDCl_3$) 2.49-1.02 (36H, m); $\delta_C$ (75 MHz, $CDCl_3$) 46.3, 43.4, 35.8, 35.1, 34.3, 32.9, 31.7, 29.7, 28.0, 26.6, 26.5, 24.0; $\nu_{max}$ 2917, 2850, 1449, 1358, 1156, 949 $cm^{-1}$.

### *5.3.3.7 Baddeley Reaction of Bicyclo[5.3.0]decane, 330*

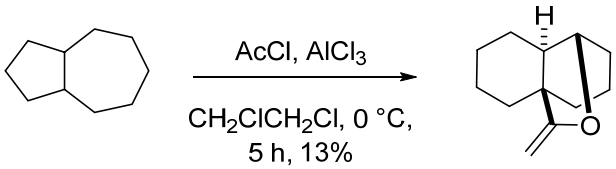


The general procedure for the Baddeley reaction was followed, using aluminium trichloride (3.65 g, 0.0274 mol), acetyl chloride (3.44 g, 0.0439 mol) and bicyclo[5.3.0]decane **330** (2.53 g, 0.0183 mol) in 1,2-dichloroethane (10 mL). Enol ether **244** was isolated in 13% yield (0.422 g).

**Enol ether 244**: $\delta_H$ (250 MHz, $CDCl_3$) 4.22 (1H, dt, *J* = 1.5, 0.5 Hz, =C*H*$_2$), 4.03 (1H, d, *J* = 4.5Hz, -C*H*-O), 3.65 (1H, d, *J* = 1.5 Hz, =$CH_2$), 1.88-1.07 (15H, m); $\delta_C$ (75 MHz, $CDCl_3$) 166.0, 80.4, 76.9, 50.0, 46.2, 39.5, 31.3, 30.2, 26.5, 24.9, 22.1, 18.9. $^{1}$H and $^{13}$C NMR data correspond to previously obtained data.

### 5.3.4 Bicyclo[5.4.0]undecane

#### *5.3.4.1 Wolff-Kishner Reduction of Benzosuber-1-one*

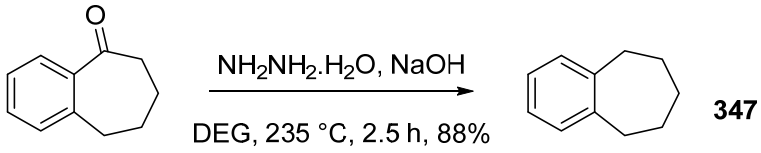


**347**

This reaction was performed in accordance with a literature procedure.[198]

Benzosuber-1-one (1.0 eq., 50.0 g, 0.310 mol), NaOH (4.0 eq., 49.8 g, 1.23 mol) and $NH_2NH_2.H_2O$ (3.3 eq., 51.6 g, 1.03 mol) were combined in diethylene glycol (200 mL) and heated to 100 °C for 1 h. Reflux apparatus was replaced with distillation apparatus; temperature of reaction flask was raised to 235 °C for 1.5 h and then allowed to cool to rt overnight. Both an organic and an aqueous layer were observed in the receiver flask and the reaction flask. Both flasks underwent the following work-up procedure. The mixture was diluted with water, transferred to separating funnel and organic product was extracted with hexane (3 × 100 mL). Hexane extracts were combined and washed with brine, dried over $MgSO_4$, and concentrated under reduced pressure. Organic layers from both flasks yielded an oily liquid identified as **347** in 88% yield (33.7 g).

**Arene 347**: $\delta_H$ (250 MHz, $CDCl_3$) 7.22 (4H, s, aryl –CH), 2.95-2.91 (4H, m, benzylic -$CH_2$), 2.00-1.93 (2H, m, -$CH_2$), 1.83-1.74 (4H, m, -$CH_2$). $\delta_C$ (62.5 MHz, $CDCl_3$) 143.5 (2C, 4°), 129.1 (2C, 3°), 126.0 (2C, 3°), 36.8 (2C, 2°), 32.9 (1C, 2°), 28.4 (2C, 2°). $^1$H and $^{13}$C NMR data correspond with literature data.[199]

#### *5.3.4.2 Birch Reduction of 347*

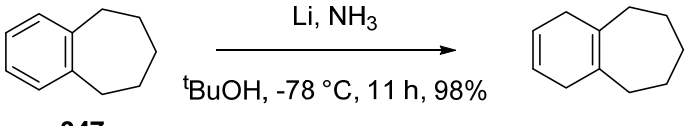


**347** **348**
Mixture of alkenes

This reaction was adapted from a literature procedure.[200]

2-necked 1 L flask and coldfinger oven dried and flushed with Ar, then cooled to -78 °C in a dry ice/acetone bath. Ammonia (200 mL) was condensed into the flask, then while stirring a mixture of $^t$BuOH (78 mL), $Et_2O$ (14 mL) and 6,7,8,9-tetrahydro-5H-benzo[7]annulene **347** (1.0 eq., 10.8 g, 0.074 mol) was added slowly. Over 6 h, Li (7.5 eq., 3.85 g, 0.555 mol) was added piecewise to the reaction mixture, turning a distinctive blue colour. After addition of Li, the reaction mixture was stirred at -78 °C for a further 5 h, then ice bath removed and $NH_3$ o/n. Solidified reaction mixture quenched by gradual addition of IPA, MeOH and $H_2O$ over 2 h, then cooled to rt, transferred to separating funnel and extracted with petrol (3 × 100 mL). Organic layers combined and washed with brine, dried over $MgSO_4$ and concentrated under reduced pressure. Crude product flushed through silica pad with hexane to give a mixture of dienes

(10.71 g, 98%) as a colourless oil. Alkene mixture was taken forward to the next step without further purification.

### *5.3.4.3 Hydrogenation of diene mixture*

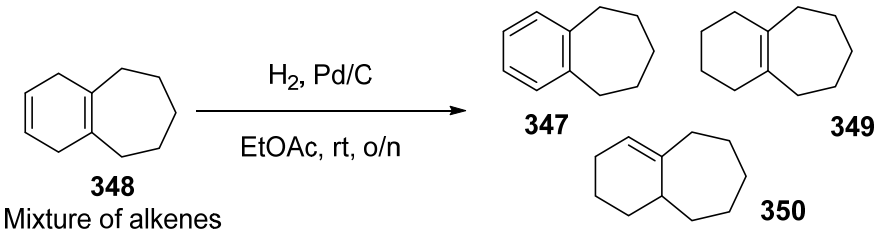


To a mixture of dienes (5.42 g) dissolved in EtOAc (100 mL) was added Pd/C (100 mg), air removed under reduced pressure and put under an atmosphere of $H_2$. The reaction was allowed to stir at rt overnight. $H_2$ was removed under vacuum and reaction vessel flushed with $N_2$. Pd/C removed by filtering through a celite pad and filtrate concentrated under reduced pressure.

Column chromatography (100% petrol) gave a mixture of alkenes **349** and **350** (visualised by $KMnO_4$ stain, $R_f$ = 0.98, 4.08 g, 74%) and 6,7,8,9-tetrahydro-5H-benzo[7]annulene **347** (visualised by UV, $R_f$ = 0.83, 0.25 g, 5%). Alkene mixture was taken forwards to further hydrogenation without further separation.

### *5.3.4.4 Hydrogenation of alkenes 349 and 350*

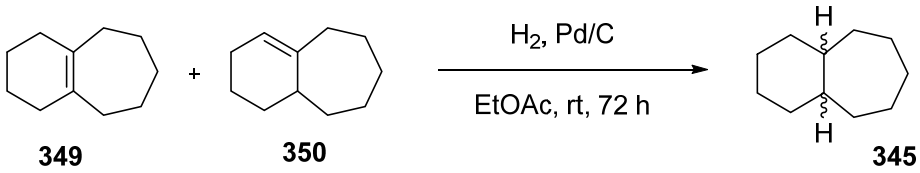


To a mixture of alkenes **349** and **350** (4.08 g) dissolved in EtOAc (100 mL) was added Pd/C (80 mg), air removed under reduced pressure and put under an atmosphere of $H_2$. The reaction was allowed to stir at rt for 72 h. $H_2$ was removed under vacuum and reaction vessel flushed with $N_2$. Pd/C removed by filtering through a celite pad and filtrate concentrated under reduced pressure. A mixture of *cis* and *trans* bicyclo[5.4.0]undecane **345** was obtained as a colourless oil (2.79 g, 68%).

**Bicyclo[5.4.0]undecane 345**: $\delta_H$ (250 MHz, $CDCl_3$) 0.80-1.80 (40H, m) ppm; $\delta_C$ (75 MHz, $CDCl_3$) 46.1, 38.6, 36.1, 36.0, 32.7, 32.4, 31.2, 27.5, 26.8, 26.5, 25.8, 24.4 ppm.

### *5.3.4.5 Baddeley Reaction of Bicyclo[5.4.0]undecane*

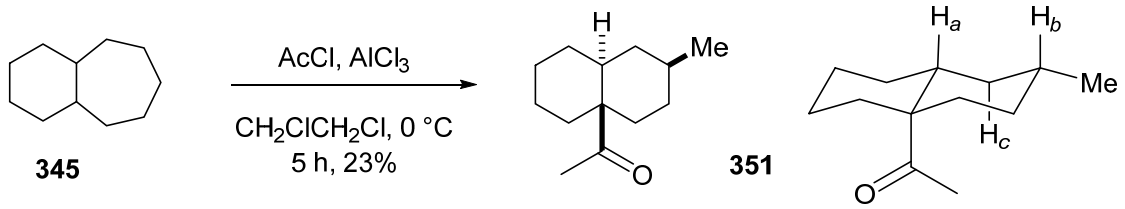


**345** **351**

The general procedure for the Baddeley reaction was followed, using aluminium trichloride (19.7 g, 0.148 mol), acetyl chloride (18.6 g, 0.236 mol) and bicyclo[5.4.0]undecane **345** (15 g, 0.099 mol) in 1,2-dichloroethane (60 mL).

Crude product purified by vacuum distillation (2.1-2.3 Torr, 76-90 °C) gave a mixture of enol ethers and **351** as the major product. This was purified further by column chromatography (100% pentane graduated to 1:99 EtOAc:pentane, $R_f$ = 0.22, 99:1 pentane/EtOAc) to give **351** as a colourless oil (4.46 g, 23%).

**Methyl ketone 351**: $\delta_H$ (400 MHz) 2.02 (3H, s, COC*H*$_3$), 2.01-1.96 (2H, m), 1.91-1.80 (1H, m), 1.75-1.68 (1H, m), 1.59-1.49 (3H, m [including 1.54, 1H, app q, *J* 11.9 Hz, H$^c$]), 1.48-1.36 (1H, m, H$^b$), 1.32-1.04 (7H, m [including 1.25-1.22, 1H, m, H$^a$]), 0.84 (3H, d, *J* 6.3 Hz, CHC*H*$_3$), 0.81-0.70 (1H, m) ppm; $\delta_C$ (100 MHz) 213.3 (C=O), 53.0 (4° *C*-C=O), 46.0 (3° H*C*-C-C=O), 37.9, 37.9, 37.8, 33.6 (*C*H-CH$_3$), 32.0, 29.0, 26.9, 26.0 (CO*C*H$_3$), 23.5, 22.4 (CH-*C*H$_3$) ppm; $\nu_{max}$ 2922, 2856, 1700, 1453, 1352, 1299, 1209, 1184, 1164, 1135, 1113, 940, 914 cm$^{-1}$; HRMS (ESI+) *m/z* calcd for $(C_{13}H_{22}O+Na)^+$ 217.1563; found 217.1564.

### 5.3.5 Isopropylcyclohexane

#### *5.3.5.1 Baddeley Reaction of isopropylcyclohexane*

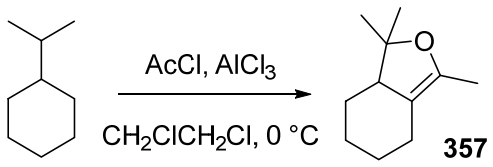


**357**

The general procedure for the Baddeley reaction was followed, using aluminium trichloride (319 g, 2.39 mol), acetyl chloride (300 g, 3.82 mol) and isopropylcyclohexane (200 g, 1.59 mol) in 1,2-dichloroethane (500 mL).

Fractional distillation was performed at rt under reduced pressure. Unreacted isopropylcyclohexane was collected in a mixture with 1-chloroethylacetate by-product. The orange residue identified as a mixture with 1,1,3-trimethyl-1,4,5,6,7,7a-hexahydroisobenzofuran **357** as the major product.

**Enol ether 357**: $\delta_H$ (250MHz, $CDCl_3$) 0.60-2.20 (18H, m) ppm; $\delta_C$ (75MHz, $CDCl_3$) 141.6 (=C(Me)-O, $4^o$), 108.2 (-C-O, $4^o$), 83.3 (C=*C*-C, $4^o$), 53.6, 29.6, 28.5, 26.6, 25.7, 24.2, 22.9, 11.2 ppm; TOF-MS (ESI+) *m/z* calcd for $(C_{11}H_{18}O+H)^+$ 167.1436; found 167.1440.

## 5.4 Experimental Procedures Relating to Chapter 4

### 5.4.1 Synthesis of Unfunctionalised Naphthalenediimides

#### *5.4.1.1 Synthesis of 397*

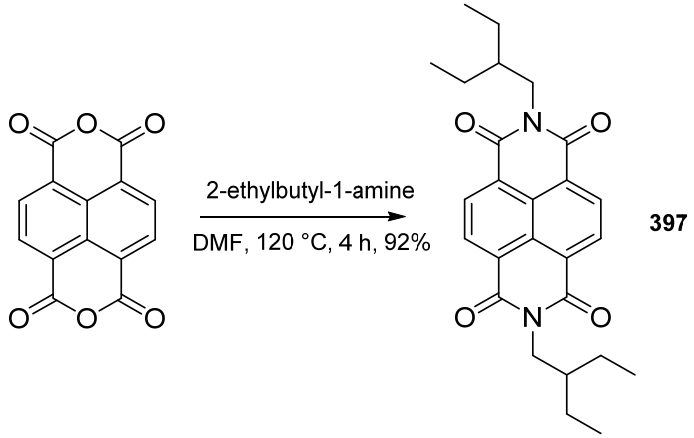


To a stirring suspension of 1,4,5,8-naphthalenetetracarboxylic dianhydride (1.0 eq., 1.00 g, 3.73 mmol) in DMF (40 mL) was added 2-ethylbutyl-1-amine (2.2 eq., 830 mg, 8.20 mmol). The resulting mixture was heated to 120 °C for 4 h. After cooling to rt, the reaction mixture was poured over 1.0M aqueous HCl (100 mL). The organic product was extracted with $CHCl_3$ (3 × 50 mL) and organic layers were washed with saturated aqueous LiCl solution and dried over $MgSO_4$. Concentration under reduced pressure afforded **397** as a pale orange solid in 92% yield (1.492 g).

**Naphthalenediimide 397**: $\delta_H$ (300 MHz, $CDCl_3$) 8.75 (4H, s, Ar-H), 4.15 (4H, d, *J* = 7.5 Hz, N-$CH_2$), 1.95-1.82 (2H, m, methine protons), 1.47-1.32 (8H, m, C$H_2$-$CH_3$), 0.95 (12H, t, *J* = 7.5 Hz, C$H_3$); $\delta_C$ (75 MHz, $CDCl_3$) 163.2 (C=O), 131.0 (Ar), 126.7 (Ar), 126.6 (Ar), 44.3 (N-*C*$H_2$), 39.3 (N-$CH_2$-*C*$H_2$), 23.4 (-*C*$H_2$-$CH_3$), 10.6 ($CH_3$); $\nu_{max}$ 2962, 2933, 2857, 1699, 1653, 1581, 1454, 1333, 1242, 1080, 770 $cm^{-1}$; TOF-MS (ESI+) *m/z* calcd for $(C_{26}H_{30}N_2O_4+H)^+$ 435.2278; found 435.2314.

#### *5.4.1.2 Synthesis of 399*

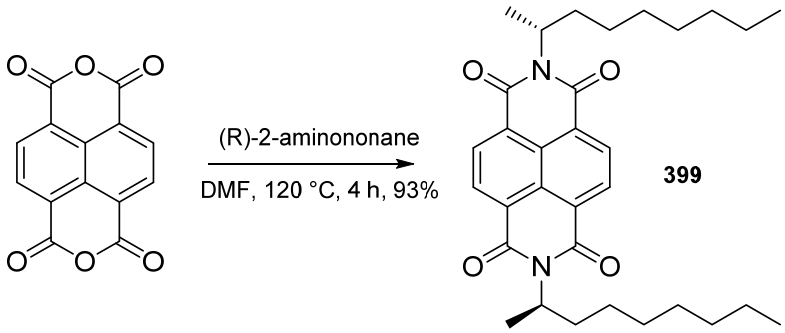


To a stirring suspension of 1,4,5,8-naphthalenetetracarboxylic dianhydride (1.0 eq., 178 mg, 0.66 mmol) in DMF (20 mL) was added (R)-2-aminononane (2.1 eq., 200 mg, 1.40 mmol). The resulting mixture was heated to 120 °C for 4 h. After cooling to rt, the reaction mixture was poured over 1.0M aqueous HCl (50 mL). The organic product was extracted with EtOAc (3 × 30 mL) and organic layers were washed with saturated aqueous LiCl solution and dried over $MgSO_4$. Concentration under reduced pressure afforded **399 as a** pale orange solid in 93% yield (329 mg).

**Naphthalenediimide 399**: $\delta_H$ (250 MHz, $CDCl_3$) 8.72 (4H, s, Naphthyl-H), 5.26 (2H, tq, *J* = 7.5 Hz, 6.5 Hz, N-CH), 2.23-2.10 (2H, m), 1.93-1.85 (2H, m), 1.58 (6H, d, *J* = 7.5 Hz, CH-C*H*$_3$), 1.33-1.16 (20H, m, $(CH_2)_5$), 0.83 (6H, t, *J* = 6.5 Hz, $CH_2$-C*H*$_3$); $\delta_C$ (75 MHz, $CDCl_3$) 163.2 (C=O), 130.8 (Ar CH), 126.7 (Ar), 126.6 (Ar), 50.3 (N-CH), 33.3 ($CH_2$), 31.7 ($CH_2$), 29.3 ($CH_2$), 29.1 ($CH_2$), 27.0 ($CH_2$), 22.5 ($CH_2$), 18.2 (CH-C*H*$_3$), 14.0 ($CH_2$-C*H*$_3$); $[\alpha]_D^{24}$= -17.8 (*c* 0.6, $CHCl_3$); $\nu_{max}$ 2952, 2922, 2854, 1709, 1648, 1582, 1454, 1333, 1246, 1184, 766 $cm^{-1}$; TOF-MS (ESI+) *m/z* calcd for $(C_{32}H_{42}N_2O_4+H)^+$ 519.3217; found 519.3258.

### *5.4.1.3 Synthesis of 401*

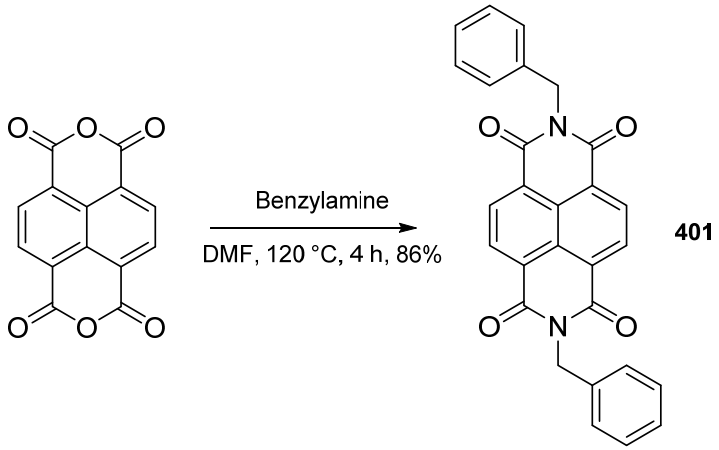


To a stirring suspension of 1,4,5,8-naphthalenetetracarboxylic dianhydride (1.0 eq., 500 mg, 1.87 mmol) in DMF (20 mL) was added benzylamine (2.2 eq., 439 mg, 4.10 mmol). The resulting mixture was heated to 120 °C for 4 h. After cooling to rt, the reaction mixture was poured over 1.0M aqueous HCl (100 mL). The organic product was extracted with EtOAc (3 × 50 mL) and organic layers were washed with saturated aqueous LiCl solution and dried over $MgSO_4$. Concentration under reduced pressure afforded **401** as a pale yellow solid in 96% yield (801 mg).

**Naphthalenediimide 401**: $\delta_H$ (300 MHz, $CDCl_3$) 8.77 (4H, s, Naphthyl-H), 7.57-7.54 (4H, m, Ph-H), 7.35-7.28 (6H, m, Ph-H), 5.39 (4H, s, $CH_2$); $\delta_C$ (75 MHz, $CDCl_3$) 162.8, 136.5, 131.1, 129.1, 128.5, 127.8, 126.7, 126.6, 44.0.

$^1$H NMR values correspond to literature values, except for the aliphatic methylene resnonance which was previously reported at 3.7 ppm.[201]

### *5.4.1.4 Synthesis of 402*

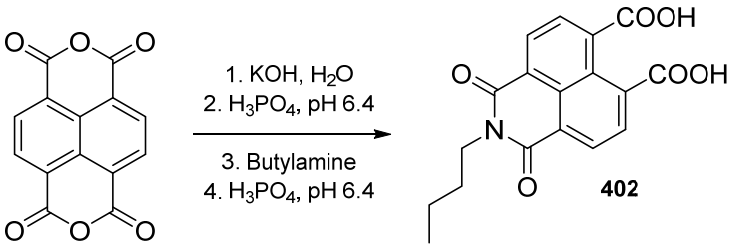


To a stirring suspension of 1,4,5,8-naphthalenetetracarboxylic dianhydride (1.0 eq., 500 mg, 1.87 mmol) in $H_2O$ (90 mL) was added aqueous KOH solution (1.0 M, 9 mL) and heated to 50 °C until 1,4,5,8-naphthalenetetracarboxylic dianhydride dissolved. Aqueous $H_3PO_4$ solution (1.0 M) was used to acidify the reaction mixture to pH 6.4, then butylamine (1.0 eq, 136 mg, 1.87 mmol) was added. Further $H_3PO_4$ solution was used to readjust the solution to pH 6.4, then heated to 110 °C for 16 h. After cooling to rt, glacial acetic acid (≈3 mL) was added and a precipitate formed. Precipitate filtered and washed with $H_2O$, then dried under vacuum giving **402** as an off-white solid, in 62% yield (396 mg).

**Naphthalene monoimide 402**: $\delta_H$ (250 MHz, DMSO-$d_6$) 8.54 (2H, d, *J* = 7.5 Hz, Naphthyl-H), 8.17 (2H, d, *J* = 7.5 Hz, Naphthyl-H), 4.04 (2H, t, *J* = 7.5 Hz, N-C*H*$_2$), 1.63 (2H, quintet, *J* = 7.5 Hz, $CH_2$-C*H*$_2$-$CH_2$), 1.36 (2H, sextet, *J* = 7.5 Hz, C*H*$_2$-$CH_3$), 0.93 (3H, t, *J* = 7.5 Hz, C*H*$_3$) ppm; $\delta_C$ (75 MHz, DMSO-$d_6$) 168.6, 162.9, 130.1, 129.1, 128.6, 125.5, 124.4, 39.6, 29.6, 19.8, 13.8 ppm.

$^1$H NMR values correspond with literature values.[202]

### *5.4.1.5 Synthesis of 403*

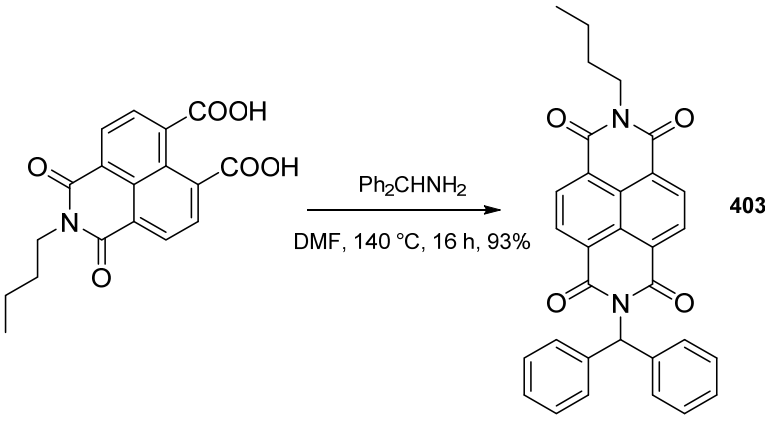


To a stirring suspension of **402** (1.0 eq., 300 mg, 0.92 mmol) in DMF (20 mL) was added benzhydrylamine (1.0 eq., 164 mg, 0.92 mmol). The resulting mixture was heated to 140 °C for 16 h. After cooling to rt, the reaction mixture was poured over 1.0 M aqueous HCl (50 mL). The organic product was extracted with $CHCl_3$ (3 × 50 mL) and organic layers were washed with saturated aqueous LiCl solution and dried over $MgSO_4$. Concentration under reduced pressure afforded the pale orange solid, **403**, in 93% yield (408 mg).

**Naphthalenediimide 403**: $\delta_H$ (300 MHz, $CDCl_3$) 8.74 (4H, s, Naphthyl-H), 7.63 (1H, s, Ph-C*H*-PH), 7.48-7.45 (4H, m, Ph-H), 7.38-7.30 (6H, m, Ph-H), 4.20 (2H, t, *J* = 7.5 Hz, N-C*H*$_2$-), 1.76-1.68 (2H,

m, $CH_2$-C*H*$_2$-$CH_2$) 1.46 (2H, sextet, *J* = 7.0 Hz, -C*H*$_2$-$CH_3$), 0.99 (3H, t, *J* = 7.0 Hz, -C*H*$_3$) ppm; $\delta_C$ (75 MHz, $CDCl_3$) 162.9 (C=O), 162.8 (C=O), 138.0 (Ar C), 131.4 (2C, Naphthyl CH), 130.9 (2C, Naphthyl CH), 130.1 (Ar C), 128.8 (4C, Ar CH), 128.3 (4C, Ar CH), 127.6 (2C, Ar CH), 126.8 (Ar C), 126.7 (Ar C), 126.7 (Ar C), 59.5 (Ph-*C*H-Ph), 40.8 (N-$CH_2$), 30.1 (N-$CH_2$-*C*$H_2$), 20.3 (*C*$H_2$-$CH_3$), 13.8 ($CH_3$) ppm; $\nu_{max}$ 3063, 2955, 1702, 1656, 1578, 1451, 1336, 1244, 770, 696 $cm^{-1}$; TOF-MS (ESI+) *m/z* calcd for $(C_{31}H_{24}N_2O_4+Na)^+$ 511.1634; found 511.1650.

### 5.4.2 General Conditions for Initial C-H Borylation Reactions

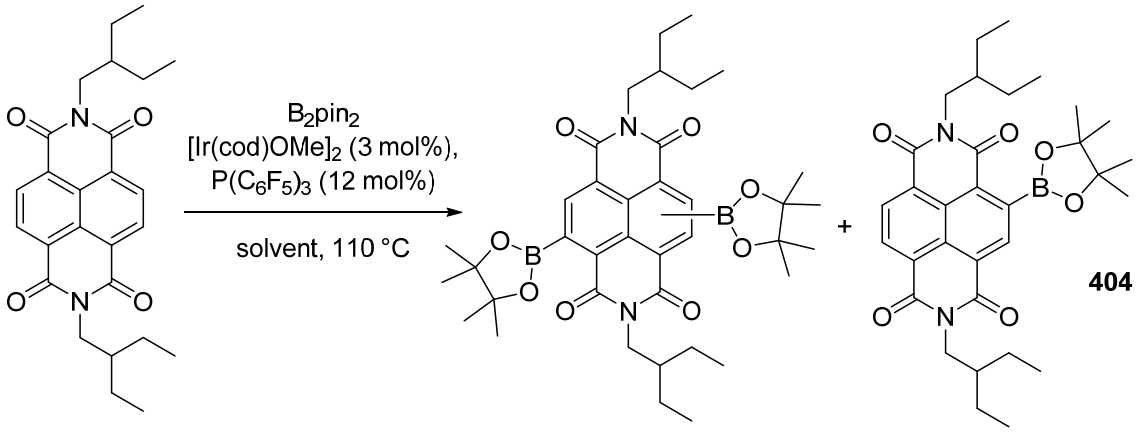


Bis(pinacolato)diboron and naphthalenediimide **397** (1.0 eq.) were weighed out into a round - bottomed flask with stirrer bar and condenser and transferred into an argon filled glovebox. $[Ir(cod)OMe]_2$ (0.03 eq.), ligand (0.12 eq.) were added, then the sealed vessel was removed from the glovebox. The solvent was added via syringe through the suba-seal. The reaction mixture was subjected to thermal heating at 110 °C for 48 h under Ar. After cooling to rt, solvent was removed under reduced pressure and where stated, products were purified via column chromatography ($CH_2Cl_2$, graduated to 5% EtOAc in $CH_2Cl_2$).

#### *5.4.2.1 C-H Borylation using PDI borylation conditions*

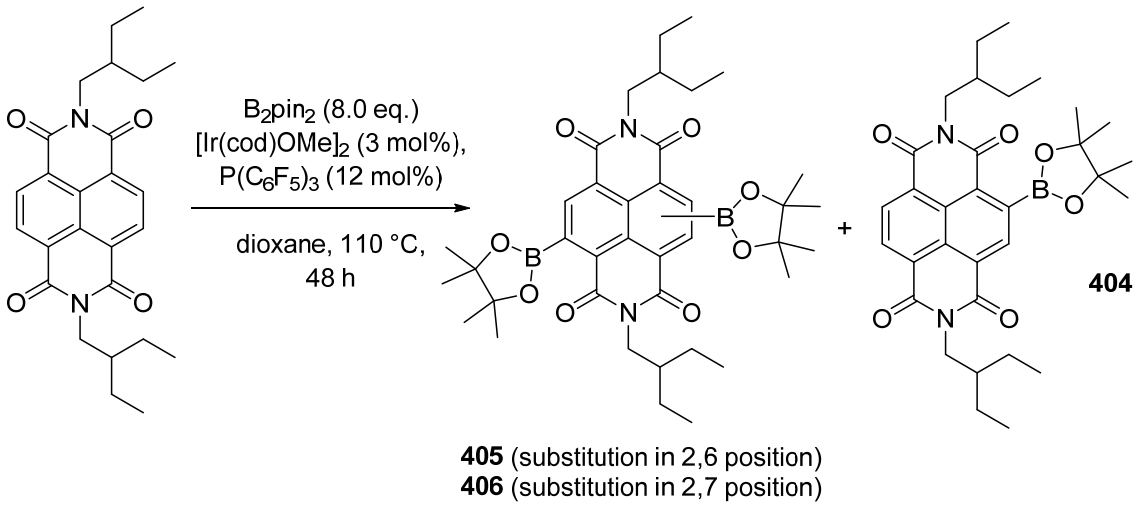


The general procedure for C-H borylation was followed, using $B_2pin_2$ (8.0 eq., 884 mg, 3.48 mmol), **397** (189 mg, 0.435 mmol), $[Ir(cod)OMe]_2$ (8.8 mg, 0.0131 mmol) and perfluorotriphenylphosphine (28 mg, 0.0506 mmol) in dioxane (7.0 mL) for 48 h. 17% conversion to monoborylated product **404** and 76% conversion to diborylated products **405** and **406** were calculated by $^1H$ NMR. 2% isolated yield of monoborylated **404** (4 mg, $R_f$ = 0.45 in 90:10 $CH_2Cl_2$/EtOAc) and 12% isolated yield of diborylated **405** and **406** (36 mg, $R_f$ = 0.21 in 90:10 $CH_2Cl_2$/EtOAc) were obtained.

**Monoborylated 404**: $\delta_H$ (400 MHz, $CDCl_3$) 8.71 (3H, s, Naphthyl-H), 4.14 (2H, d, *J* = 7.2 Hz, N-C*H*$_2$), 4.11 (2H, d, *J* = 7.2 Hz, N-C*H*$_2$), 1.91-1.81 (2H, m, methine H), 1.51 (12H, s, C-C*H*$_3$), 1.43-1.34 (8H, m, C*H*$_2$-CH$_3$), 0.95 (12H, t, *J* = 7.4 Hz, CH$_2$-C*H*$_3$); $\delta_C$ (100 MHz, $CDCl_3$) 164.8, 163.5, 163.3, 163.3, 133.9, 130.9, 130.9, 129.9, 126.7, 126.5, 126.3, 126.0, 125.1, 84.9, 44.2, 44.1, 39.4, 39.4, 24.9, 23.5, 23.4, 10.6, 10.5; $\delta_{B(11)}$ (96 MHz, $CDCl_3$) 36.9; $\nu_{max}$ 2964, 2931, 2877, 1704, 1660, 1579, 1447, 1318, 1236, 1139, 849, 786, 730 cm$^{-1}$; TOF-MS (ESI+) *m/z* calcd for $(C_{32}H_{41}BN_2O_6+Na)^+$ 583.2950; found 583.2876.

**Diborylated 405** and **406**: $\delta_H$ (500 MHz, $CDCl_3$) 8.69 (2H, s, Naphthyl-H), 8.69 (2H, s, Naphthyl-H), 4.14 (2H, d, *J* = 7.3 Hz, N-C*H*$_2$ **406**), 4.11 (4H, d, *J* = 7.1 Hz, N-C*H*$_2$ **405**), 4.08 (2H, d, *J* = 7.1 Hz, N-C*H*$_2$ **406**), 1.88-1.82 (4H, m, methine H), 1.51 (24H, B-O-C-C*H*$_3$), 1.50 (24H, B-O-C-C*H*$_3$), 1.40-1.34 (16H, m, C*H*$_2$-CH$_3$), 0.94 (12H, t, *J* = 7.3 Hz, CH$_2$-C*H*$_3$), 0.94 (12H, t, *J* = 7.3 Hz, CH$_2$-C*H*$_3$); $\delta_C$ (125 MHz, $CDCl_3$) 164.9, 164.9, 163.5, 163.5, 133.9, 133.8, 129.8, 129.6, 126.8, 126.3, 126.0, 125.3, 125.0, 125.0, 124.9, 84.9, 44.1, 44.0, 43.8, 39.5, 39.4, 39.4, 24.9, 24.9, 23.6, 23.5, 23.4, 10.7, 10.5, 10.4; $\delta_{B(11)}$ (160 MHz, $CDCl_3$) 30.6; $\nu_{max}$ 2974, 2932, 1703, 1661, 1584, 1453, 1371, 1319, 1233, 1140, 851 cm$^{-1}$; TOF-MS (ESI+) *m/z* calcd for $(C_{38}H_{52}B_2N_2O_8+Na)^+$ 709.3807; found 709.3816.

This reaction was first carried out by Montserrat Pérez-Salvia.

### *5.4.2.2 C-H Borylation with 24 h Reaction Time*

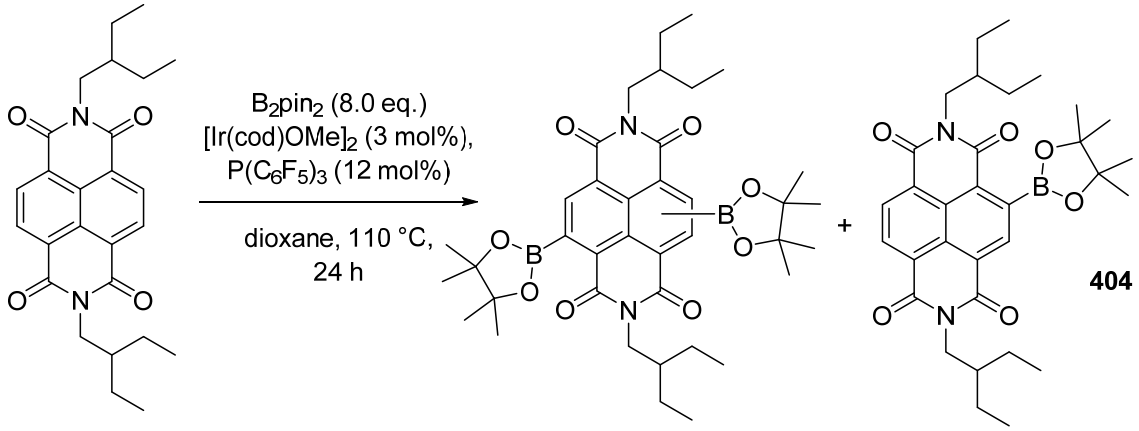


**405** (substitution in 2,6 position)
**406** (substitution in 2,7 position)

The general procedure for C-H borylation was followed, using $B_2pin_2$ (8.0 eq., 884 mg, 3.48 mmol), **397** (189 mg, 0.435 mmol), $[Ir(cod)OMe]_2$ (8.8 mg, 0.0131 mmol) and perfluorotriphenylphosphine (28 mg, 0.0506 mmol) in dioxane (7.0 mL) for 24 h. 28% conversion to monoborylated product **404** and 64% conversion to diborylated products **405** and **406** were calculated by $^1$H NMR.

### *5.4.2.3 C-H Borylation with 4.0 equivalents of $B_2pin_2$*

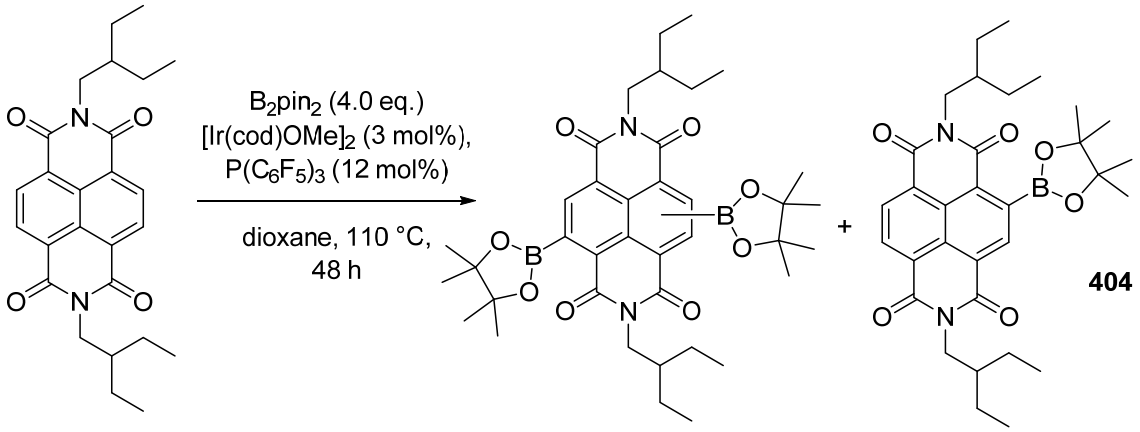


**405** (substitution in 2,6 position)
**406** (substitution in 2,7 position)

The general procedure for C-H borylation was followed, using $B_2pin_2$ (4.0 eq., 442 mg, 1.74 mmol), **397** (189 mg, 0.435 mmol), $[Ir(cod)OMe]_2$ (8.8 mg, 0.0131 mmol) and perfluorotriphenylphosphine (28 mg, 0.0506 mmol) in dioxane (7.0 mL) for 48 h. 50% conversion to monoborylated product **404** and 25% conversion to diborylated products **405** and **406** were calculated by $^1$H NMR.

### *5.4.2.4 C-H Borylation with Hexafluorobenzene*

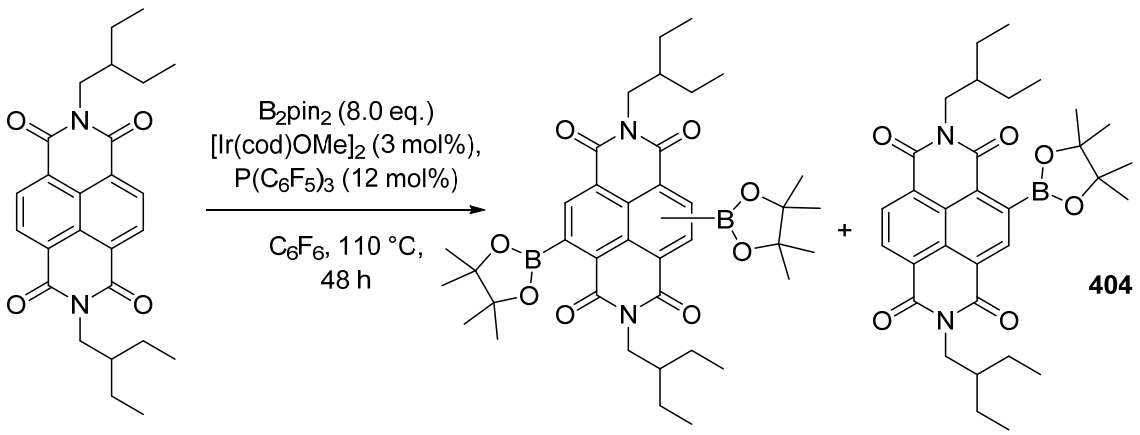


**405** (substitution in 2,6 position)
**406** (substitution in 2,7 position)

The general procedure for C-H borylation was followed, using $B_2pin_2$ (8.0 eq., 294 mg, 1.160 mmol), **397** (63 mg, 0.145 mmol), $[Ir(cod)OMe]_2$ (2.9 mg, 0.0044 mmol) and perfluorotriphenylphosphine (9.3 mg, 0.0174 mmol) in hexafluorobenzene (3.0 mL) for 48 h. 18% conversion to monoborylated product **404** and 76% conversion to diborylated products **405** and **406** were calculated by $^1$H NMR.

This reaction was first carried out by Camilla Shotton.

### 5.4.3 General Conditions for Reaction Optimisation of Microwave-Assisted C-H Borylation

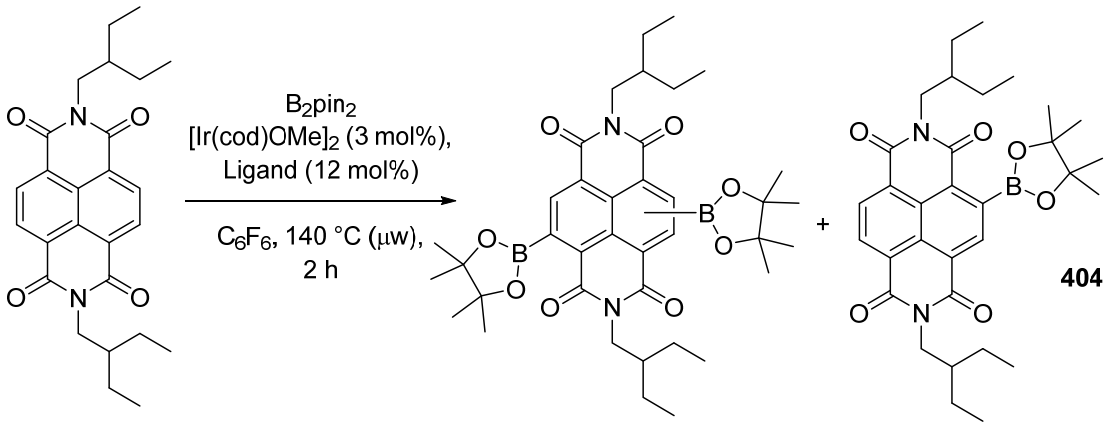


**405** (substitution in 2,6 position)
**406** (substitution in 2,7 position)

Bis(pinacolato)diboron and naphthalenediimide **397** (1.0 eq.) were weighed out into a microwave tube with stirrer bar and transferred into a glovebox. $[Ir(cod)OMe]_2$ (0.03 eq.), ligand (0.12 eq.) and hexafluorobenzene were added and the crimp cap was sealed. The reaction mixture was subjected to microwave heating at 140 °C for 2 h. After cooling to rt, solvent was removed under reduced pressure and where stated, products were purified via silica gel column chromatography (eluent $CH_2Cl_2$, graduated to 5% EtOAc in $CH_2Cl_2$, unless otherwise stated).

#### *5.4.3.1 C-H Borylation Ligand Screening*

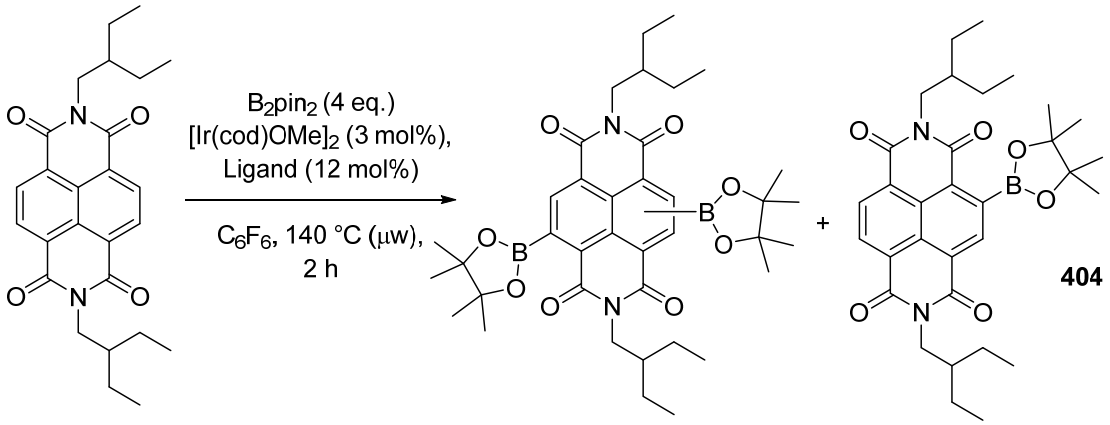


**405** (substitution in 2,6 position)
**406** (substitution in 2,7 position)

The general procedure for microwave-assisted C-H borylation was followed, using $B_2pin_2$ (4.0 eq., 147 mg, 0.580 mmol), **397** (63 mg, 0.145 mmol), $[Ir(cod)OMe]_2$ (2.9 mg, 0.0044 mmol) and ligand (0.0174 mmol) in hexafluorobenzene (3.0 mL). Conversion to monoborylated product **404** and to diborylated products **405** and **406** were calculated by $^1H$ NMR.

| Ligand | Conversion to **404** | Conversion to **405** and **406** |
|---|---|---|
| 2,2-bipyridine | 0% | 0% |
| 4,4-di-*t*butyl-2,2-bipyridine | 6% | 0% |
| triphenylphosphine | 44% | 45% |
| *Perfluorotriphenylphosphine | 12% (8% isolated yield) | 85% (67% isolated yield) |

*This reaction (without separation) was first carried out by Camilla Shotton.

### *5.4.3.2 C-H Borylation using various quantities of $B_2pin_2$*

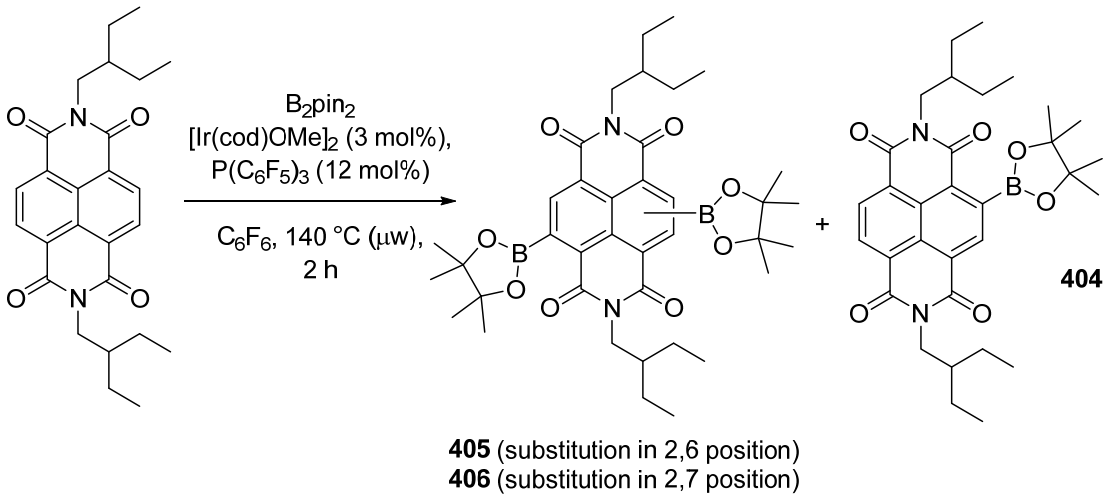


**405** (substitution in 2,6 position)
**406** (substitution in 2,7 position)

The general procedure for microwave-assisted C-H borylation was followed, using $B_2pin_2$, **397** (63 mg, 0.145 mmol), $[Ir(cod)OMe]_2$ (2.9 mg, 0.0044 mmol) and perfluorotriphenylphosphine (9.3 mg, 0.0174 mmol) in hexafluorobenzene (3.0 mL). Conversion to monoborylated product **404** and to diborylated products **405** and **406** were calculated by $^1$H NMR.

| $B_2pin_2$ | Conversion to **404** | Conversion to **405** and **406** |
|---|---|---|
| *1.0 eq., 0.145 mmol | 36% | 9% |
| *2.0 eq., 0.290 mmol | 48% | 42% |
| 3.0 eq., 0.435 mmol | 22% | 75% |
| *8.0 eq., 1.160 mmol | 7% | 84% |

*This reaction was first carried out by Camilla Shotton.

### *5.4.3.3 C-H Borylation of 399*

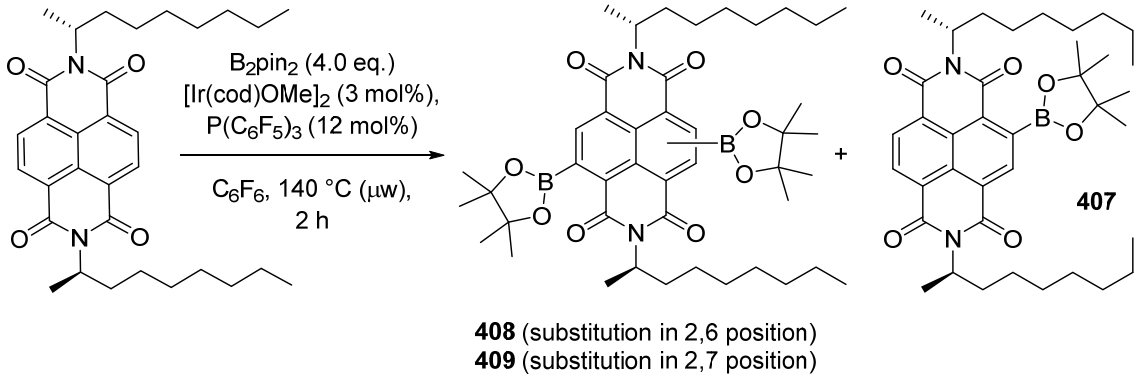


**408** (substitution in 2,6 position)
**409** (substitution in 2,7 position)

The general procedure for microwave-assisted C-H borylation was followed, using $B_2pin_2$ (4.0 eq., 147 mg, 0.580 mmol), **399** (75 mg, 0.145 mmol), $[Ir(cod)OMe]_2$ (2.9 mg, 0.0044 mmol) and perfluorotriphenylphosphine (9.3 mg, 0.0174 mmol) in hexafluorobenzene (3.0 mL). 16% conversion to monoborylated product **407** and 81% conversion to diborylated products **408** and **409** were calculated by $^1$H NMR. Monoborylated **407** was isolated in 9% yield (8 mg, $R_f$ = 0.40 in 95:5 hexane/EtOAc) and diborylated **408** and **409** were isolated as an inseparable 1:1 mixture in 61% yield (68 mg, $R_f$ = 0.23 in 95:5 hexane/EtOAc).

**Monoborylated 407**: $\delta_H$ (300 MHz, $CDCl_3$) 8.68 (3H, s, Ar-H), 5.30-5.16 (2H, m, 2 × N-C*H*), 2.24-2.07 (2H, m), 1.96-1.82 (2H, m), 1.57 (3H, d, *J* = 7.0 Hz, CH-C$H_3$), 1.56 (3H, d, *J* = 7.0 Hz, CH-C$H_3$), 1.51 (12H, s, B-O-C-C$H_3$), 1.31-1.18 (20H, m, C$H_2$), 0.84 (3H, t, *J* = 7.0 Hz, $CH_2$-C$H_3$), 0.82 (3H, t, *J* = 7.0 Hz, $CH_2$-C$H_3$); $\delta_C$ (75 MHz, $CDCl_3$) 164.9, 163.6, 163.4, 163.3, 133.8, 130.8, 130.7, 130.2, 126.6, 126.5, 125.9, 125.3, 84.8, 50.5, 50.3, 33.4, 31.8, 31.7, 29.3, 29.2, 27.0, 24.9, 24.9, 22.6, 22.6, 18.3, 18.2, 14.1, 14.0; $\delta_{B(11)}$ (96 MHz, $CDCl_3$) 33.9; $\nu_{max}$ 2961, 2925, 2856, 1704, 1653, 1582, 1270, 909, 741 cm$^{-1}$; $[\alpha]_D^{24}$= -15.0 (*c* 0.1, $CHCl_3$), TOF-MS (ESI+) *m/z* calcd for $(C_{38}H_{53}BN_2O_6+Na)^+$ 667.3894; found 667.3938.

**Diborylated 408 and 409**: $\delta_H$ (300 MHz, $CDCl_3$) 8.64 (2H, s, Naphthyl-H), 8.64 (2H, s, Naphthyl-H), 5.28-5.09 (4H, m, N-C*H*), 2.21-2.01 (4H, m), 1.95-1.81 (4H, m), 1.57 (3H, d, *J* = 6.5 Hz, CH-C$H_3$ **409**), 1.57 (6H, d, *J* = 7.0 Hz, CH-C$H_3$ **408**), 1.53 (3H, d, *J* = 7.0 Hz, CH-C$H_3$ **409**), 1.50 (24H, s, B-O-C-C$H_3$), 1.50 (24H, s, B-O-C-C$H_3$), 1.30-1.18 (40H, m, C$H_2$), 0.87-0.79 (12H, m, $CH_2$-C$H_3$); $\delta_C$ (75 MHz, $CDCl_3$) 164.9, 164.9, 163.6, 163.5, 138.3 (br), 133.8, 133.6, 130.0, 129.9, 126.7, 125.9, 125.1, 125.0, 84.8, 50.6, 50.4, 50.3, 33.4, 33.4, 31.8, 31.8, 31.7, 29.3, 29.1, 29.1, 27.0, 25.0, 24.9, 24.9, 24.8, 24.8, 22.6, 18.3, 18.2, 18.1, 14.0; $\delta_{B(11)}$ (96 MHz, $CDCl_3$) 33.2; $\nu_{max}$ 2977, 2926, 2857, 1701, 1656, 1585, 1448, 1304, 1136, 731 cm$^{-1}$; TOF-MS (ESI+) *m/z* calcd for $(C_{44}H_{64}B_2N_2O_8+Na)^+$ 793.4746; found 793.4678.

### *5.4.3.4 C-H Borylation of 401*

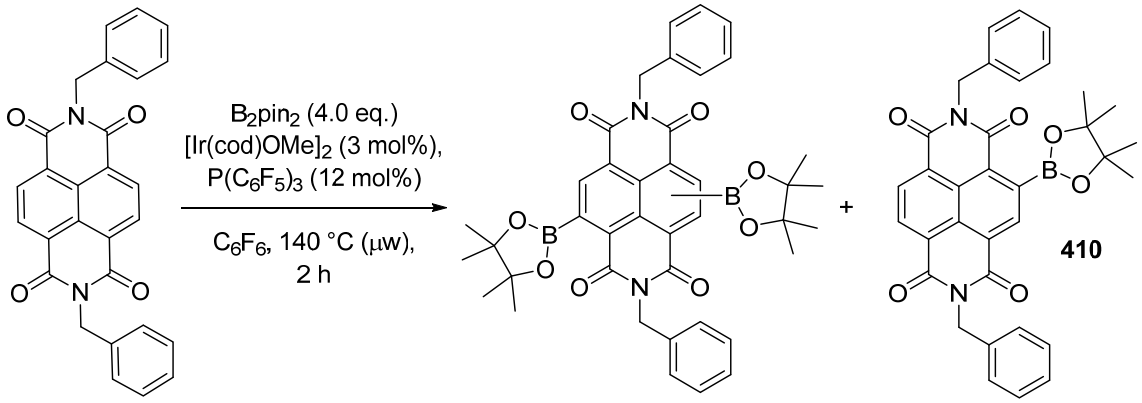


**411** (substitution in 2,6 position)
**412** (substitution in 2,7 position)

The general procedure for microwave-assisted C-H borylation was followed, using $B_2pin_2$ (4.0 eq., 147 mg, 0.580 mmol), **401** (65 mg, 0.145 mmol), $[Ir(cod)OMe]_2$ (2.9 mg, 0.0044 mmol) and perfluorotriphenylphosphine (9.3 mg, 0.0174 mmol) in hexafluorobenzene (3.0 mL). 42% conversion to monoborylated product **410** and 48% conversion to diborylated products **411** and **412** were calculated by $^1$H NMR. Monoborylated **410** was isolated in 30% yield (25 mg, $R_f$ = 0.18 in 85:15 petrol/EtOAc) and diborylated **411** and **412** were isolated as an inseparable 1:1 mixture in 34% yield (34 mg, $R_f$ = 0.08 in 85:15 petrol/EtOAc).

**Monoborylated 410**: $\delta_H$ (300 MHz, $CDCl_3$) 8.74-8.72 (3H, m, Naphthyl-H), 7.55-7.52 (4H, m, Ph-H), 7.34-7.23 (6H, m, Ph-H), 5.38 (2H, s, N-C$H_2$), 5.35 (2H, s, N-C$H_2$), 1.52 (12H, s, $CH_3$); $\delta_C$ (75 MHz, $CDCl_3$) 164.5, 163.1, 162.8, 162.8, 136.5, 136.3, 134.2, 131.1, 131.0, 129.9, 129.4, 129.1, 128.6, 128.5, 127.8, 126.7, 126.6, 126.3, 126.0, 125.1, 85.0, 44.1, 44.0, 24.9; $\delta_{B(11)}$ (96 MHz, $CDCl_3$) 33.0; $\nu_{max}$ 2977, 2931, 1704, 1661, 1447, 1320, 1237, 1132, 851, 699 cm$^{-1}$; TOF-MS (ESI+) *m/z* calcd for $(C_{34}H_{29}BN_2O_6+Na)^+$ 595.2016; found 595.2065.

**Diborylated 411 and 412**: $\delta_H$ (300 MHz, $CDCl_3$) 8.70 (2H, s, Naphthyl-H), 8.69 (2H, s, Naphthyl-H), 7.54-7.51 (8H, m, Ar-H), 7.34-7.24 (12H, m, Ar-H), 5.38 (2H, s, N-$CH_2$ **412**), 5.35 (4H, s, N-$CH_2$ **411**), 5.31 (2H, s, N-$CH_2$ **412**), 1.52 (24H, s, B-O-C-$CH_3$), 1.51 (24H, s, B-O-C-$CH_3$); $\delta_C$ (75 MHz, $CDCl_3$) 164.5, 164.4, 163.1, 163.0, 136.6, 136.4, 136.2, 134.1, 134.0, 129.8, 129.7, 129.6, 129.3, 129.1, 128.5, 128.5, 128.4, 127.8, 126.0, 125.1, 124.9, 85.0, 44.2, 44.0, 43.9, 24.9; $\delta_{B(11)}$ (96 MHz, $CDCl_3$) 33.4; $\nu_{max}$ 2977, 2931, 1703, 1660, 1584, 1448, 1313, 1232, 1133, 964, 852, 713 cm$^{-1}$; TOF-MS (ESI+) *m/z* calcd for $(C_{40}H_{40}B_2N_2O_8+Na)^+$ 721.2868; found 721.2896.

### *5.4.3.5 C-H Borylation of 403*

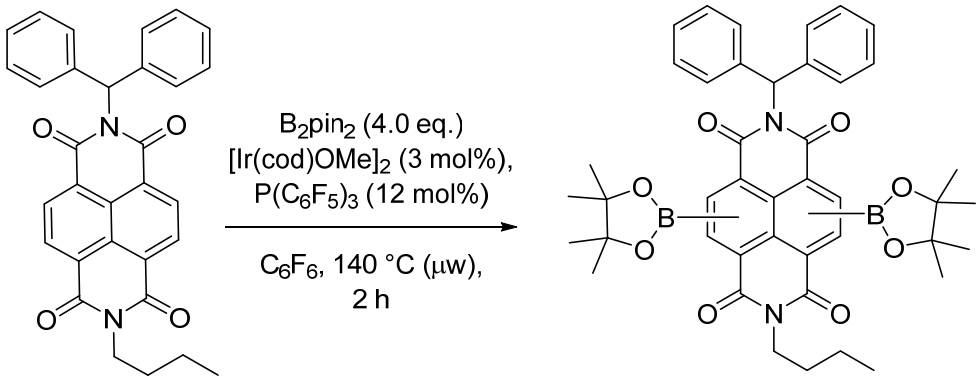


**413** (substitution in 3,6 position)
**416** (substitution in 2,6 position)
**417** (substitution in 2,7 position)

The general procedure for microwave-assisted C-H borylation was followed, using $B_2pin_2$ (4.0 eq., 147 mg, 0.580 mmol), **403** (71 mg, 0.145 mmol), $[Ir(cod)OMe]_2$ (2.9 mg, 0.0044 mmol) and perfluorotriphenylphosphine (9.3 g, 0.0174 mmol) in hexafluorobenzene (3.0 mL). Due to overlapping signals, conversion could not be determined by $^1$H NMR. Diborylated products were isolated via silica gel column chromatography (eluent $CH_2Cl_2$; graduated to 1.0% EtOAc in $CH_2Cl_2$ with $R_f$ = 0.10) in approximately a 1:2:1 ratio; **413** (17 mg, 16%), **416** (37 mg, 34%) and **417** (18 mg, 17%). Each isomer contained approximately 15% of other isomers by $^1$H NMR, which could not be further separated.

**Diborylated 416**: $\delta_H$ (500 MHz, $CDCl_3$) 8.69 (1H, s, Naphthyl-H), 8.64 (1H, s, Naphthyl-H), 7.57 (1H, s, Ph-C*H*-Ph), 7.44-7.42 (4H, m, Ph-H), 7.33-7.31 (6H, m, Ph-H), 4.16 (2H, t, *J* = 7.0 Hz, N-$CH_2$), 1.77-1.67 (2H, m, $CH_2$-C*H*$_2$-$CH_2$), 1.48 (12H, s, B-O-C-$CH_3$), 1.46 (12H, s, B-O-C-$CH_3$), 1.26-1.24 (2H, m, C*H*$_2$-$CH_3$), 0.98 (3H, t, *J* = 7.0 Hz, $CH_2$-C*H*$_3$); $\delta_C$ (125 MHz, $CDCl_3$) 164.7, 164.4, 163.1, 162.9, 138.0, 134.2, 133.8, 129.9, 129.8, 128.9, 128.7, 128.3, 128.2, 127.4, 126.2, 125.9, 125.1, 124.9, 84.9, 59.7, 40.7, 30.0, 24.9, 20.2, 13.7; $\delta_{B(11)}$ (96 MHz, $CDCl_3$) 35.4; $\nu_{max}$ 2976, 2936, 1706, 1663, 1584, 1448, 1307, 1232, 936, 851 cm$^{-1}$; TOF-MS (ESI+) *m/z* calcd for $(C_{43}H_{46}B_2N_2O_8+Na)^+$ 763.3338; found 763.3359.

**Diborylated 417**: $\delta_H$ (400 MHz, $CDCl_3$) 8.67 (2H, s, Naphthyl-H), 7.50 (1H, s, Ph-C*H*-Ph), 7.43-7.38 (4H, m, Ph-H), 7.32-7.27 (6H, m, Ph-H), 4.19 (2H, t, *J* = 7.5 Hz, N-$CH_2$), 1.74-1.66 (2H, m, $CH_2$-C*H*$_2$-$CH_2$), 1.41 (24H, s, B-O-C-$CH_3$), 1.26-1.24 (2H, m, C*H*$_2$-$CH_3$), 0.97 (3H, t, *J* = 7.5 Hz, $CH_2$-C*H*$_3$); $\delta_C$ (100 MHz, $CDCl_3$) 164.4, 163.1, 137.9, 133.8, 129.1, 128.9, 128.2, 128.1, 127.4, 127.3, 126.7, 125.1, 84.9, 60.0, 40.6, 30.1, 24.8, 20.3, 13.7; $\delta_{B(11)}$ (96 MHz, $CDCl_3$) 33.5; $\nu_{max}$ 2976, 2932, 1704, 1659, 1584, 1448, 1317, 1231, 1135, 851, 729 cm$^{-1}$; TOF-MS (ESI+) *m/z* calcd for $(C_{43}H_{46}B_2N_2O_8+Na)^+$ 763.3338; found 763.3314.

**Diborylated 413**: $\delta_H$ (500 MHz, $CDCl_3$) 8.67 (2H, s, Naphthyl-H), 7.62 (1H, s, Ph-C*H*-Ph), 7.46-7.44 (4H, m, Ph-H), 7.34-7.29 (6H, m, Ph-H), 4.14 (2H, t, *J* = 7.5 Hz, N-$CH_2$), 1.73-1.70 (2H, m, $CH_2$-C*H*$_2$-$CH_2$), 1.49 (24H, s, C-$CH_3$), 1.27-1.22 (2H, m, C*H*$_2$-$CH_3$), 0.97 (3H, t, *J* = 7.0 Hz, $CH_2$-C*H*$_3$); $\delta_C$ (125 MHz, $CDCl_3$) 164.1, 163.2, 138.1, 134.4, 134.3, 128.7, 128.3, 128.2, 128.1, 127.5, 126.1, 125.1, 85.0, 59.6, 40.8, 29.9, 24.8, 20.2, 13.8; $\nu_{max}$ 2976, 2933, 1703, 1665, 1584, 1448, 1309,

1231, 908, 851, 697 $cm^{-1}$; TOF-MS (ESI+) *m/z* calcd for $(C_{43}H_{46}\ B_2N_2O_8+Na)^+$ 763.3338; found 763.3296.

### 5.4.4 General Procedure for Suzuki Reactions

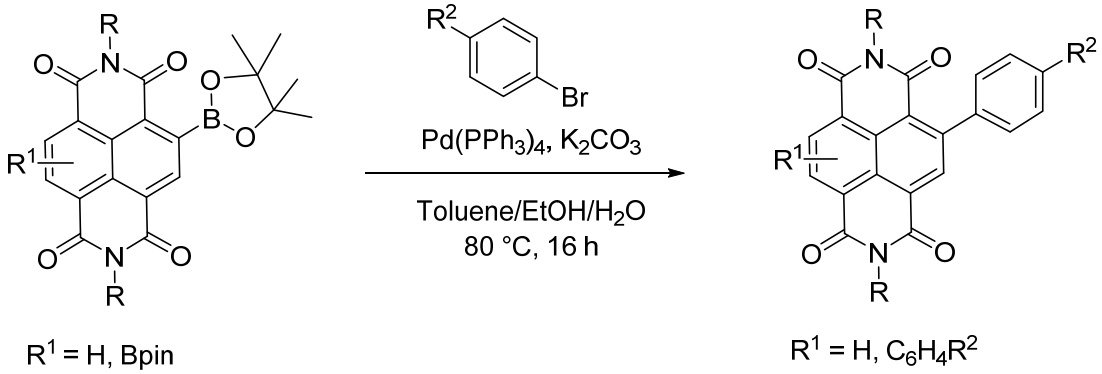


To a stirring solution of borylated NDI (1.0 eq.) and X-$C_6H_4$-Br (1.3 eq. per boronic ester) in toluene (10 mL) and EtOH (0.1 mL) under Ar was added $K_2CO_3$ (5.6 eq. per boronic ester) in $H_2O$ (1 mL) and $Pd(PPh_3)_4$ (0.15 eq.). The reaction mixture was heated to 80 °C under Ar and stirred for 16 h, before cooling to rt. The solvent was removed under reduced pressure and subjected to silica gel column chromatography with an eluent of petrol/EtOAc (graduated from 2% EtOAc to 15% EtOAc, unless otherwise stated).

#### *5.4.4.1 Suzuki Reaction of 410 and Bromobenzene*

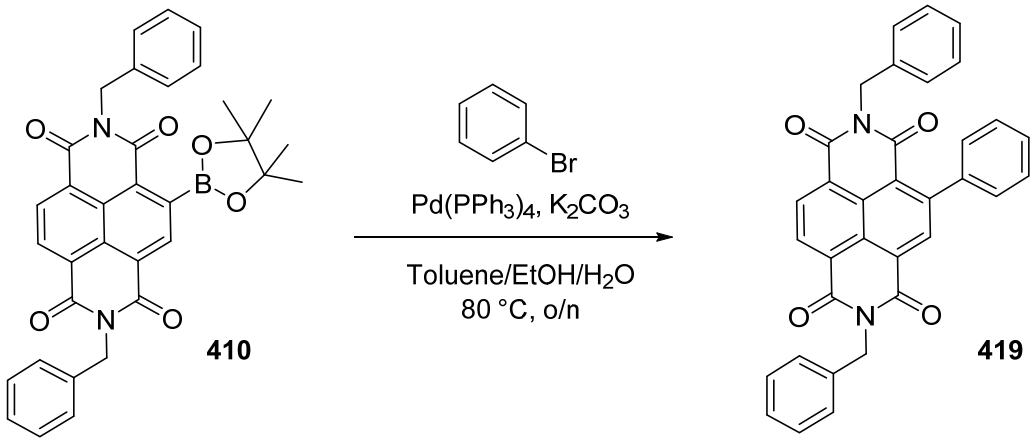


The general procedure for the Suzuki reaction was followed, using **410** (24 mg, 0.042 mmol), bromobenzene (9.0 mg, 0.055 mmol), $K_2CO_3$ (32 mg, 0.235 mmol) and $Pd(PPh_3)_4$ (7.0 mg, 0.006 mmol). **419** was isolated in 81% yield (18 mg, $R_f$ = 0.30 in 90:10 petrol/EtOAc).

**Naphthalenediimide 419**: $\delta_H$ (400 MHz, $CDCl_3$) 8.82 (1H, d, *J* = 7.7 Hz, Naphthyl-H), 8.76 (1H, d, *J* = 7.7 Hz, Naphthyl-H), 8.61 (1H, s, Naphthyl-H), 7.55-7.23 (15H, m, Ar-H), 5.39 (2H, s, N-C$H_2$), 5.28 (2H, s, N-C$H_2$); $\delta_C$ (100 MHz, $CDCl_3$) 162.9, 162.7, 162.6, 162.2, 148.5, 140.3, 136.6, 136.5, 135.8, 131.5, 130.7, 129.1, 129.0, 128.6, 128.4, 128.4, 128.4, 128.0, 127.8, 127.8, 127.6, 127.0, 126.6, 126.1, 125.3, 123.0, 44.0, 43.8; $\nu_{max}$ 3031, 2963, 2962, 1705, 1665, 1572, 1446, 1325, 1197, 753, 698 $cm^{-1}$; TOF-MS (ESI+) *m/z* calcd for $(C_{34}H_{22}N_2O_4+Na)^+$ 545.1472; found 545.1507.

### *5.4.4.2 Suzuki Reaction of 410 and p-tolylbromide*

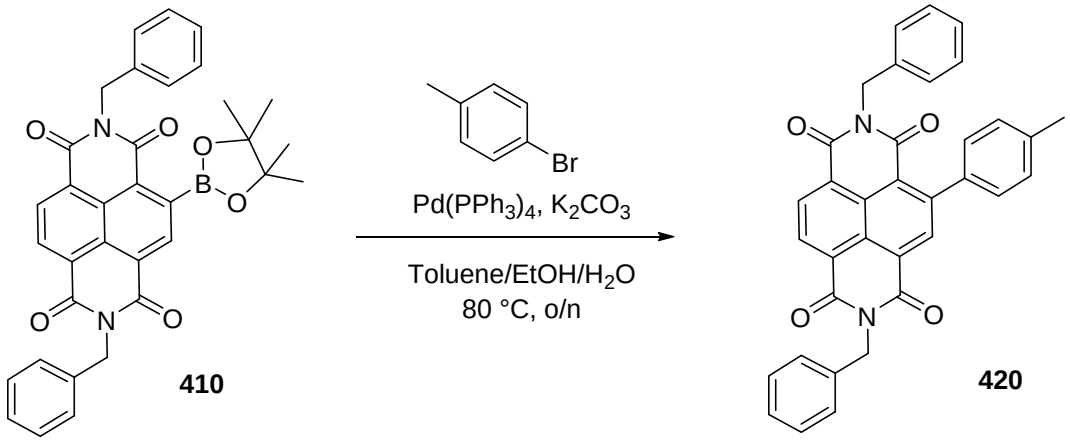


**410** **420**

The general procedure for the Suzuki reaction was followed, using **410** (15 mg, 0.026 mmol), *p*-bromotoluene (6.0 mg, 0.034 mmol), $K_2CO_3$ (20 mg, 0.147 mmol) and $Pd(PPh_3)_4$ (5.0 mg, 0.004 mmol). **420** was isolated in 56% yield (8 mg, $R_f$ = 0.34 in 90:10 petrol/EtOAc).

**Naphthalenediimide 420**: $\delta_H$ (500 MHz, $CDCl_3$) 8.80 (1H, d, *J* = 7.6 Hz, Naphthyl-H), 8.75 (1H, d, *J* = 7.6 Hz, Naphthyl-H), 8.61 (1H, s, Naphthyl-H), 7.55-7.53 (2H, m, Ar-H), 7.46-7.43 (2H, m, Ar-H), 7.33-7.23 (10H, m, Ar-H), 5.39 (2H, s, N-C$H_2$), 5.29 (2H, s, N-C$H_2$), 2.47 (3H, s, $CH_3$); $\delta_C$ (125 MHz, $CDCl_3$) 162.9, 162.7, 162.7, 162.3, 148.7, 138.4, 137.3, 136.7, 136.5, 136.1, 131.4, 130.5, 129.2, 129.1, 129.0, 128.6, 128.4, 128.1, 127.8, 127.6, 126.9, 126.6, 126.0, 125.2, 44.0, 43.8, 21.5; $\nu_{max}$ 3032, 2965, 2926, 2854, 1705, 1665, 1434, 1324, 1222, 751, 698 $cm^{-1}$; TOF-MS (ESI+) *m/z* calcd for $(C_{35}H_{24}N_2O_4+Na)^+$ 559.1628; found 559.1664.

### *5.4.4.3 Suzuki Reaction of 410 and p-methoxyphenylbromide*

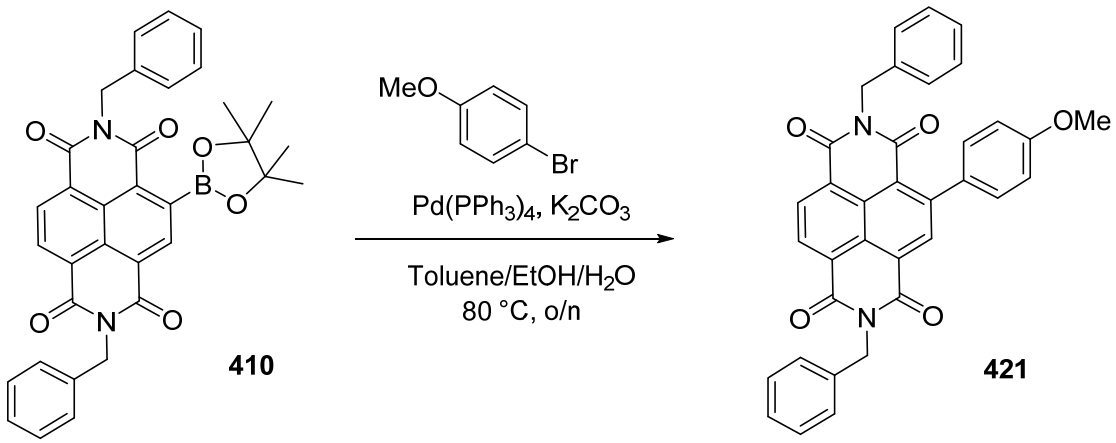


**410** **421**

The general procedure for the Suzuki reaction was followed, using **410** (23 mg, 0.040 mmol), *p*-methoxyphenylbromide (10 mg, 0.052 mmol), $K_2CO_3$ (31 mg, 0.224 mmol) and $Pd(PPh_3)_4$ (7.0 mg, 0.006 mmol). **421** was isolated in 68% yield (15 mg, $R_f$ = 0.19 in 85:15 petrol/EtOAc).

**Naphthalenediimide 421**: $\delta_H$ (400 MHz, $CDCl_3$) 8.80 (1H, d, *J* = 7.5 Hz, Naphthyl-H), 8.74 (1H, d, *J* = 7.5 Hz, Naphthyl-H), 8.62 (1H, s, Naphthyl-H), 7.54 (2H, dt, *J* = 7.0, 1.5, *o*-Ph-H), 7.46 (2H, dt, *J* = 7.0, 1.5, *o*-Ph-H), 7.47-7.44 (2H, m, Ar-H), 7.33 (2H, d, *J* = 8.8 Hz, MeO-Ar-H), 7.33-7.23 (6H,

m, Ph-H), 7.03 (2H, d, *J* = 8.8 Hz, MeO-Ar-H), 5.39 (2H, s, N-$CH_2$), 5.30 (2H, s, N-$CH_2$), 3.91 (3H, s, O-$CH_3$); $\delta_C$ (100 MHz, $CDCl_3$) 162.9, 162.8, 162.7, 162.4, 159.9, 148.4, 136.7, 136.5, 136.3, 132.3, 131.4, 130.4, 129.9, 129.1, 129.0, 128.6, 128.4, 128.0, 127.8, 127.6, 126.9, 126.6, 125.9, 125.2, 122.7, 113.9, 55.3, 44.0, 43.8; $\nu_{max}$ 3014, 2963, 2927, 2839, 1704, 1663, 1605, 1436, 1249, 1178, 750, 700 $cm^{-1}$; TOF-MS (ESI+) *m/z* calcd for $(C_{35}H_{24}N_2O_5+Na)^+$ 575.1577; found 575.1559.

### *5.4.4.4 Suzuki Reaction of 410 and p-nitrophenylbromide*

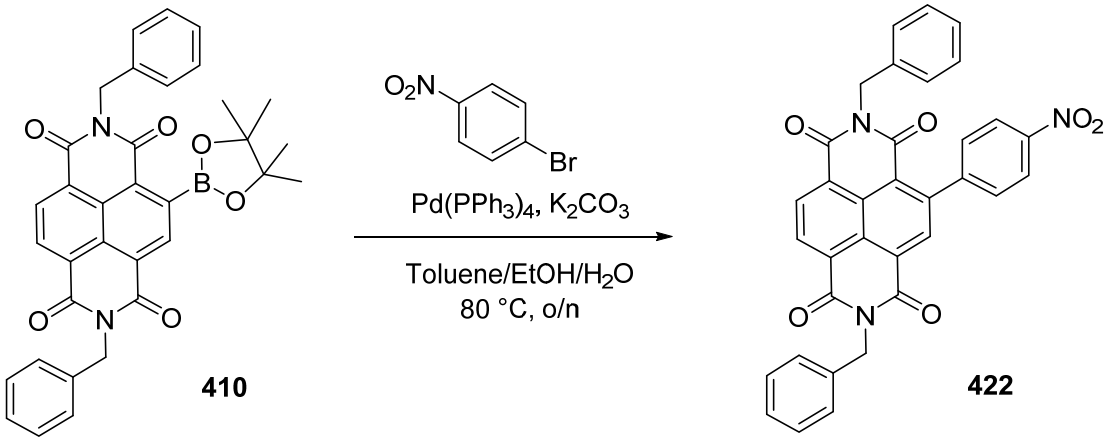


The general procedure for the Suzuki reaction was followed, using **410** (27 mg, 0.047 mmol), *p*-nitrophenylbromide (12 mg, 0.061 mmol), $K_2CO_3$ (37 mg, 0.264 mmol) and $Pd(PPh_3)_4$ (8.0 mg, 0.007 mmol). **422** was isolated in 73% yield (19 mg, $R_f$ = 0.16 in 80:20 petrol/EtOAc).

**Naphthalenediimide 422**: $\delta_H$ (400 MHz, $CDCl_3$) 8.87 (1H, d, *J* = 7.5 Hz, Naphthyl-H), 8.82 (1H, d, *J* = 7.5 Hz, Naphthyl-H), 8.53 (1H, s, Naphthyl-H), 8.37 (2H, d, *J* = 8.7 Hz, $NO_2$-Ar-H), 7.54 (2H, d, *J* = 7.2 Hz, Ph-H), 7.51 (2H, d, *J* = 8.7 Hz, $NO_2$-Ar-H), 7.43 (2H, d, *J* = 7.2 Hz, Ph-H), 7.34-7.23 (6H, m, Ar-H), 5.40 (2H, s, N-$CH_2$), 5.26 (2H, s, N-$CH_2$); $\delta_C$ (100 MHz, $CDCl_3$) 162.6, 162.4, 162.4, 162.1, 147.7, 147.1, 145.5, 136.3, 136.3, 134.3, 132.0, 131.4, 129.2, 129.1, 129.0, 128.6, 128.5, 128.0, 127.9, 127.6, 127.0, 126.7, 126.5, 125.8, 123.7, 123.3, 44.1, 44.0; $\nu_{max}$ 3030, 2926, 2854, 1705, 1665, 1518, 1439, 1346, 1310, 750, 699 $cm^{-1}$; TOF-MS (ESI+) *m/z* calcd for $(C_{34}H_{21}N_3O_6+Na)^+$ 590.1323; found 590.1361.

### *5.4.4.5 Suzuki Reaction of 410 and p-trifluoromethylphenylbromide*

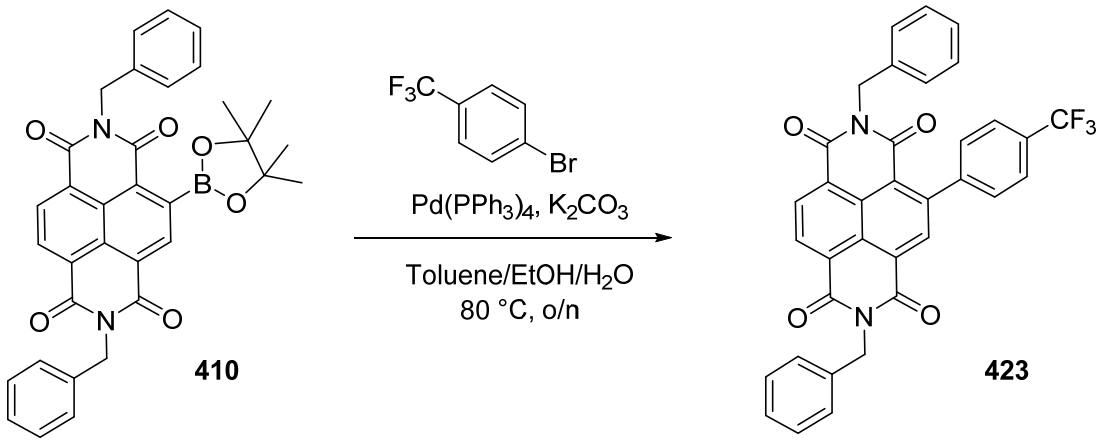


The general procedure for the Suzuki reaction was followed, using **410** (22 mg, 0.038 mmol), *p*-trifluoromethylphenylbromide (11 mg, 0.050 mmol), $K_2CO_3$ (30 mg, 0.215 mmol) and $Pd(PPh_3)_4$ (7 mg, 0.006 mmol). **423** was isolated in 69% yield (16 mg, $R_f$ = 0.31 in 90:10 petrol/EtOAc).

**Naphthalenediimide 423**: $\delta_H$ (400 MHz, $CDCl_3$) 8.85 (1H, d, *J* = 7.7 Hz, Naphthyl-H), 8.79 (1H, d, *J* = 7.7 Hz, Naphthyl-H), 8.54 (1H, s, Naphthyl-H), 7.77 (2H, d, *J* = 8.1 Hz, $F_3C$-Ar-H), 7.54 (2H, d, *J* = 7.0 Hz, Ph-H), 7.47 (2H, d, *J* = 8.1 Hz, $F_3C$-Ar-H), 7.44 (2H, d, *J* = 7.0 Hz, Ph-H), 7.34-7.23 (6H, m, Ph-H), 5.39 (2H, s, N-$CH_2$), 5.27 (2H, s, N-$CH_2$); $\delta_C$ (100 MHz, $CDCl_3$) 162.7, 162.5, 162.5, 162.1, 146.6, 144.0, 136.4, 136.4, 135.1, 131.5 (q, *J* = 59 Hz, *C*-$CF_3$), 129.1, 129.0, 128.6, 128.5, 128.4, 128.1, 127.9, 127.8, 127.7, 127.0, 126.7, 126.3, 125.4 (2C, q, *J* = 4 Hz, *C*=C-$CF_3$), 124.4 (q, *J* = 238 Hz, *C*$F_3$), 44.0, 43.9; $\delta_F$ (376 MHz, $CDCl_3$) -62.43; $\nu_{max}$ 3018, 2966, 2926, 2852, 1705, 1665, 1438, 1324, 1066, 750, 698 $cm^{-1}$; TOF-MS (ESI+) *m/z* calcd for $(C_{35}H_{21}F_3N_2O_4+Na)^+$ 613.1346; found 613.1427.

### *5.4.4.6 Suzuki Reaction of 416 and bromobenzene*

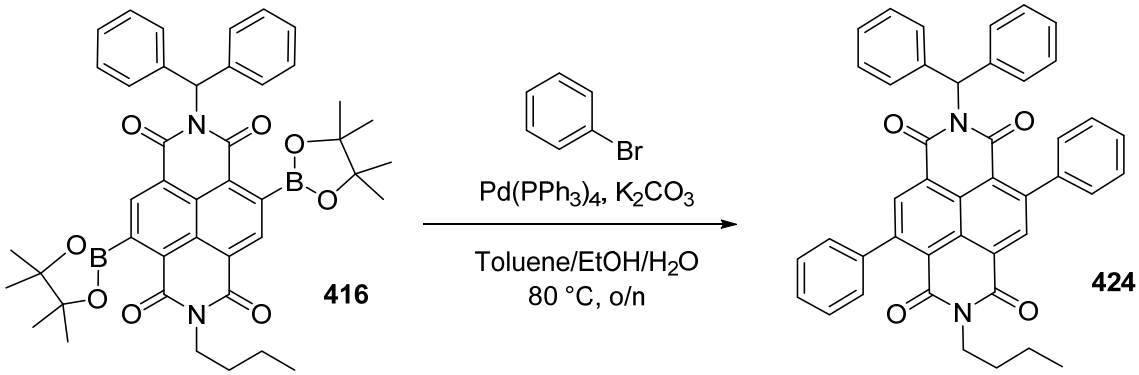


The general procedure for the Suzuki reaction was followed, using **416** (22 mg, 0.030 mmol), bromobenzene (12 mg, 0.077 mmol), $K_2CO_3$ (45 mg, 0.327 mmol) and $Pd(PPh_3)_4$ (10 mg, 0.009 mmol). **424** was isolated in 71% yield (13 mg – with 13% of **425** and **426**, $R_f$ = 0.23 in 50:50 $CH_2Cl_2$/EtOAc), using silica gel column chromatography (eluent graduated from 20% $CH_2Cl_2$ in hexane to 55% $CH_2Cl_2$ in hexane).

**Naphthalenediimide 424**: $\delta_H$ (300 MHz, $CDCl_3$) 8.68 (1H, s, Naphthyl-H), 8.61 (1H, s, Naphthyl-H), 7.51-7.27 (21H, m, Ph-H and Ph-C*H*-Ph), 4.08 (2H, t, *J* = 7.5 Hz, N-C$H_2$), 1.66-1.59 (2H, m, $CH_2$-C$H_2$-$CH_2$), 1.42-1.31 (2H, m, C$H_2$-$CH_3$), 0.92 (3H, t, *J* =7.5 Hz, $CH_3$); $\delta_C$ (75 MHz, $CDCl_3$) 162.7, 162.5 162.4, 162.2, 147.7, 147.6, 140.4, 139.9, 138.0, 136.3, 135.7, 130.1, 128.9, 128.8, 128.4, 128.3, 128.3, 128.1, 127.9, 127.8, 127.4, 127.3, 127.0, 125.7, 125.7, 123.5, 59.7, 40.8, 30.0, 20.3, 13.8; $\nu_{max}$ 3059, 3029, 2958, 2871, 1707, 1666, 1436, 1301, 1205, 765, 696, $cm^{-1}$; TOF-MS (ESI+) *m/z* calcd for $(C_{43}H_{32}N_2O_4+Na)^+$ 663.2260; found 663.2266.

### *5.4.4.7 Suzuki Reaction of 417 and bromobenzene*

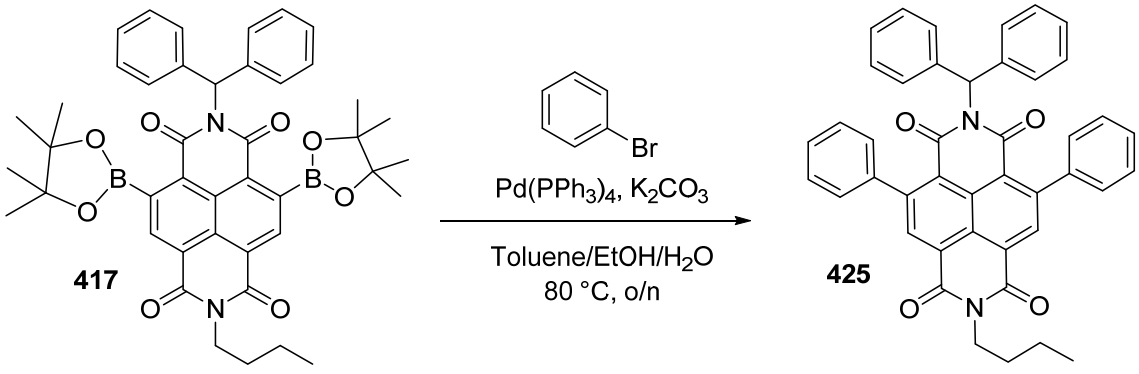


The general procedure for the Suzuki reaction was followed, using **417** (35 mg, 0.047 mmol), bromobenzene (19 mg, 0.123 mmol), $K_2CO_3$ (72 mg, 0.520 mmol) and $Pd(PPh_3)_4$ (16 mg, 0.014 mmol), in toluene (15 mL), water (1.5 mL) and EtOH (0.15 mL). **425** was isolated in 58% yield (17 mg – with 13% of **424**, $R_f$ = 0.23 in 50:50 $CH_2Cl_2$/EtOAc), using silica gel column chromatography (eluent graduated from 20% $CH_2Cl_2$ in hexane to 55% $CH_2Cl_2$ in hexane).

**Naphthalenediimide 425**: $\delta_H$ (500 MHz, $CDCl_3$) 8.61 (2H, s, Naphthyl-H), 7.43 (1H, s, Ph-C*H*-Ph), 7.41-7.27 (16H, m, Ph-H), 7.20-7.18 (4H, m, Ar-H), 4.21 (2H, t, *J* = 7.5 Hz, N-$CH_2$), 1.76-1.70 (2H, m, $CH_2$-C*H*$_2$-$CH_2$), 1.47-1.42 (2H, sextet, *J* = 7.4 Hz, C*H*$_2$-$CH_3$), 0.98 (3H, t, *J* = 7.4 Hz, -$CH_3$); $\delta_C$ (125 MHz, $CDCl_3$) 162.8, 162.5, 148.0, 140.0, 138.1, 134.8, 129.0, 128.7, 128.5, 128.5, 128.3, 128.0, 127.2, 125.2, 125.0, 124.4, 59.7, 40.7, 30.9, 20.3, 13.8; $\nu_{max}$ 3059, 3029, 2958, 2930, 2870, 1707, 1666, 1446, 1301, 1206, 734, 696 $cm^{-1}$; TOF-MS (ESI+) *m/z* calcd for $(C_{43}H_{32}N_2O_4+Na)^+$ 663.2260; found 663.2307.

### *5.4.4.8 Suzuki Reaction of 413 and bromobenzene*

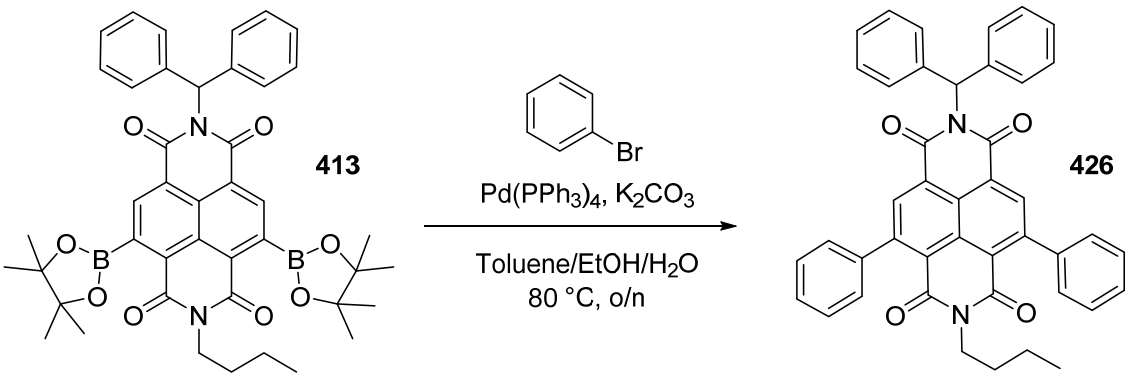


The general procedure for the Suzuki reaction was followed, using **413** (15 mg, 0.020 mmol), bromobenzene (9.0 mg, 0.053 mmol), $K_2CO_3$ (30 mg, 0.223 mmol) and $Pd(PPh_3)_4$ (7.0 mg, 0.006 mmol). **426** was isolated in 45% yield (5 mg – with 15% **424** and other contamination, $R_f$ = 0.23 in 50:50 $CH_2Cl_2$/EtOAc), using silica gel column chromatography (eluent graduated from 20% $CH_2Cl_2$ in hexane to 55% $CH_2Cl_2$ in hexane).

**Naphthalenediimide 426** (impure): $\delta_H$ (500 MHz, $CDCl_3$) 8.57 (2H, s, Naphthyl-H), 7.62 (1H, s, Ph-C*H*-Ph), 7.49-7.28 (20H, m, Ph-H) 3.93 (2H, t, *J* = 7.8 Hz, N-$CH_2$), 1.56-1.52 (2H, m, $CH_2$-C*H*$_2$-$CH_2$), 1.47-1.41 (2H, m, -C*H*$_2$-$CH_3$), 1.84 (3H, t, *J* = 7.0 Hz, -$CH_3$); $\delta_C$ (125 MHz, $CDCl_3$) 162.8, 162.0, 148.4, 140.9, 137.9, 135.6, 128.8, 128.6, 128.4, 128.3, 128.2, 127.9, 127.6, 125.5, 125.2, 123.6, 59.6, 40.9, 25.7, 20.2, 13.8; $\nu_{max}$ 3059, 3029, 2931, 2871, 1707, 1607, 1446, 1301, 1205, 1078, 765, 696 $cm^{-1}$; TOF-MS (ESI+) *m/z* calcd for $(C_{43}H_{32}N_2O_4+Na)^+$ 663.2260; found 663.2245.

### 5.4.6 Attempted Oxidation Reactions

#### *5.4.6.1 Hydrogen Peroxide*

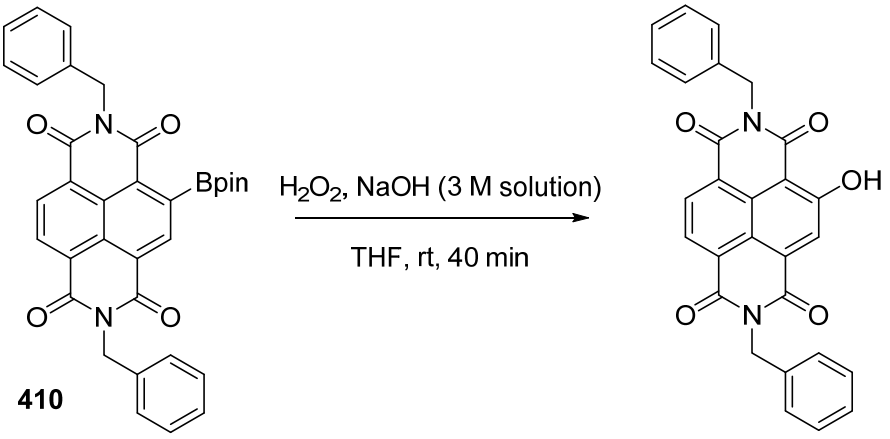


**410** (1.0 eq., 16 mg, 0.020 mmol) was dissolved in THF (1 mL) and water (40 µL). NaOH solution (3 M, 25 µL) added, followed by $H_2O_2$ solution (30% w/w, 25 µL). Reaction mixture was exothermic and turned red. Reaction mixture was left to stir for 40 min, then diluted with $CH_2Cl_2$. Organic layers washed with brine, dried over $MgSO_4$ and concentrated under reduced pressure. A yellow solid was isolated (10 mg, $R_f$ = 0.64 in $CHCl_3$) via silica gel column chromatography in $CHCl_3$, although the fraction contained several compounds that could not be identified.

$^1$H NMR shows characteristic O*H* hydrogen bonded to carbonyl oxygen.

#### *5.4.6.2 Hydroxylamine*

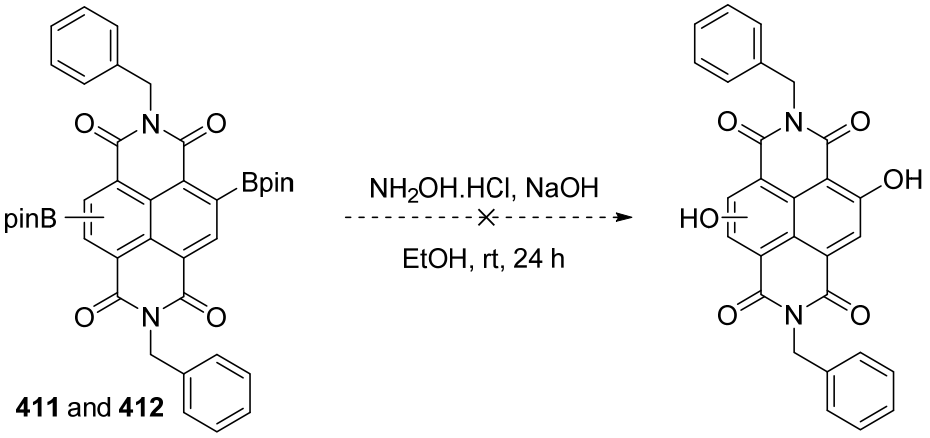


**411** and **412** (1.0 eq., 18 mg, 0.025 mmol), NaOH (2.0 eq., 2.0 mg, 0.050 mmol) and $NH_2OH.HCl$ (12.5 eq., 22 mg, 0.313 mmol) were suspended in EtOH (4 mL) and stirred at rt for 48 h. Reaction mixture was quenched with aqueoua HCl (2.0 M, ≈1 mL) and neutralised with aqueous $NaHCO_3$, then diluted with $CH_2Cl_2$. Organic layers washed with brine, dried over $MgSO_4$ and concentrated under reduced pressure. No product was observed.

### *5.4.6.3 Trimethylamine N- Oxide*

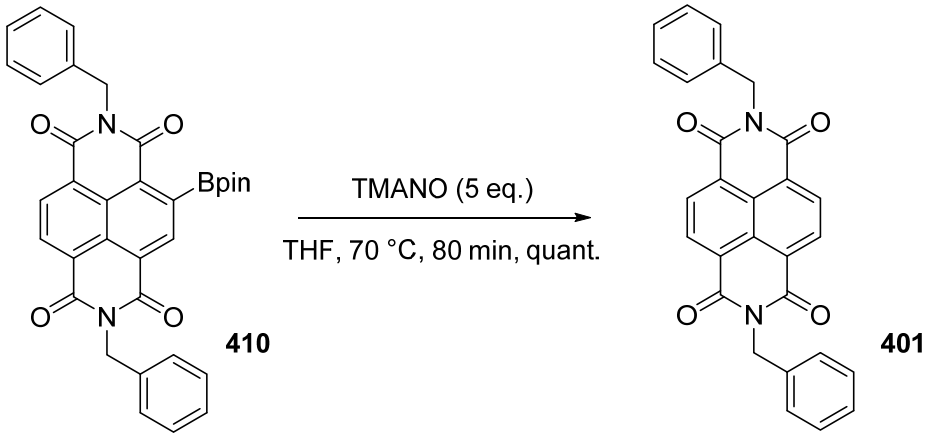


**410** **401**

**410** (1.0 eq., 20 mg, 0.035 mmol) was dissolved in THF (2.0 mL) and added to TMANO (5.0 eq., 20 mg, 0.175 mmol). Reaction mixture was heated to 70 °C under Ar and a red colour was observed. Reaction mixture cooled to rt and extracted with $Et_2O$. Organic layer washed with brine, dried over $MgSO_4$ and concentrated under reduced pressure. Protodeborylated **401** was obtained in quantitative yield (16 mg). $^1H$ values corresponded with previously obtained values.

# References


1. Labinger, J. A.; Bercaw, J. E. *Nature* **2002**, *417*, 507-514
2. Godula, K.; Sames, D. *Science* **2006**, *312*, 67-72
3. Shilov, A. E.; Shul'pin, G. B. *Chem. Rev.* **1997**, *97*, 2879-2932
4. Clayden, J.; Greeves, N.; Warren, S.; Wothers, P. *Organic Chemistry* Oxford University Press: Oxford, 2001
5. McMillen, D. F.; Golden, D. M. *Annu. Rev. Phys. Chem.* **1982**, *33*, 493-532
6. Davico, G. E.; Bierbaum, V. M.; DePuy, C. H.; Ellison, G. B.; Squire R. R. *J. Am. Chem. Soc.* **1995**, *117*, 2590-2599
7. Friedel, C.; Crafts, J. M. *C. R. Hebd. Seances Acad. Sci.* **1877**, *84*, 1392-1395; 1450-1454
8. Birch, A. J. *J. Chem. Soc.* **1944**, 430-436; Birch, A. J. *J. Chem. Soc.* **1945**, 809-813; Birch, A. J. *J. Chem. Soc.* **1946**, 593-597; Birch, A. J. *J. Chem. Soc.* **1947**, 102-105; Birch, A. J. *J. Chem. Soc.* **1947**, 1642-1648
9. Gibson, D.T.; Koch, J. R.; Kallio, R. E. *Biochemistry* **1968**, *7*, 2653-2662
10. Ley. S.V.; Sternfeld, F.; Taylor. S. *Tetrahedron Lett.*, **1987**, *20*, 225-226
11. Mattay, J. *Angew. Chem., Int. Ed.* **2007**, *46*, 663-665
12. Cornelisse, J. *Chem. Rev.* **1993**, *93*, 615-669
13. Hoffmann, N. *Synthesis* **2004**, 481-495
14. Lindlar, H. *Helv. Chim. Acta* **1952**, *35*, 446-450
15. Markownikoff, W. *Justus Liebigs Ann. Chem.* **1870**, *153*, 228-259
16. Smit, B.; Maesen, T. L. M. Nature, **2008**, 451, 671-678
17. Green, M. L. H.; Knowles, P. J. *J. Chem. Soc. D.* **1970**, 1677
18. Chatt, J.; Davidson, J. M. *J. Chem. Soc.* **1965**, 843-855
19. Hodges, R. J.; Garnett, J. L. *J. Phys. Chem.* **1969**, *78*, 1525-1539
20. Barefield, E. K.; Parshall, G. W.; Tebbe, F. N. *J. Am. Chem. Soc.* **1970**, *92*, 5234-5235
21. Moritani, I.; Fujiwara, Y. *Tetrahedron Lett.* **1967**, *8*, 1119-1122
22. Fujiwara, Y.; Moritani, I.; Asano, R.; Tanaka, H.; Teranishi, S. *Tetrahedron* **1969**, *25*, 4815-4818
23. Nishikata, T.; Lipshutz, B. H. *Org. Lett.* **2010**, *12*, 1972-1975
24. Brookhart, M.; Green, M. L. H. *J. Organomet. Chem.* **1983**, *250*, 395-408
25. Brookhart, M.; Green, M. L. H. *Proc. Nat. Acad. Sci.* **2007**, *104*, 6908-6914
26. Dawoodi, Z.; Green, M. L. H.; Mtetwa, V. S. B.; Prout, K. *J. Chem. Soc., Chem. Commun.* **1982**, 802-803
27. Perutz, R. N.; Turner, J. J. *J. Am. Chem. Soc.* **1975**, *97*, 4791-4800
28. Crabtree, R. H. *Angew. Chem., Int. Ed.* **1993**, *32*, 789-805
29. Crabtree, R. H. *J. Organomet. Chem.* **2004**, *689*, 4083-4091
30. Kubas, G. J.; Ryan, R. R.; Swanson, B. I.; Vergamani, P. J.; Wasserman, H. J. *J. Am. Chem. Soc.* **1984**, *100*, 451-452
31. Shilov, A. E.; Shulpin, G. B., *Russ. Chem. Rev.* **1987**, *56*, 442-464
32. Gol'dshleger, N. F.; Tyabin, M. B.; Shilov, A. E.; Shteinman, A. A. *Zh. Fiz. Khim.* **1969**, *43*, 2174
33. Gol'dshleger, N. F.; Es'kova, V. V.; Shilov, A. E.; Shteinman,A. A. *Zh. Fiz. Khim.* **1972**, *46*, 1353
34. Periana, R. A.; Taube, D. J.; Gamble, S.; Taube, H; Satoh, T.: Fujii, H., *Science,* **1998**, 280, 560-564

35. Periana, R.A.; Mironov. O.; Taube. D.; Bhalla. G.; Jones. C.J., *Science*, **2003**, 301, 814-818
36. Lin, M.; Sen. A., *Nature*, **1994**, 368, 613-615
37. Nizova, G.V.; Suss-Fink, G.; Stanislas. S.; Shul'pin. G.B, *Chem. Commun*., **1998,** 17, 1885-1886
38. Davies, H. M. L.; Beckwith, R. E. J. *Chem. Rev.* **2003**, *103*, 2861-2903
39. Greuter, F.; Kalvoda, J.; Jeger, O. *Proc. Chem. Soc.* **1958**, 349
40. House, H. O.; Boots, S. G.; Jones, V. K. *J. Org. Chem.* **1965**, *30*, 2519-2527
41. Brookhart, M.; Studabaker, W. B. *Chem. Rev.* **1987**, *87*, 411-432
42. Wenkert, E.; Mylari, B. L.; Davis, L. L. *J. Am. Chem. Soc.* **1968**, *90*, 3870-3872
43. Wenkert, E.; Davis, L. L.; Mylari, B. L.; Solomon, M. F.; Da Silva, R. R.; Shulman, S.; Warnet, R. J.; Ceccherelli, P.; Curini, M.; Pellicciari, R. *J. Org. Chem.* **1982**, *47*, 3242-3247
44. Corbel, B.; Hernot, D.; Haelters, J.-P.; Strutz, G. *Tetrahedron Lett.* **1987**, *28*, 6605-6608
45. Monteiro, H. J. *Tetrahedron Lett.* **1987**, *28*, 3459-3462
46. Mikołajczyk, M.; Zurawiński, R.; Kiełbasiński, P. *Tetrahedron Lett.* **1989**, *30*, 1143-1146
47. Doyle, M. P.; Westrum, L. J.; Wolthuis, W. N. E.; See, M. M.; Boone, M. P.; Bagheri, V.; Pearson, M. M. *J. Am. Chem. Soc.* **1993**, *115*, 958-964
48. Doyle, M. P. *Acc. Chem. Res.* **1986**, *19*, 348-356
49. Davies, H. M. L.; Jin, Q. *Tetrahedron: Asymmetry* **2003**, *14*, 941-949
50. Lawrence, J. D.; Takahashi, M.; Bae, C.; Hartwig, J. F. *J. Am. Chem. Soc.* **2004**, *126*, 15334-15335
51. Wei, C. S.; Jimenez-Hoyos, C. A.; Videa, M. F.; Hartwig, J. F.; Hall, M. B. *J. Am. Chem. Soc.* **2010**, *132*, 3078-3091
52. Preshlock, S. M.; Ghaffari, B.; Maligres, P. E.; Krska, S. W.; Malekzca, R. E.; Smith, M. R. *J. Am. Chem. Soc.* **2013**, *135*, 7572-7582
53. Vanchura, B. A.; Preshlock, S. M.; Roosen, P. C.; Kallepalli, V. A.; Staples, R. J.; Maleczka, R. E., Jr.; Singleton, D. A.; Smith, M. R. *Chem. Commun.* **2010**, *46*, 7724-7726
54. Tamura, H.; Yamazaki, H.; Sato, H.; Sakaki, S. *J. Am. Chem. Soc.* **2003**, *125*, 16114-16126
55. Chotana, G. A.; Vanchura, B. A., II; Tse, M. K.; Staples, R. J.; Maleczka, R. E., Jr.; Smith, M. R. *Chem. Commun.* **2009**, 5731-5733
56. Larsen, M. A.; Hartwig, J. F. *J. Am. Chem. Soc.* **2014**, ASAP article DOI: 10.1021/ja412563e
57. Kondoh, A.; Jamison, T. F. *Chem. Commun.* **2010**, *46*, 907-909
58. Mkhalid, I. A.; Coapes, R. B.; Edes, S. N.; Coventry, D. N.; Souza, F. E. S.; Thomas, R. L.; Hall, J. J.; Bi, S.-W.; Lin, Z.; Marder, T. B. *Dalton Trans.* **2008**, 1055-1064
59. Han Lam, W.; Chung Lam, K.; Lin, Z.; Shimada, S.; Perutz, R. N.; Marder, T. B. *Dalton Trans.* **2004**, 1556-1562
60. Liu. F.; Pak. E.B.; Singh. B.; Jensen. C.M.; Goldman. A.S. *J. Am. Chem. Soc.* **1999**, *121*, 4086-4087
61. Espino, C. J.; Du Bois, J. *Angew. Chem., Int. Ed.* **2001**, *40*, 598-600
62. Breslow, R.; Gellman, S. H. *J. Chem. Soc. Chem. Commun.* **1982**,1400
63. Yu, X. Q.; Huang, J. S.; Zhou, X. G.; Che, C. M. *Org. Lett.* **2000**, *2*, 2233-2236
64. Chen, M. S.; White, M. C. *Science* **2007**, *318*, 783-787
65. Chen, K.; Eschenmoser, A.; Baran, P. S. *Angew. Chem. Int. Ed.* **2009**, *48*, 9705-9708
66. Varkony, H.; Pass, S.; Mazur, Y. *J. Chem. Soc. Chem. Commun*. **1974**, 437-438

67. Newhouse, T.; Baran, P. S. *Angew. Chem. Int. Ed.* **2011**, *50*, 3362-3374
68. Proksch, E.; de Meijere, A. *Angew. Chem. Int. Ed.* **1976**, *15*, 761-762
69. Curci, R.; D'Accolti, L.; Fiorentino, M.; Fusco, C.; Adam, W.; Gonzalez-Nuez, M. E.; Mello, R. *Tetrahedron Lett.* **1992**, *33*, 4225-4227
70. Diaz-Requejo, M. M.; Belderrain, T. R.; Nicasio, M. C.; Trofimenko, S.; Perez, P. J. *J. Am. Chem. Soc.* **2002**, *124*, 896-897
71. Rhodes, C. *Chemistry & Industry*, 25 August **2008**, 21-23
72. Mazzacano, T. J.; Mankad, N. P. *J. Am. Chem. Soc.* **2013**, *135*, 17258-17261
73. Jia, F.; Li, Z. *Org. Chem. Front.* **2014**, ASAP article, DOI: 10.1039/c3qo00087g
74. Li, Z.; Yu, R.; Li, H. *Angew. Chem. Int. Ed.* **2008**, *47*, 7497-7500
75. Wang, Z.; Zhang, Y.; Fu, H.; Jiang, Y.; Zhao, Y. *Org. Lett*. **2008**,*10*, 1863-1866
76. Xia, Q.; Chen, W.; Qiu, H. *J. Org. Chem.* **2011**, *76*, 7577-7582
77. Beaud, R.; Guillot, R.; Kouklovsky, C.; Vincent, G. *Angew. Chem. Int. Ed.* **2012**, *51*, 12546-12550
78. Sarvari, M. H.;Sharghi, H. *J. Org. Chem.* **2004**, *69*, 6953-6956
79. Guchhait, S. K.; Kamble, H.; Kashyap, M. *J. Org. Chem.* **2011**, *76*, 4753-4758
80. Nishimoto, Y.; Babu, S. A.; Yasuda, M.; Baba, A. *J. Org. Chem.* **2008**, *73*, 9465-9468
81. Bensari, A.; Zaveri, N. T. *Synthesis* **2003**, 267-271
82. Caturvedi, D.; Chaturvedi, A. K.; Mishra, N.; Mishra, V. *Synlett* **2012**, *23*, 2627-2630
83. Goettmann, F.; Fischer, A.; Antonietti, M.; Thomas, A. *Chem. Commun.* **2006**, 4530-4532
84. Wilkinson, M. C. *Org. Lett.* **2011**, *13*, 2232-2235
85. Chen, L.; Zhou, F.; Shi, T.-D.; Zhou, J. *J. Org. Chem.* **2012**, *77*, 4354-4362
86. Damkaci, F.; Dallas, M.; Wagner, M. *J. Chem. Educ*. **2013**, *90*, 390-392
87. De Rosa, M.; Soriente, A. *Eur. J. Org. Chem.* **2010**, 1029-1032
88. Firouzabadi, H.; Iranpoor, N.; Nowrouzi, F. *Tetrahedron* **2004**, *60*, 10843-10850
89. McCubbin, J. A.; Hosseini, H.; Krokhin, O. V. *J. Org. Chem.* **2010**, *75*, 959-962
90. Thirupathi, P.; Soo Kim, S. *J. Org. Chem.* **2010**, *75*, 5240-5249
91. Bandini, M.; Tragni, M.; Umani-Ronchi, A. *Adv. Synth. Catal.* **2009**, *351*, 2521-2524
92. Hayashi, R.; Cook, G. R. *Org. Lett.* **2007**, *9*, 1311-1314
93. Quallich, G. J.; Williams, M. T.; Friedmann, R. C. *J. Org. Chem.* **1990**, *55,* 4971-4973
94. Fenster, E.; Fehl, C.; Aubé, J. *Org. Lett.* **2011**, *13*, 2614-2617
95. Fürstner, A.; Ackerstaff, *J. Chem. Commun.* **2008**, 2870-2872
96. Kim, K.; Kim, I. *Org. Lett*. **2010**, *12*, 5314-5317
97. Taylor, H. T. *J. Chem. Soc.* **1958**, 3922-3924
98. Jones, N.; Taylor, H. T. *J. Chem. Soc.* **1959**, 4017-4019
99. Jones, N.; Taylor, H. T.; Rudd, E. *J. Chem. Soc.* **1961**, 1342-1345
100. Jones, N.; Taylor, H. T. *J. Chem. Soc.* **1961**, 1345-1347
101. Jones, N.; Rudd, E. J.; Taylor, H. T. *J. Chem. Soc.* **1963**, 2354-2357
102. Crosby, J. A.; Rasburn, J. W. *Chem. Ind.* **1967**, 1365-1366
103. Groves, J. K.; Jones, N. *J. Chem. Soc. C.* **1968**, 2215-2217
104. Groves, J. K.; Jones, N. *J. Chem. Soc. C.* **1968**, 2898-2900
105. Groves, J. K.; Jones, N. *J. Chem. Soc.* **1969**, 608-610
106. Groves, J. K.; Jones, N. *J. Chem. Soc. C.* **1969**, 1718-1721
107. Groves, J. K.; Jones, N. *J. Chem. Soc. C.* **1969**, 2350-2352
108. Groves, J. K. *Chem. Soc. Rev.* **1972**, 73-97

109. Mayr, H.; Striepe, W. *J. Org. Chem.* **1983**, *48*, 1159-1165
110. Scharwin, W. *Ber. Dtsch. Chem. Ges*. **1902**, *35,* 2511-2515
111. Tabushi, I.; Fujita, K.; Oda, R. *Tetrahedron Lett.* **1968**, *9*, 4247-4249
112. Tabushi, I.; Fujita, K.; Oda, R. *Tetrahedron Lett.* **1968**, *9*, 5455-5458
113. Tabushi, I.; Fujita, K.; Oda, R. *Tetrahedron Lett.* **1969,** *10,* 2581-2584
114. Tavares, R. F.; Dorsky, J.; Easter, W. M. *J. Org. Chem.* **1971**, *36,* 2434-2437
115. Tardella, P. A.; Campana, F. *Gazz. Chim. Ital.* **1971**, *101*, 990-993
116. Pardo, R.; Santelli, M. *Tetrahedron Lett.* **1981**, *22*, 3843-3846
117. Akhrem, I. S.; Orlinkov, A. V.; Mysov, E. I.; Vol'pin, M. E. *Tetrahedron Lett.* **1981**, *22,* 3891-3894
118. Laguerre, M.; Grignon-Dubois, M.; Dunogues, J. *Tetrahedron* **1981**, *37,* 1161-1169
119. Harding, K. E.; Clement, K. S.; Gilbert, J. C.; Wiechman, B. *J. Org. Chem.* **1984**, *49*, 2049-2050
120. Ahra, M.; Grignon-DuBois, M. *Bull. Soc. Chim. Fr.* **1985**, 820-824
121. Ha, H.-J.; Park, K.-P. *Bull. Korean Chem. Soc.* **1988**, *9,* 411
122. Morel-Fourrier, C.; Dulcère, J.-P.; Santelli, M. *J. Am. Chem. Soc.* **1991**, *113,* 8062-8069
123. Davison, G. R.; Howard, J. A. K.; Pitchford, N. A.; Jones, A. M.; Rasburn, J. W.; Simpson, A. J. *Tetrahedron* **1993**, *49,* 10123-10132
124. Tabushi, I.; Hamuro, J.; Oda, R. *Nippon Kagaku Zasshi* **1968**, *89*, 794-797
125. Akhrem, I. S.; Orlinkov, A. V.; Vol'pin, M. E. *Russ. Chem. Rev.* **1996**, *65*, 849-863
126. Baddeley, G.; Wrench, E. *J. Chem. Soc.* **1959**, 1324-1327
127. Baddeley, G.; Heaton, B. G.; Rasburn, J. W. *J. Chem. Soc.* **1960**, 4713-4719
128. Baddeley, G.; Heaton, B. G.; Rasburn, J. W. *J. Chem. Soc.* **1961**, 3828-3835
129. Baddeley, G.; Heaton, B. G.; Rasburn, J. W. *J. Chem. Soc.* **1961**, 3835-3838
130. Ahmad, M. S.; Baddeley, G.; Heaton, B. G.; Rasburn, J. W. *Proc. Chem. Soc.* **1959**, 395
131. Ahmad, M. S.; Baddeley, G. *J. Chem. Soc.* **1961**, 4303-4306
132. Baddeley, G.; Heaton, B. G. *J. Chem. Soc.* **1961**, 4306-4307
133. Baddeley, G.; Hulme, P. *J. Chem. Soc.* **1965**, 5148
134. Emarton, R. J.; Rasburn, J. W. *J. Chem. Soc.* **1965**, 4975-4978
135. Baddeley, G.; Baylis, E. K. *J. Chem. Soc.* **1965**, 4933-4936
136. Tantillo, D. J. *Nat. Prod. Rep.* **2011**, *28*, 1035-1038
137. O'Maille, P. E.; Malone, A.; Dellas, N.; Hess Jr, B. A.; Smentek, L.; Sheehan, I.; Greenhagen, B. T.; Chappell, J.; Manning, G.; Noel, J. P. *Nat. Chem. Biol.* **2008**, *4*, 617-628
138. Karplus, M. *J. Phys. Chem.* **1959**, *30*, 11-15
139. Karplus, M. *J. Am. Chem. Soc.* **1963**, *85*, 2870-2871
140. Zelinski, N.; Turowa-Poljak, M. *Chem Ber.* **1932**, *65*, 1299-1300
141. Zlaktis, A.; Smith, E. A. *Can. J. Chem.* **1951**, *21*, 162-165
142. Bigler, P.; Schönholzer, S.; Neuenschwander, M. Helv. Chim. Acta. 1978, 61, 2059-2080
143. Bagal, S. K.; Tournier, L.; Zard, S. Z. *Synlett* **2006**, 1485-1490
144. Kaiser, E. M.; Benkeser, R. A.; Sauter, F. J.; H. O. *Org. Synth.* **1970**, *50*, 88
145. Bordeau, M.; Djamei, S. M.; Calas, R.; Dunogues, J. *Bull. Soc. Chim. Fr.* **1985**, 488-490

146. Uosis-Martin, M.; Mahon, M. F.; Yevglevskis, M.; Lewis, S. E. *Synlett* **2011**, 2211-2213
147. Uosis-Martin, M.; Pantoş, G. D.; Mahon, M. F.; Lewis, S. E. *J. Org. Chem.* **2013**, *78*, 6253-6263
148. Kishner, N. *Russ. Phys. Chem. Soc.* **1911**, *43*, 582
149. Wolff, L. *Liebigs Ann. Chem.* **1912**, *394*, 23-108
150. Huang, M. *J. Am. Chem. Soc.* **1946**, *68*, 2487-2488
151. Xu, X.; Cheng, D.; Pei, W. *J. Org. Chem.* **2006**, *71*, 6637-6639
152. Turova-Poljak, M. B.; Soshina, I. E.; Treschova, E. G. *Zh. Obshch. Khim.* **1953**, *23*, 1111-1116 (Kindly translated by Maksims Yevglevskis, University of Bath)
153. Clemmensen, E. *Chem. Ber.* **1913**, *46*, 1837-1843
154. Nyberg, N. T.; Duus, J. Ø.; Sørensen, O. W. *J. Am. Chem. Soc.* **2005**, *127*, 6154-6155
155. Nyberg, N. T.; Duus, J. Ø.; Sørensen, O. W. *Magn. Reson. Chem.* **2005**, *43*, 971-974
156. Hong, Y. J.; Tantillo, D. J. *Chem. Sci.* **2010**, *1*, 609-614
157. Bhosale, S. V.; Jani, C. H.; Langford, S. J. *Chem. Soc. Rev.* **2008**, *37*, 331-342
158. Blacker, A. J.; Jazwinski, J.; Lehn, J.-M.; Cesario, M.; Guilhem, J.; Pascard, C. *Tetrahedron Lett.* **1987**, *28*, 6057-6060
159. Ponnuswamy, N.; Cougnon, F. B. L.; Clough, J. M.; Pantoş, G. D.; Saunders, J. K. M. *Science*, **2012**, *338*, 783-785
160. Thalacker, C.; Röger, C.; Würthner, F. *J. Org. Chem.* **2006**, *71*, 8098-8105
161. Tomasulo, M.; Naistat, D. M.; White, A. P.J.; Williams, D. J.; Raymo, F. M.; *Tetrahedron Lett.* **2005**, *46*, 5695-5698
162. Mukhopadhyay, P.; Iwashita, Y.; Shirakawa, M.; Kawano, S.; Fujita, N.; Shinkai, S.; *Angew. Chem., Int. Ed.* **2006**, *45*, 1592-1595
163. Vollman, H.; Becker, H.; Corell, M.; Streeck, H. *Justus Liebigs Ann. Chem.* **1937**, *531*, 1-159
164. Würthner, F.; Ahmed, S.; Thalacker, C.; Debaerdemaeker, T. *Chem. Eur. J*. **2002**, *8*, 4742-4750
165. Chaignon, F.; Falkenström, M.; Karlsson, S.; Blart, E.; Odobel, F.; Hammarström, L. *Chem. Commun.* **2007**, 64-66
166. Bhosale, S. V.; Kalyanker, M. B.; Bhosale, S. V.; Langford, S. J.; Reid, E. F.; Hogan, C. F. *New J. Chem.* **2009**, *33*, 2409-2413
167. Jones, B. A.; Facchetti, A.; Marks, T. J.; Wasielewski, M. R. *Chem. Mater.* **2007**, *19*, 2703-2705
168. Yuan, Z.; Li, J.; Xiao, Y.; Li, Z.; Qian, X. *J. Org. Chem.* **2010**, *75*, 3007-3016
169. Bullock, J. E.; Vagnini, M. T.; Ramanan, C.; Co, D. T.; Wilson, T. M.; Dicke, J. W.; Marks, T. J.; Wasielewski, M. R. *J. Phys. Chem. B* **2010**, *114*, 1794-1802
170. Nakazono, S.; Imazaki, Y.; Yoo, H.; Yang, J.; Sasamori, T.; Tokitoh, N.; Cédric, T.; Kageyama, H.; Kim, D.; Shinokubo, H.; Osuka, A. *Chem. Eur. J.* **2009**, *15*, 7530-7533
171. Nakazono, S.; Easwaramoorthi, S.; Kim, D.; Shinokubo, H.; Osuka, A. *Org. Lett.* **2009**, *11*, 5426-5429
172. Teraoka, T.; Hiroto, S.; Shinokubo, H. *Org. Lett.* **2011**, *13*, 2532-2535
173. Battagliarin, G.; Li, C.; Enkelmann, V.; Müllen, K. *Org. Lett.* **2011**, *13*, 3012-3015
174. Pengo, P.; Pantoş, G. D.; Otto, S.; Saunders, J. K. M. *J. Org. Chem.* **2006**, *71*, 7063-7066

175. Tambara, K.; Ponnuswamy, N.; Hennrich, G.; Pantoş, G. D. *J. Org. Chem.* **2011**, *76*, 3338-3347
176. Overberger, J. E.; Aston, J. G. *Anal. Chem.* **1965**, *37*, 1167-1168
177. Fier, P. S.; Luo, J.; Hartwig, J. F. *J. Am. Chem. Soc.* **2013**, *135*, 2552-2559
178. Furuya, T.; Ritter, T. *Org. Lett.* **2009**, *11*, 2860-2863
179. James, T. D.; Sandanayake, K.R.A.S.; Shinkai, S. *Angew. Chem., Int. Ed.* **1996**, *35*, 1910-1922
180. Chan, D. M. T.; Monaco, K. L.; Li, R.; Bonne, D.; Clark, C. G.; Lam, P. Y. S. *Tetrahedron Lett.* **2003**, *44*, 3863-3865
181. Prakash, G. K. S.; Panja, C.; Mathew, T.; Surampudi, V.; Petasis, N. A.; Olah, G. A. *Org. Lett.* **2004**, *6*, 2205-2207
182. Hu, Z.; Pantoş, G. D.; Kuganathan, N.; Arrowsmith, R. L.; Jacobs, R. M. J.; Kociok-Köhn, G.; O'Byrne, J.; Jurkschat, K.; Burgos, P.; Tyrrell, R. M.; Botchway, S. W.; Sanders, J. K. M.; Pascu, S. I. *Adv. Funct. Mater.* **2012**, *22*, 503−518
183. Castellano, F. N. *Dalton Trans.* **2012**, 8493−8501
184. Earmme, T.; Hwang, Y.-J.; Murari, N. M.; Subramaniyan, S.; Jenekhe, S. A. *J. Am. Chem. Soc.* **2013**, *135*, 14960-14963
185. Dapurkar, S. E.; Kawanami, H.; Yokoyama, T.; Ikushima, Y. *New J. Chem.* **2009**, *33*, 538-544
186. Adcock, W.; Gupta, B. D.; Kitching, W. *J. Org. Chem.* **1976**, *41*, 1498-1504
187. Campbell, W. P.; Harris, G. C. *J. Am. Chem. Soc.* **1941**, *63*, 2721-2726
188. Dauben, W.; Martin, E.; Fonken, G. *J. Org. Chem.* **1958**, *23*, 1205-1235
189. Signaigo, F. K.; Cramer, P. L. *J. Am. Chem. Soc.* **1933**, *55*, 3326-3332
190. Wu, T.-C.; Xiong, H.; Rieke, R. D. *J. Org. Chem.* **1990**, *55*, 5045-5051
191. Levisalles, J.; Rudler, H.; Villemin, D. *J. Organomet. Chem.* **1980**, *192*, 195-207
192. Mahmoodi, N. O.; Fatemah; Mostagni *J. Korean. Chem. Soc.* **2002**, *46*, 52-56
193. Arnold, A.; Markert, M.; Mahrwald, R. *Synthesis*, **2006**, *7*, 1099-1102
194. Baba, T.; Avasthi, K.; Suzuki, A. *Bull. Chem. Soc. Jpn.* **1983**, *56*, 1571-1572
195. Yang, Y.; Du, Z.; Huang, Y.; Lu, F.; Wang, F.; Gao, J.; Xu, J. *Green Chem.* **2013**, *15*, 1932-1940
196. Chandler, C. L.; List B. *J. Am. Chem. Soc.* **2008**, *130*, 6737-6739
197. House, H. O.; Lee, J. H. C.; VanDerveer, D.; Wissinger, J. E. *J. Org. Chem.* **1983**, *48*, 5285-5287
198. Mayhew, M. P.; Roitberg, A. E.; Tewari, Y.; Holden, M. J.; Vanderah, D. J.; Vilker, V. L. *New J. Chem.* **2002**, *26*, 35-42
199. Demirci-Gultekin, D.; Gunbas, D. D.; Taskesenligil, Y.; Balci, M. *Tetrahedron* **2007**, *63*, 8151-8156
200. Gbara-Haj-Yahia, I.; Zvilichovsky, G.; Seri, N. *J. Org. Chem.* **2004**, *69*, 4135-4139
201. Lee, Y.-L.; Hsu, H.-L.; Chen, S.-Y.; Yew, T.-R. *J. Phys. Chem. C.* **2008**, *112*, 1694-1699
202. Ulrich, S.; Petitjean, A.; Lehn, J.-M. Eur. *J. Inorg. Chem.* **2010**, *13*, 1913-1928

# Appendices

## 6.1 Appendix 1

### 6.1.1 Crystallography Data for 312

| | |
|---|---|
| Identification code | k11sel1 |
| Empirical formula | C20 H26 N4 O4 |
| Formula weight | 386.45 |
| Temperature | 150(2) K |
| Wavelength | 0.71073 Å |
| Crystal system | Triclinic |
| Space group | P-1 |
| Unit cell dimensions | a = 10.5080(6)Å $\alpha$ = 81.989(2)$^{o}$ |
| | b = 11.6860(6)Å $\beta$ = 90.159(3)$^{o}$ |
| | c = 16.6470(10)Å $\gamma$ = 78.388(3)$^{o}$ |
| Volume | 1981.81(19) Å$^{3}$ |
| Z | 4 |
| Density (calculated) | 1.295 Mg/m$^{3}$ |
| Absorption coefficient | 0.092 mm$^{-1}$ |
| F(000) | 824 |
| Crystal size | 0.3 x 0.3 x 0.02 mm |
| Theta range for data collection | 4.04 to 25.03$^{o}$ |
| Index ranges | -12<=h<=12; -13<=k<=13; -19<=l<=19 |
| Reflections collected | 25927 |
| Independent reflections | 25927 [R(int) = 0.0000] |
| Reflections observed (>2□) | 14454 |
| Data Completeness | 0.981 |
| Absorption correction | None |
| Refinement method | Full-matrix least-squares on F$^{2}$ |
| Data / restraints / parameters | 25927 / 1 / 516 |
| Goodness-of-fit on F$^{2}$ | 1.118 |
| Final R indices [I>2□(I)] | R1 = 0.1792 wR2 = 0.3768 |
| R indices (all data) | R1 = 0.2588 wR2 = 0.4211 |
| Largest diff. peak and hole | 0.618 and -0.606 eÅ$^{-3}$ |

**Notes:**

**2 molecules in the asymmetric unit.**
**Model takes account of 50% twinning about the 0 0 1 reciprocal axis.**

Table 2. Atomic coordinates ( x $10^4$) and equivalent isotropic displacement parameters ($Å^2$ x $10^3$) for **312**.

| Atom | x | y | z | U(eq) |
|---|---|---|---|---|
| O(1) | 6724(5) | 12273(4) | 3727(3) | 48(1) |
| O(2) | 6591(5) | 11050(4) | 2875(3) | 51(1) |
| O(3) | 8445(6) | 7025(4) | 3496(3) | 55(2) |
| O(4) | 9404(5) | 6221(4) | 4651(3) | 39(1) |
| N(1) | 6927(6) | 11274(4) | 3533(4) | 35(1) |
| N(2) | 8813(5) | 7098(5) | 4187(4) | 35(1) |
| N(3) | 9473(6) | 7499(5) | 5820(3) | 36(1) |
| N(4) | 9598(5) | 7745(5) | 6620(3) | 34(1) |
| C(1) | 7622(6) | 10300(5) | 4118(4) | 32(2) |
| C(2) | 7927(6) | 9183(5) | 3900(4) | 30(2) |
| C(3) | 8563(7) | 8242(5) | 4449(4) | 34(2) |
| C(4) | 8902(6) | 8411(5) | 5256(4) | 30(2) |
| C(5) | 8585(7) | 9579(5) | 5433(4) | 36(2) |
| C(6) | 7980(7) | 10505(5) | 4884(4) | 36(2) |
| C(7) | 10134(6) | 6816(6) | 7134(4) | 33(2) |
| C(8) | 10610(8) | 5583(6) | 6943(5) | 45(2) |
| C(9) | 10324(7) | 7079(6) | 7985(4) | 38(2) |
| C(10) | 11759(8) | 7046(7) | 8167(5) | 55(2) |
| C(11) | 12009(9) | 7371(8) | 9006(5) | 59(2) |
| C(12) | 11436(7) | 6599(7) | 9651(5) | 46(2) |
| C(13) | 9990(6) | 6610(6) | 9483(4) | 38(2) |
| C(14) | 9779(7) | 6261(5) | 8641(4) | 36(2) |
| C(15) | 8341(6) | 6204(5) | 8490(4) | 29(1) |
| C(16) | 8028(7) | 5184(6) | 8406(4) | 39(2) |
| C(17) | 6669(7) | 5017(6) | 8325(5) | 44(2) |
| C(18) | 5685(9) | 6148(7) | 8163(7) | 72(3) |
| C(19) | 5973(7) | 7090(6) | 8608(5) | 52(2) |
| C(20) | 7350(7) | 7279(5) | 8475(5) | 40(2) |
| C(19A) | 2887(14) | 3208(13) | 8622(19) | 124(12) |
| O(1A) | 1731(4) | 7328(3) | 4244(3) | 41(1) |
| O(2A) | 1632(5) | 6277(4) | 3274(3) | 45(1) |
| O(3A) | 3497(5) | 2243(4) | 3603(3) | 49(2) |
| O(4A) | 4546(5) | 1289(4) | 4689(3) | 39(1) |
| N(1A) | 2013(5) | 6393(4) | 3962(4) | 32(1) |
| N(2A) | 3937(5) | 2220(4) | 4292(3) | 35(1) |
| N(3A) | 4889(5) | 2400(4) | 5907(3) | 30(1) |
| N(4A) | 5499(5) | 2530(4) | 6629(3) | 28(1) |
| C(1A) | 2768(6) | 5355(5) | 4459(4) | 29(2) |
| C(2A) | 3030(6) | 4301(5) | 4170(4) | 31(2) |
| C(3A) | 3725(6) | 3320(5) | 4646(4) | 29(2) |
| C(4A) | 4191(6) | 3373(5) | 5432(4) | 27(1) |
| C(5A) | 3922(6) | 4460(5) | 5726(4) | 31(2) |
| C(6A) | 3183(6) | 5475(6) | 5241(4) | 36(2) |
| C(7A) | 6004(6) | 1522(5) | 7051(4) | 30(2) |
| C(8A) | 5895(7) | 347(5) | 6843(4) | 35(2) |
| C(9A) | 6776(6) | 1555(5) | 7826(4) | 25(1) |
| C(10A) | 8181(7) | 960(6) | 7779(5) | 41(2) |

| | | | | |
|---|---|---|---|---|
| C(11A) | 8971(7) | 1038(6) | 8535(5) | 48(2) |
| C(12A) | 8368(7) | 527(6) | 9290(5) | 42(2) |
| C(13A) | 6939(7) | 1108(6) | 9343(5) | 42(2) |
| C(14A) | 6150(6) | 995(5) | 8586(4) | 34(2) |
| C(15A) | 4705(7) | 1488(6) | 8634(4) | 34(2) |
| C(16A) | 3851(6) | 826(6) | 8568(4) | 42(2) |
| C(17A) | 2399(7) | 1253(7) | 8589(5) | 51(2) |
| C(18A) | 1998(12) | 2619(12) | 8560(10) | 68(4) |
| C(20A) | 4297(7) | 2751(6) | 8722(5) | 45(2) |
| C(18B) | 2090(20) | 2233(19) | 8933(14) | 21(5) |
| C(19B) | 2790(40) | 3010(40) | 9000(30) | 59(12) |

Table 3. Bond lengths [Å] and angles [$^{o}$] for **312**.

| | | | |
|---|---|---|---|
| O(1)-N(1) | 1.231(6) | O(2)-N(1) | 1.228(7) |
| O(3)-N(2) | 1.233(7) | O(4)-N(2) | 1.247(7) |
| N(1)-C(1) | 1.459(8) | N(2)-C(3) | 1.438(8) |
| N(3)-C(4) | 1.356(8) | N(3)-N(4) | 1.411(7) |
| N(3)-H(3) | 0.8800 | N(4)-C(7) | 1.312(8) |
| C(1)-C(2) | 1.379(8) | C(1)-C(6) | 1.394(9) |
| C(2)-C(3) | 1.382(9) | C(2)-H(2) | 0.9500 |
| C(3)-C(4) | 1.439(9) | C(4)-C(5) | 1.410(8) |
| C(5)-C(6) | 1.362(9) | C(5)-H(5) | 0.9500 |
| C(6)-H(6) | 0.9500 | C(7)-C(8) | 1.505(9) |
| C(7)-C(9) | 1.511(9) | C(8)-H(8A) | 0.9800 |
| C(8)-H(8B) | 0.9800 | C(8)-H(8C) | 0.9800 |
| C(9)-C(10) | 1.530(10) | C(9)-C(14) | 1.539(10) |
| C(9)-H(9) | 1.0000 | C(10)-C(11) | 1.532(10) |
| C(10)-H(10A) | 0.9900 | C(10)-H(10B) | 0.9900 |
| C(11)-C(12) | 1.511(11) | C(11)-H(11A) | 0.9900 |
| C(11)-H(11B) | 0.9900 | C(12)-C(13) | 1.542(10) |
| C(12)-H(12A) | 0.9900 | C(12)-H(12B) | 0.9900 |
| C(13)-C(14) | 1.540(9) | C(13)-H(13A) | 0.9900 |
| C(13)-H(13B) | 0.9900 | C(14)-C(15) | 1.547(9) |
| C(14)-H(14) | 1.0000 | C(15)-C(16) | 1.323(8) |
| C(15)-C(20) | 1.459(8) | C(16)-C(17) | 1.488(10) |
| C(16)-H(16) | 0.9500 | C(17)-C(18) | 1.496(11) |
| C(17)-H(17A) | 0.9900 | C(17)-H(17B) | 0.9900 |
| C(18)-C(19) | 1.488(11) | C(18)-H(18A) | 0.9900 |
| C(18)-H(18B) | 0.9900 | C(19)-C(20) | 1.519(10) |
| C(19)-H(19A) | 0.9900 | C(19)-H(19B) | 0.9900 |
| C(20)-H(20A) | 0.9900 | C(20)-H(20B) | 0.9900 |
| C(19A)-C(18A) | 1.279(14) | C(19A)-C(20A) | 1.472(16) |
| C(19A)-H(19C) | 0.9900 | C(19A)-H(19D) | 0.9900 |
| O(1A)-N(1A) | 1.232(6) | O(2A)-N(1A) | 1.246(7) |
| O(3A)-N(2A) | 1.230(7) | O(4A)-N(2A) | 1.244(6) |
| N(1A)-C(1A) | 1.454(8) | N(2A)-C(3A) | 1.465(7) |
| N(3A)-C(4A) | 1.366(8) | N(3A)-N(4A) | 1.402(7) |
| N(3A)-H(3A) | 0.8800 | N(4A)-C(7A) | 1.296(8) |
| C(1A)-C(2A) | 1.361(8) | C(1A)-C(6A) | 1.405(9) |
| C(2A)-C(3A) | 1.372(9) | C(2A)-H(2A) | 0.9500 |

| | | | |
|---|---|---|---|
| C(3A)-C(4A) | 1.409(9) | C(4A)-C(5A) | 1.402(8) |
| C(5A)-C(6A) | 1.422(9) | C(5A)-H(5A) | 0.9500 |
| C(6A)-H(6A) | 0.9500 | C(7A)-C(8A) | 1.487(8) |
| C(7A)-C(9A) | 1.531(8) | C(8A)-H(8A1) | 0.9800 |
| C(8A)-H(8A2) | 0.9800 | C(8A)-H(8A3) | 0.9800 |
| C(9A)-C(10A) | 1.508(9) | C(9A)-C(14A) | 1.552(9) |
| C(9A)-H(9A) | 1.0000 | C(10A)-C(11A) | 1.529(9) |
| C(10A)-H(10C) | 0.9900 | C(10A)-H(10D) | 0.9900 |
| C(11A)-C(12A) | 1.511(11) | C(11A)-H(11C) | 0.9900 |
| C(11A)-H(11D) | 0.9900 | C(12A)-C(13A) | 1.526(10) |
| C(12A)-H(12C) | 0.9900 | C(12A)-H(12D) | 0.9900 |
| C(13A)-C(14A) | 1.541(9) | C(13A)-H(13C) | 0.9900 |
| C(13A)-H(13D) | 0.9900 | C(14A)-C(15A) | 1.519(9) |
| C(14A)-H(14A) | 1.0000 | C(15A)-C(16A) | 1.311(9) |
| C(15A)-C(20A) | 1.480(9) | C(16A)-C(17A) | 1.509(10) |
| C(16A)-H(16A) | 0.9500 | C(17A)-C(18B) | 1.33(2) |
| C(17A)-C(18A) | 1.561(15) | C(17A)-H(17C) | 0.9900 |
| C(17A)-H(17D) | 0.9900 | C(18A)-H(18C) | 0.9900 |
| C(18A)-H(18D) | 0.9900 | C(20A)-C(19B) | 1.63(5) |
| C(20A)-H(20C) | 0.9900 | C(20A)-H(20D) | 0.9900 |
| C(18B)-C(19B) | 1.29(2) | C(18B)-H(18E) | 0.9900 |
| C(18B)-H(18F) | 0.9900 | C(19B)-H(19E) | 0.9900 |
| C(19B)-H(19F) | 0.9900 | | |
| | | | |
| O(2)-N(1)-O(1) | 124.0(6) | O(2)-N(1)-C(1) | 118.0(5) |
| O(1)-N(1)-C(1) | 118.0(5) | O(3)-N(2)-O(4) | 122.0(5) |
| O(3)-N(2)-C(3) | 118.1(5) | O(4)-N(2)-C(3) | 119.9(5) |
| C(4)-N(3)-N(4) | 116.9(5) | C(4)-N(3)-H(3) | 121.5 |
| N(4)-N(3)-H(3) | 121.5 | C(7)-N(4)-N(3) | 113.5(5) |
| C(2)-C(1)-C(6) | 120.7(6) | C(2)-C(1)-N(1) | 119.2(6) |
| C(6)-C(1)-N(1) | 120.0(5) | C(1)-C(2)-C(3) | 120.3(6) |
| C(1)-C(2)-H(2) | 119.9 | C(3)-C(2)-H(2) | 119.9 |
| C(2)-C(3)-N(2) | 117.1(6) | C(2)-C(3)-C(4) | 120.6(6) |
| N(2)-C(3)-C(4) | 122.3(5) | N(3)-C(4)-C(5) | 121.8(6) |
| N(3)-C(4)-C(3) | 122.1(6) | C(5)-C(4)-C(3) | 116.1(6) |
| C(6)-C(5)-C(4) | 122.9(6) | C(6)-C(5)-H(5) | 118.5 |
| C(4)-C(5)-H(5) | 118.5 | C(5)-C(6)-C(1) | 119.2(6) |
| C(5)-C(6)-H(6) | 120.4 | C(1)-C(6)-H(6) | 120.4 |
| N(4)-C(7)-C(8) | 126.5(6) | N(4)-C(7)-C(9) | 113.9(6) |
| C(8)-C(7)-C(9) | 119.5(6) | C(7)-C(8)-H(8A) | 109.5 |
| C(7)-C(8)-H(8B) | 109.5 | H(8A)-C(8)-H(8B) | 109.5 |
| C(7)-C(8)-H(8C) | 109.5 | H(8A)-C(8)-H(8C) | 109.5 |
| H(8B)-C(8)-H(8C) | 109.5 | C(7)-C(9)-C(10) | 110.5(6) |
| C(7)-C(9)-C(14) | 113.5(5) | C(10)-C(9)-C(14) | 110.7(6) |
| C(7)-C(9)-H(9) | 107.3 | C(10)-C(9)-H(9) | 107.3 |
| C(14)-C(9)-H(9) | 107.3 | C(9)-C(10)-C(11) | 113.1(7) |
| C(9)-C(10)-H(10A) | 109.0 | C(11)-C(10)-H(10A) | 109.0 |
| C(9)-C(10)-H(10B) | 109.0 | C(11)-C(10)-H(10B) | 109.0 |
| H(10A)-C(10)-H(10B) | 107.8 | C(12)-C(11)-C(10) | 109.9(6) |
| C(12)-C(11)-H(11A) | 109.7 | C(10)-C(11)-H(11A) | 109.7 |
| C(12)-C(11)-H(11B) | 109.7 | C(10)-C(11)-H(11B) | 109.7 |

| | | | |
|---|---|---|---|
| H(11A)-C(11)-H(11B) | 108.2 | C(11)-C(12)-C(13) | 113.2(6) |
| C(11)-C(12)-H(12A) | 108.9 | C(13)-C(12)-H(12A) | 108.9 |
| C(11)-C(12)-H(12B) | 108.9 | C(13)-C(12)-H(12B) | 108.9 |
| H(12A)-C(12)-H(12B) | 107.8 | C(14)-C(13)-C(12) | 111.2(6) |
| C(14)-C(13)-H(13A) | 109.4 | C(12)-C(13)-H(13A) | 109.4 |
| C(14)-C(13)-H(13B) | 109.4 | C(12)-C(13)-H(13B) | 109.4 |
| H(13A)-C(13)-H(13B) | 108.0 | C(9)-C(14)-C(13) | 109.7(5) |
| C(9)-C(14)-C(15) | 114.3(5) | C(13)-C(14)-C(15) | 111.3(6) |
| C(9)-C(14)-H(14) | 107.0 | C(13)-C(14)-H(14) | 107.0 |
| C(15)-C(14)-H(14) | 107.0 | C(16)-C(15)-C(20) | 121.3(6) |
| C(16)-C(15)-C(14) | 119.9(6) | C(20)-C(15)-C(14) | 118.7(5) |
| C(15)-C(16)-C(17) | 124.1(6) | C(15)-C(16)-H(16) | 118.0 |
| C(17)-C(16)-H(16) | 118.0 | C(16)-C(17)-C(18) | 113.7(6) |
| C(16)-C(17)-H(17A) | 108.8 | C(18)-C(17)-H(17A) | 108.8 |
| C(16)-C(17)-H(17B) | 108.8 | C(18)-C(17)-H(17B) | 108.8 |
| H(17A)-C(17)-H(17B) | 107.7 | C(19)-C(18)-C(17) | 113.6(7) |
| C(19)-C(18)-H(18A) | 108.8 | C(17)-C(18)-H(18A) | 108.8 |
| C(19)-C(18)-H(18B) | 108.8 | C(17)-C(18)-H(18B) | 108.8 |
| H(18A)-C(18)-H(18B) | 107.7 | C(18)-C(19)-C(20) | 111.7(7) |
| C(18)-C(19)-H(19A) | 109.3 | C(20)-C(19)-H(19A) | 109.3 |
| C(18)-C(19)-H(19B) | 109.3 | C(20)-C(19)-H(19B) | 109.3 |
| H(19A)-C(19)-H(19B) | 107.9 | C(15)-C(20)-C(19) | 115.3(5) |
| C(15)-C(20)-H(20A) | 108.5 | C(19)-C(20)-H(20A) | 108.5 |
| C(15)-C(20)-H(20B) | 108.5 | C(19)-C(20)-H(20B) | 108.5 |
| H(20A)-C(20)-H(20B) | 107.5 | C(18A)-C(19A)-C(20A) | 127.6(13) |
| C(18A)-C(19A)-H(19C) | 105.4 | C(20A)-C(19A)-H(19C) | 105.4 |
| C(18A)-C(19A)-H(19D) | 105.4 | C(20A)-C(19A)-H(19D) | 105.4 |
| H(19C)-C(19A)-H(19D) | 106.0 | O(1A)-N(1A)-O(2A) | 122.8(5) |
| O(1A)-N(1A)-C(1A) | 119.4(5) | O(2A)-N(1A)-C(1A) | 117.8(5) |
| O(3A)-N(2A)-O(4A) | 121.5(5) | O(3A)-N(2A)-C(3A) | 118.6(5) |
| O(4A)-N(2A)-C(3A) | 119.9(5) | C(4A)-N(3A)-N(4A) | 119.6(5) |
| C(4A)-N(3A)-H(3A) | 120.2 | N(4A)-N(3A)-H(3A) | 120.2 |
| C(7A)-N(4A)-N(3A) | 112.1(5) | C(2A)-C(1A)-C(6A) | 121.9(6) |
| C(2A)-C(1A)-N(1A) | 120.0(6) | C(6A)-C(1A)-N(1A) | 118.1(5) |
| C(1A)-C(2A)-C(3A) | 119.8(6) | C(1A)-C(2A)-H(2A) | 120.1 |
| C(3A)-C(2A)-H(2A) | 120.1 | C(2A)-C(3A)-C(4A) | 121.6(5) |
| C(2A)-C(3A)-N(2A) | 116.1(6) | C(4A)-C(3A)-N(2A) | 122.3(5) |
| N(3A)-C(4A)-C(5A) | 119.8(6) | N(3A)-C(4A)-C(3A) | 121.8(5) |
| C(5A)-C(4A)-C(3A) | 118.4(5) | C(4A)-C(5A)-C(6A) | 120.2(6) |
| C(4A)-C(5A)-H(5A) | 119.9 | C(6A)-C(5A)-H(5A) | 119.9 |
| C(1A)-C(6A)-C(5A) | 118.0(6) | C(1A)-C(6A)-H(6A) | 121.0 |
| C(5A)-C(6A)-H(6A) | 121.0 | N(4A)-C(7A)-C(8A) | 125.5(6) |
| N(4A)-C(7A)-C(9A) | 116.7(5) | C(8A)-C(7A)-C(9A) | 117.9(5) |
| C(7A)-C(8A)-H(8A1) | 109.5 | C(7A)-C(8A)-H(8A2) | 109.5 |
| H(8A1)-C(8A)-H(8A2) | 109.5 | C(7A)-C(8A)-H(8A3) | 109.5 |
| H(8A1)-C(8A)-H(8A3) | 109.5 | H(8A2)-C(8A)-H(8A3) | 109.5 |
| C(10A)-C(9A)-C(7A) | 111.3(5) | C(10A)-C(9A)-C(14A) | 111.0(5) |
| C(7A)-C(9A)-C(14A) | 111.0(5) | C(10A)-C(9A)-H(9A) | 107.8 |
| C(7A)-C(9A)-H(9A) | 107.8 | C(14A)-C(9A)-H(9A) | 107.8 |
| C(9A)-C(10A)-C(11A) | 111.6(6) | C(9A)-C(10A)-H(10C) | 109.3 |
| C(11A)-C(10A)-H(10C) | 109.3 | C(9A)-C(10A)-H(10D) | 109.3 |

| | | | |
|---|---|---|---|
| C(11A)-C(10A)-H(10D) | 109.3 | H(10C)-C(10A)-H(10D) | 108.0 |
| C(12A)-C(11A)-C(10A) | 110.3(6) | C(12A)-C(11A)-H(11C) | 109.6 |
| C(10A)-C(11A)-H(11C) | 109.6 | C(12A)-C(11A)-H(11D) | 109.6 |
| C(10A)-C(11A)-H(11D) | 109.6 | H(11C)-C(11A)-H(11D) | 108.1 |
| C(11A)-C(12A)-C(13A) | 112.1(6) | C(11A)-C(12A)-H(12C) | 109.2 |
| C(13A)-C(12A)-H(12C) | 109.2 | C(11A)-C(12A)-H(12D) | 109.2 |
| C(13A)-C(12A)-H(12D) | 109.2 | H(12C)-C(12A)-H(12D) | 107.9 |
| C(12A)-C(13A)-C(14A) | 111.1(6) | C(12A)-C(13A)-H(13C) | 109.4 |
| C(14A)-C(13A)-H(13C) | 109.4 | C(12A)-C(13A)-H(13D) | 109.4 |
| C(14A)-C(13A)-H(13D) | 109.4 | H(13C)-C(13A)-H(13D) | 108.0 |
| C(15A)-C(14A)-C(13A) | 113.1(6) | C(15A)-C(14A)-C(9A) | 113.7(5) |
| C(13A)-C(14A)-C(9A) | 108.2(5) | C(15A)-C(14A)-H(14A) | 107.2 |
| C(13A)-C(14A)-H(14A) | 107.2 | C(9A)-C(14A)-H(14A) | 107.2 |
| C(16A)-C(15A)-C(20A) | 121.5(6) | C(16A)-C(15A)-C(14A) | 120.9(6) |
| C(20A)-C(15A)-C(14A) | 117.6(6) | C(15A)-C(16A)-C(17A) | 124.3(7) |
| C(15A)-C(16A)-H(16A) | 117.9 | C(17A)-C(16A)-H(16A) | 117.9 |
| C(18B)-C(17A)-C(16A) | 111.7(11) | C(18B)-C(17A)-C(18A) | 26.9(10) |
| C(16A)-C(17A)-C(18A) | 112.7(7) | C(18B)-C(17A)-H(17C) | 85.0 |
| C(16A)-C(17A)-H(17C) | 109.0 | C(18A)-C(17A)-H(17C) | 109.0 |
| C(18B)-C(17A)-H(17D) | 130.0 | C(16A)-C(17A)-H(17D) | 109.0 |
| C(18A)-C(17A)-H(17D) | 109.0 | H(17C)-C(17A)-H(17D) | 107.8 |
| C(19A)-C(18A)-C(17A) | 118.7(11) | C(19A)-C(18A)-H(18C) | 107.6 |
| C(17A)-C(18A)-H(18C) | 107.6 | C(19A)-C(18A)-H(18D) | 107.6 |
| C(17A)-C(18A)-H(18D) | 107.6 | H(18C)-C(18A)-H(18D) | 107.1 |
| C(19A)-C(20A)-C(15A) | 114.1(8) | C(19A)-C(20A)-C(19B) | 23(2) |
| C(15A)-C(20A)-C(19B) | 109.4(14) | C(19A)-C(20A)-H(20C) | 108.7 |
| C(15A)-C(20A)-H(20C) | 108.7 | C(19B)-C(20A)-H(20C) | 90.0 |
| C(19A)-C(20A)-H(20D) | 108.7 | C(15A)-C(20A)-H(20D) | 108.7 |
| C(19B)-C(20A)-H(20D) | 129.5 | H(20C)-C(20A)-H(20D) | 107.6 |
| C(19B)-C(18B)-C(17A) | 128(3) | C(19B)-C(18B)-H(18E) | 105.2 |
| C(17A)-C(18B)-H(18E) | 105.2 | C(19B)-C(18B)-H(18F) | 105.2 |
| C(17A)-C(18B)-H(18F) | 105.2 | H(18E)-C(18B)-H(18F) | 105.9 |
| C(18B)-C(19B)-C(20A) | 119(3) | C(18B)-C(19B)-H(19E) | 107.7 |
| C(20A)-C(19B)-H(19E) | 107.7 | C(18B)-C(19B)-H(19F) | 107.7 |
| C(20A)-C(19B)-H(19F) | 107.7 | H(19E)-C(19B)-H(19F) | 107.1 |

Table 4. Anisotropic displacement parameters ($Å^2$ x $10^3$) for **312**.

| Atom | U11 | U22 | U33 | U23 | U13 | U12 |
|---|---|---|---|---|---|---|
| O(1) | 58(3) | 36(3) | 47(3) | 3(2) | -2(3) | -9(2) |
| O(2) | 67(4) | 47(3) | 40(3) | 7(2) | -12(3) | -24(3) |
| O(3) | 86(4) | 35(3) | 41(3) | -15(2) | -14(3) | -1(3) |
| O(4) | 51(3) | 23(2) | 41(3) | -7(2) | 2(2) | -6(2) |
| N(1) | 46(4) | 23(3) | 39(4) | -6(2) | 2(3) | -11(2) |
| N(2) | 33(3) | 36(3) | 42(4) | -14(3) | 2(3) | -14(3) |
| N(3) | 50(4) | 30(3) | 28(3) | -8(2) | 1(3) | -6(3) |
| N(4) | 38(3) | 38(3) | 28(3) | -2(3) | -6(3) | -10(2) |
| C(1) | 32(4) | 26(3) | 37(4) | -2(3) | -4(3) | -1(3) |
| C(2) | 23(3) | 29(4) | 36(4) | 1(3) | -4(3) | -6(3) |
| C(3) | 44(4) | 23(3) | 32(4) | -5(3) | 10(3) | -3(3) |
| C(4) | 26(4) | 31(3) | 31(4) | -3(3) | 1(3) | -6(3) |

| | | | | | | |
|---|---|---|---|---|---|---|
| C(5) | 40(4) | 30(4) | 42(4) | -17(3) | 3(3) | -8(3) |
| C(6) | 33(4) | 25(3) | 50(5) | -8(3) | 3(3) | -7(3) |
| C(7) | 35(4) | 35(4) | 33(4) | -11(3) | 5(3) | -14(3) |
| C(8) | 53(5) | 45(4) | 37(4) | -11(3) | -5(4) | -5(3) |
| C(9) | 36(4) | 49(4) | 30(4) | 2(3) | 5(3) | -19(3) |
| C(10) | 54(5) | 73(6) | 53(5) | -26(4) | 6(4) | -36(4) |
| C(11) | 73(6) | 74(6) | 41(5) | -12(4) | -4(4) | -42(5) |
| C(12) | 51(5) | 56(5) | 37(4) | -8(3) | -7(4) | -21(4) |
| C(13) | 32(4) | 45(4) | 33(4) | -7(3) | -7(3) | -2(3) |
| C(14) | 45(4) | 26(3) | 37(4) | -7(3) | -3(3) | -4(3) |
| C(15) | 34(4) | 22(3) | 29(4) | -1(3) | 5(3) | -6(3) |
| C(16) | 50(5) | 27(4) | 42(4) | -7(3) | 2(4) | -11(3) |
| C(17) | 49(5) | 32(4) | 58(5) | -13(3) | -4(4) | -17(3) |
| C(18) | 50(5) | 52(5) | 124(9) | -25(5) | 13(5) | -25(4) |
| C(19) | 40(4) | 45(4) | 68(6) | -17(4) | -4(4) | 1(3) |
| C(20) | 42(4) | 22(3) | 58(5) | -7(3) | -7(4) | -9(3) |
| C(19A) | 19(7) | 29(8) | 320(40) | -18(15) | 9(14) | 10(6) |
| O(1A) | 42(3) | 18(2) | 61(3) | -7(2) | -9(2) | 4(2) |
| O(2A) | 55(3) | 35(3) | 43(3) | 4(2) | -15(3) | -13(2) |
| O(3A) | 77(4) | 29(3) | 41(3) | -17(2) | -11(3) | 1(2) |
| O(4A) | 49(3) | 23(2) | 42(3) | -1(2) | -7(2) | -3(2) |
| N(1A) | 34(3) | 18(3) | 47(4) | -7(2) | 7(3) | -9(2) |
| N(2A) | 40(3) | 25(3) | 38(4) | -2(3) | -1(3) | -6(2) |
| N(3A) | 39(3) | 16(3) | 34(3) | -8(2) | -7(3) | -3(2) |
| N(4A) | 20(3) | 28(3) | 31(3) | 0(2) | -3(2) | -1(2) |
| C(1A) | 31(4) | 16(3) | 36(4) | 1(3) | 1(3) | -2(3) |
| C(2A) | 21(3) | 38(4) | 35(4) | -6(3) | -2(3) | -8(3) |
| C(3A) | 37(4) | 13(3) | 38(4) | -4(3) | 5(3) | -7(3) |
| C(4A) | 34(4) | 22(3) | 27(4) | -6(3) | 8(3) | -9(3) |
| C(5A) | 46(4) | 16(3) | 36(4) | -13(3) | -8(3) | -9(3) |
| C(6A) | 30(4) | 33(4) | 51(5) | -8(3) | 5(3) | -15(3) |
| C(7A) | 22(3) | 37(4) | 33(4) | -10(3) | 2(3) | -11(3) |
| C(8A) | 42(4) | 26(3) | 37(4) | 0(3) | -5(3) | -11(3) |
| C(9A) | 22(3) | 21(3) | 34(4) | -7(3) | -7(3) | -6(2) |
| C(10A) | 36(4) | 38(4) | 46(5) | -1(3) | -3(4) | -7(3) |
| C(11A) | 32(4) | 49(5) | 63(6) | -9(4) | -14(4) | -8(3) |
| C(12A) | 27(4) | 50(4) | 45(5) | 1(3) | -19(3) | -2(3) |
| C(13A) | 36(4) | 39(4) | 48(5) | -11(3) | -9(4) | 0(3) |
| C(14A) | 37(4) | 23(3) | 42(4) | -2(3) | -13(3) | -13(3) |
| C(15A) | 37(4) | 42(4) | 23(4) | -5(3) | 4(3) | -6(3) |
| C(16A) | 29(4) | 48(4) | 47(5) | 8(3) | -4(4) | -13(3) |
| C(17A) | 43(5) | 69(5) | 45(5) | -6(4) | 11(4) | -18(4) |
| C(18A) | 35(7) | 73(9) | 79(11) | 14(9) | 4(7) | 13(7) |
| C(20A) | 29(4) | 52(5) | 56(5) | -11(4) | 4(4) | -8(3) |

Table 5. Hydrogen coordinates ( x $10^4$) and isotropic displacement parameters (Å$^2$ x $10^3$) for **312**.

| Atom | x | y | z | U(eq) |
|---|---|---|---|---|
| H(3) | 9753 | 6787 | 5693 | 43 |
| H(2) | 7700 | 9060 | 3371 | 36 |

| | | | | |
|---|---|---|---|---|
| H(5) | 8802 | 9725 | 5958 | 43 |
| H(6) | 7805 | 11283 | 5021 | 43 |
| H(8A) | 9865 | 5224 | 6855 | 68 |
| H(8B) | 11155 | 5110 | 7398 | 68 |
| H(8C) | 11122 | 5612 | 6452 | 68 |
| H(9) | 9840 | 7903 | 8008 | 45 |
| H(10A) | 12075 | 7602 | 7748 | 66 |
| H(10B) | 12265 | 6243 | 8133 | 66 |
| H(11A) | 12956 | 7263 | 9113 | 71 |
| H(11B) | 11610 | 8211 | 9021 | 71 |
| H(12A) | 11529 | 6869 | 10182 | 56 |
| H(12B) | 11936 | 5778 | 9689 | 56 |
| H(13A) | 9687 | 6051 | 9905 | 45 |
| H(13B) | 9470 | 7409 | 9510 | 45 |
| H(14) | 10304 | 5446 | 8641 | 43 |
| H(16) | 8713 | 4518 | 8397 | 47 |
| H(17A) | 6451 | 4553 | 8831 | 53 |
| H(17B) | 6614 | 4553 | 7876 | 53 |
| H(18A) | 5641 | 6436 | 7573 | 86 |
| H(18B) | 4820 | 5992 | 8317 | 86 |
| H(19A) | 5856 | 6872 | 9195 | 62 |
| H(19B) | 5350 | 7838 | 8422 | 62 |
| H(20A) | 7365 | 7775 | 7943 | 48 |
| H(20B) | 7582 | 7724 | 8898 | 48 |
| H(19C) | 2646 | 3646 | 9085 | 149 |
| H(19D) | 2772 | 3809 | 8132 | 149 |
| H(3A) | 4955 | 1696 | 5760 | 36 |
| H(2A) | 2733 | 4246 | 3641 | 37 |
| H(5A) | 4234 | 4519 | 6252 | 37 |
| H(6A) | 2976 | 6212 | 5439 | 44 |
| H(8A1) | 4981 | 342 | 6729 | 52 |
| H(8A2) | 6229 | -264 | 7301 | 52 |
| H(8A3) | 6402 | 190 | 6364 | 52 |
| H(9A) | 6746 | 2401 | 7879 | 30 |
| H(10C) | 8559 | 1339 | 7294 | 49 |
| H(10D) | 8235 | 120 | 7721 | 49 |
| H(11C) | 9874 | 597 | 8502 | 57 |
| H(11D) | 8998 | 1873 | 8564 | 57 |
| H(12C) | 8854 | 635 | 9775 | 51 |
| H(12D) | 8442 | -331 | 9290 | 51 |
| H(13C) | 6867 | 1953 | 9392 | 50 |
| H(13D) | 6575 | 729 | 9834 | 50 |
| H(14A) | 6256 | 134 | 8552 | 40 |
| H(16A) | 4167 | 24 | 8503 | 51 |
| H(17C) | 2074 | 863 | 9091 | 62 |
| H(17D) | 1982 | 1019 | 8121 | 62 |
| H(18C) | 1509 | 2942 | 8042 | 82 |
| H(18D) | 1386 | 2775 | 9002 | 82 |
| H(20C) | 4586 | 2867 | 9267 | 54 |
| H(20D) | 4743 | 3220 | 8315 | 54 |
| H(18E) | 1270 | 2677 | 8657 | 25 |

| | | | | |
|---|---|---|---|---|
| H(18F) | 1869 | 1965 | 9496 | 25 |
| H(19E) | 2785 | 3149 | 9570 | 70 |
| H(19F) | 2339 | 3763 | 8671 | 70 |

Table 6. Dihedral angles [$^{o}$] for **312**.

| Atom1 - Atom2 - Atom3 - Atom4 | Dihedral |
|---|---|
| C(4) - N(3) - N(4) - C(7) | 178.6(6) |
| O(2) - N(1) - C(1) - C(2) | 3.0(10) |
| O(1) - N(1) - C(1) - C(2) | -176.3(6) |
| O(2) - N(1) - C(1) - C(6) | -177.6(7) |
| O(1) - N(1) - C(1) - C(6) | 3.0(10) |
| C(6) - C(1) - C(2) - C(3) | 1.9(10) |
| N(1) - C(1) - C(2) - C(3) | -178.8(6) |
| C(1) - C(2) - C(3) - N(2) | 178.1(6) |
| C(1) - C(2) - C(3) - C(4) | 0.6(10) |
| O(3) - N(2) - C(3) - C(2) | -0.2(9) |
| O(4) - N(2) - C(3) - C(2) | 178.6(6) |
| O(3) - N(2) - C(3) - C(4) | 177.2(7) |
| O(4) - N(2) - C(3) - C(4) | -3.9(10) |
| N(4) - N(3) - C(4) - C(5) | 7.3(10) |
| N(4) - N(3) - C(4) - C(3) | -171.5(6) |
| C(2) - C(3) - C(4) - N(3) | 177.0(7) |
| N(2) - C(3) - C(4) - N(3) | -0.3(10) |
| C(2) - C(3) - C(4) - C(5) | -1.9(10) |
| N(2) - C(3) - C(4) - C(5) | -179.2(6) |
| N(3) - C(4) - C(5) - C(6) | -178.3(7) |
| C(3) - C(4) - C(5) - C(6) | 0.7(10) |
| C(4) - C(5) - C(6) - C(1) | 1.8(11) |
| C(2) - C(1) - C(6) - C(5) | -3.1(11) |
| N(1) - C(1) - C(6) - C(5) | 177.6(7) |
| N(3) - N(4) - C(7) - C(8) | 0.7(10) |
| N(3) - N(4) - C(7) - C(9) | 177.6(6) |
| N(4) - C(7) - C(9) - C(10) | -106.2(7) |
| C(8) - C(7) - C(9) - C(10) | 71.0(8) |
| N(4) - C(7) - C(9) - C(14) | 128.9(6) |
| C(8) - C(7) - C(9) - C(14) | -54.0(9) |
| C(7) - C(9) - C(10) - C(11) | 176.9(6) |
| C(14) - C(9) - C(10) - C(11) | -56.5(8) |
| C(9) - C(10) - C(11) - C(12) | 54.0(10) |
| C(10) - C(11) - C(12) - C(13) | -53.2(9) |
| C(11) - C(12) - C(13) - C(14) | 55.5(8) |
| C(7) - C(9) - C(14) - C(13) | -178.9(6) |
| C(10) - C(9) - C(14) - C(13) | 56.3(7) |
| C(7) - C(9) - C(14) - C(15) | -53.1(8) |
| C(10) - C(9) - C(14) - C(15) | -177.9(6) |
| C(12) - C(13) - C(14) - C(9) | -55.7(7) |
| C(12) - C(13) - C(14) - C(15) | 176.8(5) |
| C(9) - C(14) - C(15) - C(16) | 119.6(7) |
| C(13) - C(14) - C(15) - C(16) | -115.4(7) |
| C(9) - C(14) - C(15) - C(20) | -62.7(8) |

| | |
|---|---|
| C(13) - C(14) - C(15) - C(20) | 62.3(8) |
| C(20) - C(15) - C(16) - C(17) | -2.7(11) |
| C(14) - C(15) - C(16) - C(17) | 174.9(7) |
| C(15) - C(16) - C(17) - C(18) | 12.8(11) |
| C(16) - C(17) - C(18) - C(19) | -37.6(11) |
| C(17) - C(18) - C(19) - C(20) | 52.0(11) |
| C(16) - C(15) - C(20) - C(19) | 17.4(10) |
| C(14) - C(15) - C(20) - C(19) | -160.3(6) |
| C(18) - C(19) - C(20) - C(15) | -41.6(10) |
| C(4A) - N(3A) - N(4A) - C(7A) | 173.2(6) |
| O(1A) - N(1A) - C(1A) - C(2A) | 176.7(6) |
| O(2A) - N(1A) - C(1A) - C(2A) | -0.4(9) |
| O(1A) - N(1A) - C(1A) - C(6A) | -2.0(9) |
| O(2A) - N(1A) - C(1A) - C(6A) | -179.0(6) |
| C(6A) - C(1A) - C(2A) - C(3A) | -0.4(10) |
| N(1A) - C(1A) - C(2A) - C(3A) | -178.9(6) |
| C(1A) - C(2A) - C(3A) - C(4A) | -0.6(10) |
| C(1A) - C(2A) - C(3A) - N(2A) | 178.7(6) |
| O(3A) - N(2A) - C(3A) - C(2A) | 0.5(9) |
| O(4A) - N(2A) - C(3A) - C(2A) | -179.2(6) |
| O(3A) - N(2A) - C(3A) - C(4A) | 179.9(7) |
| O(4A) - N(2A) - C(3A) - C(4A) | 0.1(10) |
| N(4A) - N(3A) - C(4A) - C(5A) | -9.8(9) |
| N(4A) - N(3A) - C(4A) - C(3A) | 170.3(6) |
| C(2A) - C(3A) - C(4A) - N(3A) | -179.7(6) |
| N(2A) - C(3A) - C(4A) - N(3A) | 1.0(10) |
| C(2A) - C(3A) - C(4A) - C(5A) | 0.4(10) |
| N(2A) - C(3A) - C(4A) - C(5A) | -178.9(6) |
| N(3A) - C(4A) - C(5A) - C(6A) | -179.2(6) |
| C(3A) - C(4A) - C(5A) - C(6A) | 0.7(10) |
| C(2A) - C(1A) - C(6A) - C(5A) | 1.4(10) |
| N(1A) - C(1A) - C(6A) - C(5A) | -180.0(6) |
| C(4A) - C(5A) - C(6A) - C(1A) | -1.6(10) |
| N(3A) - N(4A) - C(7A) - C(8A) | -3.9(9) |
| N(3A) - N(4A) - C(7A) - C(9A) | 176.0(5) |
| N(4A) - C(7A) - C(9A) - C(10A) | -117.3(6) |
| C(8A) - C(7A) - C(9A) - C(10A) | 62.6(8) |
| N(4A) - C(7A) - C(9A) - C(14A) | 118.5(6) |
| C(8A) - C(7A) - C(9A) - C(14A) | -61.6(7) |
| C(7A) - C(9A) - C(10A) - C(11A) | 177.5(6) |
| C(14A) - C(9A) - C(10A) - C(11A) | -58.3(7) |
| C(9A) - C(10A) - C(11A) - C(12A) | 55.7(8) |
| C(10A) - C(11A) - C(12A) - C(13A) | -54.9(8) |
| C(11A) - C(12A) - C(13A) - C(14A) | 57.1(8) |
| C(12A) - C(13A) - C(14A) - C(15A) | 176.2(6) |
| C(12A) - C(13A) - C(14A) - C(9A) | -57.0(7) |
| C(10A) - C(9A) - C(14A) - C(15A) | -175.4(5) |
| C(7A) - C(9A) - C(14A) - C(15A) | -51.1(6) |
| C(10A) - C(9A) - C(14A) - C(13A) | 58.1(6) |
| C(7A) - C(9A) - C(14A) - C(13A) | -177.6(5) |
| C(13A) - C(14A) - C(15A) - C(16A) | -122.8(7) |

| | |
|---|---|
| C(9A) - C(14A) - C(15A) - C(16A) | 113.3(7) |
| C(13A) - C(14A) - C(15A) - C(20A) | 59.8(8) |
| C(9A) - C(14A) - C(15A) - C(20A) | -64.1(7) |
| C(20A) - C(15A) - C(16A) - C(17A) | -1.2(11) |
| C(14A) - C(15A) - C(16A) - C(17A) | -178.5(7) |
| C(15A) - C(16A) - C(17A) - C(18B) | -20.0(15) |
| C(15A) - C(16A) - C(17A) - C(18A) | 9.1(12) |
| C(20A) - C(19A) - C(18A) - C(17A) | 0(4) |
| C(18B) - C(17A) - C(18A) - C(19A) | 85(3) |
| C(16A) - C(17A) - C(18A) - C(19A) | -8(2) |
| C(18A) - C(19A) - C(20A) - C(15A) | 8(4) |
| C(18A) - C(19A) - C(20A) - C(19B) | -75(4) |
| C(16A) - C(15A) - C(20A) - C(19A) | -7.5(17) |
| C(14A) - C(15A) - C(20A) - C(19A) | 169.9(14) |
| C(16A) - C(15A) - C(20A) - C(19B) | 17.2(18) |
| C(14A) - C(15A) - C(20A) - C(19B) | -165.4(16) |
| C(16A) - C(17A) - C(18B) - C(19B) | 24(4) |
| C(18A) - C(17A) - C(18B) - C(19B) | -73(4) |
| C(17A) - C(18B) - C(19B) - C(20A) | -8(5) |
| C(19A) - C(20A) - C(19B) - C(18B) | 92(5) |
| C(15A) - C(20A) - C(19B) - C(18B) | -14(4) |

## 6.2 Appendix 2

### 6.2.1 NMR Spectra for Selected Compounds

1D spectra shown are $^{1}H$ and $^{13}C$ spectra unless otherwise stated. 2D spectra are labelled with experiment type for clarity.

**Enol ether, 244**

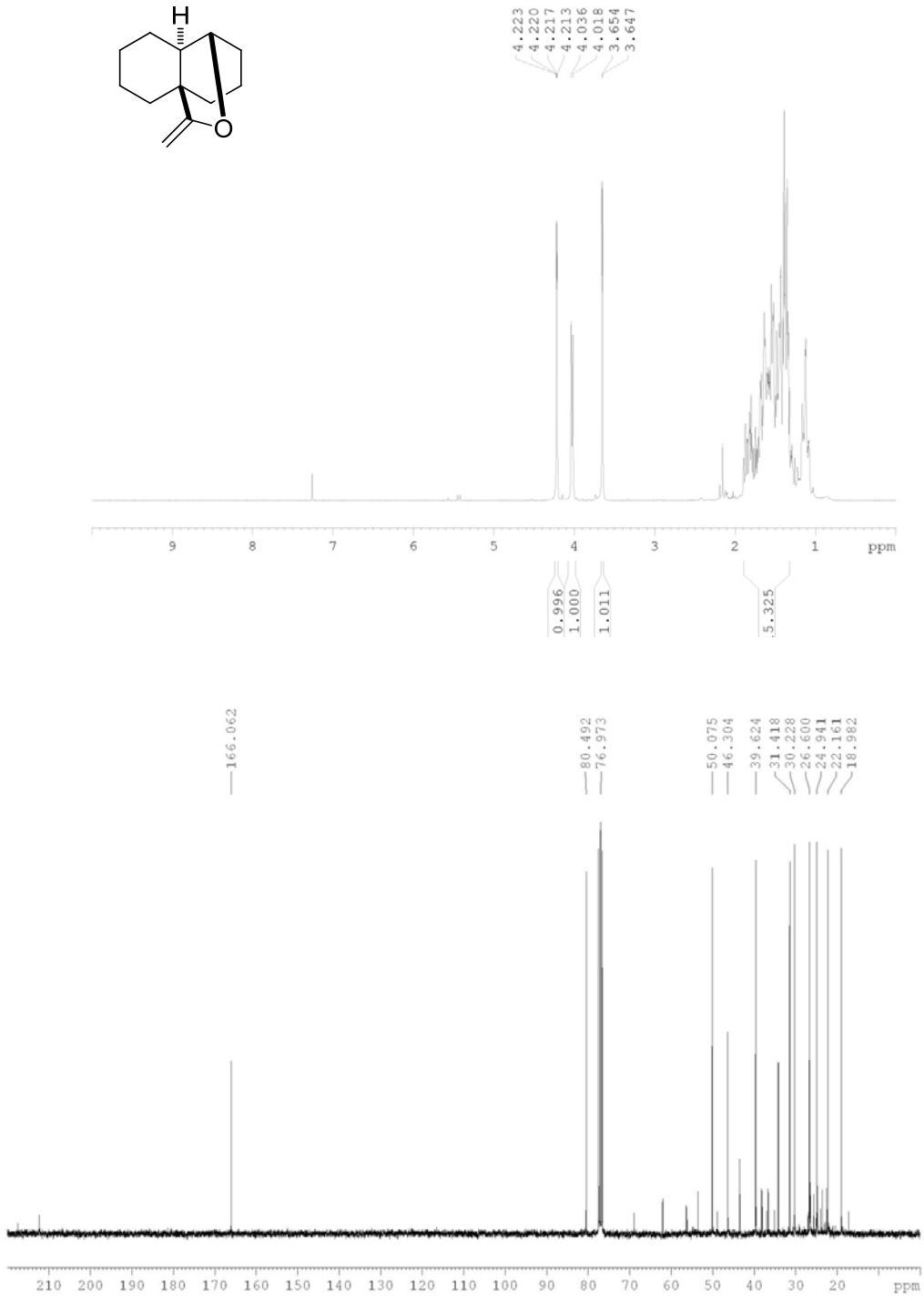

HMQC (300 MH, $CDCl_3$)

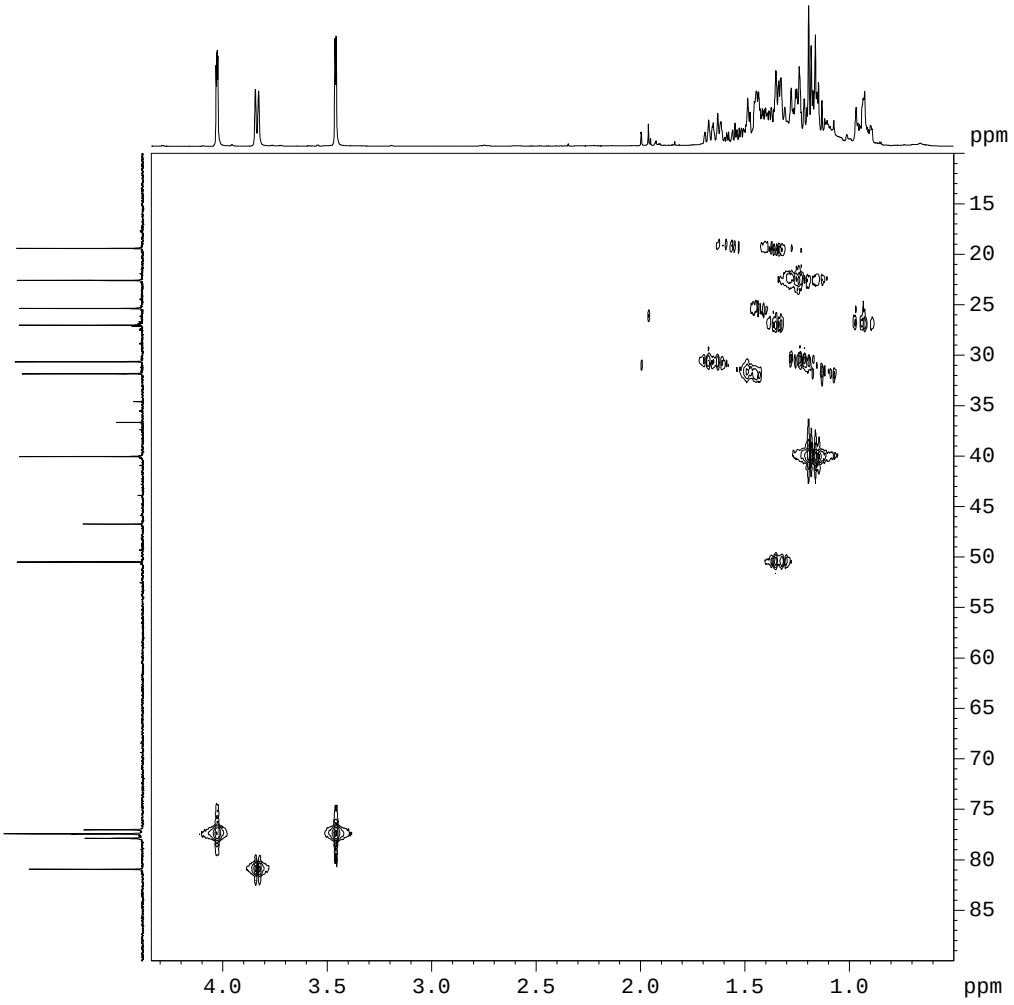

**Chloroketone, 255**

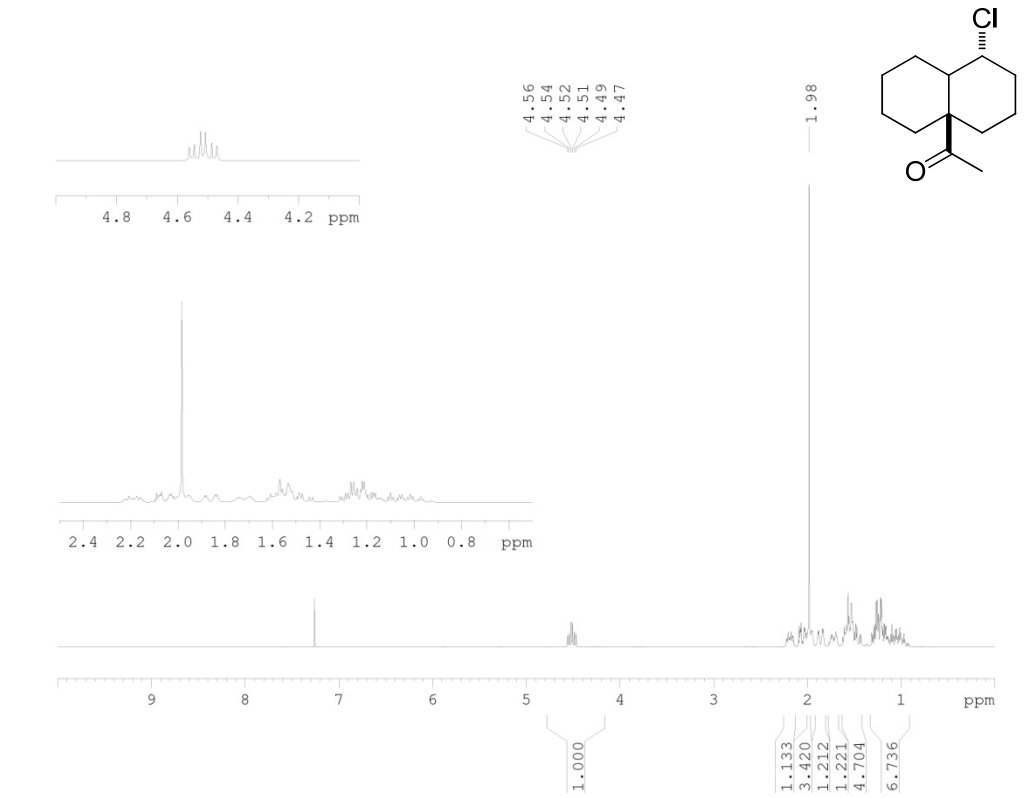


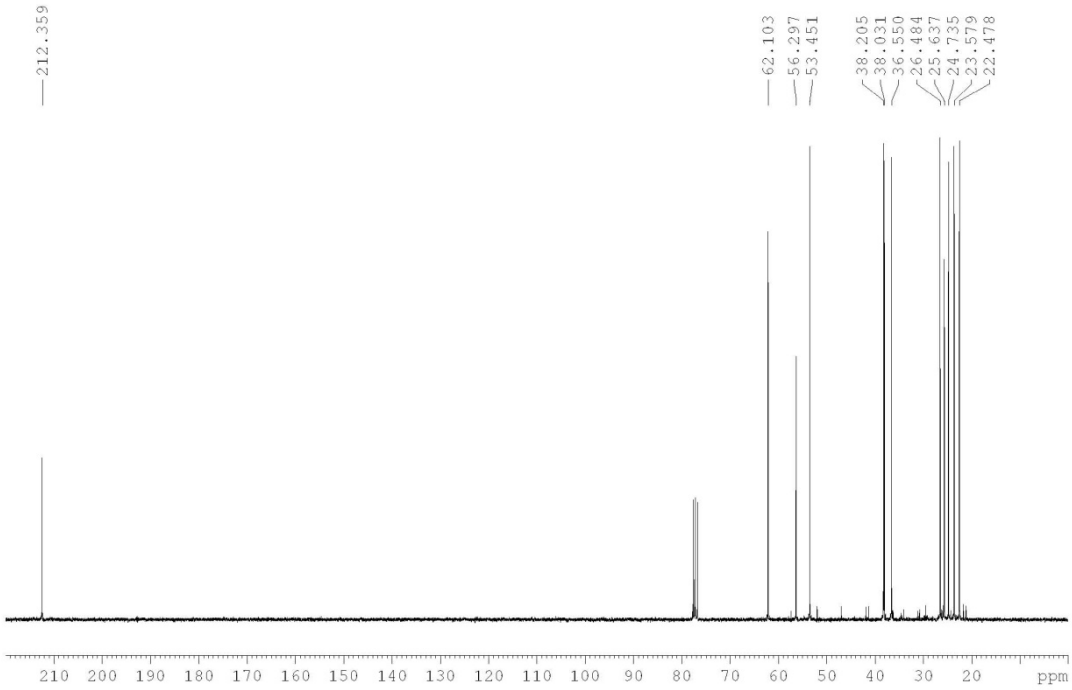

**1-chloroethyl acetate, 253**

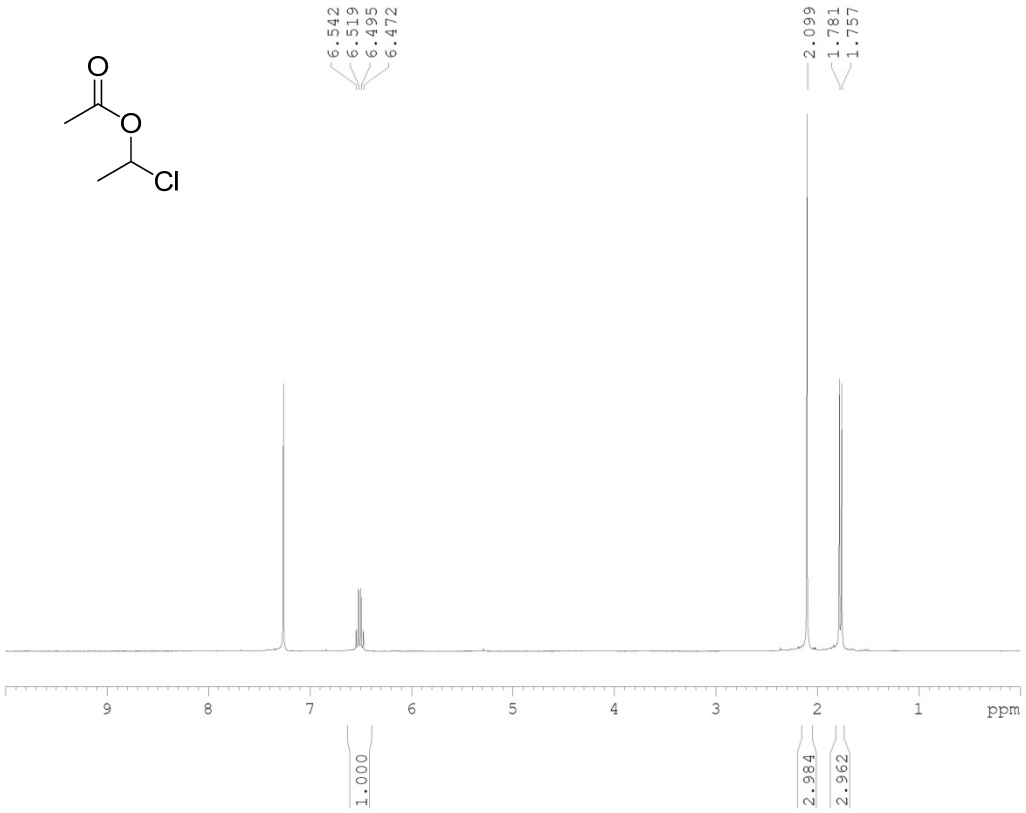


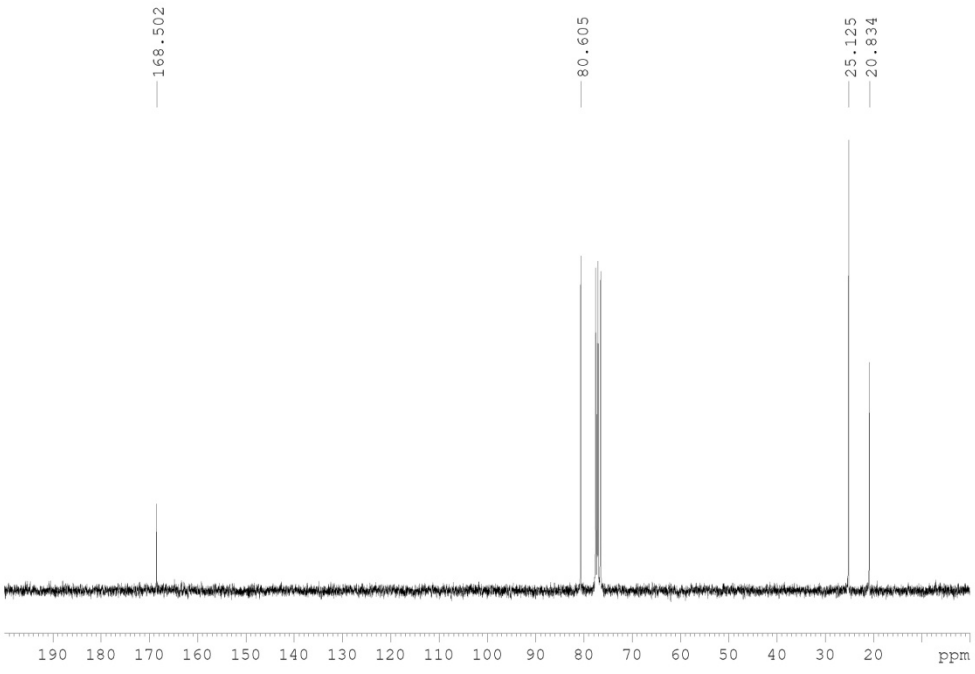

**1-chloroethyl crotonate, 255**

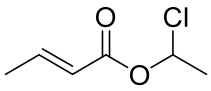


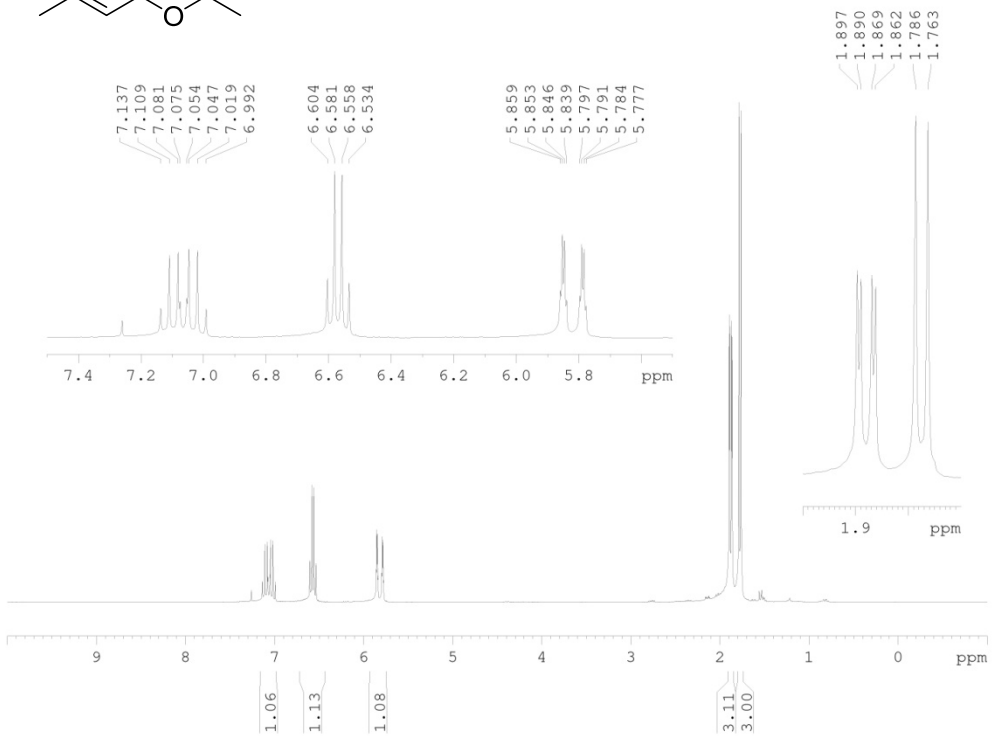


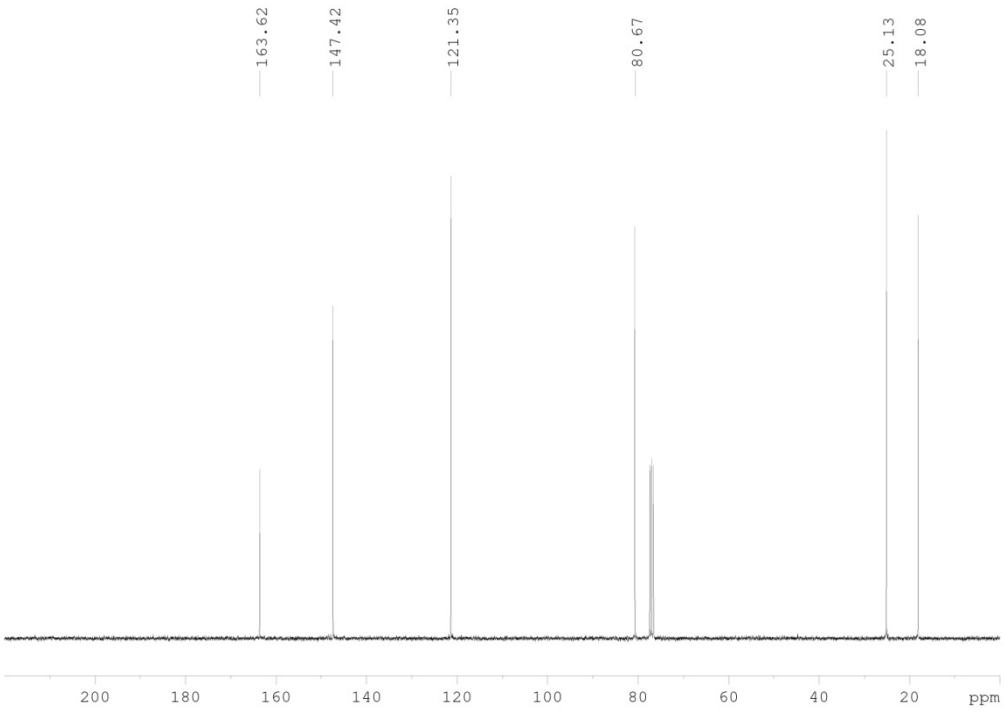

**Enol ether, 305**

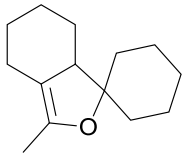





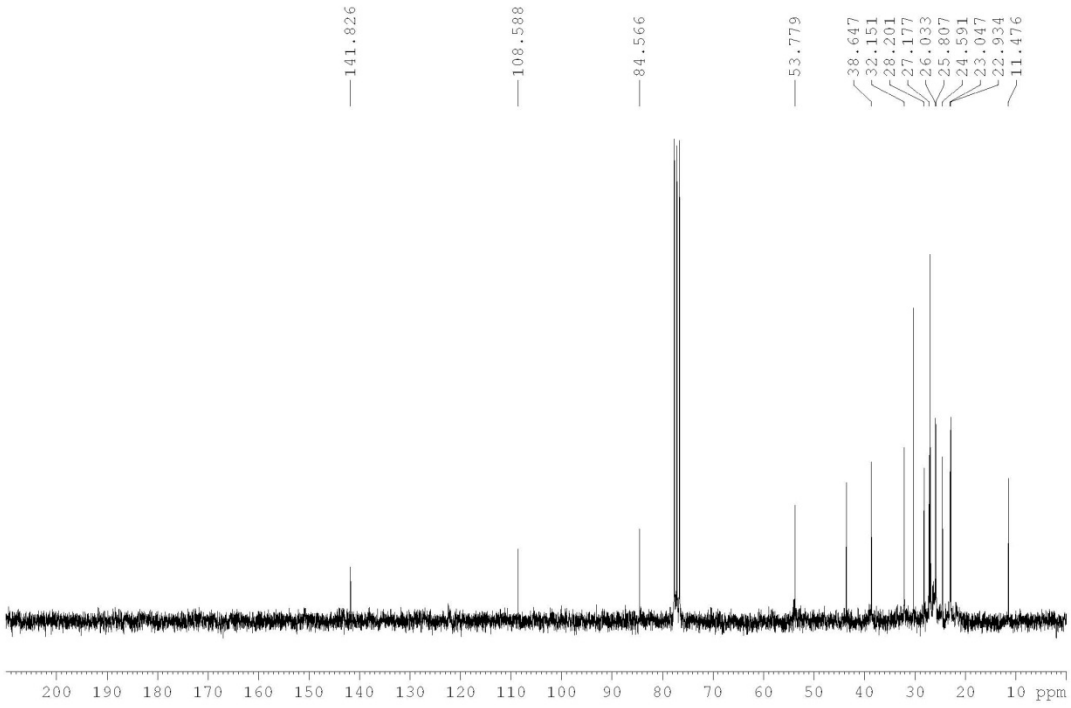

**Methyl ketone, 311**

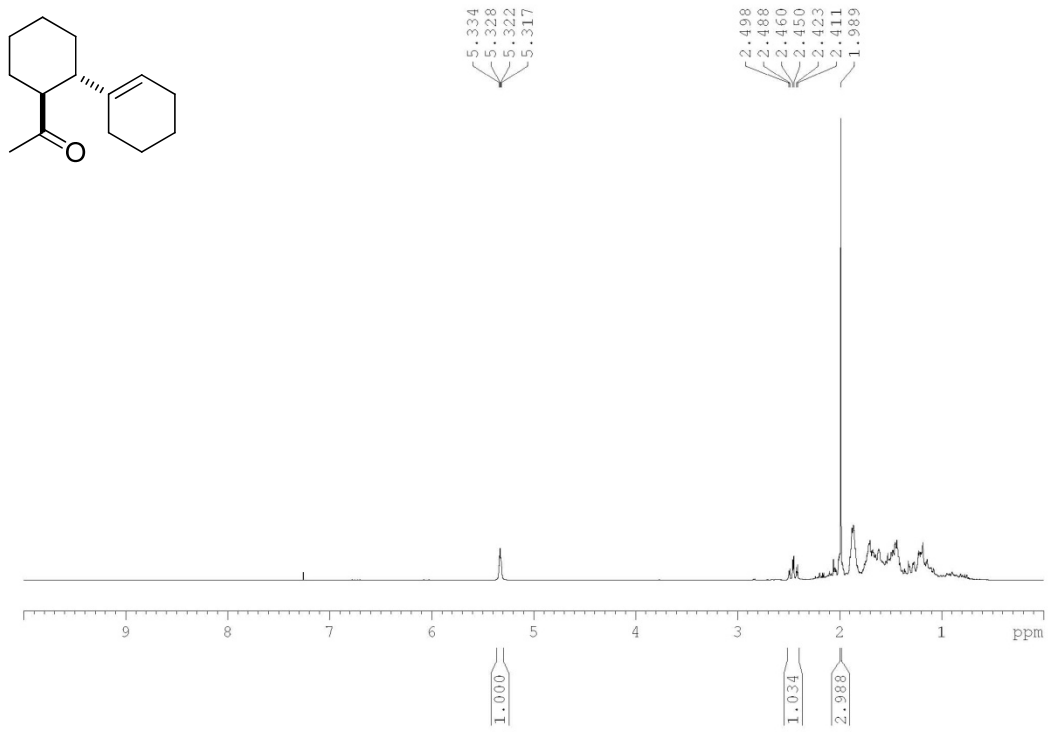


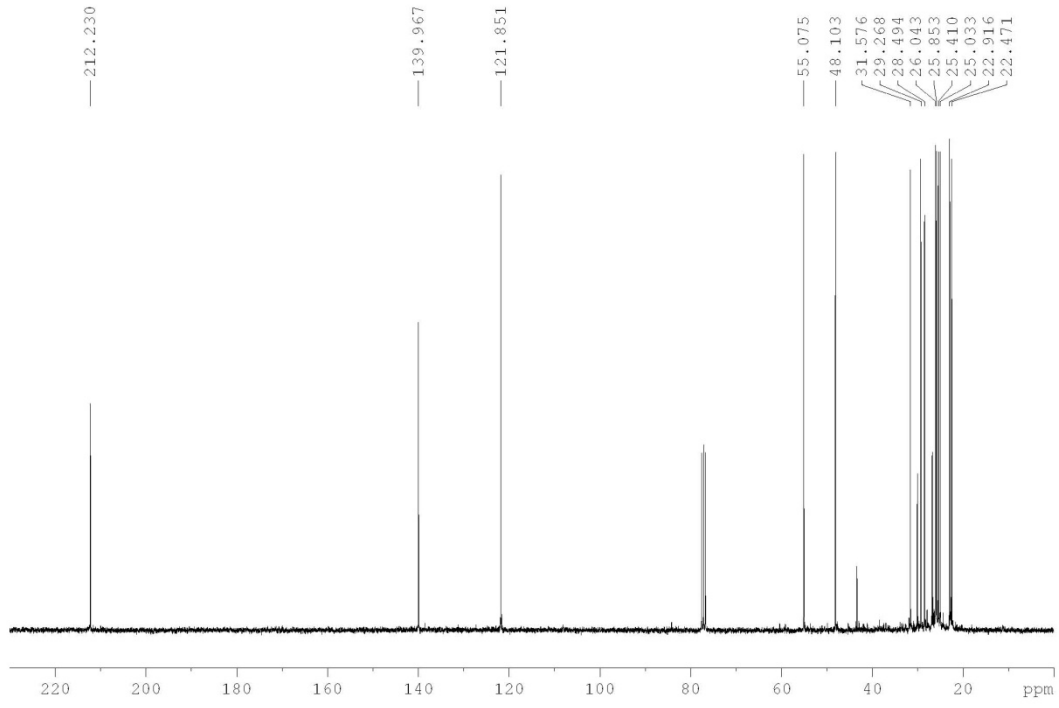

**Hydrazone, 312**

**Unsaturated ketone, 315**

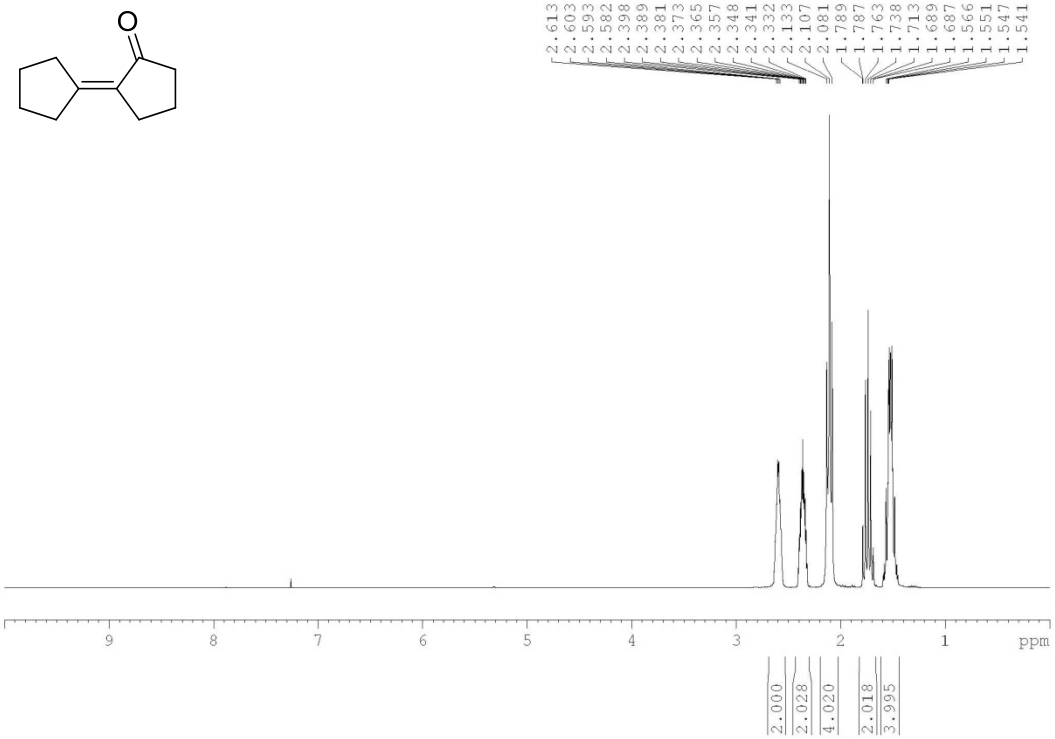


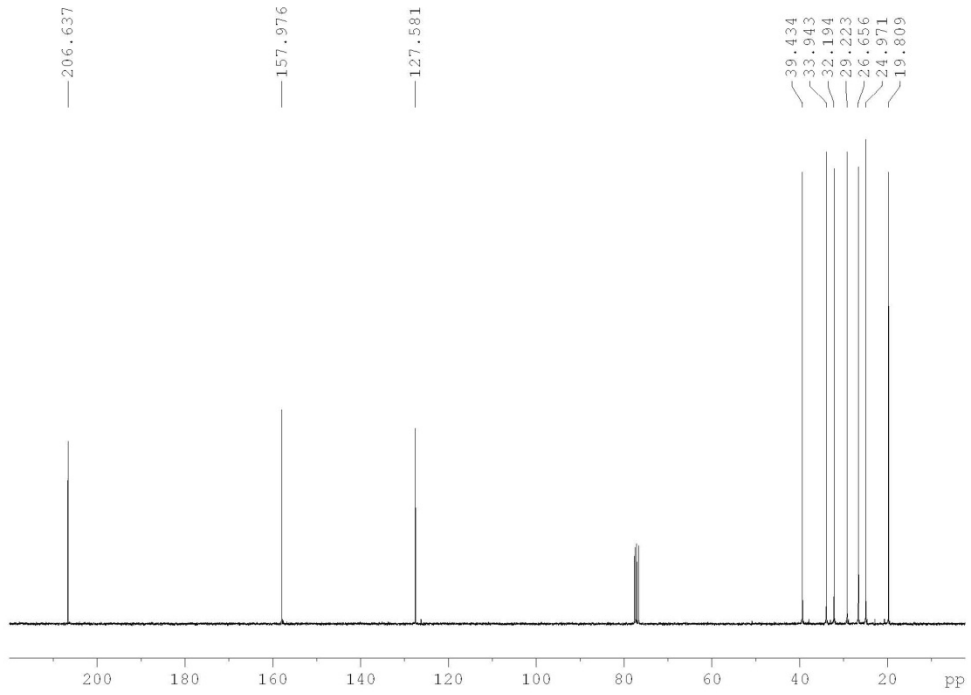

**Alkene, 317**

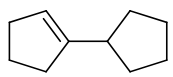


4.511
4.500
4.474
4.448
4.437
9
8
7
6
5
4
3
2
1
ppm
1.000
15.060

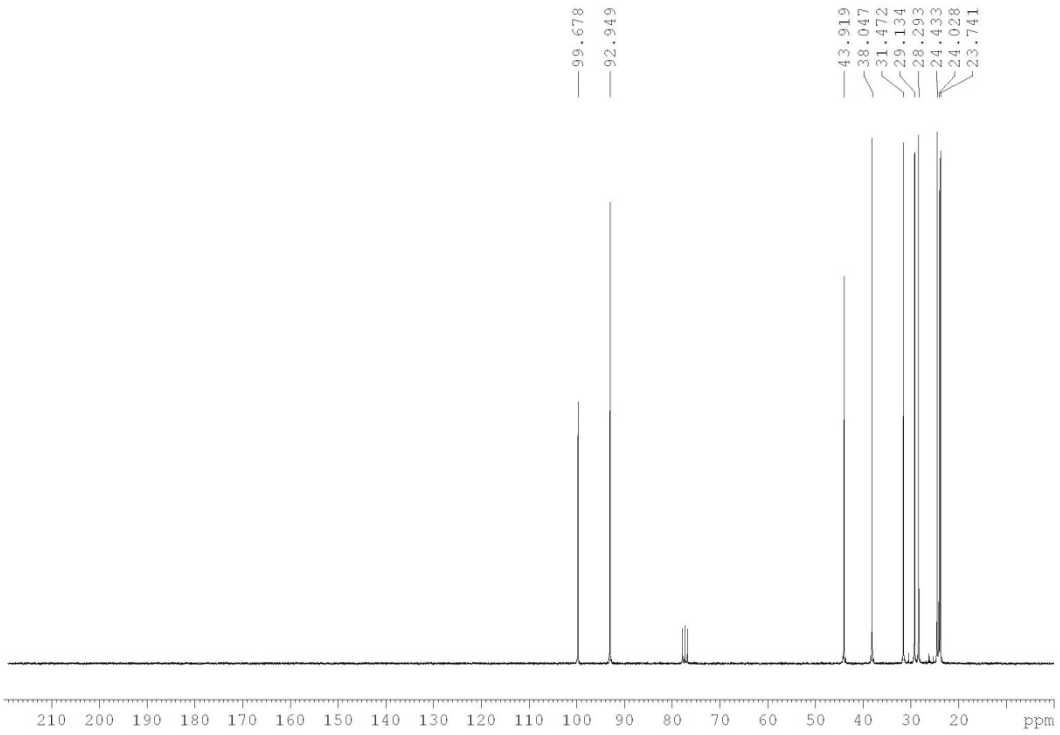
99.678
92.949
43.919
38.047
31.472
29.134
28.293
24.433
24.028
23.741
210
200
190
180
170
160
150
140
130
120
110
100
90
80
70
60
50
40
30
20
ppm

**Bicyclopentyl, 313**

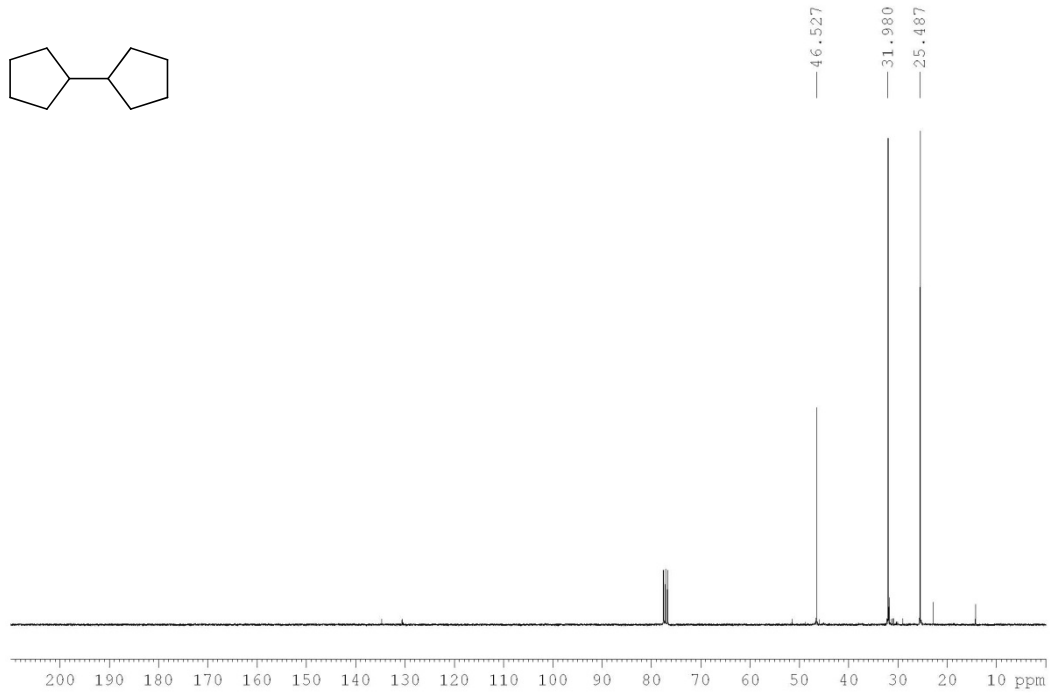

**Cyclodecane-1,6-dione, 332**

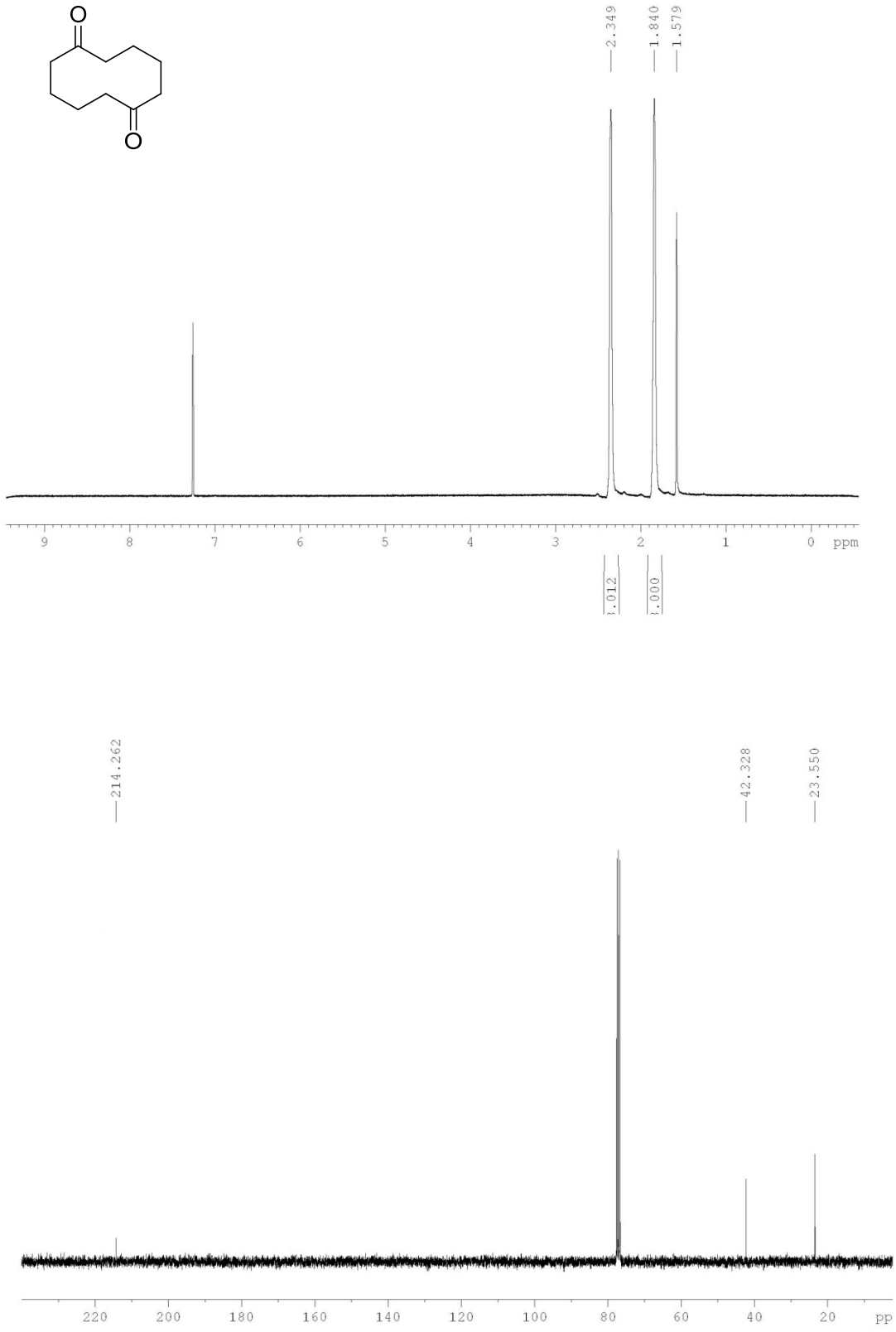

**Unsaturated ketone, 331**

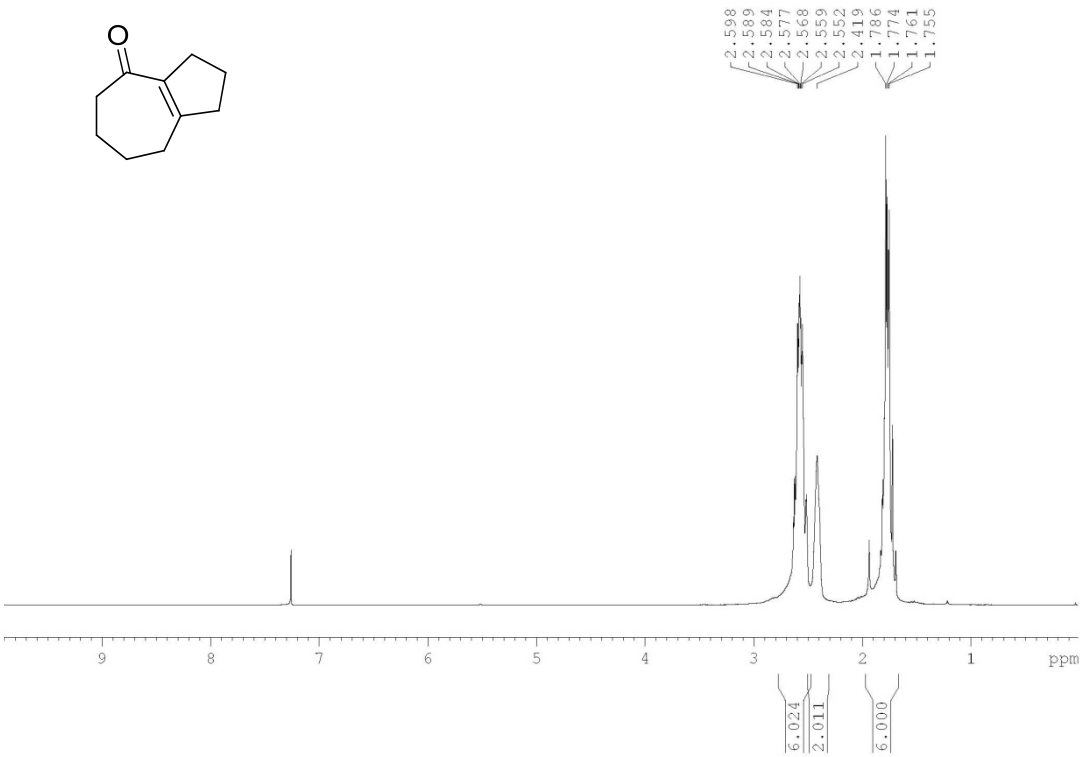


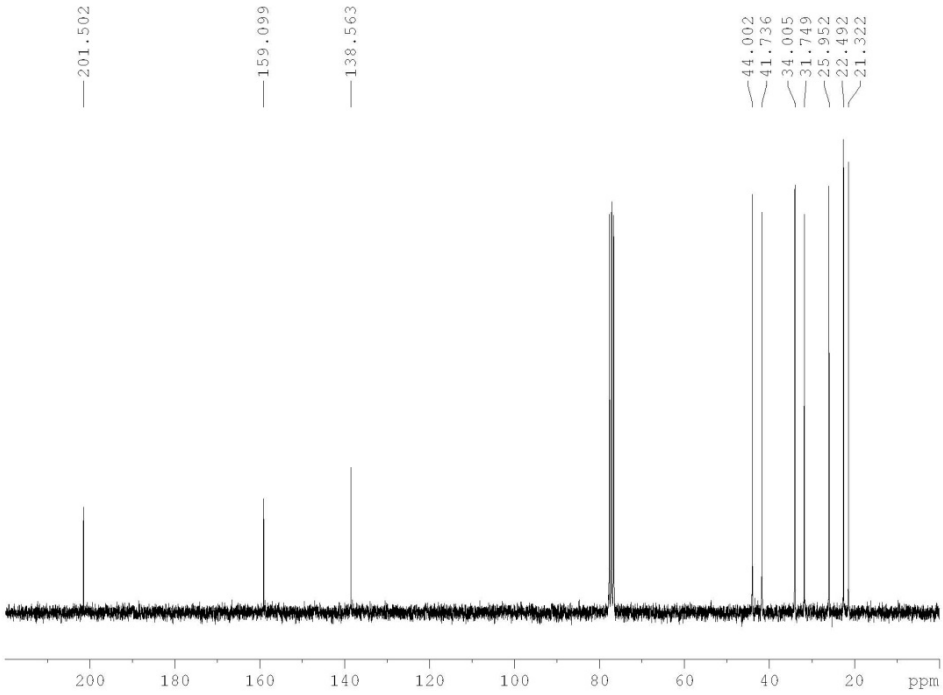

**Mixture of alkenes, 334 and 335**

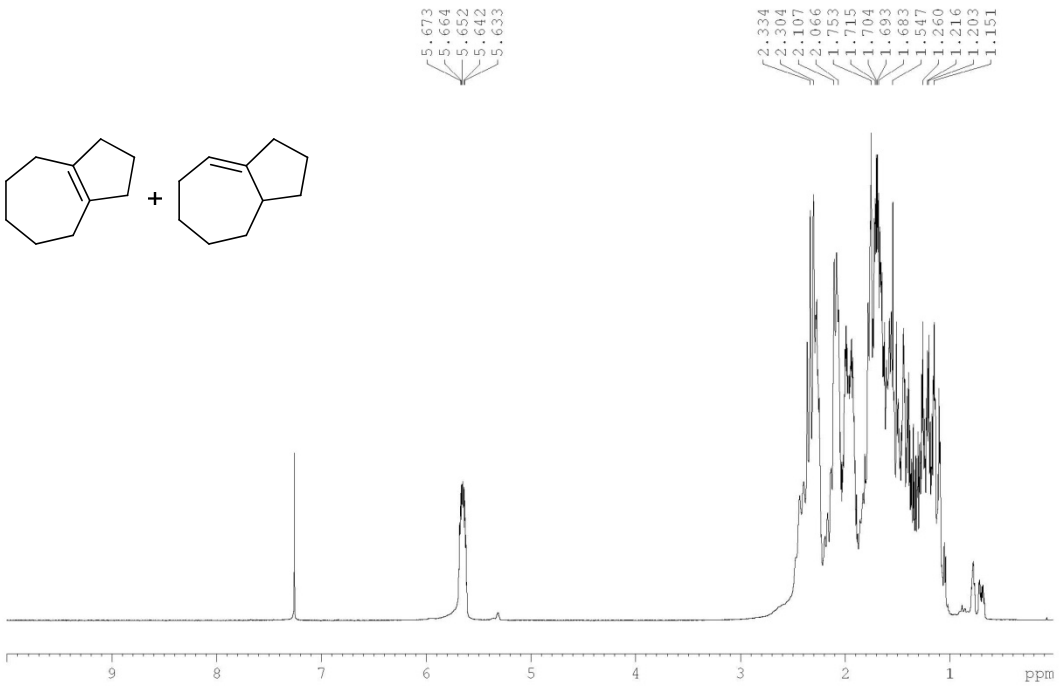


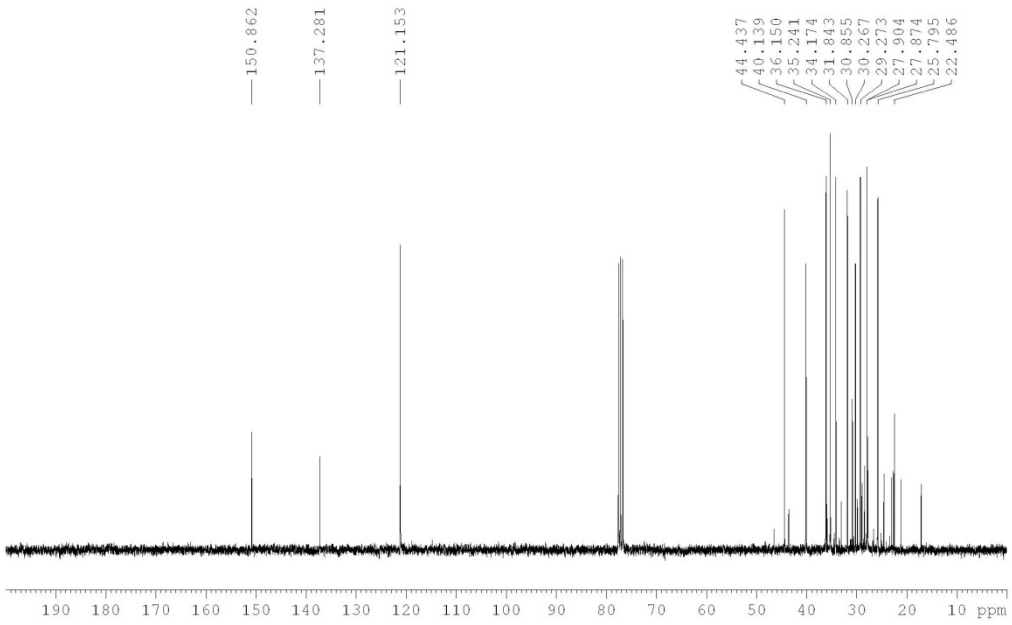

**Bicyclo[5.3.0]decane, 330**

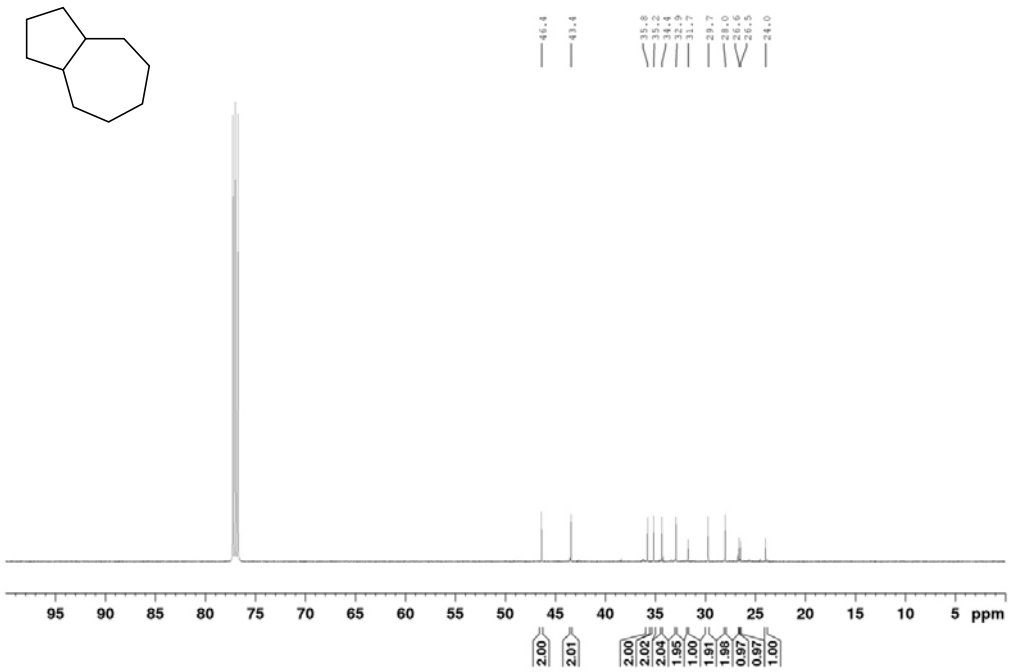

**Arene, 347**

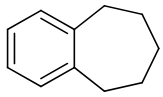


7.224
2.950
2.927
2.906
1.997
1.976
1.955
1.932
1.827
1.804
1.783
1.763
1.744
1.739
9
8
7
6
5
4
3
2
1
ppm
1.000
1.055
2.082
1.055

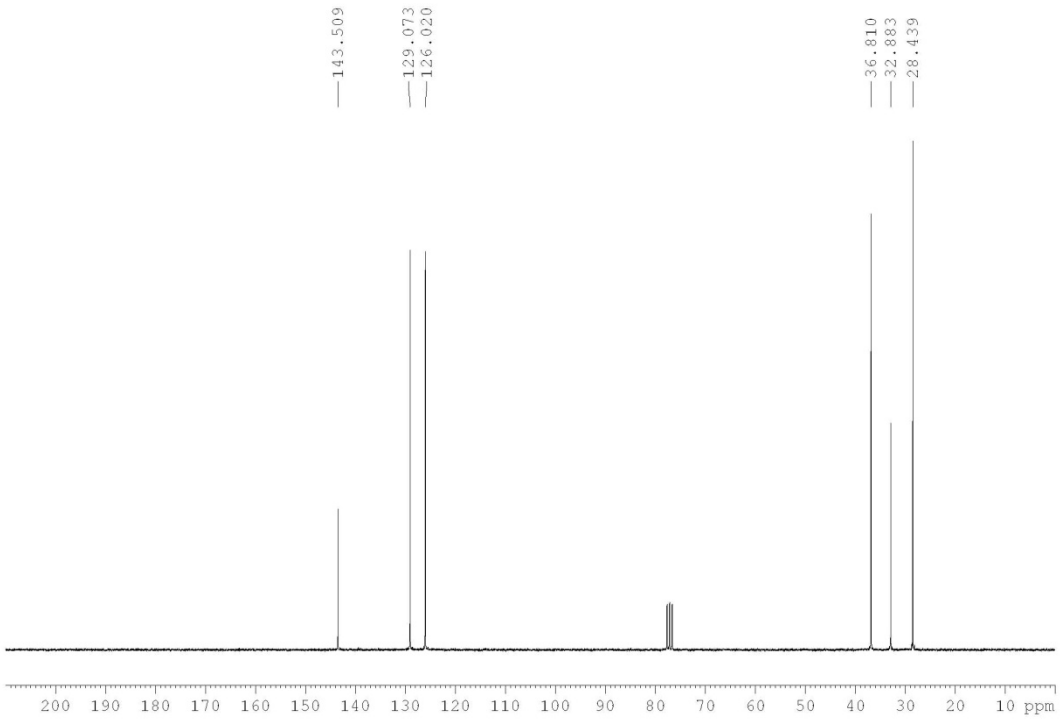
143.509
129.073
126.020
36.810
32.883
28.439
200
190
180
170
160
150
140
130
120
110
100
90
80
70
60
50
40
30
20
10 ppm

**Bicyclo[5.4.0]undecane, 345**

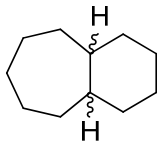





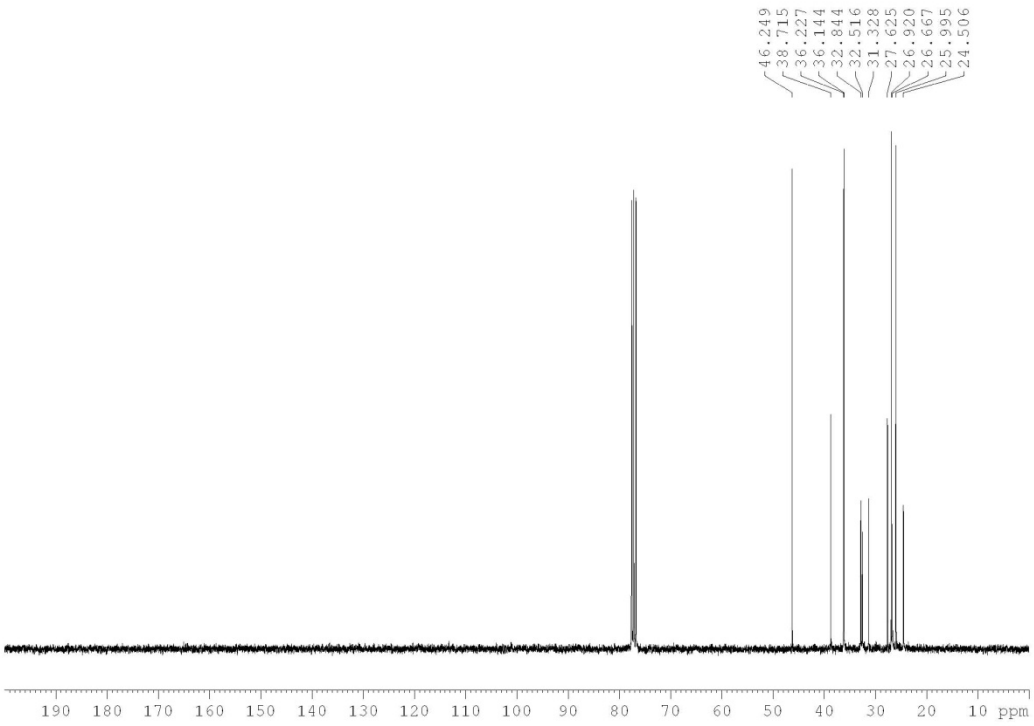

**Methyl ketone, 351**

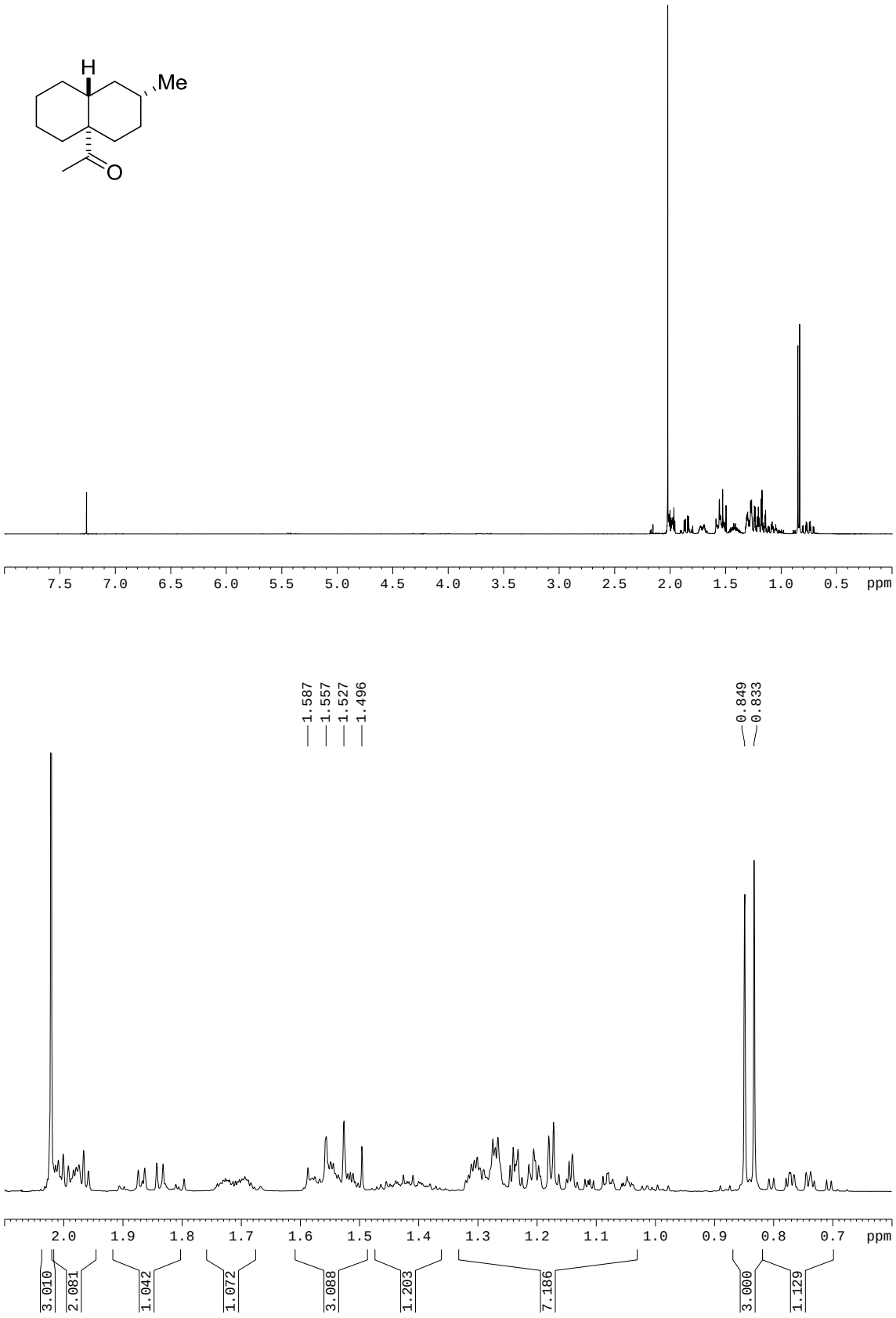

**Enol ether, 357, with isopropylcyclohexane**

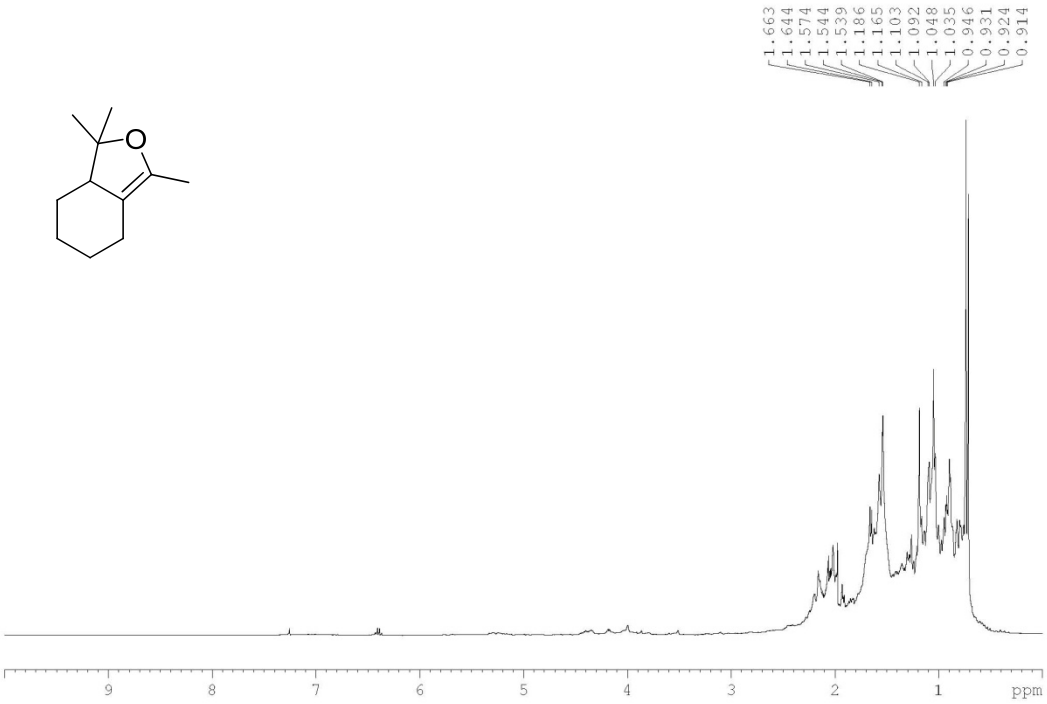


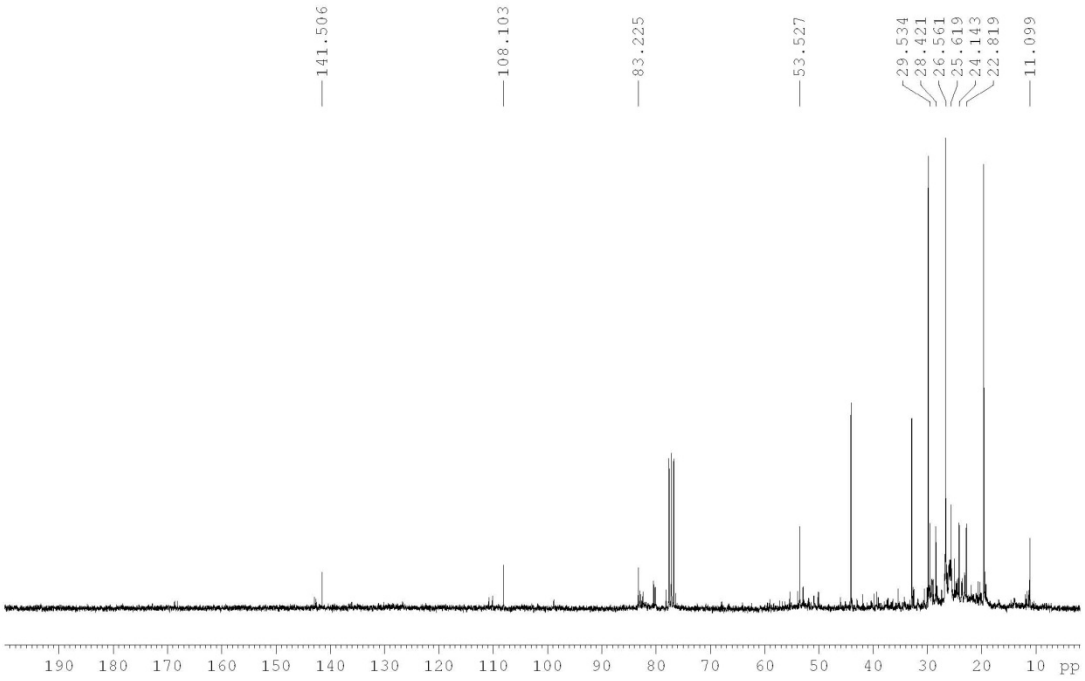

**Naphthalenediimide, 397**

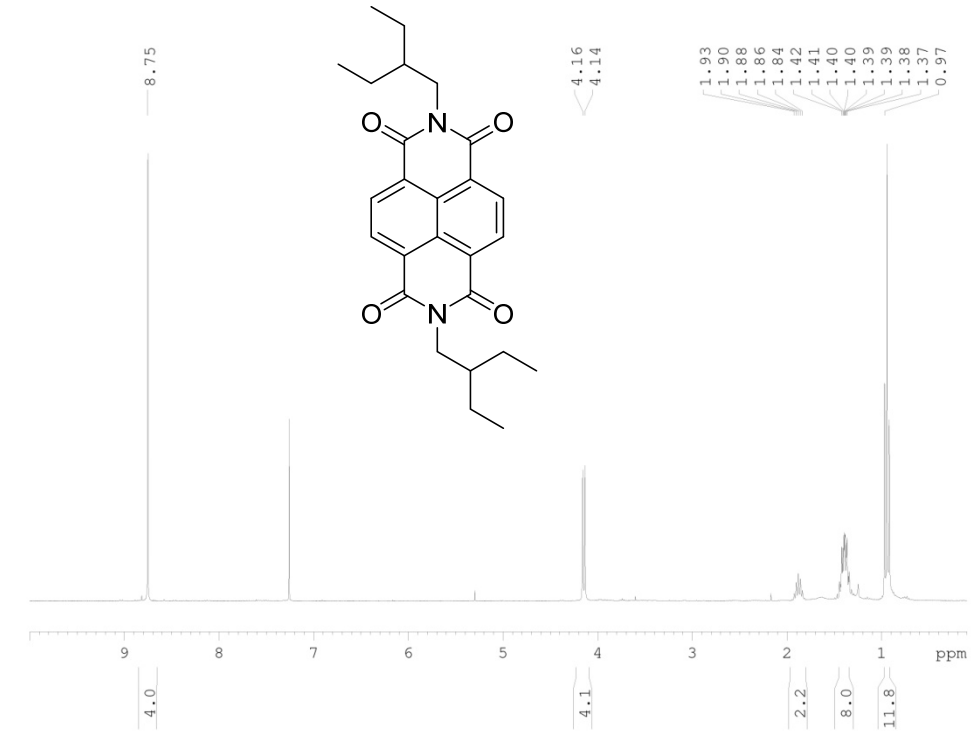


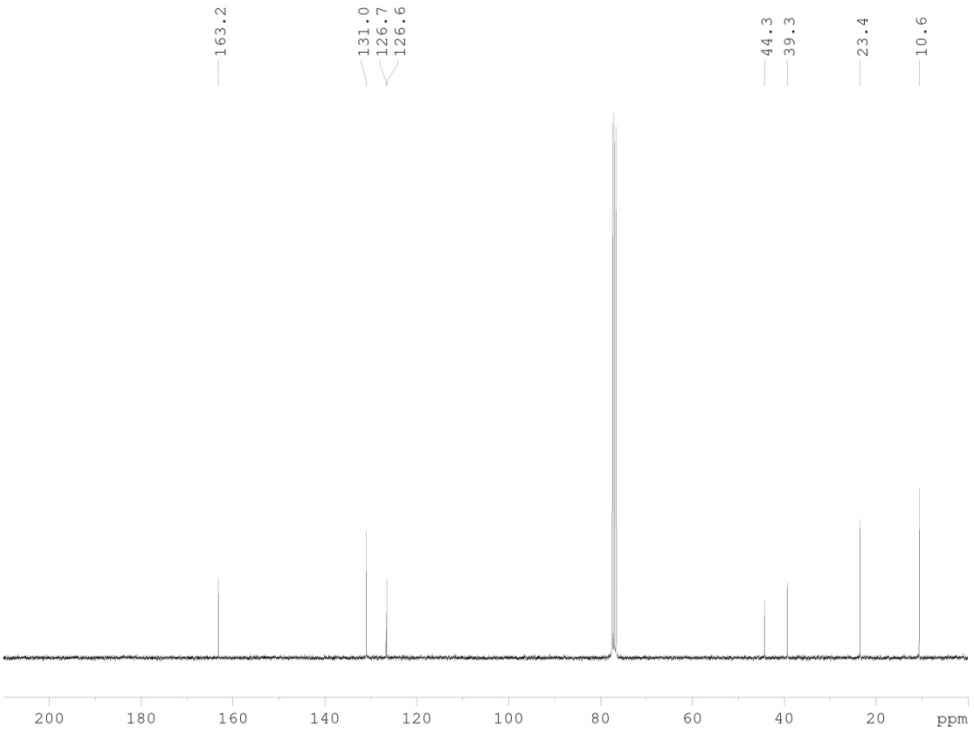

**Naphthalenediimide, 399**

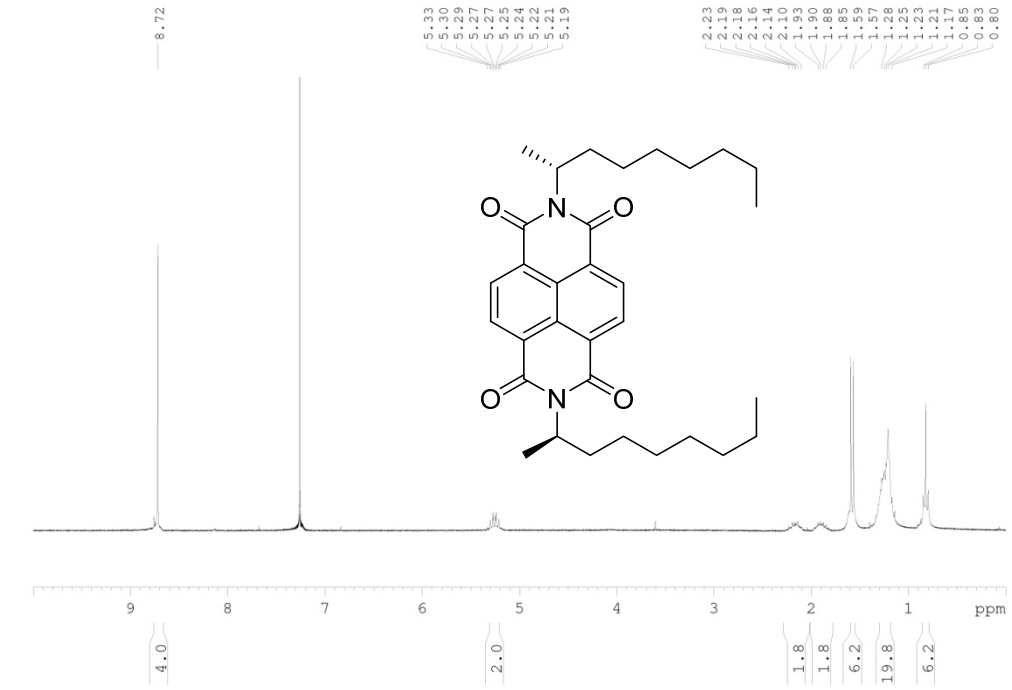


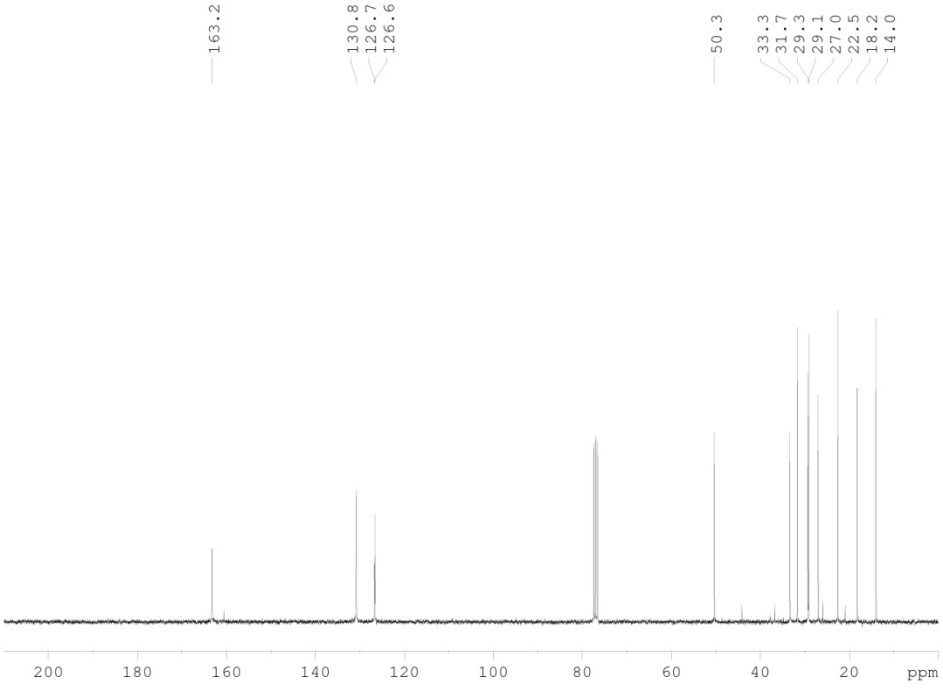

**Naphthalenediimide, 401**

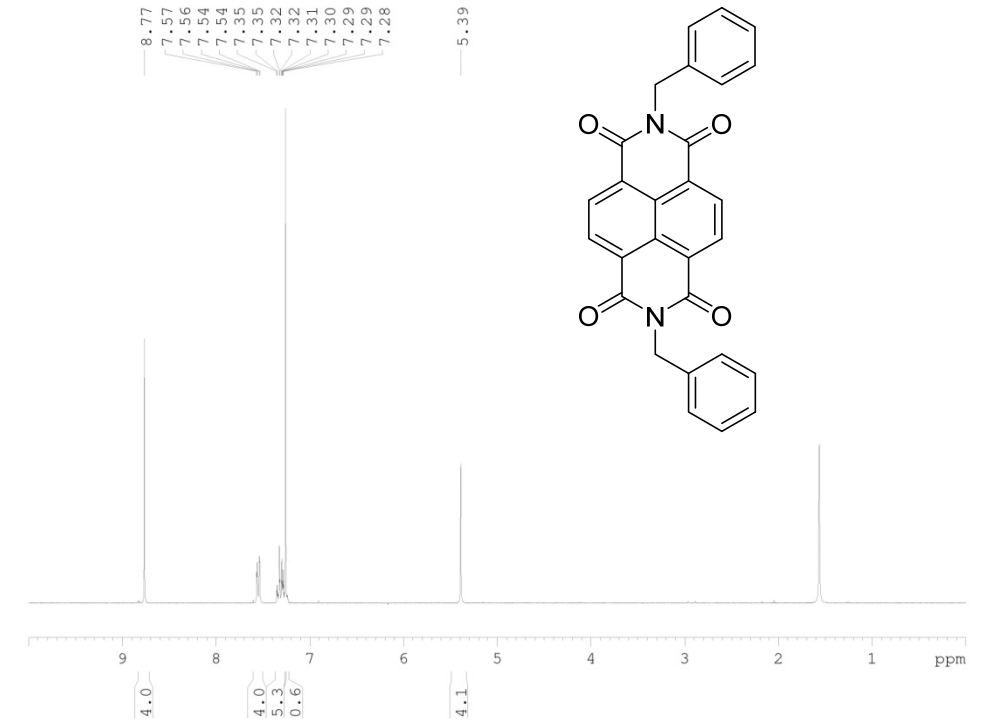


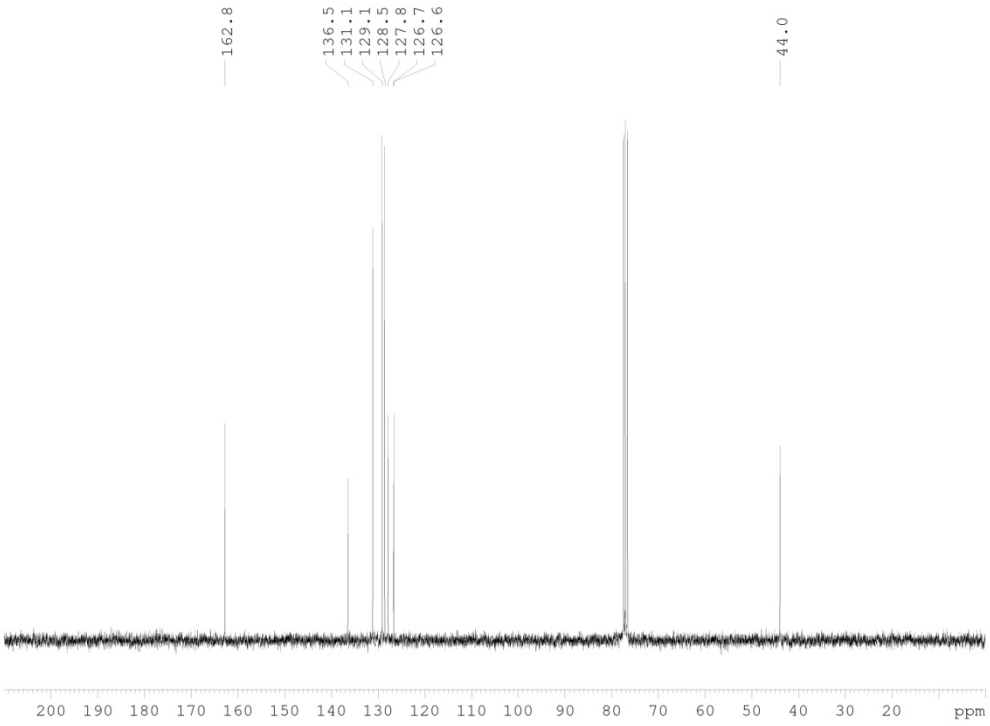

**Naphthalene monoimide, 402**

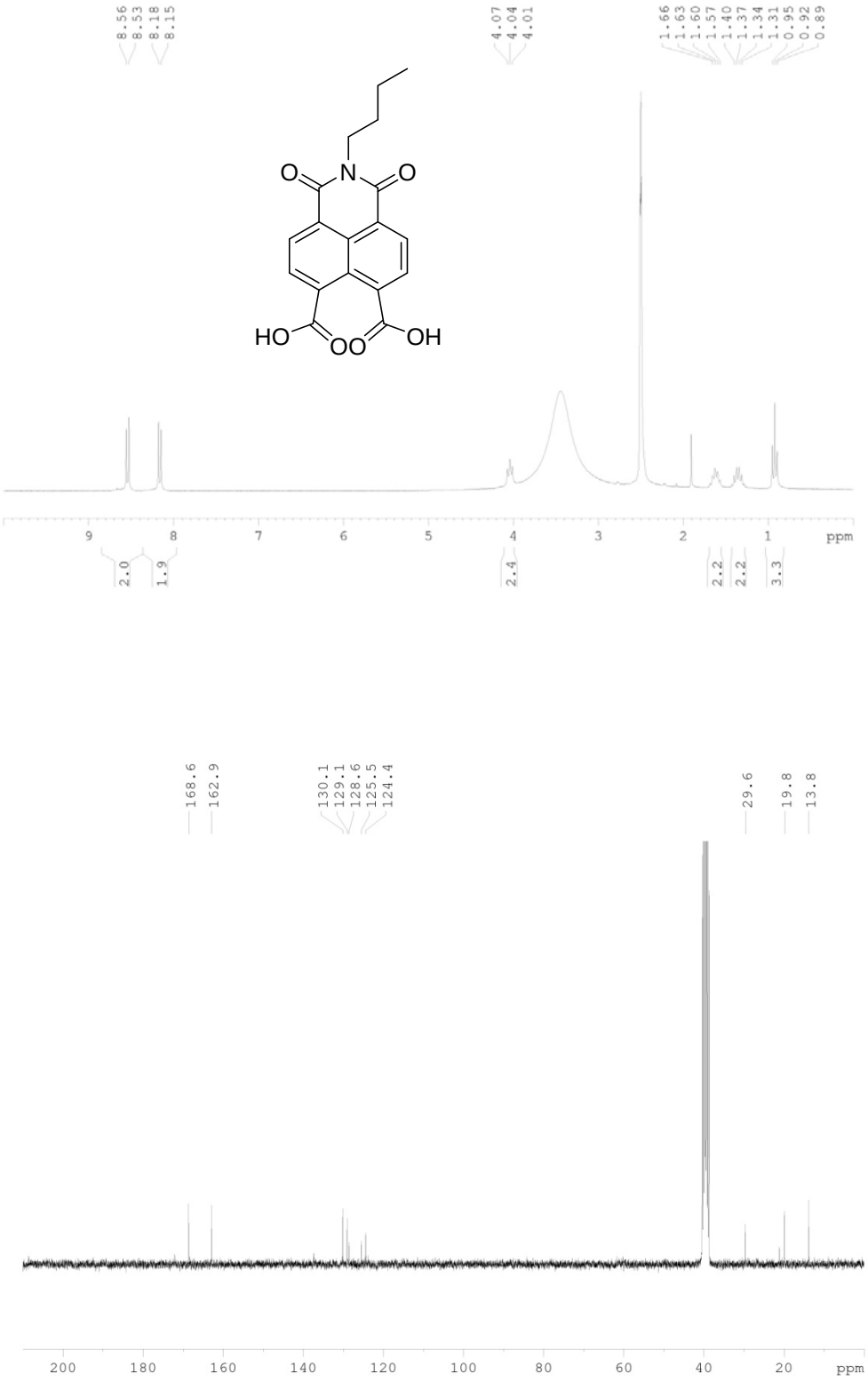

**Naphthalenediimide, 403**

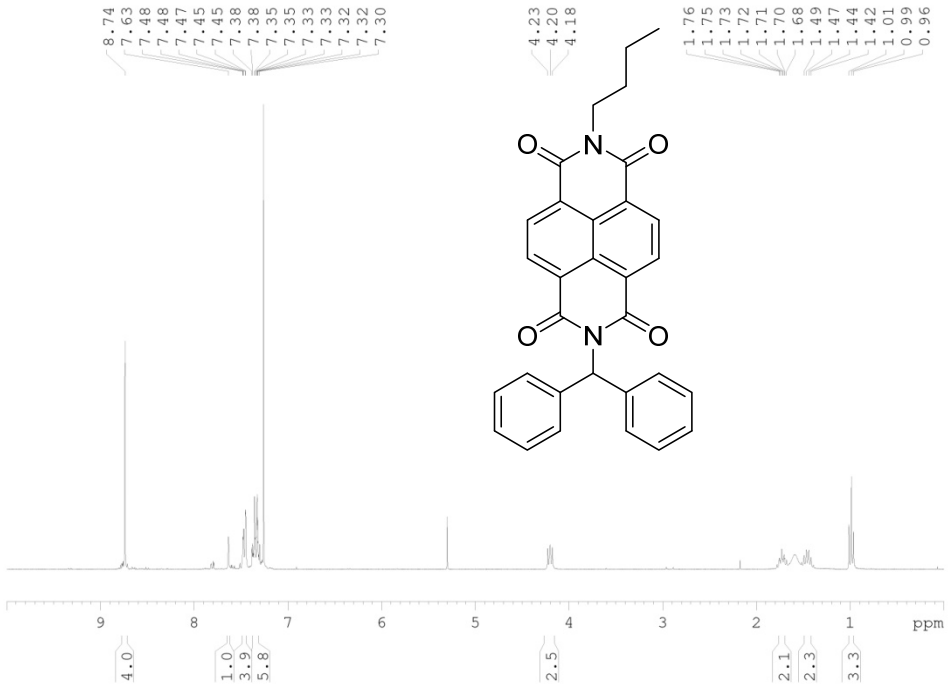


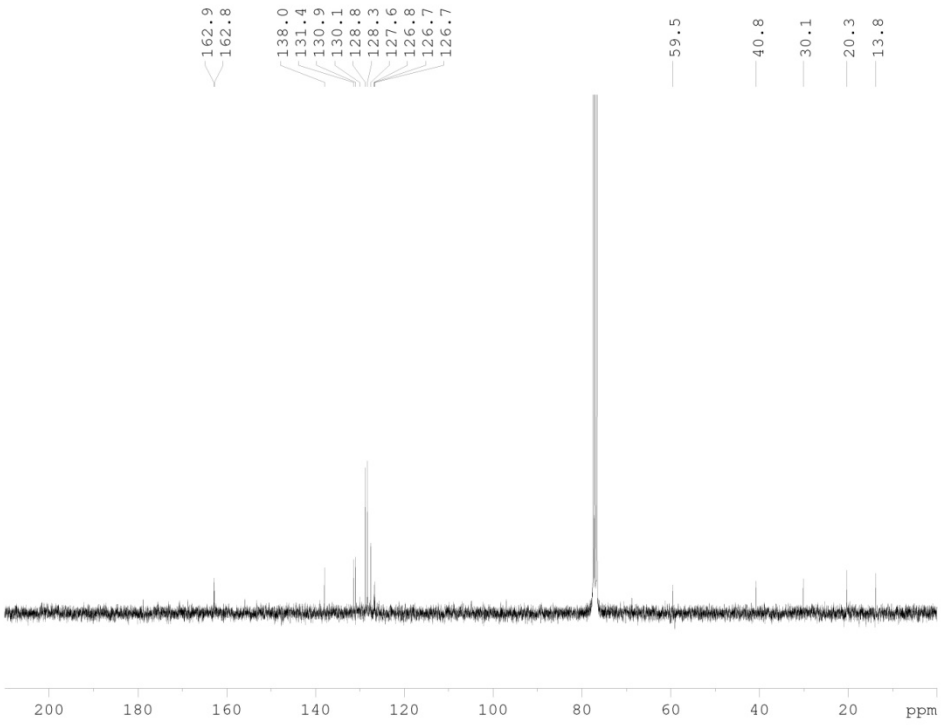

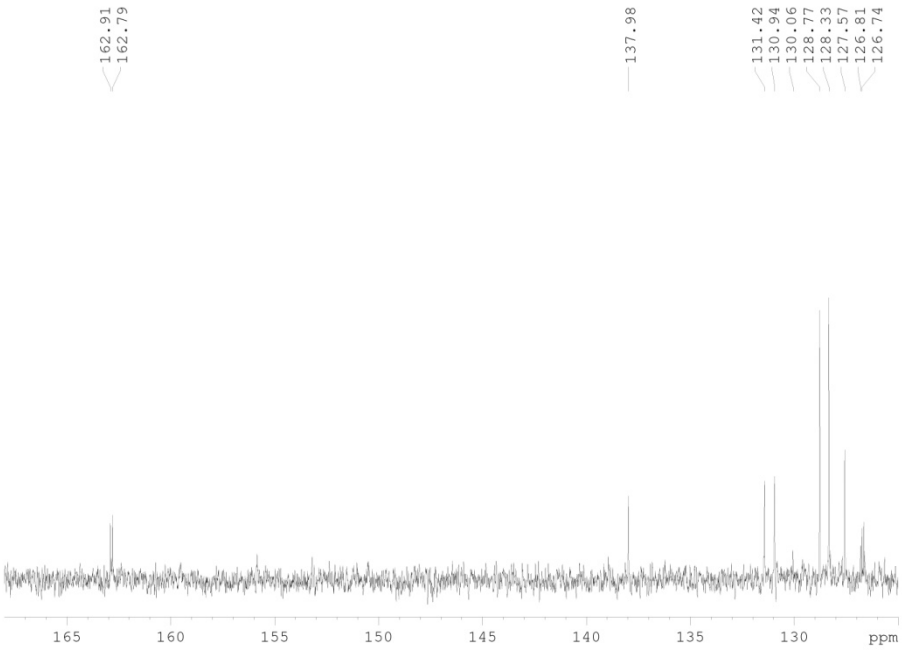


COSY (300 MHz, $CDCl_3$)

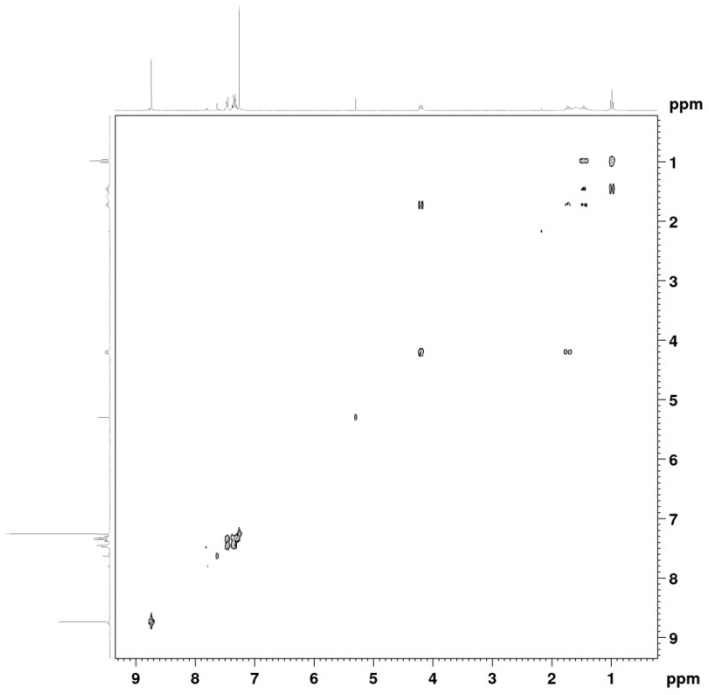

HSQC (300 MHz, $CDCl_3$)

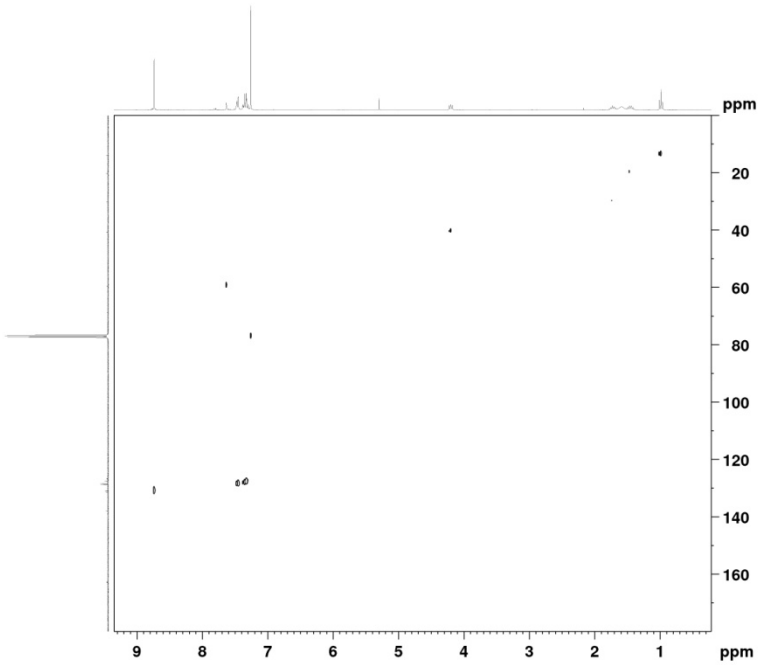


HMBC (300 MHz, $CDCl_3$)

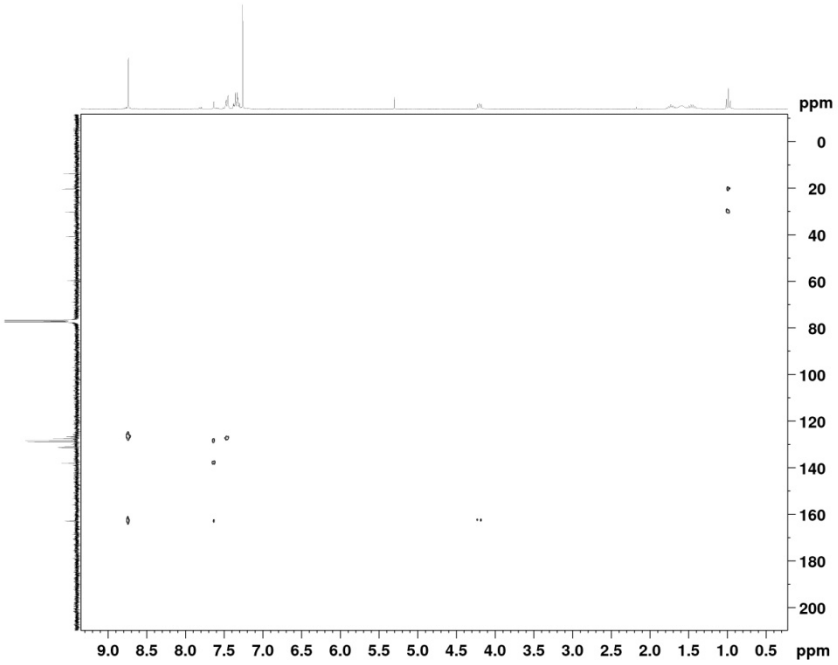

**Monoborylated NDI, 404**

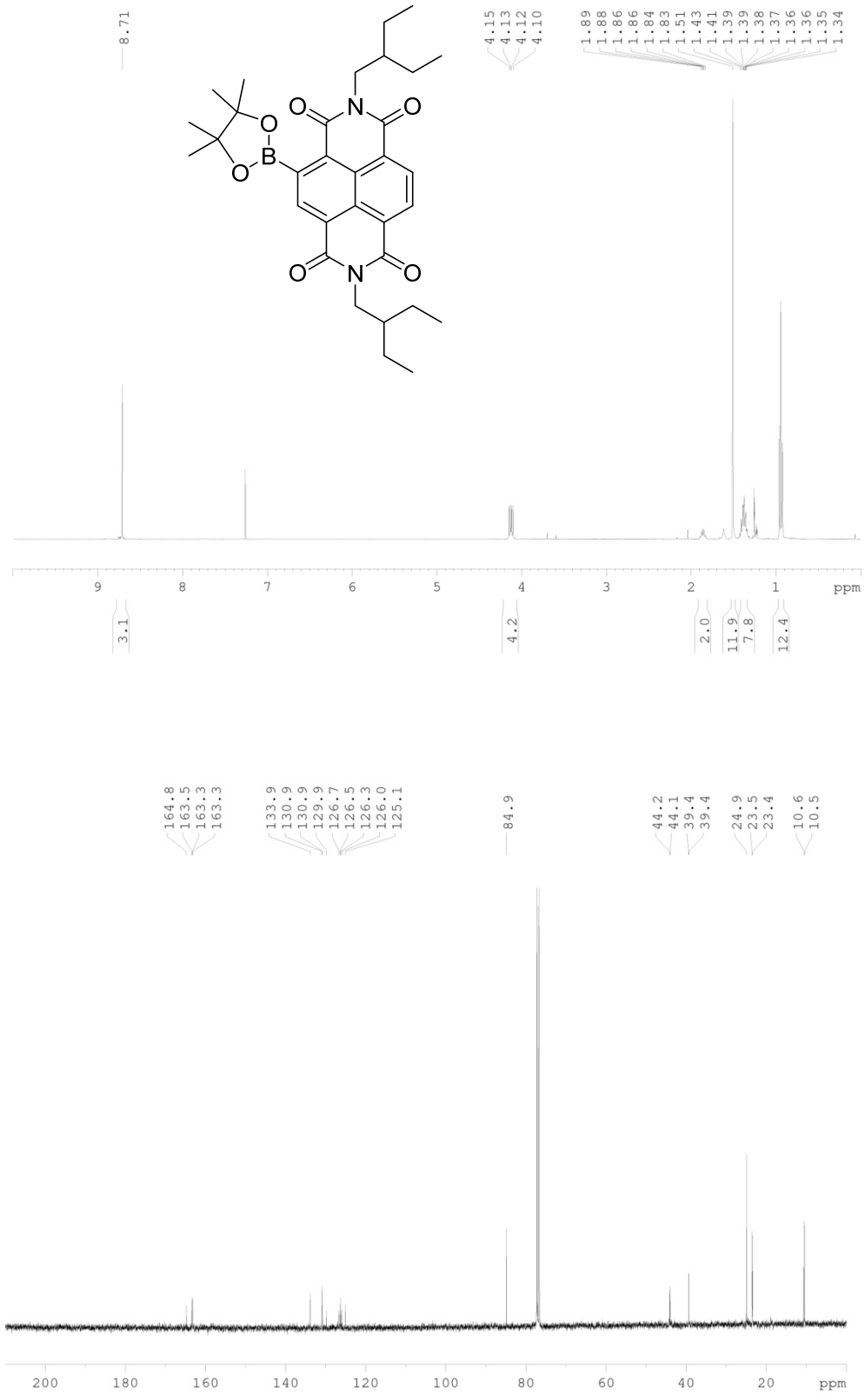

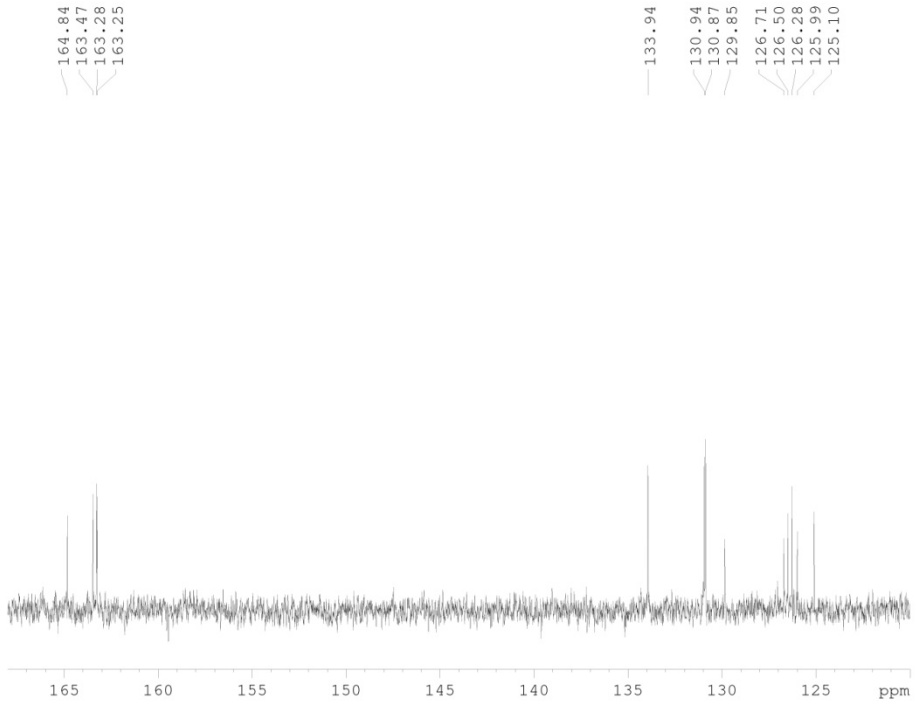


HMBC (500 MHz, $CDCl_3$)

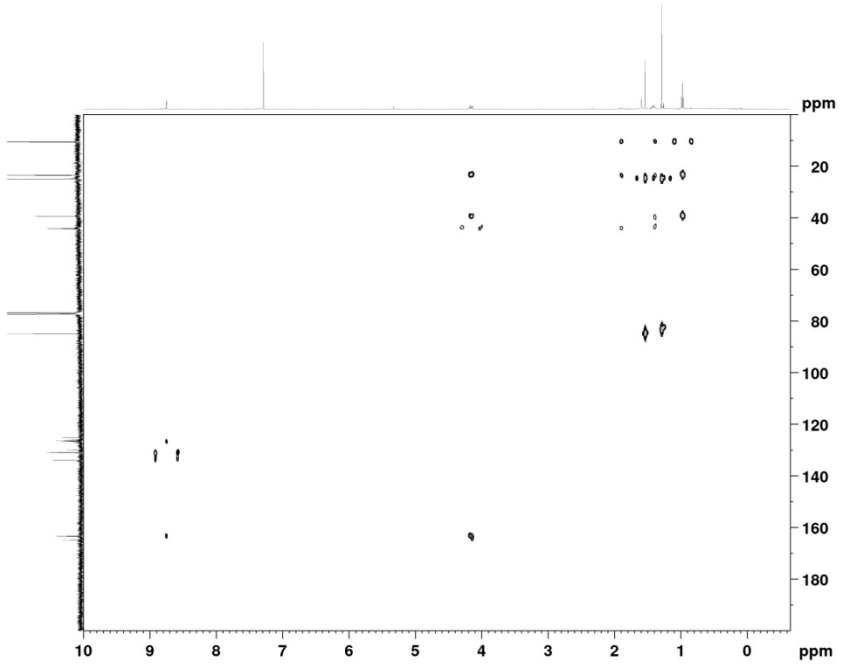

**Diborylated NDIs, 405 and 406**


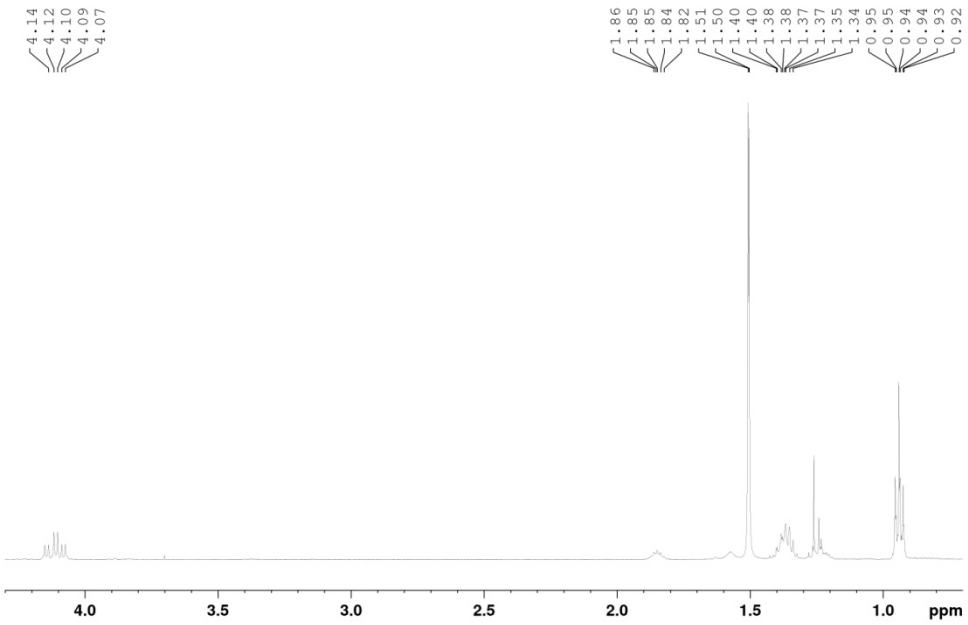

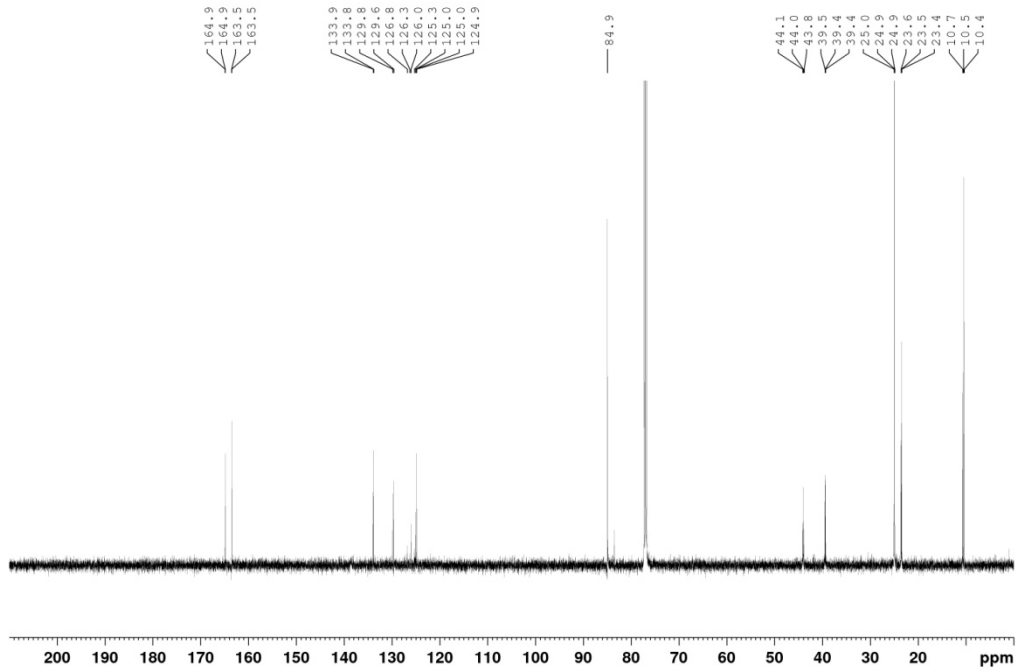
164.9
164.9
163.5
163.5
133.9
133.8
129.8
129.6
126.8
126.3
126.0
125.3
125.0
125.0
124.9
84.9
44.1
44.0
43.8
39.5
39.4
39.4
25.0
24.9
24.9
23.6
23.5
23.4
10.7
10.5
10.4
200 190 180 170 160 150 140 130 120 110 100 90 80 70 60 50 40 30 20 ppm

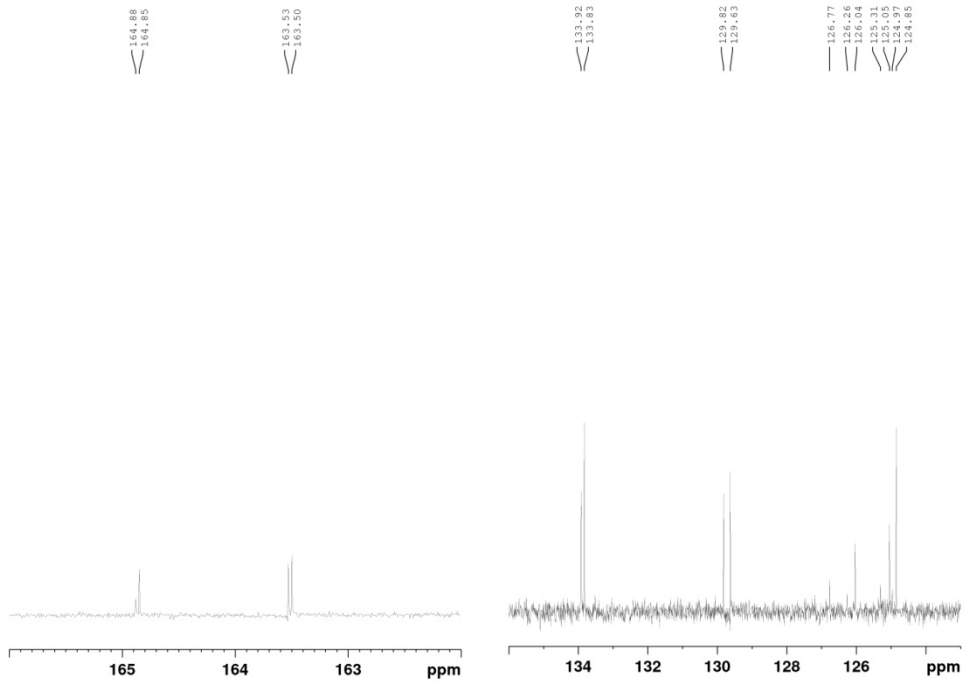
164.88
164.85
163.53
163.50
133.92
133.83
129.82
129.63
126.77
126.26
126.04
125.31
125.05
124.97
124.85
165 164 163 ppm
134 132 130 128 126 ppm

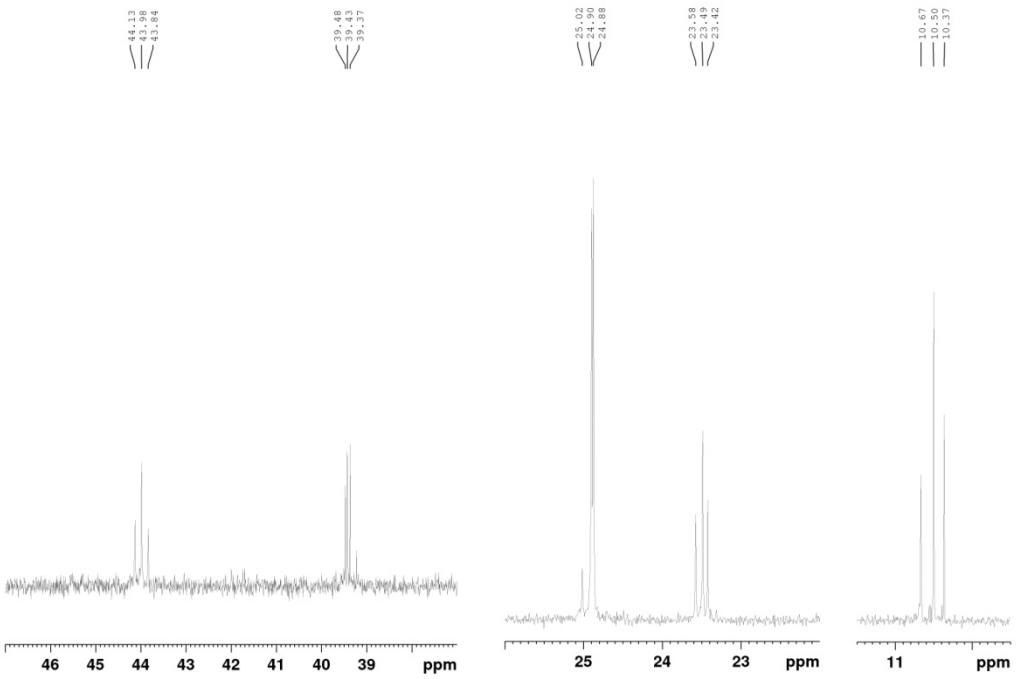


NOESY (500 MHz, $CDCl_3$ – nOe peaks in red)

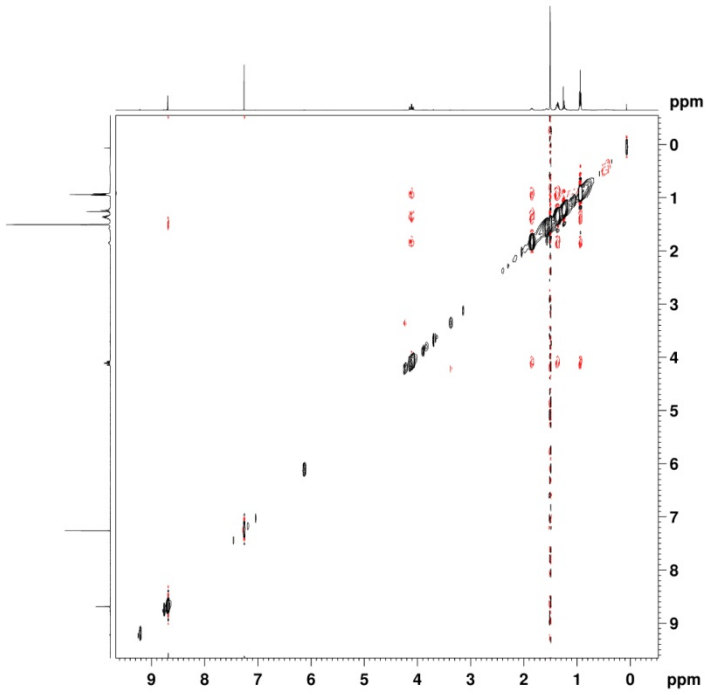

COSY (500 MHz, $CDCl_3$)

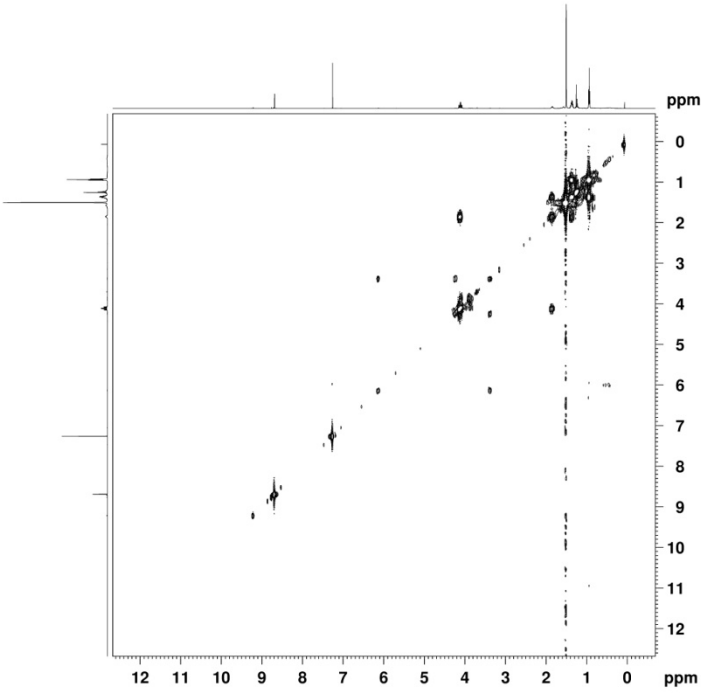

**Monoborylated NDI, 407**

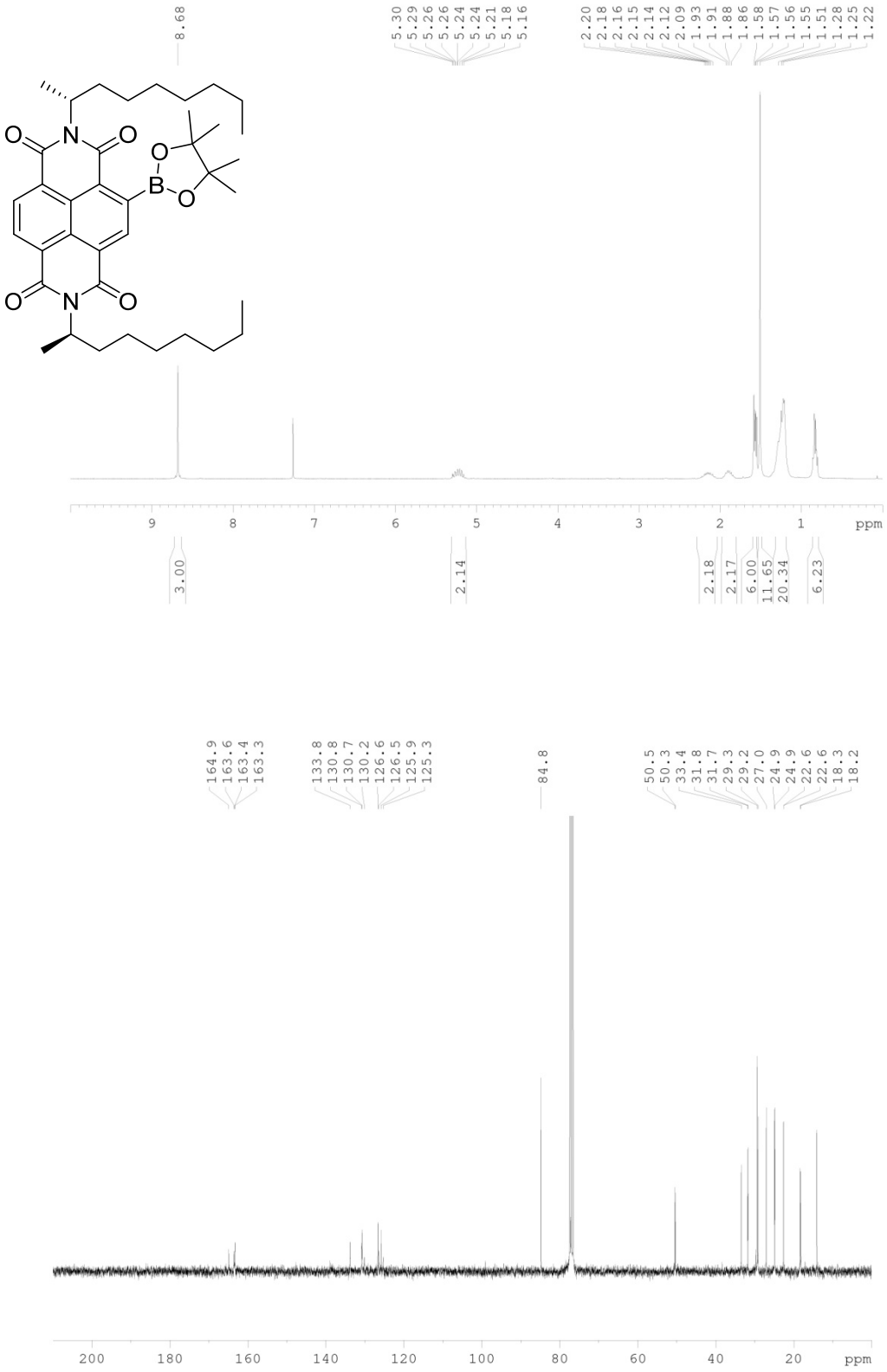

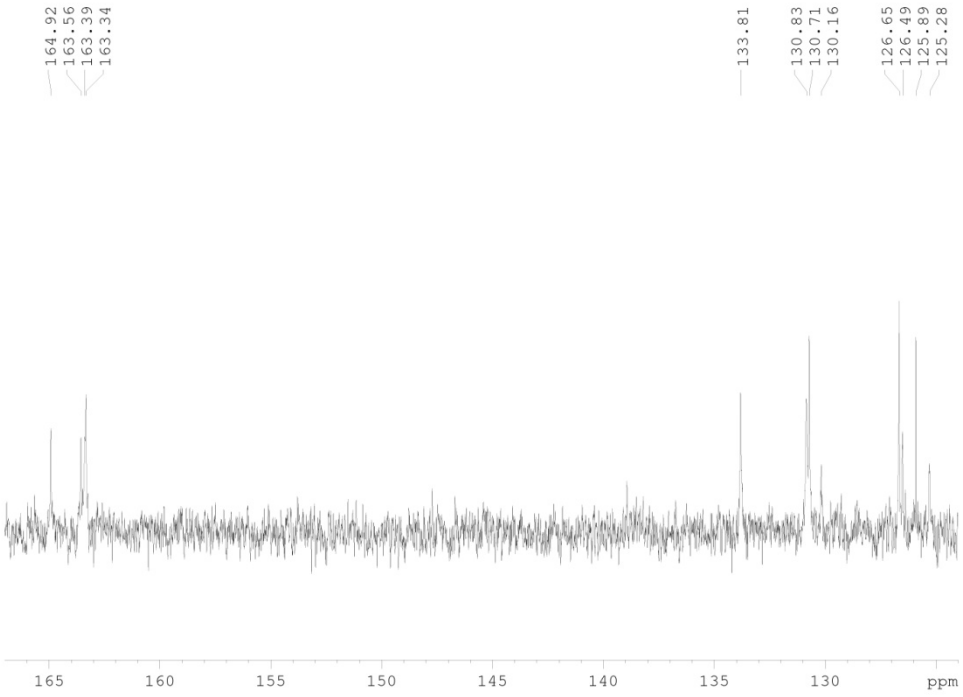
164.92
163.56
163.39
163.34
133.81
130.83
130.71
130.16
126.65
126.49
125.89
125.28
165
160
155
150
145
140
135
130
ppm

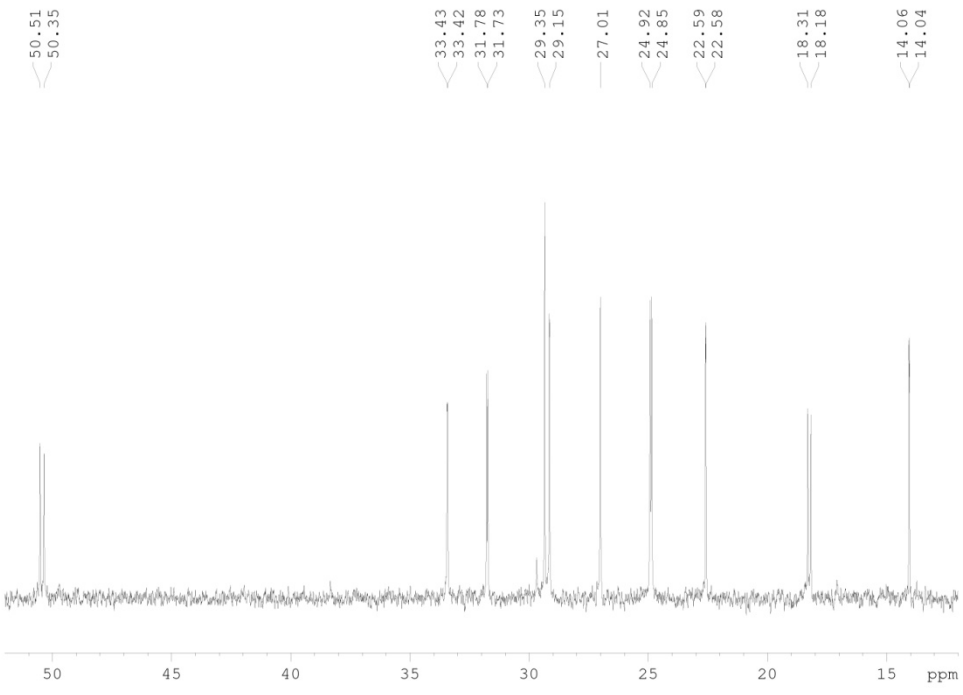
50.51
50.35
33.43
33.42
31.78
31.73
29.35
29.15
27.01
24.92
24.85
22.59
22.58
18.31
18.18
14.06
14.04
50
45
40
35
30
25
20
15
ppm

COSY (300 MHz, $CDCl_3$)

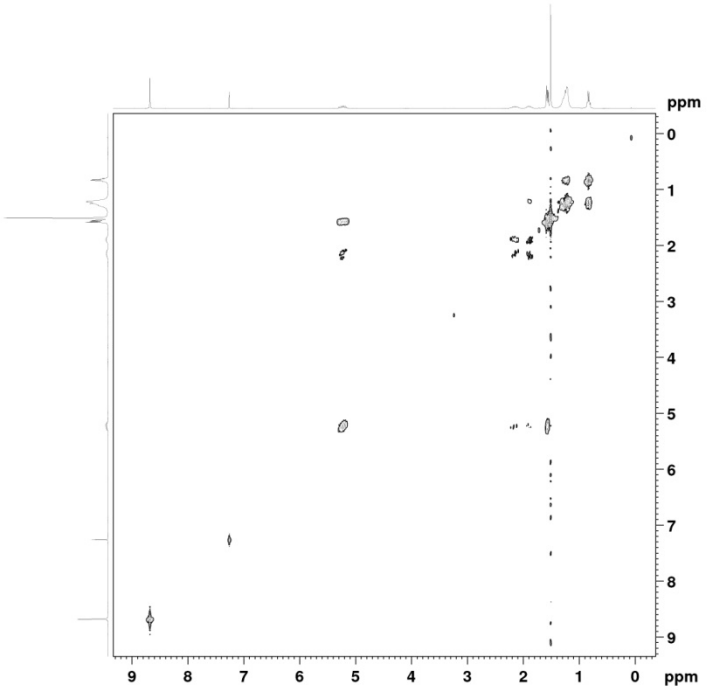


HSQC (300 MHz, $CDCl_3$)

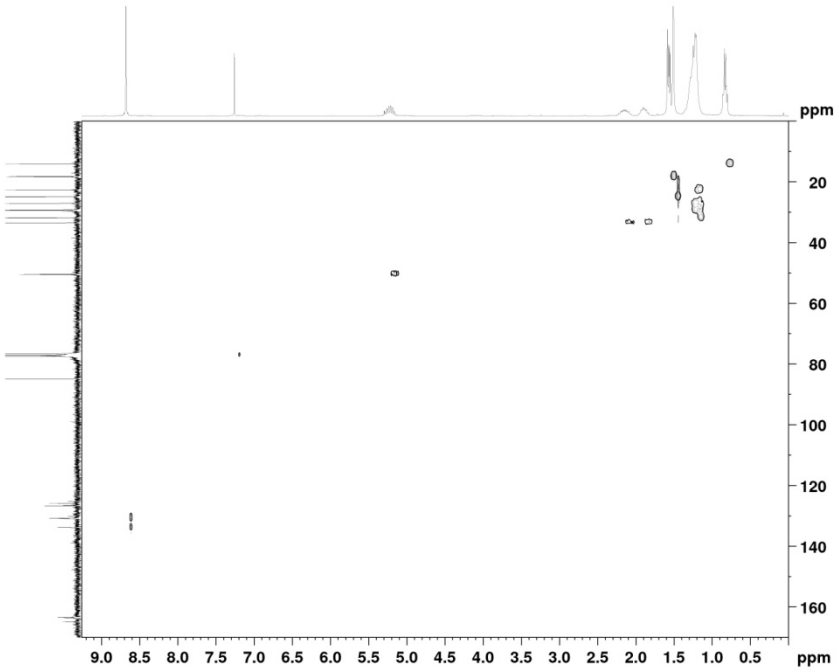

HMBC (300 MHz, $CDCl_3$)

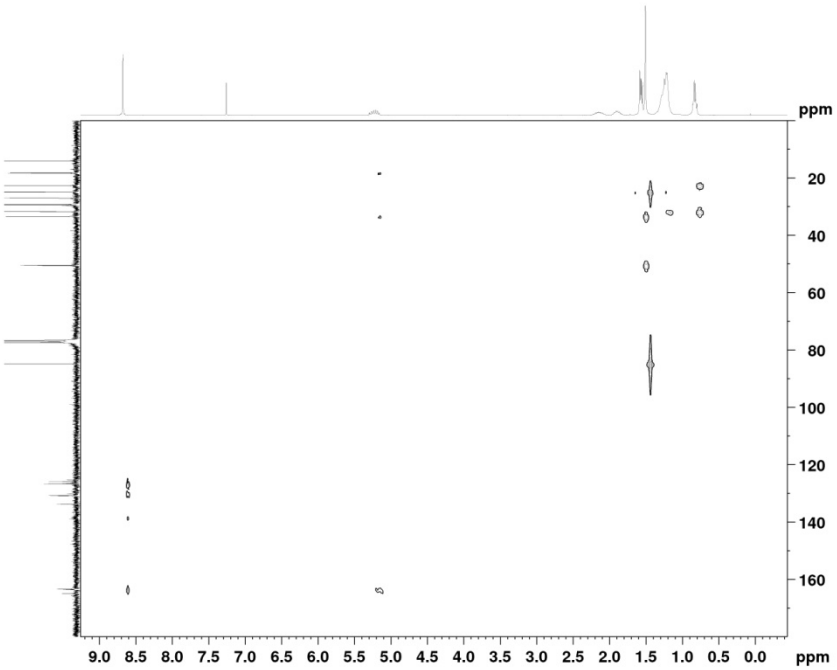

**Diborylated NDIs, 408 and 409**

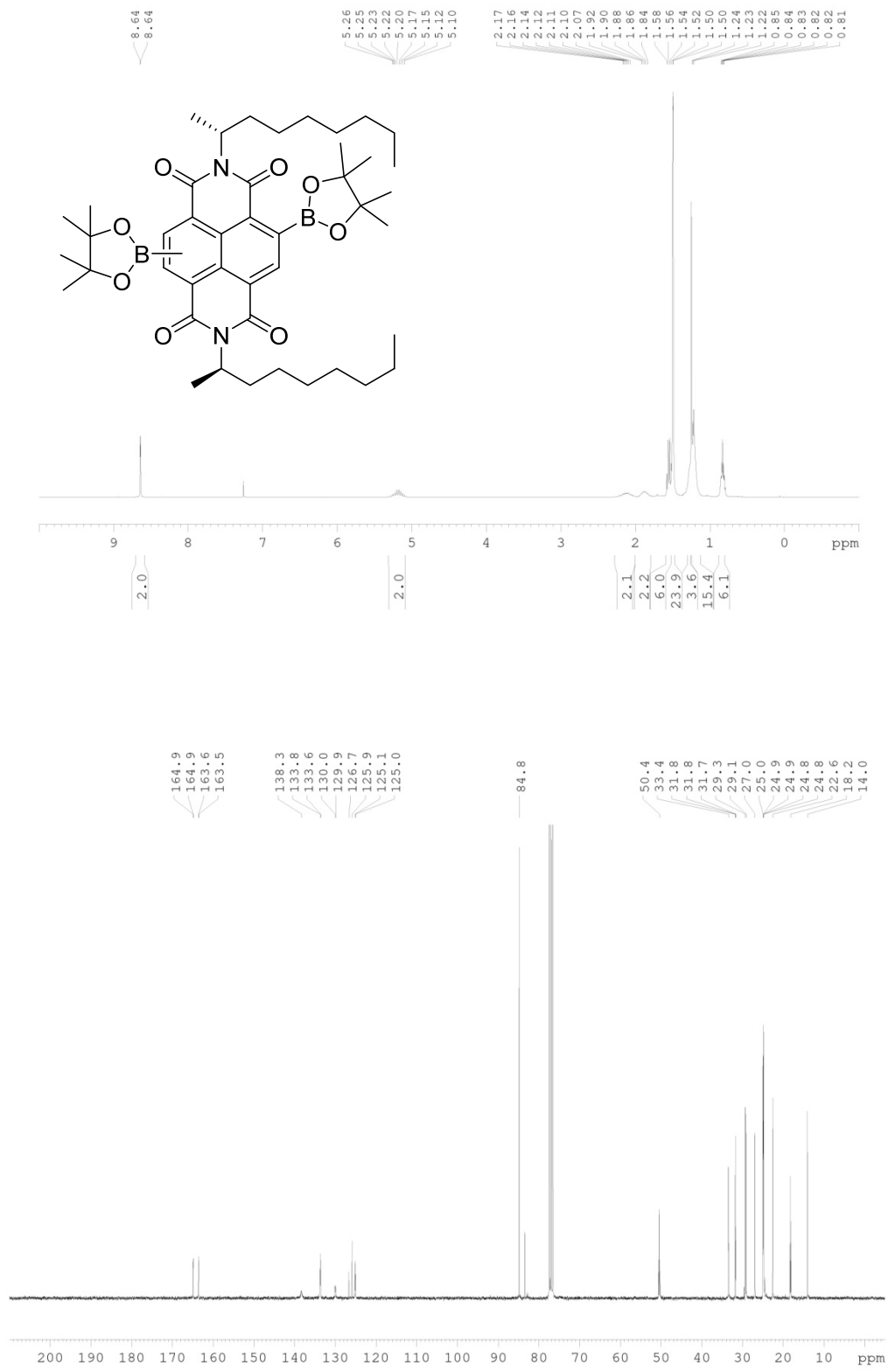

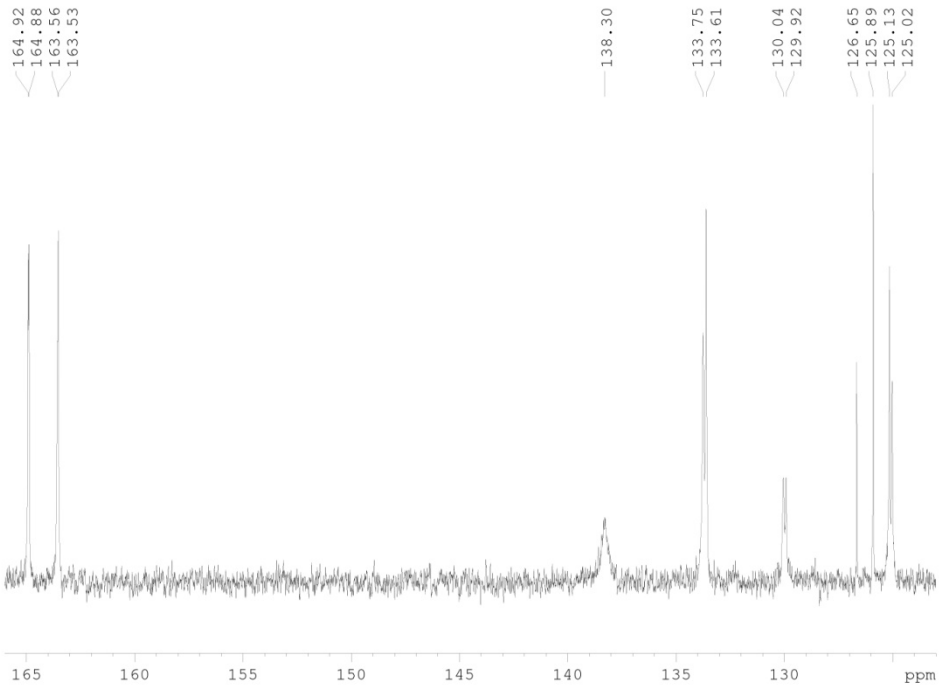
164.92
164.88
163.56
163.53
138.30
133.75
133.61
130.04
129.92
126.65
125.89
125.13
125.02
165
160
155
150
145
140
135
130
ppm

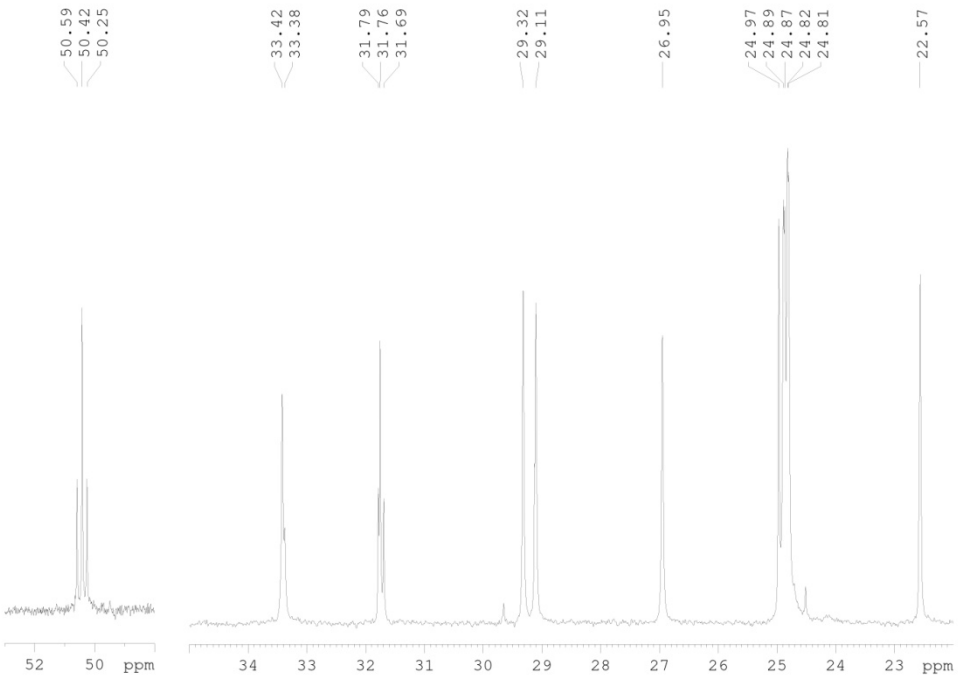
50.59
50.42
50.25
33.42
33.38
31.79
31.76
31.69
29.32
29.11
26.95
24.97
24.89
24.87
24.82
24.81
22.57
52
50
ppm
34
33
32
31
30
29
28
27
26
25
24
23
ppm

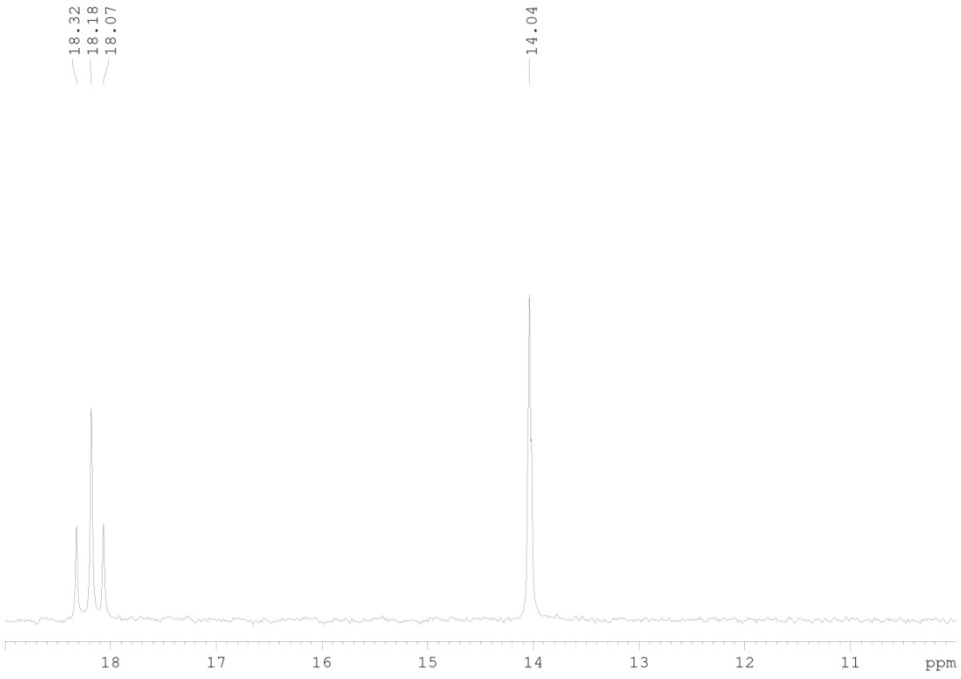


HSQC (300 MHz, $CDCl_3$)

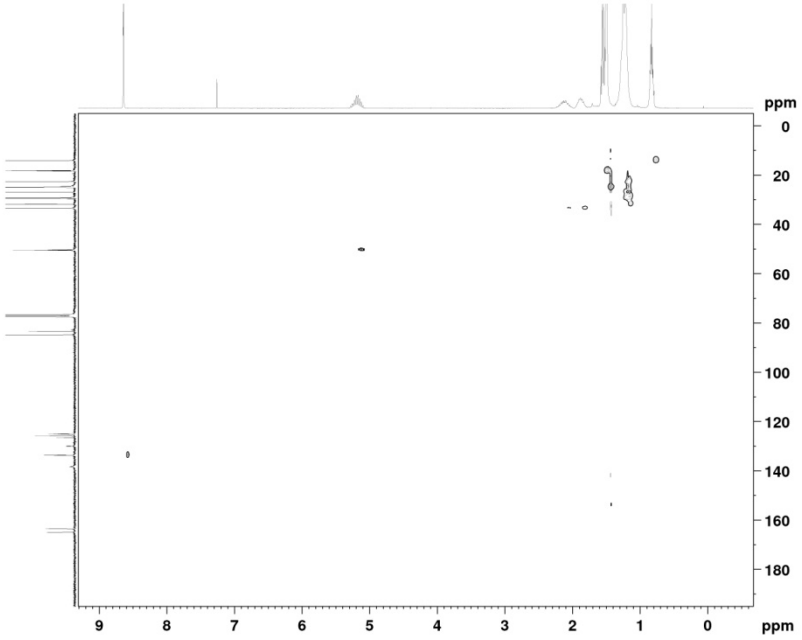

HMBC (300 MHz, $CDCl_3$)

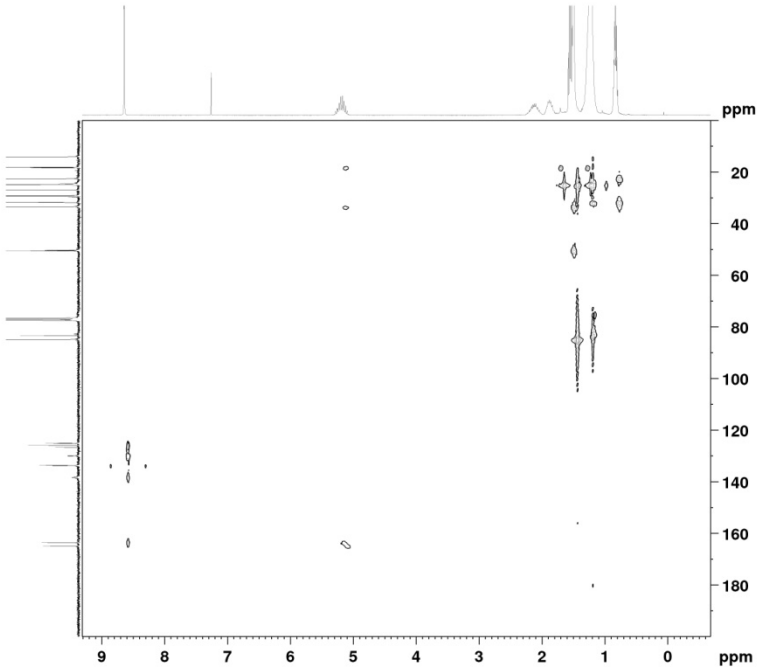

**Monoborylated NDI, 410**

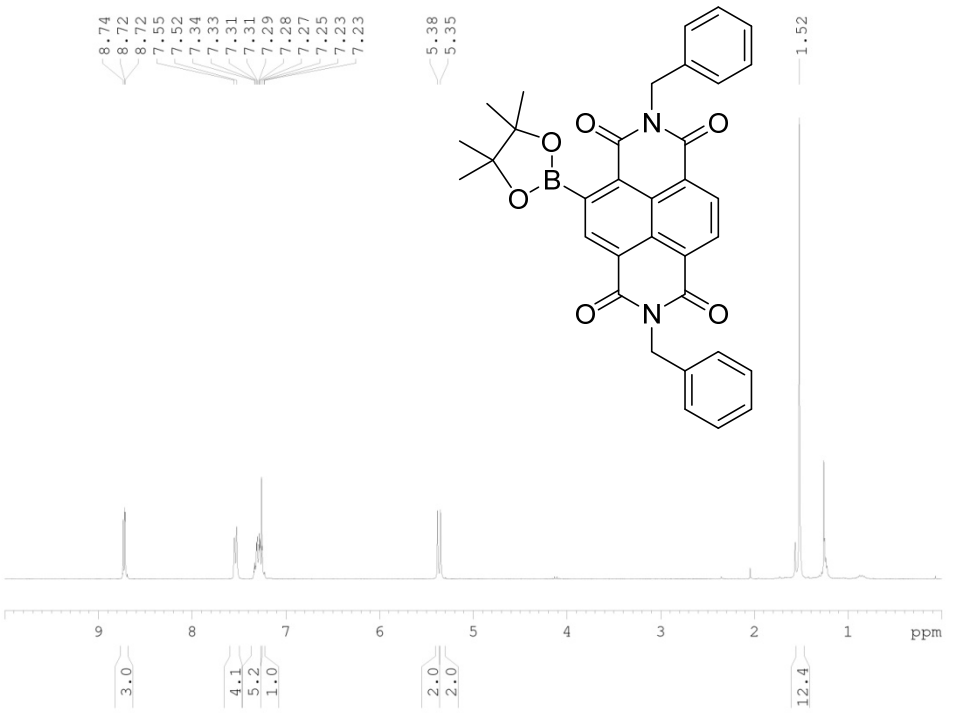


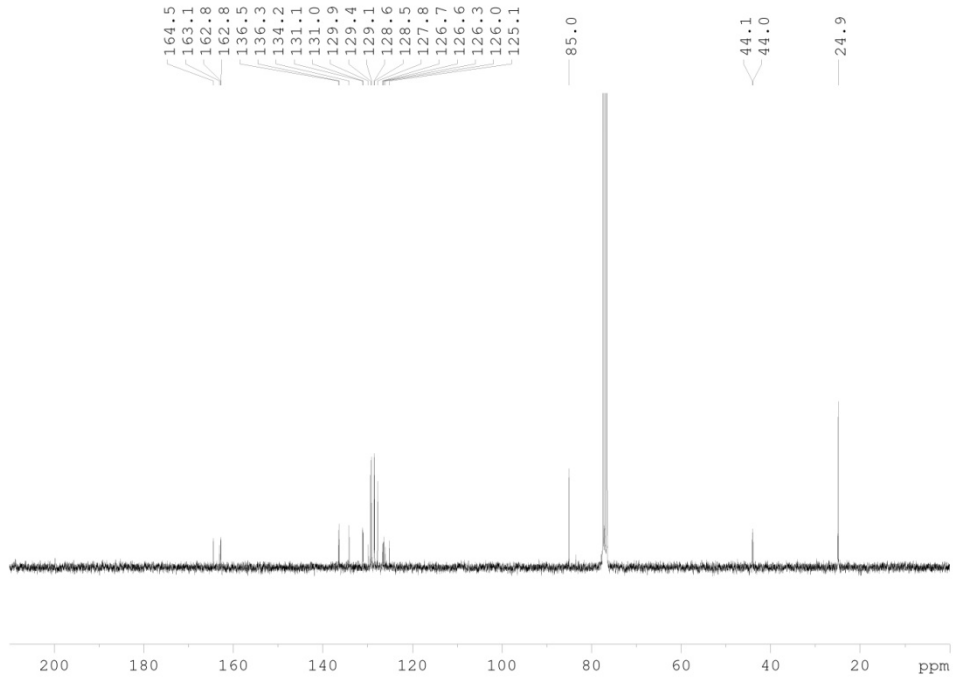

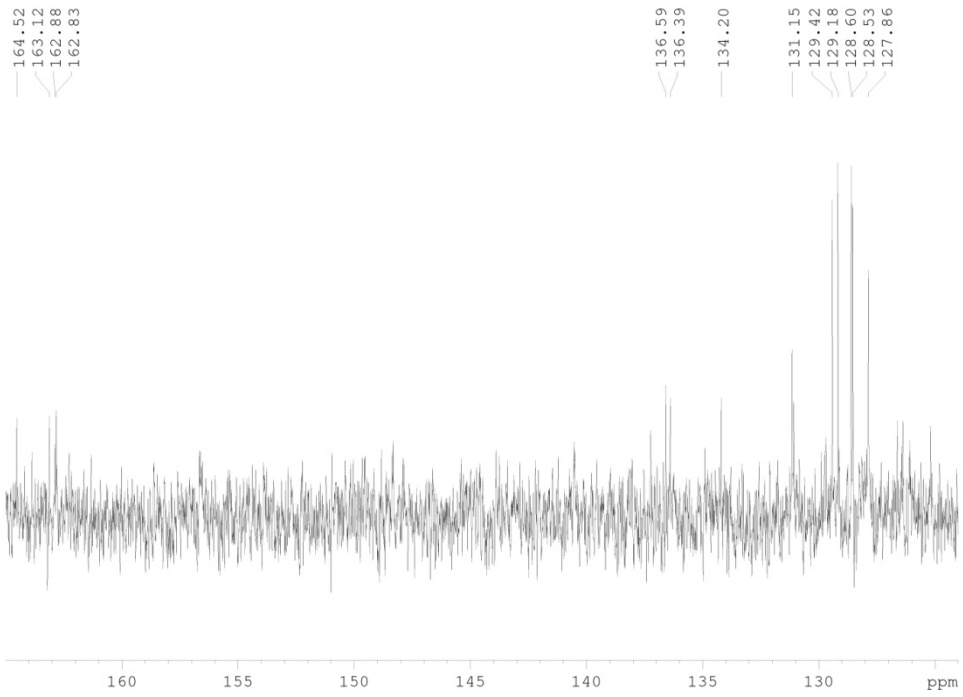


COSY (300 MHz, $CDCl_3$)

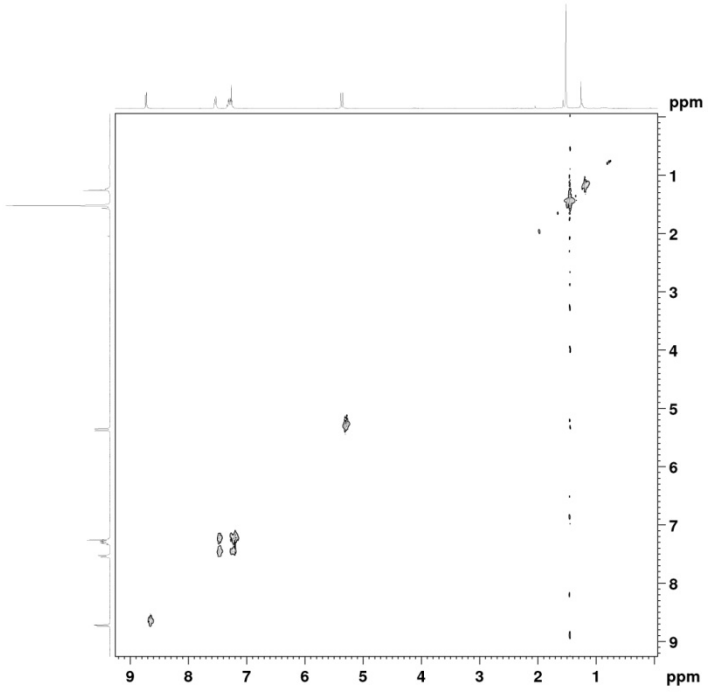

HSQC (300 MHz, $CDCl_3$)

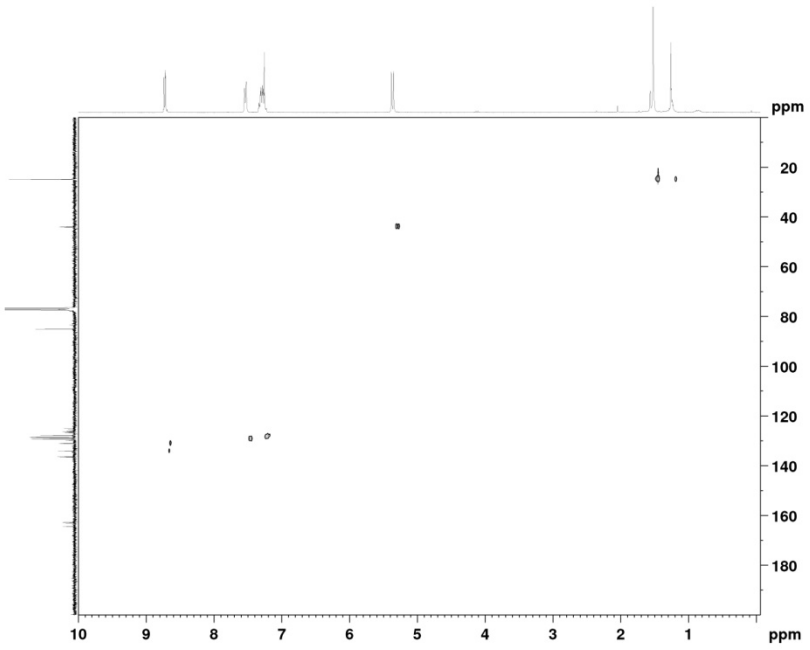


HMBC (300 MHz, $CDCl_3$)

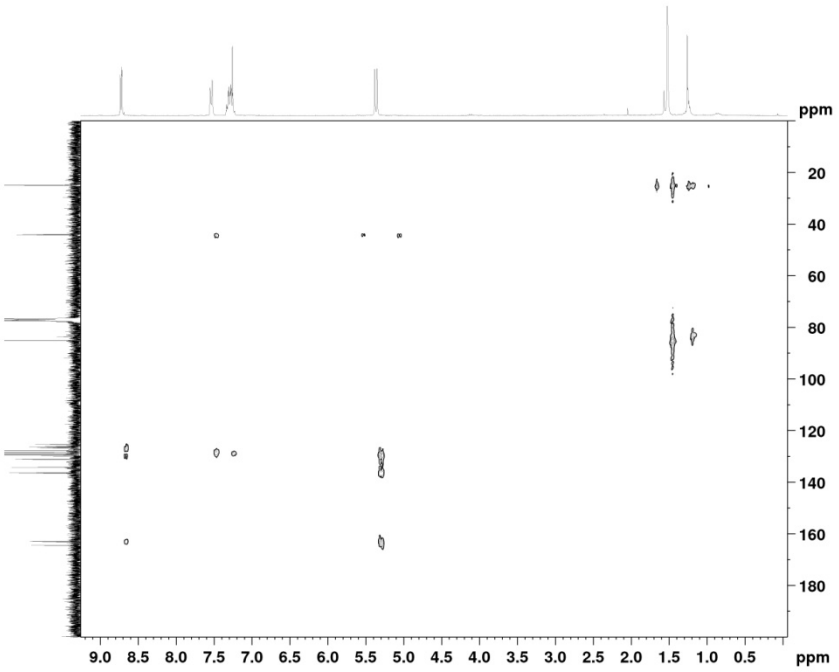

**Diborylated NDIs, 411 and 412**

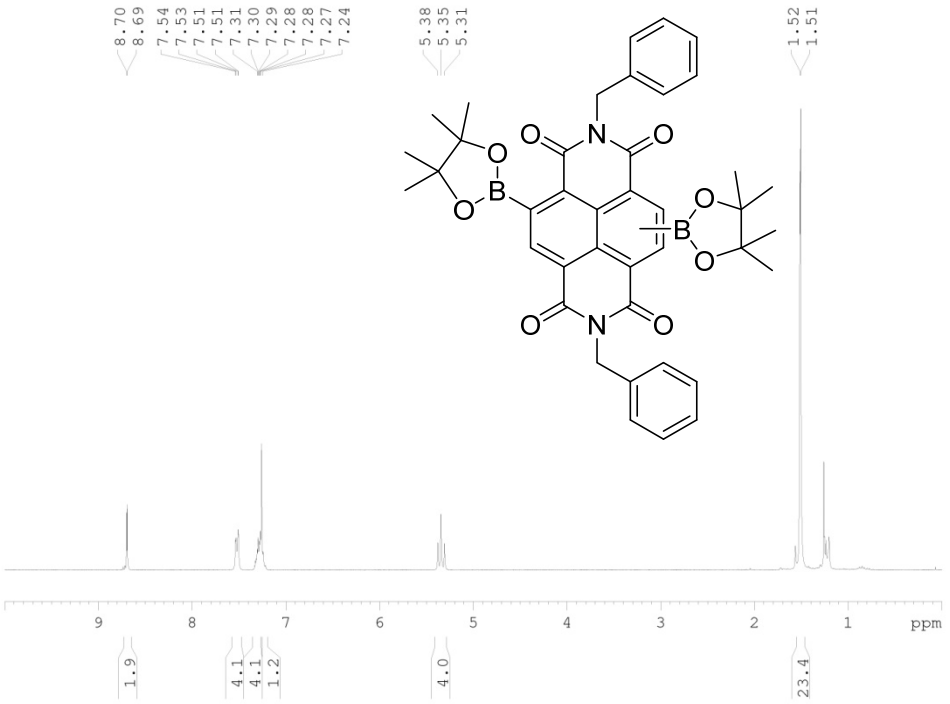


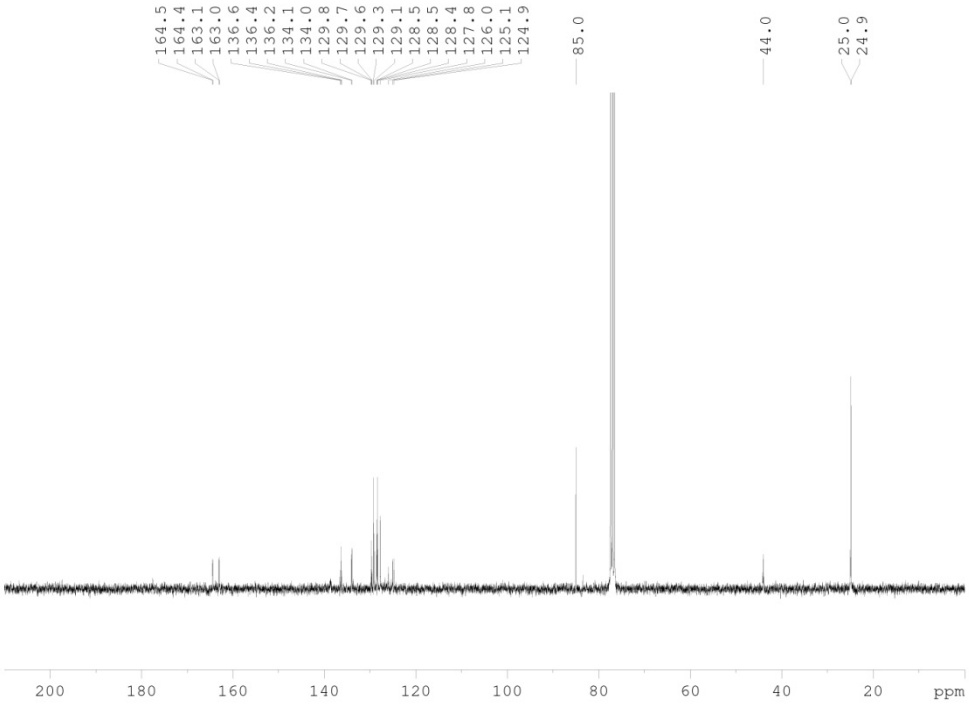

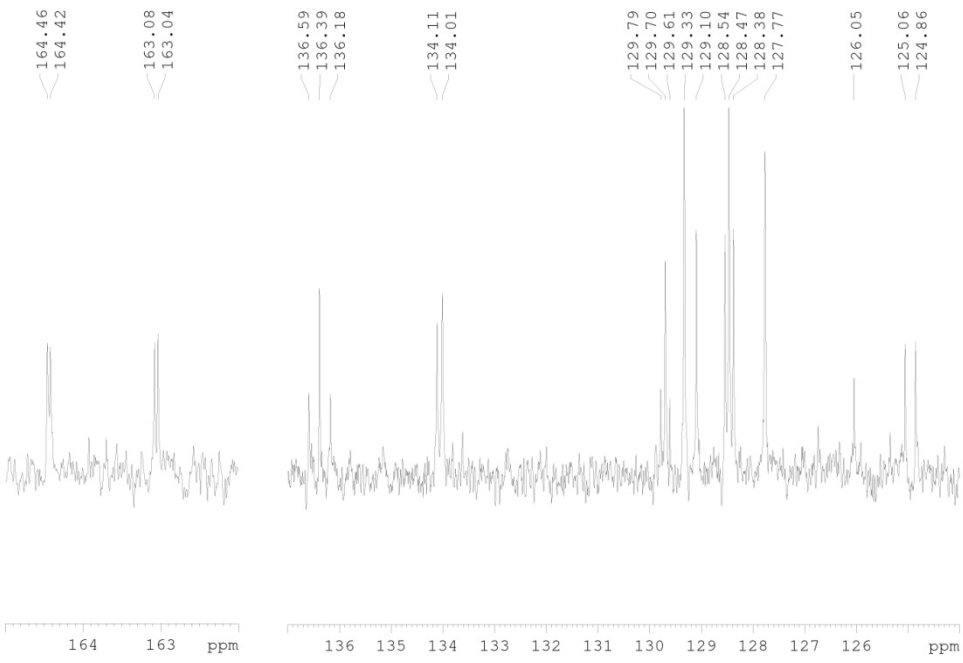
164.46
164.42
163.08
163.04
136.59
136.39
136.18
134.11
134.01
129.79
129.70
129.61
129.33
129.10
128.54
128.47
128.38
127.77
126.05
125.06
124.86
164
163
ppm
136
135
134
133
132
131
130
129
128
127
126
ppm

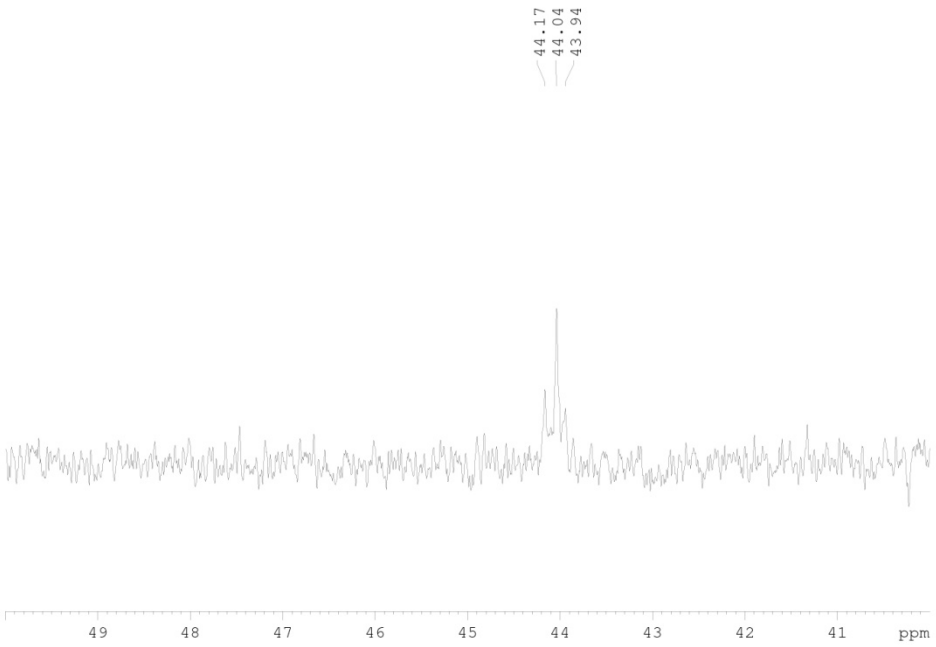
44.17
44.04
43.94
49
48
47
46
45
44
43
42
41
ppm

COSY (300 MHz, $CDCl_3$)

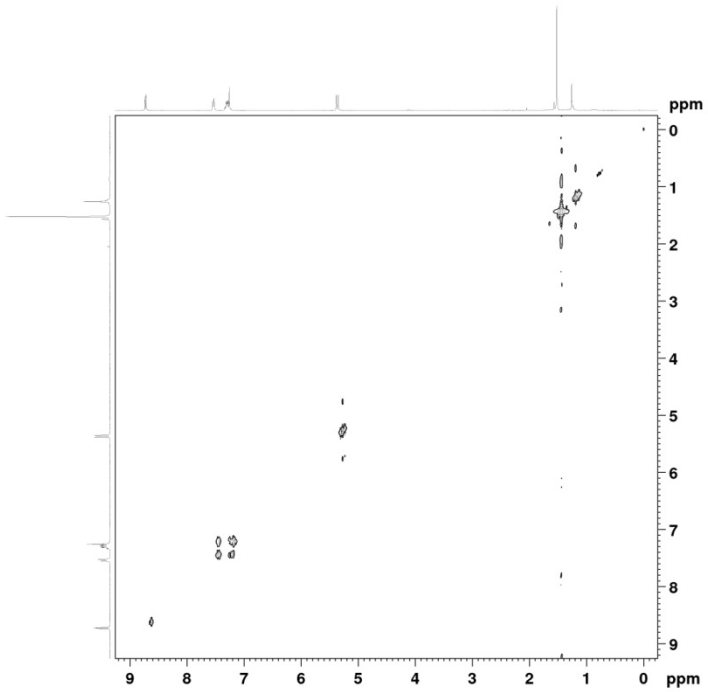


HSQC (300 MHz, $CDCl_3$)

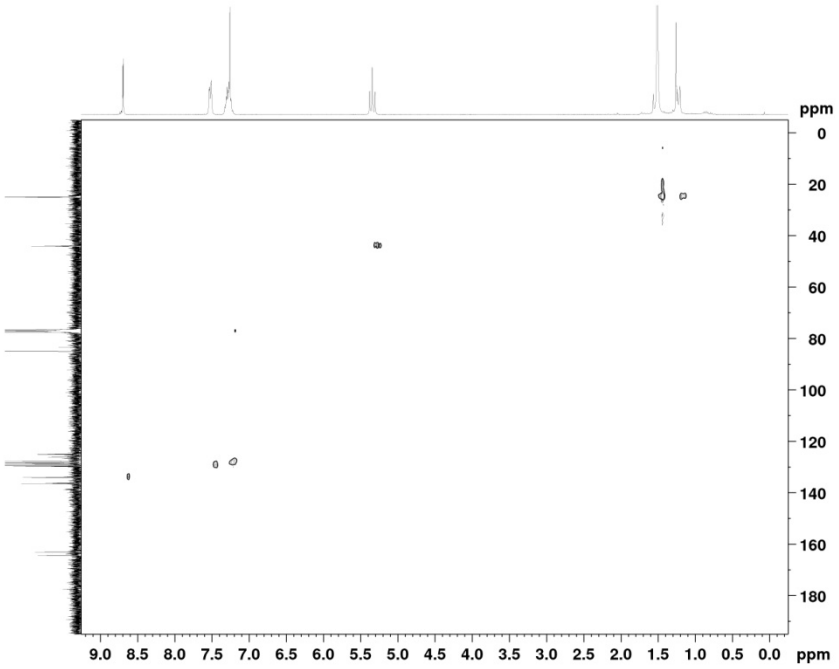

HMBC (300 MHz, $CDCl_3$)

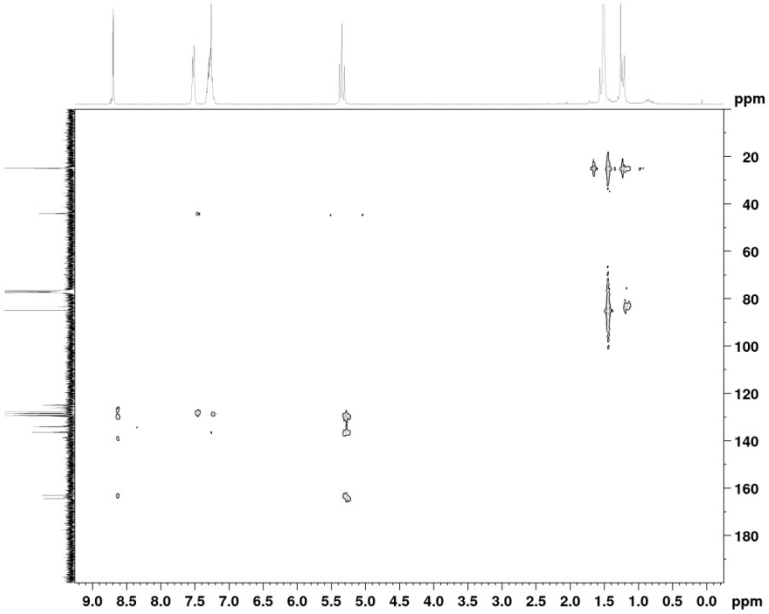

**Diborylated NDI, 416**

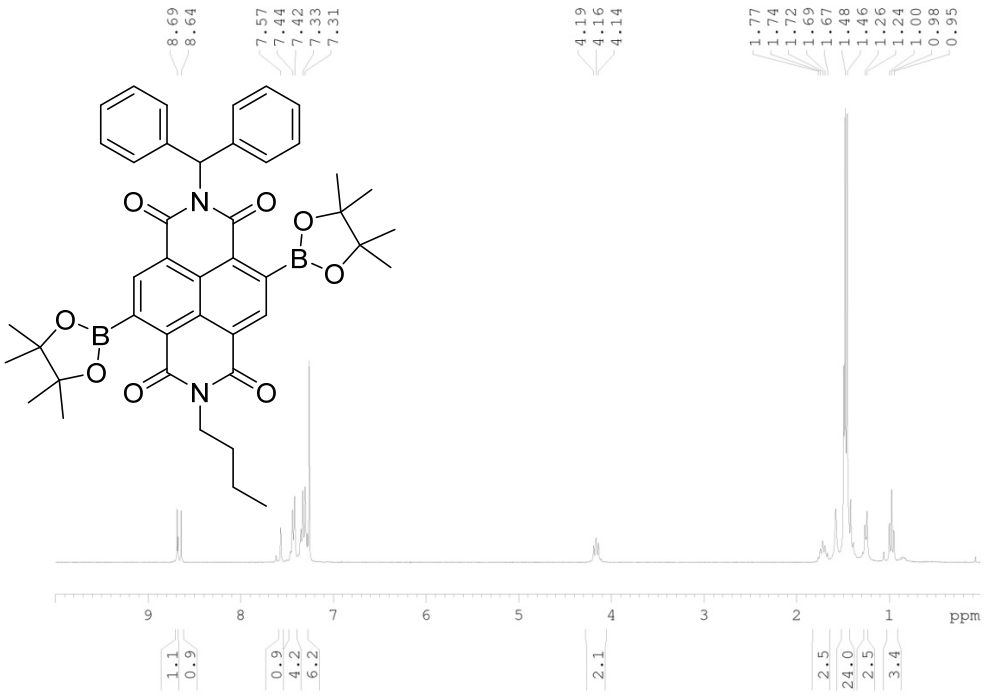


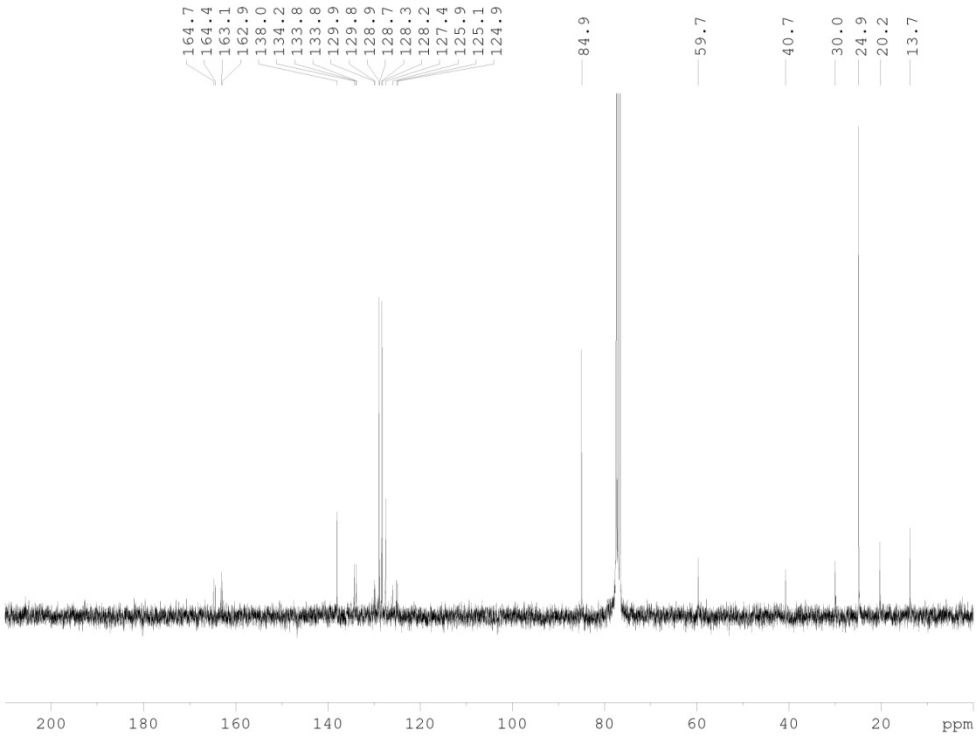

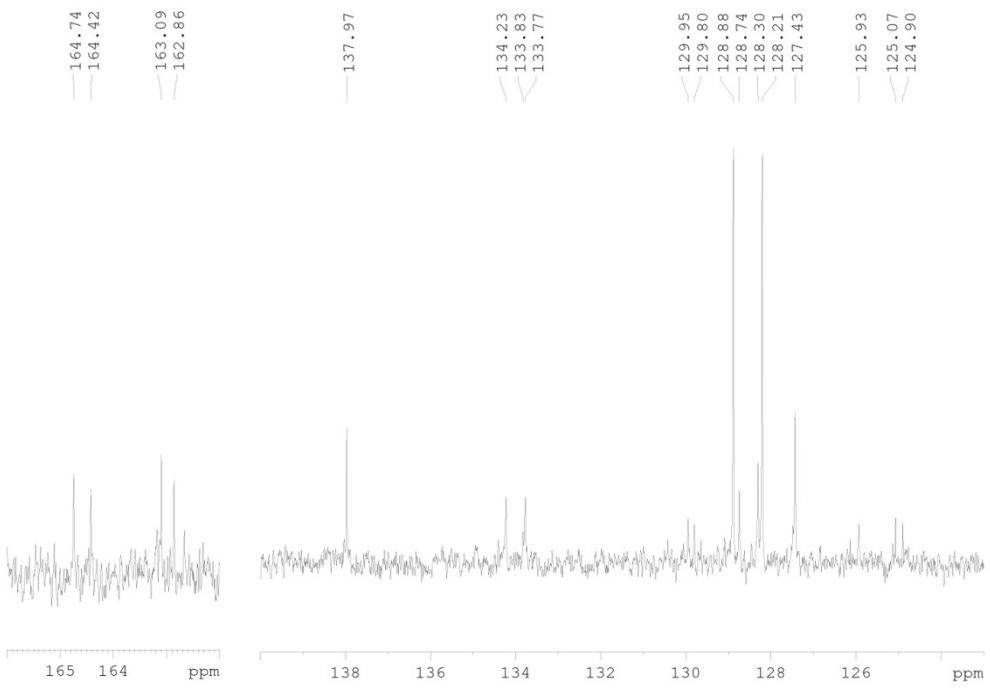


COSY (300 MHz, $CDCl_3$)

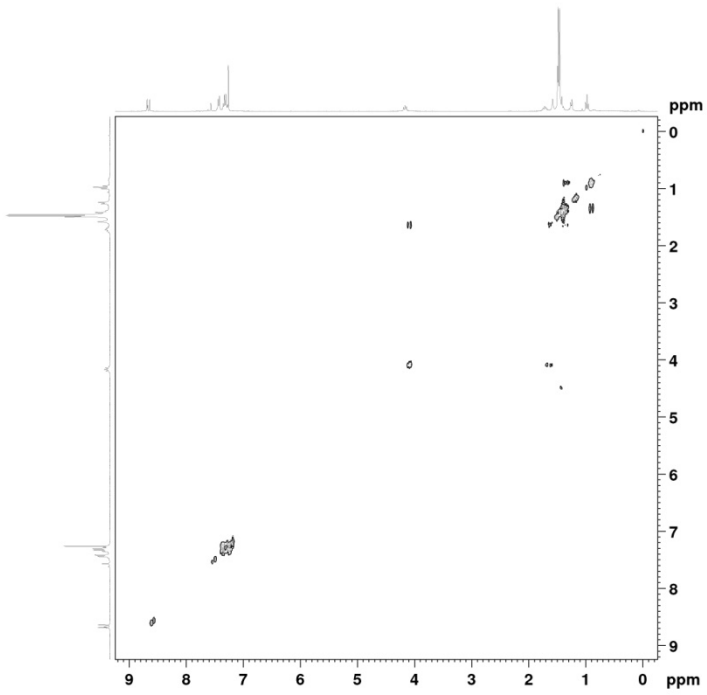

HSQC (300 MHz, $CDCl_3$)

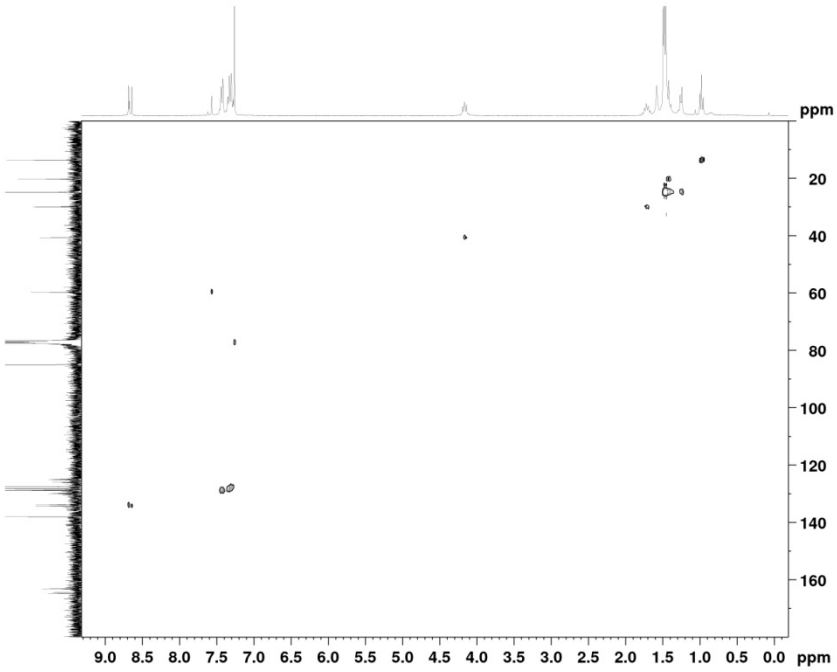


HMBC (500 MHz, $CDCl_3$)

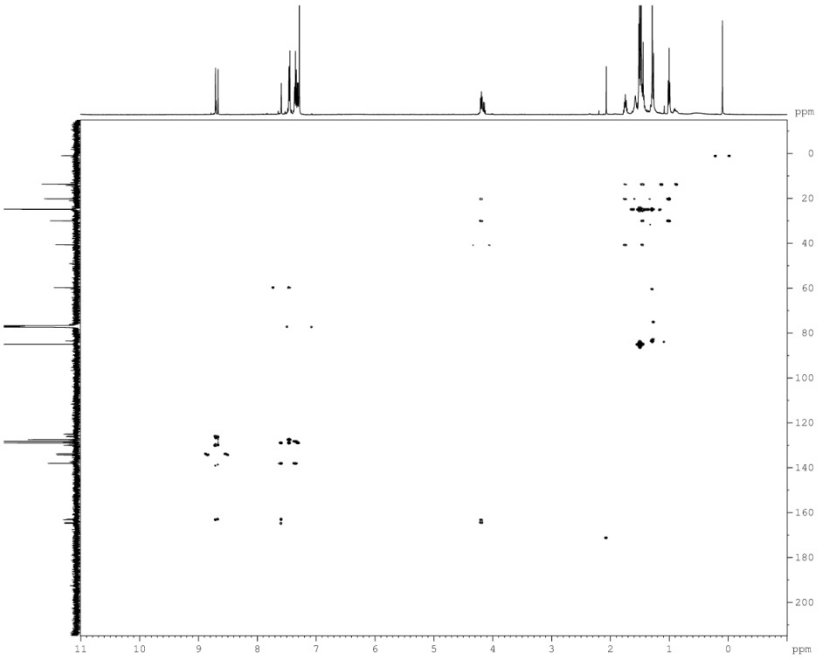

**Diborylated NDI, 417**

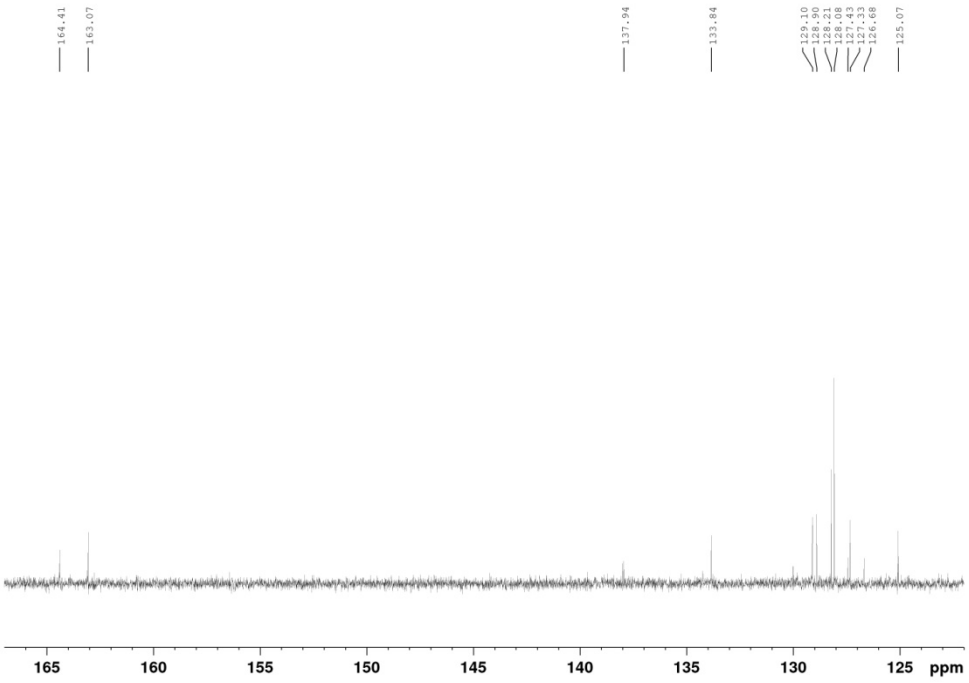


COSY (300 MHz, $CDCl_3$)

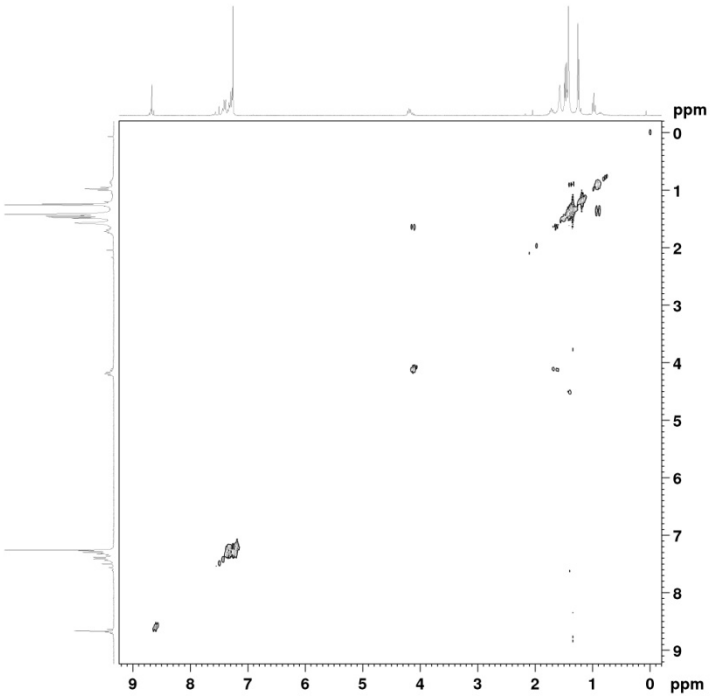

HSQC (300 MHz, $CDCl_3$)

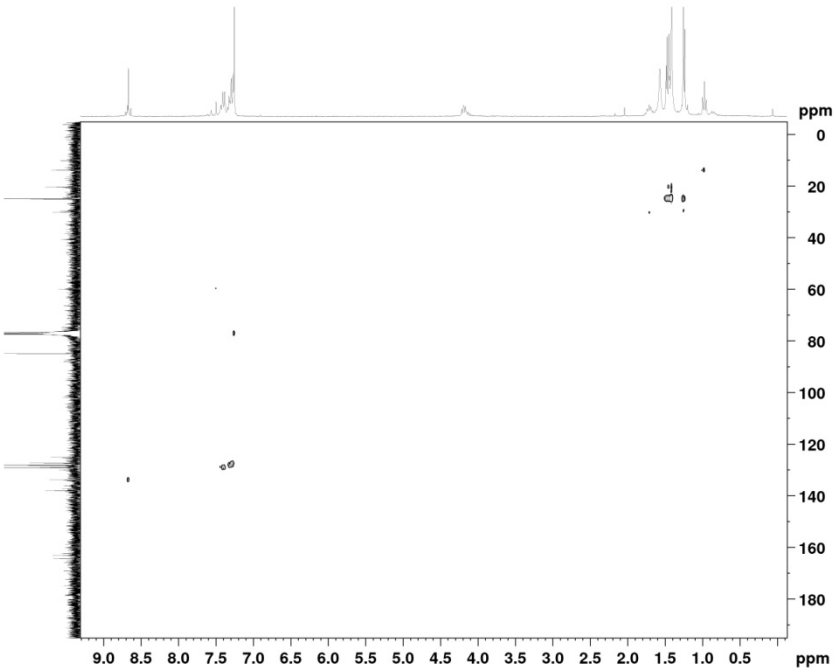


HMBC (500 MHz, $CDCl_3$)

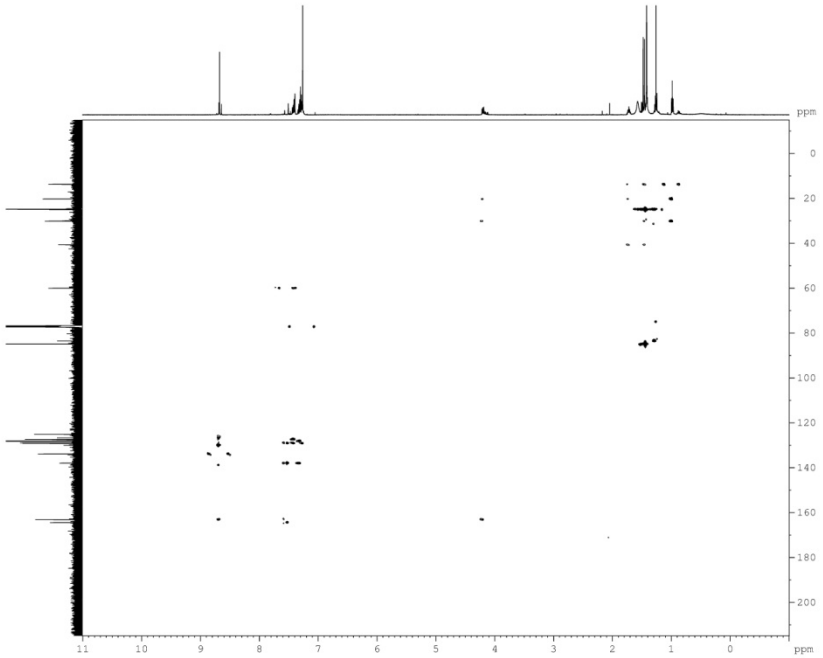

**Diborylated NDI, 413**

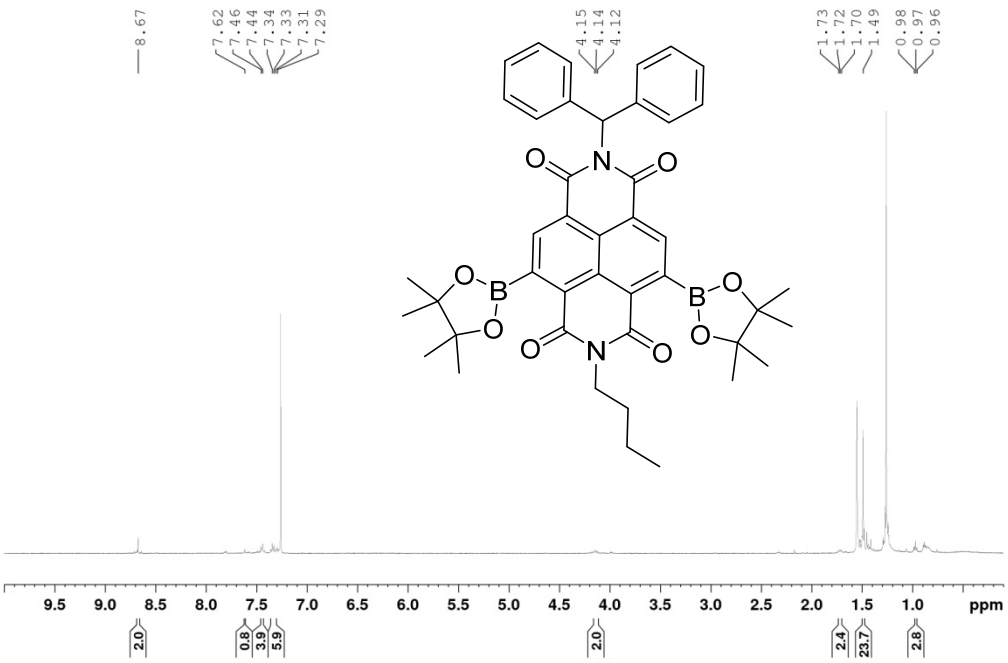


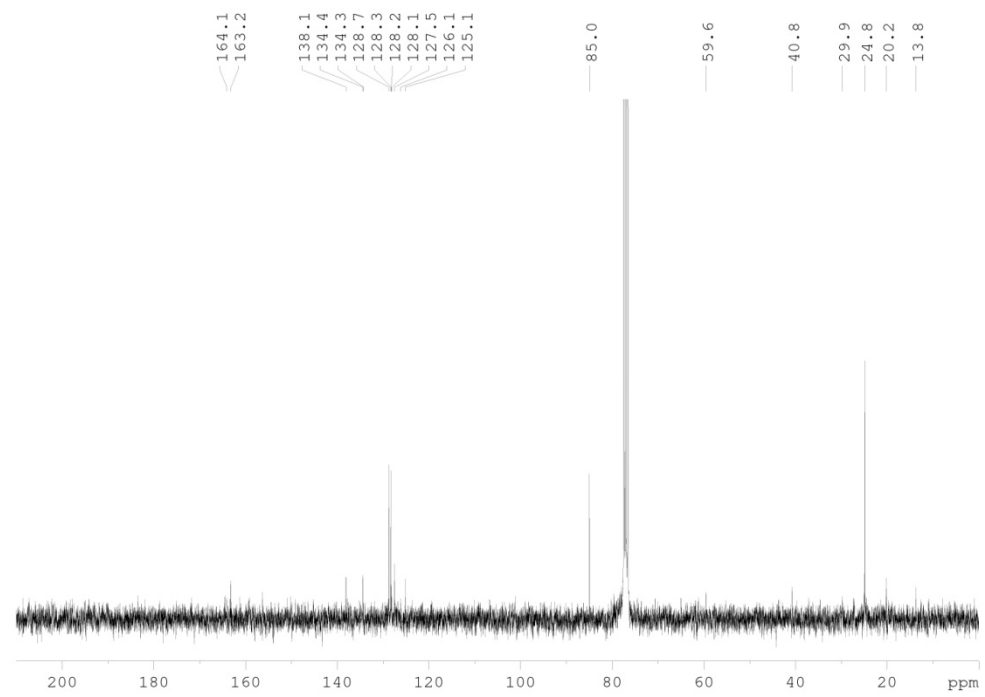

HMBC (500 MHz, $CDCl_3$)

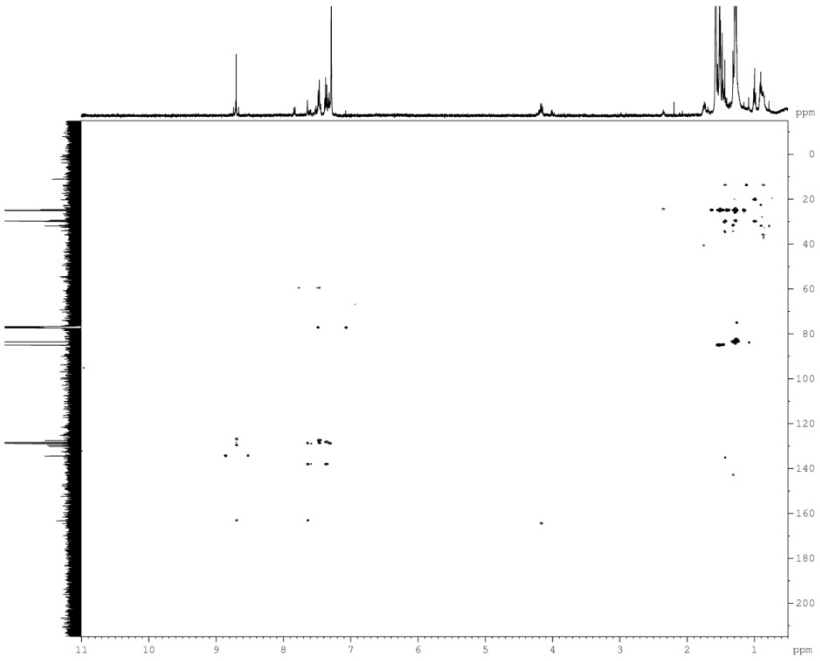

**Monofunctionalised NDI, 419**

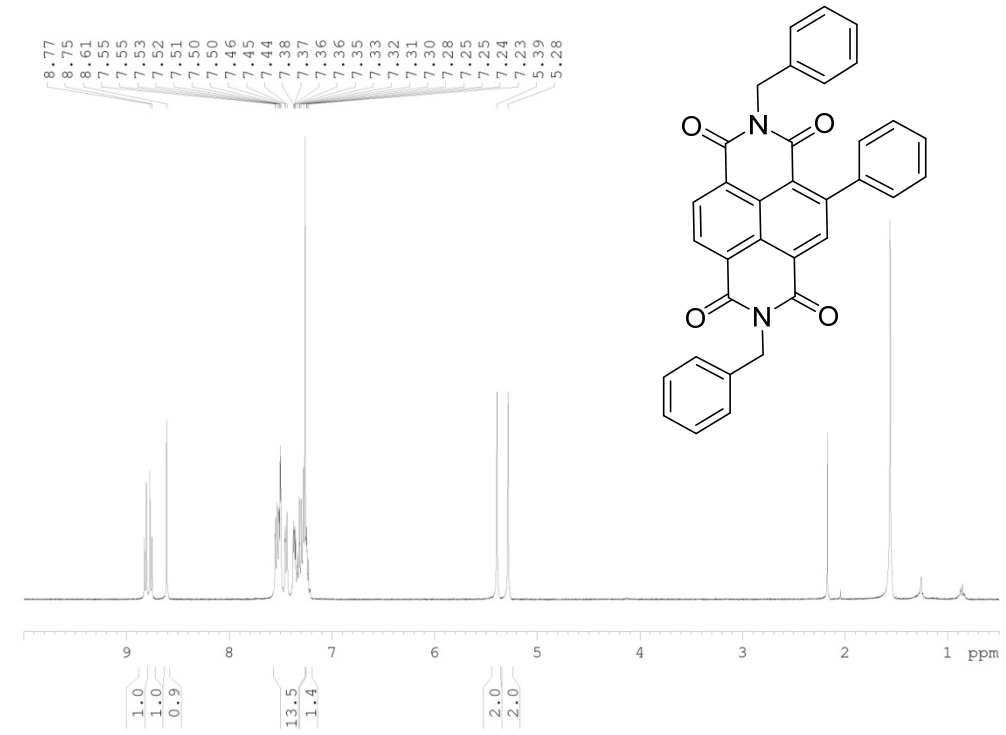


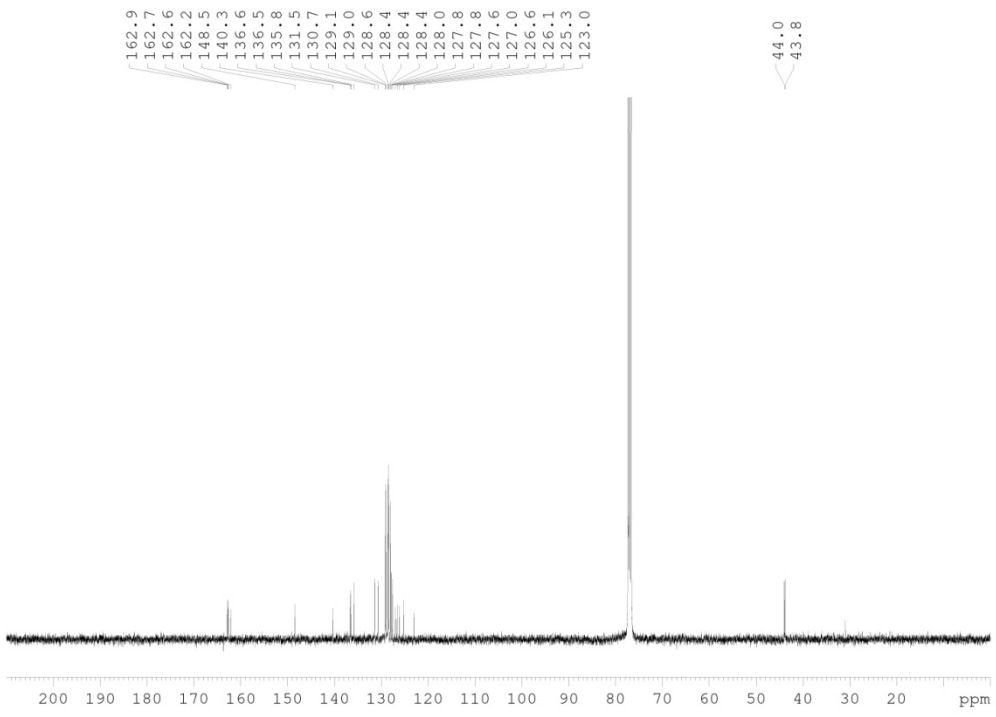

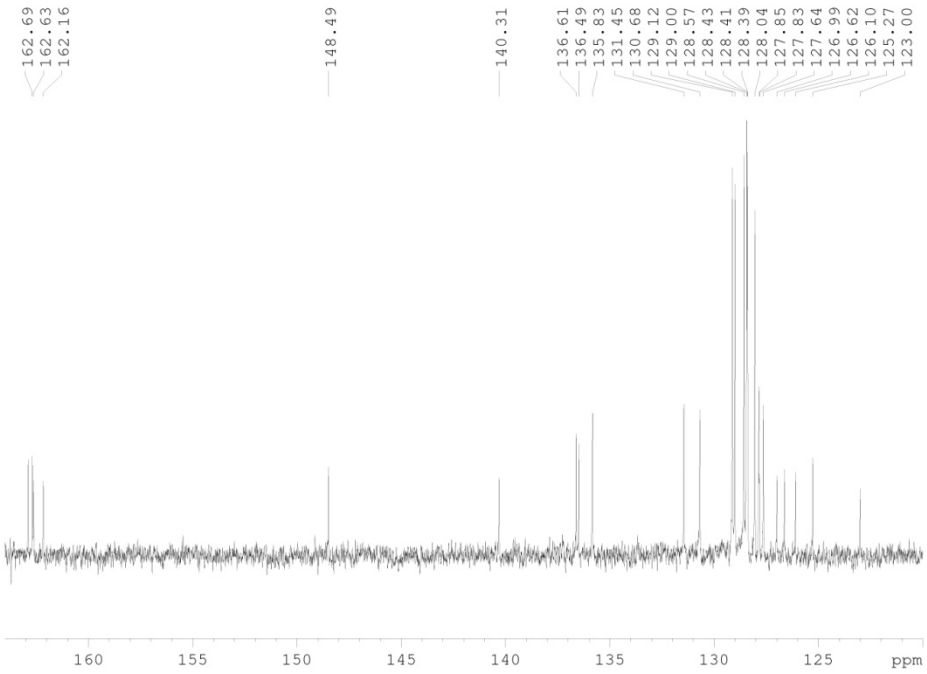
162.69
162.63
162.16
148.49
140.31
136.61
136.49
135.83
131.45
130.68
129.12
129.00
128.57
128.43
128.41
128.39
128.04
127.85
127.83
127.64
126.99
126.62
126.10
125.27
123.00
160
155
150
145
140
135
130
125
ppm

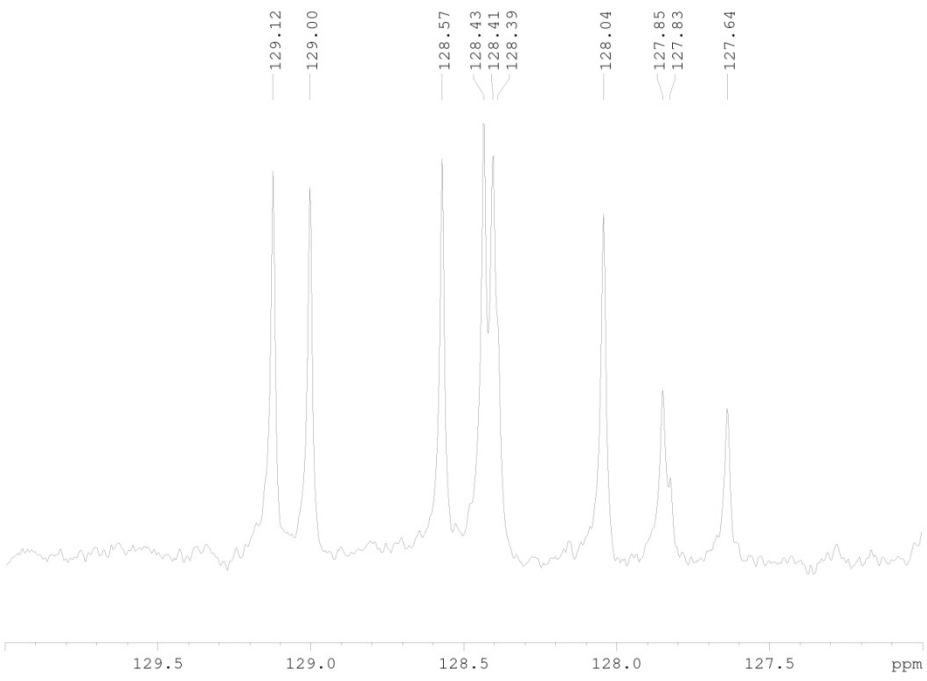
129.12
129.00
128.57
128.43
128.41
128.39
128.04
127.85
127.83
127.64
129.5
129.0
128.5
128.0
127.5
ppm

PENDANT (100 MHz, $CDCl_3$ – $CH/CH_3$ up, $C/CH_2$ down)

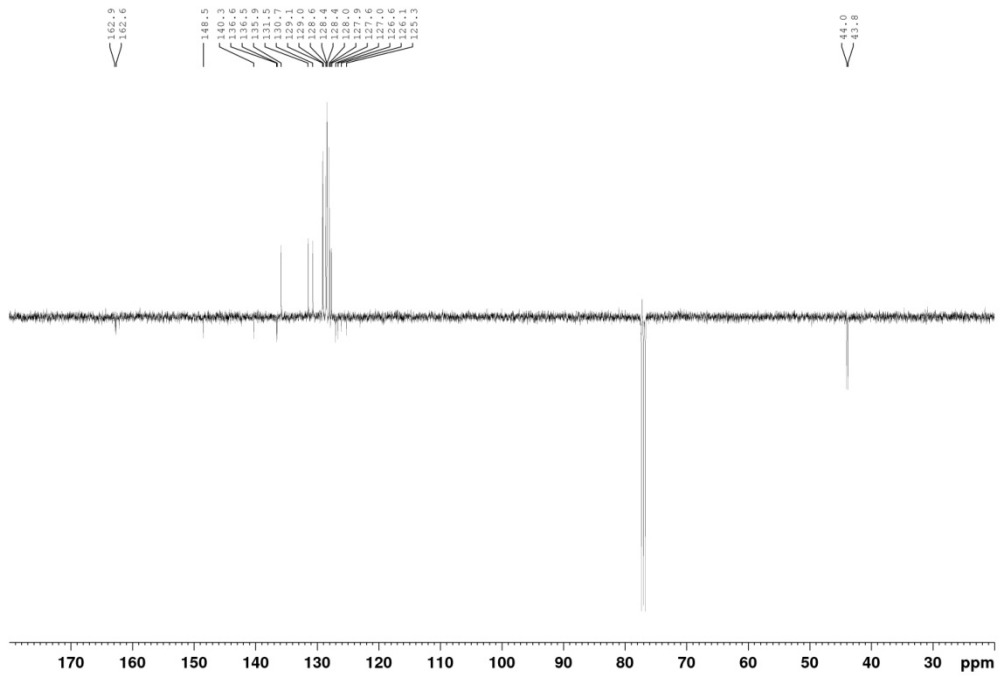


COSY (400 MHz, $CDCl_3$)

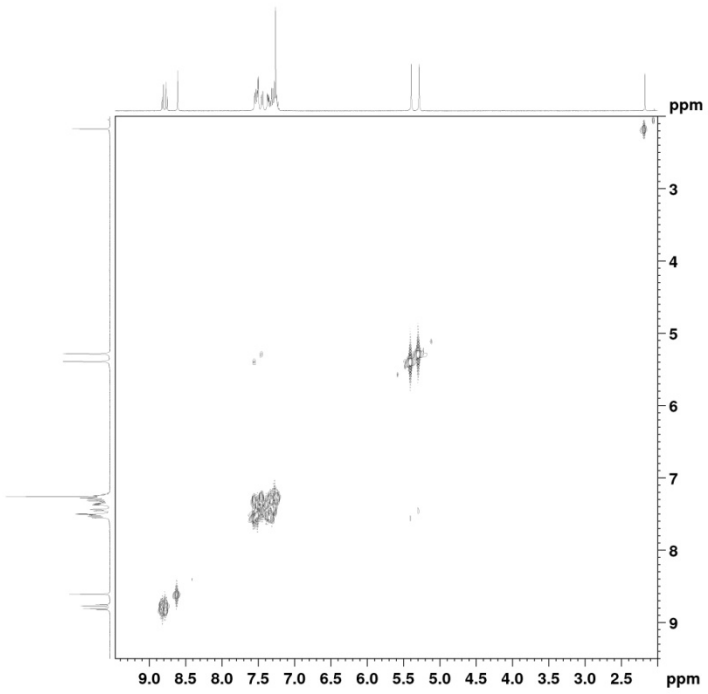

HSQC (400 MHz, $CDCl_3$)

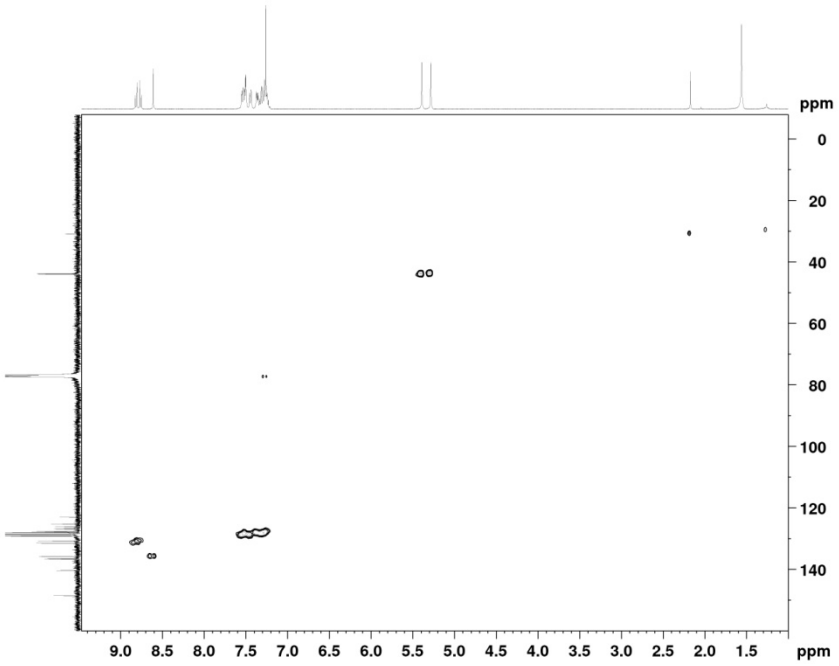


HMBC (400 MHz, $CDCl_3$)

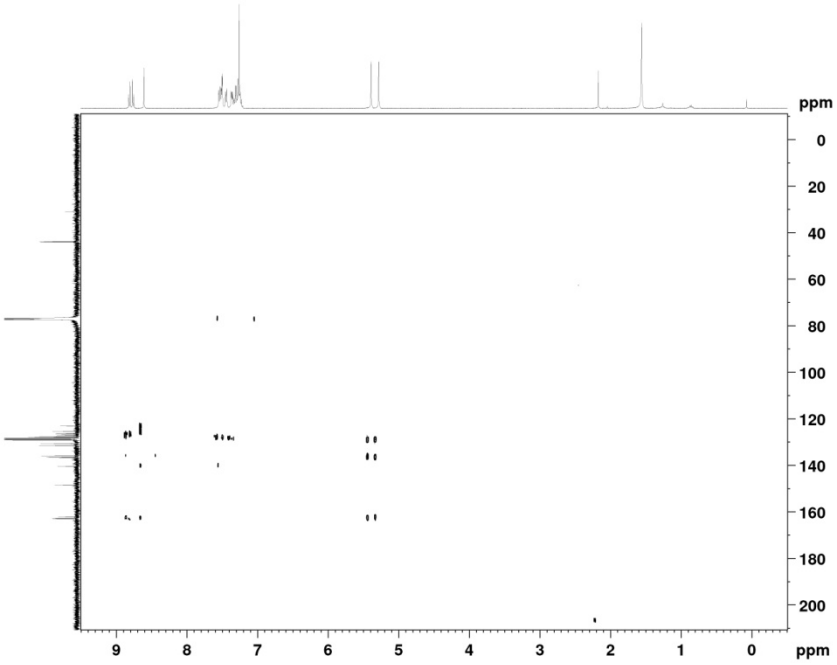

**Monofunctionalised NDI, 420**

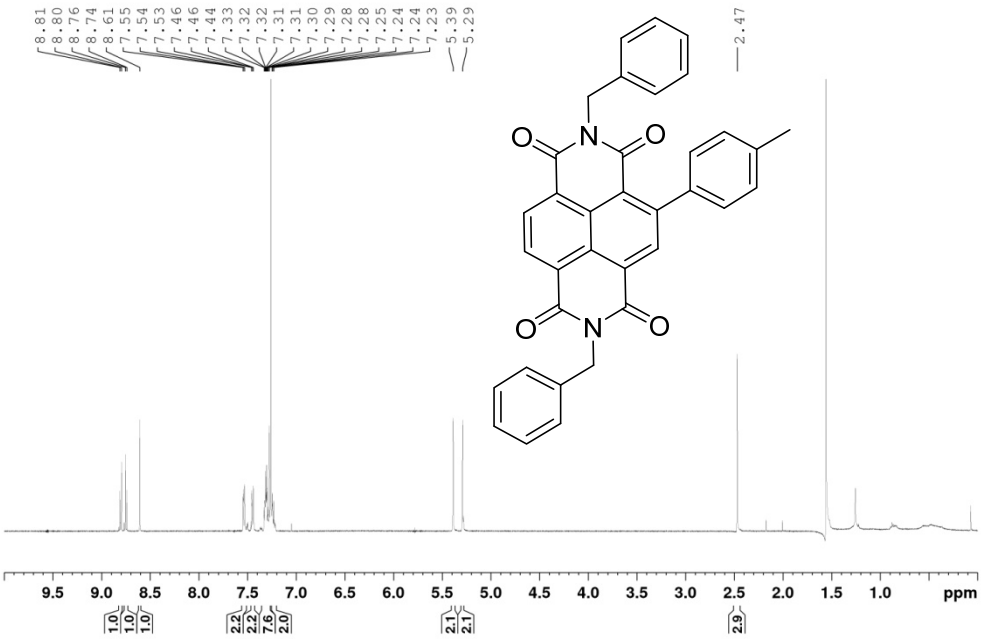


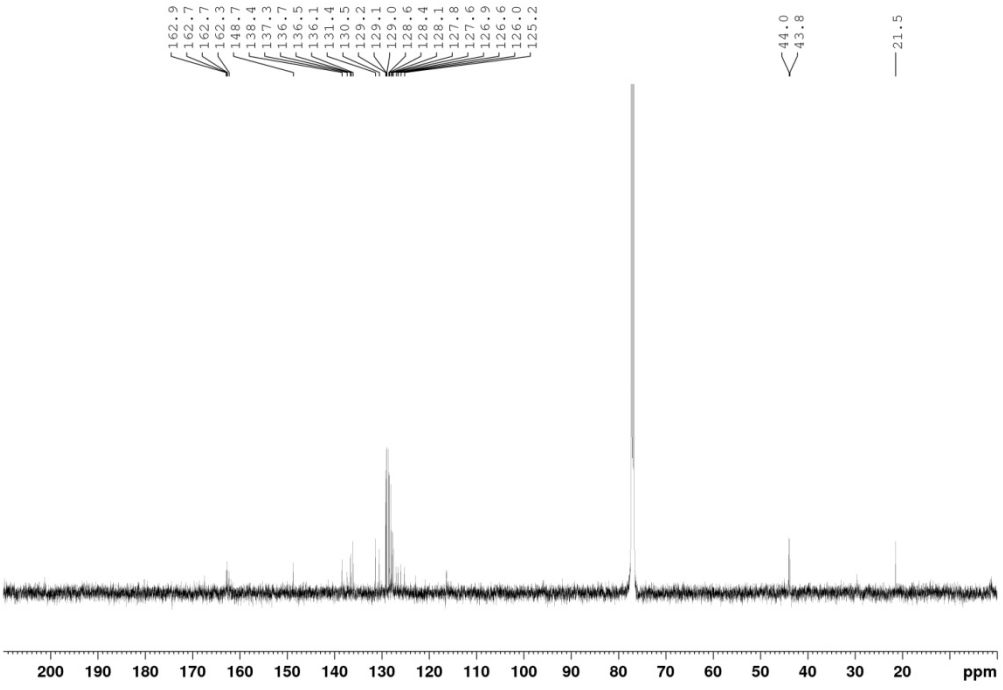

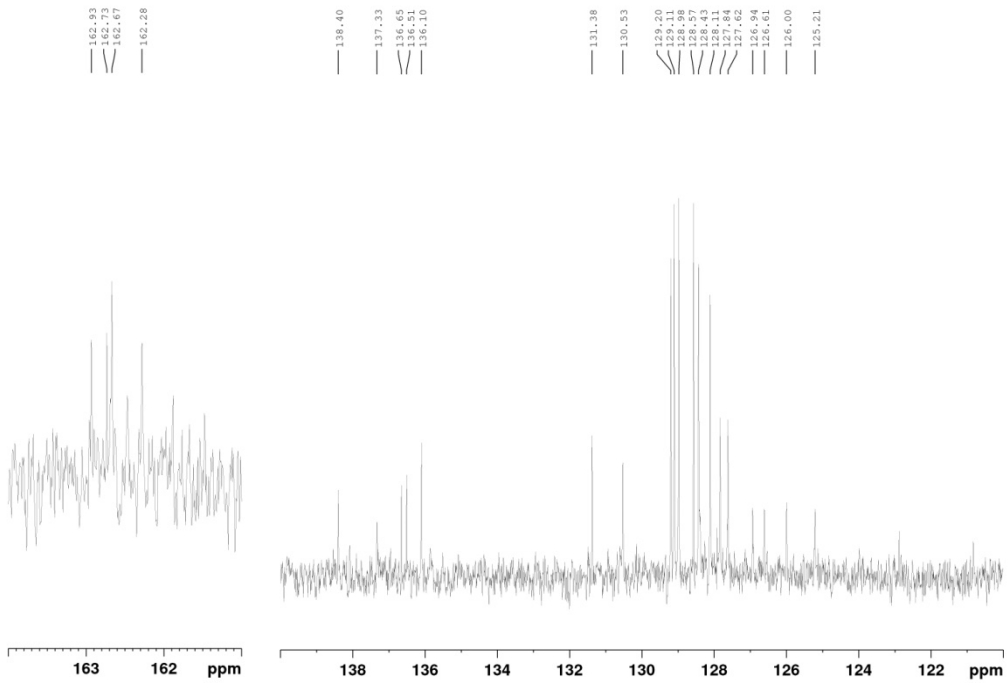


COSY (500 MHz, $CDCl_3$)

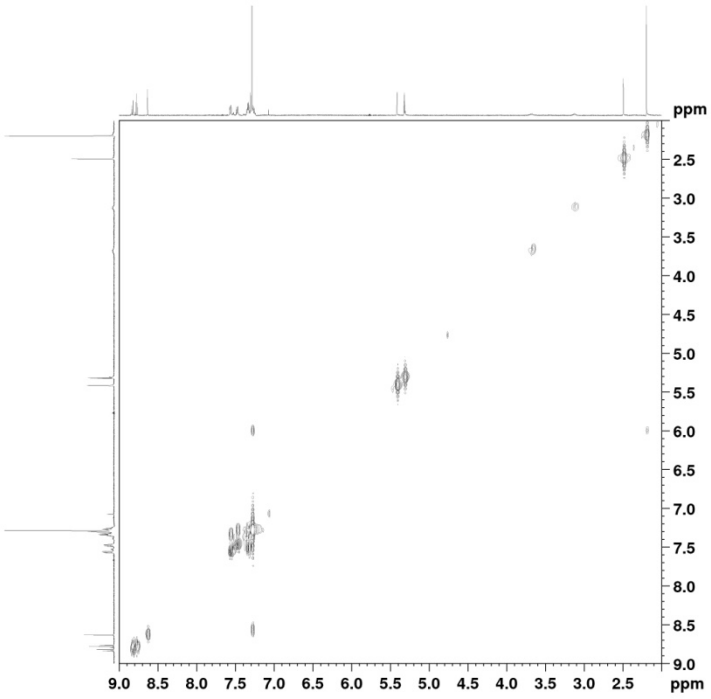

**Monofunctionalised NDI, 421**

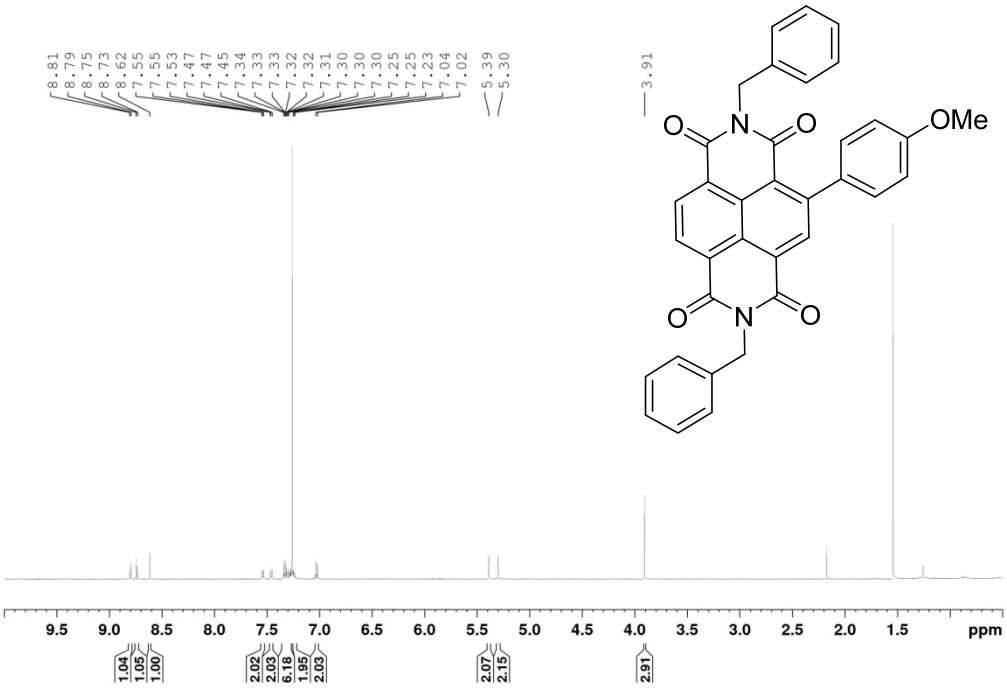


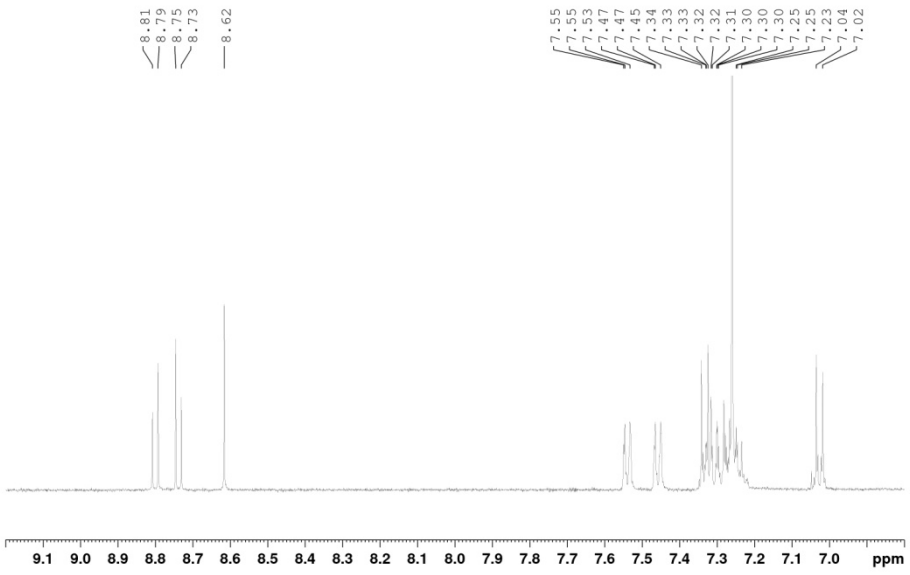

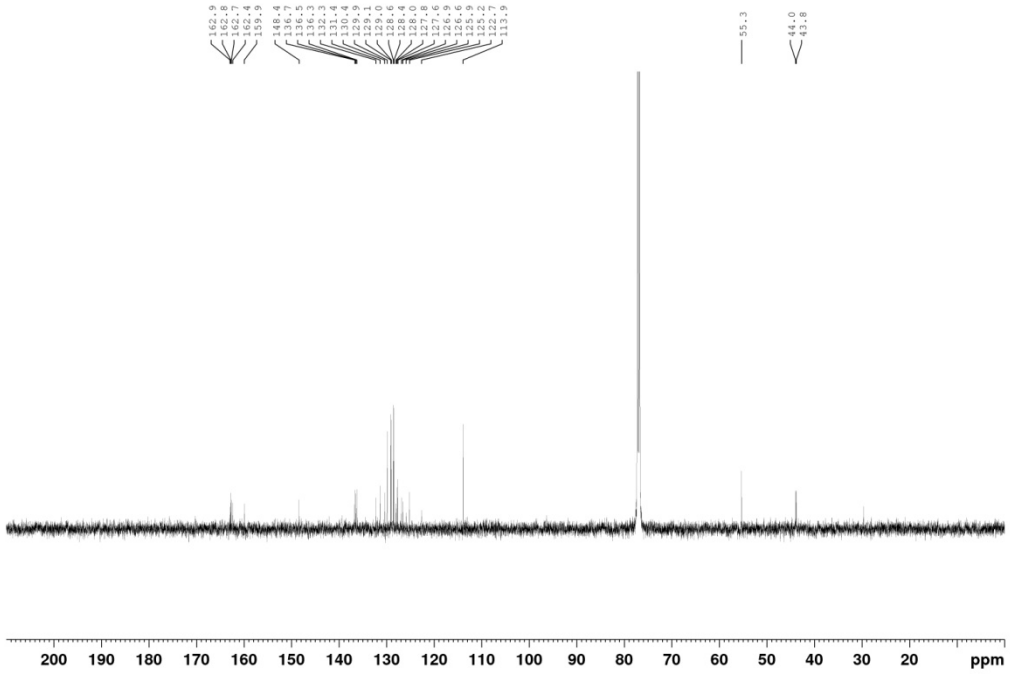
162.9
162.8
162.7
162.4
159.9
148.4
136.7
136.5
136.3
132.3
131.4
130.4
129.9
129.1
129.0
128.6
128.4
128.0
127.8
127.6
126.9
126.6
125.9
125.2
122.7
113.9
55.3
44.0
43.8
200 190 180 170 160 150 140 130 120 110 100 90 80 70 60 50 40 30 20 ppm

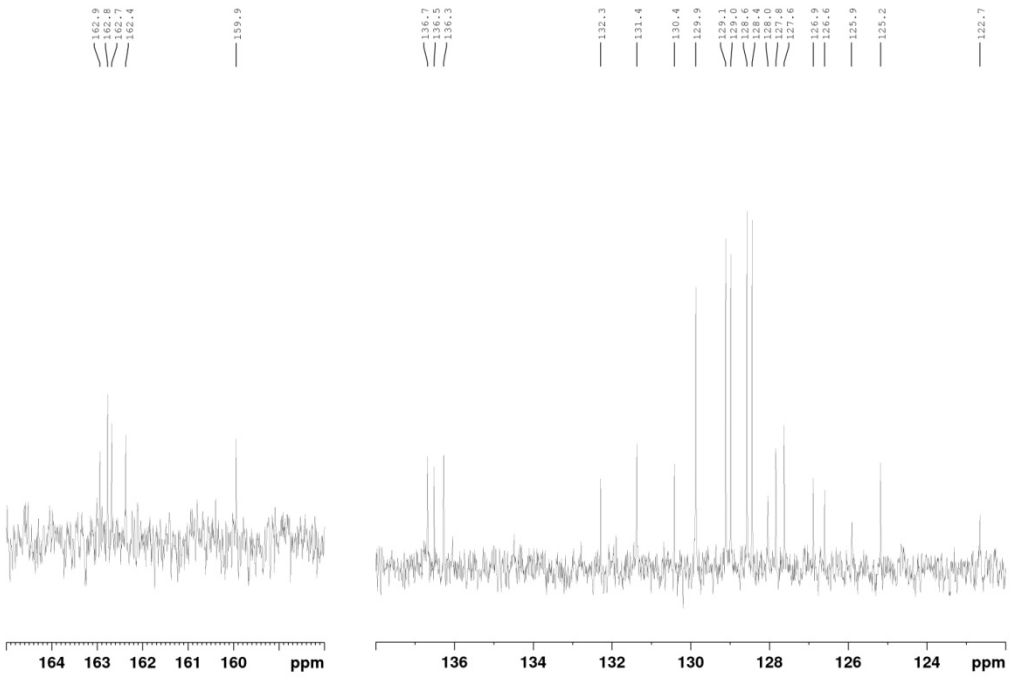
162.9
162.8
162.7
162.4
159.9
136.7
136.5
136.3
132.3
131.4
130.4
129.9
129.1
129.0
128.6
128.4
128.0
127.8
127.6
126.9
126.6
125.9
125.2
122.7
164 163 162 161 160 ppm
136 134 132 130 128 126 124 ppm

PENDANT (125 MHz, $CDCl_3$ - $CH/CH_3$ up, $C/CH_2$ down)

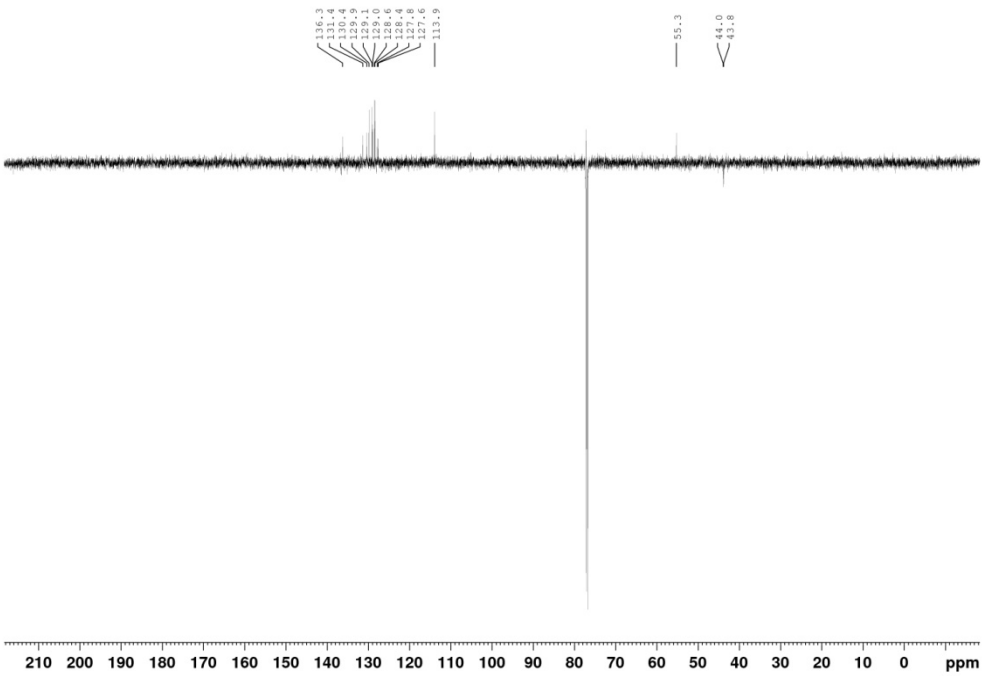


COSY (500 MHz, $CDCl_3$)

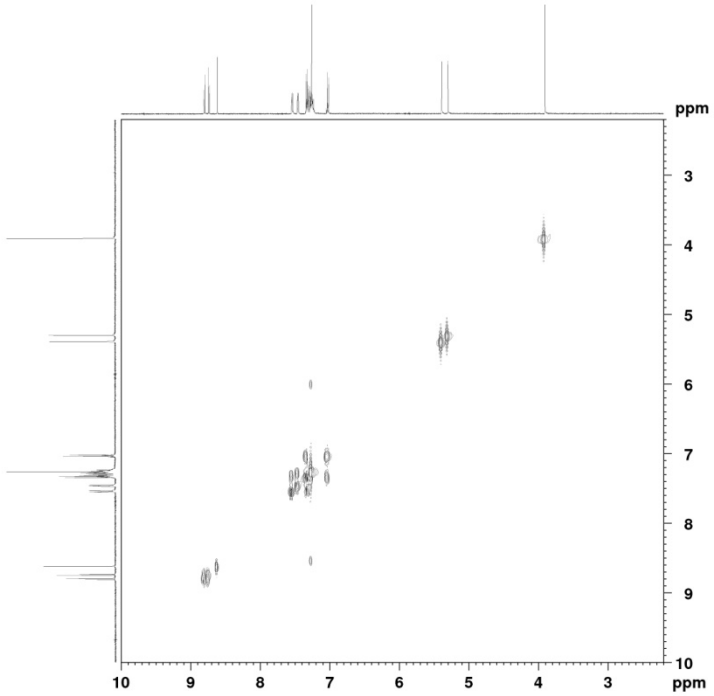

HSQC (500 MHz, $CDCl_3$)

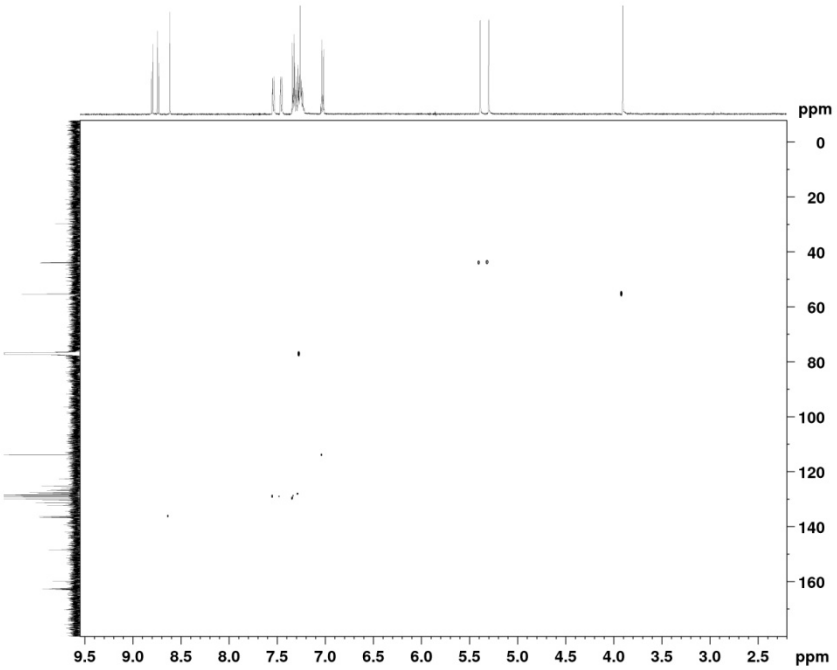


HMBC (500 MHz, $CDCl_3$)

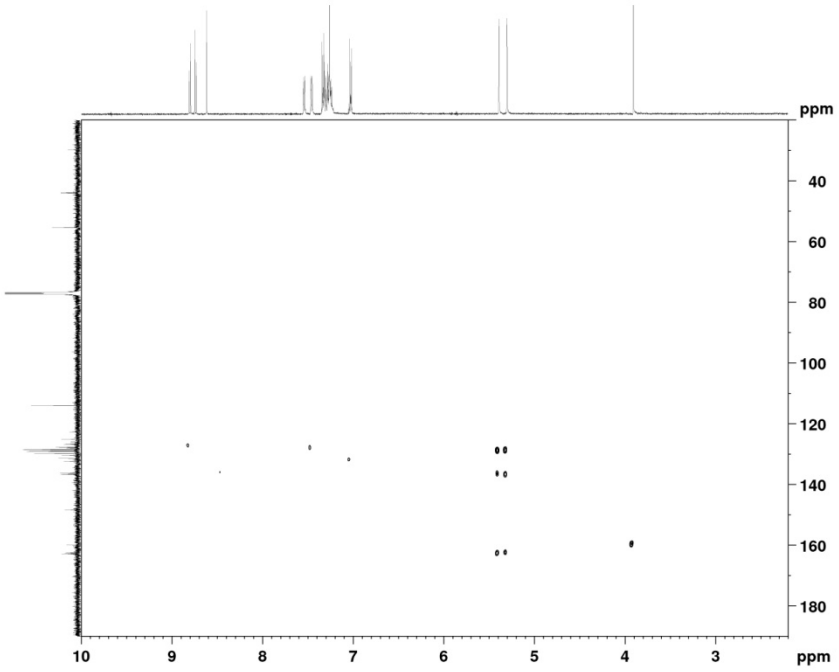

**Monofunctionalised NDI, 422**

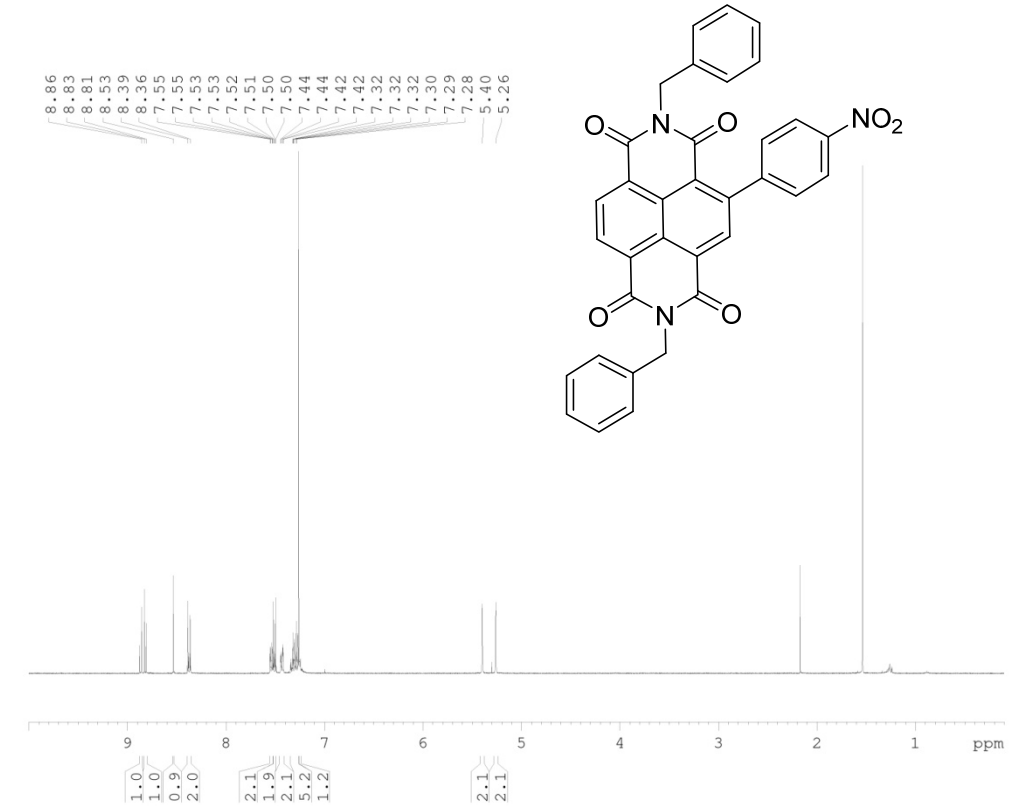


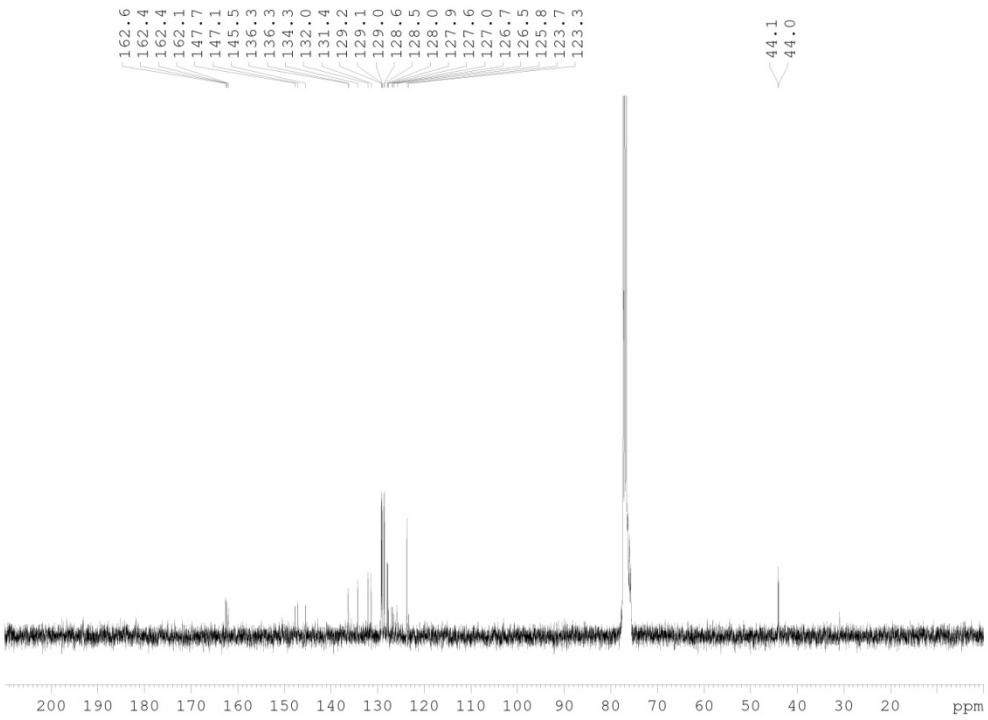

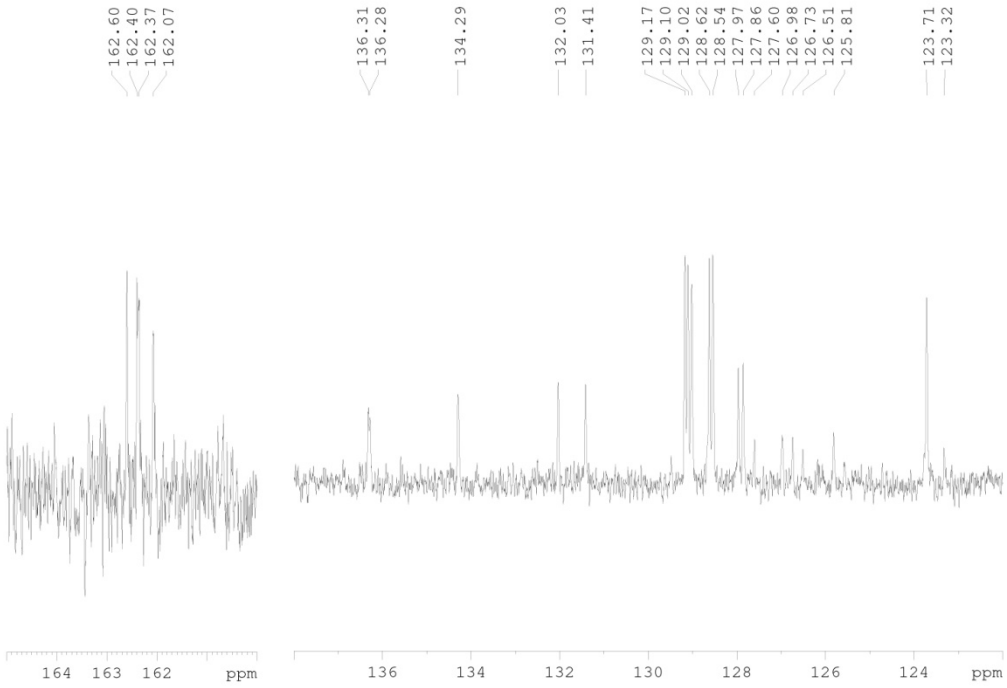


PENDANT (100 MHz, $CDCl_3$ - $CH/CH_3$ up, $C/CH_2$ down)

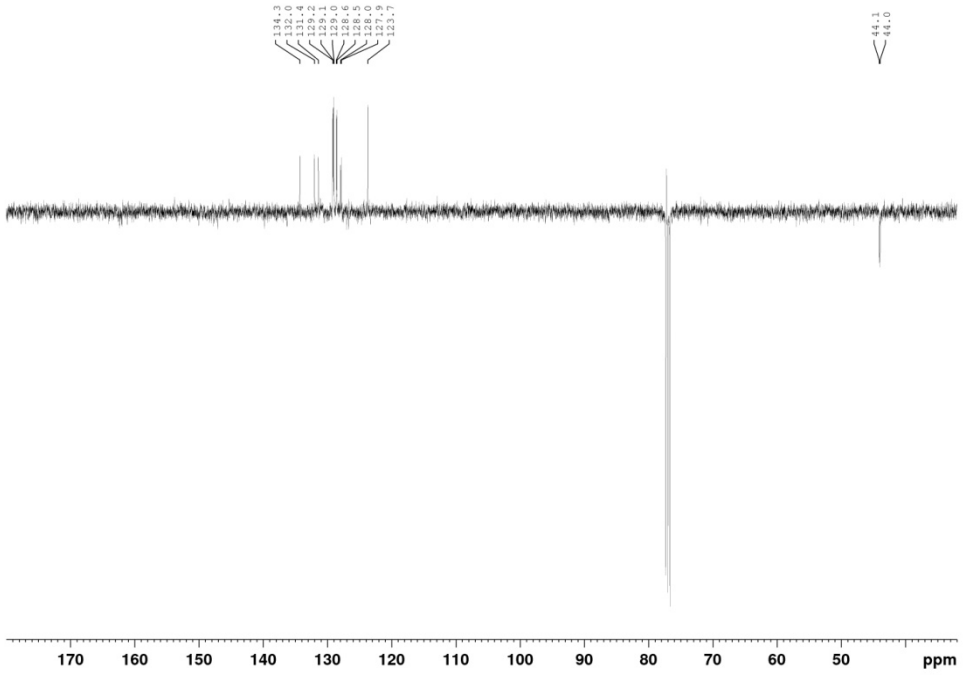

COSY (400 MHz, $CDCl_3$)

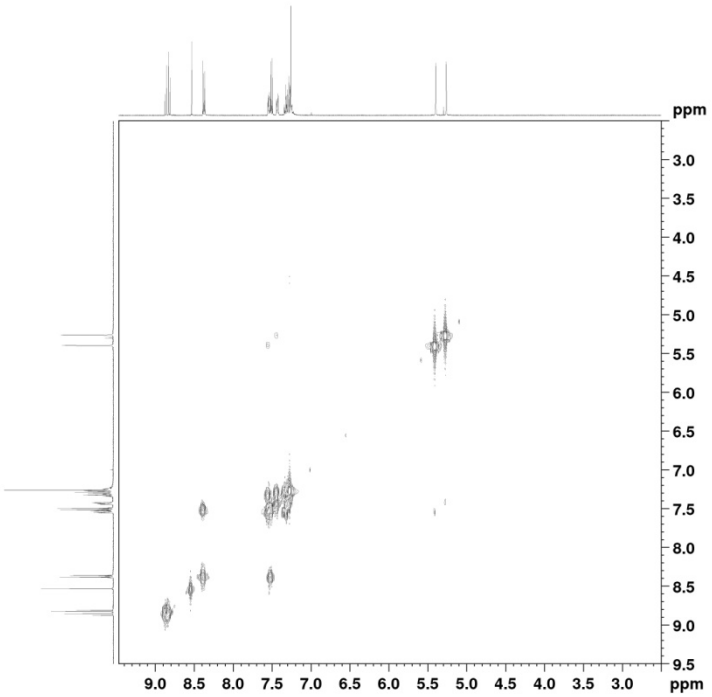


HSQC (400 MHz, $CDCl_3$)

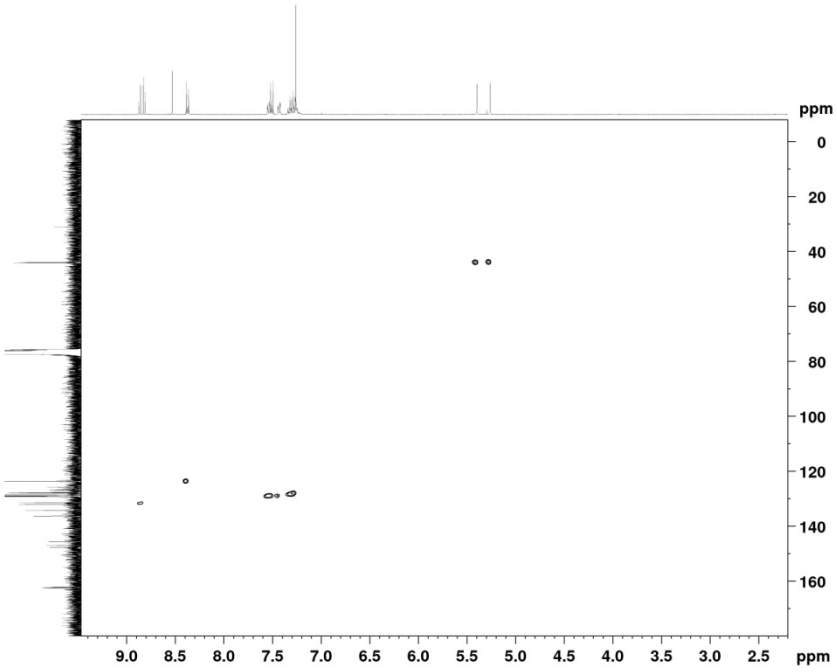

HMBC (400 MHz, $CDCl_3$)

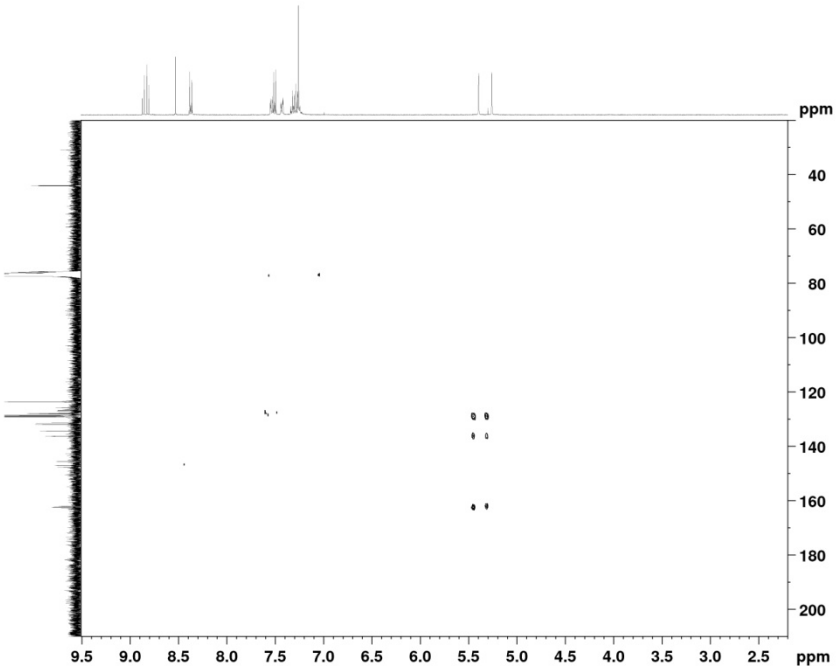

**Monofunctionalised NDI, 423**

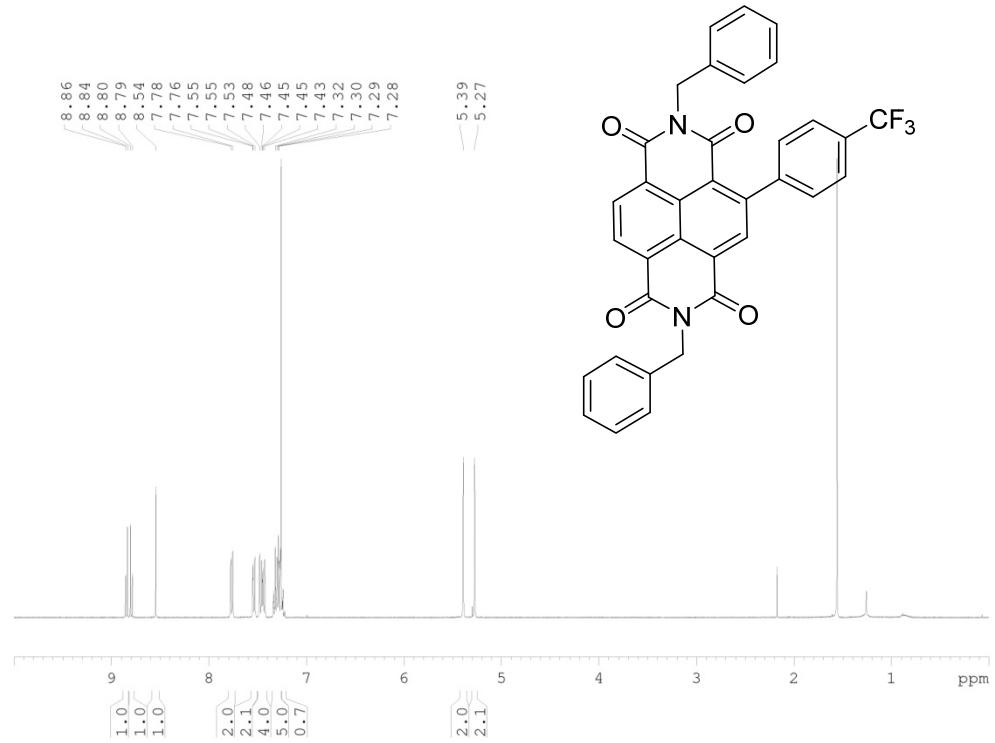


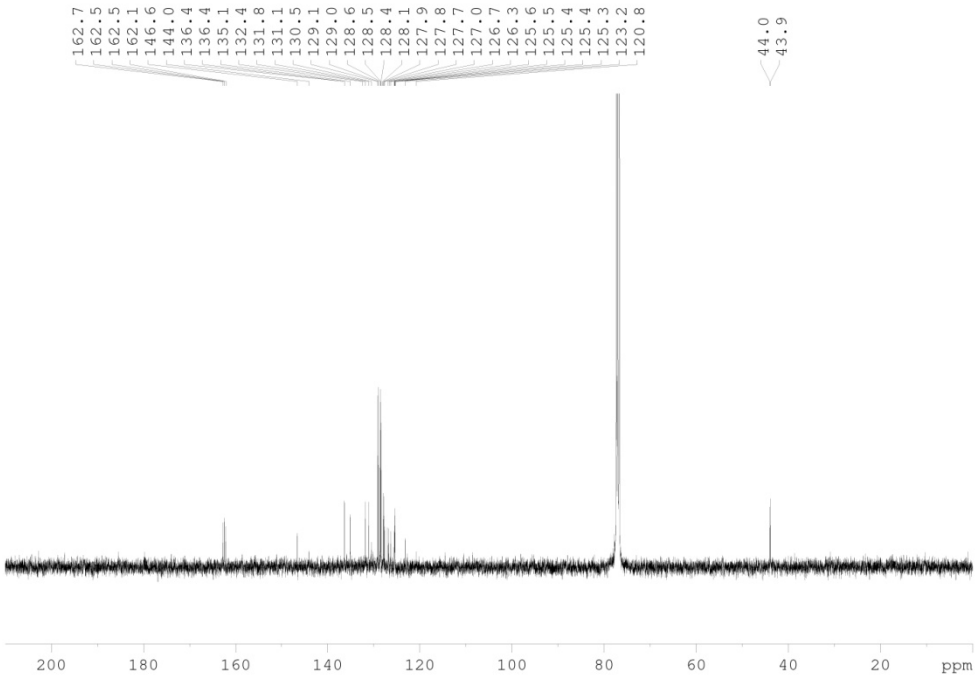

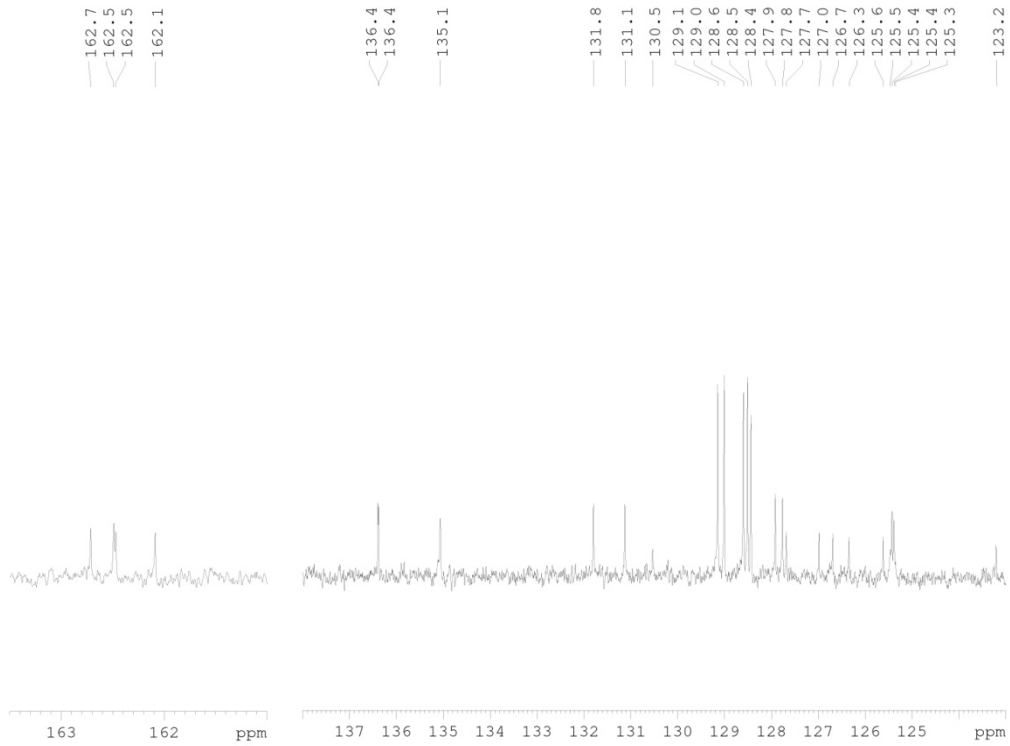
162.7
162.5
162.5
162.1
136.4
136.4
135.1
131.8
131.1
130.5
129.1
129.0
128.6
128.5
128.4
127.9
127.8
127.7
127.0
126.7
126.3
125.6
125.5
125.4
125.4
125.3
123.2
163
162
ppm
137
136
135
134
133
132
131
130
129
128
127
126
125
ppm

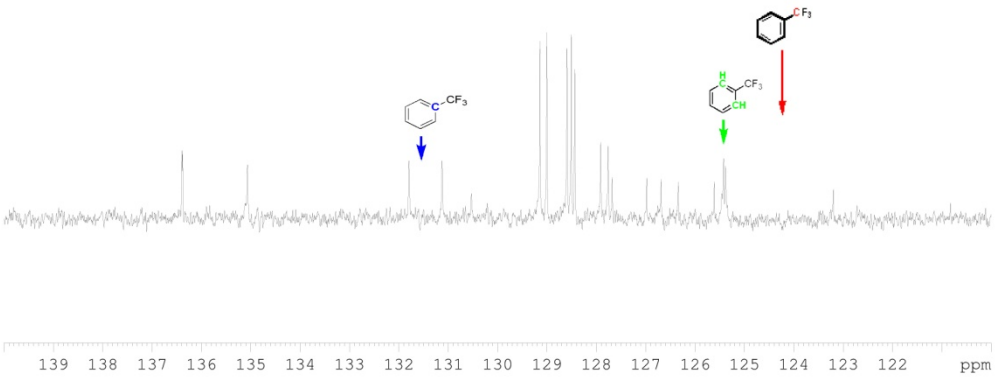
CF3
CF3
CF3
H
CH
139
138
137
136
135
134
133
132
131
130
129
128
127
126
125
124
123
122
ppm

$^{19}F$ (376 MHz, $CDCl_3$)

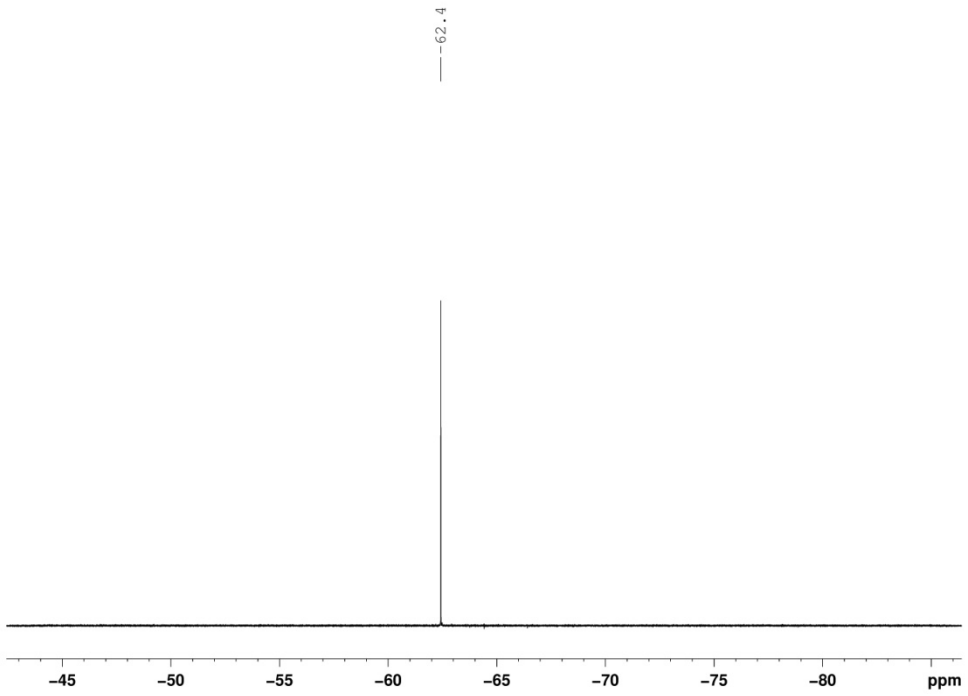


COSY (400 MHz, $CDCl_3$)

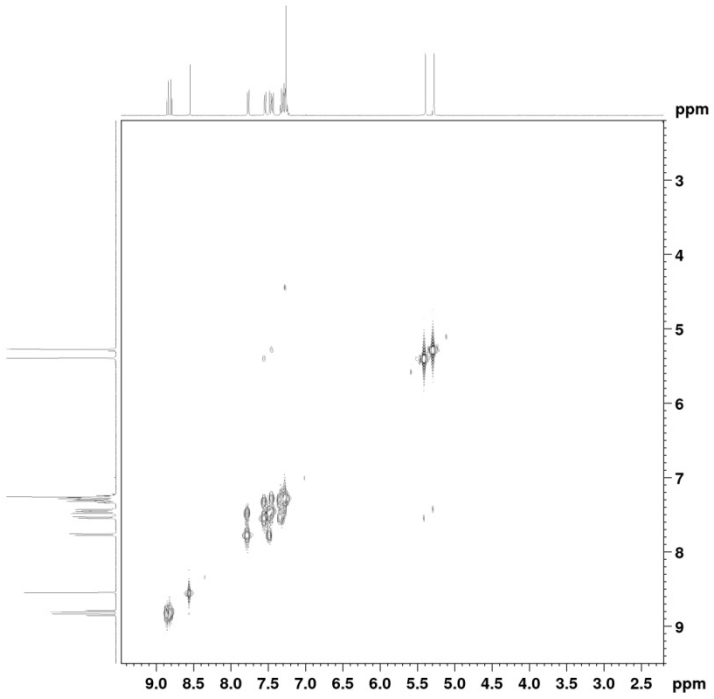

HSQC (400 MHz, $CDCl_3$)

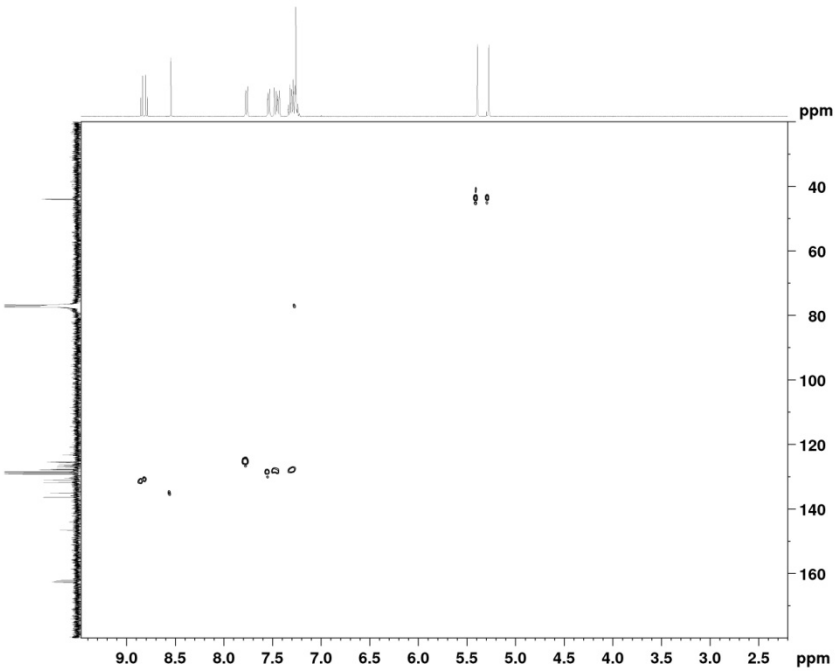


HMBC (400 MHz, $CDCl_3$)

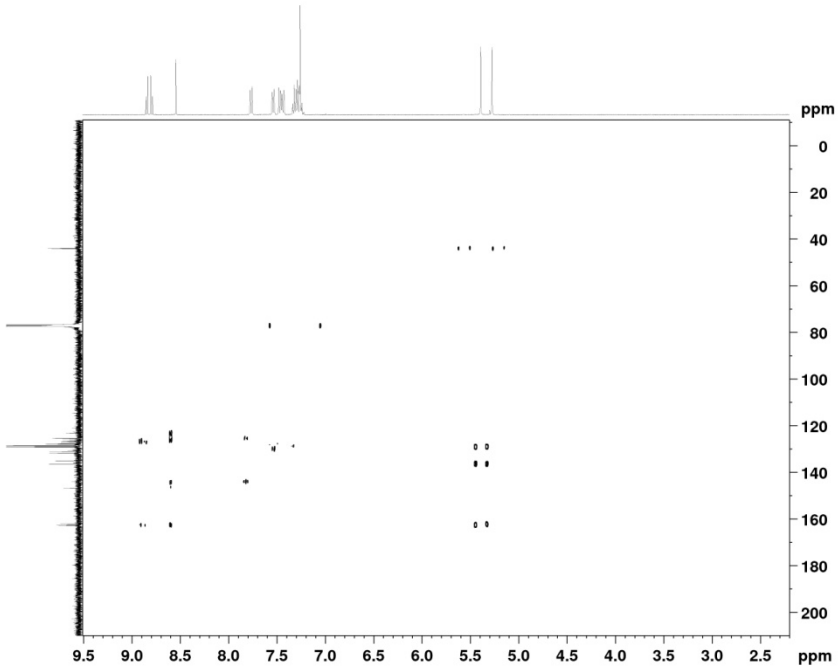

**Difunctionalised NDI, 424**

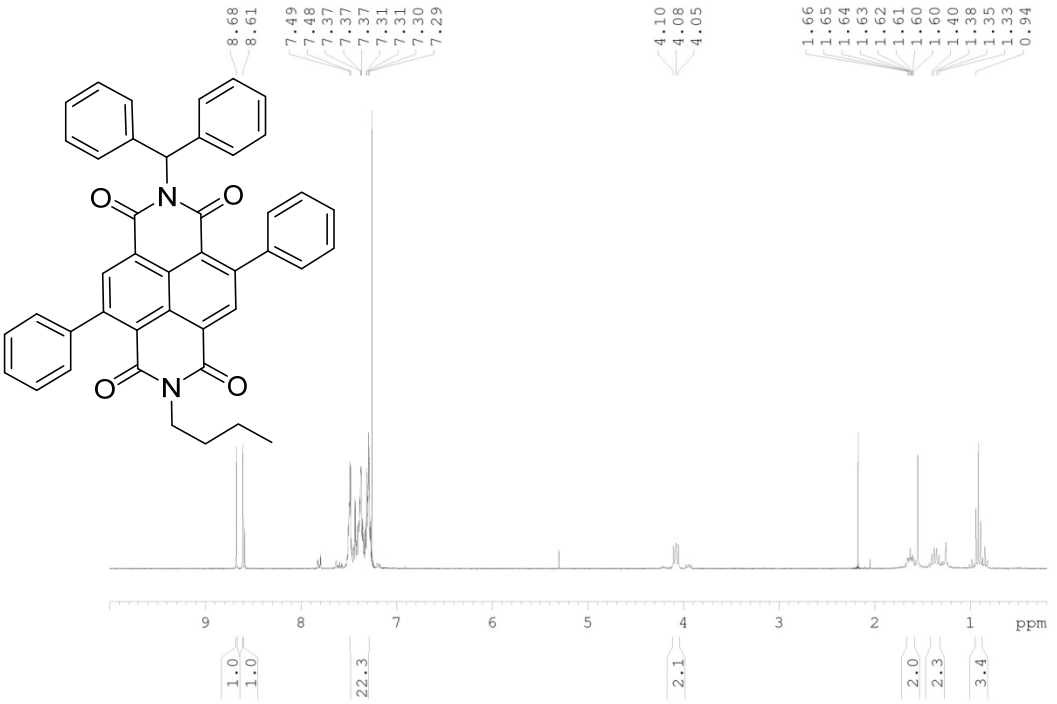


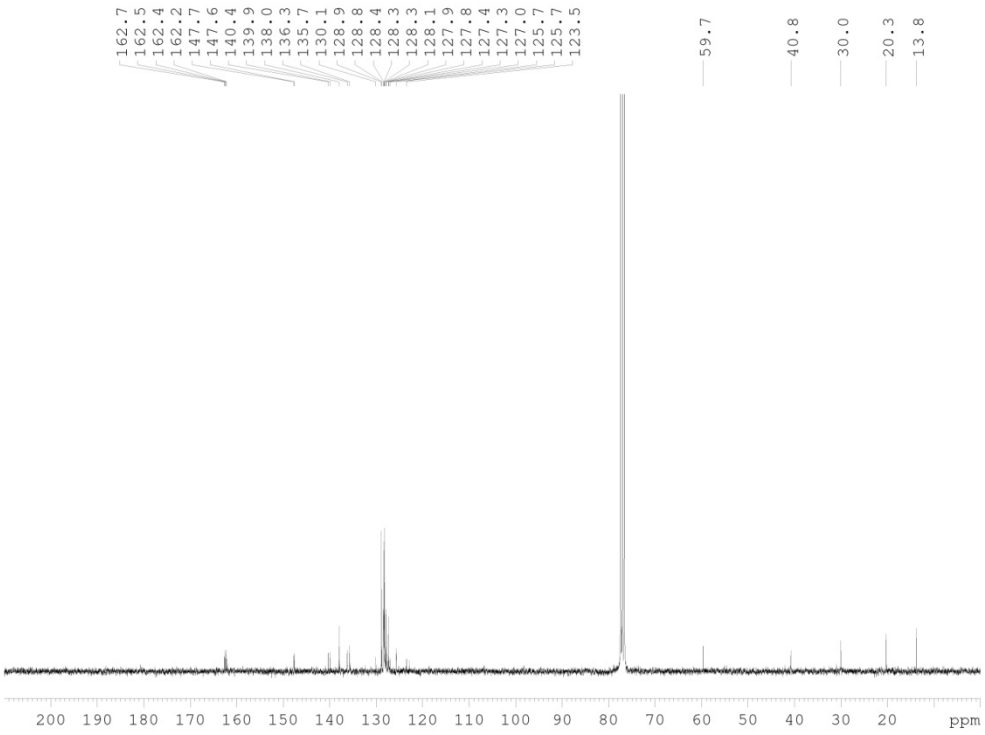

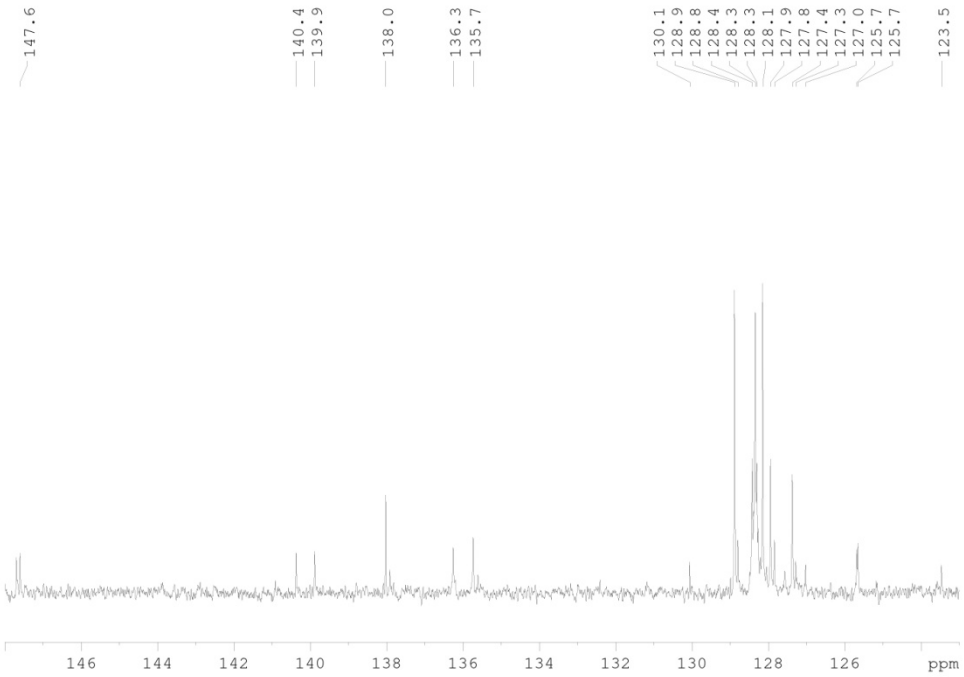


COSY (300 MHz, $CDCl_3$)

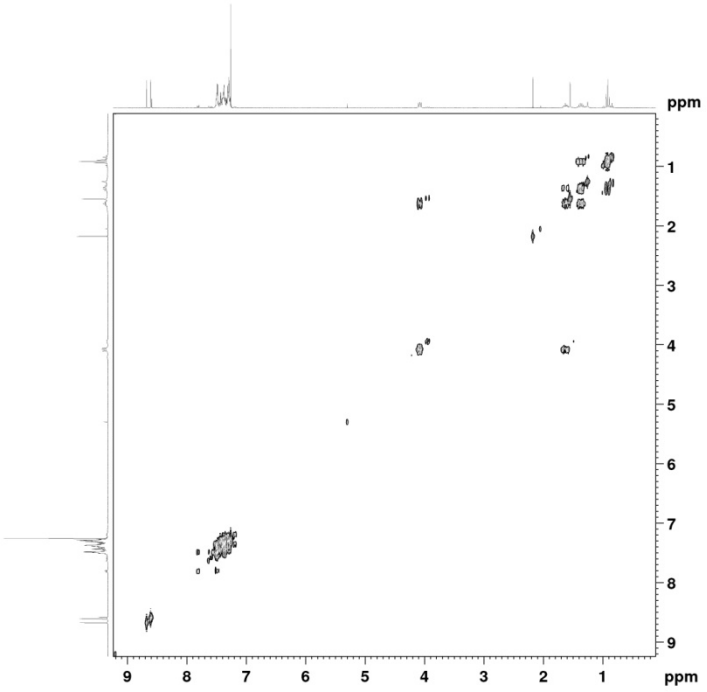

HSQC (300 MHz, $CDCl_3$)

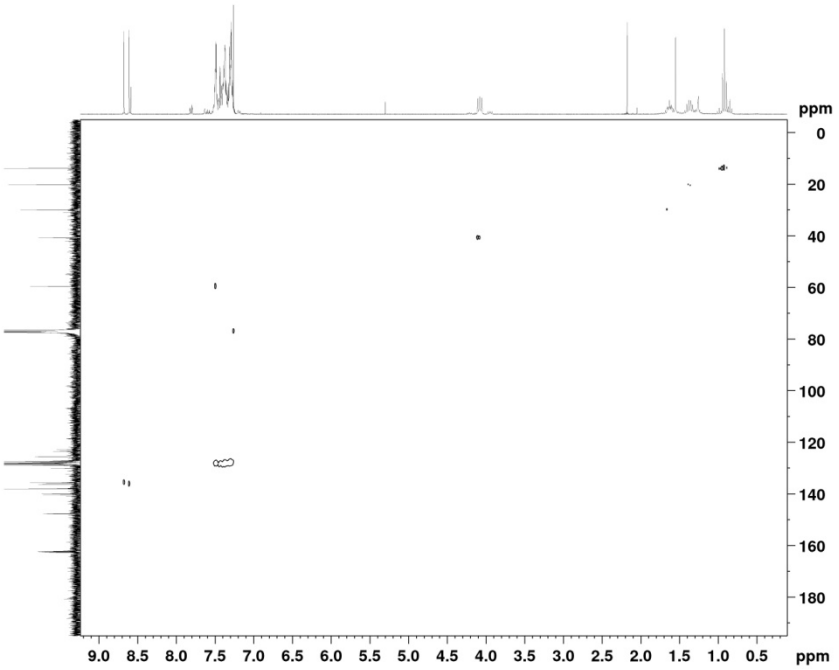


HMBC (300 MHz, $CDCl_3$)

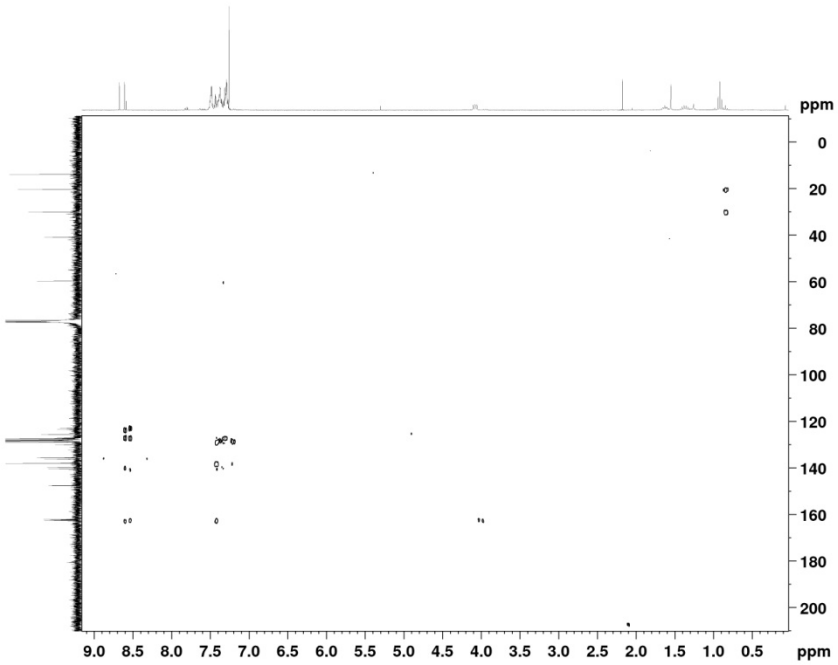

**Difunctionalised NDI, 425**

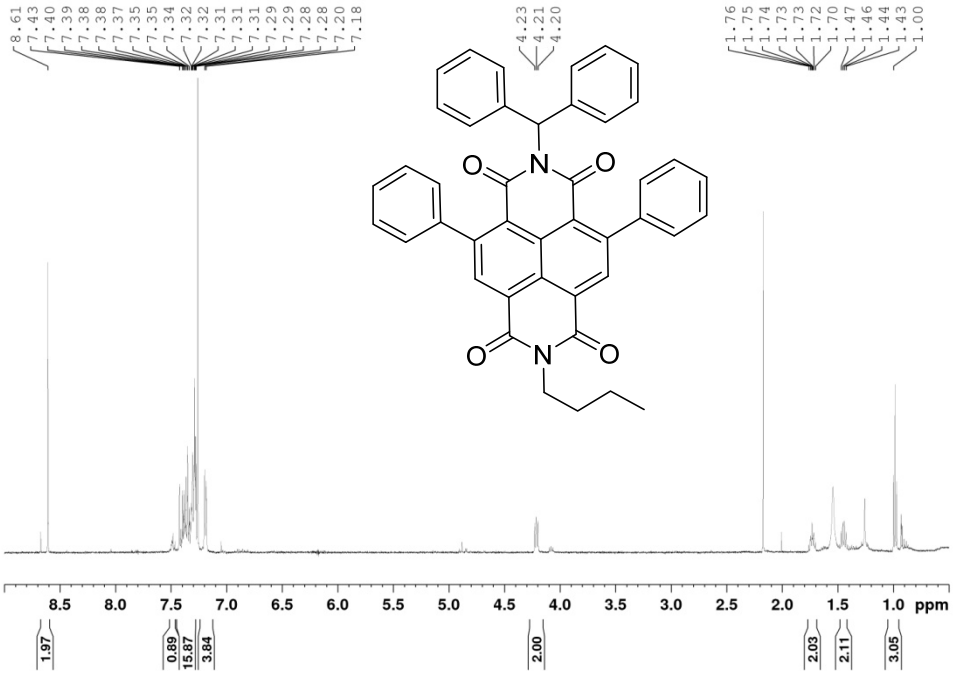


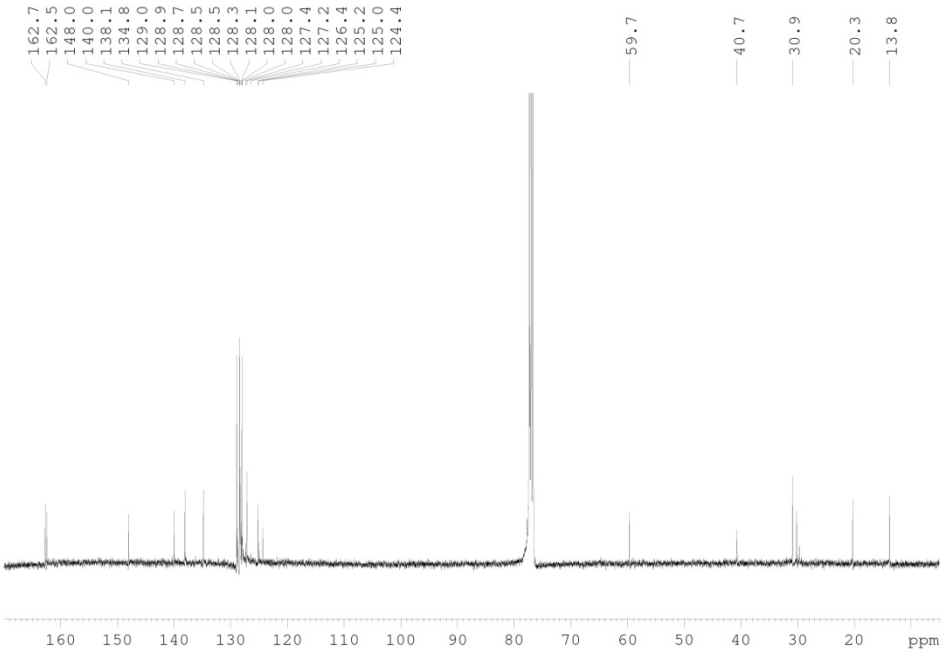

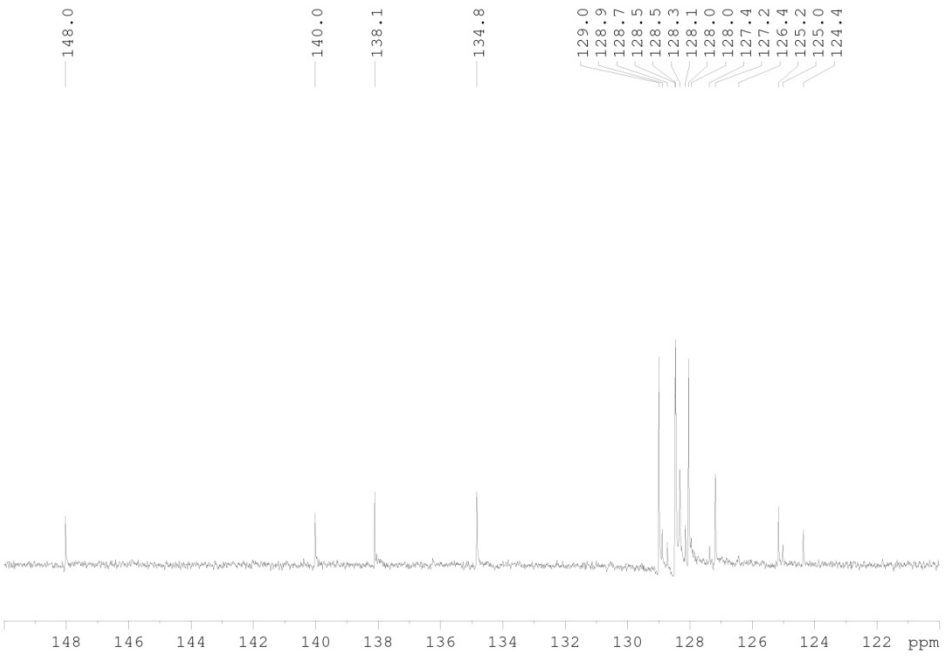


HSQC (400 MHz, $CDCl_3$)

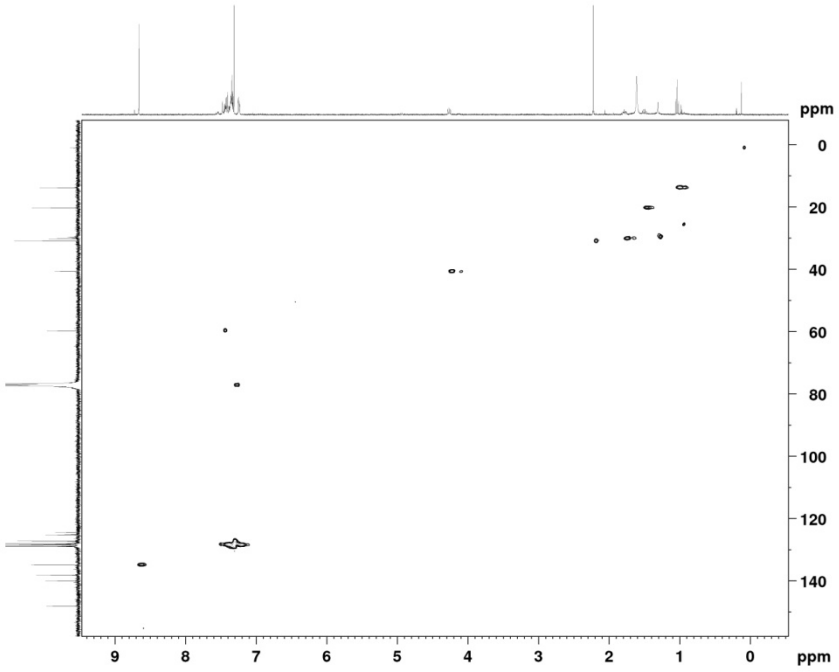

HMBC (500 MHz, $CDCl_3$)

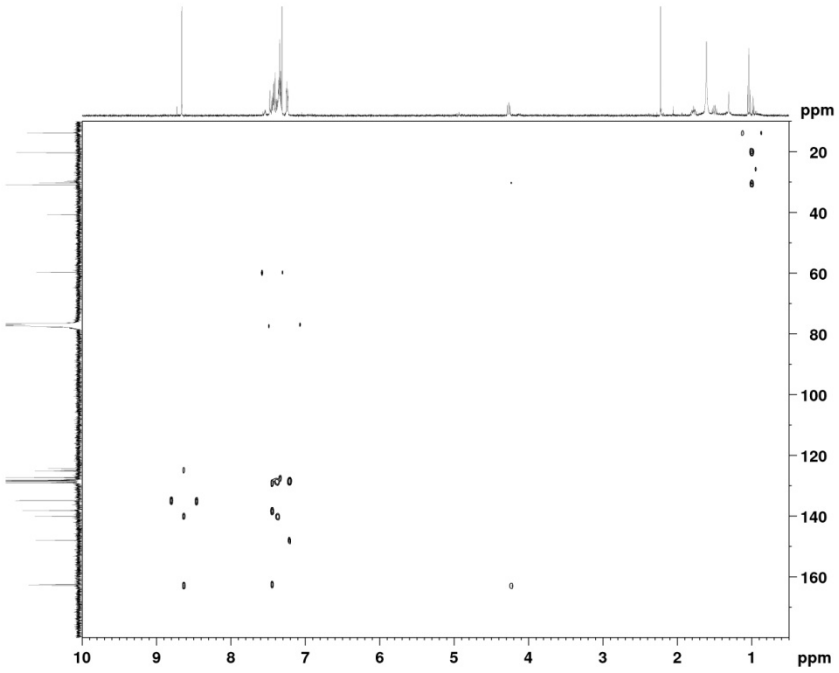

**Difunctionalised NDI, 426** (impure)

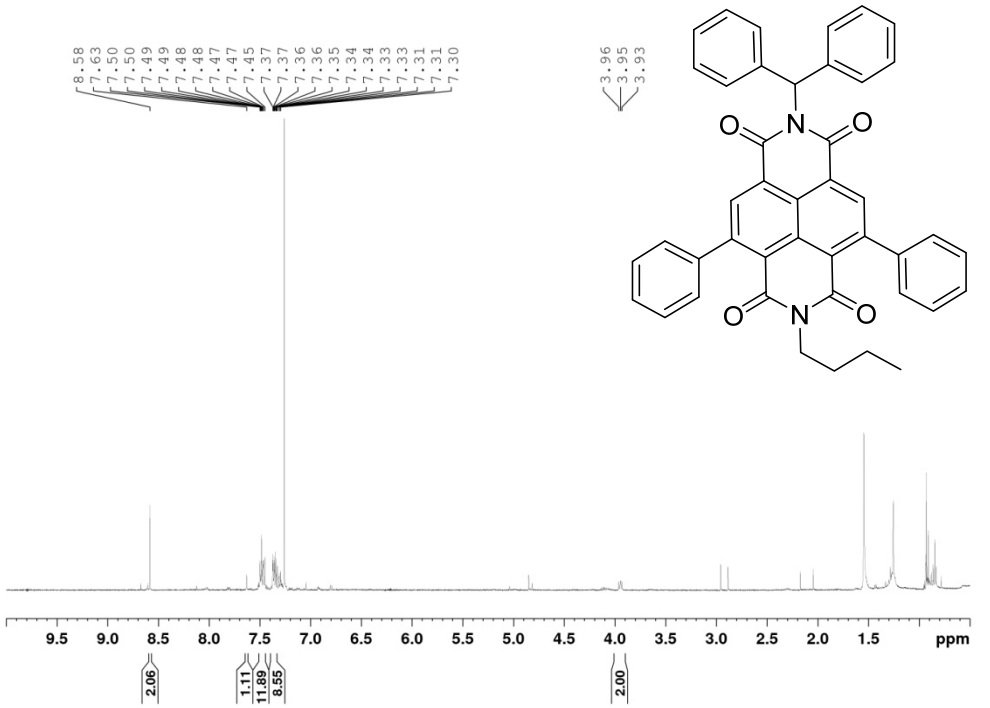


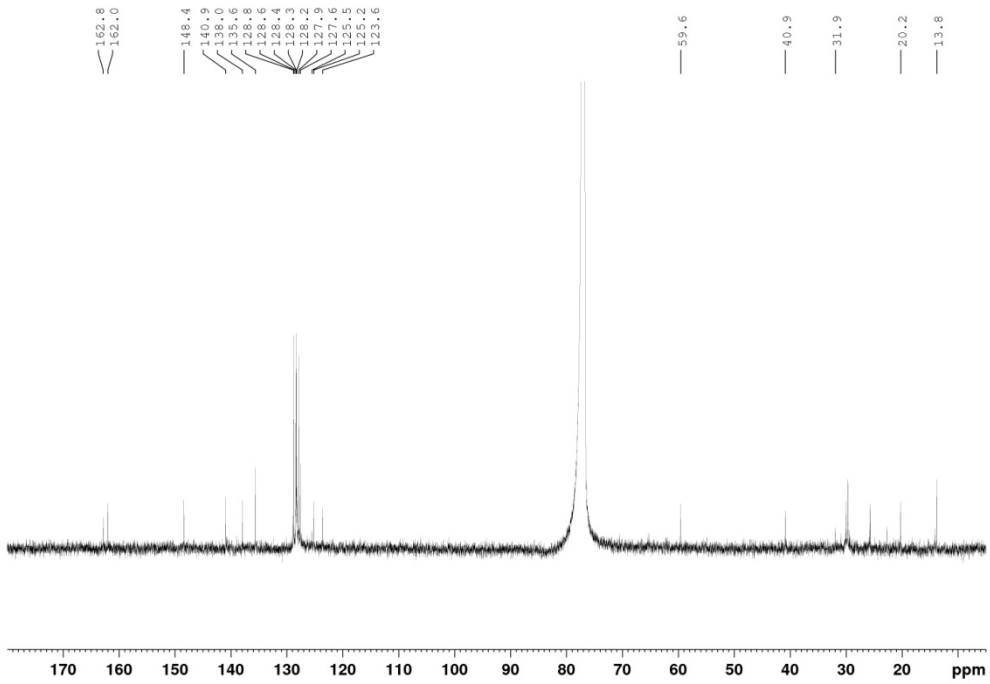

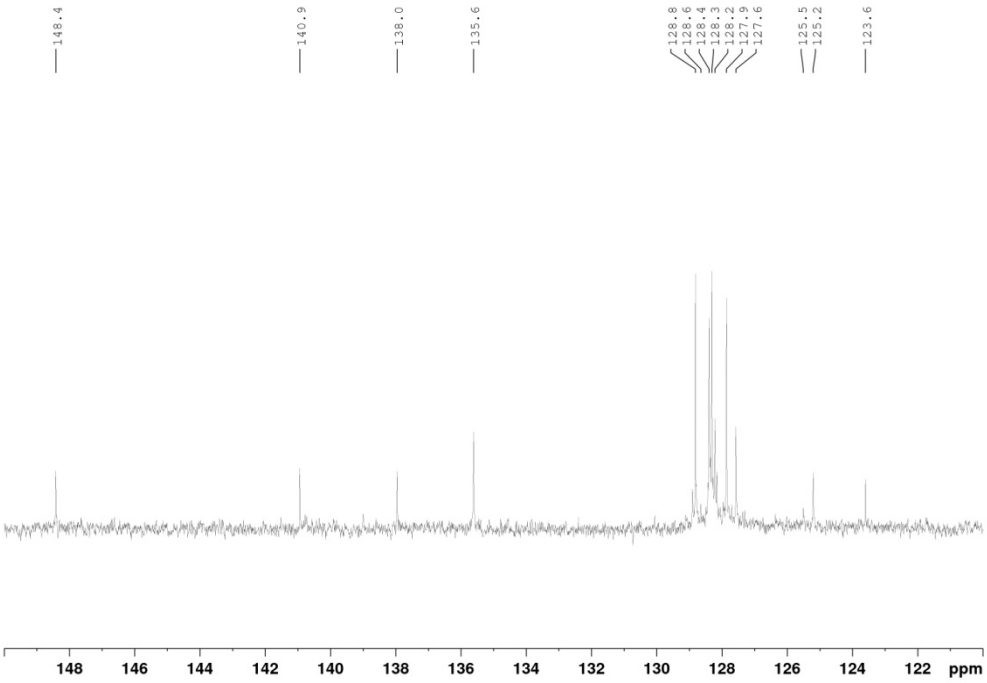


HMBC (500 MHz, $CDCl_3$)